Kamlesh kumar Yadava
Blast Furnace Operation
Malvika Steel Limited
Jagdishpur, Sultanpur.

Principles of Blast Furnace Ironmaking

Theory and Practice

ANIL K. BISWAS
University of Queensland, Brisbane, Australia

SBA PUBLICATIONS
1/1, Meredith Street, Calcutta-700072

PRINCIPLES OF BLAST FURNACE IRONMAKING

Copyright © 1981
Anil K. Biswas
First Indian edition 1984

All rights Reserved.
No part of this publication may be reproduced, stored in a retrieval system or transmitted in any form or by means: electronic, electrostatic, mechanical photocopying, magnetic tape, recording or otherwise without the prior written permission of
SBA PUBLICATIONS CALCUTTA

Library of Congress Catalog Card No. 80-65943
ISBN 0-949917-08-7 (Flexi cover)
(Students Edition)

Published by SBA PUBLICATIONS
1/1, Meredith Street,
Post Box 13315, Calcutta 700072
and
Printed by the Rekha Printers Pvt Ltd
A 102/1 Okhla Industrial Area, Phase II
NEW DELHI 110020

Symbols and conversion units

ata	=	pressure, atmosphere absolute
1 atm.	=	1 atmosphere pressure
	=	1 kilogram force per cm^2
	=	14.7 pounds force per square inch (14.7 lbs/in^2)
cal	=	calorie = 4.186 J (Joules)
kcal	=	kilocalories = 4.186 kJ
°F	=	degree Fahrenheit = 1.8 × °C + 32
ft.	=	foot = 0.3048 metre
ft^2	=	0.093 m^2
ft^3	=	0.028 m^3
gm	=	gram
h	=	hour
24 h	=	24 hours = 1 day
in.	=	1 inch = 2.54 cm
kg	=	kilogram
lb.	=	pound = 0.454 kg
m	=	metre
min.	=	minute = 60 seconds
Nm^3	=	gas volume in m^3 under standard (normal) conditions, of 1 atmosphere pressure and 0°C
s	=	second
THM	=	tonne hot metal (1000 kg of pig iron)
1 ton	=	2240 lbs
1 short ton	=	2000 lbs
η	=	viscosity
η	=	degree of utilization
η_s	=	sulphur distribution coefficient between slag and metal
ν	=	kinematic viscosity
T	=	°K
t	=	tonne (1000 kg)

To my wife
NILIMA
and to my sons
JAYDEEP and SANDEEP

and in loving memory of
MY PARENTS

Preface

The idea of writing this book came while I was engaged in the operatio of iron blast furnace and sinter plant. The behaviour of the blast furnac has always appeared to the operators as an enigma. The production o iron and the maintenance of its quality have depended greatly upon th experience and skill of the operators. It is only in the last two or thre decades that the art of ironmaking has changed to a science. This chang prompted me to collect all relevant information emanating from laborator and industrial research and operational experience and collate them i a comprehensive yet concise monograph for an easy understanding of th complicated processes occurring in the blast furnace and also for use a a text and reference by the under-graduate and graduate students, re searchers and teachers in the fields of metallurgical and chemical engineering as well as by blast furnace managers, supervisors, researchers and operators and steel plant executives.

The primary purpose of this book is to determine from theory as well as from practice the ways and means of increasing blast furnace productivity, which depends upon the fuel efficiency and flow of materials and gases through the dry and wet zones of the furnace. During teaching as well as in practice, I have felt the lack of any up-to-date single book which encompasses systematically the methods and limitations of forcing the furnace for greater productivity and increasing the fuel efficiency for decreasing the coke consumption. These have been summarized in Chapters 10 and 11 and all other chapters of the book have been largely designed as essential pre-requisites for the fulfilment of these prime objectives, containing both theory and practice.

Iron making mostly consists of interactions between various components and phases. For convenience in the discussions, the furnace has been divided into three zones based on temperature which are the logical outcome

of the various chemical reactions occurring inside the furnace. The thermodynamics and kinetics of the reactions treated in Chapters 2, 3 and 7 will be helpful in the understanding of the physico-chemical principles involved. The temperature profiles of the solids and gases in the furnace, which determine in no small way the fuel efficiency and burden descent, are discussed briefly in Chapter 4. An utmost importance has been attached to blast furnace aerodynamics which is treated in Chapter 5 and the raw materials and their properties which influence gas throughflow are described in Chapter 6. The latter chapter also includes factors that affect the reducibility of iron ores. The course of formation and the properties of primary, bosh and hearth slags are narrated in Chapter 8 and their influence on sulphur control in Chapter 9. The methods of theoretical coke rate calculations, reduction in coke rate and use of blast additives have been developed systematically in Chapter 10. The influence of the furnace profile and furnace irregularities on productivity has been treated in Chapters 12 and 13. As details have been described excellently elsewhere, only a brief outline of the furnace and its operation has been included in Chapter 1 only in order to maintain the continuity of the text as well as to provide a background to those not initiated in the blast furnace operation.

My grateful thanks to my wife Nilima for her help and support when they were most needed and for her most intimate participation in the preparation and writing of this book. I am indebted to Jaydeep Biswas and Sandeep Biswas for drawing of the figures and performing most of the calculations and also to Professors Paresh Ch. Chaudhuri, Joe Vuckovic and Saibal K. Gupta for their encouragement.

Last but not the least, is my indebtedness to the following learned Societies for permitting the use in the text illustrations drawn from their renowned journals: The American Society of Metals and the Metallurgical Society of AIME; The Iron and Steel Institute; The Metals Society; Indian Institute of Metals; Verlag Stahleisen; The Chemical Society; The Australasian Institute of Mining and Metallurgy; The Iron and Steel Institute of Japan; The American Ceramic Society; John Wiley & Sons.

November 1980

A. K. BISWAS
University of Queensland
Brisbane, Australia.

CONTENTS

		Page
	Symbols and conversion of units	vi
	Preface	vii
Chapter 1	**An Outline of the Process**	**1**
1.1	General	1
1.2	Reduction of Iron Oxides	6
1.3	Reactions in the Lower Zone	7
1.4	Reactions in the Middle Zone	11
1.5	Reactions in the Upper Zone	12
	Suggested Reading	13
Chapter 2	**The Physico-Chemical Principles**	**14**
2.1	Introduction	14
2.2	Equilibrium Constant and Activity	15
2.3	Raoult's and Henry's Laws	15
2.4	Free Energy	18
2.5	Oxygen Potential	19
2.6	Oxygen Potentials in the Blast Furnace	23
2.7	Increased and Decreased Reducibilities	24
2.8	Velocity of Gas-Solid Reactions	26
2.9	Blast Furnace Slag	48
2.10	Kinetics of Slag-Metal Reactions	57
	References	61
Chapter 3	**Systems of Importance in Ironmaking**	**64**
3.1	Introduction	64
3.2	The Fe-C System	64
3.3	The Fe-C-Metalloids System	65
3.4	The Fe-O System	66
3.5	The C-O System	69
3.6	The Fe-O-C System	72
3.7	Carburization of Iron	81
3.8	The H-O System	82
3.9	The C-O-H System	82
3.10	The Fe-O-H System	83
3.11	The Fe-O-H-C System	85
3.12	The Fe-O-Si-C-Slag System	87
3.13	The Fe-O-Mn-C-Slag System	91
3.14	The Fe-O-S-C-Slag System	92
3.15	The Fe-O-Si-Mn-S-C-Slag System	94
3.16	The FeO-SiO_2-Al_2O_3 System	98
3.17	The CaO-SiO_2-Al_2O_3 System	100
3.18	The CaO-MgO-SiO_2-Al_2O_3 System	105
3.19	The FeO-CaO-SiO_2 System	107
3.20	The FeO-CaO-Fe_2O_3 System	109
3.21	Alkali Metals and Their Compounds	110
	References	115

Chapter 4	**The Temperature Profile**	**118**
4.1	Introduction	118
4.2	Two-Stage Heat Balance	120
4.3	Factor Affecting Temperature Profile	124
4.4	The Reichhardt Diagram	133
4.5	Temperature Profile and Stock Movement	134
	References	135
Chapter 5	**Blast Furnace Aerodynamics**	**137**
5.1	Introduction	137
5.2	Importance of Uniform Gas Flow	138
5.3	Gas Flow – Static Bed of Equigranular Charge	140
5.4	Gas Flow – Multigranular Packed Bed	147
5.5	Bed Instability and Fluidization	153
5.6	Gas Flow in Wet (Bosh) Zone	157
5.7	High Top Pressure	165
5.8	Stock Distribution and Charging	169
5.9	Stock and Gas Movement	178
5.10	Variations in Stock and Gas Movement	184
	References	185
Chapter 6	**Raw Materials and Their Properties**	**188**
6.1	Introduction	188
6.2	Iron Ores and Agglomerates	188
6.3	Preparation of Ores	192
6.4	Agglomeration	194
6.5	Breakdown and Softening	208
6.6	Testing of Ores, Sinters and Pellets	214
6.7	Factors Affecting Reducibilities	222
6.8	Blast Air	243
6.9	Blast Furnace Fuels	249
	References	261
Chapter 7	**Reactions in the Blast Furnace**	**266**
7.1	General	266
7.2	Reactions in the Upper Zone	268
7.3	Reactions in the Middle Zone	273
7.4	Reactions in the Lower Zone	288
7.5	The Combustion Zone	303
7.6	Factors Affecting the Combustion Zone	308
7.7	Reoxidation of Metals	320
7.8	Thermal State of the Hearth	322
	References	326
Chapter 8	**Blast Furnace Slags**	**329**
8.1	Introduction	329
8.2	Formation of Primary and Bosh Slag	331
8.3	Formation of Bosh Slag	336
8.4	Final or Hearth Slag	343
8.5	Slag Composition and Utilization	347
	References	348

Chapter 9	**The Removal of Sulphur**	
9.1	General	
9.2	Chemistry of Sulphur Reactions	
9.3	Sulphur Reactions in the Shaft	
9.4	Sulphur Reactions in the Bosh	
9.5	Sulphur Reactions in the Hearth	
9.6	Sulphur Control	
9.7	External Desulphurization	
	References	
Chapter 10	**The Coke Rate and Fuel Efficiency**	
10.1	General	
10.2	Optimum Coke Rate Calculation	
10.3	Direct Reduction, Tuyere Carbon and Thermal Efficiency	
10.4	Reduction of Coke Rate – Methods	
10.5	Super Burden	
10.6	Stack Gas Injection	
10.7	Blast Additives	
10.8	High Top Pressure	
	References	
Chapter 11	**Blast Furnace Productivity**	**42**
11.1	General	4
11.2	Blast Furnace Production Index	4
11.3	Methods of Increasing the Productivity	4
11.4	Decrease in Coke Rate	4
11.5	Factors Limiting Productivity	4
11.6	Summary	4
	References	4
Chapter 12	**Productivity and Furnace Profile**	**48**
12.1	Introduction	48
12.2	Influence of Furnace Lines	48
12.3	Profile Calculations	48
12.4	Role of Lining Wear	49
	References	49
Chapter 13	**Furnace Irregularities and Their Control**	**496**
13.1	General	496
13.2	Channelling	496
13.3	Scaffolding	498
13.4	Scabs	502
13.5	Hanging	504
13.6	Slips	505
13.7	Ore Shift	507
13.8	Choking of Hearth	508
13.9	Chilled Hearth	509
13.10	Burning of Tuyeres	510
13.11	Coke Mess	510
	References	511
Subject Index		512

CHAPTER 1

AN OUTLINE OF THE PROCESS

1.1. General

The production of pig iron in the blast furnace ranks foremost amongst all the ironmaking processes. This is not only because of the very high production rate but also because of the great degree of heat utilization that can be obtained in such furnaces. Modern high capacity furnaces are producing as much as 12 000 THM* per day. The degree of heat utilization is to a remarkable extent of 85–90 percent which has been made possible because the blast furnace is an extremely efficient counter-current heat exchange apparatus.

The source of iron is its ores where iron exists mainly as oxides either as hematite Fe_2O_3 or magnetite Fe_3O_4 and sometimes in small proportions of hydroxides and carbonates. Of all the iron-bearing minerals used for blast furnace smelting, hematite represents the largest proportion. When chemically pure, hematite contains about 70 percent and magnetite about 72.4 percent of iron. But, usually, the iron content of the ores ranges between 50–65 percent for *rich* ores and 30–50 percent for the *lean* ones and the remainder is represented by gangue which consists mostly of silica and alumina as well as minor amounts of moisture and chemically-combined water. The ores are used either directly from the mines (*run-of-*

* THM = tonnes (1000 kg) hot metal

mine or *raw* ores) or nowadays mostly as sinters and pellets. Sintering and pelletising are processes by which iron ore fines are agglomerated into larger pieces with or without incorporation of lime and magnesia as fluxes. Other iron-bearing materials used in small quantities are scrap, open-hearth or converter slags, mill-scale. The gangue materials are insoluble in liquid iron and possess very high melting points. They, however, fuse at lower temperatures in the presence of the flux and form a slag. (Magnesia helps to lower the fusion temperature and increase the fluidity of the slag.) Lime and magnesia are *bases* and silica and alumina *acids*, their ratio known as *basicity* of the slag.

The slag and the iron can only be separated completely from each other when they are in the liquid state which requires them to be heated to above their fusion temperatures. The heat is usually supplied by burning of coke, although heating by electrical energy or by other fuels are possible but in most circumstances not economical. The reduction of iron oxides also needs sufficiently high temperatures as well as adequate amounts of reducing agents – these functions performed mainly by coke carbon. The iron also picks up 2–4.5% C from coke which lowers its melting temperature from 1534°C by 200–350°C depending upon the carbon content. The coke contains ash ranging from 6–10 percent in most of the countries to as high as 20–25 percent in a few places like India. The ash contains mainly silica and alumina which need a further amount of lime/magnesia for fluxing. The ore, coke and flux contain compounds of Si, Mn, P, S and small amounts of other impurities like Pb, Sn, Cu, Ni, Cr, Ti, alkali metals, etc., which get reduced partly or wholly and taken up by iron. (Manganese ores are usually added deliberately in order to introduce the element in the iron for the beneficial effect it has in iron- and steelmaking.) While phosphorus is almost entirely reduced and enters the iron, varying amounts of silicon from silica, manganese from Mn-bearing materials and sulphur from ore and coke are retained by the iron, depending upon the temperature and basicity of the slag. The control of sulphur in iron is the prime consideration in the fixation of slag basicity. In pig iron, the Fe component comprises about 92–93 percent, the rest being C, Si, Mn, P. S, etc.

The oxygen necessary for the burning of coke is supplied by air (blast) which is preheated in (regenerative stoves) in order to supply sensible heat from outside and thus reduce coke expenditure. Since preheating of the air is performed by the burning of the blast furnace gas (which comes out of the furnace top and contains usually 20–30% CO and 10–20% CO_2, the rest being nitrogen with a little of hydrogen and moisture), a part

of the chemical heat, i.e., unused CO, is indirectly utilized. The blast is introduced above the bottom of the furnace through water-cooled tuyeres whereas the burden materials are charged from the top with the help of skip cars or sometimes by conveyer belts.

A section of the blast furnace is shown in Fig. 1.1. The cylindrical top portion (the wall armoured for protection of refractory brick lining against falling hard burden materials) is called the *throat* and below that the *stack* or *shaft* extends with increasing diameter up to the cylindrical *belly* or *bosh-parallel*. Thereafter, the diameter decreases in the portion, known as *bosh*, which connects with the bottom-most portion, the *hearth*, where molten metal and slag accumulate.

The opening at the top is provided with a double bell or other new systems (e.g., 4-bells or bell-less top) for charging the burden which has to travel downwards for more or less about 25 metres in order to provide the ascending gases the opportunity to give up its sensible heat as well as to enable its reducing component CO (and H_2) to pre-reduce the iron oxides (*indirect* reduction). From the opening, the throat extends vertically downwards for a couple of metres or more; thereafter, the stack extends downwards to an extent of about 3/5 of the total height, its increasing diameter facilitating a uniform flow of the thermally expanding gases and burden materials. The cylindrical belly has the largest diameter in the furnace and, normally, the fusion and consequent contraction of the slag and metal start in this region. The bosh has the shape of an inverted truncated cone, the base merging with the belly and the top with the top of the hearth. The blast is introduced through a series of equidistant water-cooled *tuyeres* around the hearth periphery about 40–60 cm below its upper rim at a pressure of 1.5–2.5 atm. gauge to overcome the resistance of the materials inside the furnace. It enters the hearth at a velocity of 150–300 m/s.

The furnace profile, i.e., the shape and dimension of each individual portion (e.g., the heights, diameters and angles with the horizon), depend upon the working methods, blast temperatures, burden variety and others. The enlargement of the stack, belly and bosh and the shaft and bosh angles (cf. Fig. 1.1) must be so chosen that the burden descends smoothly and the ascending gases distribute uniformly as far as possible over the entire furnace cross-section. Modern high capacity furnaces tend towards shorter and flatter bosh.

The iron notch or *tap-hole* is situated about 50–150 cm above the hearth bottom and the *slag notch* about 1 m above the iron notch. The cold blast

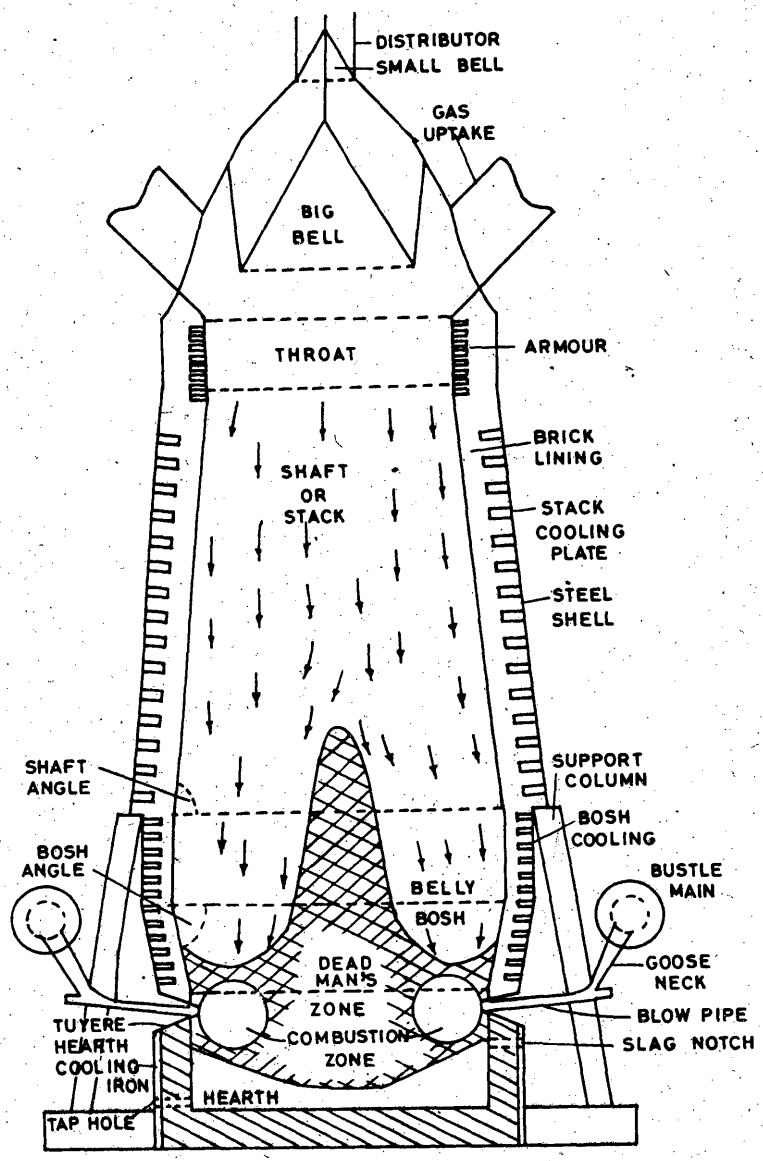


Fig. 1.1 A section of iron blast furnace showing salient features including material flow, combustion zone, etc.

from the turbo-blowers is carried through hot (regenerative *stoves*) for preheating and subsequently distributed to the tuyeres from a *bustle pipe* or *ring main* around the furnace through (*goose-necks*) and *blow pipes*.

At the top of the furnace there is a device for preventing the escape of the blast furnace gas as well as for proper distribution of the charge materials. The conventional device consists of a small and big bell, one remaining closed while the other discharges the materials on the big bell or into the furnace. The small bell rotates with a distribution hopper for delivering materials around the top of the large bell according to predetermined *charge cycle* or *sequence* and when the latter is full it is lowered to allow the materials to drop in the furnace. The (materials or the *stock* or *burden*) as they are called should be properly distributed for uniform distribution of the ascending gases. The distribution pattern at the top (*stock-line*) depends on the size and other physical characteristics of the materials as well as on the diameter and angle of the large bell and the height of fall of the materials from the large bell rim or *lip*, apart from some other variables (Sec. 5.7). Since the materials segregate during and after the fall and the stock-line pattern permeates right down to the lower portions, a proper charging of materials assumes great importance for the productivity, fuel economy and smooth running of the furnace.

The lining of the furnace consists usually of fire-clay bricks. The lower and hotter portions like the bosh and the belly should be lined with alumina-rich (40–50% alumina) high duty fire-clay bricks whereas in the upper stack they need only be resistant to abrasion. The thermally most susceptible portion is the hearth and its bottom which are lined with very high duty alumino-silicate or carbon bricks (The latter is highly refractory but is susceptible to attacks by low-carbon iron or oxidizers like ore and air.) It is better to line the hearth base with a thick layer of carbon bricks with water or air cooling underneath. The life of the bricks is enhanced by cooling with water from the hearth to the top with the help of hearth bosh and stack cooling plates.

Coke is the only component of the charge materials which descends as a solid to the tuyere level. Apart from supplying the reductant and heat for processing the burden into finished products, the coke provides mechanical support to the burden especially where it is needed most, i.e., in the bosh region where the metal and slag are liquid. These liquids flow down to the hearth through the interstices of the coke particles (coke grid). The coke rate in the blast furnace per tonne of pig iron (referred throughout the text as THM) varies from 1000 kg to as low as 450–500 kg. Low coke

rates are obtained with pre-fluxed sinters and pellets, high blast temperatures and uniform gas distribution.

The hot blast of air entering the furnace through the tuyeres burns the coke carbon to CO_2 immediately in front of them. The intense heat produced gives a flame temperature (tuyere gas temperature) of 1800–2000°C, depending upon the blast temperature. Since CO_2 is unstable in the presence of carbon above 1000°C, CO is produced according to $CO_2 + C = 2CO$. The tuyere gas, therefore, consists only of CO and nitrogen, their contents being about 35 and 65 percent respectively when dry blast is used. The coke does not fall continuously but only periodically into the tuyere zone from above.

This hot reducing gas rises through the *active coke bed* to the bosh, belly and the shaft and reduces the iron oxides (see Sec. 1.3).

1.2. Reduction of Iron Oxides

There are three forms of iron oxide: hematite (Fe_2O_3), magnetite (Fe_3O_4) and wustite (FeO).* These oxides are reduced in stages. Their reactions with CO, the equilibrium CO/CO_2 ratios and CO-utilization factors η_{CO} at 900°C are given below. The extent of utilization, i.e., the fraction or percentage of CO converted to CO_2 is denoted as,

$$\%\eta_{CO} = 100.\%CO_2/(\%CO + \%CO_2) \qquad 1.1$$

The reasons for quoting the values at 900°C will be apparent later in the text.

Reactions	*Equilibrium at 900°C*		
	CO/CO_2	η_{CO}, %	
$3Fe_2O_3 + CO = 2Fe_3O_4 + CO_2$	0	ca. 100	1.2
$Fe_3O_4 + CO = 3FeO + CO_2$	0.25	80	1.3
$FeO + CO = Fe + CO_2$	2.3	30	1.4

Since the blast furnace is a (counter-current) process, the tuyere gas with high CO-content comes into contact with the wustite which needs a very high reduction potential for conversion to Fe (Eq. 1.4). The resulting lower potential gas, as it ascends, encounters magnetite and hematite which require much smaller equilibrium CO/CO_2 ratios for reduction to lower

* Wustite is a non-stoichiometric compound of average formula $Fe_{0.95}O$ (cf. Sec. 3.4.3). For convenience only the formula FeO has been used throughout the text.

oxides. Hence, the reduction of wustite is of prime importance in iron oxide reduction, especially because about 70 percent of hematite oxygen is present as wustite.

As CO_2 represents the end combustion product of carbon, the utilization of the chemical and thermal energies of carbon will be more complete the higher the amount of oxygen removed by reactions 1.2–1.4. These reactions are called *indirect* or *gaseous* reduction and the reaction product is CO_2. The overall reaction 1.2–1.4 is mildly exothermic.

If any wustite remains unreduced in a zone where temperatures are higher than 1000°C, the CO_2 produced by reaction 1.4 is rapidly reduced by carbon according to:

$$CO_2 + C = 2CO - 41\,210 \text{ cal} \qquad 1.5$$

Combining Eqs. 1.4 and 1.5,

$$FeO + C = Fe + CO - 37\,220 \text{ cal} \qquad 1.6$$

Reaction 1.5, known variously as *Boudouard* or *solution loss* or *carbon gasification* reaction, is highly endothermic and also deteriorates CO-utilization. Reaction 1.6 is called *direct* reduction and is endothermic in contrast to *indirect* reduction but consumes less carbon for every mole of oxygen removed because the product, CO, can take part in further (gaseous) reduction.

The tuyere gas with a high flame temperature of 1800–2000°C cools down to 100–250°C at its exit during its ascent and the burden materials are heated up to 1400–1450°C during their descent. As idealized in Fig. 1.2, there are three distinct temperature zones in the furnace (for reasons, see Chapter 4) and the total heat requirement is supplied by the ascending gases in the lower and upper zones, the middle one being almost isothermal (800–1000°C) where very small heat transfer occurs. The reactions occurring in the three zones are described below.

1.3. Reactions in the Lower Zone

The lower or *melting* or *processing* zone extends from the tuyere level to 3–5 m above. The temperature of the molten materials reaches 1400–1450°C in this zone and the gas cools down to 800–1000°C (Fig. 1.2).

The burning of coke in front of the tuyeres results in a continuous creation of an empty space around the hearth periphery which permits the flow of the charge materials downwards (Fig. 1.1). The dimension and

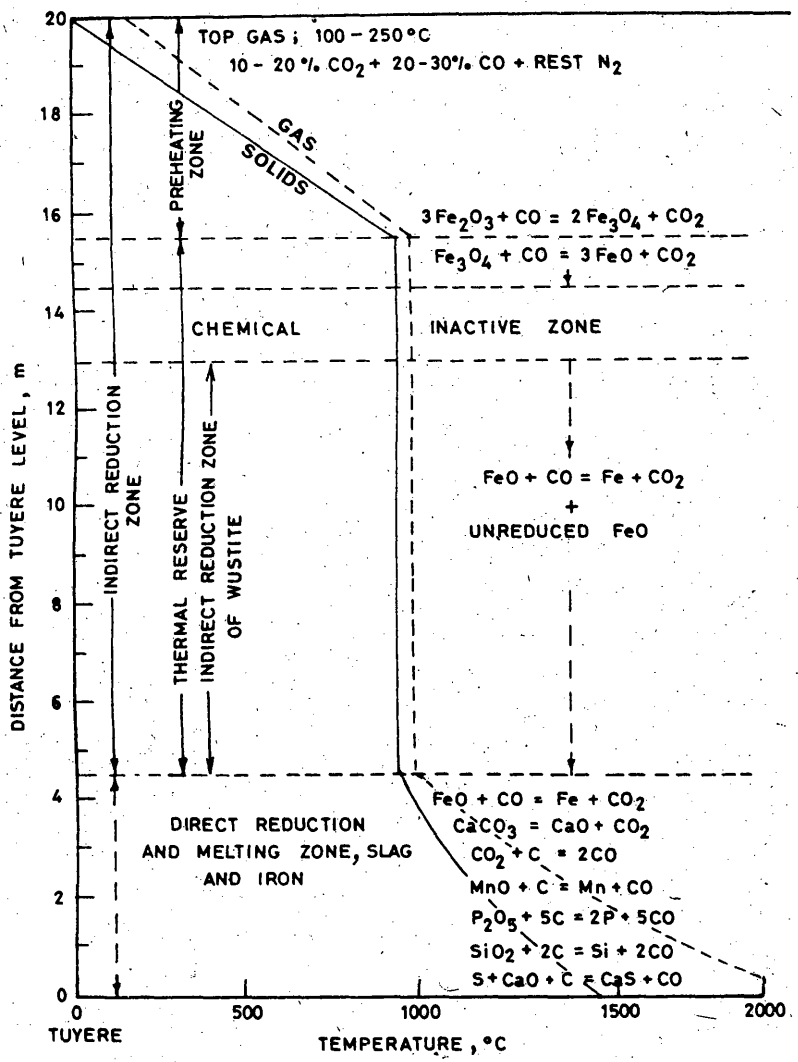


Fig. 1.2 An idealized scheme of temperature distribution of gas and solids along the height of the blast furnace and the chemical reactions occurring in the three main temperature zones.

configuration of this *combustion zone* is of importance for uniform gas distribution and stock descent. Depending upon the kinetic energy of the blast, the depth of the combustion zone is about 1–2 m. Therefore, the actual active area is a ring of 1–2 m depth, around the hearth periphery, named variously as *raceway* or *hearth annulus* or *active perimeter*. Beyond the raceway, there is a closely-packed central column of coke called *dead man's zone* (Fig. 1.1; Sec. 7.5). The coke column either floats on the liquid iron in the hearth or reaches as far as the hearth floor. Some slag and iron remain entrapped in the interstices of the coke pieces and are drained out during tapping.

The gangue in admixture with the flux starts to fuse in the belly region where two immiscible phases (partly carburized primary iron and FeO-SiO_2-Al_2O_3-MnO primary slag containing some CaO) begin to form at temperatures above 1200°C. Further down, these two liquid phases separate from each other, infiltrate through the coke grid above the raceway and collect in the hearth well from where they are tapped periodically. Since the tuyere gas also rises through the voids of the coke bed, the raceway resembles a counter-current liquid-gas exchanger, the coke providing the mechanical support. The flow of materials in this region is important because of danger of *flooding* (Sec. 5.6).

As discussed in Secs. 11.3.2.6 and 11.5, examination of the internal structure of blast furnaces quenched while in operation shows the existence of a loosely packed central coke column extending into the lower shaft. The loosely packed column is bounded by a softening-melting or cohesive zone consisting of alternate layers of coke and impervious, viscous, semi-fused mass of slag and iron through which the ascending gases are unable to flow. The permeable coke layers, called coke slits, act as gas distributors and permit the gas to flow horizontally through them. The gas ascends through the more permeable solid bed to the top. Since most of the gas has to pass through the coke slits, they should be permeable and hence greatest importance is attached to the resistance of coke to breakage, especially in large furnaces. The fusion zone and distribution of the gas through the coke slits are shown in Figs. 1.3 and 11.24. The formation and characteristics of the raceway are described in Sec. 7.5.

The primary slag picks up further lime to form bosh slag and later the coke ash released at the tuyeres and they together form the hearth slag the composition of which should be such as to provide adequate fluidity so that it flows out freely when tapped. In general, the composition of the slag is so selected that its liquidus temperature lies between 1400–1450°C and its viscosity within 10 Poise at 1500°C. This is, in general assured if the basicity ratio of the slag, expressed as $(\%CaO + \%MgO)/(\%SiO_2 + Al_2O_3)$, is about 0.9–1.2. The viscosities, basicities and liquidus temperatures of some commercial blast furnace slags are shown in Table 9.5. The slags do not contain any FeO because any

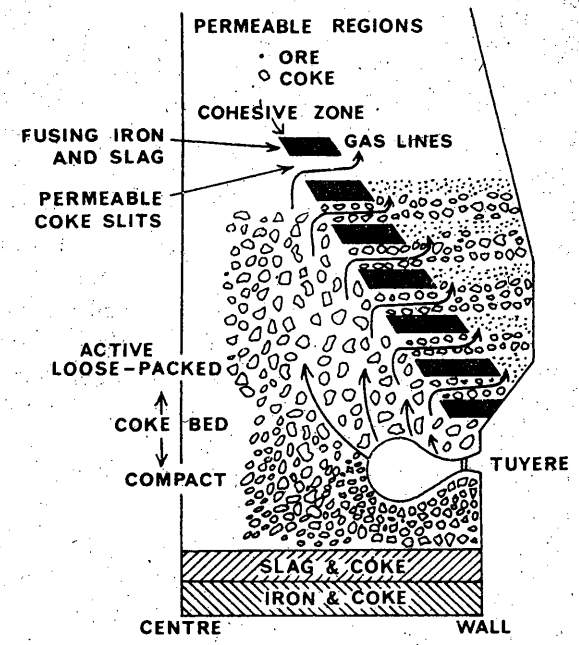


Fig. 1.3 Schematic representation of a section of the blast furnace quenched while in operation showing an inverted-V type of cohesive zone. The gases pass horizontally through the permeable coke slits interspersed with relatively impervious layers of fusing slag and iron. The coke bed, acting as percolator, is compact below the tuyere level floating on iron or reaching the hearth floor, the interstices occupied by slag and iron; it is active and loose-packed above the tuyere level because of the upward thrust of the high velocity combustion gases. The fine coke accumulates at the cavity wall in front of the tuyeres.

unreduced FeO is either completely reduced in the hearth in contact with the submerged coke column or while it percolates from the cohesive zone through the coke grid.

The minimum hearth temperature necessary for free running of the slag is termed as *critical hearth temperature* which is about 1500–1550°C in order to provide some superheat in the hearth and ensure that both slag and iron are in the liquid state under all operating conditions.

The more important chemical reactions occurring in this zone are:

i) endothermic calcination of limestone; $CaCO_3 = CaO + CO$
ii) endothermic direct reduction of FeO; $FeO + C = Fe + CO$
iii) endothermic direct reduction of SiO_2; $SiO_2 + 2C = Si + 2CO$
iv) endothermic direct reduction of MnO; $MnO + C = Mn + CO$
v) endothermic direct reduction of P_2O_5; $P_2O_5 + 5C = 2P + 5CO$

vi) endothermic sulphur removal;
$$FeS + CaO + C = CaS + Fe + CO$$
vii) exothermic combustion of carbon; $C + O_2$ (air) $= CO_2 + N_2$
viii) endothermic reduction of CO_2; $CO_2 + C = 2CO$ (>1000°C)
ix) endothermic reduction of moisture in blast;
$$C + H_2O = CO + H_2 \ (>1000°C)$$

The final temperature of iron is about 1350–1450°C and that of slag about 50–100°C higher. Depending upon the raw materials and the finished products, the heat requirement in the lower furnace including radiation and cooling losses may range between 0.7 to 1.0 million kcal per THM. This results in a rapid cooling of the tuyere gas from about 2000°C to 800–1000°C since all the above heat devouring reactions occur above 900°C. At this stage the temperatures of the gas and the charge materials approach close to each other. The thermal reserve zone starts at this point and continues up to 4–6 m below the stock level.

1.4. Reactions in the Middle Zone

The middle zone, where the temperatures of the solids and the gas are near identical (800–1000°C), is called *isothermal* or *thermal reserve* zone. Since most of the indirect reduction, especially of wustite, occurs in this zone, it is also referred to frequently in the text as 'indirect reduction' zone. In a well-run furnace this zone may occupy even 50–60 percent of the furnace volume. A major proportion of indirect reduction of iron oxides according to Eqs. 1.2–1.4 occurs in this zone.

The extent of this zone is important because the wustite should be given as much opportunity as possible for getting reduced indirectly. The factors that affect the rate of reduction of iron oxides are discussed in Secs. 2.8 and 6.7. The start of this zone depends upon the level of the furnace where the highly endothermic reactions begin and the extent upon the heat transfer efficiency and, therefore, upon homogeneous gas distribution in the various furnace cross-sections (Chapter 4).

Insertion probes into modern furnaces at different levels and analysis of gas samples show the presence of a *chemical inactive* zone inside the middle zone where very little exchange of oxygen between the ore and the gas occurs and the gas composition suffers very little change. The CO/CO_2 ratio of the gas in the inactive zone is about 2.3, a value exhibiting

an equilibrium with Fe-FeO (Eq. 1.4). This zone becomes pronounced especially in cases where the coke consumption per THM is very low.

Another reaction of importance which occurs in the middle zone is the so-called *water-gas shift* reaction:

$$CO + H_2O = CO_2 + H_2 \qquad 1.7$$

This reaction generates hydrogen which is a more active reductant than CO. The moisture is generated from reduction of iron oxides with hydrogen which itself comes from humid air or when steam and hydrocarbons are used as blast additives.

1.5. Reactions in the Upper Zone

In the upper or *preheating* or *preparation* zone, the temperature of the gas ascending from the middle zone falls rapidly from 800–1000°C to 100–250°C and that of the solids rises from ambient to 800°C.

The main reactions that occur in this zone are:

i) decomposition of carbonates other than that of calcium;
ii) vaporization of moisture and hydrated water of the burden;
iii) carbon deposition, $2CO = CO_2 + C$;
iv) partial or complete reduction of hematite and magnetite to their lower oxides.

It takes about 6–8 hours for the burden to descend from the top to the tuyere level depending upon the rate of production. The time of residence of the charge materials in each of the three zones is not known precisely. In contrast, the time of residence of the gas in the furnace varies from 1 to 10 seconds or more.

After the end of the last war, an increasing number of iron blast furnaces has been built all over the world. The number of operating furnaces is approaching 1000 with an annual production capacity of 500–600 million tonnes of pig iron.

The cost to built a modern high capacity furnace including ancillary equipment is at present about 100–120 million dollars.

The cost of production of a tonne of pig iron is about 90–100 dollars excluding the investment and amortization costs. The cost, however, depends upon the locality, price of ore and coke and others.

The purpose of this introductory chapter is to briefly familiarize the reader with the process of ironmaking in the blast furnace. The details of the principles involved and how they affect the coke consumption and productivity are outlined in the text to follow.

Suggested Reading

1. PAWLOW, M. A.: Metallurgy of pig iron, vols. 1–4 (in German), Verlag Technik, Berlin, 1953.
2. POCHWISHNEW, A. N.: Blast furnace process (in German), Verlag Technik, Berlin, 1954.
3. Blast furnace – Theory and practice, vols. 1 and 2: Edt. J. H. Strassburger, Gordon & Breach, N.Y., 1969.
4. BOGDANDY, L. v. and H-J. Engell: The reduction of iron ores (in English), Springer – Stahleisen, Düsseldorf, 1971.
5. Blast furnace ironmaking – 1977 and 1978: Edt. W. K. Lu, McMaster University, Hamilton, Canada.

CHAPTER 2

THE PHYSICO-CHEMICAL PRINCIPLES

2.1. Introduction

Iron exists in nature mainly as its oxides and the metal is obtained by their reduction. During reduction, impurities like carbon, silicon, manganese, phosphorus, sulphur and others enter the so-called pig iron. Since both iron and slag are obtained in a liquid state, their metallurgy is essentially a high temperature chemistry. A theoretical treatment of ironmaking principles, which involves heat and mass transfer, is rendered difficult by the presence of solid, liquid and gas phases on the one hand and numerous components in the system on the other. Further complications arise because of the uncertainties as to whether the interactions amongst the various phases and components reach equilibrium at all. However, even with all these difficulties it is possible to obtain an approximate estimate of the possibilities and extent of reactions from the study of thermodynamic and kinetic data.

The physico-chemical principles of metallurgical processes have been discussed by various authors.[1-10] The essentials pertaining to ironmaking are given briefly in this chapter so as to enable a better understanding of the treatment in the text that follows.

2.2. Equilibrium Constant and Activity

Equilibrium in any reacting system is reached when the forward reaction of the reactants and the reverse reaction of the products assume the same velocity. For a general reaction:

$$A + B = C + D$$

$$K = \frac{a_C . a_D}{a_A . a_B} \qquad 2.1$$

where a = activity of the components
K = equilibrium constant of the reaction

K is a function of temperature. Eq. 2.1 is known as the Law of Mass Action (LMA). As an example, for the reaction

$$Si + O_2 = SiO_2,$$

$$K = \frac{a_{SiO_2}}{a_{Si} . a_{O_2}} = \frac{a_{SiO_2}}{a_{Si} . p_{O_2}} \qquad 2.2$$

At moderate total pressures, the activity of a gaseous component can be taken as equivalent to its partial pressure.

2.3. Raoult's and Henry's Laws

In an ideal solution, the mole fraction of any component is equal to its activity and when plotted they give a straight line known as *Raoult's line* (Fig. 2.1a). This activity is with reference to the standard state of activity equal to unity when the solute is in a pure state. In non-ideal cases the extent of departure from Raoult's law is measured by the activity coefficient, γ,

$$a = \gamma . N$$

The activity coefficient is, therefore, a measure of deviation from ideality and its value is unity when the deviation is nil, greater than unity in case of positive deviation and less than unity in case of negative deviation. These are shown schematically in Fig. 2.1(a).

In non-ideal cases and in very dilute solutions the activity is, as shown by the straight-line relationship, proportional to the mole fraction though they are not equal. This is the region of *Henry's* law as shown by the Henry's line in Fig. 2.1(a) for which a standard state has been defined, i.e., the activity coefficient of a solute, γ°, is unity in an infinitely dilute solution. This is, however, a purely hypothetical situation as the linearity

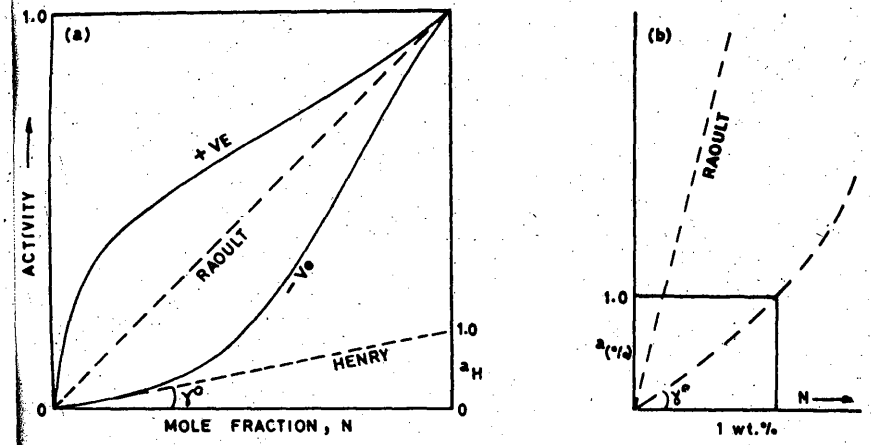


Fig. 2.1 A schematic activity diagram showing (a) the Raoult's and Henry's laws and positive and negative deviations from ideality; (b) change of scale on changing the standard state to 1 wt.%.

cannot be extended to the state of pure solute. In dilute solutions, the activity terms in the equilibrium constant equation can be replaced by mole fraction but the value of K in the LMA equation would be different. It would, however, remain constant because of the constancy of γ° within the scope of the straight-line relationship, beyond which the Henrian activity coefficient is needed to be introduced to cater for the deviation.

In ironmaking, as in the making of other metals, we deal with impurities in the metal whose concentrations are small. Therefore, a more convenient standard state can be defined where the activity is equal to unity at one weight per cent concentration of the solute, as shown schematically in Fig. 2.1(b), which is an enlarged version of Fig. 2.1(a) in the dilute region. The choice of this standard state is rendered mathematically feasible because at low concentrations the weight per cent of any solute in a solution is approximately proportional to its mole fraction. In such a case, Eq. 2.2 can be rewritten in the form of Eq. 2.3 where the equilibrium constant of the former will be different from that of the latter:

$$K' = \frac{a_{(SiO_2)}{}^*}{a_{[\%Si]} \cdot p_{O_2}} \qquad 2.3$$

$$= \frac{a_{(SiO_2)}}{(\text{wt.\%Si}) \cdot p_{O_2}}$$

Throughout the text the parenthesis will be used for the slag phase and the square bracket [ ] for the metal phase unless indicated otherwise.

However, it is more often than not that even in dilute solutions, especially in the presence of other impurity elements, Henry's law is not obeyed and the activity coefficient (γ') has to be used to obtain the constant K' (e.g., $a_{[\%Si]} = \text{wt.\%[Si]} \times \gamma'_{Si}$).

In multi-component alloys, the alloying elements affect the activity coefficients of one another. It is possible to find the activity coefficient of one component, e.g., that of sulphur in pig iron with the help of Wagner's equation:[8,9]

$$\log \gamma'_S = \log f_S^S + \log f_S^{Si} + \log f_S^{Mn} + \log f_S^P + \log f_S^C \text{ etc.} \qquad 2.4$$

where

γ'_S = overall activity coefficient of sulphur in a dilute multicomponent alloy at a given concentration of S;

f_S^S = activity coefficient of sulphur in Fe-S binary alloy at the same concentration;

f_S^{Si}, f_S^{Mn}, etc. = coefficients representing the effect of the respective elements on the activity coefficient of sulphur (interaction coefficients).

The $\log f_S^S$ values are given in Fig. 2.2.[11] The activity coefficient of sulphur in a typical pig iron is calculated[9] with the help of Eq. 2.4 and Fig. 2.2,

For 1.5% Si, $\log f_S^{Si} = +0.10$
4.0% C, $\log f_S^C = +0.52$
1.0% Mn, $\log f_S^{Mn} = -0.03$
0.06% S, $\log f_S^S = 0.00$

on adding, $\log \gamma' = 0.59$
or $\gamma' = 3.9$

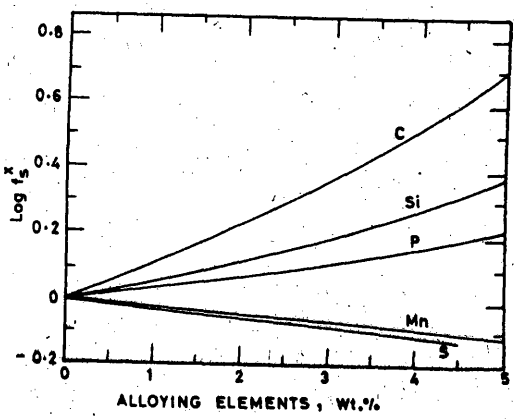


Fig. 2.2 Effect of alloying elements on the activity coefficient of sulphur in liquid iron, after Sherman and Chipman.[11] (Copyright AIME).

Due to the presence of these elements in the blast furnace iron, the activity of sulphur increases about four-fold over the normal, depending upon the concentration of the elements. In other words, in such an iron the sulphur has a four-fold tendency of escaping from the metal to slag. More recent values are also available.[5,10]

In order to facilitate calculations of the activity coefficient a term, *interaction parameter*, has been introduced valid strictly for infinitely dilute solutions. In most dilute multi-component solutions, the interaction coefficient has been found to be a logarithmic function of the concerned solute, independent of the concentration of other elements, the relation being expressed (in terms of wt.% standard state) as:

$$\left[\frac{\partial \log f_S^S}{\partial \%S}\right]_{\text{Si, Mn, etc.} = 0} = e_S^S, \qquad \left[\frac{\partial \log f_S^{Si}}{\partial \%Si}\right]_{\text{S, Mn, etc.} = 0} = e_S^{Si} \qquad 2.5$$

The interaction parameter (e) values are given in the literature for many multi-component alloys. For evaluation of the overall activity coefficient, in this case γ'_S, the following equation is used:

$$\log \gamma'_S/\gamma^\circ_S = \text{wt.\%S} \times e_S^S + \text{wt.\%Si} \times e_S^{Si} + \text{wt.\%Mn} \times e_S^{Mn} + \text{wt.\%P} \times e_S^P + \text{wt.\%C} \times e_S^C \qquad 2.6$$

Bodsworth and Bell[3] have published a list of interaction parameters of interest in iron- and steelmaking. It is, however, doubtful whether these values can be used for estimating their activity coefficients in pig iron because of fairly large concentrations of the solutes, especially of carbon.

2.4. Free Energy

The standard free energy change in a chemical reaction is expressed as:

$$\Delta G^\circ = \Delta H^\circ - T.\Delta S^\circ \text{ cal} \qquad 2.7$$

$$\Delta G^\circ = -RT \ln K \text{ cal} \qquad 2.8$$

The standard state is defined as when the solids or liquids are pure substances and the gases at 1 atm. pressure or, in other words, the reactants and products are all at unit activities. The standard free energy change

ΔG° is the maximum useful work done in transformation from unit activities to activities at equilibrium.

ΔG° value of any chemical reaction indicates whether the reaction is capable of taking place at all. If ΔG° value is negative, the reaction can possibly occur under proper conditions. A positive value denotes that the reaction does not proceed under standard conditions and the reverse reaction rather than the forward reaction is apt to take place.

When dealing with dilute alloys it is more convenient to use 1 wt.% solution as a standard state rather than the pure solute, especially as concentrations are usually given in weight percent in day to day practice.

In the case of very dilute solutions, when an element B of atomic weight W_B is transferred from pure liquid state to a state of dilute solution in a liquid solvent A of atomic weight, W_A (in this case iron), then the free energy accompanying the change in the *standard state only* is given by:

$$\Delta G^\circ = RT \ln \gamma^\circ + RT \ln \frac{W_A}{100 W_B} \qquad 2.9$$

where γ° = activity coefficient of B in an infinitely dilute solution in A.

2.5. Oxygen Potential[12]

Since in ironmaking we are primarily concerned with the reduction of iron and other impurity metals from their oxides, let us consider a three phase equilibrium at a temperature T between oxygen, a pure metal Si and its oxide:

$$Si(s) + O_2(g) = SiO_2(s) \qquad 2.10$$

Assuming the condensed phases to be pure substances at unit activities, the equilibrium constant is given by:

$$K = 1/p_{O_2} \qquad 2.11$$

Thus at any temperature there is a definite oxygen pressure with which Si and SiO_2 are in equilibrium. This is known as *oxygen dissociation pressure* and it increases with temperature for all oxides of our interest, except for CO where the p_{O_2} decreases with increasing temperature. From equations 2.8 and 2.11

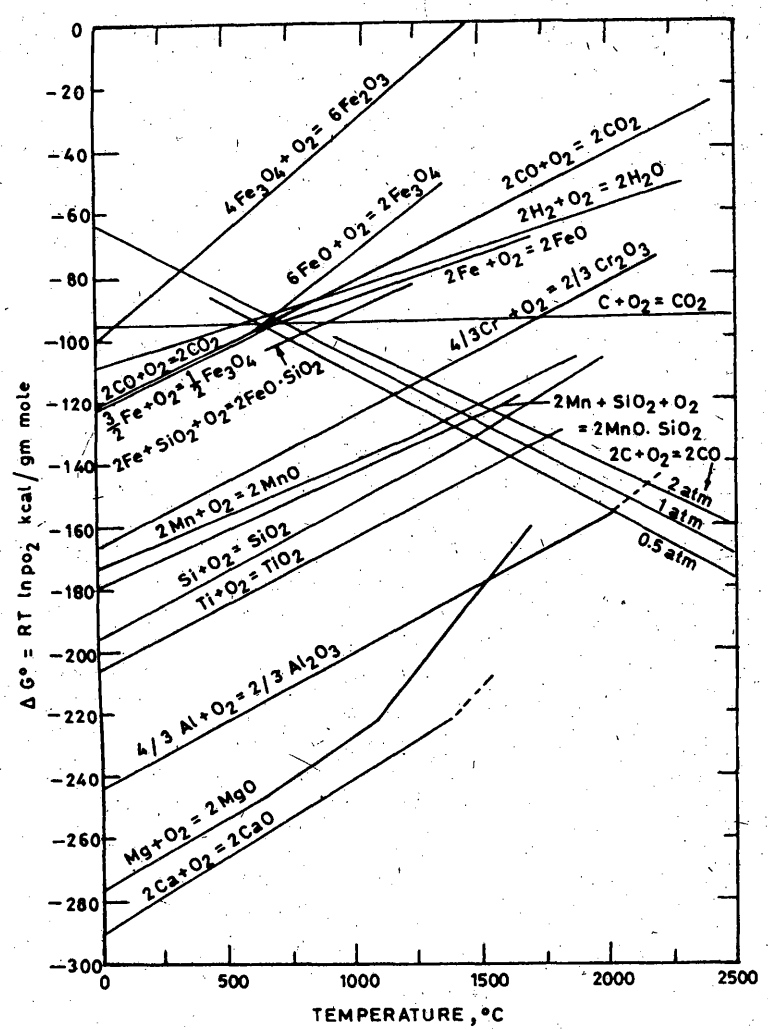


Fig. 2.3 Oxygen potentials of a few oxide systems of importance in the blast furnace.

$$\Delta G^\circ = -RT \ln K = RT \ln p_{O_2} = \Delta H^\circ - T\Delta S^\circ \qquad 2.12$$

Equation 2.12 in reality means the maximum work done during expansion of pure oxygen from 1 atm. to the equilibrium p_{O_2} of the system.

Thus, if $\Delta G^\circ = RT \ln p_{O_2}$ is drawn against T, the plots would give the variation of oxygen potential or free energy of formation of the oxides

with temperature. The free energy plots of some oxides on the basis of 1 gm mole of oxygen at 1 atm. pressure, pure metals (including hydrogen at 1 atm.) and pure oxides are shown in Fig. 2.3. There are sharp bends in the curves at points where phase transformations occur. This is because of consequent sharp changes in the entropies of the reaction. The upward slope of all the metal oxide lines shows an increase in free energy, i.e., the oxides become more unstable with increase in temperature. The line $C + O_2 = CO_2$ remains horizontal because of little change in entropy of the system while the line for $2C + O_2 = 2CO$ has downward slope because of an increase in the entropy. The entropy of solid carbon is negligible compared to that of the gases. It shows that CO becomes increasingly stable at higher temperatures. Since this reaction is dependent on pressure the free energy value will change with the partial pressure of CO, as shown in Fig. 2.3. In normal blast furnace operation $p_{CO} = 0.4$–0.5 atm. It is higher in furnaces working with high top pressure.

Fig. 2.3 gives a clear picture of the relative stability of the metal and carbon oxides. The less the free energy of an oxide (i.e., the greater the $-\Delta G^\circ$), the more stable is the compound. The lower the position of any oxide in the diagram, the lower is its oxygen pressure and the greater the affinity of the element concerned for oxygen. At any temperature an element from any lower line is theoretically capable of reducing, i.e., displacing oxygen from any oxide above it; and, the greater the vertical distance between the two, the greater is the tendency to do so. As for example, ΔG° for $Si\text{-}SiO_2$ lies below the C-CO line for $p_{CO} = 1$ atm. up to about 1550°C where both the lines meet. At this temperature $\Delta G^\circ = RT \ln p_{O_2}$ values of SiO_2 and CO are equal. Above this temperature carbon will reduce silica to Si and CO but would not do so below this temperature under standard conditions.

It can be seen from the figure that the $C\text{-}CO_2$ and C-CO lines intersect at about 700°C. Thus, the reaction $C + O_2 = CO_2$ takes place preferably below about 700°C and above this temperature CO is the main product of the two volatile oxides, according to $2C + O_2 = 2CO$. Therefore, any oxide may suffer reduction at any temperature by the process $2MO + C = 2M + CO_2$ or $2MO + 2C = 2M + 2CO$, provided the oxygen pressure or ΔG° of MO is higher than those of the carbon oxides at that temperature. At any temperature, however, there is present a third equilibrium which decides the CO/CO_2 contents of the gaseous phase ($2CO + O_2 = 2CO_2$). This line also intersects the $C\text{-}CO_2$ and C-CO lines at about 700°C.

It is possible to estimate whether a metal will be oxidised or its oxide will be reduced at a given CO/CO_2 or H_2/H_2O ratio of a mixture of gases and given temperature. If the ratio is higher than that given by the equilibrium ratio the oxide will be reduced and if the ratio is lower the metal will suffer oxidation. The equilibrium CO/CO_2 or H_2/H_2O ratios for any given oxide can be easily calculated from the free energy equations, viz:

i) $2MnO = 2Mn + O_2 : \Delta G^\circ = 183900 - 34.63\ T$ cal

ii) $2H_2 + O_2 = 2H_2O : \Delta G^\circ = -116530 + 25.62\ T$ cal

Adding (i) and (ii),

or
$$2MnO + 2H_2 = 2Mn + 2H_2O : \Delta G^\circ = 67370 - 9.01\ T \text{ cal}$$
$$MnO + H_2 = Mn + H_2O : \Delta G^\circ = 33685 - 4.50\ T \text{ cal}$$

$$K = \frac{a_{Mn} \cdot p_{H_2O}}{a_{MnO} \cdot p_{H_2}}$$

Assuming unit activities of Mn and MnO:

$$K = p_{H_2O}/p_{H_2}$$

At, say, 1500°K, $\Delta G^\circ = 33685 - 4.50 \times 1500$

$= -4.575 \times 1500 \log K$

or $K = p_{H_2O}/p_{H_2} = 1.18 \times 10^{-4}$

The ratio being very small it is difficult to reduce MnO by hydrogen.

As already mentioned, the data in Fig. 2.3 are for pure elements and their oxides, i.e., at their unit activities. For elements and their oxides in solution, due account must be taken of their activities in liquid iron and slag.

Whether oxidation or reduction will occur at a given temperature and CO/CO_2 or H_2/H_2O ratio is governed by Vant Hoff's equation:

$$\Delta G = \Delta G^\circ + RT \ln \frac{\Pi a_{products}}{\Pi a_{reactants}} \qquad 2.13$$

For $(MnO) + CO = [Mn] + CO_2$

$$\Delta G = \Delta G^\circ + RT \ln \frac{a_{[Mn]} \cdot p_{CO_2}}{a_{(MnO)} \cdot p_{CO}} \qquad 2.14$$

As ΔG° at any temperature is known from standard tables, if the activities of [Mn] and (MnO) and the CO/CO_2 values are such that ΔG is negative,

then MnO will be reduced. The oxidation-reduction reactions are further discussed in Sec. 2.7. Eq. 2.13 would also give the ΔG values for the reaction $2C + O_2 = 2CO$ at different partial pressure of CO, the standard state being $p_{CO} = 1$ atm. The ΔG values for different p_{CO} values shown in Fig. 2.3 have been calculated from Eq. 2.15 assuming $a_C = p_{O_2} = 1$.

$$\Delta G = \Delta G^\circ + RT \ln \frac{p_{CO}^2}{a_C^2 \cdot p_{O_2}} \qquad 2.15$$

2.6. Oxygen Potentials in the Blast Furnace[12]

Two basic reactions occur in the shaft of the blast furnace, namely:

i) the reaction between carbon monoxide and iron oxides producing carbon dioxide;

ii) the reaction between coke carbon and carbon dioxide producing carbon monoxide (Boudouard reaction: $CO_2 + C = 2CO$) occurring above 1000°C and its reverse reaction, i.e., carbon deposition reaction occurring at lower temperatures.

Investigations regarding the temperature and gas composition inside the blast furnace shaft at various depths and across the radius reveal that they vary systematically and as the temperature decreases the CO/CO_2 ratio also decreases. The oxygen potentials of the gases vary from furnace to furnace because of differential gas flows and temperature regimes. Goodeve[13] has described the oxidation and reduction processes occurring in the blast furnace shaft with the help of free energy diagram and the changes in the oxygen potential undergone by a mole of gas as it travels from the tuyere zone to the top of the furnace. In modern furnaces, the air enters the tuyere at about 1000°C with $p_{O_2} = 0.2$ atm. approximately, and its position is shown as A in Fig. 2.4. Its temperature rises as it reacts with incandescent coke in front of the tuyere to about 2000°C and the CO produced reaches an oxygen potential nearing the C-CO line, shown as B. As the gas ascends its temperature decreases and its oxygen potential rises as a result of reaction with iron oxides producing carbon dioxide. But as long as the temperature exceeds about 1000°C, the oxygen potential is continuously lowered by the Boudouard reaction, $CO_2 + C = 2CO$. Thus, the average oxygen potential of the gas is continuously raised and lowered as it comes into contact with ore or coke surfaces during the ascent and is shown by the wavy dotted curve in Fig. 2.4. Below 900°C the

Boudouard reaction becomes sluggish and the oxygen potential is essentially controlled by the wustite/iron and magnetite/wustite reactions. The oxygen potential may slightly rise in the region 500–900°C because of the carbon deposition reaction $2CO = C + CO_2$ as well as limestone decomposition, $CaCO_3 = CaO + CO_2$. Finally, the gas reaches near the top of the furnace at 100–250°C with an oxygen potential approaching that necessary for magnetite reduction. Modern furnaces work with gas composition near the FeO/Fe equilibrium at 800–1000°C and limestone is seldom used.

2.7. Increased and Decreased Reducibilities[7,12]

We have seen that reduction occurs when the oxide of the reductant possesses at any temperature an oxygen partial pressure lower than that of the oxide to be reduced. Thus, if an oxide is present in solution (e.g., SiO_2 or MnO in slag) its p_{O_2} will be lower than that of the pure oxide and will be relatively difficult to reduce. Similarly, it will be easier to reduce a metal oxide if the metal is obtained as an alloy. These will depend upon whether $\triangle G$ of equation 2.13 becomes less negative or more negative according to changes in the activities of the reactants or products.

As already mentioned the free energy values in Fig. 2.3 are based on pure materials where both metals and their oxides are in their unit activities. In the blast furnace the reduced elements and their oxides are present in the liquid iron and slag whereby their activities are reduced. Taking the example of silica again for a composite reaction in the blast furnace hearth, the carbon-saturated liquid iron ($a_C = 1$) droplets travelling through the slag layer:

$$(SiO_2) + 2\,[C]_{\text{sat. in Fe}} = [Si]_{Fe} + 2CO \qquad 2.16$$

$$\Delta G = \Delta G^\circ + RT \ln \frac{a_{(Si)} \cdot p_{CO}^2}{a_{SiO_2}} \qquad 2.17$$

From Eq. 2.17 at constant p_{CO}, the ΔG values will decrease or the reducibility of silica will increase if the silicon activity in the iron decreases (through an alloy formation) or the silica activity in the slag increases. If, however, these activities remain constant and the p_{CO} increases, then the ΔG value will increase, i.e., the reduction will occur either at higher temperatures or at a given temperature the activity of silicon in iron will decrease (lower Si-content of iron compared to that when $p_{CO} = 1$ atm.) Such a situation can arise in the blast furnace hearth not only because of high blast pressures resulting in high gas pressures in the hearth but

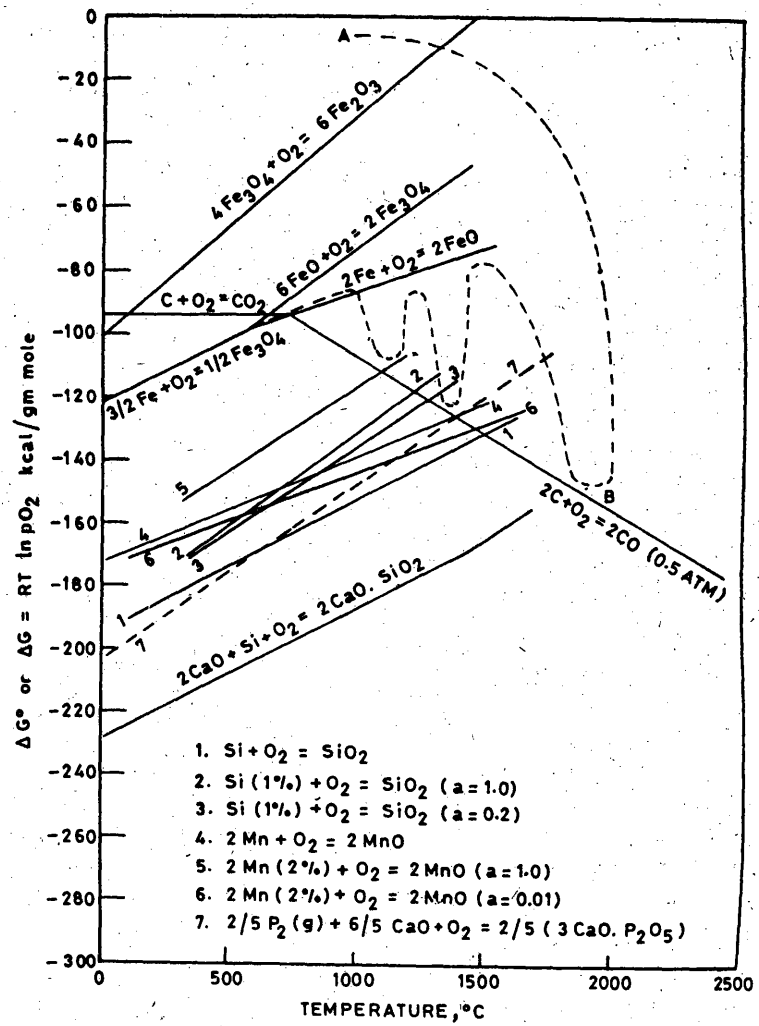


Fig. 2.4 A few metal-oxide equilibria and schematic variation of the oxygen potential of the gas in the blast furnace.

also because the CO has to evolve at a higher pressure inside the slag layer due to hydrostatic head of slag and lack of facilities for nucleation of CO bubbles, which form by the reduction of the slag oxides while the carbon-containing liquid iron droplets pass through the slag layer.

Fig. 2.4 shows examples of increased and decreased reducibilities of silica and MnO at differing activities and at $p_{CO} = 0.5$ atm. As for example, line

(1) represents the free energy of formation of pure silica from pure Si, line (2) that of pure silica from 1% Si in iron and line (3) that of silica at 0.2 activity in slag from 1% Si. In case (1), the temperature at which silica is reduced by carbon at $p_{CO} = 0.5$ atm. is given by the intersection with the corresponding C-CO line, i.e., 1500°C; for cases (2) and (3) the respective temperatures are 1225°C and 1275°C. It is obvious that the effect of dilution of SiO_2 in the slag and that of Si in iron tend to cancel each other and a significant reduction of silicon into the metal can occur under conditions where slag silica comes into contact with liquid iron, i.e., above about 1250–1300°C.

Tables of free energies of reactions and other thermochemical data have not been included in this book as they are easily available elsewhere.[2-5]

2.8. Velocity of Gas-Solid Reactions

A chemical reaction takes place with decrease in free energy. But even if a reaction is thermodynamically feasible, in practice, however, it may not proceed to equilibrium in measurable time. Calculations from thermal data do not predict the reaction rate.

Most of the reactions in the blast furnace are heterogeneous in nature and occur between different phases, e.g., reactions between gas/(ore or coke), gas/(liquid iron or slag) and liquid iron/liquid slag.

Generally, two types of variables affect the overall reaction rates in heterogeneous chemical processes, one is essentially chemical and the other physical. A chemical reaction can only take place if one reactant is transported to the other, which is a physical process. In a homogeneous reaction, this is achieved by mixing and in a heterogeneous reaction by mass transfer of one reactant to the other through diffusion or laminar and turbulent flow.

In any physico-chemical process, the chemical part is influenced by concentration, temperature and pressure of the reactants, whereas the physical one by the surface area of the solids, porosity, flow characteristics, diffusivity of the reductant molecule, etc. The overall reaction rate depends upon the relative resistance of each reaction step. The chemical resistance decreases greatly with increasing temperature but the physical (diffusion) resistance does much less so. The slowest of these steps is rate-controlling. Therefore, a high rate of chemical reaction can be obtained at high temperatures provided the mass transport restriction is eliminated or minimized.

In the blast furnace the heterogeneous reactions of greatest importance are the reduction of the iron ore lumps by CO or hydrogen and the reaction of coke carbon with blast oxygen or CO_2. These are approximately first order reactions of the type

$$A = B$$

with respect to the gaseous reactants.

From our experience the velocity of a reaction is proportional to the concentrations of the reactants. At any moment before the equilibrium is reached, the overall chemical reaction rate is given by:

$$v = -dC_A/dt = k_1 C_A - k_2 C_B \qquad 2.18$$

where

v = velocity of reaction
C = concentrations of the species A and B
k_1, k_2 = specific reaction rate constants of the forward and reverse reactions.

At equilibrium, $dC/dt = 0$ and hence the equilibrium constant K becomes,

$$K = k_1/k_2 = C_B^*/C_A^* \qquad 2.19$$

where C^* denotes the equilibrium concentrations.

In the case of a gas, the concentration term may be replaced by volume fraction or partial pressures ($p = CRT$).

The reaction rate constant is a function of temperature and the relation is given by the Arrhenius equation,

$$\ln k = \ln A - E/RT \qquad 2.20$$

where

A = frequency factor, a constant for a particular reaction in a narrow temperature range
E = activation energy.

The lower the value of E the faster the reaction. As for example, at 2000°C, a reaction with E = 30 kcal/mole will be about a million times faster than the one with E = 90 kcal/mole provided the frequency factors of the reactions do not change appreciably. However, the rate of increase of the specific reaction rate with temperature is higher the higher the activation energy.

2.8.1. Kinetics of Iron Oxide Reduction[10,14–16]

The reduction of iron ore by CO or hydrogen is a very complicated process involving a great many variables, both physical and chemical in character. The subject is so vast that it is beyond the scope of the book even to attempt to deal with it effectively. Further, the reduction process is so varied and complex that there is very little agreement amongst the investigators regarding the rate-controlling mechanism which determines the kinetics of reduction. The entire field has been covered excellently by Bogdandy and Engell[14] and reviewed by Tokuda et al.[15] and Ross.[16] A very simplified view of the rate-controlling reactions is presented here in order to enable a better understanding of the factors that influence the reducibility of ores, sinters and pellets discussed in Sec. 6.7.

The reduction sequence of hematite – hematite, magnetite, wustite and iron – as mentioned in Sec. 1.2, is given by the following equations:

$$3Fe_2O_3 + CO\ (\text{or } H_2) = 2Fe_3O_4 + CO_2(H_2O) \qquad 2.21$$

$$Fe_3O_4 + CO\ (\text{or } H_2) = 3FeO + CO_2(H_2O) \qquad 2.22$$

$$FeO + CO\ (\text{or } H_2) = Fe + CO_2(H_2O) \qquad 2.23$$

Starting with a dense sphere of hematite, an initial reaction with CO or H_2 will produce a shell or layer of metallic iron in contact with a layer of wustite (the lowest of the three oxides) beyond which there will be a layer of magnetite surrounding the core of hematite. This is shown schematically in Fig. 2.5. Such a layered structure is typical of topochemical reactions where the reacting interface between the solid reactants and solid products moves parallel to the original solid surface.

Reduction can occur through any or all of the following mechanisms:

(i)[17] Iron ions released after removal of oxygen from the wustite lattice may migrate (solid state diffusion) towards the core due to concentration gradient and reduce magnetite to wustite and hematite to magnetite without any loss of oxygen, resulting in the layered structure of Fig. 2.5:

$$Fe_3O_4 + Fe = 4FeO \qquad 2.24$$

$$4Fe_2O_3 + Fe = 3Fe_3O_4 \qquad 2.25$$

This mechanism envisages gaseous diffusion of gaseous reductant through the iron layer and transfer of oxygen from the solid phases to the gaseous phase at the wustite-iron interface only. During transformation, only hexagonal hematite undergoes structural metamorphosis to cubic close-packed

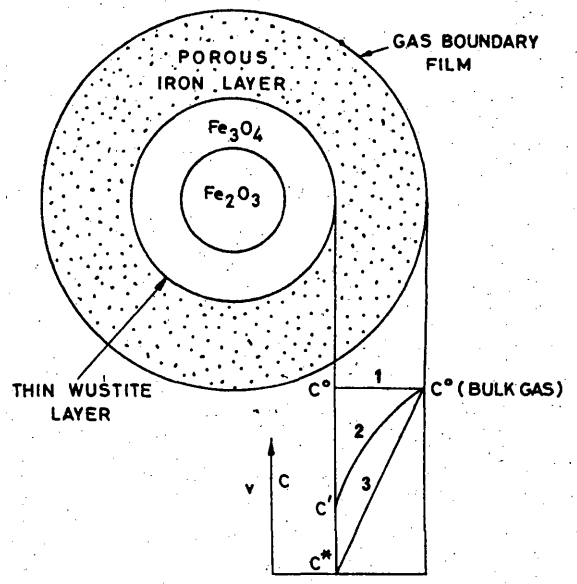


Fig. 2.5 A schematic diagram of the mode of gaseous reduction of a spherical sample of ferric oxide. Possible concentration gradients of the reducing gas across the iron layer are also shown.

magnetite lattice, the structure of wustite being similar to that of magnetite. As we will see in Sec. 3.4, wustite ($Fe_{0.95}O$) is an iron deficient non-stoichiometric compound with iron ion vacancies. The transformation of hematite to magnetite, in contrast to the transformation of magnetite to wustite, gives rise to lattice distortions. In the disturbed lattice the diffusion of iron ions is accelerated and a large vacancy concentration can arise where mass is lost. The creation of voids is thus facilitated in the defect structure and all these factors contribute to a considerable pore formation.

(ii)[18] Diffusion of gaseous reductants inwards through porous layers of iron, wustite and magnetite and reduction of all oxides simultaneously at all interfaces according to Eqs. 2.21–2.23.

(iii)[19] Gaseous diffusion cannot occur if a dense impervious layer of iron is formed. Gaseous reductant is adsorbed on iron surface and oxygen ions diffuse through the layer to react at the surface. In such cases, the reducibility of the ore will be poor and exhibit a rate minimum[19] at 700–750°C, the temperature of recrystallization and densification of the separated iron. Reduction of hematite and magnetite to wustite occurs in

the same manner as in (i) above. Such a process is inherently slow since the oxygen solubility in solid iron is negligibly small.

From the above postulates, the reduction rate will be intimately related to the formation of a porous product layer which allows gas access to the unreduced oxides in the core. This extremely useful feature of the reaction does not occur under all reduction conditions and it is important to understand that there are limitations, e.g., an alteration of reaction mechanism from porous growth can result in drastic changes in the reaction rate and product morphology.

2.8.2. The Rate Laws in Reduction[10,14–16]

The reduction of the iron oxides takes place in a series of sequential steps. The overall rate will be determined by the slowest of the process or processes in the series. The possible consecutive steps are:

i) transport of gaseous reductant from the bulk gas phase to the particle surface through a boundary gas film;
ii) molecular diffusion of the gaseous reductant through the product layer to the reaction interface;
iii) adsorption of the gaseous reductant at the interface;
iv) reaction at the interface (reaction between adsorbed reductant and oxygen of the lattice);
v) desorption of gaseous products from the interface;
vi) mass transport of iron and oxygen ions and transformations in the solid phase; formation and growth of the reaction products, viz., magnetite, wustite and iron;
vii) molecular diffusion of gaseous products through the product layer to the particle surface;
viii) transport of the gaseous products from the particle surface through the boundary gas film to the bulk gas phase.

From Fig. 2.5 and the above possibilities, the rate limiting cases are:

chemical control = steps (iii) to (vi)
diffusion control = steps (i) and (viii); (ii); (vi) and (vii)

In case CO or H_2 has free access to the reaction interface, the interface reaction rate of oxygen removal in reactions 2.21–2.23 at any given temperature can be derived with the help of Eqs. 2.18 and 2.19 in terms of partial pressures or concentrations (C = p/RT) of the reducing gas:

$$v = \frac{-d(O)}{A.dt} = k\,(p^\circ - p^*) = k'\,(C^\circ - C^*) \qquad 2.26$$

where

v = velocity of reaction per unit area of reacting surface per unit time
k, k′ = rate constants, depending upon the temperature and nature of the reductant, CO or H_2
p°, C° = partial pressure or concentration of CO or H_2 at the reaction interface
p*, C* = equilibrium partial pressure or concentration at the given temperature
$-d(O)/dt$ = rate of oxygen removal; the same equation can be used in terms of mole of CO or H_2 consumed in unit time
A = area of reacting surface

At a given temperature, the equilibrium partial pressure will depend upon which phase is being reduced:

$$Fe_2O_3 \rightarrow Fe_3O_4;\ \text{or,}\ Fe_3O_4 \rightarrow FeO;\ \text{or,}\ FeO \rightarrow Fe$$

In the blast furnace, the reduction of wustite is the most important step since its reduction rate is slow and it possesses the lowest oxygen dissociation pressure of the three (Table 3.2), highest equilibrium CO/CO_2 or H_2/H_2O ratios (Fig. 3.10) and at temperatures above 570°C it is wustite from which metallic iron is finally obtained. However, its rate of reduction itself depends upon the structural activity it inherits from the parent oxides during their reduction.

Once the surface layer of the ore (or, in the case of a porous lump, even the individual grains if they are large) has been reduced to iron, further reduction can only take place by transport of the reductant through the product layer to the shrinking reaction interface. The transport by diffusion is given by Fick's 1st Law according to which, in steady state, if dn is the amount of a substance crossing a surface of unit area perpendicular to the direction of flow in time dt (called flux J), then

$$J = \frac{dn}{A.dt} = -D\,\frac{dc}{dx} \qquad 2.27$$

where

D = coefficient of diffusion or diffusivity, cm^2/s
$-\frac{dc}{dx}$ = concentration gradient, the minus sign signifying the decrease in concentration dc along distance dx in the direction of flow.
A = surface area normal to the flux

The diffusive flux J of the reductant across the product layer (Fig. 2.5) can be derived from Eq. 2.27 and $c = p/RT$ and is given by

$$J = D.(c^\circ - c)/y \qquad 2.28$$

$$= \frac{D}{y.RT}(p^\circ - p) \qquad 2.28a$$

where

c°, c = concentrations of the reductant at the particle surface and reaction interface respectively

p°, p = corresponding partial pressures of the reductant

y = product layer thickness or pore length, cm (distance over which concentration gradient exists).

For the reaction to occur, the reactants and products must be transported to and from the reaction front through the reacted layer. In many reactions it has been found that the rate is inversely proportional to the thickness of this layer. If *y* is the thickness, then for the case of pure diffusion it can be deduced from the Fick's law that

$$y^2 = Kt \qquad 2.29$$

where the constant K includes diffusivity. Eq. 2.29 is the well-known *parabolic law*.

2.8.3. Mechanism of Iron Oxide Reduction

In the previous section the mass transfer of reductant from the bulk gas to the reaction interface and *vice versa*, steps (i) and (viii), have been included as possible rate-limiting factors. However, they are not so in the blast furnace since it is a moving bed system and the linear gas velocity far exceeds the critical velocity where the influence of boundary gas film disappears (Fig. 6.21).

The remaining six steps are discussed in the succeeding sections. However, in heterogeneous reactions, chemical and diffusion controls are not independent. Hence, in the following discussions there may be considerable overlapping between the two. Step (vi), the formation and growth of nuclei, is composed of both chemical and diffusion processes and is, therefore, treated separately in Sec. 2.8.3.3.

2.8.3.1. Chemical control

From Eqs. 2.20 and 2.26, the chemical reaction rate increases with temperature as well as concentration or partial pressure of the gaseous reductant.

From Fig. 2.5, if the product layer is very porous permitting unrestricted access of the reductant molecules to the reaction interface, at any moment the partial pressure of the reductant on the particle surface and at the reaction interface will be identical. Therefore, gaseous transport will not be rate-controlling and depending on the energy of activation the rate of reaction will increase with temperature. The rate will also increase as the term (p-p*) of Eq. 2.26 increases. In many studies on iron ore reduction, it has been found that the rate of reduction is proportional to the partial pressure of hydrogen[20,21] or of CO.[22,23]

The blast furnace being a counter-current reactor, p_{CO} or p_{H_2} decreases continuously through reaction with iron oxides and hence the term (p-p*) decreases correspondingly slowing down the reaction rate. This has been confirmed in the reduction of Fe_2O_3 to Fe in mixtures of H_2-H_2O-N_2. Although it was found that the rate increased with p_{H_2} but the rates were much slower as the ratio p_{H_2O}/p_{H_2} in the gas phase increased.[24]

Steps (iii) and (v) envisage adsorption and desorption processes. They occur on the solid reactant surface. As for example, in the reduction of wustite with CO, it is possible that CO is chemically adsorbed on the oxide surface and reacts according to:

$$CO_{ads.} + O_{lattice} = CO_{2\ ads.} \qquad 2.30$$

The reaction results in the separation of oxygen from the oxide lattice (step iv), the rate being proportional to the surface concentration of adsorbed CO at the reacting phase boundary and hence depends upon the interfacial area, partial pressure of CO and availability of vacant active sites. The extent of adsorption and, therefore, the rate of reaction increase with the total pressure. However, the rate of reaction does not increase with pressure after an optimum pressure is reached in spite of the fact that the term (p-p*) of Eq. 2.26 increases with pressure in absolute values although the ratio p/p* remains constant. This may partly be due to filling up of all available vacant sites (see also Sec. 2.8.3.2.1 and Fig. 6.25). When phase-boundary reaction is rate-controlling, the reduction in weight per unit area at any given temperature increases linearly with time (Fig. 2.6).[25] The reaction front also shrinks uniformly from the surface to the core linearly with time (topochemical reaction).

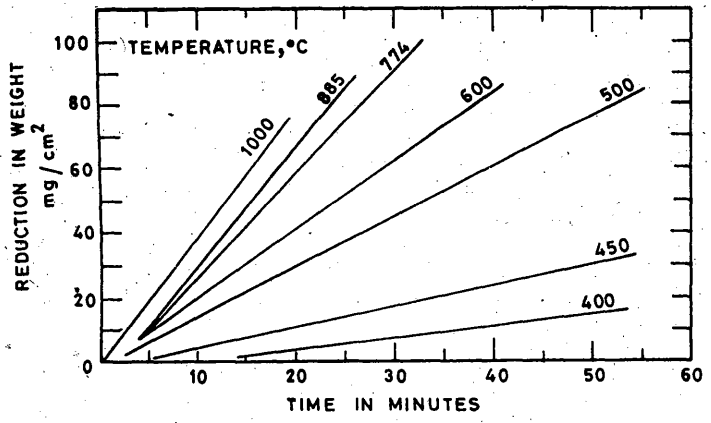


Fig. 2.6 The linear time law of the interfacial reaction in the reduction of plates of iron oxide, according to Quets et al.[25] (Copyright AIME).

The product of the reaction (CO_2) may escape as a gas or remain chemically adsorbed in equilibrium with the gas phase (step v):

$$CO_{2\ ads.} = CO_2(gas) + \square\ (\text{vacant site}) \qquad 2.31$$

If the equilibrium constant of the reaction is high, more of CO_2 will escape providing more sites for CO adsorption.

In Eq. 2.26, the reaction rate constant k is a function of temperature. In the chemical control region the rate increases exponentially with temperature. Fig. 2.6 shows that the time for a definite reduction in weight of sample decreases greatly with the increase in experimental temperature. Fig. 2.11(a) shows that the time taken for achieving the given degrees of reduction decreases as the temperature increases.

Most investigators have reported an activation energy for interfacial reaction of about 15 kcal/mole for the reduction of FeO to Fe by CO or H_2 although a value as high as 28 kcal/mole has also been quoted.[15] However, such values should be taken with caution since diffusion invariably plays a role in the reduction mechanism of iron oxides.

2.8.3.2. Diffusion control

Steps (ii) and (vii) of the rate-controlling factors involve molecular diffusion of the gaseous reductant and reaction product respectively. Step (vi, solid diffusion), which will be discussed later, is perhaps the most important since the mode of transformation of hematite into magnetite, wustite and finally into iron determines the porosity and product morphology and hence the diffusion rate. Step (vi) also involves nucleation and growth of the iron layer.

2.8.3.2.1. Gaseous diffusion

Once an iron layer is formed on the oxide, further removal of oxygen from the oxide surface occurs by transport of the reductant and withdrawal of the gaseous product to and from the surface through the pores in the iron layer. From Fig. 2.5, three cases (curves 1, 2 and 3) arise regarding the influence of porosity. For curve (1), as applicable to very porous layer and already mentioned before,

$$C^o\ (\text{bulk}) = C^o\ (\text{reaction interface})$$

In such a case, the rate is controlled by phase boundary reaction (Eq. 2.26) and it is directly proportional to the partial pressure of the reductant and surface area. Fig. 2.6 shows the linear relationship of reduction with time. Here, the diffusion of gases is not rate-limiting, i.e., the supply rate of the reductant is equal to or greater than its consumption rate.

In case the supply rate is less than its consumption, i.e., the chemical reaction rate exceeds the supply rate of the reductant gas, then gaseous diffusion becomes rate-controlling. This is shown by curve (3) of Fig. 2.5. The reductant gas concentration is about the same as the equilibrium concentration C^* at the interface, i.e., the gas reacts and attains the equilibrium value as soon as it arrives. It is the slowness of arrival that determines the reaction rate. Quantitative rate equations for gaseous diffusion have been suggested[26-28] and they take the form of Eq. 2.28 where D is the diffusion coefficient of the gas. The inward advance rate of the reaction interface should obey parabolic law which has been confirmed[29,30] from reduction of Fe_2O_3 by CO or H_2.

The diffusion of gas through the pores of the product layer is restricted, as the reaction proceeds, by the reduced cross-section available for mass transport. The porosity of the layer does not remain constant but changes with time. Therefore, the orientation of the pores relative to the diffusion path, the cross-linking and branching of the pores must be considered. These are described by the *porous or effective* diffusion coefficient, D_p, which is related to the diffusion coefficient of the gas, D, by[31]

$$D_p = D.\gamma.\xi \qquad 2.32$$

where

γ = open porosity of the layer, i.e., volume of open pores relative to the whole volume of the lump

ξ = labyrinth factor, value 0.1–0.3, to be determined experimentally. It is concerned with the degree of diffusion resistance and is affected by pore structure.

Substitution of Eq. 2.32 in Eq. 2.28 gives the total diffusive flux J_p for porous diffusion.

In case a very dense metallic layer is produced surrounding the oxide, the removal of oxygen occurs by its diffusion through the layer. The growth rate of the iron layer can be expressed by Eqs. 2.27–2.29. In this case D is the diffusivity of oxygen in metallic iron and dc the difference of oxygen concentration between the sample surface and reaction interface where the equilibrium FeO/Fe is established. The thickness of the iron product layer (y) depends upon the oxygen removed per unit area and, according to Eq. 2.29, will be proportional to the square root of time (parabolic law). This is shown by the linear relationship between the two in Fig. 2.7.[32] The obeyance of the parabolic law has also been confirmed by Ohtani et al.[33] A rate minimum has been observed where islands of wustite are surrounded by dense iron layer (Fig. 2.11b).

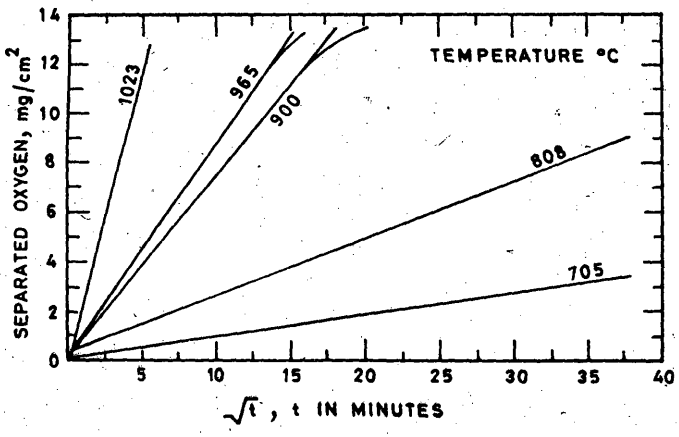


Fig. 2.7 The parabolic rate law in the reduction of wustite in hydrogen containing 2.5 percent steam at a total pressure of 700 Torr at various temperatures. Formation of dense iron layer. After Kohl and Engell.[32] (Copyright Verlag Stahleisen).

From Fig. 2.5, curve (2), the concentration of the reductant at the interface lies between C° and C*. The chemical and the diffusion rates are comparable. In this *intermediate* or *mixed-control* zone, the overall reduction processes are controlled by both diffusion and chemical reaction.[31,34,35]

2.8.3.2.2. Factors influencing diffusivity

Diffusivity, D, for gaseous diffusion depends upon various factors, such as,

i) Temperature
ii) Total pressure
iii) Density of gas or molecular weight
iv) Effective collision diameter of gas molecules

(i) Temperature dependence Apparent activation energy of gas diffusion is about 2–5 kcal/mole. From the Arrhenius equation, the temperature dependence is small. At constant pressure, the increase in D with temperature is approximately given by

$$D_2 = D_1 (T_2/T_1)^n \qquad 2.33$$

where

D_2 and D_1 = diffusivities at temperatures T_2 and T_1

$$n = 1.75 < n < 2. \qquad 2.34$$

However, the temperature dependence of ordinary gas diffusion may differ from that of porous diffusion because the term $\gamma.\xi$ in Eq. 2.32 could have its own temperature dependence. Porosity and pore structure are themselves affected by the temperature.

Since chemical reaction has higher activation energy than gaseous diffusion, the former will increase at a much greater rate with increase in temperature than the latter. Hence, a stage will arrive where diffusion will become rate-controlling. The changeover from chemical to diffusion control at 600°C in the reduction of iron oxide is illuminating from Fig. 2.8.[36] The figure shows that the lines of corrected reduction rates $v' = v/(C°-C^*)$, where (v) is the velocity of reduction, at temperatures above 600°C run parallel to the line of temperature dependence of the diffusion coefficient. The slopes of the lines in the chemical control region decrease with increasing degree of reduction (i.e., the reduction becomes increasingly diffusion controlled) and at 75 percent reduction, the reaction becomes completely diffusion controlled.

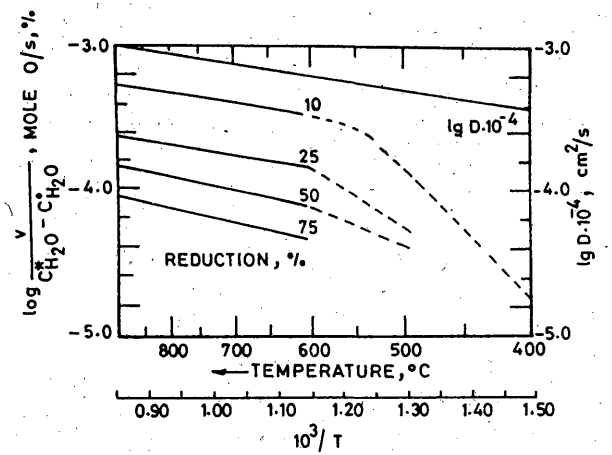


Fig. 2.8 Reduction velocity (v) and diffusion coefficient (D) in relation to temperature, according to Bogdandy et al.[36] (Copyright Verlag Stahleisen).

(ii) Pressure dependence Diffusivity is approximately inversely proportional to the total pressure,

$$D \propto 1/P \qquad 2.35$$

Therefore, according to Eq. 2.28, any increase in the total pressure P should not affect the diffusive flux since D is inversely proportional and the partial pressures of the gaseous species are directly proportional to P.

For chemical reaction control, the reaction rate would increase with the total pressure for reasons already discussed although the rate constant (k of Eq. 2.26) is independent of total pressure.

However, in considering gas diffusion through a porous layer of small pore sizes, the pore radius should exceed the mean free path of the gas molecules.[14] If the pore radius is smaller, the collisions of the gas molecules with the pore walls will be more frequent than those between the molecules, resulting in an overall decrease in the value of D. This phenomenon is described by the Knudsen diffusion coefficient, D_K:

$$D_K = \frac{d}{6}\left(\frac{8RT}{\pi M}\right)^{1/2} \qquad 2.36$$

where

d = mean diameter of the pore
M = molecular weight of the reductant gas.

For pore radii smaller than the mean free path, D_K is independent of total pressure. The mean free paths of the blast furnace gas species at 1 atm. pressure vary between $10^{-4} - 10^{-5}$ cm.

The size of the pores in the reduced product layer is approximately of the same order of magnitude as the mean free path of the reducing gases. For pore radii larger than the mean free path of the gases, i.e., where normal gas diffusion is rate-controlling, the reduction rate should not be affected by the total pressure (Eq. 2.28). For pore radii smaller than the mean free path, the gas transport occurs through Knudsen diffusion which is independent of the total pressure. But the mean free path decreases with increasing pressure. Hence, for pore sizes smaller than the mean free path, the reduction rate will increase with the total pressure according to Eq. 2.28 until the mean free path becomes smaller than the pores. Thereafter, the flux becomes independent of total pressure. This is shown in Fig. 2.9[37] where the reduction rate increases with pressure at first and ceases to do so at higher pressures, the optimum pressure being higher the smaller the pore size.

(iii) Molecular weight dependence Diffusivity of a gas molecule is approximately inversely proportional to the square root of molecular weight,

$$D \propto (1/\text{molecular weight})^{1/2} \qquad 2.37$$

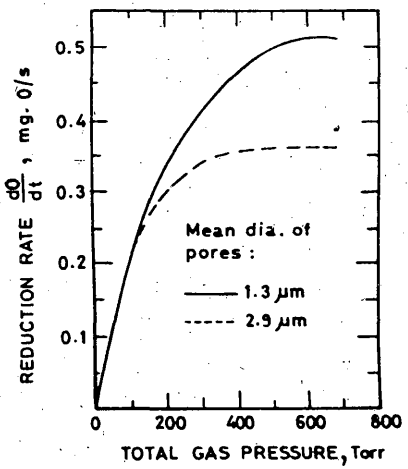


Fig. 2.9 Dependence of reduction rate of porous wustite on the total pressure, with a 50 percent degree of reduction, according to Herr.[37]

D for H_2/H_2O gas mixture is about 3–5 times the value for CO/CO_2 for ny given temperature.[92] Therefore, for purely diffusion controlled reduction, the rate of reduction with hydrogen should be 3–5 times higher than hat with CO as has been confirmed (Sec. 6.7.9).

.8.3.3. Solid state diffusion

The reaction according to step (vi), Sec. 2.8.2, involves transformations n the solid state and includes:

) diffusion of iron ions and reduction of higher to lower oxides;
) nucleation and growth of metallic iron on FeO.

(i) Diffusion of metallic iron[15] In Sec. 2.8.1 it was mentioned that the duction of higher oxides to the lower ones can occur by diffusion of on ions in the solid oxides according to Eqs. 2.24 and 2.25. The iron ns diffuse through a lattice vacancy mechanism. If the composition of e reducing gas is so adjusted that the higher oxides are reduced to the wer oxides only and no metallic iron is formed and if diffusion of iron ns only is assumed to be rate-controlling, then according to Eq. 2.29, e thickness of the lower oxide should increase in a parabolic manner d will be proportional to the square root of time. The reduction by solid te diffusion of iron ions has been confirmed by many.[38–40]

Activation energy[38,40] for the growth of FeO during reduction of Fe_3O_4 h Fe in a temperature range of 600°C to 1100°C is about 33 kcal/mole ich is consistent with the self-diffusion coefficient of iron ion in FeO.[41,42] nerally, the activation energy of solid state diffusion lies between those chemical reaction and gaseous diffusion.

(ii) Nucleation and growth This step is perhaps the most important ce the mode of transformation of wustite into iron determines the pro- ct morphology which affects the subsequent reduction rate. During the uction of hematite, its transformation from hexagonal structure to cubic gnetite generates stresses which are transmitted to wustite resulting in ice distortions and inhomogeneities in wustite activity.

When oxygen is removed from wustite, the ratio metal/oxygen increases he oxide. As the solubility limit of the metal in the oxide is reached the oxide becomes super-saturated with liberated iron ions, the metal start to precipitate. Individual nuclei will form at places where the energy of nucleation is minimum. Lattice defects, impurities, surface gularities, etc., form ideal sites for nucleation. Before the beginning ucleation the reduction rate should be slow and after an *induction*

period a rapid reduction should occur. This has been confirmed by many.[22,43,44]

Once such nucleation of iron has occurred, further removal of oxygen and consequent creation of a concentration gradient of ferrous ions across the wustite lattice induces these ions to diffuse towards the site or sites of nucleation. This diffusion is facilitated due to the presence of iron ion vacancies in the cation deficient wustite, through which these ions migrate. Due to lattice imperfections, it is possible for iron to nucleate at preferred site or sites. If such preferred sites are not numerous, a porous iron layer will be expected which will enhance the ease of gaseous diffusion and hence the reduction rate. In extreme cases of preferential nucleation, caused by a pronounced lattice distortion when a large foreign cation is introduced, the diffusion of iron ions will be greatly enhanced and they will stream towards the preferred site and the iron will grow as *needles* or *whiskers* with phenomenal volume increase (swelling, Sec. 6.7.6). The rate of reduction of iron oxides increases greatly with the introduction of soluble impurities like oxides of alkali and alkaline earth metals as shown in Fig. 2.10.[45] The increase in the reduction rate of iron oxide in the presence of foreign cations has been confirmed by others.[46]

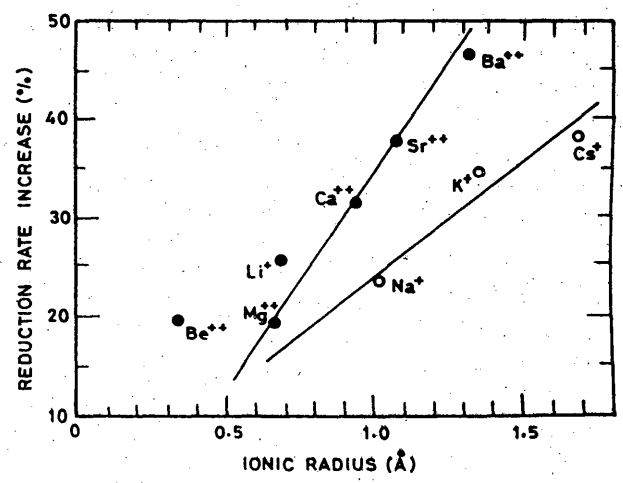


Fig. 2.10 The increase in the rate of reaction of iron oxide in the presence of alkali and alkaline earth metals of varying ionic radii, according to Khalafalla and Weston.[45] (Copyright AIME).

On the other hand, if the distribution density of nuclei is high a dense non-porous metallic layer will be expected which will inhibit gaseous diffusion and therefore retard the reduction rate. What causes the differential distribution density of nuclei is not fully known. However, it is not unlikely that the ratio, d_n,

$$d_n = \frac{\text{rate of iron ion diffusion}}{\text{rate of oxygen removal}} \qquad 2.38$$

at least partly determines the product morphology. If the ratio is high, i.e., if the rate of iron ion diffusion is much higher compared to its generation, iron ions will preferentially migrate towards the few nuclei at first formed giving a porous product. If the ratio is small, i.e., the oxygen removal rate is high, considerable super-saturation of iron ions will occur in-between the originally formed nuclei and thus cause formation of additional nuclei, resulting in the creation of a non-porous covering layer of iron (cf. Fig. 6.20). An equation similar to the above for wustite reduction has recently been suggested.[95]

It is the general experience that the reduction of hematite produces a porous product whereas that of magnetite a dense one, the pore size being larger when reduced with CO than with hydrogen in both the cases. Hydrogen being a more powerful reducing agent than CO, it will lower the ratio (Eq. 2.38) more than that with CO and tend to produce a more dense layer. On the other hand, the rate of iron ion diffusion in wustite, obtained from hematite, is much higher than that in wustite obtained from magnetite because of internal strain caused during the transformation of hematite. This will tend to increase the ratio and a more porous product will be expected during the reduction of hematite than in the case of magnetite (see also Sec. 6.7.5). It has been observed by the author[47] as well as by Turkdogan[48] that less porous iron layer is apt to form when the reaction rate is high.

Whenever a very dense impervious layer of iron is formed, islands of wustite crystals isolated from the primary wustite phase surrounded by iron have been detected. According to Lien et al.,[19] initially, when the newly formed iron layer contained many lattice defects, oxygen-ion diffusion takes place easily. However, with the passage of time and especially in the temperature range 700–750°C, recrystallization of iron removes the defects making the diffusion of oxygen ions more difficult and the rate-controlling mechanism shifts from phase-boundary to solid-state diffusion.

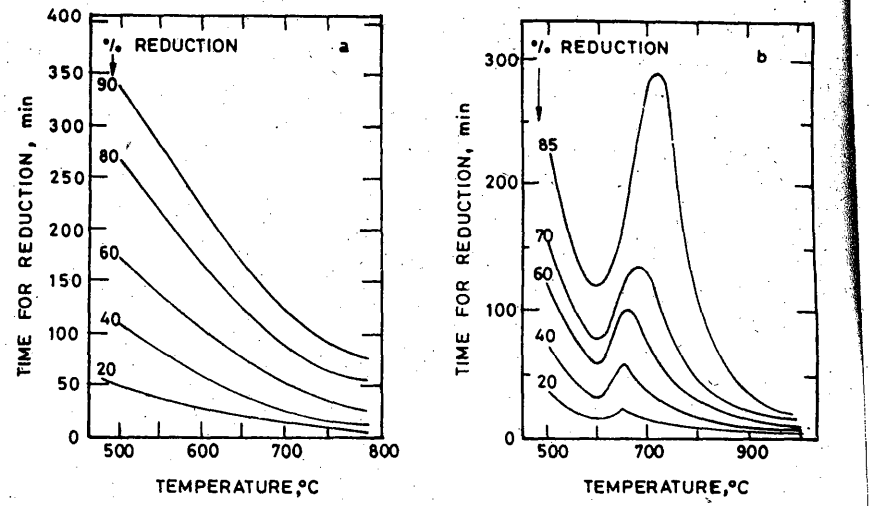


Fig. 2.11 The dependence of times for various degrees of reduction on temperature for pellets of **(a)** hematite and **(b)** magnetite, according to Ross.[16] (By permission, Indian Institute of Metals).

Some ores show a rate minimum in this temperature range and they invariably show the presence of islands of wustite in a dense iron layer.

As mentioned before, generally, hematite produces a porous spongy iron and magnetite a dense non-porous one. This shows why the latter possesses comparatively poor reducibility which can be traced to the rate minimum. This is illustrated in Fig. 2.11(b)[16] where the time for various degrees of reduction of magnetite briquettes is plotted against temperature. The reduction of hematite briquette does not show such rate inhibition (Fig. 2.11a).[16]

It is clear from the above discussions that initial reduction of iron ore at low temperatures is expected to be chemically controlled and proceeds in a topochemical fashion provided the ore is porous and coarse-grained because individual crystals are reduced topochemically. Once an iron layer is formed around the crystals, solid state diffusion of ferrous and/or oxygen ions can become rate-controlling. The relative contribution of gaseous diffusion and solid state diffusion changes with increase in time (i.e., with the degree of reduction or thickness of product layer), temperature and mode of nucleation. The grain size is important as large size inhibits solid state diffusion and a dense covering layer is apt to form.

Various physical properties of the iron ores affect the rate of reduction. They have been discussed in detail in Sec. 6.7. They are:

(a) particle size
(b) porosity
(c) crystal structure
(d) pore size
(e) volume change
(f) impurities

2.8.4. Velocity and Mechanism of Carbon Oxidation

The reaction of coke carbon with blast oxygen and carbon dioxide are of great importance in the blast furnace. The reactions are:

i) $C + O_2(air) = CO_2 + 94050$ cal 2.39

ii) $C + CO_2 = 2CO - 41210$ cal 2.40

adding,

$$2C + O_2(air) = 2CO + 52840 \text{ cal} \quad 2.41$$

Both the above reactions are approximately first order reactions with respect to the gaseous reactants at temperatures above 1000–1100°C. Reaction 2.40, the Boudouard reaction (Fig. 3.4) occurs in the lower furnace. Since it is a highly endothermic reaction and increases coke consumption, its beginning, rate, extent and temperature of occurrence are of vital importance. The rate of reaction 2.39, the combustion reaction, determines the extent of combustion in front of the tuyeres which influences in no small way the descent of the stock column.

2.8.4.1. Velocity of Boudouard reaction

As coke is a porous solid, its overall reaction with gaseous CO_2 will depend upon the various reaction steps cited in Sec. 2.8. In short, the reaction will depend upon:

i) mass transport of gaseous reactants (O_2 or CO_2) and product (CO) through a gas diffusion boundary film;
ii) mass transport of gaseous reactants and products in the coke particle, i.e., pore diffusion;
iii) adsorption and desorption of the gaseous reactants and products, i.e., chemical reaction.

The occurrence of the above three steps for the Boudouard reaction in two sizes of coke, 40 and 80 mm, from two different coking plants is shown in Fig. 2.12.[49] The rate constant k_{eff} has been defined by the following equation:[50]

$$v_c = \frac{dn_c}{dt} = k_{eff}\,(n^{\circ}_{CO_2} - n^{*}_{CO_2}) \quad 2.42$$

where

v_c = moles of carbon reacted/cm³.s
k_{eff} = effective velocity constant, 1/s
$n^{\circ}_{CO_2}$ = CO_2 concentration in gas phase, mole/cm³
$n^{*}_{CO_2}$ = CO_2 concentration in gas phase in equilibrium with C and CO (Fig. 3.4), mole/cm³.

The activation energy of reaction 2.40 is very high, about 86 000 cal/gm. mole.[14] Hence, the reaction slows down greatly at lower temperatures.

From Fig. 2.12, the rate-controlling process depends upon the temperature:[49–52]

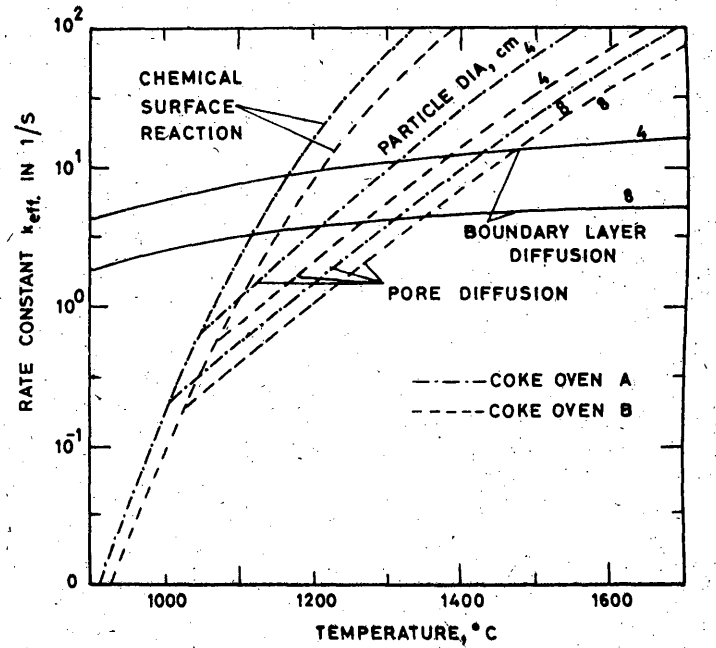


Fig. 2.12 The pattern of the dependence of the limiting curves of the effective rate constant of the Boudouard reaction on temperature for two varieties of coke, according to Heynert et al.[49] (Copyright Verlag Stahleisen).

(i) at low temperatures, up to about 1000–1050°C, the rate is greatly dependent upon the temperature and chemical reaction is rate-controlling. In this region the chemical process envisaged for the formation of CO from CO_2 is adsorption of CO_2 on the reactive coke surface, dissociation of the adsorbed molecule into adsorbed CO and O, reaction of carbon in the coke lattice with adsorbed O to form adsorbed CO and finally desorption of CO (the curves are steep);

(ii) at intermediate temperatures, porous diffusion becomes rate-controlling (the curves become flatter);

(iii) at very high temperatures, the rate is determined by diffusion through the boundary gas film (the curves are almost horizontal).

Apart from temperature, other factors like gas velocity, residence time, porosity and surface area of coke, voidage in coke bed, particle size, etc., affect the rate. Fig. 2.12 shows that pore diffusion control starts at lower temperature the larger the coke size.

According to Heynert and Willems,[52] the limits for chemical reaction control with CO_2 for blast furnace type of coke of size 80 mm and 40 mm are 960°C and 1000°C, although there is some overlapping with pore diffusion up to 1200°C. The gas film diffusion range is not reached even at 1700°C because of high gas velocity.

The use of coke with low specific inner surface area or, in other words, the use of less reactive coke is especially of importance in the chemisorption zone because the reaction rate is proportional to the surface area whereas in the pore diffusion zone, it is proportional to the square root of the surface area. Therefore, the larger the particle size and less reactive the coke, the higher will be the temperature and the lower will be the position in the furnace shaft where the carbon gasification reaction will be inoperative. This will enable a larger volume of the furnace to be effectively utilized for indirect reduction, the importance of which for fuel efficiency will be seen in Sec. 7.3. We can assume that in the blast furnace charged with average coke size of 60 mm and coke weight of about 250 kg/m³ of furnace volume, any transformation of CO_2 to CO by carbon will be negligible[52] below 1000°C.

In respect of carbon gasification reaction, Turkdogan[48] has measured the non-catalytic oxidation of coke granules in CO-CO_2 mixtures. For the limiting case of complete internal gasification, the rate of CO generation from 500 kg of coke is shown as a function of temperature (Fig. 2.13,[48] lower curve). In the blast furnace the coke size is usually much above 20 mm for which internal oxidation is minimal. The rate will be much

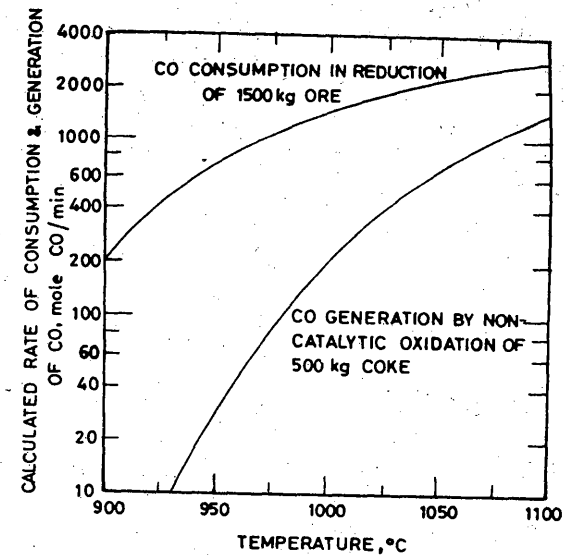


Fig. 2.13 The rate of reduction of lump hematite ore by CO and non-catalytic internal oxidation of coke by CO_2 in various gas compositions and at various temperatures, according to Turkdogan.[48] (Copyright The American Society for Metals and the Metallurgical Society of AIME 1978).

smaller if the reaction occurs on the surface alone. The upper curve of Fig. 2.13 shows the consumption of CO in the reduction of iron oxide giving rise to CO_2. One can see the rate of the latter is higher than the former. The former (Boudouard reaction) becomes prominent only above 1100°C.

In fact, however, because of the catalytic action of the alkali vapours on reaction 2.40 in the blast furnace, the rates of the Boudouard and ore reduction reactions are comparable at about 1000°C. This means that any CO_2 generated from ore reduction above 1000°C may be reduced unnecessarily by carbon. This again emphasizes the desirability, from fuel efficiency point of view, of using less porous (low specific inner surface) and less reactive coke in order to restrict the start of the endothermic gasification reaction to as high a temperature as possible.

2.8.4.2. Velocity of combustion reaction

Regarding combustion of coke by air, Heynert and Willems[52] have calculated, on the basis of certain assumptions, that 90 percent of the blast oxygen is used up at a distance of about 550 mm from the tuyere nose

with coke of 4 cm average diameter whereas with coke size of 5 cm the 90 percent limit is reached at a distance of 750 mm, causing an enlargement of the oxidising zone which facilitates stock descent (Sec. 7.5).

The combustion of coke in front of the tuyeres produces a very high gas temperature, about 2000°C or more. Apparently, the reaction should be controlled by boundary film diffusion of blast oxygen. However, the surface area to volume ratio increases with burning of coke. The Reynolds number of the main gas stream being high, it can be assumed that the combustion reaction is diffusion controlled.

2.9. Blast Furnace Slag

Metals are generally extracted from ores which are always associated with impurities, mainly oxides, called gangue. During the extraction of the metal the gangue is removed, by the addition of flux, in the form of slag which is insoluble in the metal. In the iron ores and coke ash the impurities are mainly acidic silica and alumina. The fluxes are basic lime and magnesia. The other components in the blast furnace slag which together may not amount to more than 5 percent are FeO, MnO, TiO_2, S and others.

2.9.1. Slag Structure

Liquid slags are homogeneous melts consisting of oxides of silicon and other elements. They are known to possess electrical properties and consist of simple and complex ions. Crystal analysis of solid silica shows that silicon occupies the centre of a tetrahedron surrounded by 4 oxygen atoms, one at each of the four corners. Each oxygen atom is bonded to two silicon atoms and the network is continuous in three dimensions. These tetrahedra can share only corners so that when every corner oxygen atom is shared, the substance formed will have an overall stoichiometric formula of SiO_2. An Si atom has 4 charges. As each oxygen atom of the tetrahedron has a residual valency, therefore, the SiO_4 group carries 4 negative charges, i.e. $(SiO_4)^{4-}$.

In the crystalline state the tetrahedral arrangement of the silicon and oxygen atoms is symmetrical. The solid structure does not undergo any sudden change on fusion, as expected. In molten or vitreous silica the structure becomes distorted but most of the corners remain shared. The viscosity of molten silica is very high ($\approx 10^5$ P), the corners being linked tightly in all directions in a vast network. These are apparent from Fig. 2.14.[53]

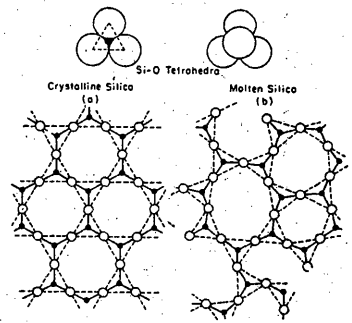


Fig. 2.14 Schematic representation of the silicate tetrahedron and crystalline and molten silica. The oxygen and silicon atoms are shown white and black respectively. In the left-hand tetrahedron as well as in the lower diagrams the apical oxygen atoms have been omitted for the sake of clarity. After Richardson.[53]

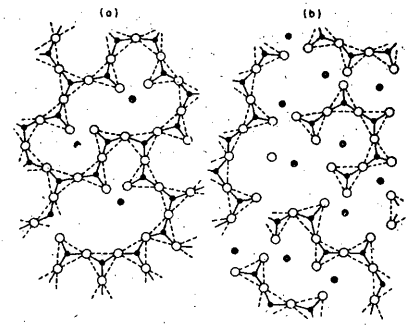


Fig. 2.15 Schematic representation of solution of a divalent metal oxide in molten silica. The shaded circles represent metal ions. After Richardson.[53]

The (SiO_4) group, which is regarded as individual tetrahedron with silicon at the centre and oxygen at the four corners, can be assumed to exist as ion in the complex silicates. Measurement of the energy of activation for electrical conductance and other results indicate that the addition of CaO, MgO or other metal oxides to molten silica results in the breakdown of the three dimensional silicon-oxygen network into silicate ions. The driving force for the breakdown process is the attraction between silicon and oxygen. This depends on their relative valencies and ionic radii.

When lime or magnesia is added to molten silica, two silicon-oxygen bonds are opened up giving rise to:[53]

$$\equiv Si - O - Si \equiv + CaO = \equiv Si - O^- + {}^-O - Si \equiv + Ca^{2+} \qquad 2.43$$

A shared corner is opened up where an oxygen is added, each oxygen at the break carrying a negative charge. The cations distribute in the interstices of the network, being localised near the charged oxygen (see Fig. 2.15).[53] As the metallic oxides are added in increasing amounts, the Si-O bonds break correspondingly, and large globular or ring-type silicate ions are formed. These become progressively smaller as the metal oxide content increases (see Fig. 2.16).[54] This continues according to Eq. 2.43 as long as the ratio of a strongly basic metallic oxide to silica in a binary slag, i.e., the ratio MO/SiO_2, is less than 2.0 and hence less than that for the orthosilicate composition $2MO.SiO_2$. The viscosity of the acidic melt falls as the network gradually breaks and ultimately a stage is reached when no corners are shared (Fig. 2.17).[53] At this stage the slag reaches the orthosilicate composition (MO/SiO_2 ratio equal to 2.0). The slag is deemed to be neutral and consists of discrete $(SiO_4)^{4-}$ ions. On attaining the stoichiometric composition of $2MO.SiO_2$, further additions of base would give oxygen ions (O^{2-}) and equivalent number of cations, i.e., when the MO/SiO_2 ratio exceeds 2.0.

It is, however, possible for oxygen ions to be present in melts having more silica than corresponding to the stoichiometric compositions $2CaO.SiO_2$ or $2MgO.SiO_2$ depending upon the temperature. Polymerized silicate groups may be present as shown:

$$2(\equiv Si - O -) = \equiv Si - O - Si\equiv + O^{2-} \qquad 2.44$$

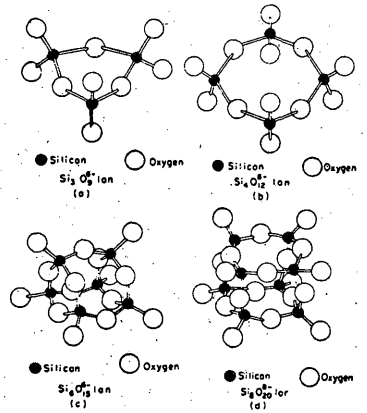


Fig. 2.16 Discrete ions in liquid silicates, after Bockris et al.[54] (Copyright Faraday Society).

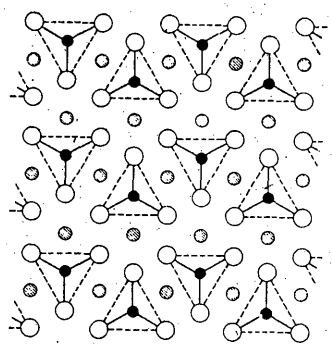


Fig. 2.17 Schematic representation of crystalline $2MgO.SiO_2$. The molten magnesium silicate will be a disordered version of this. After Richardson.[53]

There appears to exist an equilibrium of the type $2O^- = O^o + O^{2-}$ corresponding to Eq. 2.44.[53] Theoretically, the activity of the O^{2-} ions determines the basicity of the slags. In practice, arbitrary values of the base/acid ratios are selected for day to day operation.

The above discussion of slag structure is most elementary but is deemed sufficient for the purpose of understanding the blast furnace slag-metal reactions treated in the text. For more exhaustive treatment and other references, the reader may refer to the reviews by Frohberg et al.,[55] Masson[56] and Richardson.[70]

2.9.2. Electro-chemical Nature of Slag-Metal Reactions[57,58]

Although direct exchange of two atoms or ions are possible between metal and slag, the introduction of the concept of an electro-chemical mechanism of slag-metal reaction becomes a necessity since metal is non-polar and molten slag ionic in character. Hence any transfer of an element from metal to slag is accompanied with an anodic reaction, e.g.,

$$[Mn] = (Mn^{2+}) + 2e \qquad 2.45$$

To preserve electro-neutrality of the slag, a cathodic reaction must occur with the deposition of an element in the metal, e.g.,

$$(Fe^{2+}) + 2e = [Fe] \qquad 2.46$$

Hence, for the reaction,

$$[Mn] + (FeO) = (MnO) + [Fe] \qquad 2.47$$

we may write,

$$[Mn] + (Fe^{2+}) = (Mn^{2+}) + [Fe] \qquad 2.48$$

Similarly, the transfer of the following elements from iron can occur according to:

$$[C] + (O^{2-}) = CO(g) + 2e \qquad 2.49$$

$$[S] + 2e = (S^{2-}) \qquad 2.50$$

$$[Si] = (Si^{4+}) + 4e \qquad 2.51$$

$$[Al] = (Al^{3+}) + 3e \qquad 2.52$$

Slag-metal reactions take place only when they are liquid, i.e., above about 1200°C. Reduction by carbon can take place when liquid slag flows over incandescent coke in the bosh or the carbon-saturated iron droplets travel through the slag layer in the hearth. The elements, the reductions of which are of major importance in ironmaking, are silicon, manganese and sulphur. The probable electro-chemical representations of the reactions are shown below:

(a) Silicon – The reaction

$$(SiO_2) + 2[C] = [Si] + 2CO(g) \qquad 2.53$$

can be depicted electro-chemically by combination of equations 2.49 and 2.51 as

$$2[C] + (2\ O^{2-}) = 2CO(g) + 4e \qquad 2.49a$$

$$(Si^{4+}) + 4e = [Si] \qquad 2.51a$$

on adding,

$$(Si^{4+} + 2\ O^{2-} = SiO_2) + 2[C] = [Si] + 2CO \qquad 2.53$$

(b) Manganese – Manganese reduction can be depicted electro-chemically as

$$(Mn^{2+}) + 2e = [Mn] \qquad 2.45a$$

$$[C] + (O^{2-}) = CO + 2e \qquad 2.49$$

adding,

$$(Mn^{2+} + O^{2-} = MnO) + [C] = [Mn] + CO \qquad 2.54$$

Or,

$$2(Mn^{2+}) + 4e = 2[Mn] \qquad 2.45a$$

$$[Si] = (Si^{4+}) + 4e \qquad 2.51$$

Adding,

$$2(Mn^{2+}) + [Si] = (Si^{4+}) + 2[Mn] \qquad 2.55$$

(c) Sulphur – Desulphurization can be imagined to occur according to the following mechanism:

$$[C] + (O^{2-}) = CO(g) + 2e \qquad 2.49$$

$$[S] + 2e = (S^{2-}) \qquad 2.50$$

on adding,

$$[S] + [C] + (O^{2-}) = (S^{2-}) + CO(g) \qquad 2.56$$

In the absence of an electrical field across the slag-metal interface, carbon becomes oxidized to provide the electrons necessary for Eq. 2.56. Such electrons can also be provided by Eqs. 2.45, 2.51 and 2.52 with simultaneous oxidation of the elements to the slag.

The reduction of these three elements and others in the blast furnace are further discussed in Secs. 3.12–3.15 and 7.4.2.

2.9.3. Slag Basicity

The oxides, e.g., SiO_2, Al_2O_3, which accept oxygen and form anion complexes in melts are said to be acidic oxides. The basic oxides are those which break down the anion complexes, e.g., CaO, MgO, FeO, MnO, etc., by donating oxygen. In practice, the ratio of the sum of the concentration of the bases to that of the acids is called *basicity* of the slag. In ironmaking the ratio is usually depicted as CaO/SiO_2 or $(CaO + MgO)/(SiO_2 + Al_2O_3)$ although there are variations in their usage as will be seen in Chapter 8; concentrations of MgO and CaO are sometimes taken as equivalent on molar basis. In terms of wt.%, the CaO equivalence of MgO becomes %CaO = (56/40)%MgO = 1.4%MgO.

2.9.4. Slag Viscosity

We have seen in Sec. 2.9.1 that with the entry of oxygen ions from metal oxides the Si-O bonds progressively break down and the size of

the network decreases accompanied with a lowering of the viscosity of liquid slags. Since one atom of oxygen is shared by two of silicon in the tetrahedra, silicates can have isolated tetrahedra and, therefore, a low viscosity when the ratio O/Si exceeds 4 (Fig. 2.17).

In blast furnace slags alumina is always present and the AlO_4-groups form polymer units with SiO_4-groups. In slags containing CaO-MgO-SiO_2-Al_2O_3, alumina should increase the viscosity as silica does. On the other hand lime and magnesia, the suppliers of oxygen, should decrease it.

From Fig. 3.19 it is clear that the viscosity of the CaO-SiO_2-Al_2O_3 melt decreases regularly with increase of lime. The iso-viscosity lines (isokoms) run almost parallel to the lines of equal lime contents which means that on a weight percent basis, silica and alumina are nearly equivalent in their effect on viscosity. Furthermore, from Fig. 3.21 in the CaO-MgO-SiO_2-Al_2O_3 system, magnesia is slightly more effective on weight percent basis than lime in lowering the viscosity.

Viscosity of slags depends upon the composition and temperature. Low viscosity not only helps to govern the reaction rates by its effect on the diffusion of ions to and from the slag/metal reacting interface through the liquid slag but also ensures a smooth running of the furnace. Both an increase of basic oxides and that of temperature above the liquidus temperature of the slag decrease the viscosity. According to Turkdogan[59] and Bills,[60] in the CaO-MgO-Al_2O_3-SiO_2 system, alumina and silica are not equivalent on molar basis in their effect although both increase the viscosity of these melts. The effect of the former on the viscosity depends on the lime content of the slag. This is because Al^{3+} can replace Si^{4+} in the silicate network only if associated with $\frac{1}{2}Ca^{2+}$ to preserve electrical neutrality.

2.9.5. Summary of Slag Properties[61,62]

Summarising the effect of temperature and basicity, the following are of importance:

(1) Slag viscosity increases with decreasing temperature. Any presence of crystals suspended in the liquid raises the viscosity and therefore it is imperative that the melt should be all liquid, i.e., above the liquidus temperature. For most slags, the increase in viscosity is very rapid when the temperature falls below the liquidus and crystals of various phases appear in the melt.

(2) The higher the basicity, i.e., $(CaO + MgO)/(SiO_2 + Al_2O_3)$ ratio, the lower the viscosity, above the liquidus temperature. Thus, for a given alumina content, the lower the silica content the lower will be the viscosity. However, the slag should have a minimum silica content for it to be all liquid at the temperatures used. This situation is ideally suited for desulphurization and theoretically should give maximum sulphur removal (cf. Chapter 9). However, the slag becomes increasingly viscous and refractory with increasing lime/silica ratio because of escalation in the liquidus temperature and the beneficial effect on sulphur removal may be lost.

(3) At high temperatures, the difference in viscosity between slags of different basicities becomes less than at lower temperatures.

(4) The variation in the viscosity with temperature above the liquidus is greatest for slags of low basicities.

Fig. 2.18[61] shows the relationship of slag basicity and viscosity at 1500°C for 7 slags, the composition of which are given in Table 2.1. It shows in agreement with the results of Machin et al.[93,94] that the viscosity decreases regularly with increasing basicity and that the weight percent of silica and alumina are equivalent in their influence on viscosity. For example, slags

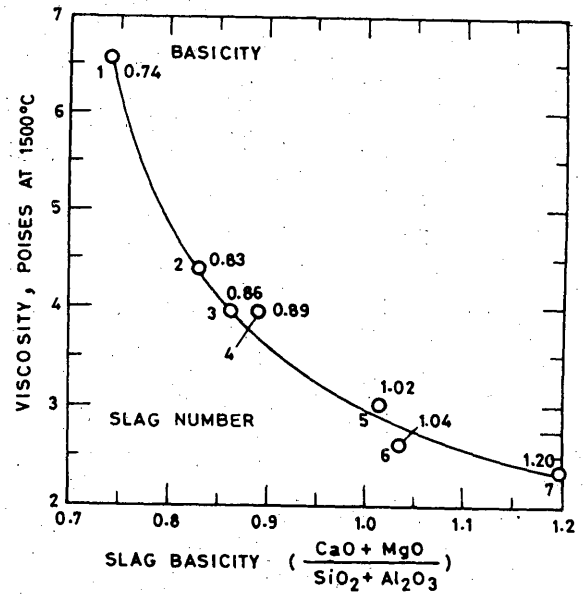


Fig. 2.18 The relationship of viscosity and basicity of slags shown in Table 2.1, after Baldwin.[61] (Copyright Iron and Steel Institute).

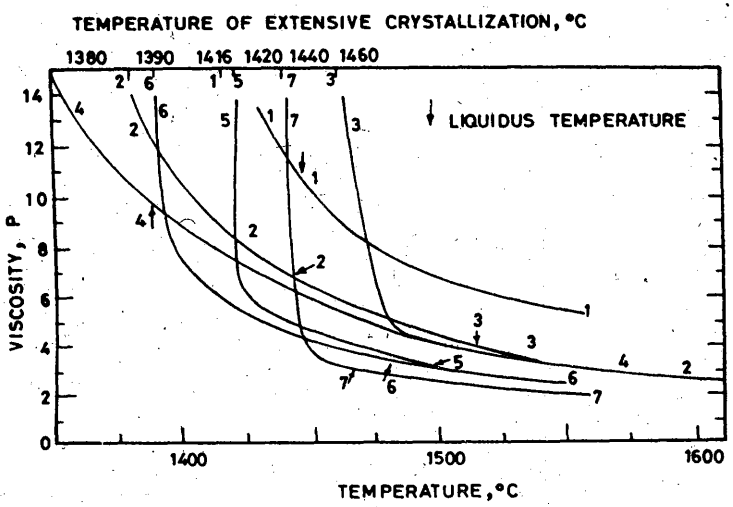


Fig. 2.19 The variation of viscosity with temperature for slags shown in Table 2.1. The liquidus temperatures and temperatures of extensive crystallization are also indicated. After Baldwin.[61] (Copyright Iron and Steel Institute).

3 and 4 with similar basicity ratios, 0.86 and 0.89, have viscosities of the same order above their liquidus temperatures, although the former contains 35.6 percent alumina and the latter only 15.2 percent. Figure 2.19[61] shows the temperature dependence of viscosity for the same 7 slags given in Table 2.1. The temperatures of extensive crystallization are also shown in Fig. 2.19.

Table 2.1[61]

Slag No.	% SiO_2	% Al_2O_3	% CaO	% MgO	% FeO	% MnO	% S	Liquidus Temp. °C measured	Liquidus Temp. °C calculated	B
1	30.4	26.1	35.5	6.4	0.4	0.3	1.4	1450	1470	0.74
2	34.1	18.7	40.6	3.4	0.7	—	0.97	1445	1460	0.83
3	17.0	35.6	44.8	0.6	—	—	—	1515	1530	0.86
4	36.0	15.2	38.5	5.1	1.0	0.7	0.79	1390	1400	0.89
5	32.2	15.2	45.1	3.5	0.8	1.3	—	1500	1500	1.02
6	33.4	13.5	45.2	3.4	0.5	0.4	—	1480	1470	1.04
7	29.7	14.8	41.6	11.9	0.3	0.8	1.4	1460	1470	1.20

$$B = \text{basicity} = (CaO + MgO)/(SiO_2 + Al_2O_3)$$

2.10. Kinetics of Slag-Metal Reactions[57,63,70]

Slag-metal reaction is a heterogeneous process. Therefore, similar to the gas-solid reactions discussed in Sec. 2.8, it includes both chemical reaction at the interface as well as mass transfer. Hence, the overall reaction rate will be controlled by the slowest of the following steps:

(a) transport of reactants from the bulk phase, slag or metal, to the reaction interface through a thin boundary layer;
(b) reaction at the interface;
(c) transport of products from the interface to the bulk phase, slag or metal, through the boundary layer.

The kinetics of the slag-metal reactions have been reviewed by Kawai and Mori.[63] In such reactions, the determination of the rate-determining step is extremely difficult since the individual steps cannot be precisely isolated and measured. One simple way is to assume that at the very high temperatures involved the chemical reaction rate is very high and therefore the reactions are diffusion controlled. In such a case, e.g., for the reaction

$$[M]_{Fe} + (FeO) = [Fe] + (MO) \qquad 2.57$$

the flux, J_M, of the element M in iron transferred from the bulk metal to the interface, similar to Eq. 2.28, is given by:

$$J_M = \frac{D}{y}(C_M^\circ - C_M) = k_m (C_M^\circ - C_M) \qquad 2.58$$

where $k_m = \frac{D}{y}$ = mass transfer coefficient
C_M° = concentration or activity of M in bulk metal
C_M = concentration or activity of M at the interface

Since $k_m = D/y$ and y, the thickness of the boundary layer, can be derived from the flow conditions and Reynolds and Schmidt numbers, the values of k_m can be calculated from the physical properties like viscosity and diffusivity. In general, the diffusivities of elements in liquid iron ($10^{-4} - 10^{-5}$ cm²/s) are about two order of magnitude higher than those in the slag and the activation energy of diffusion in slag is higher than that in iron. If diffusion of the element in iron is rate-controlling, the activation energy is about 10 kcal/mole and the value is a little higher for diffusion control in slag.

In the case where reaction 2.57 is controlled by chemical reaction at the interface, the net rate (v) is given by the difference in the rates of the forward and reverse reactions,

$$v = k_f \cdot a_{FeO} \cdot a_M - k_r \cdot a_{MO} \cdot a_{Fe} \quad 2.59$$

$$= k_f (a_{FeO} \cdot a_M - a_{MO} \cdot a_{Fe}/K) \quad 2.60$$

where k_f = rate constant for the forward reaction
k_r = rate constant for the reverse reaction
a's = activities of various species
K = equilibrium constant of reaction 2.57

The rate constant in Eq. 2.60 depends on the temperature only and not on the flow conditions. The activation energies are much higher than those for diffusion control.

Only a single rate-controlling step has been considered above. If the resistances of mass transfer and chemical reaction are of the same order, then the overall resistance is given by,[63]

$$1/k_t = 1/k_M + 1/k_S + 1/k_f \quad 2.61$$

where the subscripts t, M, S and f denote total, in metal, in slag and in chemical reaction respectively. Hence, the overall flux is given by,

$$J_M = k_t (C_M^\circ - C_M') \quad 2.62$$

where C_M° and C_M' are the concentrations or activities of M in the metal and slag respectively.

Since the slag-metal reaction is electrochemical in character, investigations have been made in this direction.[64-66] However, it is difficult to measure exactly the polarization curves of each electrode reaction.

Slag-metal reactions of major importance in the blast furnace are the reduction-oxidation of silicon, manganese, sulphur and of minor importance are those of chromium and titanium. They have been discussed in Secs. 3.12–3.15 and 7.4.2. These reactions occur in the bosh and tuyere regions and reach finality in the hearth when the iron droplets pass through the slag layer. Very little reaction is expected between the iron and slag pools in the hearth because they are relatively stagnant as well as because of relatively small surface to volume ratio of iron in contact with the slag. Stirring by thermal convection is also restricted because of fall in the temperature of iron with increasing bath depth. Therefore, once a reaction occurs at the interface and reaches equilibrium, further progress can only

be possible if the products are transported away, which is restricted not only because of increased viscosity of iron due to graphite precipitation but also that of the slag whose temperatures are merely a few degrees above the liquidus.

Assuming that carbon-saturated iron reacts with the slag, the three most important reactions are given by:

$$[C]sat. + (MnO) = [Mn] + CO \quad 2.63$$

$$[C]sat. + \tfrac{1}{2}(SiO_2) = \tfrac{1}{2}[Si] + CO \quad 2.64$$

$$[C]sat. + (CaO) + [S] = (CaS) + CO \quad 2.65$$

Equilibrium relations of these reactions are given in Secs. 3.12–3.15. However, in the blast furnace the individual equilibrium is seldom achieved. The actual Si and Mn contents of iron are more often than not lower and the S-contents higher than the equilibrium values. Even under the most favourable laboratory conditions it needs a prolonged period for the attainment of equilibrium. It is also doubtful whether diffusion is rate-controlling since stirring by CO gas does not expedite the reactions.

The rates of reduction of slag MnO have been studied by many.[67-69] Chemical reaction rate rather than diffusion control has been suggested by Daines and Pehlke.[69]

The rates of reduction of silica have been studied by several investigators.[70-77] Both chemical and diffusion control mechanisms have been suggested. However, even under the laboratory conditions and profuse agitation of the metal, the transfer of silicon from slag to metal has been found[78,79] to be small for equilibration period of 8 hours at 1425–1500°C and only a little higher at higher temperatures. However, the rate of transfer increases rapidly with temperature, the heat of activation being about 130 kcal/mole.[79] This unusually large energy requirement is attributed to the difficulty of breaking the strong Si-O bonds in the slag. The driving force of transfer increases with decreasing basicity, i.e., with increasing silica activity in the slag. Since the reaction product CO is gaseous, it is likely that the difficulty of nucleation of bubbles would increase the evolution pressure of CO. Hence, any calculations to determine equilibrium silicon contents assuming $p_{CO} = 1$ atm. may be erroneous.

Much more work appears to have been done for studying the desulphurization of pig iron by molten slag.[80-89] That the sulphur distribution, (%S)/[%S], between the slag and metal does not reach equilibrium

is indicated by the fact that the blast furnace slag has much more desulphurizing capacity than is exhibited. This has been proved by equilibration of actual blast furnace slag and metal samples in graphite crucibles under a CO atmosphere.[90]

Oelsen[91] suggested that in the oxidation-reduction reaction of metalloids in the hearth the oxygen-potential is controlled not by the C-O reaction but rather by the simultaneous coupled reactions:

$$(FeO) + \tfrac{1}{2}[Si] = [Fe] + \tfrac{1}{2}(SiO_2) \qquad 2.66$$

$$(MnO) + \tfrac{1}{2}[Si] = [Mn] + \tfrac{1}{2}(SiO_2) \qquad 2.67$$

$$[S] + (CaO) + \tfrac{1}{2}[Si] = (CaS) + \tfrac{1}{2}(SiO_2) \qquad 2.68$$

$$[S] + (CaO) + [Mn] = (CaS) + (MnO) \qquad 2.69$$

In practice, it has been found that while the reaction of silicon with manganese and sulphur strays away from equilibrium, that between manganese and sulphur is closer to equilibrium. Ward and Salmon[83] suggested from the similarity of activation energy of silicon and sulphur transfer that their rates are controlled by the same mechanism. As we have seen in Sec. 2.9.2, the cathodic reaction of sulphur ($S + 2e = S^{2-}$) can occur with simultaneous anodic reactions ($M = 2e + M^{2+}$) and hence it is likely that the rates of the anodic reactions control that of sulphur transfer to the slag and the fastest of the anodic reactions controls the overall rate.

It has been suggested that since the C-O reaction ($C + O^{2-} = CO + 2e$) is notorious for its sluggishness, this reaction is rate-controlling for sulphur removal (Eq. 2.65). However, the sulphur removal rate is affected very little when CO is bubbled through the equilibrating liquid iron. Ramachandran et al.[81,58] found that the amount of CO evolved was much less than that expected from the amount of sulphur transferred. However, the sulphur balance was obtained on summation of the CO evolved and the number of chemical equivalents of Si, Mn, Al, etc. transferred simultaneously to the slag. In Sec. 3.15 we will see that in the blast furnace it is the manganese transfer which controls sulphur transfer and it is the slowness of the reduction of MnO by silicon which retards the approach of sulphur to equilibrium values.

References

1. DARKEN, L. S. and R. W. GURRY: Physical chemistry of metals, McGraw-Hill, N.Y. 1953.
2. KUBASCHWESKI, O., E. Ll. EVANS and C. B. ALCOCK: Metallurgical Thermochemistry, 4th Ed., Pergamon Press, 1967.
3. BODSWORTH, C. and H. B. BELL: The physical chemistry of iron and steel manufacture, 2nd Ed., Longmans, London, 1972.
4. GASKELL, D. R.: Introduction to metallurgical thermodynamics, McGraw-Hill, N.Y., 1973.
5. Making, Shaping and Treating of Steel: US Steel Corp., Pittsburgh, 9th Ed., 1972, p. 242–363.
6. PARKER, R. H.: Introduction to chemical metallurgy, Pergamon Press, 1967.
7. BISWAS, A. K. and G. R. BASHFORTH: Physical chemistry of metallurgical processes, Chapman and Hall, London, 1962.
8. WAGNER, C.: Thermodynamics of alloys, Addison-Wesley, 1952.
9. CHIPMAN, J.: Basic open-hearth steelmaking, Physical Chemistry of Steelmaking Comm., AIME, 1964 Ed., Chapters 14 and 16.
10. COUDURIER, L., D. W. HOPKINS and I. WILKOMIRSKY: Fundamentals of metallurgical processes, Pergamon Press, 1978.
11. SHERMAN, C. W. and J. CHIPMAN: Trans. Met. Soc., AIME, 194, 1952, p. 597–602.
12. RICHARDSON, F. D. and J. H. E. JEFFES: J. Iron Steel Inst., 163, 1949, p. 397–420.
13. GOODEVE, C. F.: Disc. Farad. Soc., 4, 1948, p. 9–23.
14. BOGDANDY, L. v. and H.-J. ENGELL: The reduction of iron ores (in Eng.), Springer-Stahleisen, 1971.
15. TOKUDA, M., H. YOSHIKOSHI and M. OHTANI: Trans. Iron Steel Inst. Jap., 13, 1973, p. 350–368.
16. ROSS, H. U.: Recent Dev. in Met. Sci. and Tech., Iron and Steel, Silver Jub. Sym., Ind. Inst. of Metals, New Delhi, 1972, p. 1–36.
17. EDSTROM, J. O.: J. Iron Steel Inst., 175, 1953, p. 289–304.
18. McKEWAN, W. M.: Steelmaking, the Chipman Conf. (edt. J. F. Elliott), 1965, MIT Press, Camb., Mass., p. 141–155.
19. LIEN, H. O. et al.: J. Iron Steel Inst., 209, 1971, p. 541–545.
20. McKEWAN, W. M.: Trans. Met. Soc., AIME, 218, 1960, p. 2–6.
21. KNACKE, O.: Arch. Eisenhuttenw., 30, 1959, p. 581–584.
22. GERLACH, J. et al.: op. cit., 36, 1965, p. 543–547.
23. HANSEN, J. P. et al.: Proc. Blast Fce. Cokeoven Raw Mat. Comm., AIME, 19, 1960, p. 185.
24. McKEWAN, W. M.: Trans. Met. Soc., AIME, 224, 1962, p. 2–5; 387–393.
25. QUETS, J. M., M. E. WADSWORTH and J. R. LEWIS: op. cit., 218, 1960, p. 545–550.
26. BOGDANDY, L. v. and W. JANKE: Zeit. Electrochem., 61, 1957, p. 1146–1153.
27. SCHENCK, H. and H. P. SCHULZ: Arch. Eisenhuttenw., 31, 1960, p. 691–702.
28. SETH, B. B. L., and H. P. ROSS: Trans. Met. Soc., AIME, 233, 1965, p. 180–185.
29. EL-MEHAIRY, A. L.: op. cit., 200, 1954, p. 1306.
30. KAWASAKI E. et al.: J. Amer. Inst. Chem. Engg., 8, 1962, p. 48–52.
31. BOGDANDY, L. v. and H.-G. RIECKE: Arch. Eisenhuttenw., 29, 1958, p. 603–609; see also Ref. 14, p. 14.
32. KOHL, H. K. and H.-J. ENGELL: op. cit., 34, 1963, p. 411–418.

33. OHTANI, M. et al.: Jap. Soc. for Promotion of Science, No. 54, p. 1113.
34. IKEGAMI, T.: ibid., p. 1088.
35. SPITZER, R. H. et al.: Trans. Met. Soc., AIME, 236, 1966, p. 726–742.
36. BOGDANDY, L. v., P. DICKENS, W. v. d. ESCHE and J. WILLEMS: Stahl u. Eisen, 83, 1963, p. 129–139.
37. HERR, H. D.: Dr.-Ing. Thesis, Tech. Hochschule, Aachen, 1967. See also Ref. 14, p. 160.
38. EDSTROM, J. O. and G. BITSIANES: Trans. Met. Soc., AIME, 203, 1955, p. 760–.
39. EDSTROM, J. O.: Jernkont. Ann., 141, 1957, p. 809.
40. ULRICH, K. H. et al.: Arch. Eisenhuttenw., 36, 1965, p. 611–618.
41. HIMMEL, L. et al.: Trans. Met. Soc., AIME, 197, 1953, p. 827.
42. CARTER, R. F. and F. D. RICHARDSON: op. cit., 200, 1954, p. 1244.
43. FORSTER, E. et al.: Arch. Eisenhuttenw., 40, 169, p. 535.
44. ARKHAROV, V. I. and V. N. BOGOLONSKII: Zhur. F. Z. Khim (Russ.), 29, 1955, p. 272.
45. KHALAFALLA, S. E. and P. L. WESTON, Jr.: Trans. Met. Soc., AIME. 239, 1967, p. 1494.
46. PIEPENBROCK, R. et al.: Arch. Eisenhuttenw., 47, 1967, p. 141–146.
DAVIES, J. et al.: Ironmaking Steelmaking, 5, 1978, p. 151–161.
47. NAKIBOGLU, F. et al.: Australia-Japan Sym. Extract. Met., Syd., July 1980.
48. TURKDOGAN, E. T.: Met. Trans., 9B, 1978, p. 163–179.
49. HEDDEN, K.: Chem. Ing. Tech., 30, 1958, p. 125–132.
50. HEDDEN, K.: Brenstoff Chemie, 41, 1960, p. 193–203.
51. WICKE, E. et al.: Brennt, Warme Kraft, 8, 1956, p. 264–269.
52. HEYNERT, G. and J. WILLEMS: Stahl u. Eisen, 79, 1959, p. 1545–1554.
53. RICHARDSON, F. D.: Phys. Chemistry of Steelmaking, Edt. J. F. ELLIOTT, MIT, MASS., 1958, p. 55–62.
54. BOCKRIS, J. O'M., J. D. McKENZIE and J. A. KITCHNER: Trans. Farad. Soc., 51, 1955, p. 1734.
55. FROHBERG, M. G. and M. L. KAPOOR: Stahl u. Eisen, 91, 1971, p. 182–188.
FROHBERG, M. G. et al.: Arch. Eisenhuttenw., 39, 1968, p. 651–656.
KAPOOR, M. L. and M. G. FROHBERG: op. cit., 41, 1970, p. 1035–1040.
56. MASSON, C. R.: J. Iron Steel Inst., Feb. 1972, p. 89–96.
57. WAGNER, C.: Phys. Chem. of Steelmaking, Edt. J. F. Elliott, MIT, Mass., 1958, p. 237–251.
58. KING, T. B. and S. RAMACHANDRAN: ibid., p. 125–135.
59. TURKDOGAN, E. T. and P. M. BILLS: J. Amer. Cer. Soc., 39, 1960, p. 682–687.
60. BILLS, P. M.: J. Iron Steel Inst., Sept. 1963, p. 133–140.
61. BALDWIN, B. G.: op. cit., 186, 1957, p. 388–395.
62. OSBORN, E. F. et al.: J. Metals, 6, 1954, p. 33–45.
63. KAWAI, Y. and K. MORI: Trans. Iron Steel Inst. Jap., 13, 1973, p. 303–317.
64. GRIMBLE, M. et al.: J. Iron Steel Inst., 203, 1965, p. 264.
65. ASHIZUKA, M. et al.: Tetsu-to-Hagane, 54, 1968, p. 1434.
66. TOPORISCHER, G. A. et al.: Isv. VUZOV, Cher. Met., 3, 1970, p. 13.
67. TARBY, S. K. and W. O. PHILBROOK: Trans. Met. Soc., AIME, 239, 1967, p. 1005.
68. YAGI, T. and Y. ONO: Trans. Iron Steel Inst. Jap., 10, 1970, p. 36.
69. DAINES, W. L. and R. D. PEHLKE: Met. Trans., 2, 1971, p. 1203.
70. RICHARDSON, F. D.: Physical chemistry of melts in metallurgy, vol. 1 & 2, Academic Press, 1974.
71. TURKDOGAN, E. T. et al.: Trans. Met. Soc., AIME, 227, 1963, p. 1265.
72. RAWLING, J. R. and J. F. ELLIOTT: op. cit., 233, 1965, p. 1539.

73. YOSHII, C. and T. TANIMURA: Tetsu-to-Hagane, 51, 1965, p. 833; 52, 196 p. 1448.
74. KAWAI, Y. et al.: Trans. Iron Steel Inst. Jap., 12, 1972, p. 138.
75. ADACHI, A. et al.: op. cit., 9, 1969, p. 153.
76. SCHUMANN, R.: Trans. Met. Soc., 218, 1960, p. 1130.
77. FROHBERG, M. G. and H. LEYGRAF: Arch. Eisenhuttenw., 41, 1970, p. 501.
78. CHIPMAN, J. et al.: Acta Metallurg., 2, 1954, p. 439.
79. FULTON, J. C. and J. CHIPMAN: Trans. Met. Soc., AIME, 215, 1959, p. 888.
80. DERGE, G. et al.: op. cit., 180, 1950, p. 1111.
81. RAMACHANDRAN, S. et al.: op. cit., 206, 1956, p. 1549.
82. CHANG, L. C. and K. M. GOLDMAN: op. cit., 176, 1948, p. 309.
83. WARD, R. G. and K. A. SALMON: J. Iron Steel Inst., 196, 1960, p. 393–403.
84. SAITO, T. and Y. KAWAI: J. Jap. Inst. Met., 19, 1955, p. 170.
85. HATANO, M.: Tetsu-to-Hagane, 55, 1969, p. S704.
86. YOSHI, C.: ibid., p. S701.
87. TOKUDA, M. and M. OHTANI: ibid., p. S708.
88. FROHBERG, M. G. et al.: Arch. Eisenhuttenw., 40, 1969, p. 191.
89. NEUHAUS, H. et al.: Stahl u. Eisen, 85, 1965, p. 1578.
90. Anon.: Iron Coal Trd. Rev., 168, 1954, p. 1265; see Ref. 3, p. 169.
91. OELSEN, W.: Stahl u. Eisen, 68, 1948, p. 176–186; see Sec. 3.15 for other references.
92. Ref. 14, p. 50–66.
93. MACHIN, J. S. and D. L. HANNA: J. Amer. Cer. Soc., 28, 1945, p. 310–316.
94. MACHIN, J. S. and T. B. YEE: op. cit., 31, 1948, p. 200–204; 37, 1954, p. 177–186.
95. NICOLLE, R. and A. RIST: Met. Trans. B., 10B, Sept. 1979, p. 429–438.

CHAPTER 3

SYSTEMS OF IMPORTANCE IN IRONMAKING

3.1. Introduction

In the following sections an attempt has been made to collect and correlate he important data regarding the chemical reactions that occur between he materials employed in iron-making. This will help in obtaining an idea f the reactions that are possible in the blast furnace and will be useful or an understanding of the effects and limitations of these reactions on he furnace performance. The discussions will not necessarily be confined o only equilibrium relations between the various phases and components aking part in the reactions.

As usual, the concentrations of the materials present in the metal will e indicated by square brackets, in the slag by parenthesis and the gas nd the free materials without either.

3.2. The Fe-C System

Iron is generally regarded to exist in four modifications and their stability nges are as follows:

α — iron up to 906°C
γ — iron from 906°C to 1402°C

δ — iron from 1401°C to 1534°C
liquid iron above 1534°C.

However, liquid iron in contact with coke in the blast furnace dissolves considerable amounts of carbon.

The portion of iron-carbon phase diagram of our interest is shown in Fig. 3.1. The melting point of pure iron of 1534°C decreases with increasing carbon content to 1147°C at the eutectic with 4.3% C. This great lowering of the melting temperature enables blast furnace hot metal to be tapped at 1350–1450°C. Thereafter, the melting temperature increases with increasing carbon content, reaching a value of 1550°C at 6.7%.C. Some of it, usually 0.2–0.5 percent, can be present as combined carbon (Fe_3C). It is metastable and its proportion is largely dependent on the rate of cooling. The rest is present as graphite. The solubility of carbon depends upon the amount of metalloids present in iron and is discussed in the next section.

3.3. The Fe-C-Metalloids System

Fig. 3.2[2] shows that the solubility of carbon in iron at ironmaking temperatures decreases in the presence of silicon and phosphorus and increases with manganese and chromium (see also Sec. 7.4.3). The amount of combined carbon decreases and that of graphite increases with silicon. With the entry of silicon, graphite precipitates out of carbon-saturated iron and decreases its fluidity. Foundry grade iron with high silicon is, therefore, made fluid by phosphorus (0.5 to 1.5 percent) although the latter also decreases the solubility of carbon.

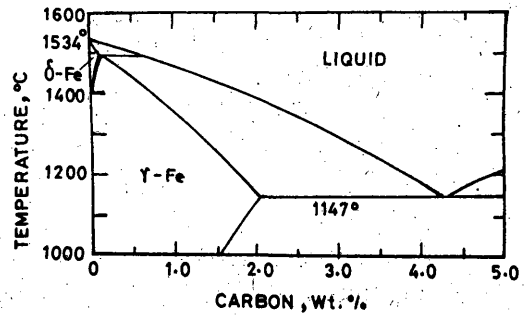


Fig. 3.1 Some features of the iron-carbon phase diagram relevant to ironmaking.

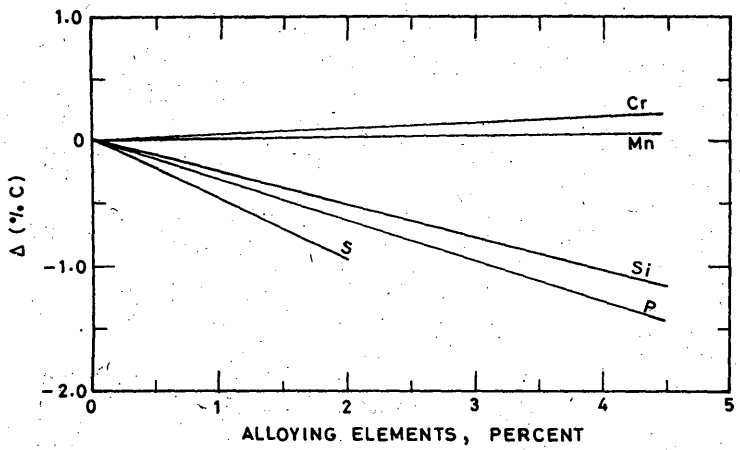


Fig. 3.2 The influence of some impurity elements on the solubility of carbon in liquid iron, after Ohtani and Gokcen.[2] (Copyright AIME).

3.4. The Fe-O System

Iron occurs in its ores predominantly in combination with oxygen. It forms three stable oxides – hematite (Fe_2O_3), magnetite (Fe_3O_4) and wustite ($FeO_{1.05}$). Their fields of existence have been studied by Darken and Gurry[3] and some important features are reproduced in Fig. 3.3 for 1 atm. total pressure. The salient features of the diagram as well as other relevant information of the three oxides are detailed below. Their heats of formation are given in Table 3.1.

3.4.1. Hematite

It contains 30.05% oxygen and at 1457°C decomposes into magnetite and oxygen (p_{O_2} = 1 atm.) The oxygen dissociation pressures of the three oxides at various temperatures are given in Table 3.2. Since the p_{O_2} values of hematite are high, it can easily dissociate into magnetite at high temperatures even in a very mildly reducing atmosphere. That is why, during sintering of iron ores (Sec. 6.4.1), a considerable amount of hematite is initially transformed into magnetite and subsequently at lower temperatures, during cooling, it is re-oxidized to *secondary* hematite.

Hematite occurs in two modifications:[4]

(a) $\alpha - Fe_2O_3$: crystal structure, hexagonal; much more prevalent;
(b) $\gamma - Fe_2O_3$: cubic lattice; forms only under special circumstances below 400–500°C; it is of no importance for our purpose.

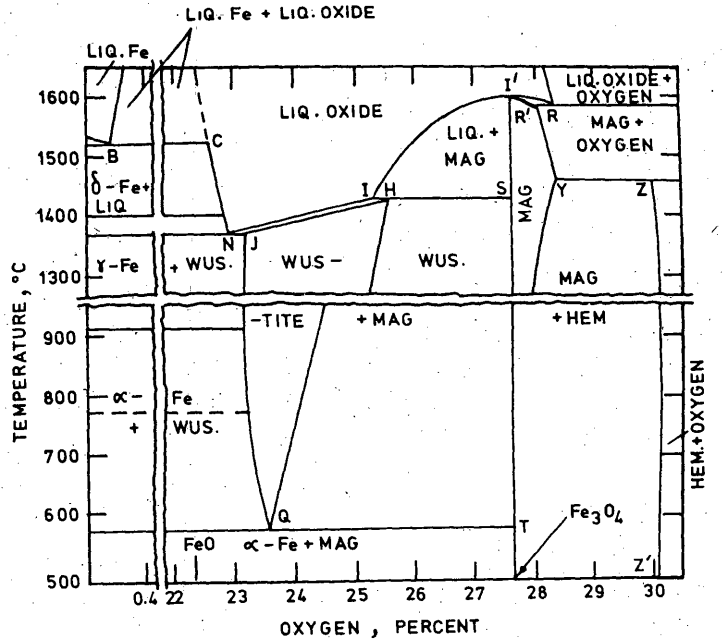


Fig. 3.3 Some important features of the iron-oxygen phase diagram taken from Darken and Gurry.[3]

3.4.2. Magnetite

It is cubic in structure and possesses a stoichiometric composition when at equilibrium with wustite and α-iron at 570°C. It forms solid solutions with hematite at higher temperatures, the O/Fe ratio becoming more than the stoichiometric. Thus, it becomes deficient in iron ions resulting in the occurrence of iron ion vacancies, i.e., while oxygen atoms occupy fixed positions in the magnetite lattice, some positions in the iron sub-lattice remain unoccupied by iron ions. Such holes or defects facilitate diffusion of iron ions (or any foreign cations of comparable size) and permit migration through them.

In contact with iron both hematite and magnetite are reduced to the lower oxides:

$$4Fe_2O_3 + Fe = 3Fe_3O_4 \qquad 3.1$$

$$Fe_3O_4 + Fe = 4FeO \qquad 3.2$$

During transformation of hematite to magnetite, the structural metamorphosis from hexagonal to cubic gives rise to volume expansion, increased porosity, cracks and fissures. In fact, as will be seen in Sec. 6.7, the reduction of hematite produces a porous product and the larger surface area thus generated results in a much higher reduction rate of hematite compared to magnetite.

Magnetite has a very high melting temperature, about 1597°C. At this point it contains 27.64% oxygen.

3.4.3. Wustite

At 1524°C, point C (Fig. 3.3), oxygen-saturated liquid iron (0.16%.O) is in equilibrium with an immiscible liquid phase of ferrous oxide containing 22.6%.O. The melting temperature of this oxide decreases with more oxygen and reaches a minimum of 1371°C in equilibrium with solid oxygen-saturated γ-iron. Thereafter, the melting temperature of ferrous oxide increases with the oxygen content.

We can see from Fig. 3.3 that stoichiometric ferrous oxide, FeO, containing 22.6%.O does not ordinarily exist. Taking an average value of 23.2%.O between 600–1371°C for wustite saturated with iron, the composition corresponds approximately to $FeO_{1.05}$ or $Fe_{0.95}O$. For convenience only, the formula for wustite used in the text is FeO. Based on $Fe_{0.95}O$, the amount of oxygen to be removed from wustite for producing 1000 kg.Fe is about 302 kg (instead of 285 kg.O based on stoichiometric FeO).

From above, wustite is deficient in divalent iron ions and in order to maintain electro-neutrality there must be present some ferric ions, the latter increasing with the oxygen content of wustite. The occurrence of iron ion vacancies greatly facilitates diffusion of iron ions through the lattice and influences the reduction rate and product morphology (Sec. 2.8 and 6.7.5).

Wustite is unstable below 570°C and, on slow cooling, it decomposes spontaneously into iron and magnetite:

$$4FeO = Fe + Fe_3O_4 \qquad 3.3$$

Table 3.1 Compositions and heats of formation of iron oxides, kcal/gm. mole

Oxide	Mol. wt.	Weight percent		ΔH° at °K		
		Fe	O	298	1000	1200
FeO	72.65*	76.8*	23.2*	− 63.64	− 54.70	− 51.94
Fe_3O_4	231.55	72.36	27.64	− 267.30	− 232.65	− 223.05
Fe_2O_3	159.68	69.94	30.06	− 197.30	− 173.26	− 166.4

* Non-stoichiometric wustite ($Fe_{0.95}O$)

Table 3.2 Oxygen dissociation pressure (p_{O_2}) in atmospheres, of iron oxides

Oxide phases	Temperature, °C			
	1100	1200	1300	1400
Fe_2O_3/Fe_3O_4	5.2×10^{-5}	1.6×10^{-3}	1.4×10^{-2}	1.3×10^{-1}
Fe_3O_4/FeO	2.0×10^{-11}	8.4×10^{-10}	2.2×10^{-8}	3.7×10^{-7}
FeO/Fe	6.0×10^{-14}	1.3×10^{-12}	2.0×10^{-11}	2.1×10^{-10}

3.5. The C-O Systems

Carbon reacts with oxygen as follows:

$$C + \tfrac{1}{2}O_2 = CO : \Delta H^\circ\ (298^\circ K) = -26.42 \text{ kcal} = -2200 \text{ kcal/kg.C} \qquad 3.4$$

$$\Delta H^\circ\ (1673^\circ K) = -28.00 \text{ kcal} = -2300 \text{ kcal/kg.C}$$

$$C + O_2 = CO_2 : \Delta H^\circ\ (298^\circ K) = -94.05 \text{ kcal} = -7840 \text{ kcal/kg.C} \qquad 3.5$$

$$\Delta H^\circ\ (1673^\circ K) = -97.8 \text{ kcal} = -8150 \text{ kcal/kg.C}$$

From above:

$$CO + \tfrac{1}{2}O_2 = CO_2 : \Delta H° \text{ (298°K)} = -67.84 \text{ kcal} \qquad 3.6$$
$$\Delta H° \text{ (1673°K)} = -69.12 \text{ kcal}$$

The burning of CO to CO_2 thus gives the major part of heat, about 5760 kcal/kg.C at 1400°C. The much lower heat evolved in Eq. 3.4 compared to Eq. 3.6 per mole of oxygen is probably due to energy consumption for breaking the C-C bonds in the carbon lattice.

The combustion of carbon to its monoxide yields only about 28 percent of the total heat possible to be obtained and only oxidation to the dioxide gives the largest amount of heat. This has a great significance in the blast furnace process where about 30–40 percent of the coke carbon is oxidised to CO_2 and the rest into CO. From Eqs. 3.4 and 3.5, in the blast furnace about half of the heating value of carbon is obtained for a top gas CO/CO_2 ratio of 2. The rest is carried away in the outgoing gas. Although a part of this heat is redeemed by burning the gas out of the furnace, it means conversion of expensive metallurgical coke to a gas which could be obtained from a less valuable fuel.

The heat values in Eqs. 3.4 and 3.5 are for pure carbon. For a good quality coke with 86% C, the respective values will be about 2000 and 7000 kcal/kg.coke.

Carbon dioxide, in the absence of carbon, is stable at high temperatures. Up to about 2000°C, its thermal dissociation is small. At atmospheric pressure, it amounts to about 2 percent.

At high temperatures, carbon dioxide is unstable in the presence of carbon and is reduced to carbon monoxide according to:

$$C + CO_2 = 2CO : \Delta H° \text{ (298°K)} = +41.21 \text{ kcal} \qquad 3.7$$
$$= +3435 \text{ kcal/kg.C}$$
$$\text{At about 1000°C} : \Delta H° \text{ (1273°K)} = +40.3 \text{ kcal}$$
$$= +3360 \text{ kcal/kg.C}$$

Equation 3.7 is generally known as *Boudouard* or *carbon gasification* reaction and is highly endothermic; the reverse reaction is exothermic and is called *carbon deposition* reaction. The former reaction is of extreme importance for the economy and smooth running of the blast furnace. It occurs at high temperatures, above about 1000°C (Sec. 2.9), and therefore consumes an enormous amount of heat in the lower third of the blast furnace. The carbon deposition reaction is most pronounced at temperatures 500–550°C and consequently takes place in the upper portion of the shaft.

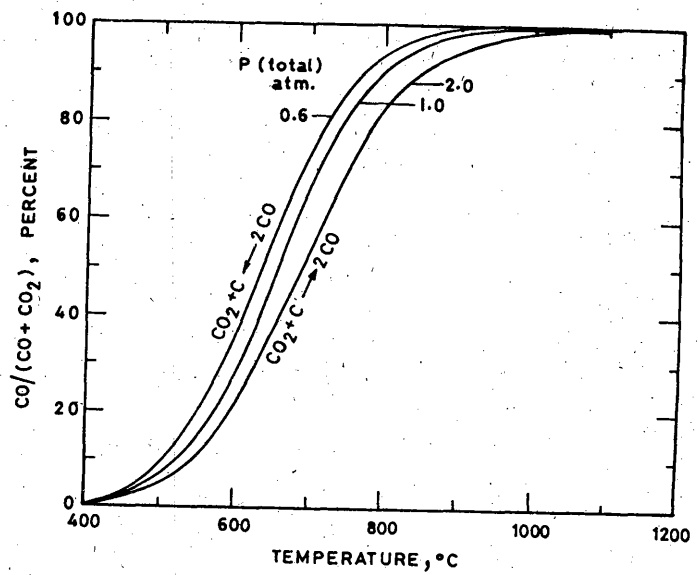


Fig. 3.4 The Boudouard or stability diagram of CO/CO_2 in the presence of carbon at various temperatures and the influence of total pressure (calculated).

Figure 3.4 shows the equilibrium relationship between the gas composition ($CO + CO_2$) in the presence of carbon at different temperatures. Since 2 moles of CO are produced from 1 mole of CO_2 (carbon being solid), reaction 3.7 is dependent on pressure. The isobars in the figure show that at any given temperature the equilibrium $\%CO_2$ increases with increasing pressure. In the normal blast furnace the average partial pressure of $CO + CO_2$ is about 0.6–0.7 atm., the furnace gas containing on an average 40% ($CO + CO_2$).

The properties of coke and the kinetics of reaction which affect the temperature of the *onset* or the *freezing* of the Boudouard reaction and the extent of the combustion zone in front of the tuyeres have been discussed in Secs. 2.8.4.1, 2.8.4.2, 7.6.1 and 7.6.5.

From Fig. 3.4, the stability of CO decreases with decreasing temperature and increasing pressure. The maximum instability is between 600 to 800°C as shown by the steep slope of the curves. The reaction velocity becomes so slow below about 400°C that a negligible amount of CO is decomposed into CO_2 and C. The reaction is accelerated in the presence of catalysts which provide nucleation sites for deposition of carbon. In the presence of catalysts, the reverse of reaction 3.7 accelerates above 400°C and reaches

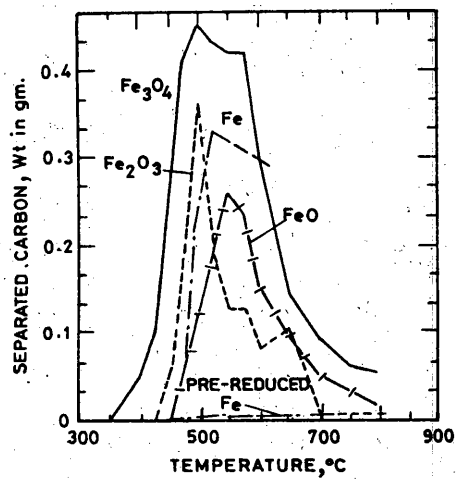


Fig. 3.5 The influence of temperature on carbon deposition in the presence of iron and its oxides after Baukloh and Schilling.[5]

a maximum between 500–550°C (Fig. 3.5).[5] Thereafter, the velocity decreases and above 850°C the reaction finally ceases. The probable catalysts are freshly reduced iron oxides or metallic iron, especially the latter.[6] Carbon deposition occurs mostly in the upper stack in smooth running furnaces. The retardation and promotion of the reaction as well as the advantages and disadvantages of carbon deposition in the blast furnace have been discussed in Sec. 7.2.5. Carbon deposition and its adverse effect on furnace refractories have been reviewed by Kohler.[5a]

The deposition of carbon has considerable importance in furnace operation because it effectively reduces the stack diameter, causes breakdown of the ferrous charge materials, retards burden descent and may ultimately lead to hanging of the furnace (Sec. 13.3).

High top pressure operation increases the overall pressure in the furnace which, theoretically, should enhance carbon deposition. However, in practice, it has been found that carbon deposition in this case is hardly different from that in the conventional furnace.

3.6. The Fe-O-C System

In the blast furnace, coke is used both for reduction reactions as well as for providing heat in order to obtain the iron and slag in a liquid state.

The burning of coke in front of the tuyeres produces only CO and nitrogen. The hot ascending gas gives up its heat to the descending burden and the CO portion of the gas reduces the iron oxides according to its reducing potential at the various temperature levels and is converted to CO_2. As already mentioned in the preceding section, above about 1000°C, CO_2 is unstable in the presence of carbon (which is always present in the furnace in an excess as coke) and CO is regenerated. This, as will be seen in Eq. 3.12, is equivalent to carbon reacting *directly* with the oxides. Thus, below about 1000°C, the reduction reactions of iron oxides are accomplished mainly by CO the reduction product being CO_2. The reactions are:

(i) $3Fe_2O_3 + CO = 2Fe_3O_4 + CO_2 + 10\,330$ cal — 3.8
$\Delta H°$ (1000°K) = − 10.43 kcal; $\Delta H°$ (1200°K) = − 10.83 kcal

(ii) $Fe_3O_4 + CO = 3FeO + CO_2 - 8750$ cal — 3.9
$\Delta H°$ (1000°K) = 3.64 kcal; $\Delta H°$ (1200°K) = 3.30 kcal

(iii) $FeO + CO = Fe + CO_2 + 3990$ cal — 3.10
$\Delta H°$ (1000°K) = − 4.58 kcal; $\Delta H°$ (1200°K) = − 3.13 kcal

(iv) Below 570°C, $Fe_3O_4 + 4CO = 3Fe + 4CO_2 + 3220$ cal — 3.11

(v) For the overall reaction, $Fe_2O_3 + 3CO = 2Fe + 3CO_2$ — 3.11a
$\Delta H°$ (1000°K) = − 10.27 kcal

The reduction reactions 3.8–3.11 are evidently independent of pressure. The reduction by CO is called *gaseous* or *indirect* reduction as opposed to direct reduction by carbon. The term direct reduction is a misnomer since it is improbable that solid coke reduces the ores by direct contact except perhaps when molten slag in the bosh flows over incandescent coke. The reaction rather occurs indirectly *via* the gas phase above 1000°C, the overall reaction being direct consumption of carbon:

$$FeO + CO = Fe + CO_2 + 3990 \text{ cal} \qquad 3.10$$

$$CO_2 + C = 2CO - 41210 \text{ cal} \qquad 3.7$$

On adding Eqs. 3.7 and 3.10,

$$FeO + C = Fe + CO - 37220 \text{ cal} \qquad 3.12$$

At 1200°C, $\Delta H°$ = + 36.16 kcal
= 3000 kcal/kg.C
or 2250 kcal/kg.O

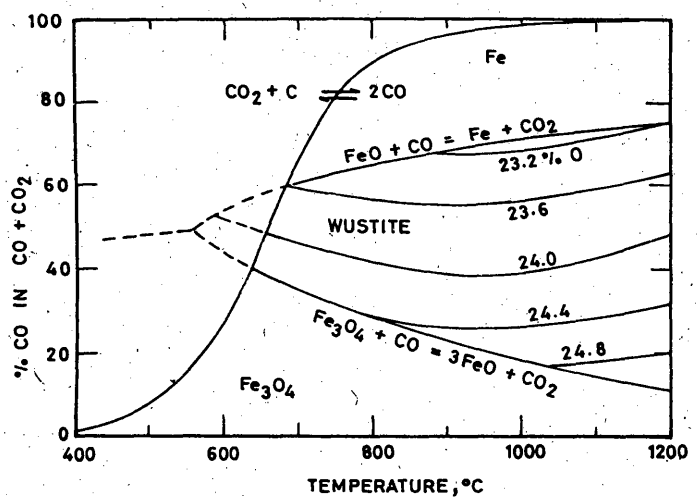


Fig. 3.6 The Fe-O-C equilibrium diagram including the Boudouard curve as well as degree of oxidation of wustite in the presence of CO and CO_2.

From calculations of the equilibrium constant of reaction 3.8, the %CO in the equilibrium mixture of CO and CO_2 at iron-making temperatures is negligible which means that the reaction is practically irreversible and proceeds entirely to the right. The stability regions of the phases of iron and its oxides in the presence of CO-CO_2 mixtures at different temperatures are shown in Fig. 3.6.[7-10] The curves show the equilibrium concentrations of CO and CO_2 (taking CO + CO_2 = 100) at a total pressure of 1 atm. for the reactions 3.9–3.11 at various temperatures. The curve for Eq. 3.10 slopes upwards because the reaction is exothermic, i.e., FeO becomes more stable with increasing temperature in the presence of CO. The curve for Eq. 3.9 slopes downwards the reaction being endothermic. At 900°C, the equilibrium concentration of CO for Fe_3O_4-FeO is 20 percent whereas that for FeO-Fe about 70 percent, i.e., for the conversion of magnetite entirely to wustite the gaseous phase must have a CO/CO_2 ratio greater than 0.25 whereas that for wustite to iron the ratio should be higher than 2.3. In other words, the extent of utilization of CO, denoted by

$$\%\eta_{CO} = 100.\%CO_2/(\%CO + \%CO_2) \qquad 3.13$$

is at a maximum of 80 percent in respect of magnetite/wustite equilibrium and only 30 percent for wustite/iron equilibrium at 900°C. For hematite/magnetite it is almost 100 percent (see Sec. 1.2). Thus, for complete

reduction of 1 mole of magnetite to wustite we need 100/80 = 1.25 moles of CO and for that of 1 mole of wustite to iron the amount is 100/30 = 3.3 moles of CO. Hence, for the respective equilibrium at 900°C, we can write

$$FeO + 3.3CO = Fe + 2.3CO + CO_2 \qquad 3.14$$

$$Fe_3O_4 + 1.25CO = 3FeO + 0.25CO + CO_2 \qquad 3.15$$

The oxygen content of wustite varies with the CO/CO_2 ratio and temperature as shown by the iso-oxygen lines inside the field of existence of wustite (Fig. 3.6).

From Table 3.1 it can be calculated that for obtaining 1000 kg Fe from hematite, 302 kg of oxygen has to be removed from wustite whereas that from Fe_2O_3 to Fe_3O_4 and from Fe_3O_4 to FeO the respective values are only 48 kg and 80 kg of oxygen, the total oxygen combined with iron as hematite being 430 kg/1000 kg.Fe. It is apparent that after reduction of 302 kg.O from FeO at η_{CO} = 30%, a CO-CO_2 gas mixture will still have sufficient reduction potential for removal of the rest of 80 kg.O from magnetite and 48 kg.O from hematite. The removal of oxygen from wustite only, therefore, assumes importance in gaseous or indirect reduction. The temperature of 900°C has been chosen because in the blast furnace the maximum extent of indirect reduction should be accomplished around 800–1000°C. Below this temperature the reduction rate of wustite is sluggish. Above this temperature, as shown by the super-imposed Boudouard curve in Fig. 3.6, any CO_2 formed from iron oxide reduction will be reduced by coke resulting in an unnecessary consumption of carbon. (It will be seen later that the carbon gasification reaction is not entirely harmful because it regenerates CO according to $CO_2 + C = 2CO$).

We have seen in Sec. 1.2 that the blast furnace is a counter-current reactor and the iron oxides are reduced in stages. However, if the blast furnace had been a single stage co-current process, then the total gas requirement for 100 percent indirect reduction of all the 430 kg.O/1000 kg.Fe would be given by

$$Fe_2O_3 + 3 \times 3.3CO = 2Fe + 3 \times 2.3CO + 3CO_2$$

since the ratio CO/CO_2 = 2.3 must always be maintained in order that all the FeO is reduced. That is, about 2000 Nm^3.CO would be required at 900°C, the total carbon consumption to produce the gas being 1060 kg.C ($C + \frac{1}{2}O_2 = CO$).

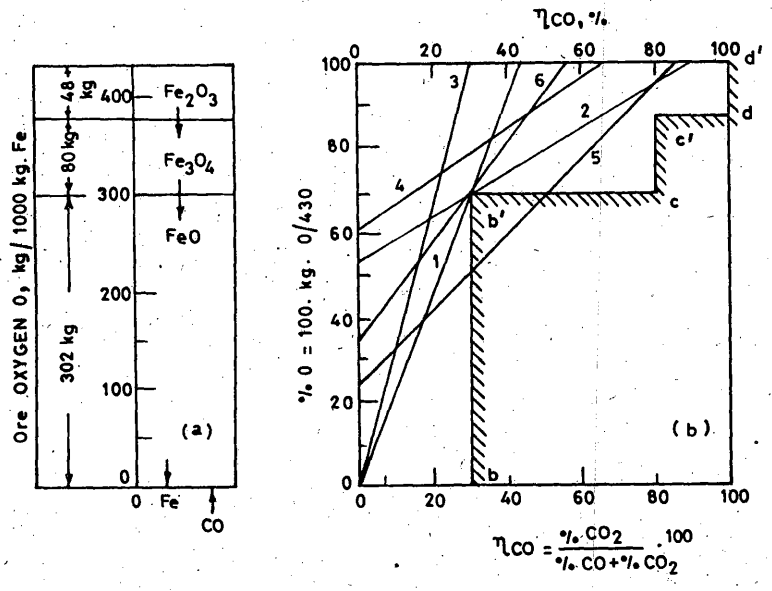


Fig. 3.7 The removal of oxygen from pure Fe_2O_3 based on 1000 kg.Fe according to (a) counter-current principle and (b) indirect reduction and CO-utilization, for the various oxide phases. The numericals 1–6 in (b) are discussed in the text.

The blast furnace is, however, theoretically a three stage counter-current process with the fresh CO reducing the wustite to iron first, the exhaust gas reacting with the magnetite to give wustite in the second and finally the gas from the second stage reducing hematite to magnetite in the third stage. Since the equilibrium CO requirements of hematite and magnetite are small, we may divide it into a two-stage process. This is very convenient from the point of view of the temperature profile of the furnace (Fig. 1.2). Most of the hematite and magnetite are reduced in the upper zone while the wustite reduction takes place in the long indirect reduction zone which occupies about 2/3 the height of the furnace shaft and where the temperature ranges between 800–1000°C, ideal for the kinetics of indirect reduction of wustite. (Gaseous reaction occurs at higher temperatures also but it becomes direct reduction because of the Boudouard reaction). The mode of reactions is shown schematically in Fig. 3.7(a).

3.6.1. Reduction and Gas Utilization[11]

In contrast to the single-stage process, for 100 percent indirect reduction of wustite in the two-stage process where the CO contacts the wustite first,

the CO requirement according to Eq. 3.14 is about 1370 Nm^3/1000 kg.Fe. This amount of CO must come from burning of 760 kg of carbon at the tuyeres. The total CO_2 formed from all the three oxides is 602 Nm^3 which gives a CO-utilization factor, η_{CO} = 44%, i.e., 56 percent of the CO supplied remains unutilized (Line 1, Fig. 3.7b). This is certainly a very inefficient use of CO.

Fig. 3.7(b) which is similar to those of Schürmann and Bülter[11] and Rist[12] shows the alteration of gas utilization with direct/indirect reduction, i.e., $\%\eta_{CO}$. For the removal of oxygen from iron, the gas utilization factor, i.e., the reducing potential of the gas, must always be on the left hand side of the shaded lines *bb'* (wustite), *cc'* (magnetite) and *dd'* (hematite). One can immediately see from the line *bb'* that about 70 percent of total oxygen is in the form of wustite and needs a highly reducing gas (η_{CO} <30% and CO/CO_2 >2.3) for its reduction.

If all the 430 kg.O is removed directly by carbon (100 percent direct reduction), about 322 kg of carbon will be needed and the gas evolved will be all CO, i.e., η_{CO} = O% (ordinate of Fig. 3.7b),

$$Fe_2O_3 + 3C = 2Fe + 3CO \qquad 3.16$$

We can see that from the reduction point of view only, direct reduction is much more economical in carbon than the indirect reduction. The carbon requirement will even be less than 322 kg, if the CO evolved in Eq. 3.16 is utilized for indirect reduction. Taking again wustite as the starting point, suppose *y* kg of wustite oxygen is removed directly by carbon and the CO evolved removes the rest (302-*y*) kg.O indirectly. Then, using Eqs. 3.12 and 3.14 for the CO balance,

$$y/16 = 3.3\ (302\text{-}y)/16 \qquad 3.17$$

or

$$y = 232\ \text{kg.O}$$

Since direct reduction is always depicted on the basis of total oxygen, the percentage optimum direct reduction = 232 x 100/430 = 54% (Line 2, Fig. 3.7b). From Eq. 3.12, the carbon requirement for 232 kg.O = 175 kg.C.

Now, 232 kg of wustite oxygen on direct reduction gives 325 Nm^3.CO which is available for indirect reduction of the rest of 430–232 = 198 kg.O. It gives rise to 277 $Nm^3.CO_2$. Hence η_{CO} = 85%. To confirm whether magnetite equilibrium is satisfied, 430-48-232 = 150 kg.O from unreduced wustite and magnetite is reduced by CO to give 210 $Nm^3.CO_2$, the η_{CO} being 65 percent, a value much less than the required 80 percent.

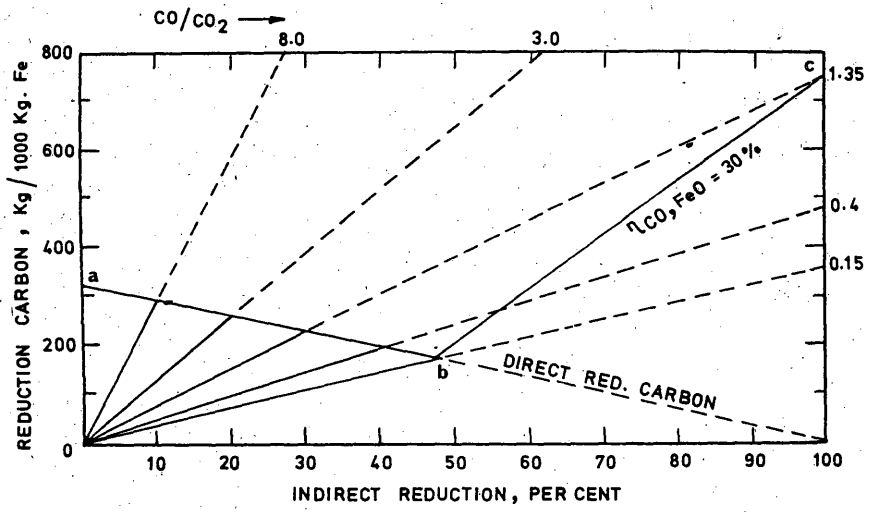


Fig. 3.8 Relationship between reduction carbon requirement for the removal of 430 kg oxygen from hematite per 1000 kg iron in accordance with CO-utilization requirements for wustite. The lines of CO/CO_2 ratios for the total oxygen are also shown.

Line 3 shows an inferior CO-utilization if the gas composition is away from the FeO/Fe equilibrium as can happen when the CO supply is in excess of 1370 Nm^3. Line 4 also shows inadequate CO-utilization if direct reduction is higher than the calculated 54 percent. If it is less than 54 percent, the CO evolved will be less than that required to reduce indirectly the residual wustite oxygen (Line 5).

We have seen that the carbon required falls from 322 kg for 100 percent direct reduction to 175 kg for 54 percent direct reduction and then rises to 760 kg for 100 percent indirect reduction. The trend of the curve *abc* for various degrees of direct/indirect reduction can be seen in Fig. 3.8 which is based on 430 kg of total oxygen and 302 kg of wustite oxygen per tonne Fe. The lines of CO/CO_2 ratios of the final gas for various degrees of indirect reduction are also drawn in Fig. 3.8. They show that the ratio decreases (higher utilization of CO) as indirect reduction increases up to the optimum point *b* and thereafter increases again as indirect reduction continues to increase. This is because of an excess CO requirement for indirect reduction beyond the optimum. Up to the optimum point, the reduction occurs by direct-cum-indirect reductions (Eqs. 3.12 and 3.14) according to which 1 kg. atom O requires 0.77 kg. atom C. On the other hand, for purely indirect reduction, 1 kg. atom O needs 3.3 kg. moles of

CO (obtained, in practice, from burning of 3.3 kg. atom C at the tuyeres).

Fig. 3.8 is based on the carbon requirements for reduction requirements only and does not consider the heat requirement of the burden. Fig. 10.2 is based both on heat and reduction requirements, 400 kg of total oxygen per THM and 280 kg of wustite oxygen per THM since pig iron contains only about 92–93% Fe. Line 6 in Fig. 3.7 is derived from Fig. 10.2 and shows optimum direct reduction for the burden given in Table 10.1.

3.6.2. Direct and Indirect Reduction[13]

Although direct reduction is endothermic in character (Eq. 3.12) and results in a thermal deficiency, it is economical of carbon and hence not entirely harmful; whereas, indirect reduction gives a thermal surplus but is expensive of carbon. This can be seen from the following considerations where both the cases are considered for the same efficiency, i.e., a CO/CO_2 ratio of 1.5 which is not uncommon in modern furnaces:

$$Fe_2O_3 + 7.5C + 3.75O_2 = 2Fe + 4.5CO + 3CO_2 \qquad 3.18$$
$$\Delta H^\circ\ (1000^\circ K) = -199.94 \text{ kcal}$$

$$Fe_2O_3 + 15/7C = 2Fe + 9/7CO + 6/7CO_2 \qquad 3.19$$
$$\Delta H^\circ\ (1000^\circ K) = +73.33 \text{ kcal}$$

From Eq. 3.18, 0.81 kg.C is required for indirect reduction of 1 kg.Fe from Fe_2O_3 and about 1790 kcal of heat is evolved in the process. From Eq. 3.19, for direct reduction of 1 kg.Fe, only 0.23 kg.C is consumed but results in an absorption of 656 kcal of heat.

In the blast furnace, the coke carbon supplies both heat and CO. Depending upon the thermal requirement, a minimum amount of carbon must be burned to produce the heat and hence a minimum amount of wustite oxygen is removed indirectly by the CO thus evolved. The final carbon requirement will depend upon the optimisation of direct/indirect reduction of the rest of the oxygen taking into consideration the heat required for direct reduction, the extra carbon burned to supply the heat and the CO evolved therefrom. A simple calculation method has been shown in Sec. 10.2 for an idealized case and the optimum is shown by Line 6 in Fig. 3.7(b).

3.6.3. Direct/Indirect Reduction-Calculation[14]

3.6.3.1. From CO_2 balance

This method does not take into consideration the moisture content of the charge materials or CO_2 from limestone and, therefore, applies to a 100 percent super-fluxed sinter. Suppose the iron-oxygen is 400 kg/THM, top gas quantity = 2000 Nm³/THM, CO_2 in top gas = 15%. Then since 16 kg.O gives 22.4 Nm³.CO_2 ($O + CO = CO_2$) and the indirect reduction r_i is given by,

$$r_i = \frac{\text{oxygen removed by CO}}{\text{total oxygen combined with iron}}$$

Therefore, $r_i \times 400 \times 22.4/16 = 2000 \times 0.15$

or $r_i = 0.61$

or percentage indirect reduction = 61%.

3.6.3.2. From nitrogen balance

Calculate the percentage indirect reduction of iron oxide from the following data:

Coke (85%C) consumption	= 700 kg/THM
Top gas volume	= 3.50 Nm³/kg coke
Top gas analysis	= 14.5% CO_2, 57% N_2 and 28.5% CO
Carbon in iron	= 3.5%C
Oxygen in air	= 21%O_2 (79%N_2)
Density of oxygen	= 1.43 kg/Nm³
Total oxygen combined with Fe	= 400 kg/THM
Carbon consumed by metalloids	= 12 kg/THM (direct reduction)

Solution

Weight of carbon in coke	= 700 × 0.85 = 595 kg
Weight of carbon in iron	= 3.5 × 10 = 35 kg
Weight of carbon for metalloids reduction	= 12 kg

Therefore, weight of carbon consumed for direct and indirect reduction of iron = 595-35-12 = 548 kg

Top gas volume	= 3.5 × 700 = 2450 Nm³/THM
Volume of nitrogen	= 57 × 2450/100 = 1397 Nm³/THM

Since nitrogen passes through the furnace unchanged,

Volume of N_2 in top gas = Volume of N_2 in blast

Therefore, volume of oxygen in the blast = 1397 × 21/79
= 371 Nm³/THM

Weight of oxygen in 371 Nm³	= 371 × 1.43 = 531 kg
Weight of carbon burnt at the tuyeres	= 24 × 531/32
	= 398 kg.C

Therefore, carbon consumed in direct reduction of iron oxides is,

548-398 = 150 kg/THM

Hence weight of iron-oxygen removed by direct reduction is equal to:

150 × 16/12 = 200 kg oxygen

Since total iron-oxygen present is 400 kg/THM, the percentage direct reduction is:

200 × 100/400 = 50 percent

Hence, indirect reduction = 50 percent

3.7. Carburization of Iron

Carbon monoxide is not only a reducing agent but, because of reverse of the Boudouard reaction, it is also a carburizing agent according to:

$$2CO = [C] + CO_2 \qquad 3.20$$

The approximate equilibrium percentage of carbon in iron in the stability field of solid iron is shown in Fig. 3.9.[15] From the figure, it is theoretically possible for iron reduced in the shaft to absorb as high as 0.5%C. More of the carbon is absorbed when liquid iron flows over the hot coke in the bosh as well as when in contact with the coke column in the hearth (Sec. 7.4.3).

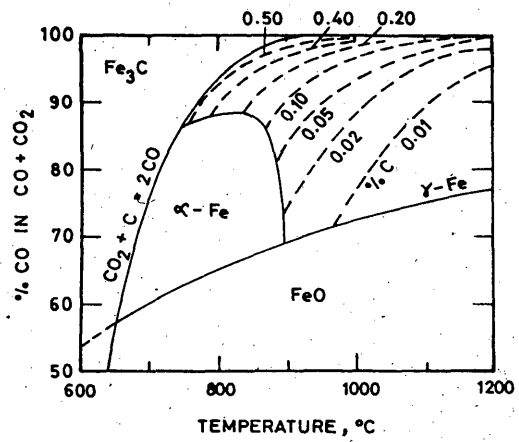


Fig. 3.9 Equilibrium carburization of iron by CO and CO_2 gas mixtures of pressure 0.4 atm. at various temperatures, according to Heynert et al.[15] (Copyright Verlag Stahleisen).

3.8. The H-O System

The dissociation reaction of water is given by:

$$2H_2O(g) = 2H_2 + O_2 - 115900 \text{ cal} \qquad 3.21$$

$$\Delta H°(298°K) = 3210 \text{ kcal/kg.}H_2O$$

Oxygen content of water = 88.9%.

3.9. The C-O-H System

The equilibrium concerning C-O-H system can be:

(i) $$C + H_2O(g) = CO + H_2 - 31530 \text{ cal} \qquad 3.22$$

$$\Delta G° = 31500 - 33.79\ T \text{ cal}$$

$$\Delta H°\ (1500°K) = 32.48 \text{ kcal}$$

1 kg.C reacting with steam at 1500°K results in absorption of 2700 kcal of heat. The reaction is similar to the Boudouard reaction and occurs above 1000°C.

(ii) CO can reduce H_2O according to the water-gas shift reaction,

$$CO + H_2O = CO_2 + H_2 + 9680 \text{ cal} \qquad 3.23$$

$$\Delta H°\ (1000\text{–}1200°K) = -7.76 \text{ kcal}$$

$$\Delta G° = -8060 + 7.18\ T$$

$$K\ (900°K) = 2.466;\ K\ (1200°K) = 0.80$$

The equilibrium ratio is unity at about 821°C. Reaction 3.23 is catalysed in the presence of freshly reduced iron and its importance in the blast furnace fuel efficiency will be seen in Sec. 3.11 and at various places in the text.

The C-O-H system has assumed importance because of an increasing use of steam (and hydrocarbons) along with air in the blast furnace. The reaction of steam with carbon or combustion of hydrocarbons with air produces hydrogen which is superior to CO as a reducing agent. Humidified blast has also a cooling effect because of the endothermic nature of reaction 3.22 which brings down the tuyere gas temperature and also tends to enlarge the combustion zone in front of the tuyeres, both helping a smoother and more extensive stock descent (Secs. 4.6 and 7.6.6).

The combustion reactions of coke carbon with air and steam, we have seen, are:

$$C + \tfrac{1}{2}O_2 = CO : \Delta H°\ (1400°C) = -2300 \text{ kcal/kg.C} \qquad 3.4$$

$$C + H_2O = CO + H_2 : \Delta H°\ (1400°C) = +2720 \text{ kcal/kg.C} \qquad 3.22$$

From Eqs. 3.4 and 3.22, moisture gives double the volume of reducing gases (CO + H_2) per mole of carbon. The combustion products, also called *bosh gas*, increase in volume according to the amount of steam injected per unit volume of the humidified blast since it contains more oxygen than normal air (steam contains 89 percent by weight of oxygen and air 23.2 percent). The various factors affected by steam injection are given in Table 6.6. The table draws out clearly that moisture increases the coke burning rate per unit volume of blast, decreases the bosh gas volume per unit of carbon and the combustion products have a higher percentage of the reducing gases (CO + H_2).

3.10. The Fe-O-H System

As with CO/CO_2 the iron oxides can also be reduced by H_2/H_2O mixtures. The reduction takes place thus:

(i) $$3Fe_2O_3 + H_2 = 2Fe_3O_4 + H_2O + 650 \text{ cal} \qquad 3.24$$

$$\Delta H°\ (1000°K) = -1.22 \text{ kcal};\ \Delta H°\ (1200°K) = -3.07 \text{ kcal}$$

(ii) $Fe_3O_4 + H_2 = 3FeO + H_2O - 18430$ cal 3.25
$\Delta H°$ (1000°K) = 12.85 kcal; $\Delta H°$ (1200°K) = 11.06 kcal

(iii) $FeO + H_2 = Fe + H_2O - 5690$ cal 3.26
$\Delta H°$ (1000°K) = 4.63 kcal; $\Delta H°$ (1200°K) = 4.63 kcal

(iv) $Fe_3O_4 + 4H_2 = 3Fe + 4H_2O - 35500$ cal 3.27

(v) For the overall reaction, $Fe_2O_3 + 3H_2 = 2Fe + 3H_2O$ 3.27a
$\Delta H°$ (1000°K) = 17.42 kcal

The above reactions are obviously independent of pressure. Reaction 3.24 is practically irreversible and hematite is reduced in the presence of even a small amount of hydrogen in the H_2/H_2O mixture. The different phases of iron oxides in equilibrium with H_2/H_2O mixtures at various temperatures are shown in Fig. 3.10[7] by the dotted lines. The reduction of FeO by H_2 is endothermic and therefore the curve inclines downwards with increasing temperature whereas the corresponding curve for reduction by CO (full line) inclines upwards because of the exothermic nature of the reaction. These two curves intersect at about 821°C, i.e., at 821°C hydrogen and CO have the same reducing power over FeO. Thermodynamically, below this temperature, the reducing power of CO is much greater, as will be seen in the next section.

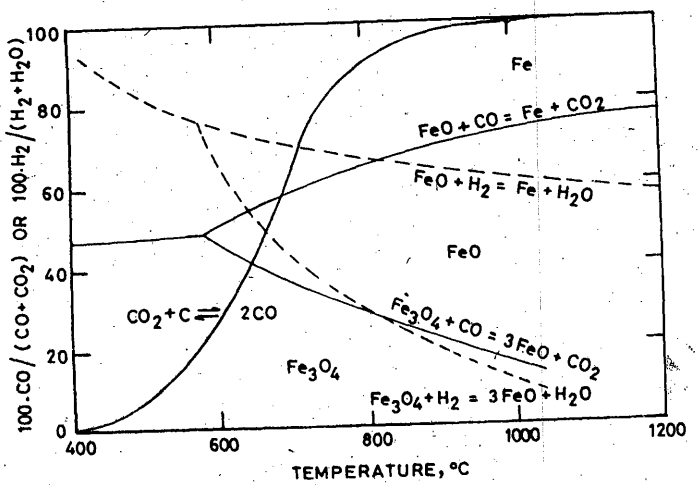


Fig. 3.10 The Fe-O-C (full) and Fe-O-H (dotted) equilibrium curves as assembled by Kalling,[7] with the superimposed Boudouard curve.

3.11. The Fe-O-H-C System

This system is a combination of the individual Fe-O-C and Fe-O-H systems (Fig. 3.10). The combined action of hydrogen and CO has assumed importance in recent years because of the increasing use of hydrogen-bearing additives in the furnace.

It is a well recognized fact that hydrogen is a very active reducing reagent. It not only reacts with and reduces iron oxide which otherwise need to be reduced by CO and thus reduces the carbon consumption but it does so with a higher rate of reduction and more efficiently from its utilization point of view. It will be seen in Sec. 6.7.9 that even 1 percent moisture in the blast increases the rate of reduction of iron oxide by CO by about 4.5–5 percent. The utilization factors of hydrogen, $\%\eta_{H_2} = 100.\%H_2O/(\%H_2 + \%H_2O)$, and $\%\eta_{CO}$ for the FeO/Fe equilibrium at different temperatures are given in Table 3.3.

Table 3.3. The equilibrium CO- and hydrogen utilization for wustite reduction at various temperatures

Temperature, °C	427	575	700	821	900	1000
$\%\eta_{H_2}$	7	20	30	33	37	40
$\%\eta_{CO}$	40	50	40	33	30	27

From Table 3.3 and as also seen in the preceding section, hydrogen gives better reduction efficiency than CO above 821°C and reverse is the case below that temperature. For the temperature of our interest, i.e., 900°C, $\eta_{H_2} = 1.2\,\eta_{CO}$. In the case of wustite reduction by hydrogen at 900°C, since the maximum η_{H_2} is 37 percent, at least 100/37 = 2.7 moles of hydrogen are necessary for each mole of wustite,

$$FeO + 2.7H_2 = Fe + 1.7H_2 + H_2O \qquad 3.28$$

From Eqs. 3.14 and 3.28, 1 kg.H is approximately equivalent to about 7.2–7.3 kg.C as far as their mutual reduction efficiency of wustite is concerned at 800–1000°C.

The water produced from Eq. 3.28 may react with CO as well as with carbon according to

$$H_2O + C = CO + H_2 - 31.53\text{ kcal} \qquad 3.22$$

$$H_2O + CO = CO_2 + H_2 + 9.68\text{ kcal} \qquad 3.23$$

Equation 3.22 resembles the Boudouard reaction and hydrogen is regenerated at temperatures above 1000°C. Below this temperature, hydrogen is regenerated through the water-gas reaction 3.23. Laboratory as well as industrial data show that when CO and H_2 are used in the reduction of ores of good reducibility, η_{H_2} and η_{CO} are inter-related and the chemical utilization of hydrogen runs parallel to that of CO. A regression analysis gave[16]

$$\eta_{H_2} = 0.88\,\eta_{CO} + 0.10 \text{ (\% explained} = 68\%) \qquad 3.29$$

This relationship is attributed to a comparatively rapid approach of the water-gas reaction to equilibrium at temperatures 800–1000°C, as confirmed in Fig. 3.11.[17] This tantamounts to a catalytic action of hydrogen on the reduction of ore by CO because hydrogen possesses, thermodynamically, a greater reducing power for wustite than CO has above 821°C, apart from a higher one from kinetic point of view (Sec. 6.7.9).

The rapid approach of the water-gas reaction towards equilibrium at 800–1000°C is presumably caused mainly by the presence of iron which acts as a catalyst.[18,19] The role of iron as a catalyst is supported by the fact that in the upper part of the furnace (up to 600–700°C level, where

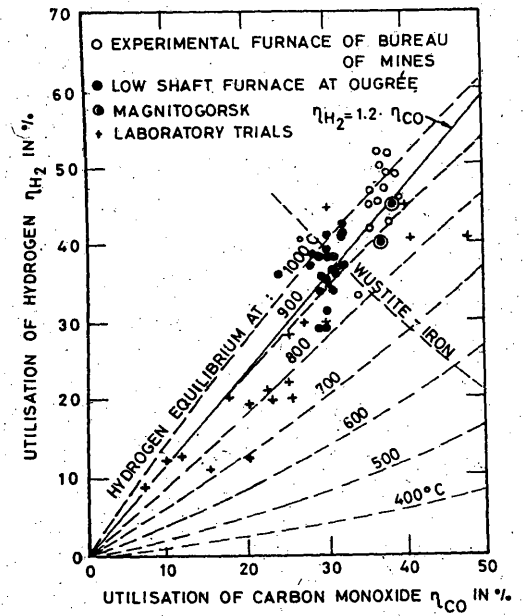


Fig. 3.11 Utilization of hydrogen and CO in the blast furnace, according to Schürmann and Bülter.[17] (Copyright Verlag Stahleisen).

metallic iron is usually not present) the water-gas equilibrium fails to set up, although the equilibrium constant of reaction 3.23 increases with decreasing temperature.

It is because of reaction 3.23 that the CO-utilization increases in the presence of H_2/H_2O. Therefore, the top gas CO/CO_2 ratio cannot be a measure of the fuel efficiency of the furnace.[25] A more acceptable ratio would be $(CO + H_2)/CO_2$ since CO_2 is produced both from reactions CO + ore as well as CO + H_2O. The corresponding utilization factor will be

$$\eta_{H_2,CO} = (CO_2 + H_2O)/(CO + CO_2 + H_2 + H_2O) \qquad 3.30$$

The reduction rate of iron oxide by CO increases greatly in the presence of hydrogen. This may be partly due to the catalytic nature of reduction by hydrogen and its regeneration from the H_2O formed and lower equilibrium partial pressure of hydrogen compared to CO (Eq. 2.26 and Table 3.3). The other factors are discussed in Secs. 2.8 and 6.7.9. Further discussions on the water-gas reaction will be found in Sec. 7.3.4.

3.12. The Fe-O-Si-C-Slag System

The reduction of silica to silicon in iron has been a subject of numerous investigations. This is because a low silicon iron is very suitable for its further processing into steel. The $\Delta G°$ for silica formation being very negative, its reduction by carbon can occur at the high temperatures prevalent only in the bosh and hearth regions (Sec. 2.7; Fig. 2.4).

Silicon enters the metallic iron in the space extending from above the hearth slag level to the belly presumably *via* gaseous silicon monoxide[20–22] (also SiS).[26] Further silicon transfer can occur through oxidation or reduction when iron droplets travel through the slag layer above the metal pool in the hearth. The two reactions are, however, different, viz.:

(i) Silicon monoxide can form when the coke burns before the tuyere and its ash-silica is reduced or when the liquid slag wets the incandescent coke in the bosh. The free energy of formation is given by

$$SiO_2(s) + C(s) = SiO(g) + CO(g) \qquad 3.31$$
$$\Delta G° = 173600 - 80.0\,T \text{ cal}$$

The reaction can also take place *via*

$$SiO_2 + CO = SiO(g) + CO_2$$
$$C + CO_2 = 2CO$$

The absorption of silicon by iron in the bosh can occur as the SiO vapour ascends along with the fast moving gases, presumably, according to:

$$\begin{aligned} SiO(g) + Fe &= [Si] + FeO \\ FeO + CO &= Fe + CO_2 \\ C + CO_2 &= 2CO \end{aligned} \qquad 3.32$$

The gaseous SiO can attain a partial pressure of 10^{-2}–10^{-3} atm. or even more depending upon the tuyere gas temperature.[23-24] The silicon content of iron reaches a maximum above the tuyeres and decreases later as iron droplets trickle through the hearth slag, the extent of which depends upon reaction with the MnO and FeO components of the slag.[22-24] These will be further discussed in Secs. 3.15 and 7.4.2.2.

(ii) As mentioned in Sec. 2.10, silica of the slag can be reduced by carbon-containing liquid iron passing through or in contact with the hearth slag. Assuming that the iron is saturated with carbon,

$$SiO_2 + 2[C]_{sat.} = [Si] + 2CO \qquad 3.33$$

The equilibrium content of silicon in carbon-saturated iron under CaO-Al_2O_3-SiO_2 slags at p_{CO} = 1 atm. has been studied by many investigators.[27-31] Although the volume of CO in the tuyere gas is about 35 percent, its partial pressure in the hearth will be about 1 atm. at 0.5 m

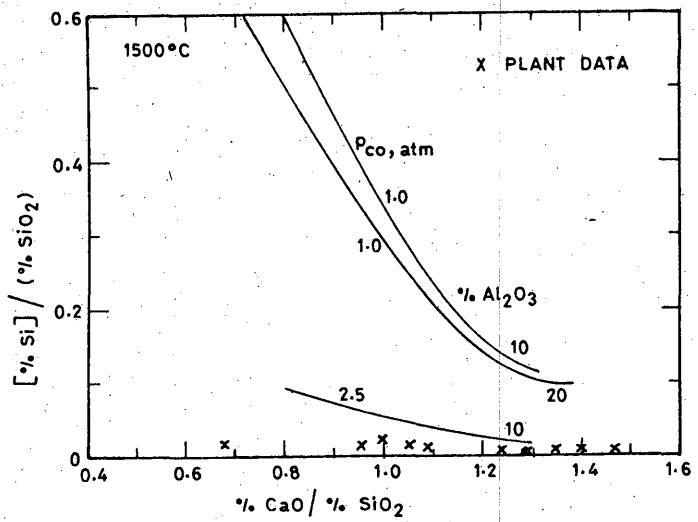


Fig. 3.12 Equilibrium metal/slag silicon distribution as a function of basicity of CaO-Al_2O_3-SiO_2 slags containing 10 or 20 percent alumina at 1500°C and CO pressures of 1.0 and 2.5 atm., reassembled from Turkdogan.[21] Plant distribution data inserted by the author.

below the slag layer, since the total pressure is approximately 0.85 of the absolute blast pressure (about 2.5 atm.) The results of the investigations compiled by Turkdogan[21] are reassembled in Fig. 3.12 for p_{CO} of 1 atm. and 2.5 atm. The figure shows the equilibrium silicon content (4–10% for p_{CO} = 1 atm., CaO/SiO_2 = 1–1.5 and SiO_2 = 36–44% at 1500°C) is several fold higher than that usually found in the blast furnace iron (<1.5 percent). Obviously, the blast furnace metal silicon fails to attain equilibrium according to Eq. 3.33.

Assuming that reaction 3.33 controls the silicon content of the metal, the failure of attainment of equilibrium has been attributed to the reaction rate being slow or the basic assumptions for comparison of laboratory or plant data erroneous. As for example,

(a) silica reduction by carbon is sluggish; a high activation energy of breaking the Si-O bonds ensures a high stability of SiO_4^{4-} ions in the slag. Very high values of activation energies, 130 and 100 kcal/mole, have been quoted.[28,31] However, the rate of silica reduction by carbon-saturated iron,[23] about 10^{-5} mole/cm².min., is unable to explain the very small absorption of silicon in the blast furnace iron, 0.5–1.5% Si;

(b) CO being a gas phase, lack of nucleation facilities may raise the evolution pressure of CO. In fact, according to Strassburger[32] if p_{CO} is assumed to be 2.5 atm., the calculated equilibrium silicon and sulphur content under the given conditions show a remarkably good agreement with the operating results;

(c) the iron may not be saturated with carbon before entering the slag layer. Carbon saturation of iron does not occur even in the hearth in contact with the central coke column. Using the activity coefficient values of carbon and silicon in iron, Taylor[33] suggests that metal silicon tends towards equilibrium in the blast furnace.

In view of the controversies regarding silica reduction, Turkdogan[21] has recently reviewed the subject from a thermodynamic viewpoint. The equilibrium constant and its temperature function for the reaction, considered on one weight percent silicon as the standard state, are

$$SiO_2(s) + 2[C]_{sat} = [\%Si] + 2CO \qquad 3.34$$
$$\Delta G^\circ = 141525 - 93.58\,T \text{ cal}$$

$$K_{Si} = \frac{[\%Si].\gamma'_{Si}.p^2_{CO}}{a_{SiO_2}.a^2_{[C]}} \qquad 3.35$$

$$\log K_{Si} = -30935/T + 20.455$$

In carbon-saturated iron, $a_C = 1$ and $\gamma'_{Si} = 15$. Hence, by appropriate transformations,

$$[\%Si].p_{CO}^2/(\%SiO_2) = 6.73 \times 10^{-4}.K_{Si}.\gamma_{SiO_2} \qquad 3.36$$

The dependence of the silicon distribution between the metal and slag on the slag basicity can be found from the value of K_{Si} at any given temperature and γ_{SiO_2} values for various basicity ratios, CaO/SiO_2 or $(CaO + MgO)/SiO_2$ (since MgO up to 20 percent does not affect γ_{SiO_2}). This is shown in Fig. 3.12 for $p_{CO} = 1$ atm. at 1500°C for two levels of alumina, 10 and 20 percent, in the $CaO\text{-}SiO_2\text{-}Al_2O_3$ slags. The values for $p_{CO} = 2.5$ atm. and 10% Al_2O_3 at 1500°C are also shown in the figure. Turkdogan[21] used the γ_{SiO_2} values derived from the data of Rein and Chipman[34] for calculations of Fig. 3.12. The actual $[\%Si]/(\%SiO_2)$ values from various modern plants inserted by the author in the figure show that they are much lower than the thermodynamic ones and hence the actual silicon contents of blast furnace metal are much less than the equilibrium values for $p_{CO} = 1$ atm. A much closer approach of the values to the line for $p_{CO} = 2.5$ atm. is obvious. Vidal and Poos[35] have shown, using 21–41% oxygen in the blast at constant blast pressure, that %Si in iron is inversely proportional to p_{CO}^2 (Eq. 3.36). According to them a major portion of silicon is reduced in the zone between the tuyere level and the hearth slag level and the silicon reduction reaction approaches equilibrium with carbon during the trickling of the hot metal and slag over hot coke.

Three important factors are immediately obvious from Fig. 3.12 and Eq. 3.35 for obtaining low silicon iron:

(i) Temperature – The lower the temperature the lower the K_{Si} and hence the lower the silicon in iron;
(ii) Basicity – An increase in the lime/silica ratio of the slag decreases γ_{SiO_2} and hence the silicon distribution;
(iii) Pressure – An increase in p_{CO} decreases the distribution ratio. Hence, operation with high top pressure may assist in lowering of the ratio.

According to Eq. 3.35, very little silicon in iron is expected below about 1300°C. As the temperature increases, the K_{Si} increases about ten-fold for every 100°C rise in temperature. For the same rise in temperature the velocity of reduction of silicon increases by 3–4 times.[36]

The silicon contents of iron in actual practice are less than the equilibrium values for $p_{CO} = 1$ atm. (Eq. 3.36) and depends upon various factors which are further discussed in Secs. 3.15 and 7.4.2.2.

From a theoretical study of the blast furnace slag-metal reactions and comparing the results with the plant data, Turkdogan[21] has come to the conclusion that since silica reduction involves three phases, slag-metal-gas, as well as simultaneous reductions of manganese, sulphur and iron from slag, it is unlikely that they will all reach equilibrium in a dynamic system like the blast furnace.

3.13. The Fe-O-Mn-C-Slag System

Higher oxides of manganese are usually present in the iron ore or are added deliberately. They are all reduced in the shaft (Sec. 7.4.2.3) and only MnO descends into the lower furnace unreduced where the temperatures are sufficiently high for its reduction to occur. Manganese does not form any gaseous species like SiO or SiS. Hence, manganese absorption by iron in the upper bosh is smaller than silicon or sulphur. Some manganese, however, enters iron when the iron and MnO-containing liquid slag flow over the incandescent coke. Most of the manganese is reduced in the hearth.

If it is assumed that manganese transfer between the slag and metal occurs during the descent of the carbon-saturated iron droplets through the slag layer in the same manner as silicon, the relevant equation is,[21]

$$MnO(s) + [C]_{sat} = [\%Mn] + CO \qquad 3.37$$

$$\Delta G^\circ = 69050 - 50.20\ T \text{ cal}$$

$$K_{Mn} = \frac{[\%Mn].\gamma'_{Mn}.p_{CO}}{a_{MnO}.a_C} \qquad 3.38$$

$$\log K_{Mn} = -15090/T + 10.97$$

Again, assuming $a_C = 1$ and $\gamma'_{Mn} = 0.8$ for carbon-saturated iron and with appropriate transformations,

$$[\%Mn].p_{CO}/(\%MnO) = 1.07 \times 10^{-2}.K_{Mn}.\gamma_{MnO} \qquad 3.39$$

From Eq. 3.38, the temperature dependence of K_{Mn} is not as high as that of K_{Si} and the value increases about 3–4 times for every 100°C rise in temperature. The influence of pressure also is not as high since K_{Si} is proportional to p_{CO} squared. However, while γ_{SiO_2} decreases, γ_{MnO} increases with increasing CaO/SiO_2 ratio. The manganese distribution as a function of basicity at $p_{CO} = 1$ atm. and 1500°C, derived from Eq. 3.39, is reassembled in Fig. 3.13 from Turkdogan's work.[21] The γ_{MnO} values were

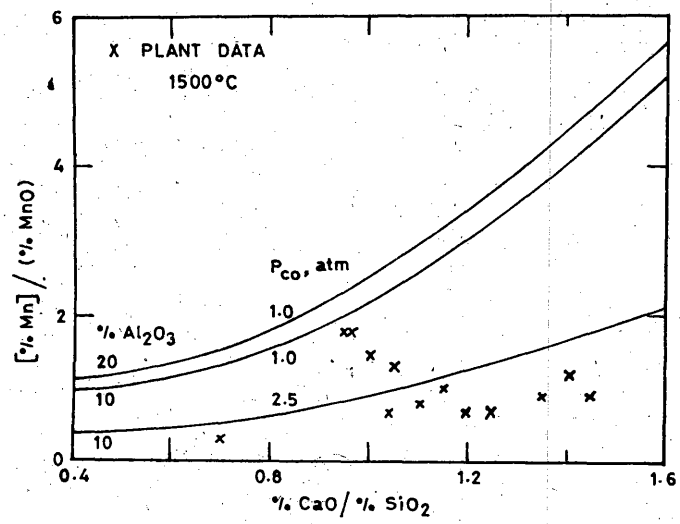


Fig. 3.13 Equilibrium metal/slag manganese distribution as a function of basicity of CaO-Al_2O_3-SiO_2 slags containing 10 or 20 percent alumina at 1500°C and CO pressures of 1.0 and 2.5 atm., reassembled from Turkdogan.[21] Plant distribution data inserted by the author.

derived by Turkdogan from the data of Abraham et al.[37] and used for calculations. The curve for $p_{CO} = 2.5$ atm. for 10%-alumina in slag is also shown in the figure. The plant distribution data inserted by the author shows the approach of manganese reduction towards equilibrium (Eq. 3.37) at $p_{CO} = 2.5$ atm. The actual [%Mn]/(%MnO) ratios, i.e., the actual Mn-contents of iron are much less than the equilibrium values for $p_{CO} = 1$ atm.

Manganese recovery is aided by

(i) high temperature
(ii) high slag basicity, i.e., high γ_{MnO}
(iii) high metal silicon (Sec. 3.15).

3.14. The Fe-O-S-C-Slag System

The mechanism of sulphur pick-up by iron in the blast furnace has been discussed in Chapter 9. Sulphur from coke is gasified in the shaft, in the bosh and in front of the tuyeres and is absorbed by iron. The absorbed sulphur, denoted as [%S], is removed by the hearth slag when sulphur-laden iron droplets pass through it.

Similar to silicon and manganese, the sulphur reaction may be represented by[21]

$$CaO(s) + [\%S] + [C]_{sat.} = CaS(s) + CO(g) \qquad 3.40$$

$$\Delta G^\circ = 27500 - 27.15\ T \text{ cal}$$

$$K_S = \frac{a_{CaS} \cdot p_{CO}}{a_{CaO} \cdot [\%S] \cdot \gamma'_S \cdot a_C} \qquad 3.41$$

$$\log K_S = -6010/T + 5.935$$

Taking $\gamma'_S = 7$ in carbon-saturated iron and with suitable transformations, the sulphur distribution ratio η_S is given by,[21]

$$\eta_S = \frac{(\%S)}{[\%S]} = 4 \frac{\gamma_{CaO}}{\gamma_{CaS}} \cdot \frac{(\%CaO) \cdot K_S}{p_{CO}} \qquad 3.43$$

The ratio $\gamma_{CaO}/\gamma_{CaS}$ for various slag basicities can be calculated from the works of Sharma and Richardson.[38] The relationships between η_S and slag basicity thus calculated from the thermodynamic data for slags containing 30 and 50 percent lime and for $p_{CO} = 1$ atm. and 2.5 atm. at 1500°C are reassembled in Fig. 3.14 from Turkdogan's work.[21] The actual plant distribution data have also been included in the figure by the author. The plant data appear to be widely scattered. Fig. 3.14 shows that the actual η_S values

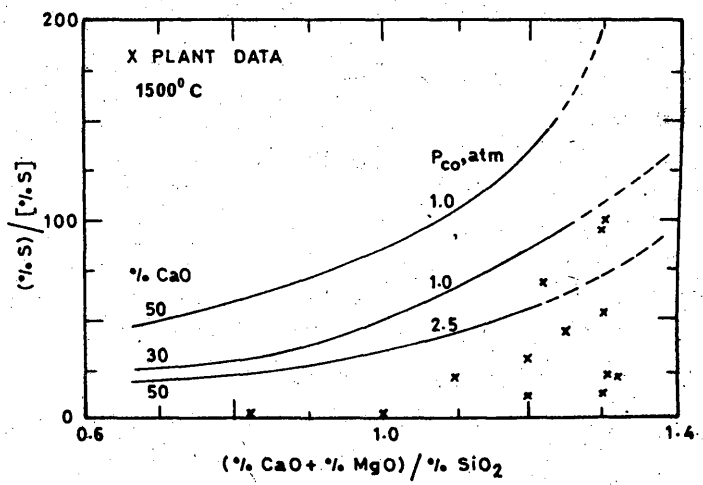


Fig. 3.14 Calculated sulphur distribution between blast-furnace-type slags and graphite-saturated iron at 1500°C and CO pressures of 1.0 and 2.5 atm. and 30 and 50 percent CaO in slags, reassembled from Turkdogan.[21] Plant data inserted by the author.

are lower than the equilibrium ones, i.e., the actual sulphur content of blast furnace iron is much higher than the equilibrium values for $p_{CO} = 1$ atm. according to Eqs. 3.40–3.43.

From Eq. 3.43 a high top pressure would deteriorate while increasing slag basicity and temperature facilitate sulphur removal.

The thermodynamic data presented show that the actual blast furnace metal silicon and manganese contents are much below and the sulphur content much above the equilibrium values with respect to C-saturated iron for $p_{CO} = 1$ atm. This subject is discussed in the next section.

3.15. The Fe-O-Si-Mn-S-C-Slag System

The deliberations in the three preceding sections show that in the blast furnace the silicon, manganese and sulphur reactions do not reach equilibrium with respect to carbon-saturated iron according to Eqs. 3.34, 3.37 and 3.40 and the actual contents of silicon and manganese in pig iron are much lower and that of sulphur higher than those found in the laboratory under calcium silicate slags. Oelsen[39,40] pointed it out over thirty years ago. Turkdogan[21] as well as Kootz[41] have also recently come to the conclusion after a comprehensive study of the thermodynamics of the reactions and plant data that reactions 3.34, 3.37 and 3.40 involving three phases – slag, metal and gas – are unlikely to attain equilibrium. The lower values of silicon and manganese and the higher ones for sulphur demonstrate that their actual contents in contact with the blast furnace slag are for oxygen potentials much higher than those determined by the C-CO equilibrium for $p_{CO} = 1$ atm.

However, Oelsen and co-workers[42–45] have shown that in the simultaneous presence of the three elements and with a thorough mixing of iron and slag, the coupled reactions between iron and FeO-containing slag for silicon, manganese and sulphur can approach an apparent equilibrium with each other but not with carbon in the carbon-saturated iron. The coupled reactions are:

$$(FeO) + \tfrac{1}{2}[Si] = [Fe] + \tfrac{1}{2}(SiO_2) \qquad 3.44$$

$$(MnO) + \tfrac{1}{2}[Si] = [Mn] + \tfrac{1}{2}(SiO_2) \qquad 3.45$$

$$[S] + (CaO) + [Mn] = (CaS) + (MnO) \qquad 3.46$$

$$[S] + (CaO) + \tfrac{1}{2}[Si] = (CaS) + \tfrac{1}{2}(SiO_2) \qquad 3.47$$

Although FeO is not expected in the hearth slag, sometimes a considerable amount may be present due to oxidation of iron in the oxidizing zone and inadequately reduced iron oxides descending in the hearth. Since the activity of silica in the slag is a function of basicity, equilibrium indices (not constants) in terms of weight percent were determined after extensive laboratory investigations. The results obtained for reactions 3.45 and 3.47 are:[46]

(i) For reverse of reaction 3.45,

$$K_{Mn,Si} = \frac{(\%Mn).[\%Si]^{1/2}}{[\%Mn]} \qquad 3.48$$

$$\log K_{Mn,Si} = -1.41\,B + 1.48 \qquad 3.49$$

(ii) For reaction 3.47,

$$K_{S,Si} = \frac{(\%S)}{[\%S]} \cdot \frac{1}{[\%Si]^{1/2}} \qquad 3.50$$

$$\log K_{S,Si} = 2.0\,B - 0.92 \qquad 3.51$$

For both cases (i) and (ii) the basicity B is given by,

$$B = (\%CaO + \%MgO)/(\%SiO_2)$$

It is understood that the K values given in weight percentages are applicable within a very narrow range of composition occurring in the blast furnace and determined for the purpose in the laboratory.

The silicon contents of actual blast furnace metal are compared in Fig. 3.15(b) with those calculated from Eqs. 3.48 and 3.49 for various (%Mn)/[%Mn] ratios, each set having the same slag basicity. Fig. 3.15(b) also shows the comparisons between Thomas iron and open-hearth iron, the former being usually tapped at lower temperatures. The silicon contents of metal samples taken from above the tuyere level are also shown in the figure. Fig. 3.15(a) shows the silicon contents expected from equilibrium with carbon-saturated iron at 1500°C for $p_{CO} = 1$ atm. valid for the same slag basicities as in Fig. 3.15(b). Fig. 3.15 shows that the actual silicon is much higher than that expected from the coupled reaction but much lower than that expected from equilibrium with C-saturated iron. Similarly, it will be seen in Fig. 3.16 that for given (%S)/[%S] ratios, the actual silicon contents are much higher than those calculated for the coupled reaction. It is thus obvious that the reduction of these three elements do not reach

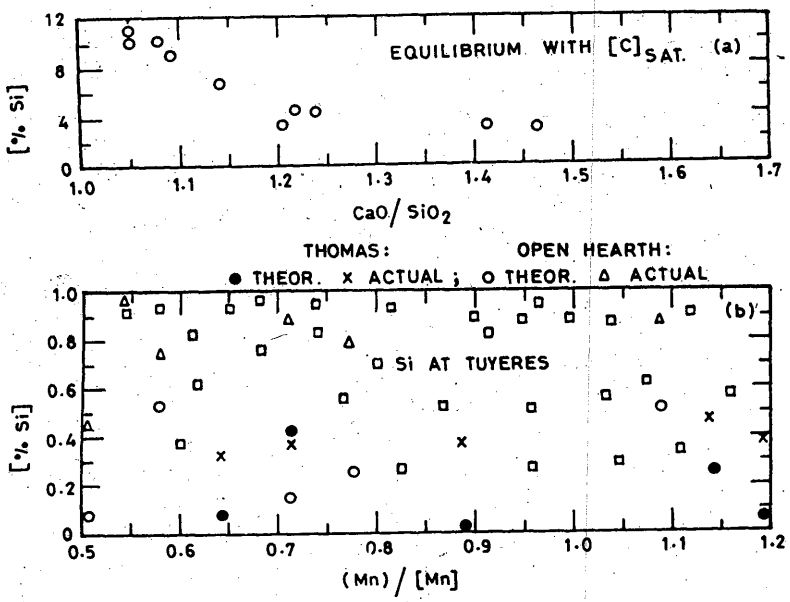


Fig. 3.15 (a) Calculated silicon content of metal in equilibrium with carbon-saturated iron at various slag basicities and CO-pressure of 1 atm.; (b) the actual and calculated silicon content of open-hearth irons and comparatively cold Thomas irons and their relation with slag-metal manganese ratios. The metal silicon at tuyere levels is also shown.

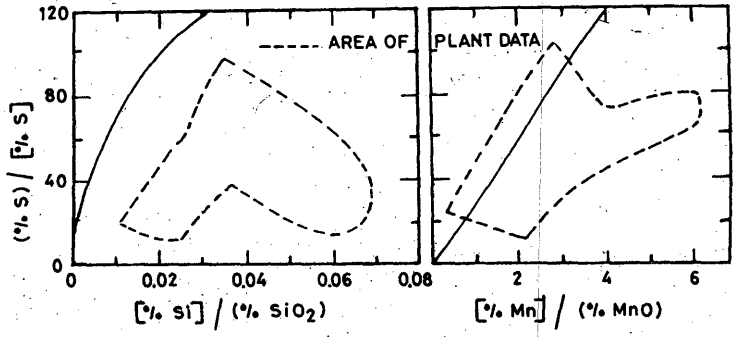


Fig. 3.16 Sulphur and silicon distribution (left) and manganese distribution (right) ratios from plant data compared with equilibrium relations at 1500°C (solid lines), after Turkdogan.[21] (Copyright The American Society for Metals and The Metallurgical Society of AIME 1978).

equilibrium either according to the coupled reactions or according to the carbon reaction.

The non-approach of the coupled reactions to equilibrium has been demonstrated by Turkdogan[21] by comparing thermodynamical and plant data. The relationships of manganese and silicon with sulphur distributions only are shown in Fig. 3.16.[21] The thermodynamic relationships are shown by the solid lines. The enclosed areas of plant data show that while in the case of manganese-sulphur reaction (Eq. 3.46) there is a closer approach to thermodynamic equilibrium, in the case for silicon-sulphur (Eq. 3.47) the data lie away from the line.

In Sec. 2.9.2 we have seen that the cathodic reaction of sulphur (Eq. 3.52) occurs with simultaneous anodic reactions (Eqs. 3.53–3.55), e.g.,

$$[S] + 2e = (S^{2-}) \qquad 3.52$$

$$[C] + (O^{2-}) = CO + 2e \qquad 3.53$$

$$[Mn] = (Mn^{2+}) + 2e \qquad 3.54$$

$$[Si] = (Si^{4+}) + 4e \qquad 3.55$$

As mentioned above, the manganese-sulphur reaction is much closer to equilibrium than the other coupled reactions. This suggests that the rate of the half-cell reaction 3.54 is much faster than those for reactions 3.53 and 3.55. Of the latter two, only reaction 3.55 is of importance since manganese, silicon and sulphur reactions approach more towards equilibrium with each other than with carbon. The similarity of activation energy of silicon and sulphur transfers (Sec. 2.10) suggests that their rates are controlled by the same mechanism, which points to the role of manganese.

That the reduction of manganese plays a substantial role in sulphur transfer from metal to slag has been demonstrated by experiments[21] in which carbon-saturated iron pellets containing silicon and sulphur were dropped through a column of molten slag containing MnO and without MnO. In the latter case, the silicon in iron increased without any change in sulphur content. On the other hand, with MnO additions, there was a rapid transfer of manganese from slag to metal and that of silicon and sulphur from metal to slag. As MnO is reduced by silicon (Eq. 3.45), sulphur transfer occurs with simultaneous oxidation of Mn to MnO. But, for some reasons, reaction 3.45 is inherently slow in the blast furnace hearth and does not reach equilibrium. If it had, the [Mn]/(MnO) ratio and consequently the (S)/[S] ratio would have been higher (Fig. 3.16). Since, as we have seen in the preceding paragraph that the half-cell reaction 3.54

is inherently fast, the faster the rate of reduction of manganese according to Eq. 3.45 the closer will be the approach of sulphur to coupled equilibrium. A large sulphur removal can, therefore, be achieved if the rate of reaction 3.45 can be increased, e.g., by working the furnace with hotter slag containing large amounts of MnO.

The only conclusion that can be derived from the available facts is that both silicon and sulphur enter the metal at a rate faster than manganese and reach maximum values at places away from the hearth[41] (formation of gaseous SiO, SiS and other sulphurous gases and their absorption by metal above the tuyeres). In the hearth, silicon in iron behaves as a poor reducing agent for manganese reduction which controls sulphur removal. The probable reasons for such a behaviour will be discussed in Sec. 7.4.2.2.

3.16. The FeO-SiO_2-Al_2O_3 System[47-49]

In the blast furnace, the gangue and flux consist mainly of silica, alumina, lime and magnesia. The source of the former two is ore and coke-ash although a small quantity may emanate from the flux itself which consists of limestone and dolomite. As long as these materials remain in the solid state, their mutual interaction and solution will be very slow. Moreover, at high temperatures, alumina and silica undergo sintering and the alumino-silicates being much more stable than the individual oxides, it is improbable that the ore picks up a significant amount of lime before the reaction products are liquid. At lower temperatures, the rate of lime dissolution will depend on the diffusion process in the solid state and the rate will be extremely slow especially because the materials are not finely divided and films of reaction products may build up between the reacting surfaces. The formation of the first slag presumably occurs through fluxing of the alumino-silicate by unreduced iron oxide. The molten slag then flows over lumps of limestone and incandescent coke and in the process picks up lime, forming what is known as *primary* slag which loses its ferrous oxide rapidly by reaction with coke at the prevailing high temperatures. These processes occur simultaneously in the belly and the bosh where most of the silica and alumina from coke ash have not been released yet. The slag formed in the region above the tuyere is termed *secondary* or *bosh* slag. The *final* or *hearth* slag is formed when the coke ash released at the tuyeres and the still undissolved lime are incorporated in the descending bosh slag which flows down to the hearth.

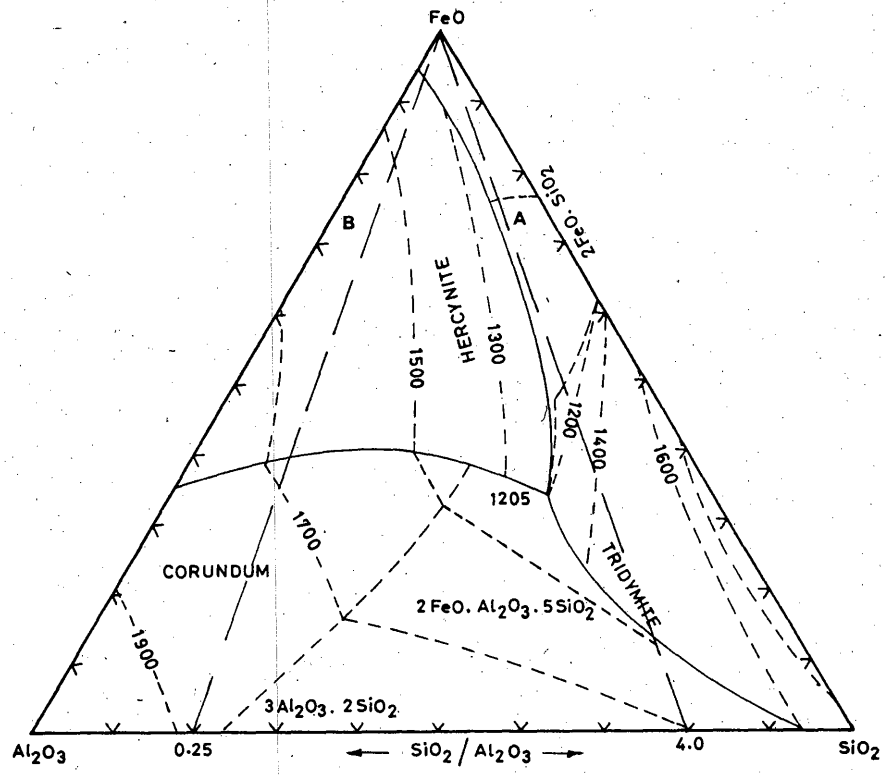


Fig. 3.17[51] Some salient features of the FeO-SiO_2-Al_2O_3 phase diagram as revised by E. F. Osborn and A. Muan. (Copyright American Ceramic Society).

From the phase diagram of the FeO-Al_2O_3-SiO_2 system (Fig. 3.17)[50] we find that the liquidus temperature of the alumino-silicates containing above 40% FeO is not more than about 1200°C. As the %FeO decreases, there is a rapid increase in the melting point to that of the FeO-free slag. Furthermore, the lowest melting points lie in the region traversed by the line (A) joining the FeO corner to 25–30% alumina on the Al_2O_3-SiO_2 base. On either side of the line, the liquidus temperatures rise progressively, especially towards the high alumina side. Therefore, the most favourable melting condition would be attained if the gangue of an ore contains a silica/alumina ratio of 2.5–4:1.

The importance of the above ternary system has been illustrated by Taylor[47-49] with regard to primary slag formation and stock movement. As discussed in Chapter 8, the proportion of direct reduction in rich ore

practice is more than that in the lean ore one and since the gangue content is also lower it is clear that the proportion of unreduced iron oxide descending in the fusion zone is much greater in the former practice. The melting point of the primary slag in rich ore practice is therefore correspondingly much lower. According to Taylor,[49] depending upon the alumina content, all the slag should be liquid at 1200–1300°C in the FeO range of 30–60 percent. As the FeO decreases below about 30 percent there is a steady increase in the liquidus temperature to that for FeO-free slags. For lean ore practice where %FeO is low the fusion temperatures are high and may extend even up to 1350°C. Thus in rich ore practice, the slag will melt at a comparatively narrow range of temperatures of about 1200°C whereas in the latter the range will be wider, 1200–1350°C. In the latter case if the efficiency of reduction is high, i.e., the unreduced ferrous oxide content is low, it would lead to the formation of semi-fused or viscous slags and *gumminess* over a wider range, resisting throughflow of gas and thereby to hanging (Sec. 8.2).

In actual practice, MnO is always present in the charge materials and pre-fluxed agglomerates are being increasingly used. They alter the pattern of softening, melting, composition and behaviour of the primary slag (Sec. 8.2).

3.17. The CaO-SiO_2-Al_2O_3 System

The primary slag of relatively low melting point which forms in the lower part of the stack or in the belly consists of FeO-containing silicates and aluminates with varying amounts of lime which has become incorporated depending upon the degree of calcination undergone (for composition, see Sec. 8.2.4). As the slag descends, ferrous oxide is rapidly reduced by carbon as well as by CO. As the lime is continually absorbed, the original FeO-SiO_2-Al_2O_3 system rapidly changes to the CaO-SiO_2-Al_2O_3 system with some minor impurities accompanying the burden. The dissolution of lime and the approach to the CaO-SiO_2-Al_2O_3 system is more pronounced, the lower the viscosity and liquidus temperature of the primary slag and the higher the temperature. It should be noted, however, that as the liquid primary slag runs down the bosh and loses its fluxing constituent FeO, the liquidus temperature also increases. If, therefore, the slag has to remain liquid it must move down to hotter parts of the furnace as rapidly as its melting point is raised. If the reduction of FeO is almost complete above the tuyeres the resulting bosh slag, composed mainly of CaO-SiO_2-Al_2O_3,

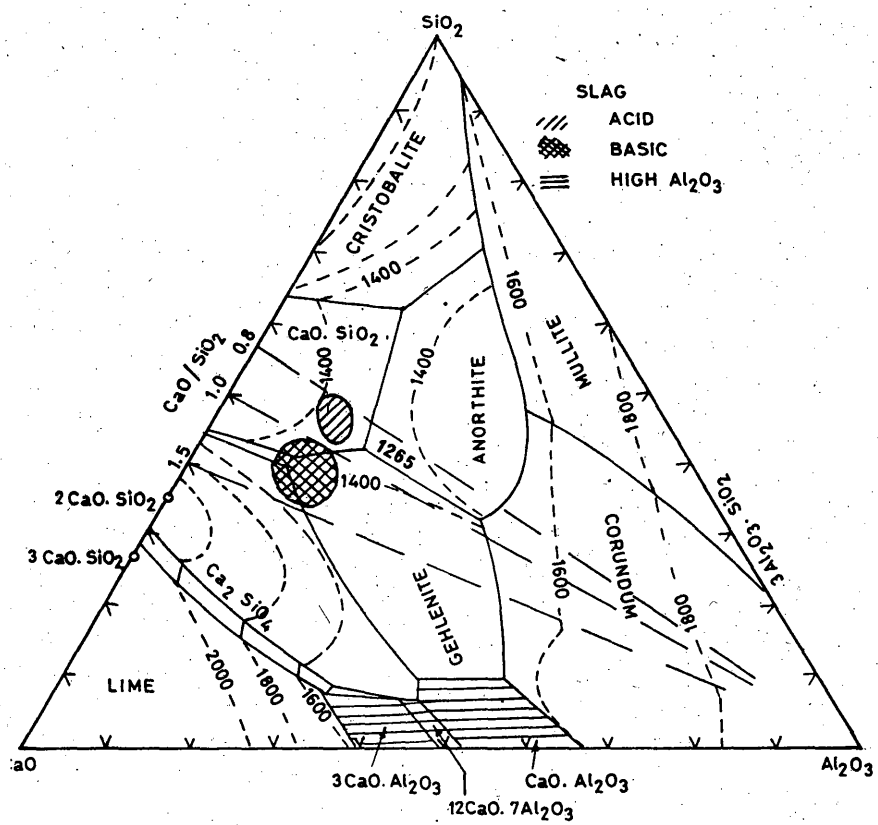


Fig. 3.18[51] Basic features of the lime-alumina-silica system taken from the phase diagram as revised by E. F. Osborn and A. Muan. (Copyright American Ceramic Society).

should also be liquid and sufficiently fluid so as to descend freely to the hearth. (Slag flowing down along the central coke column may contain considerable amounts of FeO). If the bosh slag is viscous or refractory, it will not only resist stock descent but also gas throughflow, leading to irregular furnace operation and hanging. We should also remember that since the entire lime is not usually absorbed in the bosh, the slag here is rather on the acid side of the theoretical bosh slag composition and more basic than the final slag because more acids from the coke ash are absorbed at the tuyeres and below (Sec. 8.3).

Having discussed the course of formation of the bosh slag we would now consider the probable composition of slag which would give liquid

and fluid product at the operating temperatures. The operating temperatures are limited by the excessive coke consumption and high silicon in metal at high temperatures on one side and the danger of solidification and high viscosity of the slag at low temperatures on the other. For a smooth operation, the slag must be free-running and above the *critical hearth temperature*. Figs. 3.18[51] and 3.19[52] show the phase and viscosity diagrams of the CaO-SiO_2-Al_2O_3 system from which the composition of a low melting and low viscosity region can be evaluated. In selecting the most favourable composition, it should be remembered that the primary function of blast furnace slags is not only to bind the gangue and flux into a low melting liquid but also to control sulphur and silicon and recover manganese all of which need a basic slag with a basicity ratio higher than unity. The region of normal basic blast furnace slags is shown in Fig. 3.18, lying between the isobasicity ratio lines of 1.0–1.5 and that of acid slags between 0.8–1.0.

Under blast furnace conditions, the compounds that may be present in the slag as can be seen in Fig. 3.18 are $CaO.SiO_2$ (pseudo-wollastonite or calcium bisilicate), $2CaO.SiO_2$ (calcium orthosilicate), $CaO.Al_2O_3.2SiO_2$ (anorthite), $2CaO.Al_2O_3.SiO_2$ (gehlenite). Their melting points and lime/silica ratios are given in Table 3.4.[53] It will be seen that anorthite has the least lime/silica ratio and therefore any slag inclined to this region should possess higher silica activity and result in higher sulphur and silicon in the metal.

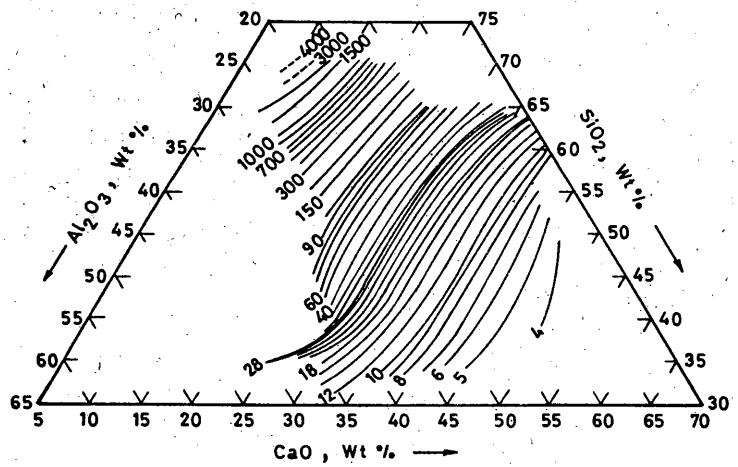


Fig. 3.19 Isoviscosity coefficients (isokoms) in Poise of lime-alumina-silica melts at 1500°C, according to Machin and Yee.[52] (Copyright American Ceramic Society).

Table 3.4[53]

	SiO_2	Al_2O_3	MgO	CaO	$\frac{(CaO + MgO)}{SiO_2}$	$\frac{CaO}{SiO_2}$	m.p. °C
$CaO.SiO_2$ (cal.silicate)	51.72			48.28		0.93	1544
$2CaO.SiO_2$ (cal.orthosilicate)	34.88			65.12		1.87	1700
$3CaO.2SiO_2$ (cal. sesquisilicate)	41.66			58.34		1.40	1700
$CaO.Al_2O_3.2SiO_2$ (Anorthite)	43.19	36.65		20.16		0.47	1700
$2CaO.Al_2O_3.SiO_2$ (Gehlenite)	21.91	37.18		40.91		1.87	1580
$2CaO.MgO.2SiO_2$ (Akermanite)	44.07		14.79	41.14	1.27	0.93	1350–1400
$2CaO.MgO.SiO_2$ (Monticellite)	38.39		25.77	35.84	1.60	0.93	1500

The minimum temperature of liquid formation appears to be around 1265°C, the ternary eutectic of wollastonite, gehlenite and anorthite having a basicity of less than unity. From the point of view of fuel efficiency, a ratio of unity or even less may be ideal provided the principal function of the slag, i.e., desulphurization of metal, is done outside the furnace. An increase in anorthite would, however, lead to increased viscosity of the slag. Calculation of slag composition should always take into consideration the bosh slag which has higher melting point and viscosity and, therefore, will be sticking on the bosh if the lime content is excessive. As magnesia lowers the melting point as well as the viscosity, nowadays more than 95 percent of the blast furnace slags are composed of lime, alumina, silica and magnesia which will be discussed in the next section.

The liquidus temperature and viscosity are not inter-related.[53] A eutectic with 23.25% CaO, 14.75% Al_2O_3 and 62% SiO_2 melts at 1170°C but is extremely viscous till about 1600°C. On the other hand, high liquidus tem-

perature (about 1700°C) as with slags with excessive lime does not necessarily mean that the smelting process will be hindered. With high temperature blast, it is possible to work with slags having 30% SiO_2 and 5–20% Al_2O_3 and most of the rest CaO, since the actual liquidus temperature is lowered by about 100°C due to the presence of FeO, MnO, CaS and others.

As already mentioned in Sec. 2.9.4, the viscosity of slags decreases with increasing lime/(alumina + silica) ratio. A decrease in the ratio makes the slag *gummy*; it solidifies slowly and gradually turns into a glassy phase. As the ratio increases to unity, the slag becomes increasingly thinner, solidifies fast and is amorphous on fracture. With further increase of lime the slag becomes thicker because of increasing liquidus temperature and on cooling it disintegrates. The slag is, however, not viscous above the liquidus. The liquidus temperatures of some slags consisting of CaO, Al_2O_3, MgO and SiO_2 and their viscosities are shown in Table 9.5.

For more detailed information on the viscosity of the lime-silica-alumina system, the work of Kozakevitch,[54,55] Machin and co-workers[56,57] and Turkdogan and Bills[58] may be consulted. Normally, for a given alumina content, the viscosity of the melt increases with increasing silica content and for a given basicity, the viscosity does not vary so much with alumina in the medium basicity range; however, it increases in the high basicity region and decreases in the low basicity region. Alumina appears to behave as an amphoteric oxide being acidic, i.e., net-work former in basic slags and basic, i.e., net-work breaker in the acid region. The viscosity increases with decreasing temperature for all slags (see also Sec. 2.9).

There is another region[59] in the CaO-SiO_2-Al_2O_3 system where the slag is low melting with sufficient fluidity, having silica less than 20 percent. This field of low liquidus temperature slags is shown by the shaded area in Fig. 3.18 at the CaO-Al_2O_3 base. The calcium aluminates, $CaO.Al_2O_3$, $12CaO.7Al_2O_3$ and $3CaO.Al_2O_3$, are soluble in the slag. When the lime content is high and the slag is cooled down slowly, most of the alumina is present as $12CaO.7Al_2O_3$. The aluminates are soluble in water and alkali, and hence can be extracted and used for portland cement manufacture.

For smelting of iron in this slag region we require high alumina/silica ratio. Ores having high Al_2O_3/SiO_2 ratio would be more suitable than the use of raw bauxite for attaining the composition. A typical slag composition for open hearth hot metal was 12.3% SiO_2, 30.56% Al_2O_3, 53.8% CaO with tapping temperatures 1350–1420°C. The ore burden contained a major part from the Indian Goa area with Al_2O_3/SiO_2 ratio of 3–4:1.

3.18. The CaO-MgO-SiO_2-Al_2O_3 System[60]

Magnesia is known to lower the liquidus temperature as well as the viscosity of lime-alumina-silica slags. Most of the blast furnaces nowadays work with slags containing magnesia and therefore the above system has assumed greater importance. The clarification of this system has been due to the outstanding work of Osborn et al.[60] Since the principal function of the blast furnace slag is to hold sulphur, they have also indicated the optimum slag composition for desulphurization which fortunately coincides with minimum viscosity since the latter decreases with increasing ratio of base to acid, necessary for sulphur removal.

In order to determine the influence of MgO on the CaO-Al_2O_3-SiO_2 system, the liquidus temperatures of the boundaries of the different phases present in the system have been determined from mixtures of the four components containing from 5 to 35 percent alumina. These are pseudo-ternary diagrams where the liquidus temperatures were measured with additions of alumina to mixtures of CaO, MgO and SiO_2. There are several phases present depending upon the alumina content and they are shown only in Fig. 3.20[60] as an example for 10%-alumina. As we are primarily interested in blast furnace type slags, only relevant portions of the diagram are shown. For higher and lower alumina contents and detailed information, the original paper may be consulted.

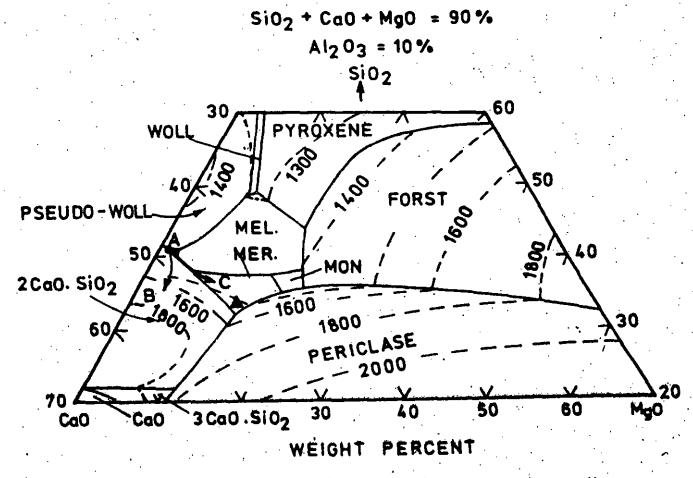


Fig. 3.20 Some important features of the CaO-SiO_2-MgO-Al_2O_3 phase diagram containing 10 percent alumina taken from the work of E. F. Osborn et al.[60]

For the significance of the diagrams we shall consider Fig. 3.20 for 10% alumina, assuming the slag temperature to be around 1500°C. At the foot of the steep temperature slope of the liquidus surfaces of the fields of dicalcium silicate and periclase, there is a region of low liquidus valley where merwinite ($3CaO.MgO.2SiO_2$), monticellite ($CaO.MgO.SiO_2$) and melilite (solid solution of akermanite $2CaO.MgO.2SiO_2$ and gehlenite $2CaO.Al_2O_3.SiO_2$) are the primary phases. Here, the slag will be liquid at the operating conditions and silica will be low. The lowest silica with optimum desulphurizing capacity will of course be near the corner of the dicalcium-silicate/periclase boundary shown by the solid triangle (44% CaO, 14%MgO and 32% SiO_2). For 10% alumina, silica content lower than 32 percent is not possible. If more lime or magnesia is added to increase the basicity (thereby reducing silica), the composition will enter the higher liquidus regions and crystals of dicalcium silicate or periclase (in equilibrium with the liquid) will separate out and appear in the liquid which will be at 1500°C and will have silica no less than 32 percent. On the other hand, if the crystals have lower silica-content than that of the mixture, the resulting co-existing liquid will have silica higher than that of the mixture and the purpose will not only be self-defeating but rather the desulphurizing power of the slag will be decreased. Furthermore, the appearance of crystals in the liquid melt will decrease the fluidity and promote *stickiness* of the slag. In order to avoid the appearance of crystals and assure a smooth operation of the furnace, the selected composition should be farther back from the dicalcium silicate and periclase boundaries since any fluctuation of silica content of the raw materials may move the composition into the high melting zones. As long as the slag composition lies in the trough with respect to the four components, the slag is expected to be all liquid, as normally the temperatures in the furnace are sufficiently high. Any contemplated change in the lime or magnesia content of the slag should be done taking into consideration the nearness of the slag composition to the dicalcium silicate or periclase fields. Further addition of MgO to a slag lying close to the periclase field will cause separation of crystals and increase of viscosity, whereas lime can be added safely. Similarly, magnesia can be added to slag near the dicalcium silicate field without endangering the slag properties (compare lines AB and AC in Fig. 3.20). MgO or CaO can be interchanged freely if the composition lies away from either of the two boundaries.

According to Osborn et al.,[60] the actual slag temperature will be about 1400°C instead of 1500°C as selected by them for determining the optimum

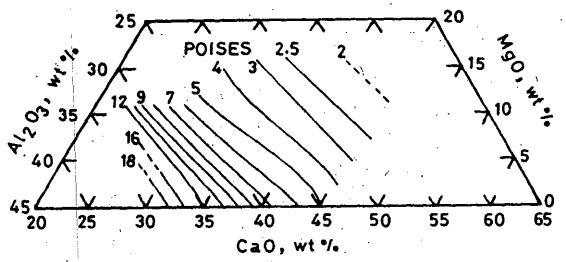


Fig. 3.21 Isoviscosity coefficients (isokoms) in Poise of MgO containing blast furnace type slags containing 35 percent silica at 1500°C, after Machin et al.[57] (Copyright American Ceramic Society).

slag compositions since the impurities present lower the liquidus temperatures by about 100°C, providing sufficient allowance for absorbing the shocks of temperature variations in the furnace. However, according to Baldwin,[61] at least for British blast furnaces, the actual slag liquidus temperatures are not far below those calculated from Osborn's diagrams. For safety, the slag composition should be chosen for liquidus temperatures of about 1450°C rather than 1500°C.

The viscosity of MgO-containing blast furnace slags with 35% SiO_2 is shown in Fig. 3.21[57] for 1500°C. A comparison with Fig. 3.19 shows that on addition of MgO to the $CaO-SiO_2-Al_2O_3$ slags, the viscosity decreases. Turkdogan and Bills[58] have shown that the viscosity changes little if lime is replaced by magnesia on a molar basis. Also, both silica and alumina increase the viscosity of these slags, although the two effects are not equivalent on molar basis (Sec. 2.9.4).

3.19. The $FeO-CaO-SiO_2$ System

This system has importance for lime-bearing sinters[62] (Sec. 6.4.3). Because of the presence of a reducing atmosphere around coke particles in the sinter mix some quantities of the higher iron oxides are invariably reduced to FeO which, depending upon its amount, can form several equilibrium phases in combination with CaO and SiO_2. However, the heating (1300–1400°C) and cooling cycles in the sintering process being very fast the phases formed often do not represent those expected from the overall composition of the sinter mix nor do the phase reactions have sufficient time to attain equilibrium due to rapid solidification during recrystallization.

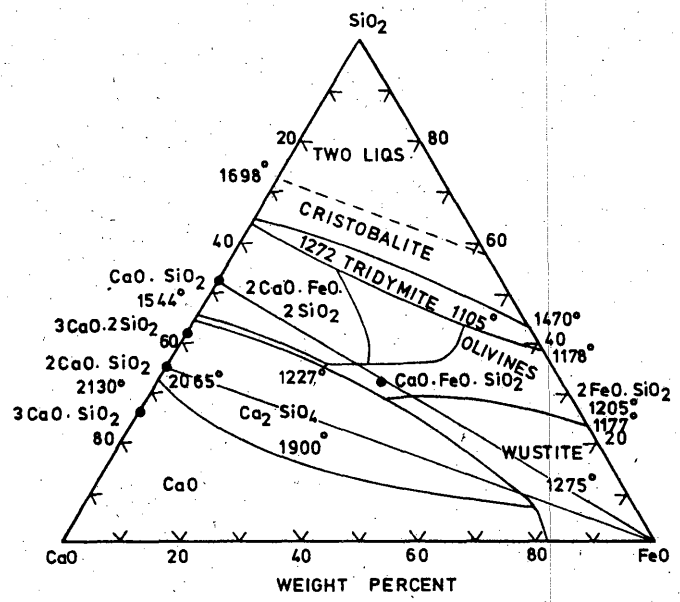


Fig. 3.22[63] Some relevant features of the FeO-CaO-SiO_2 phase diagram, revised by E. F. Osborn and A. Muan. (Copyright American Ceramic Society).

The FeO-CaO-SiO_2 system is shown in Fig. 3.22.[63] In acid sinters, in the absence of lime, the base FeO-SiO_2 is relevant. Fayalite, $2FeO.SiO_2$, of melting point about 1210°C, can form in a reducing atmosphere, the extent depending upon the relative amounts of silica and iron oxides, temperature and amount of coke in the mix. Since some alumina is always present in the ore, it is also incorporated in fayalite. The relevant FeO-Al_2O_3-SiO_2 phase diagram is shown in Fig. 3.17.

In the presence of lime, it is possible that the phases – $CaO.SiO_2$, $2CaO.SiO_2$ and $3CaO.SiO_2$ – may form, depending upon the composition of the sinter mix (Fig. 3.22). During cooling, fayalite can separate out from the residual melt below 1210°C. Fayalite is soluble in $CaO.SiO_2$ as well as in β-$2CaO.SiO_2$. The latter undergoes spontaneous transformation to γ-form during cooling accompanied by about 10 percent volume expansion, resulting in its breakdown called *dusting* or *falling*. Sinters with large amounts of β-dicalcium silicate are weak, liable to cracking and breakage during handling and in the furnace itself. Fayalite stabilizes the β-form and increases the sinter strength.

During cooling, the various phases that can form are:[64]

$2FeO.SiO_2$; $CaO.FeO.SiO_2$ (olivines of general composition $Ca_x.Fe_{2-x}.SiO_4, x>2$); $2CaO.SiO_2$; $CaO.SiO_2$; $3CaO.SiO_2$.

A varying amount of these silicates along with the main body of uncrystallized combination of FeO, CaO, Al_2O_3, SiO_2 form a glassy matrix which serves as a bonding medium between the ore particles, especially in the range of lime/silica ratio of 0.0 to 1.0. As the ratio increases from 1.0 to 1.2, the devitrification[64] of the above silicate glass occurs with the separation of $2CaO.SiO_2$ crystallites and a calcium ferrite constituent. With increasing lime additions, the amount of the glassy phase decreases and the relative proportion between calcium ferrite and dicalcium silicate continuously increases and ultimately the FeO-CaO-SiO_2 system changes over predominantly to the FeO-CaO-Fe_2O_3 system discussed in the next section.

3.20. The FeO-CaO-Fe_2O_3 System

A revised version of this system after Phillips and Muan is shown in Fig. 3.23.[65] The most important compounds of the system are:

Calcium diferrite, $CaO.2Fe_2O_3$; calcium ferrite, $CaO.Fe_2O_3$; and dicalcium ferrite, $2CaO.Fe_2O_3$.

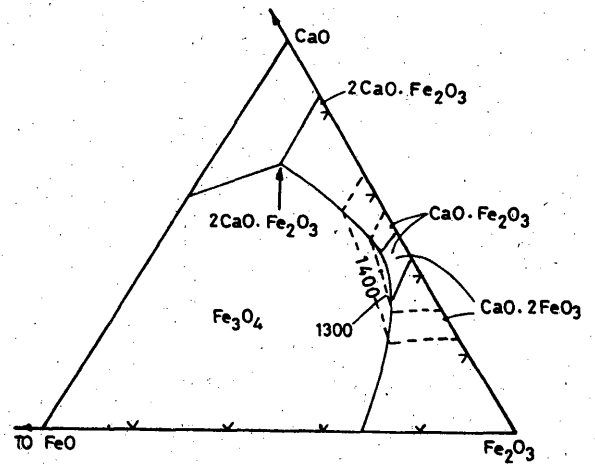


Fig. 3.23 The FeO-CaO-Fe_2O_3 phase diagram, after B. Phillips and A. Muan.[65] (Copyright American Ceramic Society and AIME).

Under reducing conditions, some other ferrites containing FeO (especially $CaO.FeO.Fe_2O_3$) are also possible.[66]

The lowest melting phase is $CaO.Fe_2O_3$, the melting temperature just above 1200°C. Fig. 3.23 shows that the lowest eutectic temperature of $CaO.Fe_2O_3$ containing some FeO, which inevitably forms during the actual sintering process, will lie below 1200°C. The ferrites solidify as needles and plates which form strong bonds with the ore particles. According to Edstrom,[67] $CaO.2Fe_2O_3$ is the most important of all ferrites as bonding medium for basic sinters.

In the solid state CaO stabilizes the magnetic phase rich in Fe^{2+} and in the liquid phase lime increases the Fe^{3+}/Fe^{2+} ratio.[66] Thus once a liquid is formed, the degree of oxidation of the final sinter will increase which is beneficial for sinter reducibility. The strength and reducibility of limey sinters are further discussed in Secs. 6.4.3.2 and 6.7.2.

3.21. Alkali Metals and their Compounds[69-73]

The presence of alkali metals, sodium and potassium, in the form of their compounds has invariably been detected in the neighbourhood of scaffolds and scabs in the higher levels of the furnace. It has been surmised that the slagging of refractories which precedes scaffold formation is caused by these metals or their compounds. A thermodynamic study of their behaviour is important on account of the following:

(i) slagging action of alkali on blast furnace and stove refractories (Sec. 13.3);
(ii) formation of scaffolds and scabs leading to furnace irregularities like hanging and slipping (Sec. 13.3–13.6);
(iii) catalytic effect on reaction of CO_2 with coke carbon resulting in the Boudouard reaction occurring at lower temperatures (Sec. 6.9.1.2);
(iv) catastrophic swelling, especially of pellets, caused by alkali impregnation (Sec. 6.7.6);
(v) formation of a recirculation load of alkali (also zinc) in the temperature zone 800–1100°C in the furnace;
(vi) loss of strength of ferrous burden as well as that of coke (Secs. 6.5.1 and 6.9.1.2).

Sodium and potassium accompany the burden materials in roughly equal amounts as complex silicates. Their input may range up to about 10 kg/THM. In the outgoing slags, their concentration seldom exceeds 2

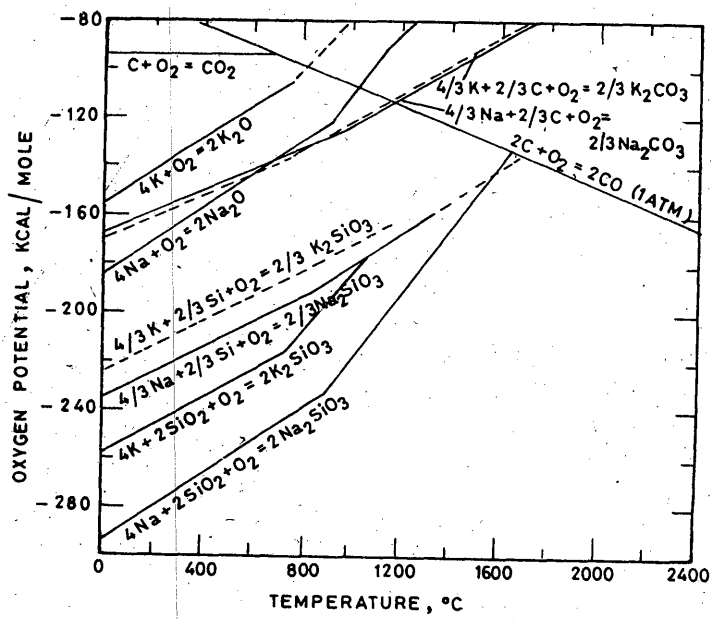


Fig. 3.24 Standard free energies of formation of oxides and silicates of alkali metals.

percent. A material balance shows that the alkali input is much higher than that passing out in the slag. Some of the deficit escape with the flue dust and top gas in a finely divided state and the rest is absorbed in the stack refractories.

The thermodynamics of oxidation-reduction of alkali oxides, silicates and carbonates in the blast furnace can be understood from the oxygen-potential diagrams of Richardson and Jeffes.[69] A modified diagram using latest available data is shown in Fig. 3.24 but that does not affect the basic mechanisms of the reaction involved. Fig. 3.24 shows that alkali silicates are much more resistant to reduction than their oxides or carbonates. Depending upon the temperature and the activities of various components, the silicates may be reduced to alkali vapour and silica or alkali vapour and silicon at the intersection of the C-CO line with those of:

$$4K \text{ (or } Na) + 2SiO_2 + O_2 = 2K_2SiO_3 \ (2Na_2SiO_3) \qquad 3.56$$

$$4/3K \text{ (or } Na) + 2/3Si + O_2 = 2/3K_2SiO_3 \ (2/3Na_2SiO_3) \qquad 3.57$$

At an assumed $p_{CO} = 1.0$ atm. in the lower furnace, pure sodium silicate can be reduced by carbon to Na-vapour at 1 atm. and pure silicon above

about 1650°C, the corresponding temperature for potassium being 1550°C. Richardson and Jeffes[69] have estimated the vapour pressures of Na and K built up in the tuyere gas to be 0.015 atm. and 0.025 atm., assuming activity values of the respective silicates of 0.02 and 0.06 between 1400–1500°C. However, on the one hand, dissolution of silicon in iron (decrease in Si-activity) would increase the alkali vapour pressure, while on the other the fast ascending gas stream would tend to lower it. Richardson and Jeffes have assumed pressures between 0.001–0.002 atm.

As the alkali-laden gases ascend to the medium temperature thermal reserve zone (800–1000°C) where the CO/CO_2 ratio is in the neighbourhood of 2.5–3, they can be reoxidized to oxides or carbonates according to their relative stabilities under the prevailing conditions. The relevant equations are:

$$K_2O\ (Na_2O) + CO = 2K\ (2Na),\ g + CO_2 \qquad 3.58$$

$$K_2CO_3(Na_2CO_3) + CO = 2K\ (2Na),\ g + 2CO_2 \qquad 3.59$$

$$2/3K_2CO_3\ (2/3Na_2CO_3) = 4/3K\ (Na),\ g + 2/3C + O_2 \qquad 3.60$$

From Fig. 3.24, it is not likely that the carbonates are stable above 1100–1200°C with CO and alkali vapours of 1 atm. However, with alkali vapour pressures of 0.001–0.002 atm. and CO/CO_2 of 2.5–3, it is possible for carbonates to form below about 900–1000°C. In the temperature and CO/CO_2 ranges quoted above, the oxides are less stable than the carbonates, the equilibrium partial pressures according to Eq. 3.58 being 0.55 atm. for K and 0.06 atm. for Na vapours.

We can expect the alkali vapours to be oxidized by CO_2 in the middle zone of the furnace to finely divided solid carbonate particles, some of which may escape with the top gas, some react with the refractories and the rest caught up by the descending burden, brought down to the high temperature zone and get reduced. Therefore, a much higher alkali metal pressure and concentration may be built up between the reduction and re-oxidation zones of the furnace than apparent from the overall concentration in the burden or from a straight alkali balance (Fig. 13.1). Liquid carbonates may form above 850°C since the melting points of sodium and potassium carbonates are about 850 and 900°C respectively.

A reoxidation of the alkali metals to silicates is also possible through reaction with CO and silica of the ore or the refractories even in the presence of carbon. This may happen at about 700°C with alkali vapour pressures of 0.001–0.002 atm. Thus the furnace linings are open to attack, the

danger being more for a furnace moving along the walls. The formation of scaffolds resulting from slagging of the refractories will be discussed in Chapter 13.

Apart from the formation of carbonates and silicates, it is possible for the alkali metals to form stable cyanides according to:

$$2K\ (Na),\ g + 2C + N_2 = 2KCN\ (2NaCN) \qquad 3.61$$

The free energies of formation are slightly negative. In the presence of solid carbon and p_{N_2} = 1.5–2 atm. approx., it is likely that cyanides are formed in the bosh and tuyere zones. The melting points of KCN and NaCN are 622°C and 562°C and their boiling points 1625°C and 1530°C respectively. As such they should form liquids in the bosh and lower shaft and gases in the tuyere zone. Whether they would exist as stable cyanides depends upon the relative stabilities of the cyanides, oxides and silicates. Fig. 3.25 shows that cyanides are more stable than oxides, the lines of $\Delta G°$ of formation of oxides from cyanides being higher than the CO line. However, they are very unstable in the presence of silica both at high or low activities and at all temperatures in the blast furnace. Below about 1000°C, cyanides are apt to form carbonates the overall reaction being:

$$2KCN\ (2NaCN),\ g + 4CO_2 = K_2CO_3\ (Na_2CO_3) + N_2 + 5CO_3 \qquad 3.62$$

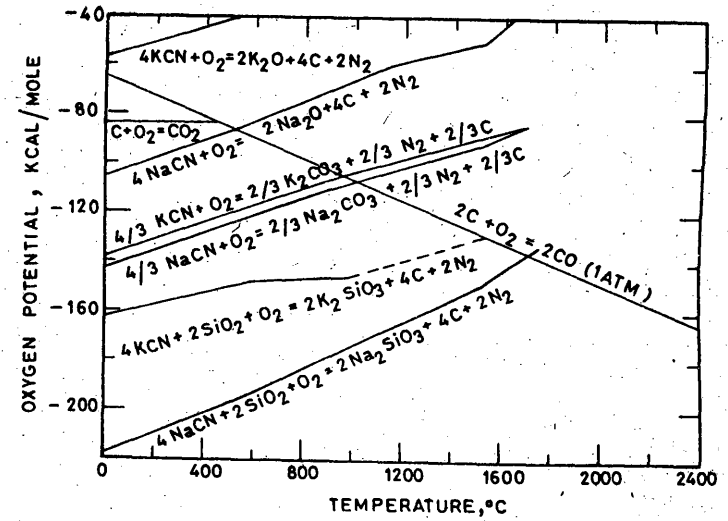


Fig. 3.25 Standard free energies of formation of oxides and silicates of alkali metals from their cyanides.

Reaction 3.62 would occur when the CO/CO_2 ratio and the temperature of the gas in the middle zone of the furnace are favourable for carbonate formation.

Normally, cyanides should be reoxidized to silicates in the lower furnace but would need the presence of solid or liquid silicate phase. However, because of the heterogeneity of the burden and fast-moving gas stream, the cyanide vapours may ascend to cooler, high oxygen potential regions and form finely divided solid carbonates through oxidation by CO_2. A part of the solid carbonates may escape through the top gas. Since the top gas is used for firing the hot blast stoves, the gas should be thoroughly cleaned to avoid fluxing of the stove refractories.

3.21.1. The alkali cycle[69-73]

We have seen that alkalis are volatilized as elements or their cyanides in the tuyere and bosh zones and carried up along with the furnace gas. In the cooler regions where the oxygen potential is also high, part of the vapour reacts with the refractory lining or burden material to form compounds according to their relative stability. The compounds that deposit on the burden are carried down to hotter regions, get reduced and ascend again to form a recirculating load of alkalis.

Willems et al.[74] found a concentration of sodium and potassium (and also zinc) in the furnace in the temperature range 800–1100°C which far exceeded the amount introduced with the raw materials. Although approximately equal amounts of sodium and potassium were introduced and approximately equal amounts were present in the slag, about four-fifths of the total alkali in the samples was potassium. Consequently, the predominant alkali in the flue dust would be expected to be sodium which was indeed borne out by the mass balance. The Na_2O in the top gas constituted about 55 percent and K_2O 15 percent of the input.

The extent of recirculating load a furnace can tolerate depends upon the operation practice. When a critical load is reached, the alkalis can cause severe operating troubles due to their harmful effects on the reactivity and loss of strength of coke, and swelling and loss of strength of the ferrous burden both at low and high temperatures. An increase in the coke gasification rate would increase direct reduction resulting in a thermal disturbance while an increased break-down would reduce the bed permeability and decrease production.

The bed permeability is further reduced because small particles may be glued together by the liquid cyanides and carbonates. Further, small

coke particles of different sizes will decrease the voidage of the coke bed in the wet zone and also increase the coke surface area, both of which promote flooding and hanging (Sec. 5.6). Breakage of coke also promotes choking of the hearth, and burning of tuyeres and slag notch (Secs. 13.8 and 13.10).

Fig. 11.10 is an illuminating example of how the permeability and production are affected by an increased alkali input. Fig. 11.9 shows the breakdown of coke in the region where an excessive amount of alkali accumulates.

Since, for a given burden the alkali input cannot be controlled, only operational controls can minimize the adverse effects. They are:

(i) operation with lower flame temperature since alkali gasification from the silicates increases with temperature (Fig. 3.24);
(ii) operation with high p_{CO} since it opposes alkali gasification reaction. This can be achieved by oxygen-enrichment or high top pressure;
(iii) decrease in slag basicity since lime and magnesia bind silica more strongly than do alkali oxides and hence increase the activity coefficient of the oxides;
(iv) increase in slag volume to decrease alkali oxides activity.

The subject will be further discussed in Chapter 13.

References

1. HANSEN, M. and K. ANDERKO: Constitution of binary alloys, 2nd Ed., McGraw-Hill, N.Y. 1958.
2. OHTANI, M. and N. A. GOKCEN: Trans. Met. Soc., AIME, 216, 1960, p. 533.
3. DARKEN, L. S. and R. W. GURRY: The physical chemistry of metals, McGraw-Hill, N.Y. 1953.
4. BOGDANDY, L. v and H.-J. ENGELL: The reduction of iron ores (in Eng.), Springer-Stahleisen, 1971.
5. BAUKLOH, W. and H. J. SCHILLING: Tonind.-Ztg., 64, 1940, p. 397–399; see also Ref. 5a.
5a. KÖHLER, E. K.: Stahl u. Eisen, 81, 1961, p. 1297–1301.
6. TURKDOGAN, E. T. and J. V. VINTERS: Met. Trans., 5, 1974, p. 11.
7. KALLING, B.: The phys. chem. of steelmaking, Edt. J. F. Elliott, MIT, 1958.
8. EDSTROM, J. O.: J. Iron Steel Inst., 175, 1953, p. 289–301.
9. WIBERG, M.: Jernkont, Ann., 124, 1940, p. 129.
10. HOVGARD, N. A. and P. N. JENSFELT: op. cit., 140, 1956, p. 467.
11. SCHURMANN, E. and D. BULTER: Stahl u. Eisen, 81, 1961, p. 1565–1575.
12. RIST, A. and G. BONNIVARD: Rev. de Metallur., 59, 1962, p. 401; 60, 1963, p. 23.
13. TAYLOR, J.: J. West Scot. Iron Steel Inst., 1947–48, p. 137–176.
14. DURRER, R.: Verhuetten von Eisenerzen, Verlag Stahleisen, 1954.

15. HEYNERT, G., E. SCHURMANN and J. WILLEMS: Stahl u. Eisen, 78, 1958, p. 1493–1505.
16. BOGDANDY, L. v. and W. SCHAEFERS: op. cit., 82, 1962, p. 1–18.
17. SCHÜRMANN, E. and D. BULTER: Arch. Eisenhuttenw., 35, 1964, p. 677–698.
18. GOLDSHTEIN, N. L. and N. S. KHROMCHENKO: Stal in German, 5, 1965, p. 611–615.
19. Ref. 4, p. 201.
20. DECKER, A. and R. SCIMAR: CNRM, Met. Rep., 12 Sept. 1967, p. 37.
21. TURKDOGAN, E. T.: Met. Trans., 9B, 1978, p. 163–178.
22. FUKUSHIMA, T.: Rep. 54, Comm. Jap. Soc. for Promotion of Science, July 1970, p. 54–1157.
23. TOKUDA, M. et al.: Tetsu-to-Hagane, 58, 1972, p. 219.
24. TSUCHIYA, N. et al.: Met. Trans., 7B, 1976, p. 315–320.
25. HODGE, A. L.: J. Iron Steel Inst., Sept. 1961, p. 6–15.
26. OELSEN, W. and H. MAETZ: Arch. Eisenhuttenw., 13, 1939–40, p. 465–474.
27. FULTON, J. C. et al.: Trans. Met. Soc., AIME, 193, 1953, p. 185–190.
28. FULTON, J. C. and J. CHIPMAN: op. cit., 200, 1954, p. 1136–1146; 215, 1959, p. 888–891.
29. LANGENBERG, F. C. and J. CHIPMAN: op. cit., 215, 1959, p. 958–962.
30. REIN, R. H. and J. CHIPMAN: op. cit., 227, 1963, p. 1193–1203.
31. KAWAI, Y. et al.: Trans. Iron Steel Inst. Jap., 12, 1972, p. 138–145.
32. Blast Furnace – Theory and Practice, vol. 2, Edt. J. H. Strassburger, Gordon and Breach Science Pub., 1969, p. 918–922.
33. TAYLOR, J.: J. Iron Steel Inst., 1964, p. 420.
34. REIN, R. H. and J. CHIPMAN: Trans. Met. Soc., AIME, 233, 1965, p. 415–425.
35. VIDAL, R. and A. POOS: Journ. Intn. de Siderur., Amsterdam, 1965, p. 189–192; Blast furnace technology, Edt. J. Szekely, Dekkar, N.Y. 1972, p. 201–232.
36. FROHBERG, M. G. and H. LEYGRAF: Arch. Eisenhuttenw., 41, 1970, p. 501–508.
37. ABRAHAM, K. P. et al.: J. Iron Steel Inst., 196, 1960, p. 82–89.
38. SHARMA, R. A. and F. D. RICHARDSON: op. cit., 200, 1962, p. 373–379.
39. OELSEN, W.: Stahl u. Eisen, 68, 1948, p. 75–86.
40. OELSEN, W. and H. MAETZ: op. cit., 69, 1949, p. 147–153; Arch. Eisenhuttenw., 20, 1949, p. 53–58.
41. KOOTZ, Th.: Recent dev. in met. sci. and tech., Iron and Steel, Silver Jub. Sym., Ind. Inst. Metals, New Delhi, 1972, p. 247–271.
42. OELSEN, W.: Arch. Eisenhuttenw., 35, 1964, p. 1–2; p. 699–711; p. 713–724.
43. OELSEN, W. et al.: op cit., 36, 1965, p. 779–790; 40, 1969, p. 277–293.
44. OELSEN, W. and H. G. SCHUBERT: op cit., 35, 1964, p. 1115–1122 and p. 1039–1057; 39, 1968, p. 881–891; 40, 1969, p. 1–14.
45. OELSEN, W. and H. BROCKMANN: op. cit., 40, 1969, p. 767–781.
46. OELSEN, W. et al.: op. cit., 38, 1967, p. 675. (See also Y. Kawai and K. Mori, Trans. Iron Steel Inst. Jap., 13, 1973, p. 303–317).
47. TAYLOR, J.: Ironmaking, Met. Progress-3, Iron & Steel, London, 1953, p. 2–22.
48. TAYLOR, J.: J. Iron Steel Inst., Feb. 1950, p. 129–136.
49. TAYLOR, J.: op. cit., Sept. 1962, p. 701–703.
50. The Phase Diagram for Ceramists: Levin et al., Amer. Cer. Soc., 1964.
51. See Ref. 50.
52. MACHIN, J. S. and Y. B. YEE: J. Amer. Cer. Soc., 31, 1948, p. 200–204.
53. HOPKINS, D. W.: Phys. Chem. of metal extn., Garnet & Miller, London, 1954, p. 173.

54. KOZAKEVICH, J.: Phys. chem. of process met., Interscience Pub., N.Y. 1961, 97–116.
55. KOZAKEVICH, P.: Rev. de Met., 51, 1954, p. 569–587; 46, 1949, p. 505.
56. MACHIN, J. S. and D. L. HANNA: J. Amer. Cer. Soc., 28, 1945, p. 310–316.
56a. MACHIN, J. S. and T. B. YEE: op. cit., 37, 1954, p. 177–186.
57. MACHIN, J. S. et al.: op. cit., 35, 1952, p. 322–325.
58. TURKDOGAN, E. T. and P. M. BILLS: op. cit., 39, 1960, p. 682–687.
59. VORWERK et al.: Tech. Mitteilung, Hüttenwerke Rheinhausen, No. 4, Dec. 1955, p. 197–209.
60. OSBORN, E. F., R. C. DEVRIES, K. G. GEE and H. M. KRANER: J. Metals, 6, 1954, p. 33–45.
61. BALDWIN, B. G.: J. Iron Steel Inst., Aug. 1957, p. 388–395.
62. BOGDANDY, L. v and H.-J. ENGELL: see Ref. 4, p. 41.
63. See Ref. 50.
64. KNEPPER, W. A. et al.: In Agglomeration, Edt. by W. A. Knepper, Interscience Pub., N.Y. 1962, p. 787–807.
65. See Ref. 50; See also Trans. Met. Soc., AIME, 218, 1960, p. 1112–1118.
66. NYQUIST, O.: See Ref. 64, p. 809–864.
67. EDSTRÖM, J. O.: Jernkont. Ann., 140, 1956, p. 101–113.
68. WATANABE, S.: See Ref. 64, p. 865–890.
69. RICHARDSON, F. D. and J. H. E. JEFFES: J. Iron Steel Inst., 163, 1949, p. 397–420.
70. ABRAHAM, K. P. and L. I. STEFFANSSON: J. Scand. Inst. Met., 4, 1975, p. 193–204.
71. Proc. Sym. on alkalis in blast fce. – State of art, McMaster Univ., Hamilton, Ont., 28 June 1973.
72. RANKIN, W. J. and J. B. SEE: Alkalis in blast fce., Rep. No. 1879, Nat. Inst. Met., Johannesburg, 1977.
73. DAVIES, J. et al.: Ironmaking Steelmaking, 4, 1978, p. 151–161.
74. WILLEMS et al.: Stahl u. Eisen, 84, 1964, p. 57–62.

CHAPTER 4

THE TEMPERATURE PROFILE

4.1. Introduction

The processing of the burden in the blast furnace needs an enormous amount of heat not only to obtain metallic iron and slag in the liquid state but also for the sustenance of other heat consuming items like volatilization of moisture and dissociation of hydrates, calcination of carbonates, direct reduction of part of wustite and oxides of other metalloids, radiation and cooling losses, sensible heat loss in exit gases. The actual amount of heat required ranges from 2.1–2.8 $\times$ 10^6 kcal per THM, of which an overwhelming amount of about 1.7 $\times$ 10^6 kcal is required for dissociation of ferric oxide to iron. The rest 0.4–1.1 $\times$ 10^6 kcal/THM is consumed for other aforesaid endothermic heat requirements the extent of which depends upon the quality and richness of the ore and the type of pig iron made.

The minimum carbon requirement, from the point of view of reduction of ferric oxide alone by carbon, is about 175 kg/THM (Sec. 3.6.1). This small amount relates to the reduction requirement only and the process is entirely feasible if the heat requirement is supplied from outside, as for example, by electrical energy. In practice, the carbon requirement in the blast furnace is much higher, 450–750 kg.C/THM, because carbon is used both as a reductant as well as a producer of heat. The heat supplied

depends upon the amount of carbon burned at the tuyeres and blast preheat.

The amount of heat available from the calorific value of carbon together with the amount supplied by the blast must satisfy, in the first instance, the overall heat requirement including physical and chemical heat losses. Therefore,

$$8000C + 0.333V_bt_b = 2.1 \times 10^6 + 350S + 0.337V_gt_g + 3020.10^{-2}V_g.\%CO_g \quad 4.1$$

where,

C	=	carbon (gasified), kg/THM
V_b	=	volume of blast, Nm^3/THM
t_b	=	blast temperature, °C
S	=	slag bulk, kg/THM
V_g	=	top gas volume, Nm^3/THM
t_g	=	top gas temperature, °C
$\%CO_g$	=	top gas CO-content, % volume
8000	=	calorific value of carbon, kcal/kg.C
3020	=	calorific value of CO, kcal/Nm^3
0.333	=	heat capacity of air, kcal/Nm^3.°C
0.337	=	heat capacity of furnace gas, kcal/Nm^3.°C
350	=	sensible heat of slag, kcal/kg.slag
2.1 $\times$ 10^6	=	heat of dissociation of ferric oxide plus sensible heat of liquid iron, cooling losses, etc., kcal/THM

The large heat deficit on the right hand side of the above equation is provided for by the calorific value of carbon and the blast heat on the left hand side. However, the heat requirement is not constant throughout the range from the ambient to the processed products temperature of 1400–1450°C. As will be seen later, the major heat consuming reactions occur above 900–1000°C. Since, according to the second law of thermodynamics, heat can flow naturally only from a higher to a lower temperature potential, it is not the overall heat balance that is important. The temperature and the heat content of the gas must be higher than those of the stock at every temperature level to ensure adequate heat transfer and satisfy the thermal demands of physical and chemical reactions.

In view of the above, a multi-stage thermal balance, e.g., at every 100°C temperature increment, is preferable to the overall one. In such a case, the heat required and the heat supplied at each temperature level must

be estimated. However, the heat required for raising the temperature of the solid stock by 1°C is more or less a constant quantity up to 900–1000°C. At about this temperature, the heat requirement increases suddenly and enormously due to the commencement of highly endothermic reactions, viz., calcination of limestone, direct reduction of FeO and metalloid oxides, fusion of metal and slag, radiation and cooling losses, etc. (Only the formation of slag is slightly exothermic). As against the two distinctly different stock thermal capacities per THM, the gas can be assumed to possess a constant mean heat capacity of about 0.337 kcal/Nm³.°C. Hence, instead of a multi-stage thermal balance, we can for all practical purposes use a two-stage one,[1,2] the dividing line between the two being approximately 900°C. Thus, the tuyere gas while cooling down from the flame temperature to 900°C must be able to supply all the heat required to raise the temperature of the stock from 900°C to that of the processed products, approx. 1400°C. Thereafter, the gas while cooling down from 900°C to the exit gas temperature must supply the heat required to raise the stock from the ambient temperature to 900°C.

4.2. Two-Stage Heat Balance

A schematic two-stage heat supply and requirement is shown in Fig. 4.1. The dotted gas lines FH, F'H', etc., represent the average thermal capacity of the gas per THM per °C, based on total gas required to smelt one THM in Nm³ multiplied by the mean specific heat, kcal/Nm³.°C. The full line JK denotes the average heat requirement of the burden per THM per °C between the temperature range 0–900°C and lines BC, B'C' those between temperatures 900–1400°C. The areas under the lines between any two temperatures represent the total heat available from the gas and that required by the burden, all per THM. The calculations are based on the following assumptions:

Stock heat requirement, 0–900°C	= 450000 kcal/THM
Stock mean thermal capacity, <900°C	= 500 kcal/THM.°C
Stock heat requirement, 900–1400°C	= 850000 kcal/THM
Stock mean thermal capacity, >900°C	= 1700 kcal/THM.°C
Tuyere carbon rate	= 370 kg/THM
Gas produced from tuyere carbon	= 2000 Nm³
Mean thermal capacity of gas, per THM	= 2000 × 0.337
	= 675 kcal/THM.°C
Flame (gas) temperature	= 2160°C

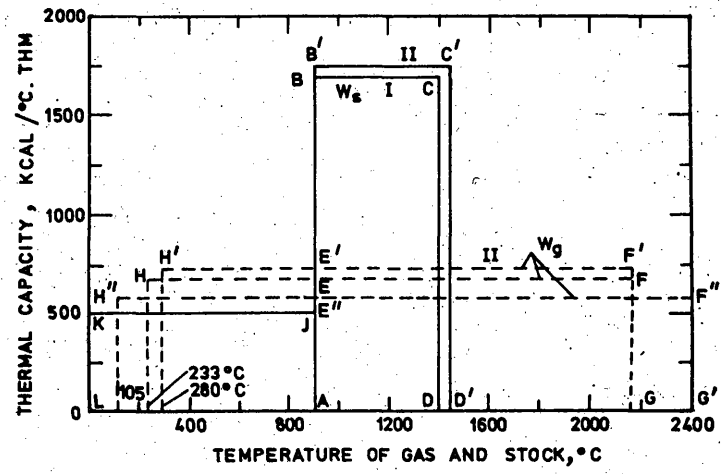


Fig. 4.1 The course of the average thermal capacities of burden and gas per THM and per °C. The relative values change greatly above 900°C.

[The carbon rate has been calculated on the basis that 1 kg.C produces 5.376 Nm³ of tuyere gas (Sec. 6.8). Therefore, the total heat available from the gas per kg.C while cooling down from the flame temperature 2160°C to 900°C is 5.376 × 0.337 × (2160 − 900) = 2300 kcal. Since the heat required between 900 and 1400°C = 850,000 kcal per THM, therefore,

$$\text{Tuyere carbon requirement} = \frac{850{,}000}{2300} = 370 \text{ kg}]$$

It is clear from above that the thermal capacity of the stock is more than three times higher at temperatures above 900°C than it is below 900°C.

A salient feature of Fig. 4.1 is the intersection of the thermal capacity lines of the stock and gas at 900°C. If we designate the thermal capacity per THM per °C as water equivalent W and subscripts g and s for gas and stock respectively, then from Fig. 4.1 we can see that,

$$\text{above } 900°\text{C: } W_s \gg W_g \text{ or } W_s/W_g \gg 1$$

$$\text{below } 900°\text{C: } W_s < W_g \text{ or } W_s/W_g < 1$$

$$\text{hence, at } 900°\text{C: } W_s = W_g \text{ or } W_s/W_g = 1$$

4.2.1. Furnace Temperature Profile

According to Kitaev et al.,[3,4] such differing thermal capacities in the blast furnace would provide a temperature profile as in Fig. 4.2(a). It shows a sharp increase in stock temperature to 800°C within 3–5 m from the stock level. Then there is a close approach of the stock and gas temperatures at 900°C and this trend continues downwards to within 3–5 m above the tuyere level. In this lower third section there is a sharp increase in the stock temperature to 1400°C and very sharp fall of the gas temperature from about 2000°C to 900°C to provide for the enormous heat requirements. Such a temperature profile has been substantiated by the investigations of Firket,[5] Bonnaure,[6] Schürmann[7] and others,[8,9] (See also Fig. 7.3).

The convexity at the top and the concavity at the bottom of the ζ-curve is the logical outcome of the differential thermal capacities of the stock and the gas on the left and right hand sides of the inter-section in Fig. 4.1. Thus, ideally, the blast furnace can be divided thermally into three distinct zones:

(i) the upper or preparation zone, where there is a sharp heat exchange and where $W_s < W_g$, is mainly a preheating and preparation zone; ideally, in this zone the indirect reduction of hematite and magnetite to wustite can occur (Fig. 1.2);
(ii) the middle or thermal reserve zone where $W_s \approx W_g$ and there occurs very little heat exchange but most of the indirect reduction, especially of wustite (Fig. 1.2); the stock and gas temperatures can approach to within 5–10°C in furnaces working with well-prepared burden (Fig. 1.2); this zone is also sometimes called *thermal pinch point*;
(iii) the lower or processing or melting zone where $W_s \gg W_g$ and where all the highly endothermic reactions occur (Fig. 1.2).

At first sight, it may appear surprising that the gas temperature falls from about 2000°C to 900°C and the stock is processed within 3–5 m from the tuyere level. But then, all the necessary conditions for rapid heat transfer are present in the lower furnace. They are:

(i) high value of heat transfer coefficient and great temperature difference between stock and gas;
(ii) intimate gas-solid contact for endothermic gasification reaction ($FeO + CO = Fe + CO_2$ and $CO_2 + C = 2CO$);
(iii) presence of liquid droplets of slag and iron in the bosh in the form of an emulsion which exposes a large surface for rapid heat transfer;
(iv) highly endothermic reduction of metalloids whose intensity increases with increasing temperature.

The thermal reserve zone occupies about 50–60 percent of the furnace height. Such a long zone may appear to be useless from the heat exchange point of view but is *important* for indirect reduction. As the temperature 800–1000°C is ideal for the kinetics of indirect reduction of wustite (without the interference of the Boudouard reaction) the more vertically elongated the zone is, the better. The height can be manipulated to a certain extent, as will be seen in Sec. 4.3.

In an operating furnace, the heat requirements and consumptions do not remain constant at the various temperature levels. As such, while the thermal capacity of the gas (W_g) remains approximately constant, that of the burden (W_s) will not be so sharply delineated as in Fig. 4.1. The intensity of heat exchange is maximum in the lower zone with a gas-burden temperature difference of 500–600°C. In this zone, after the slag and iron have melted and a substantial part of 'direct reduction FeO' has been reduced in the bosh, the W_s becomes less and the ratio W_s/W_g can even approach unity or less because of an enormous amount of heat evolved during re-oxidation of pig iron in the oxidizing zone (Sec. 7.7). Further, the highly endothermic direct reduction of any unreduced FeO or re-oxidized pig iron descending into the hearth would result in an increase in the water equivalent ratio to above unity. Thus, a third heat-exchange zone can exist in the hearth as shown in Fig. 7.22. The variations in W_s and W_g along the furnace height are also shown in Fig. 7.22.

The appearance of the thermal reserve zone of moderate temperature where the temperatures of the gas and burden are very close (within 10–20°C) shows that the heat exchange in the lower zone is complete. The closer the temperature difference to zero, the more efficient the blast furnace as a counter-current heat exchanger. The temperature of stabilization of the isothermal zone, i.e., the point of nearest approach of burden and gas temperatures or the line A-B (temperature of intersection) of Fig. 4.1, can shift towards the right or left according to the temperature of commencement of the highly endothermal reactions. Calcination of limestone starts at about 900°C. In its absence (e.g., in the case of super-fluxed sinter), the temperature of beginning of the first endothermal reaction, that of the Boudouard reaction, will be about 1000°C and the line A-B will

shift towards the right, i.e., to a lower level in the furnace, thus extending the isothermal zone vertically.

The thermal reserve zone occupies about 70 percent of the shaft volume. Although it is called isothermal zone, the actual temperature ranges between 800–1000°C because of various exothermal and endothermal reactions occurring therein. The zone is, however, maintained because their heat effects tend to cancel each other. From Sec. 3.6, it can be calculated that for 50% indirect reduction of magnetite to iron occurring in the shaft the heat evolved is 10,000 kcal per THM which is about 2 percent of the required heat in the upper furnace. This amount of heat probably compensates for the heat losses in radiation and cooling, and calcination of limestone and Boudouard reaction, the latter two occurring to a little extent in the shaft.

In the upper heat exchange zone, the temperature difference between the burden and the gas at the exit point is about 200°C. The top temperature of the gas depends upon its amount and the burden heat requirement below 900°C. In modern furnaces, the sensible heat lost in the gas does not exceed 5 percent of the total heat released from the coke burned at the tuyeres. The heat exchange is thus more or less complete in the upper zone as well. The presence of the isothermal zone *guarantees* the completeness of heat exchange in the blast furnace. The loss of sensible heat in the exit gas is inherent in the heat exchange scheme and depends only upon the heat content of the gas and heat requirement of the burden in the upper zone.

The ζ-profile is more pronounced, the more uniform the gas flow and the better the heat exchange. The slopes of the curves measure the rate of heat transfer. The pattern of temperature distribution, however, changes from furnace to furnace depending upon various factors, such as, burden heat requirement, coke rate, blast temperature, blast volume (production rate), nature of coke and charge materials, uniformity of gas flow, etc. Some of these are discussed below and some will be found in the text at appropriate places.

4.3. Factors Affecting Temperature Profile

4.3.1. Blast Volume

If the blast volume in unit time is increased to produce more iron, the increased velocity of movement of gas and stock will affect heat transfer and hence the pattern of the ζ-profile.

Assuming a convective heat transfer in the blast furnace, the rate of transfer (in kcal in unit time) from the gas to solid across an infinitesimal surface is expressed by the product of heat transfer coefficient α and temperature difference, T_1-T_2,

$$J_h = \text{heat flux} = \alpha\,(T_1 - T_2)$$

where,

J_h = heat flow, kcal/m².s
α = heat transfer coefficient, kcal/m².s.°C
T_1 and T_2 = temperature of gas and solid, °K.

The heat transfer coefficient α depends upon various factors, the interrelationships being given by,[10]

$$\alpha = Nu.\lambda/d$$
$$Nu = 1.5\ Re^{0.5-0.6}$$
$$Re = w.d/\nu$$

where,

α = heat transfer coefficient, kcal/m².s.°C
d = particle diameter, m
λ = thermal conductivity, kcal/m.s.°C
w = gas velocity, m/s
ν = kinematic viscosity of gas, m²/s
Nu = Nusselt number, dimensionless
Re = Reynolds number, dimensionless

From above, heat transfer from the gas to the stock depends upon various factors, such as, conductivity of the materials, velocity and kinematic viscosity of gas, voidage (size and size fraction). With all other variables constant, α increases with 0.5–0.6th power of the gas velocity. However, although α increases with the gas velocity (blast volume), the heat transfer efficiency decreases at the same time because the production rate increases with the blast rate with consequent decrease in time of residence of the stock in the furnace. The adverse effect of decreased gas-solid contact time on heat transfer efficiency is only partially compensated by the increased α. It is difficult to assess the effect of the two opposing influences on the temperature profile. Presumably, an increase in the blast volume of 20–30 percent will shorten the isothermal zone approximately by 10–15 percent. This, in fact, means that the ζ profile will become flatter (Fig. 4.2b). How-

ever, the top gas temperature will not increase as long as the reserve zone exists. The effect of a high driving rate is an enlargement of the upper and lower heat exchange zones at the expense of the reserve zone. Only when the driving rate becomes so high that the height of the isothermal zone becomes almost zero, will the top temperature begin to rise.

More important than heat transfer, which does not decrease as rapidly, is the decrease in the residence time of the ore in the shortened isothermal zone where most of the indirect reduction occurs. The consequences on the coke rate and production rate are discussed in Sec. 11.3.2.8.

4.3.2. Coke Rate

We have seen that the thermal capacity of the gas per THM must satisfy, in the first instance, the heat requirement of the lower furnace, i.e., the area AEFG should be equal to ABCD (Fig. 4.1). If 400 kg.C is burned instead of 370 kg.C as in Sec. 4.1, under otherwise the same conditions, then:

amount of tuyere gas	= 2150 Nm^3
thermal capacity (line F'H')	= 725 kcal/THM.°C
flame temperature	= 2160°C
heat given up, 2160°C-900°C	= 913000 kcal
heat requirement, originally	= 850000 kcal
excess heat available	= 63000 kcal

Since the heat exchange must be complete in the lower furnace, the surplus heat will increase endothermic reactions, e.g., increased silicon reduction, increased metal and slag temperature, etc.[1] In other words, W_s will increase as shown schematically by B'C' (Fig. 4.1). The area AE'F'G will be equal to the area AB'C'D'. Since the extra endothermic reactions would need more furnace volume, the isothermal zone will start at a higher level in the furnace as shown by case II as compared to the base case I in Fig. 4.2a.

Now we will examine what happens in the upper part of the furnace. Neglecting any gas generated through direct reduction, in case I,

heat content of gas at 900°C	= 607500 kcal
heat requirement, <900°C	= 450000 kcal
excess heat in gas	= 157500 kcal
top gas temperature	= 233°C

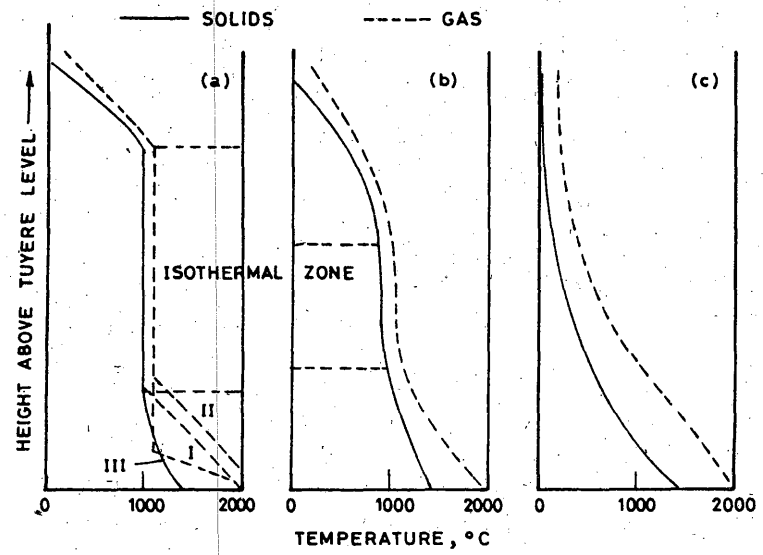


Fig. 4.2 Variations in the gas and solids temperature profiles and the extent of the isothermal zone, depending upon the temperature and amount of gas.

In case II,

heat content of gas at 900°C	= 652000 kcal
heat requirement, <900°C	= 450000 kcal
excess heat in gas	= 202500 kcal
top gas temperature	= 280°C

We can see from the above two examples (cf. Fig. 4.1) that the exit gas carries away an enormous amount of heat. The top gas temperature can only be reduced by decreasing the W_g. One of the possibilities of accomplishing this is by decreasing the coke rate (i.e., decreasing the gas volume) and compensating the consequent lowered heat input in the lower furnace by delivering more sensible heat from outside, as for example, by increasing the blast temperature.

4.3.3. Blast Temperature

A very simplified and approximate method of calculating the theoretical flame temperature based on pure carbon has been shown in Sec. 6.8. If the flame temperature in example 4.3.2 is increased to 2400°C from 2160°C

by increasing the blast temperature, a tuyere carbon rate 312 kg/THM*, a gas volume of 1680 Nm^3 of thermal capacity 566 kcal/THM.°C (line H″F″, Fig. 4.1) will satisfy the lower furnace heat requirement, i.e.

$$\text{area AE″F″G′} = \text{area ABCD.}$$

The heat content of the gas at 900°C exceeds the heat requirement at the top by 59600 kcal with an estimated top temperature of 105°C.

The steeper temperature gradient in the lower furnace with increased flame temperature and the decreased ratio of gas volume/unit charge materials will presumably bring the isothermal zone downwards as shown by line III in Fig. 4.2(a). It has been corroborated in practice and exemplified in Sec. 7.3.3.2. We will see in Sec. 4.5 that depending upon the burden quality such a steep temperature gradient may bring down the primary slag fusion zone and affect the flow of gases.

It is clear from Fig. 4.1 that the H-E (W_g) lines approach W_s (line J-K) as the gas volume per THM decreases, i.e., as W_g approaches W_s (<900°C). If the flame temperature is so high and the gas volume so small that $W_s > W_g$ in the upper furnace, then the temperature pattern will resemble that in the lower furnace, resulting in a thermal imbalance. Such a case can arise when using oxygen-enriched blast (Fig. 4.2c and Sec. 4.3.4).

The thermal balance diagram Fig. 4.1 can be drawn differently as can be seen from the so-called Reichardt diagram, Sec. 4.4 and Fig. 4.5.

4.3.4. Oxygen-enriched Blast

At first sight it would appear that an enormous amount of heat is carried away by nitrogen present in the top gas. However, nitrogen brings in also an enormous amount of heat through hot blast, its mean heat capacity being 0.337 kcal/Nm^3.°C. The hot blast supplies about 10–20 percent of the total blast furnace heat requirement. If some of the nitrogen is replaced by oxygen, the volume of air for burning 1 kg.C and that of gas produced both decrease and hence the sensible heat input through the air as well as the thermal capacity of the tuyere gas will become lower (Fig. 6.26).

The volumes of air and gas produced per kg.C and the respective flame temperatures for cases of 21, 25, 30, 35 and 40 percent oxygen in air and

* The tuyere carbon rate of 312 kg has been calculated assuming that the heat requirement in the lower furnace remains constant. Therefore,

$$C = \frac{850000}{5.376 \times 0.337\ (2400 - 900)} = 312\ \text{kg.}$$

1000°C blast temperatures are shown in Table 4.1. They have been calculated according to Eq. 6.10.

Table 4.1. Effect of oxygen enrichment on flame temperature

% O_2 in air	Blast volume Nm^3/kg.C	Tuyere gas volume Nm^3/kg.C	Tuyere gas heat content kcal/kg.C	Blast temperature °C	Flame temperature °C
21	4.44	5.37	4337	1000	2394
25	3.73	4.66	4097	1000	2608
30	3.11	4.05	3888	1000	2848
35	2.48	3.60	3675	1000	3029
40	2.33	3.26	3625	1000	3300

For the case, 1000°C normal blast with corresponding 2394°C flame temperature, and following the same method of calculations as in Secs. 4.1, 4.3.2, 4.3.3,

tuyere carbon	= 314 kg.C
W_g	= 567 kcal/THM.°C
W_s (0–900°C)	= 500 kcal/THM.°C
top gas temperature	= 106°C
W_s/W_g	= 0.88

Provided the reduction requirement is satisfied, the above carbon consumption rate and normal blast at 1000°C are just suitable for processing the given burden.

Now, if the air is enriched to 25% oxygen, the same method of calculation will show,

tuyere carbon	= 316 kg
flame temperature	= 2608°C
W_g	= 498 kcal/THM.°C
W_s (0–900°C)	= 500 kcal/THM.°C
W_s/W_g	= 1.006

The water equivalent ratio being similar to that in the lower furnace, the upper furnace temperature profile will also be similar as shown in Fig.

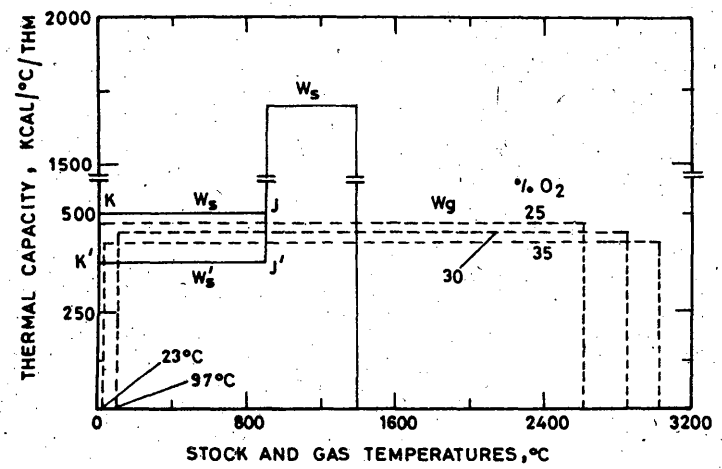


Fig. 4.3 The course of the average thermal capacities of the burden and gas per THM and per °C using oxygen-enriched blast.

4.2(c). The heat content of the gas has become so deficient that the entire pattern has completely changed. The W_g lines of the gas for blasts containing 25%, 30% and 35% oxygen at a temperature of 1000°C and two values of W_s (<900°C) lines J-K and J'-K', are shown in Fig. 4.3.

The temperature profile can be restored by increasing the thermal capacity of the gas, i.e., when $W_g > W_s$. This can be achieved by increasing the amount of tuyere gas per THM through injection of coolants in the tuyeres, e.g., steam, natural gas, oil etc. (Secs. 4.3.5 and 10.7).

Oxygen injection is helpful when the upper furnace heat requirement is small compared to that of the lower one and a large volume of gas leaves the furnace with unutilized sensible heat. We have seen above that, for the particular case, even a 25% oxygen-enrichment leads to thermal imbalance. However, if the upper furnace thermal load is decreased from 450000 kcal to 350000 kcal/THM through ore preparation (line J'-K', Fig. 4.3), even a 30%-enrichment is feasible with top gas temperature of 97°C. With 35%-oxygen the top temperature will be 23°C and hence theoretically possible to work but not in practice. With 40%-oxygen, the thermal capacity of the gas falls below that of the stock and hence unworkable. Under these circumstances, the burden and gas temperature profiles will resemble Fig. 4.2(c) without the formation of any thermal reserve zone.

4.3.5. Oil Injection

Injection of oil or any other coolant additives reduces the flame temperature for constant blast temperature (Table 6.7). The volume of gas from combustion of 1 kg carbon by normal air is 5.376 Nm^3 and that from 1 kg oil it is 5.86 Nm^3 (Table 6.8), their respective heats of combustion being 2300 and 1466 kcal per kg. From above, the total volume of gas produced at the tuyeres will increase or decrease depending upon the amount of tuyere carbon (in the base case) replaced by oil.

The heat supply in the lower furnace is a product of the thermal capacity of gas (volume × mean heat capacity/Nm^3.°C) and t_f-900. As the flame temperature t_f decreases considerably, the gas volume must increase in order to maintain the same heat supply. The lower thermal potential gas needs a greater furnace volume to heat the processed products and hence the thermal reserve zone starts at a higher level with increasing amount of oil (Fig. 4.4). The lowering of the starting levels with oxygen-enrichment is also shown – the levels depending mainly upon the flame temperature and the thermal capacity of the gas. The latter decreases with increasing oxygen enrichment. Fig. 4.4 is a schematic diagram drawn from the results of investigations of Schulz and Bülter.[11]

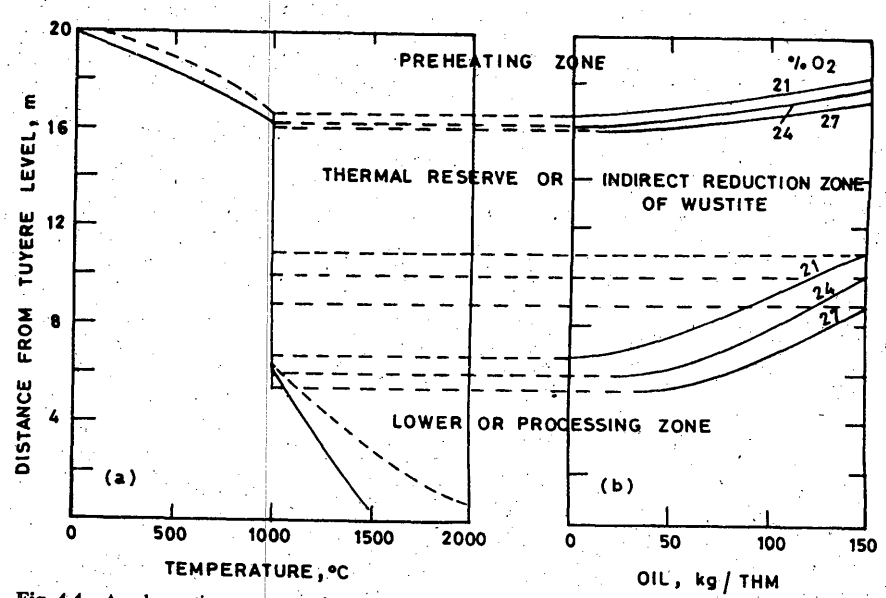


Fig. 4.4 A schematic representation of the effect of oxygen-enrichment of the blast and oil injection on the extent of the thermal reserve zone in the blast furnace.

The upper furnace temperature profile does not change so dramatically. The preheating zone becomes narrower but at a much slower rate because although the thermal capacity of the gas has increased the potential remains the same as in the base case when the gas emanates from the isothermal zone (1000°C in this case, in the absence of limestone).

From Fig. 4.4(b), the thermal reserve zone contracts, with increasing oil input, the more so with the normal than with the oxygenated blast. The short residence time of ores in the contracted reserve zone decreases indirect reduction with its consequential adverse effects on direct reduction, CO-utilization, carbon rate, top gas temperature, etc. These will be discussed in Secs. 7.3.3 and 10.7. It should be remembered that the heat requirement of the furnace, especially in the lower section, does not remain the same while using oil or other hydrogen-bearers. Hydrogen, being a better reducing agent, increases indirect reduction and lowers the direct reduction heat requirement.

What is true with oil is also valid for all other injectants like natural gas, coke-oven gas, steam, coal, oil-coal slurry, etc., their overall effect depending upon the flame temperature, necessary gas volume and altered heat requirements.

4.3.6. Hot Charge Materials

When charging hot sinter or when a large amount of heat is evolved in the upper furnace, e.g., during reduction of hematite pellets, the isothermal zone extends vertically upwards, shortening the upper heat-exchange zone and increasing the top gas temperature. This shows a close resemblance of the upper furnace with recuperators.[3]

4.3.7. Furnace Height and Stock Level[3]

The two heat-exchange zones separated by the isothermal zone exist in all normal operating furnaces, big or small. An increase in the furnace height only increases the vertical height of the reserve zone and does not affect the top temperature significantly.

A change in the stock depth is equivalent to change in the furnace height with its attendant variations in the height of the isothermal zone which would affect the gaseous reduction of wustite and hence the coke rate. For uniformity of furnace operation and metal quality, the stock level must be maintained constant by accelerated or delayed charging. Apart from the above, variations in the stock level result in differential segregation of the charge materials which deteriorates bed permeability and uniformity

of gas distribution. An even distribution of gas over the furnace cross-section promotes an extensive heat-exchange.

4.3.8. Nature of Charge Materials

Small particle size promotes better heat-exchange. Kitaev et al.[3] cite an example where crushed ore and limestone were charged and the temperature of 800°C was reached within 3.5–5 m in the upper heat-exchange zone compared to 7–8 m with uncrushed materials. It means an accelerated heat-exchange with smaller sizes and an extension of the isothermal zone.

It can be concluded that the upper heat-exchange zone operates independently and automatically and it does not affect the operation in the lower zone. The lower heat-exchange zone is controlled by the endothermal reactions and the isothermal zone begins when the carbon gasification reaction virtually ceases. It will cease the earlier the lower the coke reactivity and *vice-versa*.

4.4. Reichardt Diagram[12,13]

The thermal balance diagrams such as Figs. 4.1 and 4.3 can be drawn differently as can be seen from the so-called Reichardt diagram (Fig. 4.5). A schematic heat requirement at various temperature levels is shown

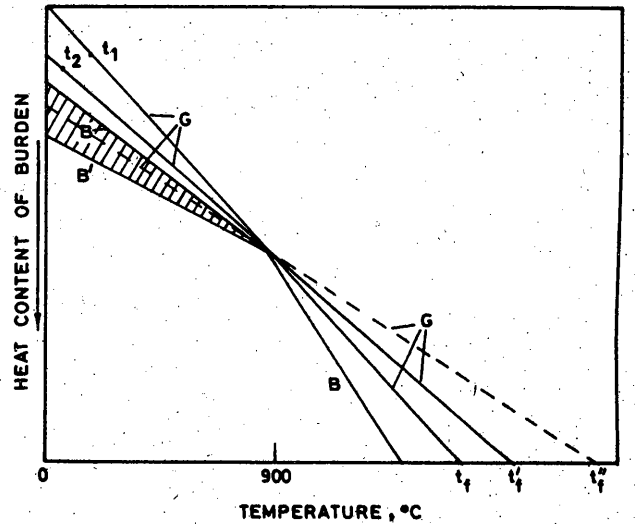


Fig. 4.5 A typical schematic Reichardt diagram showing the heat balance of the gas and the solids.

by the burden line B and the heat supply by the gas line G. The slopes of the lines in reality mean the thermal capacities of each per THM per °C. As discussed previously, the gas line should approach the burden line at around 900°C. Below this temperature, the upper furnace heat requirement being usually smaller than in the lower furnace, the slope of line B changes and becomes flatter. It may be assumed that the burden heat requirement per °C above and below 900°C is constant. When the flame temperature is t_f, the coke rate and hence the gas volume need to be high in order to meet the high temperature heat requirement. As a consequence, the top gas temperature will be high (t_1, Fig. 4.5). If the flame temperature is increased to t_f', the coke rate, gas volume (therefore, thermal capacity) and top temperature will all be lower (t_2, Fig. 4.5). When the flame temperature is t_f'', the heat requirement >900°C will still be satisfied but not that for <900°C. Hence, a thermal imbalance will result. However, the same flame temperature can be used if the heat requirement <900°C is reduced by ore preparation (line B′).

The thermal balance does not forecast whether the furnace will run smoothly with very high flame temperature. Furnace irregularities arising from the use of high flame temperature are treated in the succeeding section.

4.5. Temperature Profile and Stock Movement[14-16]

We have seen in Figs. 4.2(a) and 4.4(a) that an increased flame temperature, caused by high blast temperature and/or oxygen-enrichment, results in a steeper temperature gradient in the lower furnace. This is also evident from Fig. 4.6.[16] The temperature gradient at 800°C blast temperature (B) is much steeper than at 600°C (A). Assuming that slag fusion occurs at 1200°C in the belly at a height D from the tuyeres for case A, on raising the blast temperature to 800°C the fusion zone (1200°C) shifts downwards to the bosh incline (D′). Since the large cross-section of the belly allows reasonable flow of gas, any formation of a sticky semi-fused slag in the narrow bosh incline is likely to cause impedance to gas throughflow and material descent. The *gumminess* of slag in this sector results in sluggishness of movement and causes *bosh hanging*. This irregularity can be rectified by raising the 1200°C level to D. This can be achieved by restoring the flame temperature to the original value for 600°C blast temperature by injection of suitable coolants along with the blast. Line C, Fig. 4.6, shows the flattening of the temperature gradient of line B and approach to line

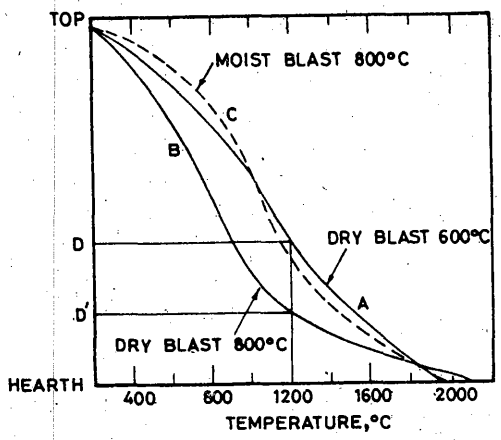


Fig. 4.6 Temperature gradient in a blast furnace with dry and moist blast, according to Grieve.[16] (Copyright Iron & Steel Institute).

A when the 800°C blast is humidified with steam. Any other coolant like, oil, natural gas, etc., will produce the same result.

It is the experience of blast furnace operators that the burden hangs when the blast temperature is raised by a fair degree. However, the cause is not yet fully known. The following are a few possibilities:

(i) descent of slag fusion zone to the bosh incline;
(ii) increased formation of gaseous silicon monoxide at high flame temperatures and its subsequent reoxidation and condensation at higher levels, blockage of voidage hindering gas flow;
(iii) increased volatilization of alkali metals, Na and K, at high flame temperatures, formation of their cyanides, condensation of cyanides to viscous liquids which glue the burden materials together, choke the voids, and hence retard gas flow;
(iv) flooding of slag in the coke grid due to increased tuyere gas velocity (Sec. 5.6).

References

1. BÜLTER, D. and A. KLITZING: Stahl u. Eisen, 88, 1968, p. 108–119.
2. SCHULZ, D. et al.: op. cit, 92, 1972, p. 629–637.
3. KITAEV, B. I., Yu. G. YAROSHENKO and V. D. SUCHKOV: Heat exchange in shaft furnace, Pergamon Press, Oxford, 1967.
4. KITAEV, B. I. et al.: Trans. Ind. Inst. Met., 11, (12), 1958, p. 3–20.
5. FIRKET, A. and J. MOLDERETZ: Rev. univ. mines, Ser. 9, 102, No. 2, 1959, p. 93–106.

6. BONNAURE, E.: Stahl u. Eisen, 79, 1959, p. 1105–1119.
7. SCHÜRMANN, E. et al.: op. cit., 80, 1960, p. 854–861.
8. HEYNERT, G. and J. WILLEMS: op. cit., 79, 1959, p. 1545–1554.
9. ASTIER, J. E. et al.: J. Iron Steel Inst., Oct. 1961, p. 143–148.
10. BEER, H. and G. HEYNERT: Stahl u. Eisen, 84, 1964, p. 1353–1365.
11. SCHULZ, D. and D. BÜLTER: op. cit., 92, 1972, p. 1179–1188.
12. REICHHARDT, P.: Arch. Eisenhüttenw.: 1, 1927, p. 77–101.
13. GERSTENBERG, B. and Th. KOOTZ: Stahl u. Eisen, 84, 1964, p. 1105–1120.
14. TAYLOR, J.: J. Iron Steel Inst., 164, Feb. 1950, p. 129–140.
15. TAYLOR, J.: Ironmaking, Met. Progress, Iron & Steel, London, Feb. 1953, p. 3.
16. GRIEVE, A.: J. Iron Steel Inst., 194, Jan. 1960, p. 37–43.

CHAPTER 5

BLAST FURNACE AERODYNAMICS

5.1. Introduction

The blast furnace can be considered to be both a chemical reactor as well as a counter-current heat exchanger. The burden and coke are charged from the top and they descend due to gravity because of the continuous creation of voids by the combustion of coke at the tuyeres and removal of iron and slag to the hearth bottom. The hot reducing gaseous product of combustion ascends through the coke grid wetted with molten slag and iron above the raceway and travels upwards through a column of dry lumpy materials, imparting its heat to the descending charge and itself cooling down in the process. It further performs the duty of reducing the iron oxides.

Mechanical flow of gas depends upon the resistance it encounters during its ascent while its chemical and thermal utilization will depend upon the uniformity, intimacy and time of contact with the charge apart from the chemical aspects which will be dealt with in Chapter 7. In this chapter we shall discuss at first the counter-flow of the charge and gas from a mechanical point of view and will later consider the variations in temperature, pressure and composition of the gas during its ascent. Irregularities in stock and gas movements and their causes will be discussed in Chapter 13. The part played by furnace profile has been left for Chapter 12.

5.2. Importance of Uniform Gas Flow

The interstices or voids between the lumps in the charge bed enable the gas to flow upwards. Therefore, the physical characteristics of the feed materials should determine the uniformity of gas distribution, i.e., the velocities and temperatures of the gas. The distribution is, however, affected not only by the stock pattern in the dry zone but the processes occurring lower down in the furnace also have far-reaching effect on the flow of gases. An increased productivity of a given furnace depends on the increased blast intake and therefore on an increased throughflow of gas and also on a decreased coke consumption. The latter can be achieved by the best possible utilization of the chemical and thermal energies of the gases which is closely related to uniformity of gas flow.

The disturbance to gas flow can occur mainly in three regimes although maldistribution can take place anywhere. These are illustrated in Fig. 5.1.

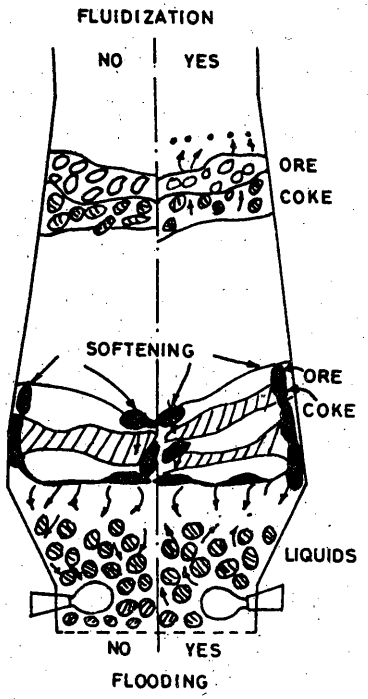


Fig. 5.1 A schematic representation of the regimes in the blast furnace where disturbances to gas flow can occur due to fluidization, softening of the burden and flooding of slag.

They are:

(i) fluidization of small particles when the local gas velocity is excessive;
(ii) diminution of voidage due to swelling and softening-melting (Fig. 11.24);
(iii) flooding of slag in the bosh zone when the slag volume and gas velocity are excessive.

The gas flow through the blast furnace has attained greatest importance to-day because of emphasis on larger and larger furnaces. This is so because of confinement of the gas flow more and more towards the periphery as the hearth diameter increases. On the basis of the presence of an active annulus where the coke burns and burden descends, a simple calculation will show the great decrease in the percentage of *active zone* as the diameter increases. Assuming a ring of 2 m around the hearth periphery which is active (Fig. 5.2), the total and active hearth areas as well as their percentages are shown in Table 5.1. However, there is an increasing evidence that the blast penetration increases with increasing furnace size.

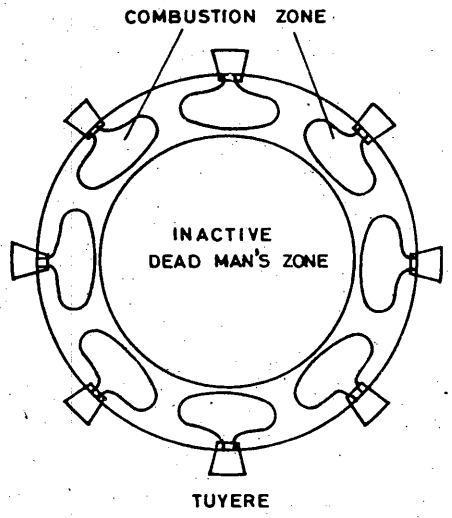


Fig. 5.2 A schematic plan view of the combustion zone at the tuyere level of a blast furnace showing the raceway around the hearth periphery and the inactive zone.

Table 5.1. Proportion of active and inactive areas in the hearth

Furnace dia, m	4	6	8	10	12	14
Total hearth area, m^2	12.6	28.3	50.3	78.5	113.1	154.0
Active hearth area, m^2	12.6	25.2	37.7	50.2	62.8	75.4
Active ring zone, %	100	89.0	75.0	64.0	56.0	49.0
Inactive centre zone, %	0	11.0	25.0	36.0	44.0	51.0

The gas formed in the combustion zone undergoes two different types of flow patterns, viz.:

(i) flow through voids of descending beds of solid materials of different shape, size and density; the voids do not remain constant in the vertical or horizontal cross-sections due to continuous motion, pulverization of coke and ore (caused by abrasion, impact, compression and disintegration), carbon deposition, softening and swelling of ores, etc.;

(ii) flow through voids of the coke grid wetted by a mass of flowing liquid iron and slag in the bosh, causing changes in the condition of gas motion; the resistance offered is two-fold, one caused by fluid and/or viscous liquid in the interstices between coke pieces (i.e., diminution of voids), and the other, by the contraction of the active annulus due to the blast striking against the rapidly trickling mass in front of the tuyeres.

We shall now discuss each of the two broad patterns of counter-flow which embody the aerodynamics of gas stream and the mechanics of gas flow through the dry as well as irrigated beds of loose particles.

5.3. Gas Flow – Static Bed of Equigranular Charge

The basic concept regarding flow of a gas through a layer of lumpy materials is the resistance to flow, i.e., the pressure-fall along the bed height (dissipation of energy). In the blast furnace the primary aim is to obtain a uniform and unhindered gas throughflow which is associated with a bed of uniform permeability and as small a pressure-drop as possible.

When a gas of volume V flows through a pipe of cross-sectional area A, the so-called *empty tube velocity* (w) is given by

$$w = V/A \qquad 5.1$$

If the gas flow rate is small (laminar region), at first a relatively small pressure drop occurs. In this laminar flow region, the pressure loss is directly proportional to the velocity and is caused by the viscous energy losses of the gas. As the velocity increases and enters the turbulent region, the pressure loss increases as the product of gas density and square of the velocity. This pressure loss is related to kinetic energy losses. It is customary to use dimensionless parameters to express the flow characteristics, e.g., by

$$\lambda = f(\mathrm{Re}) \qquad 5.2$$

where, λ = friction factor
and Re = Reynolds number

The significance of the terms as given by D'arcy is,

$$\lambda = \frac{2\,\Delta P}{H} \cdot \frac{D}{\rho . w^2} \qquad 5.3$$

$$\mathrm{Re} = \frac{w.D.\rho}{\eta} = \frac{w.D}{\nu} \qquad 5.4$$

where,

ΔP = pressure drop, $gm.cm^{-1}.sec.^{-2}$
H = length of pipe, cm
D = diameter of pipe, cm
ρ = operational density of gas, $gm.cm^{-3}$
w = operational velocity of gas (empty tube), $cm.sec^{-1}$
η = operational viscosity of gas, $gm.cm^{-1}.sec.^{-1}$
ν = η/ρ, operational kinematic viscosity of gas, $cm^2.sec^{-1}$

If the empty pipe is now packed with spherical solid particles of uniform diameter, the gas flow will be blocked by the charge and the gas will flow only through the voids between the solid particles. If the porosity or voidage is ε, then the actual velocity (w') will increase according to

$$w' = w/\varepsilon \qquad 5.5$$

In Eq. 5.5, it is assumed uniform voidage of any cross-section of the bed perpendicular to the direction of flow. It is emphasized that any porous bed is a non-uniform flow system and the actual velocity and flow rate of the gas at different localities may vary widely from the average because of different voidage and also because of different transverse dimensions

along the furnace height. However, it is customary to use the empty tube velocity (w) in gas flow equations.

The same gas flow concept according to Eqs. 5.3 and 5.4 can be applied to flow of gases through a bed of packed materials, assuming the voids between the particles to resemble a bundle of parallel capillary tubes of very thin walls, the space between them sealed. The mathematical relationships of resistance to flow of gases through such beds have been formulated by Carman,[1] Kozeny,[2] Ergun[3] and others.[4–13] The relationship is given by Eq. 5.6, the validity of which has been verified by numerous experimental investigations using cold models. Such models can be extended to blast furnace conditions.

$$\frac{\Delta P}{H} = \psi . \frac{1-\varepsilon}{\varepsilon^3} . \frac{\rho}{d} . w^2 \qquad 5.6$$

where,

ψ = friction factor, dimensionless
ε = porosity or voidage
$1-\varepsilon$ = fraction of bed volume occupied by solids
d = diameter of particles, cm.

In case the particle deviates from spherical shape, the equivalent diameter (d_e) of the irregular particle, which may be substituted in place of (d) in Eq. 5.6, can be estimated from the following equation,

$$d_e = d_1 . \phi \qquad 5.7$$

where,

d_1 = diameter of a sphere equivalent in volume to the irregular particle
ϕ = sphericity or form factor, i.e., the ratio between the specific surface of the equivalent sphere and the specific surface of the irregular particle.

ϕ = 1 for spheres and pellets;
ϕ = 0.70–0.75 for coke, ore, sinter, etc.

The values of (ρ) and (w) in Eq. 5.6 are operational quantities. Based on standard conditions

$$\rho . w^2 = \rho_o . w_o^2 . \frac{T}{T_o} . \frac{P_o}{P} \qquad 5.8$$

where subscript o is for standard conditions and T and P are absolute temperature and pressure respectively, i.e., T_o = 273°K and P_o = 1 atm. absolute. Therefore, Eq. 5.6 becomes

$$\frac{\Delta P}{H} = \psi . \frac{1-\varepsilon}{\varepsilon^3 . d} . \rho_o . w_o^2 . \frac{T}{T_o} . \frac{P_o}{P} \qquad 5.9$$

Eq. 5.9 shows qualitatively that the pressure drop or the resistance to flow of gas decreases with:

(i) increase in voidage;
(ii) increased pressure in the column;
(iii) increase in particle diameter;
(iv) decrease in gas density;
(v) decrease in gas velocity.

In order to calculate the pressure drop, the value of ψ must be known apart from other variables. Measurements of Ergun[3] with Reynolds number varying from 1 to 2500 gave the following relationship between ψ and Re′ as shown in Fig. 5.3,

$$\psi = 1.75 + \frac{150}{Re'} \qquad 5.10$$

where $$Re' = \frac{\rho . w . d.}{\eta\,(1-\varepsilon)} = \frac{Re}{1-\varepsilon} \qquad 5.11$$

Since ρ.w does not change with temperature or pressure,

$$Re' = \frac{\rho_o . w_o . d}{\eta\,(1-\varepsilon)} \qquad 5.12$$

For finding the values of Re′, the value of the viscosity of the gas must be known under experimental conditions. The gas viscosity does not change significantly with pressure. The viscosities of the blast furnace gas and hydrogen at 300°C and 1000°C are given below:

	Viscosity, η, gm.cm^{-1}.sec^{-1} × 10^{-6}	
	300°C	1000°C
Blast furnace gas	275	480
Hydrogen	140	240

In the blast furnace stack, the actual gas velocities may range from 2 to 20 m or more per second and the Reynolds numbers vary from 500

to 3000 depending upon the locality, voidage and particle diameter. On an average, $\psi = 1.75$ may be regarded as a constant. However, Brauer[11] has shown that Eq. 5.13 is more applicable for $Re' > 2000$ in beds of uniform spherical particles. The relationship is shown in Fig. 5.3 and the equation that fits the curve is given by,

$$\psi = 160\ (Re')^{-1} + 3.1\ (Re')^{-0.1} \qquad 5.13$$

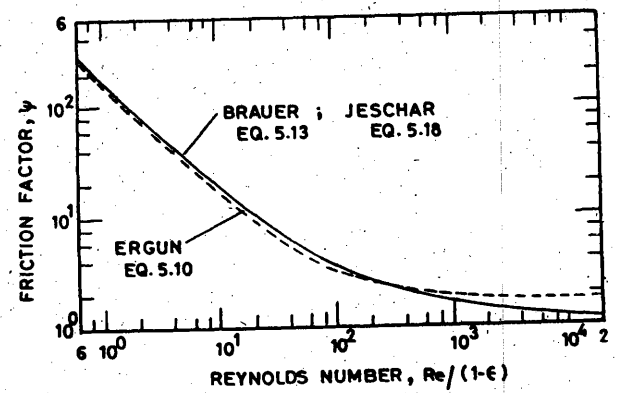


Fig. 5.3 Friction factors for flow of gas through unirrigated packed bed.

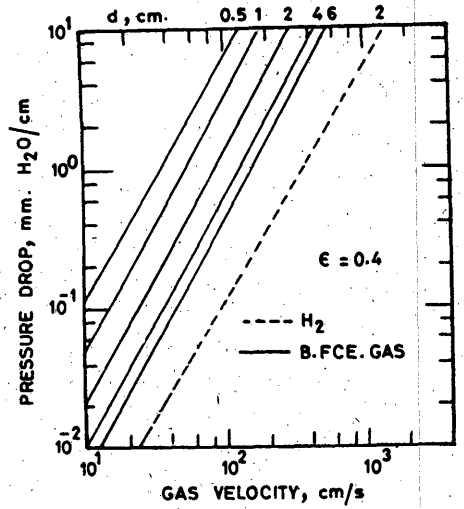


Fig. 5.4 Dependence of pressure drop on the velocity of two different gases in a packed column of spheres of varying diameters and fixed bed voidage (calculated).

For a fixed voidage, the relative effects of particle diameter and gas velocity on pressure drop per unit height of a column packed with spherical solids are shown in Fig. 5.4. The calculations are based on Eqs. 5.9, 5.12 and 5.13. One can see from the figure that the pressure drop increases as the particle diameter decreases and/or the gas velocity increases. The beneficial effect of lower density and viscosity is shown by the hydrogen line. This has some relevance in modern blast furnaces, most of which use hydrogen-bearers, like oil and natural gas. A sample method of calculation of pressure drop using Eqs. 5.9, 5.12 and 5.13 is shown below.

Blast furnace gas at 1000°C; flow rate $= 4000\ Nm^3/m^2.h$; $\rho_o = 1.5 \times 10^{-3}\ gm.cm^{-3}$; viscosity (1000°C) $= 480 \times 10^{-6}\ gm.cm^{-1}\ sec^{-1}$; particle diameter $= 4$ cm; voidage, $\epsilon = 0.35$; average pressure $= 1.6$ ata. From Eq. 5.8,

$$\rho.w^2 = 1.5 \times 10^{-3}\left(\frac{4000 \times 10}{3600}\right)^2 \cdot \frac{1273}{273} \cdot \frac{1}{1.6} \qquad 5.14$$

$$= 53.97$$

From Eq. 5.12,

$$Re' = \frac{1.5 \times 10^{-3}}{480 \times 10^{-6}} \cdot \frac{4000 \times 10^2}{3600} \cdot \frac{4}{(1\text{-}0.35)} \qquad 5.15$$

$$= 2137$$

Hence from Eq. 5.13,

$$\psi = 1.515 \qquad 5.16$$

Therefore from Eq. 5.9,

$$\frac{\Delta P}{H} = 310\ gm/sec^2.cm^2 \qquad 5.17$$

$$\equiv 3.16\ mm\ H_2O/cm$$

The influence of voidage on pressure drop is shown in Fig. 5.5. For a given size, if the voidage decreases by 0.1 the pressure drop increases 3–5 times and even more when the voidage is small. The effect can be staggering if it is borne in mind that only one-fifth to one-tenth of the furnace cross-section is available for gas throughflow. However, a saving feature is that the bed in the blast furnace is not stationary and the actual voidage increases at a rate depending upon the rate of stock descent, the higher the rate the higher the voidage in general.

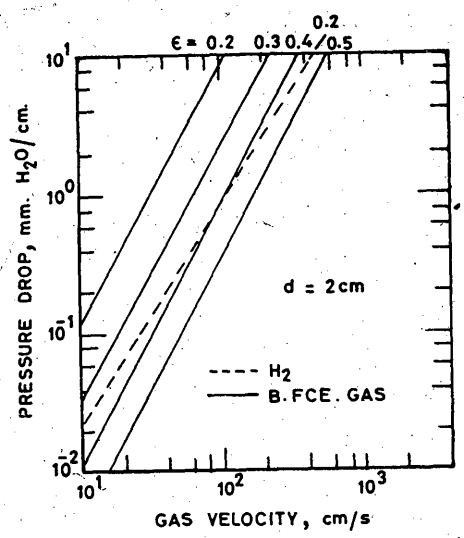


Fig. 5.5 Dependence of pressure drop on the velocity of two different gases in a packed column of uniform spheres of fixed diameter and varying bed voidage (calculated).

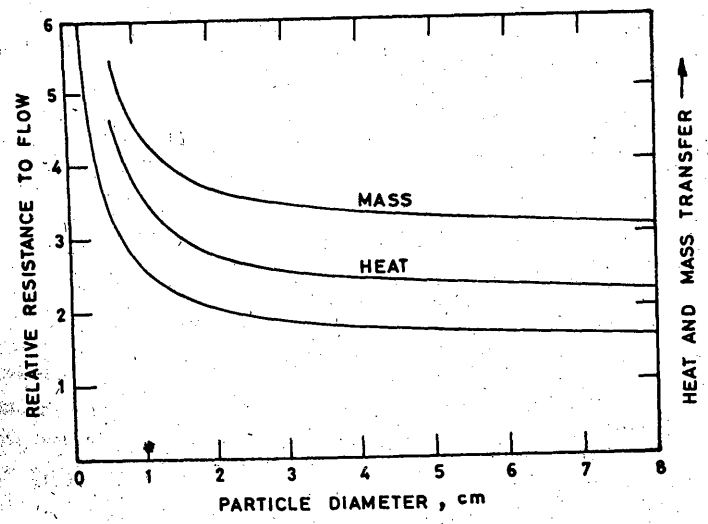


Fig. 5.6 Influence of particle diameters on the relative resistance to flow of gases. The influence of the size on heat and mass transfer is also shown schematically.

The influence of particle size on resistance to flow is not as clear in Fig. 5.4 as it is in Fig. 5.6 which shows that the relative resistance to flow increases rapidly as the particle diameter decreases. The increase is not great with decrease in size up to about 10 mm and the rise is steep below 3–4 mm.[14] This means if the burden contains a substantial amount of fines or breaks down into fines in the furnace, the resistance to gas flow will be so great that the furnace cannot be run effectively. The blast pressure will increase steeply and ejection of material and/or gas break-through in a certain portion of the impermeable bed may occur, resulting in excessive flue dust losses or in channelling. The fines may deposit by gravity in less permeable areas where the gas velocity and hence its kinetic energy is low. This reduces the voidage in those areas which further aggravates the flow difficulties which will be clear in the next section (cf. Ore Shift, Sec. 13.7).

5.4. Gas Flow – Multi-granular Packed Bed

For resistance to gas flow, more important than the particle diameter is the relative size of the materials in the bed.[14] In a mixed bed of widely varying particle size, the small particles land in the interstices of the large ones and decrease the voidage (Fig. 5.7a). Fig. 5.7(b)[15] shows the variation in voidage of spheres, sinters and ores of two different size fractions with differing particle diameter ratios. The term V_t is the total volume of the particles and V_s and V_l are the volumes of the small and large particles respectively with particle diameters d_s and d_l. The void fraction of the uniform sized bed is denoted by ε and that of the mixed bed by ε_m. For the case of spheres the values of ε are approximately 0.36–0.38 (voidage ranges from 25.95 to 47.64 percent for rhombohedral to cubic packing).[16,17] Starting with large uniform spheres, the voidage decreases as the small ones are introduced and the bed becomes more and more compact as the proportion of the latter increases. The bed is most dense, i.e., the voidage is minimum when 60–70 percent of the total volume of the particles consists of the large ones for about all the cases. The ε_m increases on either side of the minimum, i.e., with increasing or decreasing volume fraction of the small particles (approaching more uniformity of the size distribution). The pattern of pressure drop in such beds will be seen later (Fig. 5.9).

Fig. 5.7 also points to the influence of size ratios of the two different particles. The voidage decreases greatly as the ratio d_s/d_l decreases. This shows that for a good and uniform permeability and low resistance to

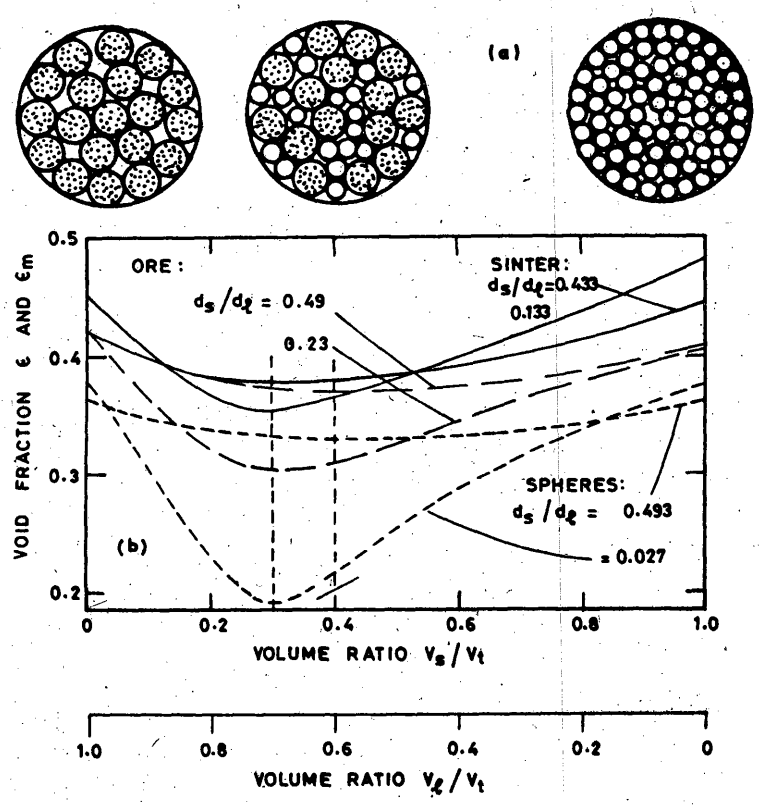


Fig. 5.7 (a) Left and right figures show packings of uniform large and small spheres and the middle that of a mixed packing of large and small spheres; (b) void fractions of mixtures of two sizes of ores, sinters and spheres of different size ratios, according to Jeschar et al.[15] (By kind permission).

gas flow in a mixed bed, the size fractions should be as narrow as possible. One can also visualize the adverse effects of a multi-granulur bed of particles of varying diameters on the voidage.

Simulation studies[7,8] on gas flow through multi-granular beds show that Eq. 5.6 can still be applied if the voidage is experimentally determined and the values of the diameters of uniform spheres modified to a *single equivalent diameter* as defined by Eq. 5.19. However, the relationship between the resistance parameter ψ and the Reynolds number Re′ changes slightly from Eq. 5.13 and is given by Jeschar[7] as,

$$\psi = \left(\frac{160}{Re'} + \frac{3.1}{Re'^{(0.1)}}\right)\left(\frac{\varepsilon_s}{\varepsilon_m}\right)^{0.75} \qquad 5.18$$

where,

ε_s = void fraction of bed of smallest diameter particles (uniform spherical)

ε_m = void fraction of bed of mixed spherical particles.

The equivalent diameter (d_e) of a particle in a mixed bed of uniform spheres is given by,[7]

$$d_e = \frac{1}{v_1/(v_t.d_1) + v_2/(v_t.d_2) + \ldots + v_n/(v_t.d_n)} \qquad 5.19$$

where,

$v_1, v_2, \ldots v_n$ = volumes of particles of each size fraction

v_t = total volume of all particles of different sizes

$d_1, d_2, \ldots d_n$ = diameters of particles of each type.

Polthier[8,15] has shown that Eq. 5.6 also holds good for packed bed of non-spherical particles if the diameter (d) is replaced by a representative diameter (d_r) which is defined as

$$d_r = \frac{1}{v_1/(v_t.d_{r_1}.\phi_1) + v_2/(v_t.d_{r_2}.\phi_2) + \ldots + v_n/(v_t.d_{r_2}.\phi_n)} \qquad 5.20$$

where,

d_r = mean diameter of spheres equal in volume to the non-spherical particles

$d_{r_1}, d_{r_2} \ldots d_{r_n}$ = diameters of spheres equal in volume for each type of non-spherical particles

$\phi_1, \phi_2 \ldots \phi_n$ = sphericity or form factor of particles of each fraction (Eq. 5.7).

From Eq. 5.6, the ΔP or ψ is not so much dependent upon the diameter of the particle as upon the voidage ε because of the factor $(1-\varepsilon)/\varepsilon^3$. Hence, for accurate calculations of pressure drop, the voidage should be determined experimentally and is given by

$$\varepsilon = 1 - \frac{M}{\pi r^2.\rho_s.H} \qquad 5.21$$

where,

M = mass of solids in a uniform column
r = radius of the column
ρ_s = density of the solids
H = height of the column

The importance of accurate determination of ε is shown in Fig. 5.8,[15] where the factor $(1-\varepsilon)/\varepsilon^3$ for uniform and mixed beds of some of the blast furnace charge materials is drawn against ε. It can be seen that the former term increases from 3 to 26 as the void fraction decreases from 0.53 for sinter of equal size to 0.30 for a mixed bed of spheres.

In the blast furnace, the charge may be assumed to consist of two components, coke and ore (or sinter, pellet) of varying sizes in alternate layers. For each component, an equivalent or representative diameter can be calculated using Eq. 5.19 or Eq. 5.20 and hence each layer be considered as a bed of particles of 'uniform size'. The relationship of ψ and Re′ also follows Eq. 5.13, valid for a bed of uniform size. The use of Eq. 5.6 would give pressure drop for each individual layers (Δp_1, Δp_2, etc.) which on summing up yield the total pressure drop ΔP for the entire bed height,[7]

$$\Delta P = \Delta p_1 + \Delta p_2 + \Delta p_3 + \ldots + \Delta p_n \qquad 5.22$$

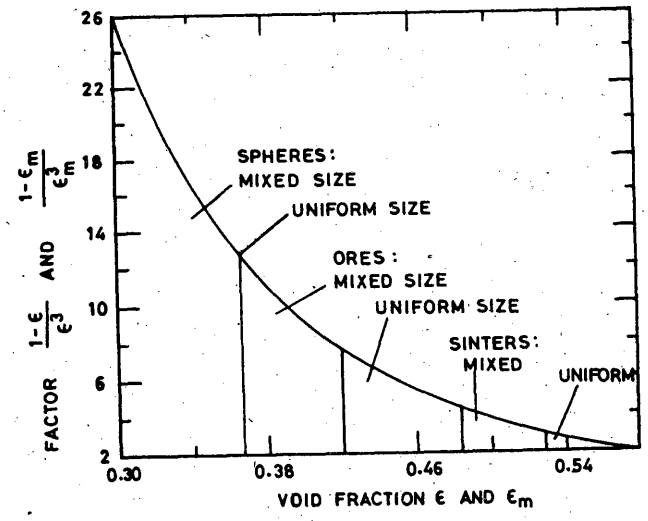


Fig. 5.8 Void fractions of blast furnace charge materials, according to Jeschar et al.[15] (By kind permission).

For each layer the pressure drop is given by

$$\frac{\Delta p_i}{H_i} = \psi_i \cdot \frac{1-\varepsilon_i}{\varepsilon_i^3} \cdot \frac{\rho_g \cdot w^2}{d_{r,i}} \qquad 5.23$$

During stock descent in the furnace shaft, the alternate layered structure changes to a mixed bed due to intermixing, especially at the phase boundary between the coke and ore, which greatly decreases the voidage and hence increases the pressure drop. This is illustrated in Fig. 5.9[15] in which a dimensionless *reduced pressure drop* of the form $(\Delta p.d_s)/(\rho_g.w_g^2.H)$ is shown as a function of the volume fractions V_s/V_t and V_l/V_t with variations of the parameter d_s/d_l. The voidage of the non-mixed bed has been taken as 0.38 whether for small or large spheres. Although Fig. 5.9 has been estimated for spherical particles, it should at least supply qualitative information in the case of a bed of non-spherical particles when the diameters are suitably modified as in Eq. 5.20.

For Fig. 5.9, the Reynolds number of the gas phase $Re = (w_g.d_s)/\nu_g = 1500$ has been calculated using the diameter of the smaller spheres. The diagram shows that the pressure drop increases several fold for the mixed bed compared to the layered one and that the pressure drop is higher the larger the size difference, i.e., the lower the d_s/d_l ratio. The

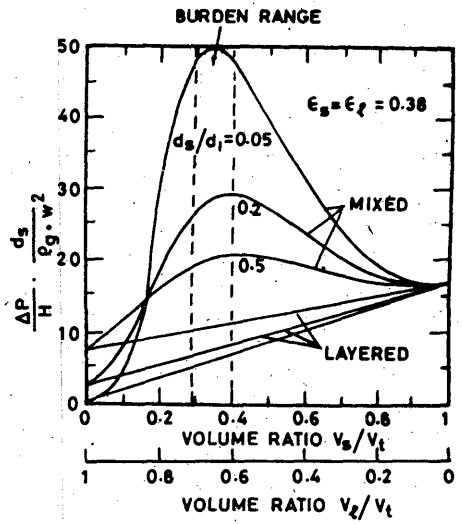


Fig. 5.9 Reduced gas pressure drops for separate layers and mixtures of spheres of two sizes and of different size ratios, according to Jeschar et al.[15] (By kind permission).

much smaller and linear rise in pressure drop as the V_s/V_t ratio approaches 1.0 in the layered beds is due to the effect of small diameter (Eq. 5.6). Since the size of the coke in the blast furnace is much larger than that of the ore, it is apparent that for any given size of the ore (selected for good reducibility and heat transfer) the larger the coke size the greater the pressure drop in a mixed bed while reverse is the case in the layered bed. It is unfortunate that for any given d_s/d_l ratio the maximum pressure drop is at V_l/V_t ratio of about 60 percent. In the blast furnace, the coke occupies about 60–70 percent of the furnace volume. Therefore, in the shaft where the materials are still solid, the optimum gas throughflow will be assured if the coke and ore are of similar size. However, as will be seen later, the liquid flow through the coke grid in the bosh is facilitated if the coke size is large and simulation studies of Bredehöft and Jeschar[18] have shown that a minimum pressure drop in the furnace is expected if the coke/ore size ratio is about 3–5.

The volume of voids which has the greatest influence on permeability is a function of close size range. According to Thibaut,[19] it is not the actual sizes but high size ratios that give higher voidage. As for example, coke size range 80–100 mm or size ratio 80/100 = 0.8 and 60–80 mm or size ratio 60/80 = 0.75 will have almost the same voidage, about 55 percent. Hence, the size ratios for any component should ideally be about 0.7, viz., size range of 40–60 mm, 30–40 mm, 20–30 mm etc.

The necessary close size fractions can be attained by proper crushing, screening and removal of fines before charging. However, the size fractions are not maintained during stock descent. Both ore and coke break down in the furnace due to abrasion, impact, compression, temperature and chemical actions. The ore undergoes cracking and decrepitation during reduction, generating fines. It also undergoes shrinkage, expansion (swelling) and compacting due to softening on load. All these changes lead to decrease in voidage or increased resistance to flow. Hence, for high productivity, the charge materials should possess high mechanical strength to withstand abrasion, impact and load as also minimal tendency of generation of fines, softening, swelling, etc. during reduction.

For higher production, an increasing volume of blast is necessary which will result in higher gas velocity in the furnace. From Eqs. 5.6, 5.11 and 5.13, in the laminar region the ΔP is directly proportional to gas velocity (w) and to $(w)^{1.9}$ in the turbulent region. Hence, as the velocity increases the dynamic pressure ΔP increases as $(w)^{1.9}$ and may give rise to instability of the bed if sufficient voidage is not provided.[13]

5.5. Bed Instability and Fluidization[13,20–22]

The charge in the blast furnace descends under gravity against the frictional forces of solids and buoyancy of gas. With increasing gas velocity, the pressure drop increases approximately quadratically until the upward thrust of the gas and downward thrust of the solids are held in balance. When this critical velocity is exceeded (the point of incipient fluidization), the packing in the bed becomes loose, the finer particles begin to *teeter* and the pressure drop ceases to increase, i.e., the resistance to gas flow drops (due to increase in voidage at places where the fines become suspended).

Mathematically, at the critical point, the pressure drop becomes equal to the bed weight per unit area, or

$$\Delta P/H = (1-\varepsilon_c).(\rho_s-\rho_g).g \qquad 5.24$$

where,

ρ_s = average density of solids, kg/m³
ρ_g = density of gas, kg/m³
g = gravitational acceleration, 9.81 m/sec²
ε_c = voidage at critical point.

From Eqs. 5.6 and 5.24, the critical gas velocity of fluidization (w_c) is given by

$$w_c^2 = \frac{(\rho_s-\rho_g).g.\varepsilon_c^3.d}{\psi.\rho_g} \qquad 5.25$$

From Eq. 5.25, under otherwise same conditions, the critical gas velocity which when exceeded the bed becomes unstable and solids may be blown up will be lower the lighter the particle and the smaller its diameter. The critical size (d_c) below which the particles will fluidize for a given gas velocity is derived from Eq. 5.25, assuming spherical shape of the particles and $\phi = 1$.

$$d_c = \frac{\psi.\rho_g.w_c^2}{(\rho_s-\rho_g).g.\varepsilon_c^3} \qquad 5.25$$

Neglecting ρ_g because of its very small value compared to ρ_s and converting to standard conditions (subscript o) with the help of Eq. 5.8,

$$d_c = \frac{\rho_{o,g}.\psi.w_o^2}{\rho_s.\varepsilon_c^3.g} \cdot \frac{T}{T_o} \cdot \frac{P_o}{P} \qquad 5.26$$

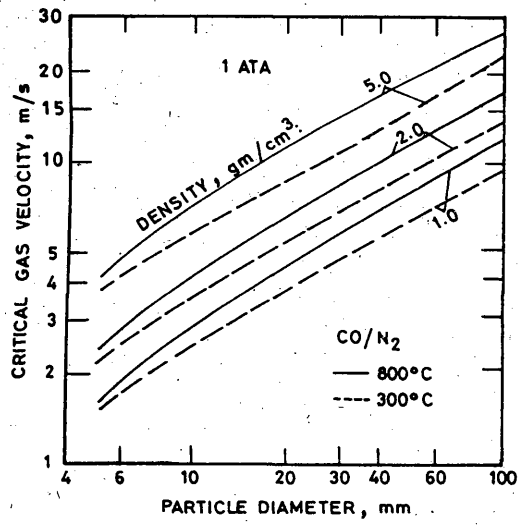


Fig. 5.10 Critical empty tube gas velocities of fluidization for different particle sizes and densities, according to Bogdandy et al.[22] (Copyright Verlag Stahleisen).

The critical empty tube velocities of fluidization for different densities and particle size are shown in Fig. 5.10.[22] The figure shows that for any given particle size, the lighter particles fluidize at lower gas velocities than the heavier ones. The densities of 5, 2 and 1 gm/cm³ approximate those of ore, limestone and coke respectively.

The nomogram (Fig. 11.21) shows the relationships between the critical particle size, furnace gas velocity (or gas throughput per unit shaft area), gas temperature, gas pressure and voidage. From Fig. 11.21, one can find out the critical fluidization particle diameter for any gas throughput (i.e., empty tube velocity) or the critical gas throughput for minimum ore and coke size. (The densities are, ore = 5000 kg/m³ and coke = 1000 kg/m³). If the voidage decreases locally at some place due to accumulation of fines or for any other reason, the critical diameter of the fluidizing particle will increase, depending upon its density. The coke being lighter than ore will be affected earlier. Fig. 11.21 also shows that the critical size can be decreased by the use of high top pressure which decreases the linear gas velocity (Table 5.3).

The relative increase in pressure drop with decrease in voidage can be seen from Eq. 5.29 derived from Eq. 5.6,

$$(\Delta P_2/H)/(\Delta P_1/H) = \frac{(1-\varepsilon_2)/\varepsilon_2^3}{(1-\varepsilon_1)/\varepsilon_1^3} \qquad 5.29$$

where subscripts 1 and 2 denote the change in pressure drop with the change in voidage from ε_1 to ε_2.

From Eq. 5.29, a decrease in voidage, say, from 40 to 30 percent can increase the pressure drop by about 300 percent. This means that in order to avoid charge instability (fluidization or ejection of solids from the shaft) and thus facilitate burden descent, the gas velocity (therefore, blast volume) has to be decreased which means a lowering of furnace productivity.

The radial distribution of gas in the furnace is inversely proportional to the resistance encountered and the gas flows along the line of best permeability. Since the size and density of the charge materials are different, they are distributed non-uniformly over the furnace cross-section and hence the critical gas velocity may be exceeded at some places. Normally, the fine particles are stationary in the interstices of large particles. On approach of the critical gas velocity the bed becomes loose, the finer particles are lifted up and remain in a suspended state and the pressure drop ceases to increase. As the resistance decreases, more and more of the gas rushes in the region. Finally, the finer particles, especially coke because of its much lower density, are blown out of the bed and, depending upon the density and particle size, are either emitted as flue dust or deposit as pockets where the gas velocity or permeability is lower. This *ore shift* (so-

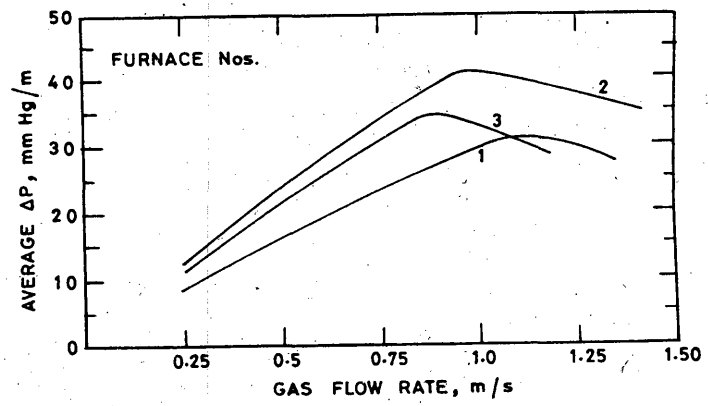


Fig. 5.11 Pressure drop in blast furnaces, according to Kegel.[23] (Copyright Verlag Stahleisen).

called because the ore being heavier settles down preferentially) leads to compactness of less permeable areas, further contributing to unevenness. The gas then flows through a system of distinct channels (called preferential flow of gases or channelling). The ore shift results in maldistribution of the gas and contributes to poor gas-solid contact; it may also cause hanging in the upper portion of the shaft, slipping and other furnace irregularities (Chapter 13).

An example of the adverse effects of high rate of blowing is found in the work of Kegel.[23] Fig. 5.11 shows an increasing pressure drop with increasing gas velocity in three blast furnaces charged with unprepared ores. The pressure drop ceases to increase when the gas velocity exceeds 1 m/s. Thereafter, the furnace takes more blast without any increase in blast pressure, indicating channelling. The ill effects of such preferential flow are:

(i) higher top gas temperature;
(ii) inadequate heating of stock;
(iii) high top gas CO/CO_2 ratio (inferior indirect reduction, i.e., inadequate utilization of chemical energy);
(iv) increased coke consumption rate;
(v) higher flue dust emission;
(vi) erratic metal quality.

It should be noted that the bed does not return to normalcy even when the blast rate is reduced to the value that caused 'teetering'. According to Furnas,[14] there is a hysteresis effect and the blast pressure is sometimes required to be brought down to as low as 0.1–0.2 atm. (gauge).

The importance of close size range of the charge materials, removal of fines, use of materials of adequate strength that do not break down in the furnace, is immediately obvious for forcing of the blast furnace for higher production. For ferrous materials, since smaller size facilitates heat and mass transfer (Fig. 5.6) but increases the resistance to flow of gases, a suitable compromise is usually made. The ideal will be the largest possible surface area and minimum possible resistance to flow of gases. Since resistance to flow does not increase greatly above particle diameter of 10–12 mm (Fig. 5.6), large new surface can be created by crushing lumps into small pieces, as is apparent from Table 5.2. As for example, one 8 cm lump is equivalent in volume to 512 of 1 cm pieces. The surface area per unit volume of 1 cm piece is eight times that of 8 cm piece and new surface generated is 1536 cm^2 compared to 192 cm^2 in the case of 8 cm lump.

Table 5.2. Approx. relationship between surface area and volume of spheres

Diameter, cm	Surface/ volume ratio	Number of small spheres of different sizes which occupy the same volume		
		2 cm	1.5 cm	1 cm
8	0.75	64	150	512
6	1.00	27	64	217
4	1.50	8	19	64
2	3.00	1	2.5	8
1	6.00	–	–	1

We have hitherto considered resistance to gas flow through a bed of solids. Depending upon the nature of ferrous charge, temperature and extent of reduction, these materials soften prior to melting in the blast furnace, resulting in the diminution of voidage. The larger the temperature range of softening, i.e., the greater the vertical distance of existence of the softened materials the greater will be the overall resistance to gas flow (Eq. 5.22). This affects the gas distribution in the shaft and hence gas utilization and thus exerts a great influence on the coke consumption rate and iron production. The effect of diminution of voidage by softening is apparent from Eq. 5.29.

Fortunately, due to pre-burning and pre-fluxing of the ferrous materials (sintering and pelletising), the softening temperature range has narrowed down and softening temperatures have also increased from 700–800°C for raw ores to above 1000°C for the prepared burden. This has helped in a phenomenal increase in blast furnace output over the last two decades (see also Secs. 6.5.2 and 11.5).

5.6. Gas Flow in Bosh (Wet) Zone

Productivity may be limited by either excessive pressure drop leading to fluidization of solids in the shaft or by liquids hold-up in the bosh. In the bosh region, coke is the only solid material present and the tuyere gas flows upwards and the liquids (liquid iron and fluid or semi-viscous slag) downwards through the interstices of the coke grid. Since these liquids

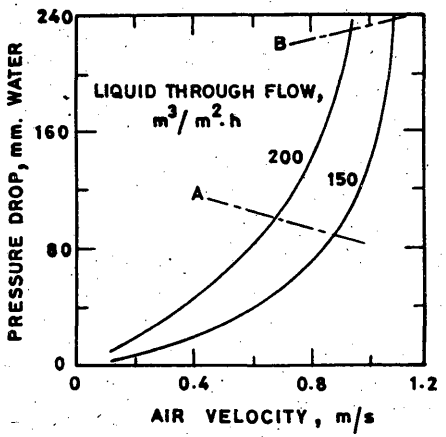


Fig. 5.12 Dependence of pressure drop in an irrigated packed column on the gas velocity and liquid flow rate, according to Hansen.[24] (Copyright Verlag Stahleisen).

reduce the free cross-section available for the flow of gases, the pressure drop will increase with increased liquids throughput for constant gas velocity or for a fixed liquids throughput it would do so with increased gas velocity. This increased resistance to gas flow may result in liquid hold-up (*loading*) in the coke voids. This would lead to further diminution of free volume, steep rise in pressure drop with slightest increase in gas velocity and finally as the gas has to bubble through a mass of liquids, much of the latter may be carried upwards mechanically leading to the so-called *flooding*. The phenomenon is shown schematically in Fig. 5.12,[24] where A and B are the *loading* and *flooding points* respectively.

The relation between gas and liquid flow through a packed column has been studied by Sherwood et al.[25] and others.[12,22,26-28] Beer and Heynert[28] have used the Sherwood equations to determine the flooding limits in blast furnaces, calculating the *flooding factor*, f and the *fluid ratio*, k. The limiting flooding curve is shown in Fig. 5.13[28] which is approximately represented by Eq. 5.30.[22] The flooding or *hanging* factor is essentially a balance between the opposing forces of the gas and liquid in the coke grid and the fluid ratio is relative mass flow of liquids and gases:

$$\log f = -0.559 \log k - 1.519 \qquad 5.30$$

where,

$$f\ (\text{flooding factor}) = \frac{w^2}{g}\frac{F_s}{\varepsilon^3}\cdot\frac{\rho_g}{\rho_l}\cdot\eta^{0.2} \qquad 5.31$$

$$k\ (\text{fluid ratio}) = \frac{L}{G}\left(\frac{\rho_g}{\rho_l}\right)^{1/2} \qquad 5.32$$

From Eq. 5.30, the critical condition for hanging is,

$$f^2.k \approx 10^{-3} \qquad 5.30a$$

and the furnace may start to hang if $f^2.k$ exceeds 0.001.

The meaning of the various terms are:

w = superficial tuyere gas velocity (empty tube), m/s
F_s = surface area of coke, m^2/m^3 of packed column
ρ_g = density of tuyere gas, kg/m^3
ρ_l = density of bosh slag, kg/m^3
L = superficial mass flow rate of bosh slag, kg/m^2h
G = superficial mass flow rate of tuyere gas, kg/m^2h
ε = voidage of coke grid
η = viscosity of bosh slag, cP
g = gravitational acceleration, m/sec^2

From Eqs. 5.31 and 5.32, the flooding factor depends mainly on the gas velocity (blast volume) and the fluid ratio on the slag quantity, provided other quantities in the equations remain constant, which they usually do in a furnace running with fixed raw materials. It is assumed that, iron being heavier, flooding confines to the slag which is lighter. However, liquid

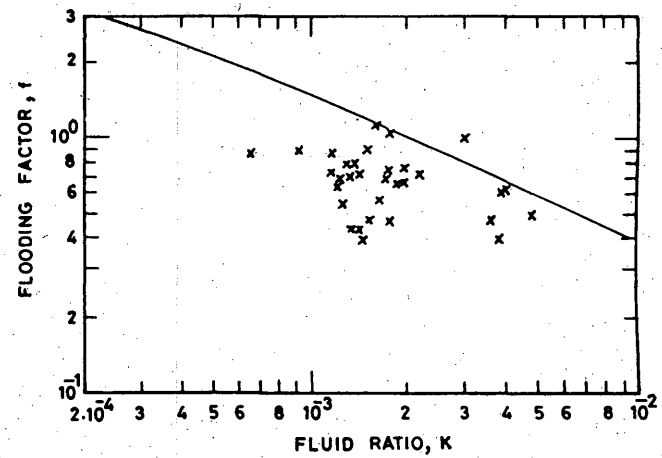


Fig. 5.13 Relationship between flooding factor and fluid ratio. The values calculated from the data of various furnaces are shown by the crosses. After Beer and Heynert.[28] (Copyright Verlag Stahleisen).

iron also decreases the voidage in the coke grid. Hence, Polthier[21] has taken into account the mass of iron also for calculating the irrigation density in Fig. 5.14.

If the blast volume is increased to obtain a greater driving rate, loading may start at first at a place where conditions are adverse. The resulting local non-uniform flow of slag and gas would raise the gas velocity elsewhere. The resistance to gas flow will increase which will be accentuated the more viscous the slag. Hence, new sites will become loaded and the number of partially blocked voids will increase progressively till the gas permeability becomes very low in the entire cross-section of the bosh. The blast pressure would increase continuously and the kinetic energy of the gas would push the slag up and flood the bed. In extreme cases, the slag may be carried upwards into the lower temperature zone where it will freeze and choke the voids, further aggravating an already bad situation. As a consequence of flooding the furnace refuses to take substantial quantities of blast and starts to hang. On decreasing the blast velocity by decreasing the blast volume and/or temperature, the slag will again flow and the furnace take air. In case the re-solidified slag has formed a strong arch above the bosh, continued blowing of air burns the coke underneath. This may result in a sudden collapse or slip and the descent of relatively cold and inadequately pre-reduced material into the hearth is apt to seriously deteriorate the thermal state of the hearth or even chill it. It can even cause damage to bosh refractories. Thus the blast volume, which determines the coke burning rate and hence the productivity, is limited by the liquids volume (and also slag viscosity). Running with lower blast temperature increases the coke consumption per tonne of iron which again lowers the productivity.

The limiting flooding curve is drawn in Fig. 5.13. The curve falls as the fluid ratio increases which means the productivity will fall with decrease in burden yield (higher slag volume) because lower blast volume and lower blast temperature have to be used for smooth running of the furnace. Eq. 5.31 also shows the benefit of low viscosity and high density of bosh slag and that of low coke surface area. Since the larger the coke size the smaller the surface area, use of large strong coke lumps which retain their optimum size during descent to the bosh facilitates gas and liquids throughflow in the bosh zone. However, large coke/ore size ratio increases the pressure drop in the dry zone (shaft) and hence a suitable comprise is made. As mentioned earlier, coke size 3–5 times larger than the ore has been suggested for optimum gas throughflow in both the dry and wet zones.[18]

The operational viscosity of the bosh slag increases several fold because of formation of foam and emulsion as the bosh gas churns through the streaming liquids. The increased viscosity is apt to promote flooding. However, according to Rikhter et al.[29] the gas permeability in the wet zone is affected less by the viscosity than by the density of the slag since, with the pressure drop prevailing in the lower furnace, about 60 percent of the slag must descend along with the coke in the grid. The amount of gas at which flooding begins increases by:

(i) 3 percent if the slag viscosity decreases by 0.1 Poise;
(ii) 1 percent if the slag density increases by 0.1 gm/cm^3;
(iii) 1 percent if the slag bulk decreases by 100 kg/THM.

Fig. 5.13 shows the values of flooding factor and fluid ratio for some small, medium and large furnaces. The larger furnaces generally work much below the flooding limit. In the figure, the furnaces which are near the flooding limit are either small ones or are working with high operating intensity.

The Sherwood diagram (Fig. 5.13) suffers from the drawback that both the coordinates contain gas terms and the ordinate is not dimensionless which render the interpretation of the diagram difficult. A new loading and flooding diagram has been suggested by Mersmann[30] who used it originally to study countercurrent flow of gas and liquid in an irrigated packed-bed column where the liquid descends as a film along the column wall. In this diagram (Fig. 5.14) the calculated dimensionless pressure drop in the dry (non-irrigated) bed is shown as a function of dimensionless irrigation density. The dimensionless irrigation density b is given by[21,30]

$$b = \sqrt[3]{\frac{\nu_l.B.(1-\varepsilon)}{g^2.\phi.d_r.\varepsilon}} \qquad 5.33$$

and the dimensionless pressure drop in the dry bed by

$$\Delta p_t/g.\rho_l.H = \psi.\frac{\rho_g.w_g^2.(1-\varepsilon)}{g.\phi.d_r.\rho_l.\varepsilon^3} \qquad 5.34$$

Most of the terms have been discussed in Eq. 5.6. The new terms are:

ν_l = η_l/ρ_l = kinematic viscosity of slag, m^2/s
g = gravitational acceleration, 9.81 m/s
B = irrigational density of iron and slag, m^3/m^2.s
$\phi.d_r$ = form factor x representative diameter of coke, m

w = operational gas velocity, m/s
Δp_t = pressure drop in dry, non-irrigated bed.

Fig. 5.14 shows the loading and flooding limits.[21,31] For constant irrigational density, the dry bed pressure drop Δp_t increases with increasing gas velocity and a stage will be reached when the coke grid will be flooded. On the other hand, as the flooding curve slopes steeply downwards, the limit is reached at much lower gas velocities with increasing irrigational density. The figure also contains lines of constant dimensionless total pressure loss $\Delta p/g.\rho_l.H$ in the irrigated bed as well as lines (dotted) of constant relative liquid to void volume ratio V_l/V_ε, i.e., the liquid-filled fraction of the voids which should attain a value of unity at the flooding limit. The latter vertical lines depend only upon the irrigational density under the loading limit.

Polthier[21] has calculated the dimensionless terms from operational data of three groups of furnaces based on hearth diameters. The calculations show that while most furnaces operate above the loading level, the larger ones do so far below the flooding level. Furnaces with very high operating intensity work almost at the flooding limit (Fig. 5.14). This tendency is

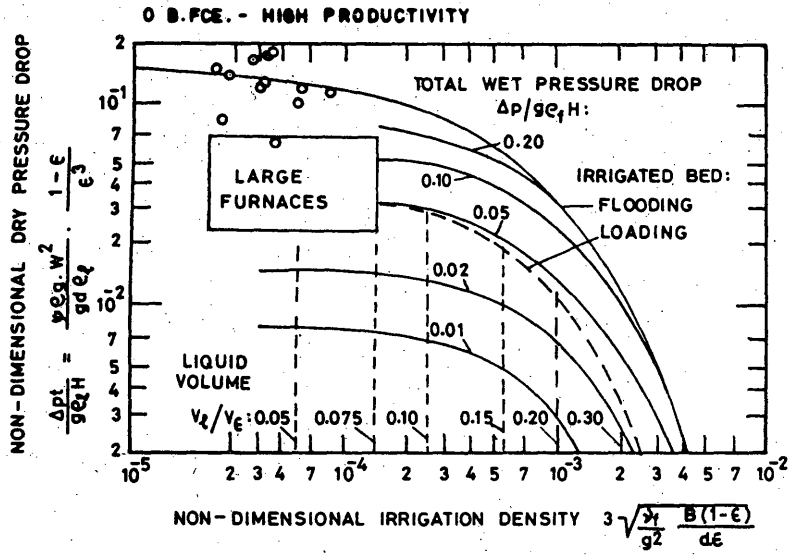


Fig. 5.14 Flooding diagram with some blast furnace performance; large furnaces work below the flooding limit and the limit is approached as the furnace diameter decreases and/or the operating intensity increases. After Polthier[21] and Jeschar et al.[31]

also apparent from Sherwood's flooding limit (Fig. 5.13). This suggests that the productivity of modern high capacity furnaces is not limited by the flooding in the wet zone but rather by the bed instability and fluidization in the upper dry zone. One must however bear in mind that for Figs 5.13 and 5.14 the gas velocities for the flooding limits were calculated on the basis of total hearth area without consideration of the dead man's zone or maldistribution of the liquids and gas over the furnace cross-section. These velocities would be much larger if the raceway area only is taken into account for calculating the gas velocities. Since the depth of blast penetration in the raceway is only 1–2 metres, the ratio of raceway area/hearth area is smaller the larger the furnace. Hence, the larger furnaces appear to operate much below the flooding limit. The author has calculated some values based on 2 m raceway and they show that the flooding limit is approached in the high capacity furnaces as well. That flooding may actually limit productivity is discussed in Sec. 11.5. In addition, the operational slag viscosity is much higher than that determined in the laboratory.

The nature of the flooding curve also depends upon the wetting properties of slag and coke. Although no work has yet been done in this field, it appears that the surface tension of the slag may have a bearing on the flooding level. Cold model experiments with various liquids show that the level increases with increasing surface tension of the liquids as is shown in Fig. 5.15.[32] Flooding limit is higher with non-wetting slag than with the wetting ones. The limit is lowered when the slag tends to froth. Low surface tension and the presence of FeO and $2CaO.SiO_2$ increase the frothing tendency.[33]

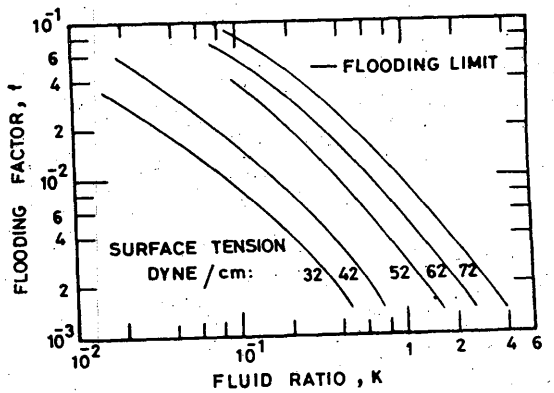


Fig. 5.15 Influence of surface tension of the liquid on flooding limits in irrigated beds.[32]

According to Warner,[34] the Sherwood equation which is applicable to irrigated packed-beds in chemical engineering may not apply to the very different conditions prevailing in the blast furnace bosh zone. This is because the volume of the coke voids occupied by liquids is small, the volume being about 0.18 percent of the total bosh volume. This small amount of liquid and the non-wetting tendency of the coke surface by the slag are not expected to affect the gas flow to any great extent. Warner suggests a different mechanism of slag hold-up in the bosh based on the Archimedes Principle expressed as *an object will float when its density is equal to the pressure gradient in the medium within which it is immersed.*

The slag, being much lighter than iron, while flowing down through the coke grid will become suspended by the upward thrust of the gas when the gas-pressure gradient is equal to the downward force of gravity. The equation describing the slag hold-up by means of buoyancy is given by:

$$dp/dH = \rho_s . g/g_c$$

where,

dp/dH = gas-pressure gradient
ρ_s = slag density
g/g_c = ratio of gravitational acceleration and gravitational constants.

Warner has successfully used the above equation for describing slag hold-up in Port Kembla blast furnaces.

Two major areas where slag hold-up may be caused by this phenomenon are:[35]

(i) softening-melting zone (Fig. 11.24), where the burden materials begin to soften resulting in areas of low permeability and, therefore, of high pressure gradients;
(ii) raceway zone immediately above the tuyeres, where the gas velocity is high because of high blast temperature and the gas distribution across the cross-sectional area is poor.

According to Jourde and Huck,[36] it is the total quantity of slag and iron that flows through the coke grid which determines the blast intake of a furnace since the gas has to pass through the descending liquid mass in the coke voids. They suggest a limit of 15–17 m^3 of the total iron and slag volume per m^2 of the hearth area per day. The author has also arrived at the same figure from calculations of data of furnaces producing

6000–12 000 tonnes of iron per day. What significance this figure has is difficult to surmise.

5.7. High Top Pressure (HTP)

If it is desired to blow more air to increase the furnace output, a stage may reach when the gas velocity exceeds the critical limit of flooding or fluidization, resulting in hanging, slips and irregular furnace operation. However, furnaces can be forced even with conventional burden materials if the linear gas velocity is reduced with the help of HTP or oxygenated blast. Since the furnace output increases as more coke is burnt per unit time, both the above methods permit an increased oxygen input without any simultaneous increase in pressure fall. In the conventional furnace the top is almost open to atmosphere. If the top pressure is increased with suitable valves and seals at the top, an increased blast pressure will be needed at the bottom to maintain the same pressure drop. For a constant blast volume the average gas pressure in the furnace and, therefore, the density of the gas will increase with corresponding decrease in the volume and linear velocity of the gas. As a consequence, for the same pressure drop from the hearth to the top, a greater volume or mass of blast can be blown (because of increased gas density) than in the conventional furnaces using the same raw materials and producing the same amount of flue dust.

At a constant blast rate (hence gas rate), a given furnace and raw materials and other identical conditions, the relationships between the blast pressure, top pressure, linear gas velocity, etc. can be calculated approximately with the help of Eq. 5.9.

From Eqs. 5.9, 5.11 and 5.13, the pressure drop varies as w_o^n where $1<n<1.9$ depending upon the extent of turbulence. Combining some of the constants of Eq. 5.9 into a factor K and rewriting the equation in a differential form,

$$-\frac{P\,dP}{dH} = K.T.\,w_o^n \qquad 5.35$$

Since under constant working conditions T and w_o are also constants, therefore, integrating Eq. 5.35 between P_b and P_t along the furnace height from the tuyere to the stock level, i.e., from 0 to H, we get

$$P_b^2 - P_t^2 = 2KTw_o^n H \qquad 5.36$$

$$\approx K'V^n \qquad 5.37$$

where,

P_b = bottom (tuyere) pressure
P_t = top gas pressure
K,K′ = factors depending upon the given furnace, its height, temperature profile, raw materials, blast volume, etc.
V = volume of blast (or tuyere gas since they are inter-related), usually depicted as Nm^3 per m^2 of hearth area per unit time.

Using subscripts 1 and 2 for the cases *before* and *after* introduction of HTP, from Eq. 5.37,

$$(P_{b_1} + P_{t_1})(P_{b_1} - P_{t_1}) = 2P_1.\Delta P_1 \approx K'.V^n \qquad 5.38$$

where,

ΔP_1 = pressure drop without HTP
P_1 = average furnace gas pressure without HTP
$= (P_{b_1} + P_{t_1})/2$

Also

$$P_{b_2}^2 - P_{t_2}^2 \approx K'.V^n = 2P_2.\Delta P_2 \qquad 5.39$$

From Eqs. 5.38 and 5.39, assuming factor K′ to be constant,

$$P_{b_2} = (2P_1.\Delta P_1 + P_{t_2}^2)^{1/2} \qquad 5.40$$

$= $ bottom pressure with HTP

Suppose a furnace of volume 1200 m^3 and blast rate of 2400 $Nm^3/m^2.h$ is working with $P_{t_1} = 1.1$ ata and $P_{b_1} = 2.5$ ata so that the pressure drop,

$$\Delta P_1 = 2.5 - 1.1 = 1.4 \text{ atm.}$$

And,

$$P_1 = (2.5 + 1.1)/2 = 1.8 \text{ ata}$$

If now the pressure at the top (P_{t_2}) is raised, the respective bottom pressures calculated from Eq. 5.40, the corresponding pressure falls and percentage decrease in linear gas velocities will be as shown in Table 5.3.

Table 5.3. Variations of blast pressure, pressure fall and percent decrease in gas velocity with HTP

P_{t_2} (HTP) ata	P_{b_2} (HTP) ata	Pressure drop		Decrease in linear gas velocity, percent (approx.)
		ΔP atm.	Percent	
1.1	2.5	1.4	100	0
1.5	2.7	1.2	85.7	14.3
2.0	3.0	1.0	72.1	24.9
2.5	3.36	0.86	61.4	38.6
3.0	3.75	0.75	53.6	46.4

It will be seen from Table 5.3 that the pressure drop is steep with HTP in the beginning and it later flattens with increasing top pressure. The linear gas velocity decreases greatly.

If we intend to blow 30 percent more blast, i.e., 3100 Nm^3 instead of 2400 $Nm^3/m^2.h$ in order to increase the coke burning rate (hence productivity) by approximately 30 percent at the same time keeping the linear gas velocity and the pressure drop the same, i.e., $\Delta P_1 = \Delta P_2 = 1.4$ atm., the bottom and top pressures necessary for achieving this can be calculated as follows:

From Eqs. 5.38 and 5.39, assuming K′ = constant, n = 1.75 and $V_2 = 1.3\ V_1$,

$$\frac{P_2}{P_1} = 1.3^{1.75} = 1.565$$

where,

P_2 = average gas pressure with HTP
$= (P_{b_2} + P_{t_2})/2$

In the example quoted above,

$$P_1 = 1.8 \text{ ata}$$

Therefore,

$$P_2 = 1.8 \times 1.565$$
$$= 2.82$$

Since $\Delta P_2 = 1.4$ atm. (identical to that before HTP), therefore,

$$P_{b_2} = P_{t_2} + 1.4$$

However,

$$P_2 = 2.82 \text{ ata} = \frac{P_{b_2} + P_{t_2}}{2}$$

$$= \frac{(P_{t_2} + 1.4) + P_{t_2}}{2}$$

Therefore,

$$P_{t_2} = 2.1 \text{ ata}$$

and

$$P_{b_2} = 2.1 + 1.4 = 3.5 \text{ ata}$$

The blast volume and therefore the coke throughput can be increased by 30 percent with the maintenance of identical pressure drop and gas velocity conditions in the blast furnace by increasing the top pressure to 2.1 from 1.1 ata and bottom pressure to 3.5 from 2.5 ata under the given blowing conditions.

5.7.1. Advantages of HTP

The preceding section showed an approximate estimate of expected increase in output with the use of HTP. However, the actual benefits likely to accrue depend upon the raw materials and other blast furnace parameters. The advantages are:

(i) for the same volume flow rate, a greater mass of air (hence, oxygen) can be blown with HTP; higher output;
(ii) increased reduction rate with increased total pressure and hence decrease in direct reduction (fuel saving);
(iii) suppression of Boudouard reaction ($CO_2 + C = 2CO$) and hence savings in fuel;
(iv) increased carbon deposition ($2CO = CO_2 + C$) has both advantages and disadvantages (Secs. 3.5 and 7.2.5);
(v) more uniform distribution of gas velocity and reduction across furnace cross-section; smoother furnace operation due to increased permeability;

(vi) lower input of iron oxides in the hearth, improved hearth temperature, lower silicon and sulphur in iron;
(vii) less fluidization of fines and less number of slips;
(viii) less flooding tendency in the wet zone and less number of checks;
(ix) less flue dust losses, less variation of coke input, better maintenance of the thermal state of the hearth, more uniform iron analysis; less thermal reserve in the stove necessary;
(x) benefits higher with unprepared burden or super-large furnaces due to lowered gas velocity and more uniform radial gas distribution;
(xi) increase in the metal tapping rate.[37,38]

5.7.2. HTP Equipment

High top pressure necessitates providing of equipment for operation up to 4 ata. The use of HTP leads to excessive wear of the bell seats, leakage of gas, wear of refractories, charging difficulties etc. The details of the improvements in the design, equipment and operation necessary have been described.[37,38]

5.8. Stock Distribution and Charging

Blast furnace productivity depends upon the quantity of air that can be blown in unit time. The quantity of gas that can be accepted is governed by the uniformity of voidage and particle size both of which depend upon proper material distribution in the stock column. We have seen that the resistance to gas flow (as measured by Δp) can increase by 300 percent for a decrease in voidage by 10 percent. Since the ascending gas finds the path of least resistance, the gas will prefer to flow through areas of best permeability, i.e., areas where the largest and uniform sized particles accumulate. The resulting non-uniform flow of the gas in other localities leads to an inadequate utilization of its thermal and chemical energies and hence to an inferior fuel efficiency.

The blast furnace charge consists of different sizes of coke and ore (also sinter, pellet, limestone) with different physical properties and it is difficult to distribute them at the top of the stock column, with our conventional system of charging at the periphery, in a manner that the entire vertical and horizontal cross-sections of the furnace would offer equal resistance to gas flow. During charging, the materials tend to segregate radially according to their nature, size and density. Non-uniform radial distribution of charge materials results in a non-uniform radial distribution of particle

size, voidage and hence that of permeability of the stock column. The resulting non-uniform radial distribution of the gas flow rate affects the charge flow rate and *vice versa*. As the stock line pattern has been found to persist during descent (cf. Fig. 7.4), much attention has been given to obtain an optimal material distribution at the top.[39,45] Proper charging is also of much importance even at present although modern furnaces use more uniform sized materials compared to earlier methods of charging raw ores with their fines, rubbles and lumps and coke of varying sizes. It should, however, be noted that an uneven distribution of material helps in forcing of the furnace for greater production although it increases the coke rate. It promotes the throughflow of gas and enhances the rate of material descent.

Model experiments of Peetz and Winzer[44] show that the stock line cross-section can be divided into three zones:

(i) peripheral;
(ii) intermediate;
(iii) central.

The intermediate zone consists of about 50 percent of the total cross-sectional area and 30–35 percent of the total gas passes through this area. Each of the peripheral and central zones consists of about 25 percent of the area and irrespective of radial segregation 65–70 percent of the gas always passes through them. Actual blast furnace data studied by the author tend to approximately confirm this. Since a major quantity of the gas passes through the outer and inner zones, a uniform permeability in these two regions is desirable. It is possible to attain this aim to a certain extent by proper material distribution at the top with the help of proper charging cycles and gears.

Although the blast furnace produces iron continuously, the charging is performed intermittently. In our conventional charging system, the skip unloads the materials into a rotatable hopper or distributor (Fig. 5.19) mounted on the small bell, the latter emptying the mass into the big bell for final discharge or *dumping* in the furnace (the distributor rotates in order to distribute the material around the big bell circumference). Usually six (sometimes three or four) small bell charges make up a big bell charge after which the latter is dumped. The charge sequence is usually written as, for example, OOCCOO/ where O denotes ore, C coke and the stroke 'dumping'. Sinter, pellet, limestone are denoted by S, P and L.

The distribution of materials when dumped in a heap on a stationary bed has largely to do with two natural laws:

(i) the finer particles tend to accumulate in a peak or ridge and the rubbles and lumps slide down to a distance according to their kinetic energies, the largest going the farthest;
(ii) two different materials dumped under the same conditions tend to have their surfaces at different angles with the horizon, i.e., they have different angles of repose. The angles of repose of ore and coke layers generally vary between 30–35° and 34–40° respectively, depending upon their moisture content, coefficient of friction and size, the smaller particles having greater angles than the larger ones. The angles of repose of some of the charging materials are shown in Table 5.4. However, in an operating furnace the material distribution does not occur as expected from the angles of repose.

When the big bell is dumped, the charge slides down the bell surface and takes a parabolic path during the fall. This results in a varied nature of accumulation of the materials on the stock surface, the chief influences on it being:[39,43]

(a) friction of the materials on bell surface; the larger particles having smaller coefficients of friction than the finer ones;
(b) bell angle, usually between 50–55°. This angle assures a rapid slide of the materials and they do not stick on the surface;
(c) bell/throat (diameter) ratio or the distance between the bell lip and throat inwall, i.e., whether the materials will hit the inwall directly on bell lowering;
(d) charging distance or stock depth, i.e., height of the bell bottom, when fully lowered, above the stock line;
(e) bell lowering time.

Table 5.4.[46] Angles of repose of blast furnace charge materials

Material	Sinter	Pellet	Coke	Raw ore
Angle of repose in degrees	31–34	26–28	35–38	33–35
Mean size, mm	20	11	45	18
Size range, mm	5–30	8–14	25–75	10–30

On dumping, as the materials fall on the stock surface, they take a parabolic path and mainly two different profiles of the accumulated mass emerge depending upon whether the particles hit the inwall directly (V-

shape) or the stock surface (M-shape). The V-shape is generally obtained corresponding to the parabola of fall when the bell lip is near to the inwall, i.e., the bell/throat diameter ratio is high or the charging distance is large (Fig. 5.16, right).[44] In such a profile, the ore fines because of high coefficient of friction and higher angle of repose will tend to accumulate at the place where the material falls on the stock surface whereas the larger pieces roll down and spread towards the centre. The coke particles are much larger than the ore in size and hence they also spread towards the centre and much more so than the ore. Thus, the coarse material is generally in the centre (predominantly coke) and the finer material accumulates in an annulus directly under the bell circumference. Hence in a V-profile the periphery becomes partially blocked (the extent depending upon the size distribution of ore before charging) and a major volume of the gas will tend to pass through the centre and its thermal and reduction potential only partly utilized because of the predominance of coke in the region. A probe in the region should show high temperature and CO/CO_2 ratio or low η_{CO} of the gas. This is confirmed in Fig. 7.4 where the ore/coke ratio is the lowest in the centre at all furnace levels. (See also Fig. 7.5).

For a more uniform distribution of gas, both the periphery as well as the centre should be loosely packed (too much peripheral flow is avoided when the inwall becomes overheated since the ore, if there is a lot of fines,

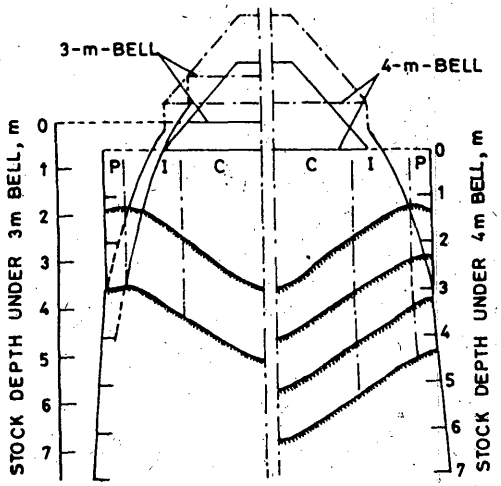


Fig. 5.16 Parabola of fall of charge materials and the burden profile when using 3 m and 4 m bells, according to Peetz and Winzer.[44] P = peripheral, I = intermediate and C = central zones. (Copyright Verlag Stahleisen).

may stick on the refractory and also to reduce wall-heat losses). Such an even distribution of permeability is obtained from an M-shaped profile where the fines accumulate on the ridge and larger particles roll down on either side of the peak. The M-profile itself is generally obtained if the material strikes the stock surface. This happens when the bell/throat diameter ratio is small (larger bell-inwall distance) or the charging distance is small (Fig. 5.16, left). It is clear that the peak of the M-contour approaches the inwall (hence the peripheral permeability decreases) as the charging distance increases and ultimately the M changes to V profile. This will happen earlier the larger the bell/throat diameter ratio (compare left and right sides of Fig. 5.16). The percentage of gas passing through the periphery will increase as the ridge extends towards the centre and the central flow decreases correspondingly due to axial compaction. The concentration of larger particles will increase towards the inwall as the peak moves farther away, stimulating peripheral flow.

The above discussion can be summed up with the help of the model experiment of Peetz and Winzer[44] (Fig. 5.17). The left side of the figure

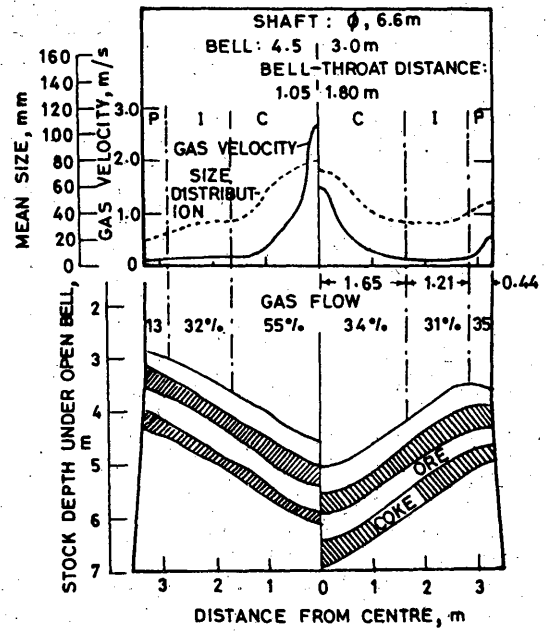


Fig. 5.17 Gas velocity and particle size distribution with V and M burden profiles. The relative gas flows in the P, I and C zones (cf. Fig. 5.16) are also shown. After Peetz and Winzer.[44] (Copyright Verlag Stahleisen).

shows a V-contour with 4.5 m bell diameter and the right side an M-contour with 3 m bell diameter, the distances between the bell lip and the throat inwall being 1.05 and 1.80 m respectively. The distribution of gas velocity and particle size as well as the percentage of gas flow through the three zones are also shown. These are, as expected, more uniform in the case of M-contour. In the case of V-contour, the peripheral and central gas distributions were 13 and 55 percent compared to 35 and 34 percent respectively for the M-contour. The concentration of larger particles and high gas velocity in the centre are immediately obvious in the case of V-contour.

In an operating furnace, it is not possible to alter the bell-throat diameter ratio and hence the stock profile can only be modified by adjusting the

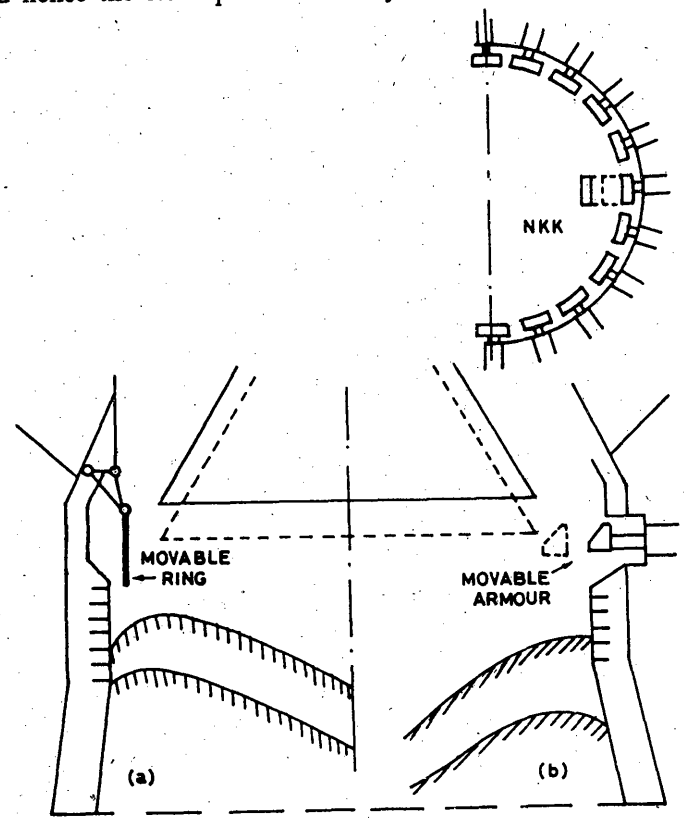


Fig. 5.18 **(a)** Control of burden profile with movable deflecting ring; **(b)** control of burden profile with movable armour at NKK, according to Higuchi et al.[36] (By kind permission).

charging distance (by accelerated or delayed dumping) and finding out the optimum gas distribution. This is done by inserting gas probes radially below the stock level and lower down in the shaft at different distances from the inwall towards the centre. A low temperature and high $\%CO_2$ of the gas indicate compactness of the area and reverse is the case at places of excessive gas throughflow.

It is possible to alter the profile if the furnace is fitted with *deflecting ring* placed in-between the bell and the throat inwall, capable of moving vertically up and down (Fig. 5.18a). The ring may be raised or lowered to place the burden on the stockline and obtain an M or a V profile according to will at any charging distance. A more versatile system (movable armour) operates by pushing segments of the ring horizontally from the sides of the throat (NKK type – Fig. 5.18b).[38] The great increase in productivity by the use of NKK gears is discussed in Sec. 11.3.2.10.

In addition to material segregation discussed above, the distribution pattern can also be affected by the ratio of the height and the diameter of the receiving hopper. Fig. 5.19(a)[47] shows too small a ratio and a considerable segregation can occur from the small to the big bell which is apt to persist in the furnace itself as is clear from the lower diagram. Fig. 5.19(b)[47] shows a narrower and taller hopper where the material distribution is uniform. According to Pawlow,[48] the diameter of the hopper should not exceed 1.5 m with a maximum of 1.8 m for large furnaces, the height/diameter ratio ranging from 3 to 4. Wrong dimensions can lead

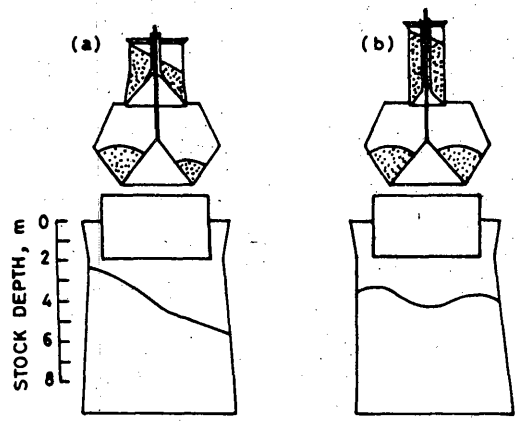


Fig. 5.19 Material distribution pattern in a blast furnace with the use of different height to diameter ratios of the receiving hopper, according to Brandi et al.[45] (Copyright Verlag Stahleisen).

to higher flue dust emission, higher coke rate and irregular furnace movement.

An important development of the 1970s is the use of bell-less top gear which enables the charge to be distributed selectively over the entire furnace throat cross-section by means of a rotating distribution chute.[37,60] The advantage of bell-less top in the manipulation of the shape of the softening-melting zone in the furnace will be seen in Sec. 11.5.

5.8.1. Charging Cycle[45]

There is one further operating variable, the charging cycle or sequence, which has been found to be very useful for changing the gas distribution and stock descent in a running furnace. In a model experiment by Wild,[40] it was demonstrated that the material placed first on the big bell will accumulate near the inwall of the furnace. Consequently, if the ore is placed first, the material near the wall will be predominantly ore and the same will happen with coke if it is placed first. Since the coke bed is more permeable than the ore bed, the gas distribution can be altered by charging ore-coke (OC) or coke-ore(CO). The following is a summary of some charging methods that can be used to change the gas distribution pattern to overcome furnace irregularities, such as, uneven material distribution, channelling, scabs, scaffolds, hanging etc. Further details are given in Chapters 11 and 13.

For a mixed burden of ore, sinter and pellet, the stock distribution pattern changes according to their proportions and placement on the large bell. If 50–75% pellet is charged above the ore in the big bell, on dumping the ratio (ore + pellet)/coke at the centre is large but if it is reversed there is more uniform distribution in the radial direction. In the case of 100% sinter or pellet, the ratio lies in-between the two cases. By proper manipulation of pellet and ore, the output can be increased and the coke rate decreased significantly.[46]

5.8.1.1. Normal filling

In this type, the ore is placed first in the big bell and the coke comes over it. As already indicated this helps the periphery to retain the ore and the coke travels to the axis which is thus loosened. The charge is expressed as OOLCCC/ or OOCC/OLCC/. This filling is desirable if the amount of the fines is small and hence their nearness to the wall will not cause formation of accretions on the wall. A lower coke rate is usually obtained because of better peripheral utilization of CO.

5.8.1.2. Reverse filling

Coke is placed first in the big bell, e.g., CCCOOL/. Here, the coke falling ahead of ore forms a slope and the ore rolls to the centre, loosening the periphery. This filling makes the inwall hotter because of smaller specific heat of coke and results in higher coke rate (inferior utilization of CO). However, this filling can be used in charges where they tend to form accretions on the wall, e.g., some varieties of ores and fluxed sinter. However, occasional change-over from the normal to the reverse helps in *cleaning up* of the inwalls.

5.8.1.3. Mixed filling

As for example, OCOLC/CLCOC/. It is specially suitable for ores or sinters having a lot of fines. It helps in the distribution of ore both in the periphery as well as in the centre. Some of the fines are also carried to the centre along with the rolling coke.

5.8.1.4. Separate filling

Only part of the charge is brought in the big bell and then lowered, e.g., OOL/CCC/. The time interval between the two dumpings is smaller, the stock slope remains steeper and more of ore moves to the centre. It helps loosening of the periphery. This filling is very suitable for closely graded material because size segregation is promoted in this method.

5.8.1.5. Weight variation

Since in a thermally smooth running furnace, the ore/coke ratio by weight is a fixed quantity, the weight of coke per charge must be increased if that of the ore is desired to be increased. If more ore is desired in the centre, a larger quantity of ore will help because it will spread to a greater extent. Thus, for greater peripheral flow, the ore quantity (and, therefore, coke quantity) per charge should be increased and for greater peripheral compactness they should be decreased.

The charge weight is directly related with blast volume, burden permeability and furnace cross-section. In large furnaces, the ores or agglomerates need to be spread more towards the centre. A big charge results in a more uniform burden distribution over the furnace cross-section and a better utilization of the reducing gases. A more permeable bed with close size range and the elimination of fines also enable a bigger charge to be used. A statistical study shows:[49]

$$P = 5 \times 10^{-4}.Q^{1.34}$$

where,

P = charge size, tonnes
Q = blast volume, Nm^3/min, since gas volume is proportional to blast volume.

5.9. Stock and Gas Movement

A proper, steady and smooth descent of the stock against the buoyant forces of the ascending gas and wall friction is of vital importance for efficient working and productivity of the blast furnace as well as for iron quality.

5.9.1. Stock Movement

Apart from the differential permeability caused by burden segregation, the stock descent depends upon various other factors, viz.,

(i) furnace profile;
(ii) blast temperature and volume;
(iii) nature and composition of burden;
(iv) quality of iron made;
(v) incrustations and accretions on the bosh and shaft brickwork;
(vi) sticky or resolidified primary slag;
(vii) formation of arches, bridges and scaffolds due to fusion or bulging out of bricks by the fluxing action of compounds of sodium, potassium and zinc and incorporation of ore and coke therein.

These have been or will be treated at proper places in the text.

As the stock descends due to gravity, the solids in the shaft from the peripheral, intermediate and central zones converge past the dead man's zone towards the raceway as shown in Fig. 1.1. Hence, the stock flow across any horizontal section of the furnace is not uniform. This is also so because the combustion of coke which takes place in localized zones in front of the tuyeres is not uniform since the feeding of the coke in the combustion zone is intermittent and hence the stock descent rate is neither uniform nor constant in time. The effect of this unequal combustion in the individual tuyere zones is transmitted to the stock column in the entire distance from the tuyere to the stock level.

When the furnace is charged, the stock forms a funnel in the centre with steep wall. In a normally working furnace, the peripheral flow of

solids is faster than the other two flows (intermediate and axial) and hence the angle of the stock funnel becomes flatter; this is still more so because there is a time interval between dumpings during which period the material moves down. This means that the ore when charged will spread less towards the centre, opening up the axis. This, in its turn, will result in a steeper cavity at the centre due to increased axial flow and the subsequent ore charge will roll towards the centre and make it more compact, thereby decreasing the axial flow. Thus, in a smooth running furnace the gas distribution and stock descent are adjusted automatically and uniformly. For a balanced stock movement, the rate of peripheral descent should be about 40–60 percent higher than the rate of central descent.

However, the rate of stock descent is seldom uniform and is different in different cross-sectional levels and even at different localities in the same level due to continuous intermixing and breakdown of materials. In large furnaces, the faster descent usually occurs in the peripheral zones but sometimes rapid flow in the intermediate and central zones has been experienced. In case of a slowing down due to resistance offered by accretions or tightening of the furnace in a certain area, the gas velocity and stock descent can increase in the neighbouring areas.

Some stock descent rates are available from Russian experiments.[50] In a Magnitogorsk furnace, the rates of descent were found to be 111 mm/min at the wall near the stockline, 20 mm/min at the axis and 67 mm/min in the intermediate zone. In 'Azowstal', a smooth running furnace showed the following average rates: 63 mm/min at the wall; 84 mm/min, 0.5 m from the wall; 36.5 mm/min, 1.8 m from the wall; and 41 mm/min at the axis. The respective rates during a tight running were: 20.2 mm/min; 19.6 mm/min; 37.8 mm/min; and 50.0 mm/min. The faster movement at the axis in the tightened furnace was probably due to occasional slips. The usual smaller descent rate at the axis compared to the peripheral movement indicates and confirms the presence of a relatively inert stock column extending from the dead man's zone almost to the top.

The stock descent rate also depends on the blast volume and increases as the volume increases. An investigation at the Zaporhstal works showed the rates to be 70.5 mm/min and 64.9 mm/min at the wall for blowing rates of 2500 and 2000 Nm^3/min respectively at blowing pressures of 2.35–2.48 ata and 2.16–2.20 ata.

It is natural to expect that the gas flow in modern furnaces will encounter more resistance compared to the older ones because of continuous improvement in the coke rate, resulting in an increased amount of ore charged

per unit weight of coke. In fact, the ore/coke weight ratio has increased from about 2 to 4 in the last couple of decades. However, such fears have not been substantiated yet perhaps because low coke rates are associated with the use of closely graded sinter and coke giving highly permeable beds. On the other hand, if the ore/coke ratio increases due to the use of heavy oil or natural gas, the gas volume per unit of coke increases greatly which is apt to increase the factor K′ in Eq. 5.37, resulting in retarded gas throughflow and other troubles. Kase[51] suggests oxygen-enrichment of the blast to reduce the bosh gas volume and stabilize the furnace conditions in such cases.

It was also feared that an increase in the throat diameter in large furnaces (necessitated by the high operating intensity to reduce the top gas velocity and hence an excessive emission of flue dust) would result in an undue concentration of the ore in the peripheral and intermediate zones. Hence, a sufficient quantity of ore would not reach the centre, leading to an inefficient utilization of the thermal and chemical energies of the gas. This has indeed been substantiated by the measurements of the ore/coke ratio at the stock level in 2000 m³ and 2700 m³ furnaces with respective throat diameters of 7.3 and 8.1 m with throat-bell clearance of 0.95 m. In the former[52] (Fig. 7.4) the ore/coke ratios at the peripheral, intermediate and central zones were approximately 2.8, 4.0 and 1.0 whereas in the latter[53] the respective ratios were 2.0, 5.0 and 0.0. That is, in the larger furnace the ore hump in the intermediate zone contained large amounts of ore while the centre was devoid of ore and contained mostly coke. Hence, it is natural to expect that a major amount of the gas will pass through the peripheral and axial areas where the gas permeability will be greater than in the region where the main ore hump is located.

To improve heat transfer and gas utilization in the intermediate zone, it is necessary to redistribute the ferrous materials more uniformly towards the centre without disturbing the gas permeability in the peripheral or the axial zones. This can be done by increasing the blast volume, charge weight, throat-bell distance (say, from 0.95 m to 1.05 m and using moveable rings), and by improving the size of the charge materials. Also, due to paucity of ore in the centre, a dynamic equilibrium[54] is set up there between the gas temperature, CO-utilization and direct/indirect reduction (Sec. 7.3.2).

It is difficult to confirm the results of laboratory experiments on voidage and resistance to flow of gas from blast furnace measurements. This is due to everchanging voidage on account of intermixing, breakage and vol-

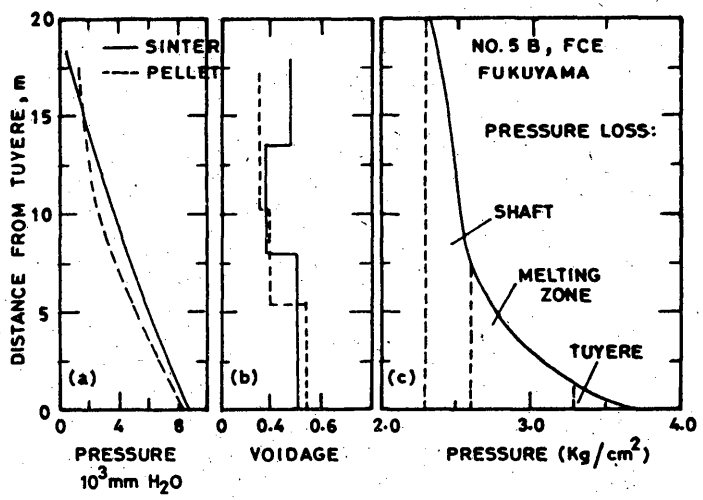


Fig. 5.20 (a) and (b) – Pattern of variations of pressure and voidage along the furnace height for sinter and pellet, according to Engel et al.[54] (Copyright Stahleisen); (c) Pattern of pressure variation in Fukuyama No. 5 blast furnace of diameter 14 m with HTP, according to Higuchi et al.[55] (By kind permission).

ume changes of the burden materials on the one hand and continuous changes of the gas velocity in the vertical and horizontal cross-sections of the furnace on the other. However, the pressure fall is the highest between the tuyere zone and the belly, sometimes 50–60 percent of the total. This is also expected because of the high velocity of the hot gases which have to pass through the wet zone in the bosh and viscous, semi-fused mass in the belly.

Fig. 5.20(a)[55] shows the pressure drops from the tuyere zone to the top for furnaces working with sinters and pellets. In the former case, 35–55 percent of the total pressure fall occurred in the lower zone (0–8 m from the tuyere nose) and about 45 percent in the shaft, whereas in the latter the respective figures were 50–60 percent and 30–35 percent. The steep pressure fall in the lower third of high capacity furnaces is illustrated in Fig. 5.20(c).[56]

The estimated voidage in the furnace, however, does not vary. Fig. 5.20(b)[55] shows that the average voidage in the lower zone is 50–60 percent whereas it is about 40 percent in the middle and upper shaft. The high pressure drop in the high voidage area in the lower furnace is presumably due to high velocity of the hot gases as well as liquids flow through the coke grid.

5.9.2. Pressure of Charge Column[57,58]

The charge materials descend into the raceway due to gravity. However, the downward pressure of the charge depends upon several factors, viz., friction against the furnace wall and the central coke column protruding into the belly or lower shaft, upward thrust of the gas and the bulk density of the materials, which increases as they soften and occupy the voids.

When the charge is dumped, the materials at the throat become compacted and less porous due to dynamic (impact) energy of the falling materials, resulting in a rapid rise of the lateral pressure on the wall. This decreases the vertical downward pressure. If the stock level is low and/or the resistance to flow of gases is increased in the presence of fines, scabs or scaffolds, it might lead to top hanging which can be countered to some extent by charging at high stockline level to reduce material compaction.

With increasing distance from the stock level the effect of dynamic load gets weaker and the consolidated materials loosen up because of stack batter. Therefore, the downward pressure increases with increase in cross-sectional area, stock height and bulk density (contraction due to softening) and decrease in lateral pressure.

Theoretically, the stock pressure at the tuyere level should be maximum. However, under blast furnace conditions as seen in Fig. 1.1, the descending charge undergoes considerable friction against the relatively stationary central coke column because of peripheral location of the combustion zone (Fig. 5.2). As a result, the value of the actual pressure is reduced to one-sixth[57] of that expected.

If the bosh angle is increased, the distance of the tuyeres from the centre increases, resulting in a transverse enlargement of the coke column which causes the frictional forces to increase and the vertical pressure to decrease. Elimination of the bosh has resulted in operational failures in practice because the tuyeres move farthest away from the centre and the stock pressure at the tuyere level is decreased to one-tenth, compared to one-sixth in furnaces with bosh. A decrease in the slope of the bosh ensures greater permeability and higher driving rate. This feature has been adopted in modern furnaces with large hearth diameters (Table 12.1).

In blast furnaces with conventional lines, the greatest downward pressure is encountered at the foot of the shaft or the belly (0.2–0.7 with an average of 0.47 kg/cm^2) and the lowest at the throat and tuyere levels. It is there where the charge usually hangs. The gas flow supports 60–80 percent of the charge weight at the top. Disturbance of the stock movement can occur at any cross-section if the lifting force of the gas exceeds the weight of the materials in the vertical space above the cross-section.[59]

5.9.3. Gas Movement

The gases produced opposite the tuyeres reach temperatures of about 2000°C. The very high temperatures increase the gas volume enormously. The flow of this enormous volume of gas through the wet zone is very unfavourable but is taken care of by the relevant furnace lines. The decreasing section of the shaft above the belly is not a hindrance since the gas cools off and its volume decreases greatly because of the endothermic reactions of direct reduction, fusion and calcination. The gas pressure, as seen before, also falls greatly at first and then more gradually in the shaft because a dry porous bed is normally available there.

The velocity of the ascending gas is not uniform at all places. It changes according to the resistance encountered in the bed. Generally, the velocity is highest in the axis because of the presence of a comparatively highly porous bed (more coke than ore), intermediate along the inwall and the least in the intermediate zone. It is not possible to give the velocity figures for the innumerable furnace measurements all over the world. Some recent measurements[55] in furnaces using sinters and pellets show gas velocities of 3–4 m/s in the intermediate zone and 6–9 m/s in the peripheral and central zones, the periphery having a lower velocity on an average than the centre. The time of residence of the gas in the furnace ranged from 2.5–6 seconds. However, the residence time depends upon the blast volume as well as furnace volume.

A small residence time of the gas is unfavourable for fuel efficiency (inadequate CO-utilization, Sec. 11.3.2.8). The disadvantage of high linear velocity of the gas and small solid surface of the ore is made up by increasing the time of residence, i.e., by increasing the shaft height or furnace volume. However, a high rate of heat and mass transfer is obtained in the blast furnace in spite of large ore particles presenting relatively small surface area because the gas forcibly finds its way through them at high speed. The expansion, compression and change of direction of the gas through the tortuous path offered by the voids greatly increase the turbulence and effective gas/solid contact. More important than the heat transfer efficiency (which does not decrease as rapidly) is the decrease in indirect reduction of the ore which suffers greatly because of the decrease in residence time.

A very broad relationship exists between the gas velocity and gas temperature.[55] A difference of gas temperature of even 600°C is possible at

the same level, depending upon the local gas velocity. However, the changes in gas temperature must be interpreted in conjunction with the rate of stock descent. The temperature of the gas should depend upon the relative thermal capacities of the gas and the solids, i.e., W_g/W_s ratio (subscripts g and s are for gas and burden; W = mass flow, kg/m².s × specific heat). The gas temperature will increase if the ratio in any sector increases either because of an increase in the mass flow rate of the gas for constant burden descent rate or a decrease in the stock descent rate for the same gas flow rate. This usually happens in the axis or along the wall and also in the case of furnace irregularities. The increase in gas temperature in one sector will cool down the neighbouring sectors.

On the other hand, a decrease in the gas temperature may be caused either by a higher burden flow rate for the same gas flow rate or a lower gas rate for the same burden flow rate. This is confirmed by the minimum temperature of the gas in the intermediate zone where the gas flow rate is small and uniform (see Fig. 7.4) compared to the burden flow rate. The burden/gas ratio in this zone is on an average higher than in the other two zones because the productivity of large furnaces depends greatly upon a developed central (ore/coke ratio the lowest) and a moderate peripheral flow due to higher permeabilities in these zones.

The region of lowest temperature lies in the intermediate zone where the ore/coke ratio is the highest. The gas temperature falls most rapidly in the intermediate zone at all heights. The weighted mean gas temperature falls from 1180°C at the bosh parallel to 610°C at the throat, or on an average of 33°C/metre of stack height.[52] The temperature distribution in a 2000 m³ blast furnace shaft is shown in Fig. 7.4. The gas utilization forms almost a mirror image of temperature distribution, i.e., the $\%CO_2$ is the highest in the intermediate zone where most of the ore is concentrated (Fig. 7.5) and the burden/gas ratio is the highest (Fig. 7.4). The changes in the gas composition in the furnace are further discussed in Sec. 7.3.2.

5.10. Variations in Stock and Gas Movement

The operating intensity and, therefore, the rate of stock descent in a smoothly running furnace is proportional to the consumption of blast oxygen and depends upon various factors, such as:

(i) increased supply of oxygen per unit time for burning coke;
(ii) decreased coke rate per THM;

(iii) proper composition and fluidity of the primary and bosh slag;
(iv) optimum size distribution of the charge;
(v) optimum blast distribution and dimension of the combustion zone (blast control);
(vi) distribution of materials at the stock surface (charging control);
(vii) furnace lines;
(viii) furnace irregularities.

These have been or will be discussed at various places in the text.

All changes in the stock movement are reflected in the variation of temperature and composition of the gas across the cross-section as well as at various levels of the stock, the optimum values being different for different furnaces. Generally, a higher temperature and lower $\%CO_2$ in the gas indicate a coarse permeable bed whereas a low temperature and high $\%CO_2$ shows compactness of ore in the area and efficient utilization of the thermal and chemical energies (Sec. 7.3).

A non-uniform or violent furnace movement may be caused by any or more of the following irregularities:

(a) channelling;
(b) uneven distribution;
(c) slips;
(d) scabs;
(e) scaffolds;
(f) lowering of slag fusion zone.

These irregularities can be controlled by controlling the chemical composition, ore/coke ratio, blast (flame temperature, blast volume, diameter and length of tuyeres), charging sequence and weight of the charge. Indication of non-uniformity is shown by: temperature and composition of the gas; temperature at the inwall at different levels and radial cross-sections; temperature of iron and slag; iron quality; peaks, depressions and oscillations in the blast and top pressure charts. These are discussed at appropriate places, especially in Chapters 11 and 13.

References

1. CARMAN, P. C.: Trans. Inst. Chem. Engg., 15, 1937, p. 150–166.
2. KOZENY, J.: Ber. Wiener Akad., 136a, 1927, p. 271.
3. ERGUN, S.: Chem. Engg. Progress, 48, 1952, p. 89–94.
4. MORCOM, A. R.: Trans. Inst. Chem. Engg., 24, 1946, p. 30.
5. ROSIN, P. O.: op. cit., 15, 1937, p. 167.

6. HANSEN, M.: Arch. Eisenhüttenw., 34, 1963, p. 151–157.
7. JESCHAR, R.: op. cit., 35, 1964, p. 91–108.
8. POLTHIER, K.: op. cit., 37, 1966, p. 365–374.
9. JESCHAR, R.: Stahl u. Eisen, 88, 1968, p. 1144–1153.
10. BRAUER, H.: Chem. Ing. Tech., 29, 1957, p. 785–790.
11. BRAUER, H.: Dechema Monogr., 37, 1960, p. 7–77.
12. Blast Furnace Aerodynamics: Proc. Sym. Aus. I.M.M.: Edt. N. Standish, Wollongong, 1975.
13. BOGDANDY, L. v. and H.-J. ENGELL: The reduction of iron ores, (in English), Springer-Stahleisen, 1971.
14. FURNAS, C. C.: US Bur. Mines Bull., No. 307, 1929, p. 1–144.
15. JESCHAR, R. et al.: Ref. 12, p. 136–147.
16. GRATON, L. C. and H. J. FRAZER: J. Geol., 1935.
17. MARTIN, J. J. et al.: Chem. Ing. Prog., 47, 1951.
18. BREDEHÖFT, R. and R. JESCHAR: Stahl u. Eisen, 93, 1973, p. 55–60.
19. THIBAUT, Ch. G.: Circ. Inform. Techn., 15, 1958, p. 1863–1877.
20. LEVA, M.: Fluidization, N.Y.: 1959.
21. POLTHIER, K.: Stahl u. Eisen, 90, 1970, p. 246–246.
22. BOGDANDY, L. v. et. al.: op. cit., 88, 1968, p. 1177–1188.
23. KEGEL, H.: op. cit., 70, 1950, p. 730–740.
24. HANSEN, M.: op. cit., 82, 1962, p. 1061.
25. SHERWOOD, T. K. et al.: Ind. Eng. Chem., 30, 1938, p. 765–769.
26. ELLIOTT, J. F. et al.: J. Metals, July 1952, p. 709–717.
27. KODAMA, K. et al.: Tetsu-to-Hagane, 49, 1963, p. 883–888.
28. BEER, H. and G. HEYNERT: Stahl u. Eisen. 84, 1964, p. 1353–1365.
29. RIKHTER, R. G. et al.: Steel in USSR, Sept. 1974, p. 692.
30. MERSMANN, A.: Chem. Ing. Tech., 37, 1965, p. 218–226.
31. JESCHAR, R. et al.: Stahl u. Eisen, 91, 1971, p. 665–678.
32. NEWTON, et al.: Tower packings and packed tower design, Max Leva, Consult. Chem. Eng., 1953; See M. Hansen, Stahl u. Eisen, 82, 1962, p. 1061.
33. STANDISH, N. and J. B. DRINKWATER: J. Metals, Feb. 1972, p. 43–45.
34. WARNER, R. E.: Ref. 12, p. 23–29.
35. DARTNELL, J.: Ironmaking Steelmaking, 5, 1978, p. 18–24.
36. JOURDE, P. and J. HUCK: Stahl u. Eisen, 84, 1964, p. 1656.
37. Developments in ironmaking practice: Proc. Conf. Iron and Steel Inst., London, Nov. 22–23, 1972.
38. HIGUCHI, M. et al.: Trans. Iron Steel Inst. Jap., 16, 1976, p. 453–464.
39. SAUNDERS, H. L. and R. WILD: J. Iron Steel Inst., 152, 1945, p. 259–290.
40. WILD, R.: op. cit., 166, 1950, p. 339.
41. REDKO, A. N.: Stal, 2, 1948, p. 117.
42. WINTERS, Ch.: Stahl u. Eisen, 80, 1960, p. 465–473.
43. HEYNERT, G. et al.: ibid., p. 473–483.
44. PEETZ, E. and G. WINZER: op. cit., 81, 1961, p. 1101–1107.
45. Blast furnace – Theory and practice, vol. 1, Edt. H. Strassburger, Gorden and Breach, N.Y., 1969.
46. SUZUKI, G. et al.: Recent developments in met. sci. and tech., Iron & Steel, Silver Jub. Sym., Ind. Inst. Met., N. Delhi., 1972, p. 199.
47. BRANDI, H. Th., P. ISCHEBECK and G. HEYNERT: Stahl u. Eisen, 80, 1960, p. 65–78.
48. PAWLOW, M. A.: Metallurgy of pig iron, vol. 3, Verlag Technik, Berlin, 1953.

49. BONDARENKO, A. I. and M. Ya OSTROUKHOV: Steel in USSR, April 1973, p. 278.
50. POCHVISNEV, A. N.: Blast furnace process, Verlag Technik, Berlin, 1954, p. 256.
51. KASE, T.: Ref. 46, p. 207–219.
52. NEKRASOV, Z. I. and M. T. BUZOVERYA: Stal in Eng., Feb. 1969, p. 141–147.
53. NEKRASOV, Z. I. et al.: op. cit., July 1970, p. 502–509.
54. KITAEV, B. I. and B. M. SHAVEL'ZON: Steel in USSR, June 1976, p. 300.
55. ENGEL, K., S. MAYER and K. POLTHIER: Stahl u. Eisen, 93, 1973, p. 1–6.
56. HIGUCHI, M. et al.: Ref. 12, p. 129–135.
57. BABARYKIN, N. N. et al.: Stal in Eng., Apr. 1959, p. 249; Sept. 1962, p. 667–672; Sept. 1969, p. 772–7.
58 POLTHIER, K.: Reviews, Stahl u. Eisen, 87, 1967, p. 960–962.
59. GREKOV, P. N. and V. E. GRUGINOV: Stal in Eng., April 1964, p. 259.
60. HEYNERT, G. et al.: Iron and Steelmaker, No. 3, 5, 1978, p. 15–24.

CHAPTER 6

RAW MATERIALS AND THEIR PROPERTIES

6.1. Introduction

Blast furnace raw materials have changed in character greatly in the last two or three decades. Formerly, they used to be raw iron ores, raw limestone and coke. They are being increasingly replaced by pre-fluxed sinters and pellets and liquid and gaseous fuels. Their preparation and properties are discussed in this chapter. Since the air blast is also one of the raw materials, it is discussed in terms of pre-heating as well as humidification, oxygenation and addition of hydrocarbon fuels.

6.2. Iron Ores and Agglomerates

Iron ores are iron-bearing minerals associated with varying proportions of waste or *gangue* materials which generally contain silica, alumina and sometimes lime and magnesia as well. In addition, they contain very small amounts (generally from below 1 percent to a few percent) of other constituents like compounds of Zn, Cu, Ti, Cr, Mn, As, Sb, Sn, Pb, Ni, V, Na, K, S and P. Since by definition an ore is a mineral from which the desired element can be extracted economically, any iron-bearing material can become an ore provided the cost of mining, transporting, preparing and smelting it is such that the iron thus obtained is competitive in price

and saleable at a profit. Iron ore fines, which a few decades ago used to be considered as waste because of their adverse effects in the blast furnace are now beneficiated and agglomerated into lumps, mainly by sintering and pelletising processes, and the decrease in coke rate, increase in production and reduction in cost by their use have been of considerable magnitude.

The most commonly used iron-bearing minerals contain the iron compounds as: hematite, Fe_2O_3 (70% Fe); magnetite, Fe_3O_4 (72.4% Fe). Of much less importance are: limonite, $2Fe_2O_3.3H_2O$ (60% Fe); siderite, $FeCO_3$ (48.3% Fe); pyrites, FeS_2 (46.6% Fe).

The iron percentages calculated above are from their pure states and in ores the iron content is lowered according to the amount of impurities present. The names and analyses of some common ores are given in Table 6.1.

6.2.1. Characteristics of Iron Ore

The essential characteristics of the iron ore are:

(i) Reducibility;
(ii) Size and size distribution;
(iii) Strength;
(iv) Temperature and range of softening;
(v) Iron, moisture and gangue contents;
(vi) Swelling and volume change.

Reducibility is the ease with which the oxygen combined with iron can be removed *indirectly*. A higher reducibility means a greater extent of indirect reduction that may be obtained in the blast furnace resulting in a lowered coke rate and higher productivity. Reducibility is of vital importance and will therefore be discussed separately in Sec. 6.7.

The importance of size and size distribution for a uniform flow of gas through the charge bed has been discussed in Sec. 5.4. The present practice is to grade the ore so that the upper size limit is about 2–3 times the lower one. This range gives a good ratio between the surface and volume of the lumps and ensures an adequate gas/solid contact. The minimum diameter should be about 6–8 mm because particles smaller than that would increase the resistance to flow of gases steeply. The upper limit (60–70 mm) is restricted by the reduction rate which should be 0.5–1.0 percent per minute of oxygen combined with iron. Therefore, the size grad-

Table 6.1. Chemical composition of iron ores from various countries in percent

Ore	Country	Fe	SiO_2	Al_2O_3	CaO	MgO	P	S	Mn	Cr
Bakal	USSR	60.7	2.4	2.0	1.2	0.2	0.004	0.03	1.50	
Bomi Hills	Liberia	69.5	0.1	0.2	0.02	0.15	0.05	–	0.15	–
Carol Lake	Canada	64.7	3.9	0.35	–	–	0.005	–	0.2	–
Cerro Boliver	Venezuela	63.7	0.75	1.0	0.3	0.25	0.09	0.03	0.02	–
Conakry	W. Africa	53.8	1.5	8.7	0.1	0.4	0.09	–	0.12	1.5
Conception	Newfoundland	51.4	11.9	4.4	2.9	0.7	0.9	0.04	–	–
Goa	India	57.8	2.5	6.5	0.7	0.3	0.04	0.02	–	–
Gellivara	Sweden	60.1	5.9	1.1	3.3	1.0	0.9	0.04	0.15	–
Goldsworthy	Australia	63.2	4.9	1.6	–	–	0.035	–	–	–
Itabira	Brazil	68.9	0.35	0.6	–	–	0.03	0.01	0.05	–
Kiruna	Sweden	66.5	1.9	0.5	2.3	0.9	0.5	0.005	0.1	–
Kriwoi Rog	USSR	62.8	6.2	2.4	0.6	0.2	0.04	0.1	0.05	–
Labrador	Canada	53.9	6.3	1.1	–	–	0.08	0.01	1.03	–
Marcona	Peru	60.5	7.0	1.2	1.0	0.15	0.09	0.03	0.02	–
Mesabi	USA	57.5	10.1	0.7	0.05	0.05	0.06	0.01	0.5	–
Minnesota	USA	54.3	6.8	0.4	0.25	0.10	0.23	–	1.0	–
Minette	Belgium	38.7	15.7	6.1	5.6	1.6	0.9	–	0.3	–
Reserve-pellet	USA	63.0	8.1	0.4	0.45	0.55	0.025	.003	0.25	–
Tula	USSR	52.2	10.1	1.25	0.3	0.1	0.6	0.1	0.35	–

ings should be in the range 10–25 mm, 20–50 mm, 30–60 mm etc. A narrow size distribution has the following advantages:

(a) charge permeability increases and the gas distribution is more uniform with better utilization of the chemical and thermal energies of the gases;
(b) more even material distribution at the stock level and less material segregation in the shaft during descent;
(c) gas flow is not impeded if the size ratio is within limits but at the same time gives rise to a tortuous flow of gases with continuous changing of flow directions, providing a larger gas/solid contact time.

In the furnace, whether the ores as charged will maintain their size depends on their strength. They should be resistant to abrasion and possess high crushing strength. Their breakage in the furnace due to impact, abrasion, compression and volume changes at high temperatures in a reducing atmosphere generates smaller particles, resulting in choking of the voids. Hence, the purpose of size gradings will be lost. However, such breakage cannot be avoided completely as all ores during reduction undergo disintegration in varying degrees.

The porosity of the bed can also be affected by the softening of the materials. Although the compounds associated in the ore have more or less definite melting temperatures, they undergo intermixing and sintering in the furnace, the result being formation of materials of lower melting temperatures. Since the products belong to multi-component systems, the melting occurs between a range of temperatures, e.g., between the solidus and liquidus of the complex oxide systems. For ores the range may be wide, 700–1350°C, and that for sinters and pellets much narrower, 1000–1350°C. The smaller the range of softening, i.e., the shorter the vertical distance in which the highly viscous semi-fused mass forms and exists, the better the gas flow and the higher the productivity.

The moisture content of the ores varies according to the conditions under which they are mined, stored, transported and also according to season, humidity, etc. Moisture increases the thermal load and therefore the fuel rate. In addition, it adds to extra and useless transport charges and loading and unloading difficulties, especially in the cold countries. On the other hand, if it is deficient it can lead to handling difficulties due to dust formation.

The richer the ore, i.e., the higher the iron content, the more economical the blast furnace smelting. The minimum iron content, however, has not

been specified and depends upon the technical and economic conditions of the area. Ores having basic or predominantly basic gangue but with low iron content are being smelted economically. Some self-fluxing ores (containing lime) having 25–30% Fe may have even lower coke consumption than siliceous ores with higher Fe-content.

Some pellets have the tendency to swell enormously in a reducing atmosphere at 800–1000°C. The consequent loss of strength and compaction under load decrease the voidage and resist the flow of gases. The operation of the blast furnace under such circumstances becomes very difficult.

6.3. Preparation of Ores

The preparation of ores consists of all the processes involved in the conversion of raw *run-of-mine* ores into products more suitable for blast furnace charge. It includes crushing, grinding, screening, washing, blending, concentrating or upgrading, agglomerating, etc. The purpose of ore preparation is to improve the raw material condition so as to increase blast furnace efficiency and produce cheaper iron. All the processes mentioned above except agglomeration are included in a broader term called *beneficiation*. The entire field of burden preparation, agglomeration and physical testing of ferrous materials has been covered excellently by Ball et al.[1] They are discussed briefly here.

6.3.1. Beneficiation of Iron Ores[1–4]

6.3.1.1. Crushing, grinding and screening

Run-of-mine ore contains various sizes of lumps as well as fines. Fines below about 6 mm adversely affect the permeability of the charge bed and the upper size limit is fixed by reducibility which should be above 0.5–1 percent of Fe-oxygen per minute. Depending upon the quality of the ores, they should normally be crushed to a size range of about 6 to 60 mm. On screening, the oversize goes for further crushing and the undersize for agglomeration like sintering. Since the size range 6–60 mm is too large for uniform gas flow, these can be re-screened to various narrow size fractions, e.g. 6–20 mm, 20–40 mm, 40–60 mm etc., and each fraction charged separately into the blast furnace.

6.3.1.2. Concentrating

Concentration is a process of enrichment of ores in its iron content at the expense of gangue and harmful components. The diminution of the

gangue acids decreases the thermal load. If, for example, 40–50 kg of silica per THM is removed from the ore, the required limestone for fluxing the acids drops by about 100–130 kg. This amounts to a decrease in slag volume of 100 kg and decrease in the amount of CO_2 to be removed in the endothermic calcination reaction by about 50 kg. These two factors together means a coke saving of about 40–60 kg per THM. A simultaneous increase in the production by 5–10 percent is also likely to occur.

The general guideline for deciding whether an ore should be concentrated or not depends upon the acids and CaO (MgO) contents of the ore. Concentration is very effective, under certain circumstances, even when the ore is rich in iron. Certain Indian ores with 60–65% Fe contain large amounts of alumina in the gangue which when smelted give a highly viscous slag. It is very difficult to work with such slags and the removal of alumina from the ore, if possible, should increase the furnace output, lower the coke rate and improve the iron quality.

The usual methods of concentrating iron ores are:

(i) washing
(ii) heavy media separation
(iii) flotation
(iv) magnetic separation.

The above processes have been described by Ball et al.[1] and others.[2–4]

6.3.1.3. Blending

A uniform operation and, therefore, an increased blast intake, decreased fuel rate, uniform iron quality and decreased downtime depend greatly upon the stability of the blast furnace. The stability can only be ensured by a uniform burden quality and constant heat supply.

A uniform chemical composition of all the raw materials including the ash and moisture content of the coke assures a uniformity of softening temperature and reduction of ores, uniformity of melting of iron and slag as also of slag formation zones, thus permitting a uniformity in the combustion process and gas throughflow. This also permits to maintain a lower thermal reserve in the hot blast stoves without endangering the furnace operation. Hence, a more efficient use of the effective furnace volume can be achieved by employing higher blast heat (near to stove capacity) and heavier ore charges.

A uniform chemical composition of the burden materials can be obtained by blending (mixing).[4,5] Blending assumes greater importance for those

plants where the supply of raw materials comes from different sources. For the purpose, large storage and *bedding* areas are necessary. The economics of blending is very difficult to evaluate. However, tests carried out in the Soviet Union showed[4] an increase in output by 7 percent, decrease in fuel rate by 4 percent, decrease in iron cost by 2.5 percent and capital savings of 4.5 percent by blending as compared to unblended ores.

6.4. Agglomeration

An enormous amount of fines (40–50 percent) is generated during mining and ore dressing operations. Since the fines cannot be charged directly in the blast furnace, it is necessary to agglomerate them into lumps which is performed predominantly by sintering and pelletising processes. An important prerequisite of sinter or pellet is their adequate reducibility and strength to withstand handling hazards, and impact, abrasion and compression in the blast furnace.

6.4.1. Sintering[1-3,6-11]

Agglomeration by sintering is achieved by the application of heat which results in the conversion of ore fines into large, hard, porous lumps. The formation of such lumps is caused by:

(a) an incipient fusion of ore particles at the contact surface which binds them together;
(b) formation of *diffusion bonds* through recrystallization and crystal growth of hematite and magnetite which keep the particles together without melting.

Both these are made possible through combustion of small sized coke breeze which are intimately mixed with moistened ore fines. Due to complete combustion of carbon, a temperature of 1300–1400°C is easily attained. The process is performed in stationary or in more commonly used Dwight-Lloyd type continuous travelling grate machines, on the grate of which is fed a 40–50 cm thick layer of the sinter mix. Combustion of the coke breeze in the top layer is initiated by burning oil or natural gas through burners and is maintained by continuously sucking free air through the charge from under, the suction being usually about 800–1000 mm water gauge, depending upon the permeability of the sinter mix. Before charging the mix the grates are initially covered with 4–5 cm thick layer of coke-free return sinter of size − 10, + 8 mm in order to prevent leakage of the

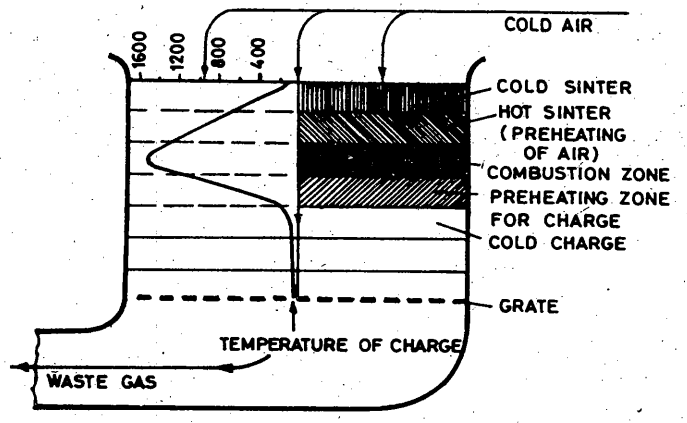


Fig. 6.1 Temperatures prevailing in a sinter bed 3 minutes after ignition, according to Wendeborn.[8] (Copyright Iron and Steel Institute).

mix through the grate openings as well as to protect the grates from overheating during the final stages of the process. The sinter mix usually contains other materials like flue dust, return fines, limestone/dolomite, etc., in order to control the properties of the product as well as to utilize industrial wastes. Return sinter fines having lower fusion temperature than the raw mix serve as seeds for initiation of the sintering process.[12] A vertical section of the sinter strand is shown in Fig. 6.1.[8]

6.4.1.1. Combustion

The burning of the coke breeze occurs in thin horizontal layers proceeding successively vertically downwards. The temperature in each layer reaches more than 1400°C very quickly because of double regeneration of heat as is clear from Fig. 6.1. The air, burning the coke breeze in a particular combustion layer, is preheated while passing through the hot layer of sinter above it and the hot gaseous combustion product preheats the mix in the layers below, itself cooling down in the process. This preheating of air and cold mix and the complete combustion of the fuel to CO_2 make the process thermally very efficient. Theoretically, about 4–8 percent coke breeze in the sinter mix should suffice to raise the temperature to 1400°C.

The preheating of layers below the combustion zone results in the evaporation of moisture and hydrated water and dissociation of carbonates. The moisture-laden hot gases cool down in the process and the water recondenses in the still lower layers when the dew point is reached (usually

50–60°C). The process continues in successive layers up to the last one when due to the absence of any cold mix (except return sinter) the waste gas temperature shoots up to 300–350°C.

The rate of sintering is very fast and depending upon the permeability and thickness of the bed it takes 15–20 minutes for completion. The permeability depends upon the moisture content which through its surface tension forces prevents segregation and occupation of the voids in the interstices of the larger particles by the lighter and/or smaller ones like coke, return fines, dust, etc.

The size distribution of a typical sinter charge is shown in Table 6.2.[13] For obtaining optimum permeability the water content of the sinter mix may range from 5 to 20 percent, the content increasing with increasing degree of fineness. Too low an amount results in a non-uniform permeability and, hence, non-uniform sinter quality. Too large an amount decreases the permeability through flooding of the voids which is aggravated due to recondensation of water in the lower layers. With high water content, an addition of hot return sinter to the mix helps in reducing the amount of condensation water and thus increasing the output even up to 30 percent.[14,15] Addition of CaO as part replacement of limestone in basic sinters serves the same purpose.

Table 6.2.[13] Particle size of ore fines suitable for sintering and pelletising

Size, mm	% size fraction	
	Sinter	Pellet
+ 10.00	4.1	+
+ 8.00	2.3	–
+ 3.00	11.7	–
+ 1.00	7.0	–
+ 0.50	27.1	–
+ 0.30	18.2	–
+ 0.15	20.3	0.4
+ 0.09	2.1	11.6
+ 0.075	4.1	–
+ 0.06	3.1	11.3
– 0.06	–	76.7

For adequate voidage and heat transfer the ore size should not exceed 5–6 mm and coke and limestone 3 mm. For a given fuel rate, if the coke size is too large, a local overheating, excessive liquid formation and reduction of iron oxides to difficultly reducible fayalite can occur. At the same time an inadequate heating at other places will deteriorate sinter bond strength (formation of pockets of unsintered material). In the case of limestone as well, calcination will be incomplete with too large a size which would affect the sinter strength adversely. For uniformity of sinter quality, both physical and chemical, the coke and limestone both should be mixed uniformly with the ore before charging. The optimum coke rate varies between 4–8 percent to give at least 65–70 percent of +12 mm fraction in the finished sinter. The fuel requirement is higher if the melting temperatures and viscosity of the slag are high since the intention is to produce a melt which is well-dispersed throughout the sinter matrix in order to obtain adequate strength. The amount of limestone added depends upon the basicity, reducibility and strength of the sinter desired. It is much cheaper to calcine limestone in the sinter strand with low-cost fuel than in the blast furnace. Lime also increases the reducibility of the sinters greatly.

The influence of these factors on sinter mineralogy, strength and reducibility will be discussed in later sections.

6.4.2. Types of Sinter

Depending upon whether bases have been incorporated in the sinter mix, sinters are divided into two broad classes:

(i) **Non-fluxed or acid sinters** Those where no flux is present in the ore or is added.

(ii) **Fluxed sinters** Those where flux has been added or is present in the ore. Depending upon the relative amounts of bases and acids, these are further categorized into two sub-classes according to basicity:

  (a) **Self-fluxing sinter** Those where sufficient flux has been added in the sinter mix to provide a basicity that is desired in the final slag, taking into consideration only the burden acids. An extra flux is added to the burden while charging to cater to coke ash acids.

  (b) **Super-fluxed sinter** In such sinters, an additional flux is added to the mix to provide for the desired final slag basicity, taking into account the acids content of both the ore as well as the coke ash.

If any flux is naturally present in the ores, then they are called self-fluxing ores.

6.4.3. Sinter Mineralogy[1-3,11,16-28]

A wide variety of minerals is observed in the final sinter, depending upon the chemical constituents of the ore and flux as well as the fuel rate. The types of minerals produced and their liquidus temperatures are of great importance for the primary requirement of a good sinter, i.e., good reducibility and high strength. Usually, the higher the amount of hematite (Fe^{3+} content) or degree of oxidation and the lower the amount of magnetite or wustite (Fe^{2+}) in the sinter, the greater the reducibility. (For reasons, see Sec. 6.7). Since most sinters break down into fines due to impact and abrasion under load in a mildly reducing atmosphere at lower temperatures, their low-temperature breakdown (LTB) properties are of utmost importance for blast furnace productivity. The testing methods of physical and chemical properties are given in Sec. 6.6. The degree of oxidation is given by:[29]

$$\frac{\text{amount of actual oxygen combined with Fe}}{\text{theoretical amount of oxygen necessary to form } Fe_2O_3} \qquad 6.1$$

or,

$$\% \text{ degree of oxidation} = (1 - Fe^{2+}/3\Sigma Fe) \times 100$$

The degrees of oxidation of the three iron oxides are:

$$FeO \approx 70\%;\ Fe_3O_4 = 88.9\%;\ Fe_2O_3 = 100\%.$$

The mineralogical constituents expected in the sinter have been briefly described in Secs. 3.19 and 3.20. However, due to the rapidity of the process and the comparatively large size of the materials present, equilibrium conditions are seldom achieved. During sintering a predominant part is initially transformed to magnetite because the combustion gas is slightly reducing[30] to hematite and the latter's high oxygen dissociation pressure (Sec. 3.4). However, during the passage of cold air and falling temperature of the sintered layers, a varying amount of magnetite is reoxidized to *secondary* hematite. The presence of hematites, depending upon their amounts and types, deteriorates the LTB properties of sinters.[21,31]

The sinter bond strength is achieved by:[3]

(i) slag or fusion bond – partial or complete embedding of crystalline constituents in the matrix of a fused glassy melt, the extent depending upon the volume and wettability of the liquid phase. The bond strength depends upon the amount of glass and the amounts and types of the constituents. These depend upon the fuel rate and impurities SiO_2, CaO, MgO and Al_2O_3, added or present.

(ii) diffusion bond – recrystallization and crystal growth of hematite (and magnetite). Hematite diffusion plays an important role, especially above 1250–1300°C, because of surface mobility at high temperatures. Diffusion bonded sinters are more porous, accessible to reducing gases and hence easily reducible. Such bonds are, however, obtained in Fe-rich low-silica ores, since the impurities in lean ores form low-melting liquids before the 'diffusion' temperatures are reached. In rich sinters the slag bond is of minor importance, the main bond being due to crystallization, oxidation and recrystallization of magnetite and hematite.[23]

Sinter mineralogy and its relation to strength and reducibility have been investigated by innumerable workers. Only a few have been quoted. In commercial furnaces, the phases undergo transformations during reduction.[23,32] The relationship between sinter mineralogy and quality are summed up below, with regard to the effect of lime/silica ratio.[11,21] The variations of mineralogy in sinters of optimum properties with the CaO/SiO_2 ratios at low MgO and Al_2O_3 contents are shown in Fig. 6.2.[21]

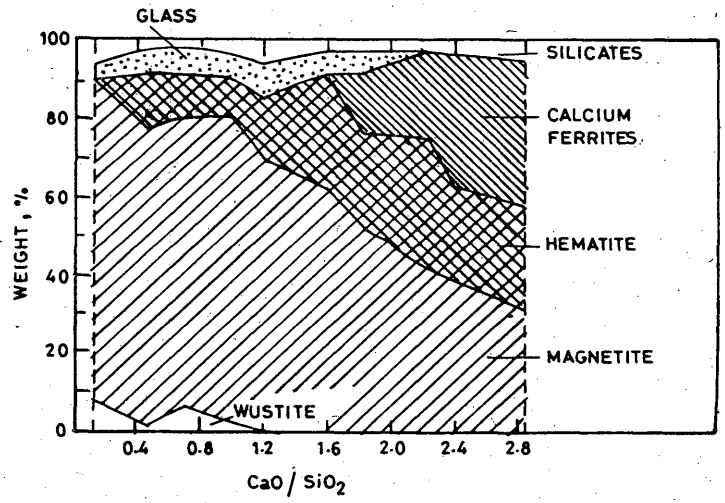


Fig. 6.2 Variation in mineralogy of sinter of optimum strength with CaO/SiO_2 ratio at 0.5% magnesia and 1.5% alumina, after Price and Wasse.[21] (Copyright Iron and Steel Institute).

CaO/SiO_2 ratio 0.0: In acid sinters when no lime is present, the major constituent is fayalite which can form from magnetite or directly from hematite. Fayalite (m.p. 1210°C) in the presence of SiO_2, FeO, Fe_3O_4 forms low-melting multi-component liquid whose viscosity increases with the silica content. When silica and fuel are high, large amounts of liquid will form and a strong sinter with a low degree of oxidation and poor reducibility will be obtained, having Fe^{2+}, 20–30 percent. For low silica and/or low fuel rate, the sinter is weak but more reducible with high degree of oxidation, having Fe^{2+}, 10–15 percent. In this case, diffusion may contribute a share to bond strength. These are clear from Fig. 6.3 which shows schematically the relationship between the coke rate, sinter strength, reducibility, degree of oxidation and fayalite content of acid sinters (see also Fig. 6.12). The strength, however, starts to decrease after an optimum fayalite content is reached.[33]

CaO/SiO_2 ratio 0–0.8: As the basicity increases, the slag volume increases and the crystalline silicates are increasingly replaced by glass. Lime makes the glass less viscous requiring lower temperature and hence less fuel, thus increasing the degree of oxidation and hematite content, both original and secondary. Hence, the sinter strength decreases and the reducibility increases (Fig. 6.12).

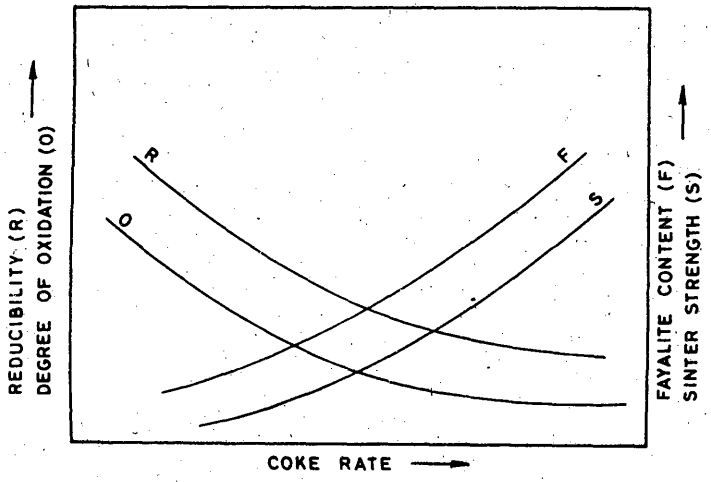


Fig. 6.3 Schematic trends in the increase of fayalite content and sinter strength and in the decrease of reducibility and degree of oxidation with increasing fuel rate in the sinter mix.

CaO/SiO_2 ratio 0.8–1.4:[21] With increasing basicity, the amount of glass increases and the fuel rate decreases and hence the strength continues to decrease and the reducibility to increase (or sometimes even decrease). At a ratio of 1.2, calcium ferrites begin to appear and at 1.4–1.6 the crystallization of β-$2CaO.SiO_2$ occurs. At this stage, the volume of glass is maximum and the sinter strength minimum. This is perhaps because of volume expansion accompanying the phase transformation of β- to γ-dicalcium silicate during cooling which generates points of weakness and cracks. The basicity of minimum strength varies according to sinter composition and hence the trends are shown only schematically in Fig. 6.4 with regard to sinter yield from sinter strand and tumbler indices, both normal and under reducing conditions (cf. Sec. 6.6).

CaO/SiO_2 ratio 1.4–2.8: As the basicity increases above 1.4, the glassy matrix is replaced by calcium silicate and ferrites, the latter increasingly taking over as bonding medium with simultaneous steady increase in sinter strength (needle-like ferrite precipitates hold the ore grains together). Reducibility also continues to increase.

The reducibility of the various phases (Sec. 6.7.2) varies according to:[6,20,34]

$$Fe_2O_3 > CaO.2Fe_2O_3 > CaO.Fe_2O_3 > 2CaO.Fe_2O_3 > \text{magnetite} > \text{olivines} > \text{fayalite}.$$

Because of strong bonds created by ferrites a lower fuel rate can be used for achieving the same strength for limey sinters compared to acid sinters, with resulting higher degree of oxidation and higher reducibility. The viscosity of ferrites at 1300–1600°C is of the order of 0.35–0.15 Poise and that of corresponding silicates about 10 times higher.[35,36]

The susceptibility of sinter breakdown at basicity 1.4–1.6 can be somewhat decreased by the use of MgO and Al_2O_3. According to Price and Wasse,[21] sinters containing 4.5% MgO plus 6.5% Al_2O_3 have excellent LTB property and the strength minimum is hardly detectable. Alumina enlarges the solidification range of dolomite-sinters, relieves the cooling stress, increases the mechanical strength and improves reducibility.[17] It also increases the degree of oxidation.[20]

The approach of the mineralogical composition of the finished sinter to the equilibrium conditions of crystallization within the bonding silicate material depends upon the temperature and duration of sintering. When

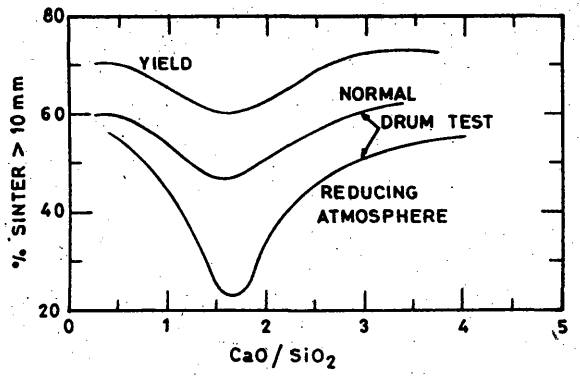


Fig. 6.4 Schematic trends of loss of strength of sinters with increasing lime/silica ratio with a minimum at medium basicity range as revealed by sinter yield and drum test, normal as well as in a reducing atmosphere.

cooling is rapid (quenching) as happens in the top part of the sinter cake due to inadequate preheating of air, the structure is glassy and breaks down easily. A stronger sinter with more yield can apparently be made by using preheated air.[37]. Since the crystallization of molten phase finishes at 800–900°C, a retarded cooling to 600–700°C gives better sinter strength because of the decrease in thermal stress and the disappearance of glassy phase from the microstructure.[38]

6.4.4. Advantages of Sintering

6.4.4.1. Acid sinter

(i) agglomeration of fines into hard, strong and irregular porous lumps which give good bed permeability. In fact the gas throughflow is better in a sinter bed than in a pellet bed for the same size range because of higher voidage (cf. Fig. 5.8);

(ii) elimination of 60–70 percent of ore sulphur and arsenic (if present) during sintering;

(iii) elimination of moisture, hydrated water and other volatiles on the sinter strand with a cheap fuel;

(iv) increase in softening temperature and narrowing down of the softening range.

6.4.4.2. Fluxed sinter

Apart from the benefits mentioned above, fluxed sinters have the following additional advantages:

(i) calcination of limestone inside the blast furnace is very expensive of carbon. Approximately 60–70 kg C/100 kg of CO_2 (230 kg.$CaCO_3$) are saved by transferring the calcination work to the sinter strand (Sec. 10.4.2.4);

(ii) since incorporation of lime lowers the viscosity and the liquidus temperature of the bonding slag, less coke (lower temperature) can be used for the same strength and hence a high degree of oxidation and reducibility can be achieved[20] (Sec. 6.7.2). The increased strength of highly fluxed sinters during reduction may be due to the fact that calcium ferrites retain a compact structure without forming pores during the entire reduction process;[36]

(iii) lime increases the activity coefficient of FeO in the silicate and increases sinter reducibility (Sec. 6.7.2);

(iv) super-fluxing saves much more coke in the furnace. (However, the large amount of limestone needed results in an inadequate calcination during the short sintering time and the consequent presence of undissociated stone deteriorates sinter strength. For adequate strength either finely ground stone or calcined lime should be used but both these increase the cost of sintering. Hence, very few plants resort to super-fluxing);

(v) lime in sinter stabilizes the liquidus temperature of the primary FeO-Al_2O_3-SiO_2 slag the melting point of which would otherwise rise steeply as the FeO is reduced in the bosh;

(vi) lime-rich bosh slag hinders reduction of silica, absorbs vaporized silicon and sulphur to produce low-Si, low-S iron;

(vii) primary slag formed from fluxed sinter possesses lower viscosity and liquidus temperatures and more uniform composition than in the case of raw ores or acid sinters or pellets and hence permits smoother furnace operation. The slag characteristics are partly attained in the sinter itself so that the transformation to the final slag is rapid but gradual and occurs at a relatively lower and narrower temperature range;[36]

(viii) softening temperatures higher and the range closer than in the case of acid sinters because of lower amount of glassy silicates. Dolomitized sinters have higher softening temperatures than limey-sinters;[39]

(ix) sintering rate is higher than in acid sinters;[36]

(x) high blast furnace productivity, better than even with pellets; ideal blast furnace feed material because of by far the best high-temperature gas permeability.[40]

6.4.5. Pelletising[1-3,11,41-43]

During mining and ore dressing operations, especially where very fine grinding is necessary for wet concentration, a large amount of − 0.05 mm fines is generated which are not amenable to sintering because of very low permeability of the bed. They can, however, be agglomerated by balling them up in the presence of moisture and suitable additives like bentonite, lime, etc. into 8–20 mm or larger size. These *green* pellets are subsequently *hardened* for handling and transport by firing or *indurating* at temperatures of 1200–1350°C.

The balling stage is the most important part of the process and determines the strength, size, compactness and other pellet properties. The operation is performed in rotating devices like drums, discs (with flange on the rim) and cones, the most used being the former two. The effectiveness of the plain drum can be increased by fixing baffles inside. The ball formation occurs because of surface tension forces of water and collisions between particles. Initially, small nuclei of pellet are formed on addition of water and the nuclei grow bigger into balls and then into pellets as they pick up loose grain particles during their travel through the drum which is slightly tilted. The angle of tilt determines the time of residence, pellet size and productivity. The size and shape of the drum should be such as to obtain the most favourable condition of motion and pressure, i.e., more of rolling (moving up along the drum wall and dropping) as opposed to sliding action. This ensures more effective collisions between the particles. The capillary action of water in the interstices of the grains causes a contracting effect on them.[29] The pressure of water in the pores of the ball is sufficiently high so as to compact the constituent grains into a dense mass. The compressive force is directly proportional to fineness of the grains since the capillary action rises with the decrease in pore radius and the latter decreases with increasing fineness. An optimum moisture is important since too little of water introduces air inclusions in the pores

and too much of water would cause flooding and destruction of capillary action. The optimum moisture content usually lies between 5–10 percent or more, the finer the grains the larger the requirement.

A typical grain size distribution of ore suitable for pelletising is shown in Table 6.2. For full capillary effect the concentrate must be sufficiently fine-grained having about 95–100 percent + 0.01 mm and 60–90 percent − 0.05 mm. Under optimum conditions, very compact green pellets of sufficient strength are obtained for handling prior, during and after indurating. Such dense packing enables burning and hardening of pellets at temperatures lower than those required for sintering, especially for magnetic fines.

The firing can be performed either in shaft furnaces or in continuous travelling grates. In the latter drying, preheating, burning and cooling are all done in successive stages. During firing a critical stage is reached when the moisture is evaporated and yet the temperature attained is too low for any bond formation. The addition of even a small amount of bentonite or lime (0.5%) helps in maintaining some degree of cohesion among the grains during this period.[43]

The use of cement, concentrate and 100%-humidified air has been suggested for making cold-bound pellets.[44]

6.4.6. Pellet Bond[29,45]

6.4.6.1. Acid pellets

Depending upon the initial iron oxides, silica content and art of firing, the bonding forces for acid pellets are:

(a) Magnetite During firing at 1100–1250°C, magnetite is oxidized to hematite with an evolution of 55 kcal/mole of heat which ensures a uniform temperature distribution in the mass. In an excess of oxygen, the bonding is performed by bridging of magnetite grains through the hematite crystals formed. The strengthening of the pellets occurs due to high surface mobility of the atoms during oxidation, recrystallization and crystal growth of hematite. In a neutral atmosphere the bond is formed through recrystallization and grain growth of magnetite.

(b) Hematite In the absence of any exothermic heat of oxidation, the bonding and strengthening effect is obtained by recrystallization process involving coalescence of ferric oxide particles in the grain. Such a process needs higher temperature, usually 1300–1350°C. Hence, the firing time for hematite ore pellets is also higher.

The formation of bridges and hence pellet strength can be increased by fine grinding and also by intensification of crystallization with the use of pre-burnt or pre-reduced material.[45]

(c) Slag bond In cases where silica, lime, etc. are present, slag formation above 1200°C can also contribute as bonding agent. Such bonds give a glazed surface and retard the reduction rate but they yield pellets stronger than sinters.[46]

The pellet specifications as suggested by Traice and Lappin[41] are given in Table 6.3.[41]

Table 6.3.[41] Pellet specifications

Test	Suggested value
Size range	minimum 85%, + 9 mm − 16 mm
Compression strength (Sec. 6.6.2)	minimum 200 kg
ASTM index	minimum 94%, + 6.3 mm maximum 5%, − 500 μm
Reducibility (dR/dt 60%)	0.65% O/min
LTBT (Sec. 6.6.2)	minimum 80%, + 6.3 mm maximum 7.5%, − 500 μm
Swelling (Sec. 6.6.2)	maximum 20%

6.4.7. Fluxed Pellets[43,46–48]

It is possible to incorporate limestone in the pellet to obtain fluxed pellets. The stone needs to be ground to match ore fineness which is a costly process. Technical difficulties also arise during firing because of sticking of pellets, probably due to earlier softening caused by the formation of calcium silicate. Such stickiness does not arise in acid pellets because low-melting fayalite does not form in the oxidizing atmosphere.

In fluxed pellets, even if obtained from rich ores, an important role in bonding is played by glass. Main factors governing the strength of pellets are partial sintering of hematite or magnetite grains, some recrystallization of hematite and cementing of these two together by glass.[49] In dolomitized pellets, MgO is concentrated in magnetite and calcium ferrite and on reduction forms[50] higher melting solid solution 'magnesio-wustite'.

Fluxed pellets have the disadvantage of poor compressive strength, sensitiveness to weathering and decreased reducibility due to glazed surface. To make fluxed pellets less liable to breakdown during reduction, Khokhlov[51] suggests the use of high grade bentonite to reduce limestone consumption, an increase in the MgO level and firing temperatures to form more of difficultly reducible compounds of MgO with the iron oxides as well as to improve oxidation, and slow heating in the range 800–1000°C as maximum gas evolution occurs at these temperatures. Fine grinding of limestone also increases the pellet strength.[52] Self-fluxing pellets have been successfully made by Tyama et al.[53] Breakdown of fluxed pellets has been discussed by Khokhlov.[51]

Fluxed pellets are not used widely because of cost or other aforesaid disadvantages.

6.4.8. Advantages and Disadvantages of Pellets

6.4.8.1. Advantages

(i) minimum closure of pores by fusion or slagging; open pore system; very good reducibility due to high microporosity (porosity 25–35 percent). Slag bonded are less reducible;

(ii) spherical (egg) shape and small uniform size (10–20 mm) give very good bed permeability. The shape, size and low angle of repose give minimal segregation and an even charge distribution in the furnace, extending more towards the axis;

(iii) more accessible surface per unit weight and more iron per unit of furnace volume because of high bulk density, 3–3.5 tonnes/m^3. Larger surface and increased time of residence per unit weight of iron give better and longer gas/solid contact and improved heat exchange;

(iv) high iron content and more uniform chemical composition because of fine grinding and upgrading during ore dressing. Hence lower flux and fuel requirement in the furnace. Lower slag volume;

(v) high softening temperature, 1200–1350°C with narrow range; dolomitized pellets have a softening temperature about 80°C higher than the corresponding limey pellets;[54]

(vi) high strength – average compression strength about 150–250 kg or more for acid pellets;

(vii) heat consumption much less than that for sintering;

(viii) ease in handling, e.g., by pneumatic methods;

(ix) ideal for direct reduction processes;

(x) maintenance of size during reduction in the blast furnace, much more than in the case of ores and sinters especially in the lower temperature regions;[55]
(xi) acid pellets are stronger than fluxed sinters or pellets.[56] Reducibility of fluxed pellets is higher than that of fluxed sinter or acid pellets;[45,46]
(xii) fluxed pellets are more economical than fluxed sinters;[57]
(xiii) alkali attack on fluxed pellets is less than that on acid pellets.[58]

6.4.7.2. Disadvantages

(i) high cost of production due to grinding and firing especially with oil burners;
(ii) swelling and loss of strength inside the furnace;
(iii) sticking during firing;
(iv) resistance to flow of gas more than that in sinter for the *same size range* due to lower voidage (cf. Fig. 5.8);
(v) difficulty of producing fluxed pellets;
(vi) fluxed pellets break down under reducing conditions much more than acid and basic sinters and acid pellets;[56]
(vii) strong highly fluxed sinters, especially containing MgO, are being increasingly preferred to pellets.

6.5. Breakdown and Softening

It is well-known to operators that ores, sinters and pellets disintegrate and soften in the blast furnace in varying degrees. The diminution of voidage due to softening and generation of fines affect furnace output. It is, therefore, necessary to study the causes of such undesirable properties and how to avoid or minimize their occurrence.

6.5.1. Breakdown

Iron ores, sinters and pellets are composed of iron oxides associated intimately with impurities. When such materials are subjected to mechanical stresses at normal conditions as well as at higher temperatures in reducing atmospheres, their disintegration starts at points of weakness. Also, during reduction, new pore systems are developed which may result in further flaws and failures.

The mechanical properties of raw ores cannot be altered but it is possible to do so in the case of sinters and pellets. Experience shows that the mechanical stability of sinters varies widely depending upon the mineralogical composition and method of production. Fig. 6.4 shows schematically the variations in the strength of basic sinters as determined by yield from sinter strand and also by the tumbler test (abradability, Sec. 6.6.2.1). They show a minimum at medium basicity range.[18,59] The same tests carried out in a reducing atmosphere (top gas composition) below 700°C show a more marked degree of disintegration. Limey sinters of medium basicity show a very small percentage of larger size. Surely, if such breakdown occurs in the blast furnace, it would greatly reduce the furnace output.

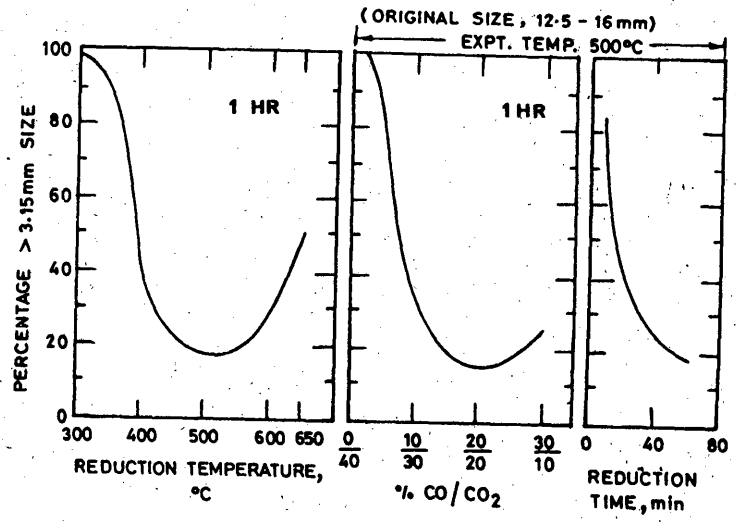


Fig. 6.5 Influence of temperature, gas composition and reduction time on sinter breakdown, according to vom Ende and Grebe.[59] (Copyright Verlag Stahleisen).

The extent of disintegration depends upon reduction temperature, reducing potential of gas and reduction time (Fig. 6.5).[59] Maximum breakdown occurs between 400–600°C with a CO/CO_2 ratio of about 1.0 and a longer reduction time. Obviously, the furnace will run smoother if the burden descends through the critical temperature zone of 400–600°C as fast as possible. In this respect, high productivity furnaces will be least affected. The cause of maximum breakdown of fluxed sinters of basicity 1–1.5 prior to or during reduction probably lies in the inherent weaknesses engendered by volume expansion associated with the transformation of dicalcium silicate from the β- to γ-phase as the sinter cools down from the strand (Sec. 6.4.3.2). The maximum breakdown between 400–600°C during reduction is sometimes attributed[60] to carbon deposition which is maximum between

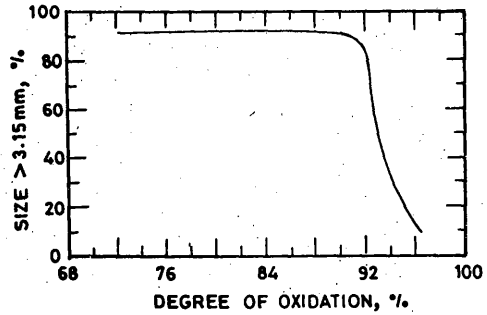


Fig. 6.6 Relation between sinter strength and degree of oxidation during reduction, according to vom Ende and Grebe.[59] (Copyright Verlag Stahleisen).

450–550°C. The breakdown is less when reduced with hydrogen[61] than with CO.

It is likely that the susceptibility of sinter (ore, pellet) to breakdown during reduction is intimately connected with the presence of hematite.[61,62] Fig. 6.6[59] shows that disintegration starts as the degree of oxidation exceeds 90 percent, that of magnetite being 89 percent. The loss of strength is initiated through cracks and fissures caused by volume changes while heating hematitic materials in a reducing atmosphere.

The normal volume increase of hematite (apart from catastrophic swelling to be seen in Sec. 6.7.6) during reduction to magnetite is of the order of 15–20 percent, and is associated with the structural metamorphosis of hexagonal hematite to cubic magnetite[29,63] (Sec. 3.4).

According to Ottow,[64] the degradation of iron-rich hematite pellets during reduction is partly due to an inward migration of iron ions from the reduced layer *a* and an increase in thickness (11 percent) of the underlying magnetite layer *b* (Fig. 6.7a).[64] When reduction occurs on all sides, there is a preferential expansion of magnetite in the directions of reduction leading to cracks (Fig. 6.7a).

One of the causes of crack formation is the directional nature of reduction velocity (anisotropy). The changeover from hematite to magnetite involves a rearrangement of oxygen ions. The transformation occurs when the (111) plane of the growing magnetite lies parallel to the basal plane (0001) of the hematite since it involves the lowest activation energy. This means that hematite will be reduced to magnetite preferably parallel to the basal plane (perpendicular to C-axis) as shown in Fig. 6.7(b).[64] The directional reduction results in unequal volume changes in different direc-

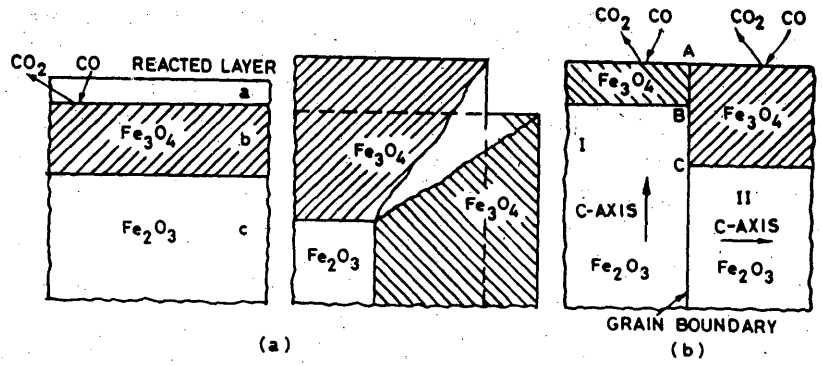


Fig. 6.7 **(a)** Change in volume during reduction of hematite; **(b)** anisotropy of the reduction rate in a single hematite grain, according to Ottow et al.[64] (Copyright Verlag Stahleisen).

tions during the formation of magnetite as shown for two neighbouring crystals of a hematite grain. This results in stress on the boundary BC where fissures appear. Whether the differential expansion results in fine, large or no cracks would depend upon the bond strength and crystal growth pressure. The reducibility will depend upon the extent of exposure of fresh surfaces created by the fissures.

Calcium silicate and ferrites increase the LTB strength during reduction.[65] Silicate bonding of hematite increases the strength, reduces cracking but deteriorates reducibility. Reduction cracking of sinters can be changed with the CaO/SiO_2 ratio.[66] Initial strength of sinters increases with up to 15–20 percent of slag constituents and it drops rapidly up to 10–20 percent reduction.[67] Once a sufficiently thick layer of iron is formed, the strength starts to increase.

6.5.1.1. Alkali attack

A further cause of breakdown of ferrous materials is the presence of alkali metals. The mode of action may be different at higher and lower temperatures.

At higher temperatures, around 1000°C, the presence of alkali metals causes excessive swelling of ferrous burden, especially of iron-rich pellets. Such enlarged volume leads to a soft, highly porous material without any significant strength and easily amenable to compaction and breakdown, causing serious impedance to gas flow. This subject has been dealt with in Sec. 6.7.6.

The alkali metal compounds which are stable at low temperatures can contaminate the charge materials in the upper furnace, having been carried along with the gases as fine solid particles. According to Davies et al.,[130] low-temperature-breakdown (LTB) tests carried out with various types of sinters and pellets at 600°C in a mildly reducing atmosphere, while being tumbled, showed that alkali carbonates can have detrimental effect on the resistance of sinters and pellets to LTB, the extent of which depends upon the concentration of alkalis. The causes of LTB are not known but they may be connected with the increased reduction rate of iron oxides in the presence of alkalis (Secs. 2.8 and 6.7.6). According to Davies et al.,[130] the alkalis catalyse the surface reduction of hematite to magnetite and increase the reduction rate so much that the stresses generated during transformation of hexagonal hematite to cubic magnetite do not recover due to insufficiency of time, resulting in extensive crack formations. On this basis, the LTB results of different materials can be explained. As for example,[130]

(i) acid pellets without alkali do not normally disintegrate much during LTB tests because the matrixes are comprised of directly bonded hematite grains. In the presence of alkalis, the direct bonds are weakened and the pellets break up due to stresses generated during transition of hematite to magnetite;

(ii) fluxed pellets plus alkalis do not show any adverse LTB properties, probably because of more effective and increased slag bonding of such pellets;

(iii) in the case of sinters, the LTB properties depend upon the ability of the slag matrix to withstand the stresses generated; as we have already seen in this section, sinters of medium basicity have the most adverse LTB properties. The addition of alkalis to fluxed sinters increases the reducibility accompanied by a marked cracking and disintegration at low temperatures.

6.5.2. Softening[68-75]

Softening, plastic flow or premature fusion of raw ores can occur in a wide range of temperature, 700–1350°C. In sinters and pellets they occur at a higher and in a much narrower range, 1000–1350°C. Any softening below 1000°C is detrimental to indirect reduction due to premature closure of pores which is aggravated by the mechanical load of the charge. In addition, any decrease in voidage caused by softening and consequent compacting of the bed of charge materials in the dry zone of the shaft results in an increased resistance to flow and decreased furnace output (Eq. 5.29).

A wide range of softening temperature is also detrimental because of formation of a large zone of sticky materials which lowers the bed permeability in a vertically extended zone in the furnace. Since the formation of a sticky fusion zone cannot be avoided (because the gangue and flux have to melt anyway), it is desirable to restrict the range of this zone of low permeability to the minimum (Eq. 5.22).

Softening characteristics depend upon various factors, such as, temperature, crystal structure, porosity, degree of reduction, particle size, iron content, initial state of oxidation, nature and amount of gangue, basicity, etc. The presence of alkali metal oxide may lower the softening temperature greatly.[76] According to Grieve,[78] softening can start above a degree of reduction of 20 percent (i.e., when essentially wustite is formed). Poos and Decker[71] showed that the minimum temperature for 25 percent decrease in sample height (denoting end of softening, Sec. 6.6.2.6) occurred at a degree of reduction greater than 50–60 percent.

According to Bogdandy and Engell[75] the higher the porosity the lower the incipient softening temperature. A high and narrow range of softening at degrees of reduction above 50 percent creates the most favourable conditions for smooth and efficient furnace operation.

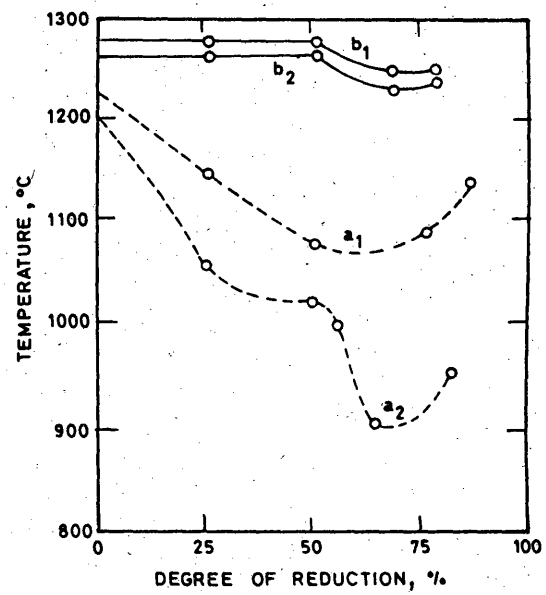


Fig. 6.8 Influence of degree of reduction of two different varieties of iron ores on the softening temperature, after Davison.[77] (By permission, Indian Institute of Metals).

Measurement of softenability is discussed in Sec. 6.6.2.6. The range is given as beginning (3 percent height reduction) and end of softening (25 percent height reduction). From Fig. 6.8,[77] the material (*a*), which has a wide range, is likely to result in a larger zone of viscous semi-fused mass and a large pressure drop in the lower furnace leading to maldistribution of gas, non-uniform material descent, hanging, scab formation, etc. On the other hand, material (*b*) is not expected to give any of the above troubles provided it is not susceptible to low-temperature breakdown or swelling.

Sintering and pelletising not only raise the softening temperatures but also narrow down the range. This is more so with fluxed agglomerates. Acid sinters show comparatively lower softening temperatures (1000–1150°C) because of flow of fayalite. The much higher softening temperatures of fluxed sinters (1100–1250°C) cause less disturbance and the reducibility of such sinters is also very much higher. From the softening point of view acid pellets are as good as fluxed sinters but their reducibility is inferior.

The softening and melting of the charge materials occur in a range of temperature. The patterns of the softening-melting zones in the blast furnace are shown schematically in Figs. 5.1 and 11.24.

The size and zone of softening-melting can be affected by alkali metals. They lower the liquidus temperatures of the burden materials. They also accumulate to a maximum extent in the recirculating zone of 700–1200°C. If an optimum quantity is exceeded the position and extent of the zones will be affected which may be detrimental to gas throughflow and furnace productivity (cf. Sec. 11.5).

6.6. Testing of Ores, Sinters and Pellets

The principal purpose of burden preparation is to obtain optimum coke rate and furnace productivity. Even if an apparently optimum material is charged in the furnace, it can undergo degradation occurring by impact, abrasion, compression, decrepitation, attrition, temperature, carbon deposition, reduction, etc. In addition, they can undergo softening and swelling. The alterations in the bed permeability caused by the above occurrences may occasion severe impedance to gas throughflow. It is, therefore, imperative that all burden materials are tested for their suitability with regard to their physical strength and breakdown properties under ambient as well as blast furnace conditions. Similarly, their reducibility should also be

ascertained in order to determine the extent of gaseous (indirect) reduction likely to be obtained under the same conditions.

Reducibility, reducibility testing and physical testing methods are described very briefly in the following sections. For more details of the testing methods, the coverage by Ball et al.[1] and by Davison[77,78] may be consulted. The various factors affecting reducibility are discussed in Sec. 6.7.

6.6.1. Reducibility Testing[1,6]

It has been stressed at various places in the text that it is desirable for fuel efficiency, smooth furnace operation and iron quality that the ferrous materials are reduced as far as possible in the zone of indirect reduction (<1000°C) during their time of residence in this critical temperature regime. As different materials behave differently, it is necessary to evaluate the various factors that contribute to their differential rates of reduction.

The possible mechanisms of iron oxide reduction have been discussed in Sec. 2.8. In commercial ores the individual reaction mechanisms are subject to overlapping influences of various physical and chemical factors. Without taking the mechanism of reduction into consideration, the overall reduction velocity, similar to Eq. 2.26, can be written broadly as,[6]

$$-\,d(O)/dt = f\phi,\ A,\ (C^* - C^\circ) \qquad 6.2$$

where,

$-\,d(O)/dt$ = rate of oxygen removal, mole/unit time
ϕ = factor (similar to rate constant) depending upon temperature, degree of reduction, nature of ore, etc.
A = available surface area for reduction
C^* = equilibrium CO_2 or H_2O concentration of gas for the oxide (generally wustite)
C° = actual CO_2 or H_2O concentration in the gas.

Reducibility is the ease with which the oxygen combined with iron can be removed *indirectly*. There is no universally accepted standard method of ascertaining it. Since, for a given ore, the reduction rate is greatly dependent on particle size, reducibility tests on the ore crushed to various sizes can and do give sufficient information for selection of suitable feed material.

In the case of raw ore, very little can be done for improving reducibility except by crushing to smaller sizes. In the case of prepared burden, the various parameters on the right hand side of Eq. 6.2 can be suitably varied

in order to increase the reduction rate, e.g., the available surface area A can be increased by increasing the porosity of the sinter or pellet or C* can be increased by suitable alteration of the mineralogical composition. Even ϕ can also be advantageously altered by encouraging formation of wustite lattice distortions during reduction.

6.6.1.1. Reducibility testing methods[1,6]

Reducibility of ferrous materials is characterized by their fractional oxygen removal rates in gaseous reducing atmosphere. The percent degree of reduction or percent fractional oxygen removal is given by

$$\% \text{ degree of reduction} = \frac{n_o - n}{n_o} \times 100 \qquad 6.3$$

where,

n_o = number of moles of oxygen originally combined with iron only;
n = number of moles of oxygen left combined with iron after experimental time, t.

The amount of oxygen removed is measured by weight loss of the sample or through material balance of the oxidized and reducing gas. The degree

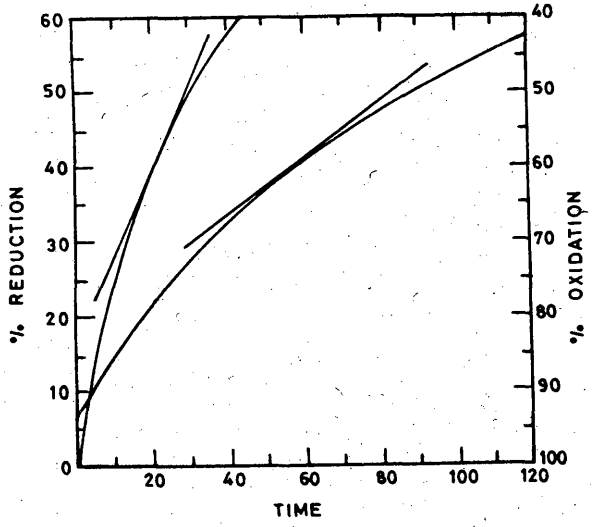


Fig. 6.9 A schematic representation of relationship between reduction at 40% degree of reduction and 60% degree of oxidation levels, after Davison.[77] (By permission, Indian Institute of Metals).

of reduction is plotted against time, the slope of the curve giving the velocity of reduction at any time or at any particular degree of reduction. Since the reduction rate is critical after a metallic iron layer is formed from wustite, the reducibilities are generally compared at 40 percent degree of reduction, dR/dt(40%).

However, by this process, hematite which contains more oxygen is compared unfavourably with magnetite. A more fair comparison is the rate at 60 percent oxidation level, dR/dt(60%), i.e., when O/Fe = 0.9, which is the same as dR/dt(40%) when two hematites or two magnetites are being compared. Nowadays, the percent oxygen removed per minute, dR/dt(60%), is being increasingly quoted for reduction rates. These two procedures are illustrated in Fig. 6.9.[77]

Reducibility testing includes determination of reduction rate of the ore or agglomerate samples, usually by three different methods:

(a) reduction rate at one temperature or during continuous heating;
(b) reduction at one or two temperatures and determining the degradation of materials after experimentation (static method);
(c) combined reducibility and degradation measurements during continuous heating (dynamic method).

Only a few methods are quoted briefly below:

(i) Isothermal test[79-81] It involves reduction of ore or agglomerate samples of different sizes at any temperature between 800 and 1000°C by CO or H_2 or a mixture of both, or either or both mixed with N_2 and/or CO_2. The temperature 800–1000°C is selected because the reduction rate of wustite in this range is critical for gaseous reduction (Fig. 1.2).

(ii) Non-isothermal test[82-86] An alternative to the above method is continuous heating of the sample in a desired reducing gas at a rate of 4–6°C per minute from 20 to 1000°C so as to simulate descent through the blast furnace shaft and simultaneous and continuous monitoring of oxygen removal.

(iii) C.N.R.M. test[82,87] Reduction at 1000°C for one hour. Total amount of reduction measured by weight loss or chemical analysis.

(iv) Linder test[88] It is a combination of degradation and reducibility tests. It simulates in a rotating cylinder the various reducing atmospheres and temperatures to which ferrous materials are exposed in the blast furnace. After going through pre-determined heating-cum-reduction cycles up to 1000°C, the sample is cooled, screened and -0.5 mm and -1.7,

+ 0.5 mm fractions expressed as percentage of the final product and results correlated with blast furnace performance.

Chiba[89] dynamic test is similar but measures low-temperature breakdown (LTB) up to 600°C.

(v) Gakushin test[90,91] This test, widely used in Japan, employs a gas of fixed composition, 30% CO + 70% N_2, at 900°C for 3 hours. The extent of reduction is measured by CO-CO_2 analysis or weight loss. It can also be suitably modified for measuring pellet swelling. The strength of materials after reduction is obtained from a tumbler test of the reduced material. The breakdown occurring during reduction can also be estimated.

(vi) Chiba test[89] It is similar to Gakushin test but the reducibility is converted into an interface speed index in mm/hour. The gas composition used is 35% CO + 65% N_2.

(vii) BoRist test[92] Bonnivard and Rist have developed a testing method for determining the minimum residence time of an ore in the shaft for obtaining a chemical inactive zone when the blast furnace gas is in equilibrium with wustite (Sec. 3.6). If the residence time is small, furnace productivity can be increased without endangering the formation of an inactive zone. If it is too high, the ore would need preparation (crushing to small size, etc.) to increase the reduction rate. Thus, the critical residence time can be used as a measure of reducibility index.

(viii) Bulk burden reducibility index[77,78] Blast furnace feed materials consist of ores, sinters and pellets of different varieties and sizes. Bulk reducibility index of each component is determined from intrinsic reducibility of each size. The bulk reducibility indices of all the components are then summed up to give the 'Bulk burden reducibility index' for correlation with the blast furnace coke consumption rate.

The most useful tests are those which include reduction rate along with degradation, pressure drop, compressive loading, etc. Some more testing methods are given in the next section.

6.6.2. Physical Testing[1,77,78]

Since ores, sinters and pellets possess inherent mechanical instability or they develop it during heating and reduction, a few methods are used to determine their cold strength as well as their physical behaviour during hot reduction. To ascertain these properties some testing methods have

been developed which broadly fall into the following categories. The adverse effects of some of the inferior properties have already been discussed.

1. Cold strength
2. Porosity
3. Decrepitation
4. Low-temperature breakdown under reducing conditions (LTB)
5. Hot compression strength
6. Softening temperature and range
7. Swelling and volume change
8. High-temperature bed permeability under compressive load and reducing conditions.

6.6.2.1. Cold strength[93,94]

Cold strength measurement comprises of tumbler or drum test for abradibility, shatter test for impact and compression test for load during storage.

(i) Tumbler or drum test[93] It measures the susceptibility of ferrous materials (coke as well) to breakage due to abrasion during handling, transportation, charging on to the blast furnace bells as well as inside the furnace itself. In this test, a certain weight of the material within a selected size range is rotated in a drum of given size for a given time with certain number of revolutions. The abrasion strength is given by the percentage weight of + 6.3 mm surviving the test and dust index by the percentage of − 0.6 mm. For good pellets the respective percentages are 85–95 and 3–7, for sinters 60–80 and 5–10 and for ores they vary greatly, 60–95 and 2–25.

In order to minimize the amount of fines delivered to the furnace, a practice attracting an interest is to deliberately subject the materials, especially coke and sinter, to mechanical breakdown and stabilize the charge, e.g., by means of vibrating screens. They break where the bonds are weak and the undersize screened out. However, it cannot be helped if any fines are generated between charging into the skip car and then into the furnace. The testing by hot abrasion has been investigated by Janke.[94]

(ii) Shatter test[93] It measures the susceptibility to breakdown due to impact during loading, unloading and charging into the furnace. In this test a certain weight of material is allowed to fall on a steel plate from

a certain height for a pre-determined number of times and the amount of undersize measured. For strong sinters the percentage + 10 mm surviving is above 80.

(iii) Compression test[95] It is used mainly for pellets. Pellets, unreduced or reduced to various degrees, are subjected to compressive load at ambient or high temperatures and the percentage of + 5 mm yield measured and correlated with blast furnace performance.

6.6.2.2. Porosity[95,96]

While ores and pellets possess mostly open pores, in sinters there are macro- and micro-pores as well as open and closed pores (cut off from outside and cannot be reached by gas).

True porosity and hence closed porosity can be determined from open porosity which can be measured from the true and bulk densities.

Although reducibility increases with increasing open porosity, the latter changes continuously during reduction on load. Generally, a high initial porosity results in earlier softening of the material.

6.6.2.3. Decrepitation[93,97,98]

Dust formation can occur during transportation or while charging in the skips and in the furnace in case of materials having a low tumbler or shatter index or due to decrepitation in the throat of the furnace where the temperature is as high as 400–600°C. Decrepitation can occur due to internal pressure developed from evaporation of moisture and chemically combined water or crack-formation arising from sudden heating and expansion. It can be measured from percentage − 5 mm and − 0.5 mm generated from samples after heating in a nitrogen or in a mildly reducing atmosphere at temperatures 400–600°C.

Decrepitation is a property which is not in the hands of blast furnace operators. The only remedy is to screen out all fines below − 6 mm or − 10 mm prior to charging. Also, such ores can be mixed with sinter or pellet (they do not decrepitate) in such proportions as to obtain the least furnace disturbance.

6.6.2.4. LTB tests under reducing conditions

After being charged in the furnace, apart from decrepitation at lower temperatures, the materials undergo further degradation by abrasion, compression and chemical reactions for reasons already seen in Sec. 6.5. For forecasting their behaviour, testing methods have been devised[1] some

of which have already been described in Sec. 6.6.1. Sinters of medium basicity are most susceptible to breakdown in a mildly reducing atmosphere at 500–600°C. Bisra LTBT method involves rotation of sample during reduction at 600°C and the indices for + 6.3 mm and − 0.5 mm and the degree of reduction are recorded.[99]

It has been invariably found that materials having inferior LTB properties or inferior reduction strength under conditions of temperature and reducing atmosphere as prevailing in the blast furnace shaft, when charged, result in poor performance, hanging, slipping, etc.[100,101]

6.6.2.5. Hot compression strength[102]

Usually employed for pellets, it is used under conditions simulating their descent to various levels in the furnace. As the formation of wustite and iron increases, the hot compression strength of the pellets (also ores and sinters)[103] decreases greatly and they lose their ability to withstand load half way down the furnace stack.

6.6.2.6. Softening

Ferrous materials soften in a range of temperature depending upon the degree of reduction, applied load and rate of heating. The C.N.R.M. method[104] consists of using pellets as delivered and ores and sinters ground to definite size fractions, all pre-reduced to various degrees. Beds of these are subjected to slow heating in nitrogen under load (approx. 2 kg/cm^2) to 1350°C. The temperatures at which decrease of 3 and 25 percent of the initial bed height occurs are taken as the beginning and end of softening. These are plotted against the degree of reduction (Fig. 6.8). The importance of such tests has been seen in Sec. 6.5.2.

6.6.2.7. Swelling[104]

Swelling or volume change occurs when hematite pellets in general are reduced in a hot reducing atmosphere. The volume changes are determined either by dilatometer for single pellets or, for more representative results, by measuring the volume through mercury displacement of a batch of pellets before and after experiments at various temperatures and stages of reduction. Maximum volume change occurs at 900–1000°C and at a degree of reduction of 45–50 percent.

6.6.2.8. High-temperature bed permeability test

This very useful test simulates blast furnace shaft conditions.[101,105] It combines reducibility, swelling, softening, disintegration and decrepitation

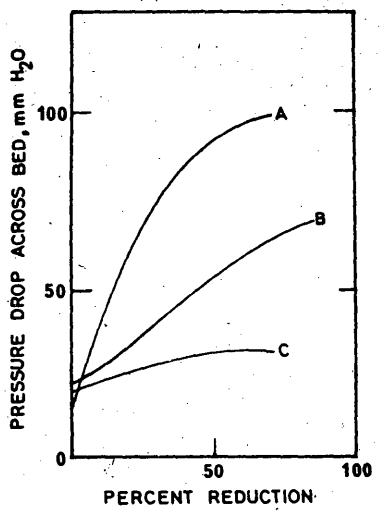


Fig. 6.10 A typical example of Burghardt test applied to 3 different ores which shows the favourable properties of Ore C, after Davison.[77] (By permission, Indian Institute of Metals).

under load and includes pressure drop measurement across the column of sample for ascertaining bed permeability. In the Burghardt method[105] which particularly furnishes loss of permeability due to softening and swelling, the alteration of bed height and pressure drop are measured while reduction is proceeding isothermally at 1000–1050°C under load (0.5–0.8 kg/cm²). Results are quoted for 80 percent reduction. Fig. 6.10[77] is a typical example of such a test which shows the possible deleterious effects of ores A and B compared to C. A higher resistance to gas flow and a lower furnace output is expected with the use of the former two in the blast furnace.

Sinters do not swell or soften under Burghardt test conditions. Special tests[106] have been developed where they are subjected to a programmed temperature increase up to 1200°C and reduction-gas composition under a load of 2 kg/cm².

6.7. Factors Affecting Reducibility

The various factors that affect the rate of reduction of iron ores, sinters and pellets are discussed in the following sub-sections.

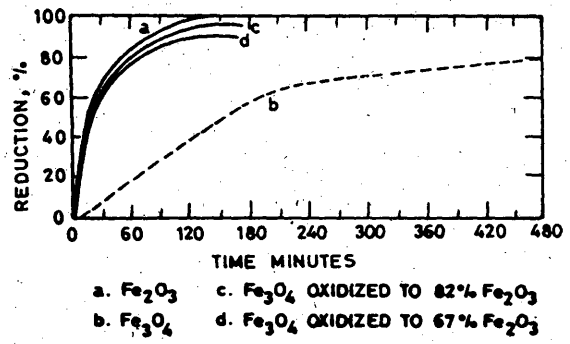


Fig. 6.11 Reduction of single crystals of hematite and magnetite as well as of magnetite oxidized to hematite in varying degrees, according to Edström.[63] (Copyright Iron and Steel Institute).

6.7.1. Ore Quality

Reduction of natural hematite ores by CO or H_2 starts between 200–500°C, depending upon the physical characteristics and mineralogical composition. However, the rate below 500°C is sluggish.

Hematite is more reducible than magnetite although the amount of oxygen to be removed per unit weight of iron is about 12 percent higher in the former. Fig. 6.11[63] shows that the reduction rate increases with increasing degree of oxidation of magnetite. The better reducibility of hematite may be due to:

(i) formation of porous wustite from hematite, easily accessible to reducer gas whereas magnetite forms dense wustite during reduction;
(ii) tendency of hematite to break down and expose larger surface due to expansion in volume during reduction to magnetite as already discussed in Sec. 6.5.1;
(iii) pores in hematite are more elongated and the microporosity larger; magnetite has larger grain size and is more closely packed;
(iv) a higher value of overall rate constant (ϕ, Eq. 6.2) for wustite reduction since the wustite lattice formed during reduction of hematite exhibits a higher degree of disorder than that formed from magnetite.

A logical result of the inferior reducibility of magnetite is its conversion to hematite by oxidising roasting. It is economical[107–109] and in Sweden the coke rates have been brought down to as low as 650 kg/THM.

The mineralogical composition of ores affects reducibility both physically and chemically.

6.7.1.1. Physical influence

Breakdown due to expansion of gangue materials. As for example, quartz changes to α-phase at 575°C and to tridymite at 875°C, both transformations being accompanied by volume increase.

Iron may be present as hydrates and carbonates. They are of little interest now-a-days because most blast furnace feed materials are sintered or pelletised. Both of them decompose endothermically at temperatures 400–600°C:

$$FeCO_3 = Fe + CO_2 - 82950 \text{ cal} \qquad 6.4$$

$$Fe(OH)_2 = FeO + H_2O - 15000 \text{ cal (approx.)} \qquad 6.5$$

Apart from a thermal load in the upper shaft, the CO_2 and H_2O evolved decrease the term in the parenthesis of Eq. 6.2 and hence the reduction rate. However, the decrease in volume and evolution pressure of the gases cause extensive breakdown and increase in surface area, facilitating reduction although at the same time causing severe impedance to gas flow.

Decrepitation is also caused by physically absorbed or adsorbed or hydrated water during their evaporation.

6.7.1.2. Chemical influence

We have seen in Sec. 2.8 and also elsewhere in the text that the reduction rate of wustite is critical in the overall kinetics of iron oxide reduction. In the reaction,

$$FeO + CO = Fe + CO_2 \qquad 6.6$$

$$K = \frac{a_{Fe} \cdot p_{CO_2}}{a_{FeO} \cdot p_{CO}} \qquad 6.7$$

the equilibrium partial pressure or concentration of CO_2 would decrease if a_{FeO} is lowered by solution and/or compound formation. Hence, from Eq. 6.2, the reduction rate would also decrease.

Natural ores can contain iron oxides as compounds with gangue materials, such as, $2FeO.SiO_2$, $FeO.Al_2O_3$, $FeO.Cr_2O_3$, $FeO.TiO_2$, etc., where wustite exists in a state of low activity. Even in the absence of these compounds, the activity of wustite can decrease at higher temperatures during descent of the burden in the blast furnace when it undergoes sintering with the impurities present (or added), such as, SiO_2, Al_2O_3, CaO, MgO, etc. The reduction of such wustite would occur at higher temperatures as shown, for example, by the free-energy line of $2FeO.SiO_2$ in Fig. 2.3. If the reduction occurs in the field of the Boudouard reaction (above 1000°C), the gaseous reduction becomes equivalent to direct reduction and hence expensive of coke.

6.7.2. Sinter and Pellet Quality

Perhaps the most reducible form of iron oxide is hematite. During the making of acid sinter a considerable quantity of difficultly reducible fayalite is formed depending upon the silica content of the ore and fuel rate in the sinter mix. As the fuel rate and hence the amount of fayalite increases, the reducibility also decreases simultaneously. This was seen schematically in Fig. 6.3 and is clarified from the experimental values, valid for $CaO/SiO_2 = 0$, shown in Fig. 6.12.[21] Since the sinter strength increases with the fayalite content, in making an acid sinter of sufficient strength and reducibility, a compromise is usually made.

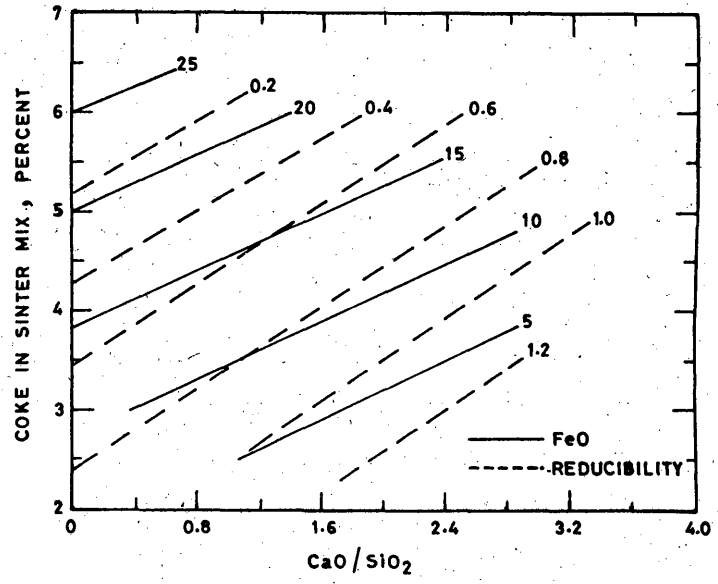


Fig. 6.12 Variation of Sinter FeO and reducibility dR/dt(60%) with sinter coke rate and CaO/SiO_2 ratio at 0.5% magnesia and 1.5% alumina, according to Price and Wasse.[21] (Copyright Iron and Steel Institute).

The probable causes of low reducibility of acid sinters are:

(i) low activity coefficient of FeO in fayalite;
(ii) closure of pores by liquid slag making them less accessible to reducing gases;
(iii) low degree of oxidation, i.e., low Fe^{3+}/Fe^{2+} ratio; the higher the ratio, i.e., the higher the hematite content the greater the degree of volume expansion, cracks and fissures, and porosity of the product during reduction. (Acid pellets do not suffer from these physical disadvantages to any great extent).

A sinter with both sufficient strength and reducibility is obtained if lime is incorporated in the sinter mix. Fig. 6.12 shows the reducibility and FeO content as functions of CaO/SiO_2 ratio and coke rate. The reducibility has been measured as %O/min removed at dR/dt (60%). For any basicity ratio, the lower the coke rate the higher the reducibility and the smaller the FeO content. This means, for a desired oxygen removal rate, the sinter coke rate can be increased to obtain adequate strength by increasing the basicity correspondingly. In limey sinters the fayalite bonding medium is increasingly replaced by calcium ferrites as the basicity increases (Sec. 6.4.3.2).

Some results of reduction experiments with various sinter constituents and ore are shown in Fig. 6.13[36] and Table 6.4.[20] A comparison between them shows that except $2CaO.Fe_2O_3$ and $4CaO.Al_2O_3.Fe_2O_3$, all the lime-bearing constituents are as much or more reducible than hematite. Magnetite is even less reducible than dicalcium ferrite. The least reducible constituent is $CaO.FeO.SiO_2$, similar to fayalite in acid sinters.

Table 6.4.[20] Degree of reduction of sinter minerals after reduction for 40 minutes in pure CO at 850°C

Constituents	Percentage reduction
Fe_2O_3 (Brazilian)	49.4
$CaO.Fe_2O_3$	49.2
$CaO.2Fe_2O_3$	58.4
$3CaO.FeO.7Fe_2O_3$	59.6
$CaO.Al_2O_3.2Fe_2O_3$	57.3
$2CaO.Fe_2O_3$	25.5
$4CaO.Al_2O_3.Fe_2O_3$	23.4

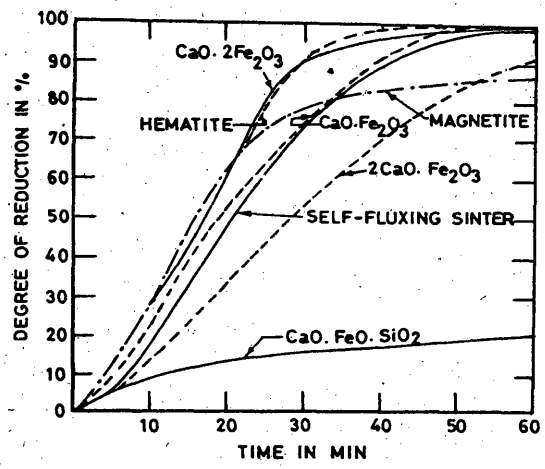


Fig. 6.13 Reducibilities of various ores and sinter constituents in hydrogen at 800°C, according to Watanabe.[36] (Copyright John Wiley).

The cause of increased reducibility of limey sinters (or pellets) is not still very clear. It may be due to one or more of the following:

(i) increase of lime decreases the amount of iron-bearing silicates by forming preferably calcium silicates. It also raises the activity coefficient of wustite;
(ii) limey hematite tends to form disordered and hence more reactive wustite, especially from pellets (Secs. 2.8 and 6.7.6) which enhances the rate of wustite reduction;
(iii)[6,110] iron oxides and iron-rich ferrites are at first reduced to FeO and $2CaO.Fe_2O_3$.

The reducer gas then attacks the dicalcium ferrite preferably according to:

$$2CaO.Fe_2O_3 + H_2 = 2CaO + 2Fe + 3H_2O \qquad 6.8$$

The ferrite is reformed through reaction of wustite with the liberated lime:

$$2CaO + 3FeO = 2CaO.Fe_2O_3 + Fe \qquad 6.9$$

Since the newly formed ferrite is in a highly reactive state, it is immediately reduced by hydrogen;

(iv)[111] high porosity of iron layer surrounding the unreduced lime-containing wustite, giving high reaction rate in contrast to lime-free wustite (Sec. 6.7.5).

The reducibility of pellets is usually higher than that of sinter. However, if the pellets are fired at high temperatures, usually a glazed surface is produced which hinders gas accessibility to the interior. Fluxed pellets are also superior to fluxed sinters in reducibility but inferior in mechanical properties.

6.7.3. Ore Size

Apart from the mineralogical composition and internal physical structure, reducibility is a function of external size of the ore, sinter or pellet. The influence of outer visible surface, i.e., ore size, decreases as the invisible ore surface, i.e., porosity increases. In general, the size and compactness both assume importance in reduction.

In practice, the furnace operator has little control over the porosity or mineralogical composition of the ore with the exception of sinters and pellets. Hence, the only alternative for achieving a desirable rate of reduction of ore is to crush it and expose a greater surface per unit volume. From practical viewpoint, a minimum rate of oxygen removal of 0.5–1.0 percent per minute at 40 percent degree of reduction is adequate for optimum

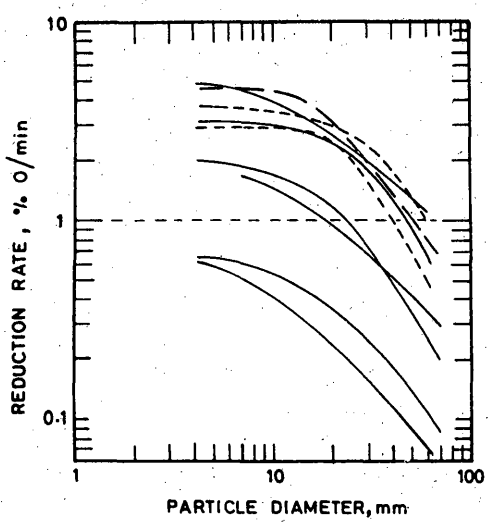


Fig. 6.14 Relationship between reduction rate and size of iron ores from various sources, according to Birnbaum and Bogdandy.[112] (Copyright Verlag Stahleisen).

indirect reduction in the blast furnace shaft. Different ores should be crushed and graded into suitable size to obtain the above reduction rate.

Fig. 6.14[112] shows the relationship between ore size (diameter, d) and velocity of reduction (v) for various ores at 800°C in a stream of hydrogen, the diameters ranging between 7 and 70 mm. For each variety, below a certain size, the velocity remains more or less constant. It would be uneconomical to crush the ore below this optimum size. Regarding the relationship between the reduction velocity and particle diameter, the following have been confirmed statistically from experimental values:[113]

(i) for very small size, v is proportional to d^0, i.e. independent of size;
(ii) for medium size, v is proportional to d^{-1};
(iii) for large size, v is proportional to d^{-2}.

Although the limits between these three regions are different for different varieties of ores, from the viewpoint of practical interest, i.e., between 6 to 70 mm, all the three fields are crossed as is apparent from Fig. 6.14.

6.7.4. Degree of Oxidation

The degree of oxidation of magnetite is about 89 percent. The presence of hematite starts above this figure. Hematite is much more reducible than magnetite, the reasons for which have already been discussed in Sec. 6.7.1.

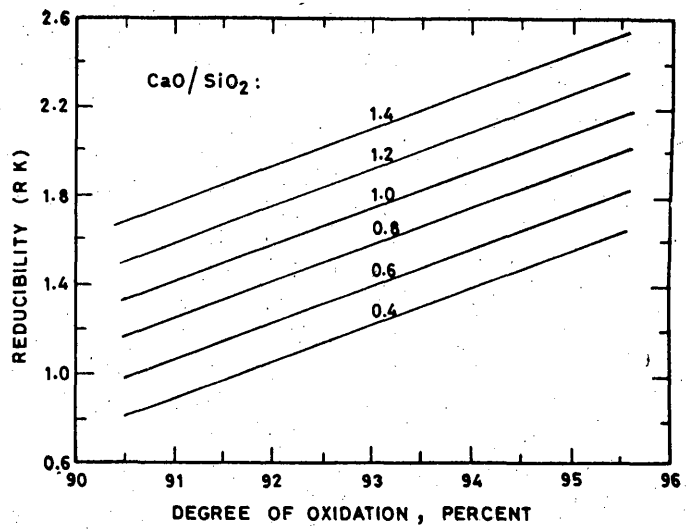


Fig. 6.15 Increasing reducibility of sinters with increasing degree of oxidation as well as basicity, according to Schwabe and Rellermeyer.[10] (Copyright Verlag Stahleisen).

Hence, the greater the degree of oxidation, i.e., the larger the amount of hematite, the better the reducibility. The trends are shown in Fig. 6.15[10] for different iso-basicity lines. The figure also confirms that reducibility increases with increase in basicity.

We have seen in Fig. 6.12 that the FeO-content in sinters decreases, i.e., the degree of oxidation increases with decreasing coke rate in the sinter mix or for the same coke rate it does so with increasing basicity. Therefore, a highly oxidized sinter can be produced with comparatively small coke rate with increased lime content in the sinter.

6.7.5. Porosity

Reduction of ores by a reducing gas is greatly facilitated if access is available into the interior of the ore lump. Also, the higher the porosity the larger the inner surface area available for reduction. Hence, it is expected that the reduction rate will be higher the higher the porosity. It was recognized by Joseph[114] in 1936 who showed that, for 90 percent reduction, the reciprocal of time varied linearly with percent porosity. This is confirmed by the investigations of El-Mehairy (Fig. 6.16).[115]

However, classification of ores according to their reducibilities based on initial porosities has no absolute significance since the initial porosity found in ferrous materials undergoes profound changes during their descent in the blast furnace. Porosity changes continuously as the reduction progresses because of removal of oxygen from oxide lattices, removal of gaseous pro-

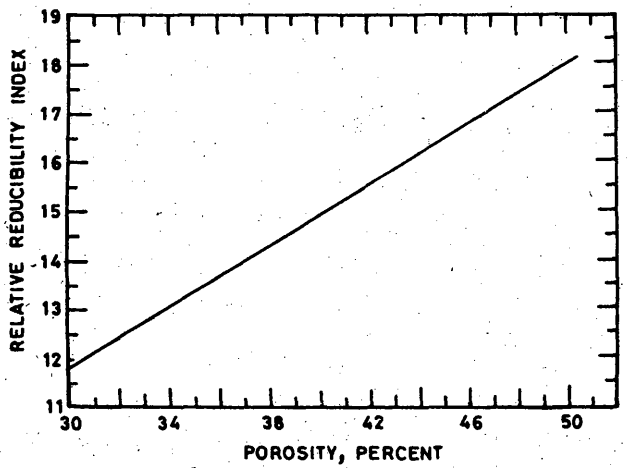


Fig. 6.16 Reducibility is directly proportional to porosity provided the pore size remains the same, according to El-Mehairy.[115] (Copyright Iron and Steel Institute).

ducts, lattice disturbances, phase transformations, decrepitation and volume changes, compressive load, softening and recrystallization of iron, softening of gangue and filling up of pores, etc.

The difference between the modes of reduction of dense and porous hematite lumps is shown by the photomicrographs[111] of partially reduced specimens in Fig. 6.17(a) and (b) respectively. In the former case a layered structure with inward advance of iron, wustite and magnetite phases is clearly visible (Fig. 6.17a). The formation of such a structure is typical of a slow diffusion of reducing gas particularly through the iron layer.[116,117] Similar figures are also obtained when the driving force of reduction is high, e.g., when reducing with 100%H_2.

In the case of porous lumps (Fig. 6.17b), gaseous diffusion through the pores is easy and hence there is a rapid *internal* reduction of hematite to wustite and subsequent reduction of the latter to iron. Such a diffuse product structure (absence of distinct layers) is also obtained when the reduction rate is slow, furnishing more time to the reducing gas to diffuse into the pores, as for example, when a dense specimen is reduced with a CO/CO_2 ratio of 9, the rate of reduction being[111] one-tenth that with 100% H_2. It is likely that the difference in the product morphology in the dense specimen when reduced with high and low reduction potential gases is caused by the relative rates of iron ion diffusion and oxygen removal from the oxide lattice as suggested by Eq. 2.38 in Sec. 2.8.3.3.

The pattern of Fig. 6.17 has indeed been confirmed by partly reduced sinter samples taken from the blast furnace shaft. The layered structure of iron, wustite and magnetite surrounding the hematite core is maintained in the case of dense materials. In the case of very porous sinter, there is an extensive internal reduction and only the wustite phase could be identified.[118]

Generally, a dense covering layer is expected when the density of distribution of nuclei of iron in-between the originally formed nuclei increases which is possible when the degree of disorder in the wustite is small (i.e., rate of diffusion of iron ions is small, e.g., when magnetite is reduced) and/or the reaction rate high (high rate of super-saturation). Photomicrographs[119] of spongy porous and non-porous iron films are shown in Fig. 6.18(a) and (b).

We are aware that a considerable amount of wustite, depending upon the coke rate (i.e., amount of CO generated at the tuyeres), is perforce reduced directly at high temperatures in the belly and the bosh. The higher the level above the tuyeres at which this highly endothermic direct reduc-

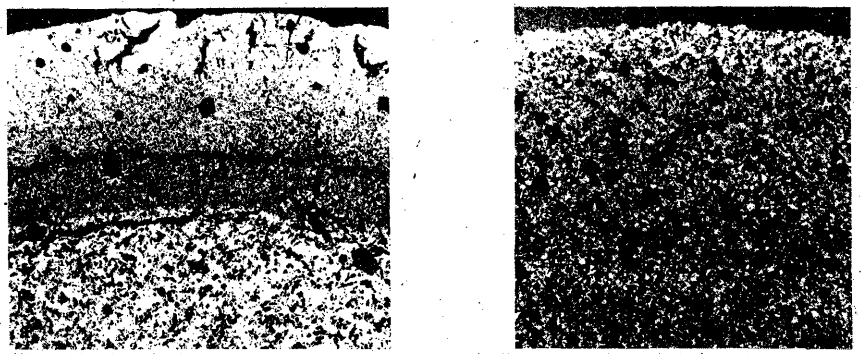


Fig. 6.17 Polished sections of sintered hematite pellets partially reduced in hydrogen at 900°C; **(a)** distinct reduction layers with dense hematite pellets; **(b)** no reduction layers, extensive internal reduction with porous ore pellet. After Turkdogan.[111] (Copyright The American Society for Metals and the Metallurgical Society of AIME 1978).

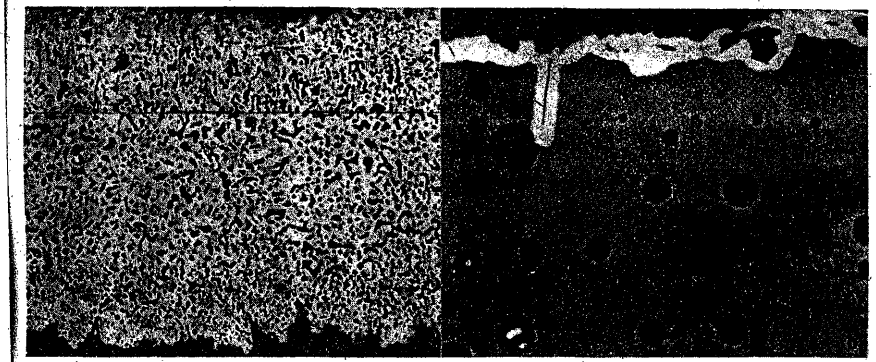


Fig. 6.18 Typical examples of **(a)** spongy porous and **(b)** dense non-porous iron films, after Kohl and Engell.[119] (Copyright Verlag Stahleisen).

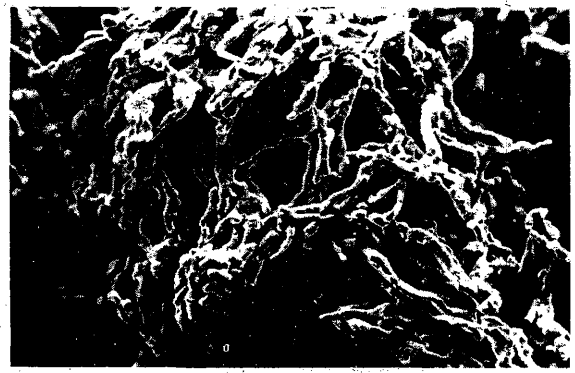


Fig. 6.19 Swelling and whisker formation of a sample of iron oxide during reduction in a CO/CO_2 atmosphere at 900°C.

tion occurs, the lower will be the wustite input in the hearth and consequently the higher will be the hearth temperature and the more uniformly will it be maintained (Sec. 7.8). Hence, high temperature reducibility of the burden also assumes importance. In acid sinters, the difficulty of reduction of partially reduced wustite descending from the stack is attributed to residual wustite forming fayalite above 1100°C.

Turkdogan[111] has shown that acid pellets partially reduced at 1000°C (to simulate shaft reaction) and subsequently reduced at 1350°C promote the formation of a dense layer of iron which retards the final reduction. Whereas, in the case of fluxed pellets, the reduction is much faster and a porous surrounding iron layer with connected pores throughout is formed. Evidently, the basicity of the pellet in some way increases the porosity of the reduced iron layer.

The relationship between the reduction velocity and porosity of iron oxide pellets has been studied extensively by Putzier.[120,121]

6.7.6. Swelling[122-132]

Apart from normal volume expansion as seen in Sec. 6.5.1, some pellets show an abnormal or *catastrophic* swelling with volume increase even up to 400 percent. Photomicrograph in Fig. 6.19 demonstrates an extraordinary growth of iron needles or *whiskers* during reduction of such a pellet. Such enlarged volume leads to a soft, highly porous material without any significant mechanical strength. In the blast furnace, the compaction of such a material under load reduces bed voidage and causes serious impedance to gas throughflow. However, swelling increases the rate of iron oxide reduction because of the formation of highly porous reduction products.[130]

Maximum swelling occurs[127,132] during reduction at temperatures 900–1000°C. The cause of such abnormal swelling has not yet been fully established. Some pellets swell while others do not. Ores and sinters seldom swell to such a degree. According to Wahlster,[133] swelling is associated with the art of making and indurating of the pellets, for ores and sinters of similar porosity and composition do not swell to any great extent. Generally, iron-rich pellets are prone to swelling.

The phenomenon of swelling is intimately associated with the mode of nucleation and growth during the reduction of wustite. Results of various investigators including those of the author[132] show that the whisker formation occurs during the reduction stage wustite/iron from pellets impreg-

nated with oxides of sodium, potassium and calcium. Their ionic radii as well as those of other likely impurities are given in Table 6.5.

Table 6.5. Ionic radii of some likely impurity elements

Elements	Na^+	K^+	Ca^{2+}	Fe^{2+}	Mg^{2+}	Mn^{2+}
Ionic radius, 10^{-8} cm	0.95	1.34	0.98	0.74	0.66	0.80

The causes of formation of a porous or dense growth of iron on wustite have been discussed in Sec. 2.8.3.3. The growth of whiskers may be deemed to be an extreme case of preferential nucleation which occurs when the relative rates of iron ion diffusion and oxygen removal (Eq. 2.38) are comparatively high, i.e., when the reduction potential of the gas is low and the iron ion diffusion high. It is likely that pronounced lattice disturbances occurring due to diffusion of ions larger than Fe^{2+} into the wustite lattice and consequent expansion of the wustite unit cell gives rise to preferential sites of nucleation of iron on the wustite surface. Freshly reduced iron ions tend to diffuse towards these rather than form new nuclei (especially when the reducing potential is low, absence of excessive super-saturation of iron), resulting in further elongation and growth of the whiskers (Fig. 6.20a). That the swelling is predominant at 900–1000°C is probably due to about 100 times higher mobility[134,135] of ferrous ions at 900°C than at 600°C. More frequent swelling in modern furnaces with stack gas composition near wustite/iron equilibrium tends to support this view. The author has also experienced a pronounced swelling when freshly reduced wustite from lime-impregnated hematite is further reduced to iron at 900–1000°C with CO/CO_2 gas composition near equilibrium with wustite/iron. The swelling decreases as the gas mixture is made more reducing.

If the wustite lattice is less disturbed (absence of impurities or when they are distributed homogeneously by prolonged induration), the formation of nuclei will be indiscriminate and iron would cover the whole surface of the grain. This can also happen when the reduction potential is high (low ratio, Eq. 2.38) and consequently a rapid and excessive super-saturation of iron ions occurs. In these circumstances the pellets may not swell. That pellets containing large amounts of silica do not swell may be due to the fact that the impurity oxides preferentially form silicates and do not cause excessive lattice imperfections.

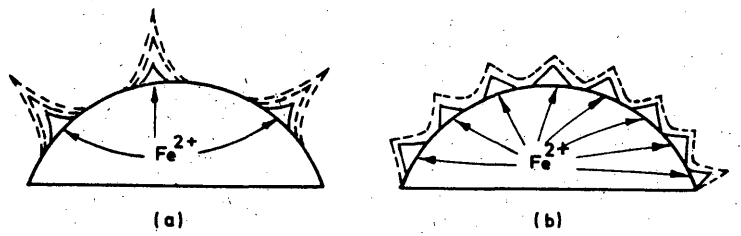


Fig. 6.20 A schematic representation of the mechanism of growth of **(a)** porous whiskery growth and **(b)** dense covering layer during reduction of iron oxide pellets.

From the viewpoint of above mechanism, Fig. 6.20 is self-explanatory. Fig. 6.20(a) shows schematically the formation of a nucleus at a preferred site, diffusion of iron ions generated from oxygen removal towards the site, growth of nucleus and consequent whisker formation. On the other hand, Fig. 6.20(b) shows the diffusion of iron ions towards a number of nuclei and in such a case a layer of iron will form without preferential growth.

However, the above explanations need substantiation. Swelling of pellets depends upon various factors, such as:

(i) composition, nature and quantity of impurities;
(ii) time and temperature of induration;
(iii) degree of oxidation (extent of magnetite);
(iv) time, temperature and degree of reduction;
(v) gas composition;
(vi) porosity, before and during reduction.

The swelling can be avoided or minimized by the following measures:

(i) prolonged induration of lime-containing pellets at high temperatures. It encourages excessive growth of hematite grains. Pellets fired at low temperatures are more susceptible to swelling. To decrease swelling, Fuwa and Ban-ya[136] suggest to hold pellets at 1300°C, or add Al_2O_3 or SiO_2 to pellet feed and hold at 1200°C;
(ii) addition of pre-reduced ore or return fines or certain ores from different sources;[45]
(iii) presence of silica in large amounts; add some silica to very rich ores before making lime-impregnated pellets;
(iv) avoidance or minimization of alkali metals input through ore or coke in the blast furnace as they promote swelling;

(v) avoidance of use of high flame temperatures in the blast furnace as it promotes reduction of alkali metal compounds from the slag;
(vi) introduction of hydrogen in the furnace (33% less swelling).[62]

The addition of specific fine-grained metal oxides for influencing swelling in cold-bound auto-claved pellets and the theory behind it have been recently suggested by Hässler.[137]

6.7.7. Linear Gas Velocity

The reduction rate of ore increases with increase in linear velocity of the reducing gas due to the reduction of the boundary layer thickness at the bulk-gas/particle interface (Sec. 2.8). After a critical gas velocity is reached, there is no further increase in the rate[84,85] with increasing gas velocity since the overall rate becomes controlled or limited by other processes. This is borne out in Fig. 6.21[84] which shows the limit at only 0.4 m/s. The figure also shows that the critical velocity is independent of the degree of oxidation. In blast furnace, the linear gas velocity does not affect the reduction rate since it ranges between 1–20 m/s and is often exceeded.

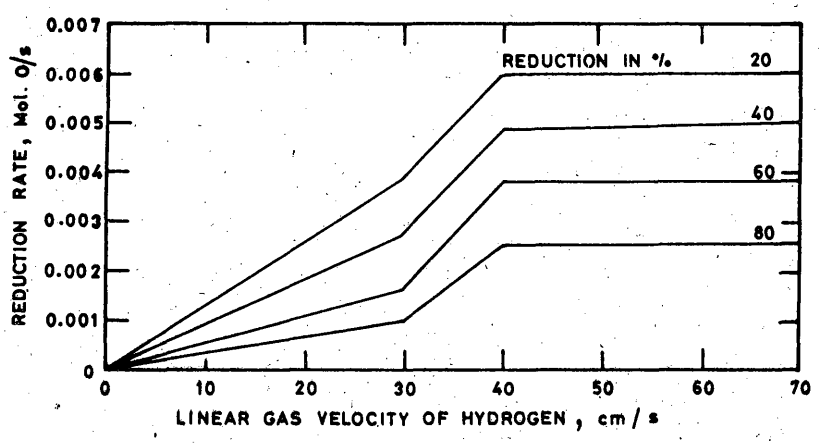


Fig. 6.21 Variations of reduction rate with linear velocity of hydrogen. After a critical velocity, the reduction rate of iron oxide becomes independent of gas velocity for all degrees of reduction, according to Bogdandy et al.[84] (Copyright Verlag Stahleisen).

6.7.8. Temperature

This subject has been discussed in Sec. 2.8.3.2.1. For the reduction of iron ores the reducing gas has to diffuse into the interior of the body where transformations can occur. In general, the reduction rate increases with temperature but the degree depends upon the mechanism of the reaction (Sec. 2.8.3). The overall reduction rate depends upon the relative contributions of chemical control and gaseous mass transport and hence depends upon the particular reactions occurring and the reaction temperature. Depending upon the degree of reduction, at lower temperatures of about 500–600°C, the chemical reaction rate controls the reduction rate forming what is known as the *kinetic* region in the blast furnace (Fig. 2.8). At temperatures above 600°C, gaseous diffusion becomes the dominant rate-controlling mechanism. The temperature regime in the blast furnace shaft is such that it can be assumed a zone of mixed-control exists.

For gaseous reduction the maximum beneficial temperature is 1000°C above which the Boudouard reaction sets in. In this respect, the formation of the thermal reserve zone in the shaft at 800–1000°C is ideally suited for indirect reduction of the ore. In practice, the temperature of the charge

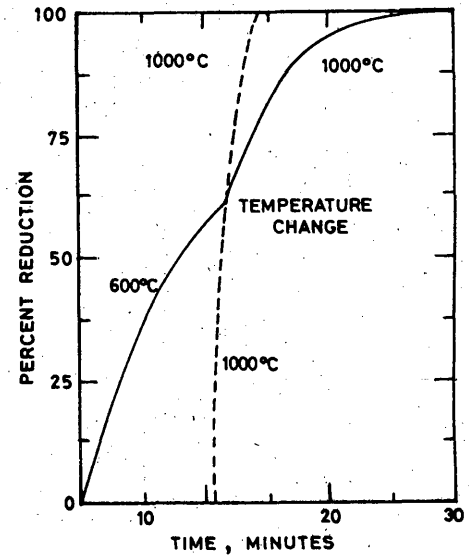


Fig. 6.22 Difference between reduction rate of a spherical hematite pellet reduced at first to 60% at 600°C and the remainder at 1000°C (solid lines) and that of a pellet reduced fully at 1000°C (dotted line), according to Turkdogan.[111] (Copyright The American Society for Metals and the Metallurgical Society of AIME 1978).

and that of the gas vary in the entire horizontal and vertical cross-sections of the furnace (Fig. 7.4).

The temperature of reduction can affect the morphology of iron produced and hence the reduction rate. Turkdogan[111,116] advocates that reducibility tests should include both high and low temperature ones. At low temperatures the iron layer formed around the ore is fine-grained, dense and compact whereas at high temperatures the pore structure becomes coarser[116] and permits an increased gas diffusion in the sample. Further, once a fine-grained structure is produced it does not readily coarsen at higher temperatures. Hence, due to non-uniform gas distribution if any metallic iron is produced in the upper shaft the ore may suffer a retarded reduction in the lower shaft. This is demonstrated in Fig. 6.22[111] where a spherical hematite pellet was first reduced to about 60 percent by hydrogen at 600°C and the remainder at 1000°C. The superimposed dotted curve is for the entire reduction performed at 1000°C. This shows that the iron layer of fine porosity initially formed at lower temperature does indeed retard reduction at higher temperature.

The more porous structure at 1000°C compared to 600°C can again be explained by Eq. 2.38. Assuming an activation energy of about 15 kcal/mole the increase in the rate of reduction will be about 10–15 times in the above temperature range whereas that for iron ion diffusion it is more than 100 times (Secs. 2.8.3.3 and 6.7.6).

6.7.9. Gas Composition

In the blast furnace, the reducing gas is predominantly CO with varying amounts of hydrogen depending upon the moisture content of the blast and other blast additives like fuel oil or natural gas. The equilibrium gas compositions (CO/CO_2 or H_2/H_2O) in the Fe-O-C and Fe-O-H systems are shown in Fig. 3.10. At 821°C the ratios in equilibrium with wustite are identical. Thermodynamically, for wustite reduction, CO is more efficient than H_2 below 821°C and H_2 more efficient than CO above 821°C. From Eqs. 2.26 and 6.2, an overall increase in the concentration of the reducing species would enhance the reduction rate, e.g., when using oxygenated or humidified blast or hydrogen-bearing additives or eliminating limestone from the burden which would otherwise dilute the furnace gas with CO_2.

The reduction rate of iron oxides by CO is much less than that by hydrogen. It may be due to the diffusivity of CO being much smaller as well

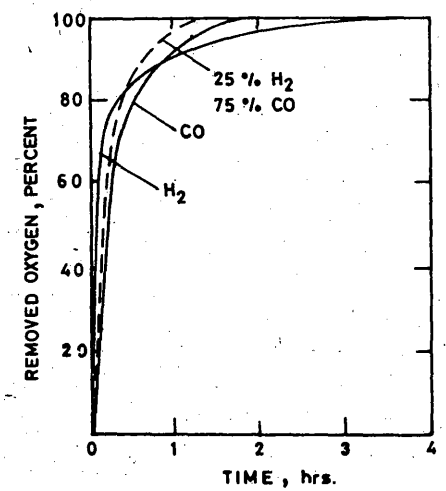


Fig. 6.23 Differences in the reduction rates of iron oxide with pure CO and H_2 and their mixtures, according to Wiberg.[139]

as the probability of blockage by deposited carbon of the pores of the initially formed solid iron[138] ($2CO = CO_2 + C$).

According to Wiberg,[139] pure hydrogen is a superior reducing agent at first but later at a high degree of reduction the rate slows down. In the case of CO, the last portion of iron oxygen is removed more quickly although initially the rate is sluggish as can be seen in Fig. 6.23.[139] The longer time taken by hydrogen for complete reduction is probably due to the formation of a dense non-porous iron shell.[139,140]

Fig. 6.23 also shows that a much quicker reduction than attainable either with hydrogen or with CO can be effected if both of them are present in the reducing gas. With pure CO, when an initial iron layer is formed, the CO carburizes the iron. The carbon diffuses to the wustite/iron interface, reacts to form $CO + CO_2$ and a high gas over-pressure is built up inside which breaks the surrounding iron film,[63,141] thus permitting further gas exchange at the oxide/metal interface. In the case of hydrogen only, the steam over-pressure is not sufficient to burst open the shell. With $CO + H_2$ gas mixture, the CO performs the bursting operation, opening up the passage for hydrogen with its greater reducing power. Fig. 6.23 shows that reduction with 75% CO + 25% H_2 is complete in 90 minutes whereas the times taken for pure CO and pure hydrogen are 2 and 4 hours respectively. A mixture of CO and hydrogen appears to be a more

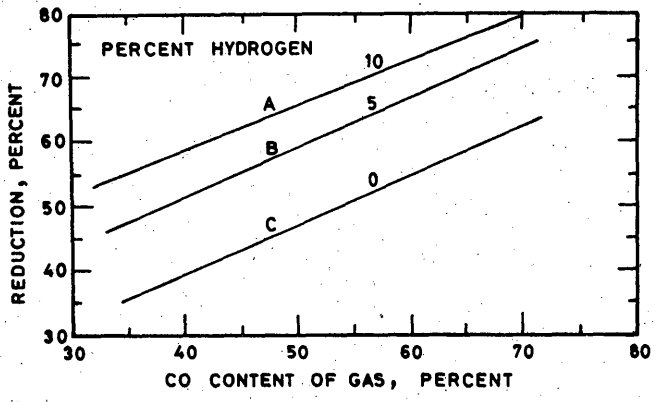


Fig. 6.24 Influence of increasing hydrogen in the presence of CO on the percent reduction of iron oxide for a given time of experiment.[145-147]

efficient reductant than either of them. This has been confirmed from actual blast furnace results. Working with 100 percent self-fluxing sinter, Cordier[142] has shown that an increase of 1% H_2 in the tuyere gas increases indirect reduction coefficient by about 3 percent and in the case of raw burden by about 4.5 percent. Hydrogen is especially beneficial for sinters of poor reducibility.[143,144] For sinters having a large quantity of small pores, an increase in hydrogen accelerates the reduction rate.[144]

The increase in the reduction rate of iron oxides by hydrogen is shown in Fig. 6.24.[145] It shows that while 0–5% H_2 in the CO-mixture increases the degree of reduction greatly (2–5% increase for each 1% H_2), a further 5 percent gives much less improvement (1% for each 1% additional H_2).[145-147]

The efficacy of hydrogen is due to the 3–5 times higher diffusivity of H_2/H_2O compared to CO/CO_2 (Sec. 2.8.3.2.1), which enables hydrogen to penetrate the innermost core of the ore particle at a much faster rate than CO. For porous ores of radii 3–20 mm and when porous diffusion is rate controlling, the ratios[148] of the rates of reduction by hydrogen and CO are about 1.5–5. When phase-boundary is rate-controlling, a ratio of reduction rates of about 40 has been reported.[149] The initial substantial increase in the rate on addition of hydrogen in Fig. 6.24 is probably due to the combined effect of higher hydrogen diffusivity and regeneration of hydrogen ($CO + H_2O = CO_2 + H_2$). The smaller increase in the rate with more hydrogen is caused presumably by diffusivity alone since the regeneration does not depend so much on the amount of hydrogen.

The consensus at present is that hydrogen both accelerates ore reduction as well as improves indirect reduction. Experiments with ores and $CO + H_2$ in the reducing gas show higher and increasing hydrogen utilization with increasing temperature and hydrogen content of the gas. The CO-utilization also improves when hydrogen is between 1–5 percent in the gas, due to the formation of CO_2 in the regeneration mechanism.

6.7.10. Gas Pressure

The gaseous reduction of iron oxides by CO or hydrogen does not involve any change of volume of the gaseous reduction products. Therefore, the equilibrium concentrations of the gases do not depend upon the total pressure. However, from Sec. 2.8.3.2.1, the reaction rate is a function of the absolute partial pressures of the components and hence an increase in the reduction rate is expected with increased total pressure (e.g., in high top pressure furnaces).

Diepschlag[150] investigated the reduction of hematite, 1–2 mm size, in atmospheres of hydrogen and CO at temperatures of 400, 600 and 800°C

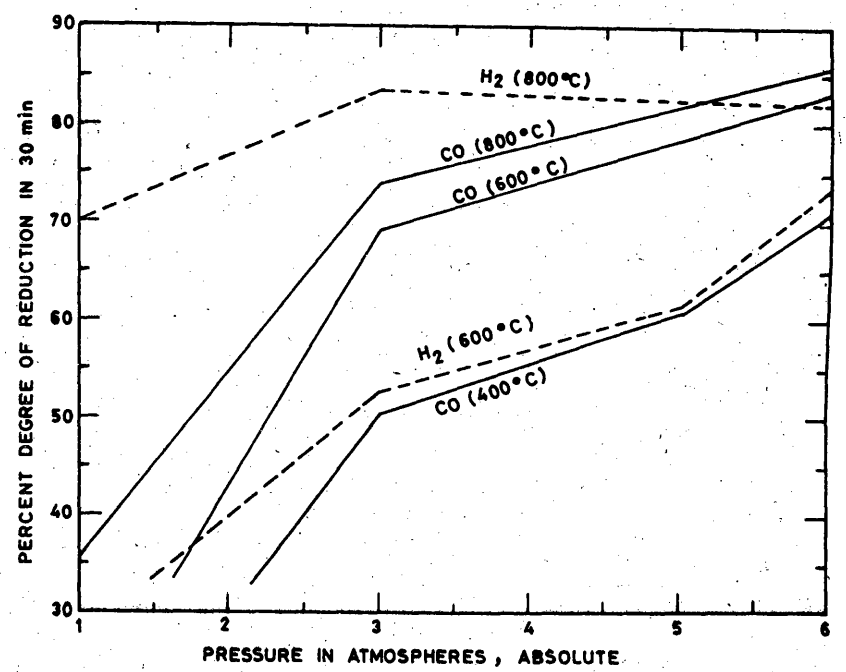


Fig. 6.25 The course of reduction of iron oxide with different reductants, temperatures and total gas pressures, after Diepschlag.[150]

and at pressures of 2, 4, 6 and 8 atm. The experimental duration was 30 minutes. The results are shown in Fig. 6.25. An increase in pressure accelerated the reduction rate, especially in the range of 2–4 atm. The rate was faster with hydrogen than with CO at 800°C but it reversed at 600°C. In all cases, the rates increased steadily as the pressure increased up to about 3 atm. and thence there was a slowing down in the increase. This may be due to reasons discussed in Sec. 2.8.3.2.1. Strassburger[151] has also found an increase in the reduction rate with hydrogen at 2 atm. pressure.

In the diffusion range, no benefit is expected to be accrued with increased pressure since diffusive flux is independent of total pressure, although variations in the mean free path and velocity of molecules may have some influence. On the other hand, the carbon deposition reaction $2CO = C + CO_2$ will be shifted to the right with increased pressure in the blast furnace and will augment carbon deposition inside the pores of the ore particles, enhance cracking of the ore and thus expose larger surface to the reacting gases.

6.7.11. Time of Contact

We have seen in Sec. 2.8 and in the various preceding sub-sections that in the temperature range 800–1000°C, i.e., in the indirect reduction zone of wustite, once an iron layer is formed the rate-controlling steps are those of mass transfer of gas through the porous product layer or oxygen diffusion through the dense covering layer of iron. As reduction proceeds, gaseous diffusion control slowly changes over to solid-state diffusion becoming rate-controlling. In the case of solid-state diffusion an increased concentration or diffusivity of the reductant component will be of little help in improving gaseous reduction. In either case, however, an increased gas/solid contact time would increase gaseous reduction. In any case, hydrogen with its low viscosity and high diffusivity should be more advantageous than CO as a reducing agent.

In practice, however, it is doubtful whether a smaller transit time in high capacity furnaces affects reduction. From an analysis of data of several blast furnaces, Bell and Taylor[152] have concluded that the highest indirect reduction values are obtained with well-prepared burdens with a high proportion of self-fluxing sinters even when the driving rate is very high (transit time of burden small). It may be that the optimum residence time is not reached in these furnaces because the improved burden lowers the coke rate and increases the ore/coke ratio. In contrast, Fig. 11.11 shows

a definite deterioration in η_{CO} when the residence time of gas in the furnace decreased below about 9 seconds.

We have discussed briefly in the preceding sub-sections the various physical and chemical factors that affect the gaseous reduction efficiency of the ores, sinters and pellets. However, it must be noted that complete reduction of iron oxides in the blast furnace does not depend upon their reducibilities. Any variety of ore will be reduced in the furnace irrespective of its origin, physical structure, associated impurities, size, shape, porosity, degree of oxidation, etc. The point is that an ore may, because of its adverse properties, descend inadequately reduced into the high temperature zone (>1000°C) where the CO_2 evolved from gaseous reduction is unstable in the presence of carbon and unnecessarily reacts to give CO and hence decreases the fuel efficiency, *although the furnace gas possessed sufficient reduction potential for further gaseous reduction.*

6.8. Blast Air

An enormous amount of air (about 5 kg) is used for combustion of 1 kg coke at the tuyeres. For efficient carbon utilization the air is preheated which increases the heat input at well as the tuyere gas temperature, i.e., flame temperature. A very simplified method of calculating the theoretical flame temperature assuming that all the heat produced is conserved and based on burning of hot pure carbon at 1400°C is presented here. Such calculations, though very approximate, have been used throughout the text in order to avoid complications. The actual tuyere gas temperature seldom exceeds 2000°C because coke and not carbon is used for burning and there are considerable heat losses in the tuyere region. We have already seen in Sec. 3.5 that at high temperatures carbon is oxidized only to CO. Therefore, depending upon the oxygen content of air,

$$C + \tfrac{1}{2}O_2 + \tfrac{1}{2}.\frac{(100 - \%O_2)}{\%O_2} N_2 = CO + \tfrac{1}{2}.\frac{(100 - \%O_2)}{\%O_2} N_2 \qquad 6.10$$

For normal air blast containing 21% O_2 by volume

$$C + \tfrac{1}{2}O_2 + 1.88N_2 = CO + 1.88N_2 \qquad 6.11$$

Therefore,

volume of air = 2.38 moles/mole C
= 4.44 Nm^3/kg.C 6.12

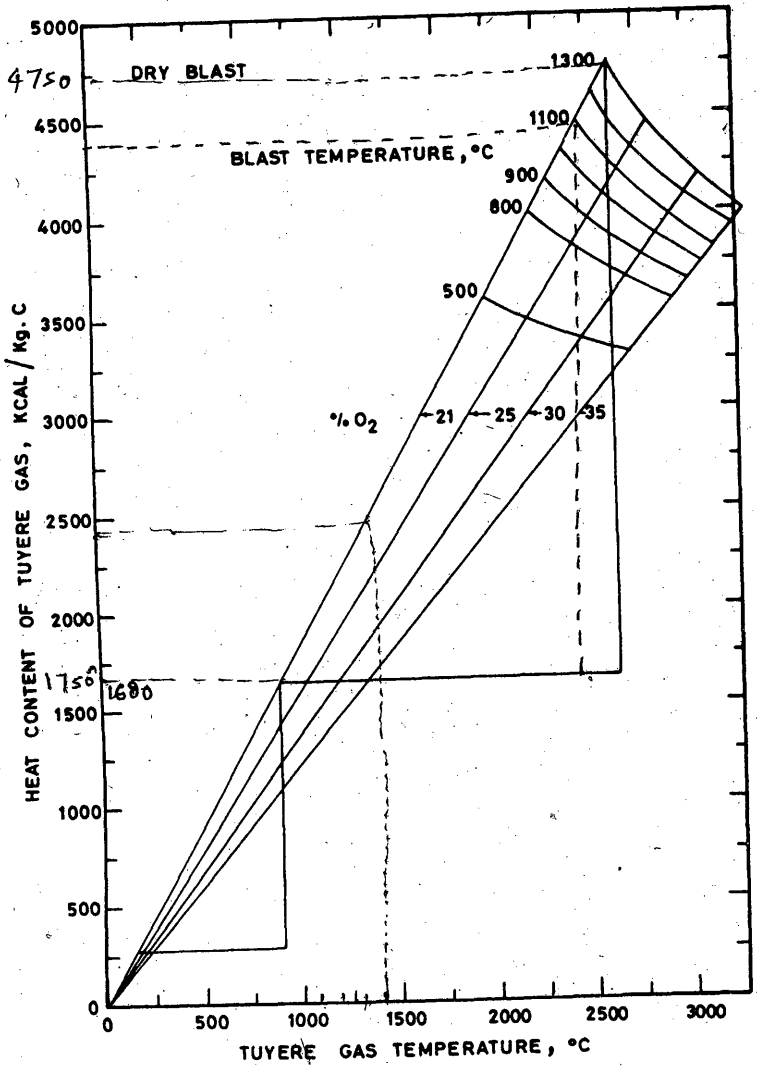


Fig. 6.26 Theoretical flame temperature and heat content of tuyere gas formed on combustion of 1 kg.C at 1400°C with dry air and dry oxygenated air at temperatures 500–1300°C.

Volume of tuyere gas = 2.88 moles/mole C
= 5.376 Nm^3kg.C 6.13

If t_b and t_f are the blast and flame temperatures in °C respectively,

$$2300 + 540 + 4.44 \times 0.333\, t_b = 5.376 \times 0.338\, t_f \qquad 6.14$$

where,

2300 = heat of combustion[187] of C to CO, kcal/kg.C
540 = heat content of carbon at 1400°C, kcal/kg.C
0.333 = heat capacity of air, kcal/Nm^3.°C,
0.338 = heat capacity of tuyere gas, kcal/Nm^3.°C.

The left hand side of Eq. 6.14 represents the heat input, i.e., the heat content of the tuyere gas. The calculated theoretical flame temperatures and heat contents of tuyere gas for different blast temperatures and oxygen-enrichments of dry air are plotted in Fig. 6.26. It is clear from the figure that both oxygenation and increase in blast temperature increase the flame temperature greatly. The total available heat per kg.C becomes smaller with increasing oxygen content but larger with increasing blast temperature. The decrease in the heat content with oxygenation is due to the diminution of the blast volume consequent upon decreased nitrogen input per kg.C. That nitrogen is not a useless ballast and carries a considerable amount of sensible heat into the blast furnace is highlighted by the figure. The use of the figure for calculating theoretical carbon consumption in the blast furnace will be seen in Sec. 10.2.

6.8.1. Humidified Air

We have seen in Sec. 4.6 that the blast furnace operation can become erratic if the flame temperature increases beyond a limit depending upon the burden characteristics and furnace profile. In such cases, the blast temperature can be increased without any increase in flame temperature if some coolant additives are injected along with the blast. Steam can be employed as a corrective for high blast temperatures because of its endothermic nature of reaction with carbon:

$$C + H_2O = CO + H_2 \qquad 6.15$$
$$\Delta H°(1200°C) = + 2700 \text{ kcal/kg.C}$$
$$= + 1800 \text{ kcal/kg.}H_2O$$

Since from Eqs. 6.10 and 6.15 the moisture gives double the volume of the reducing gas ($CO + H_2$) per mole of carbon, the bosh gas volume will

increase per unit of blast volume according to the amount of steam injected. Steam is incorporated in the blast prior to entry in the stoves and the amount is depicted in gm/Nm³ blast. Hence, with steam addition although the amount of blast oxygen and nitrogen will decrease slightly, the oxidising power per unit volume of blast will increase since oxygen composes about 89 percent of H_2O. Therefore, the bosh gas volume will increase per unit volume of blast but it will decrease per unit weight of carbon burnt. The various factors affected by steam addition are given in Table 6.6. It shows that moisture increases the coke burning rate, the tuyere gas is enriched with reducing gases ($CO + H_2$) and there is a decrease in total gas volume per kg carbon.[145]

Table 6.6. Variations of tuyere gas volume and composition with steam injection

Moisture gm/Nm³ blast	0	10	20	40	60
Increase in carbon burnt at tuyeres, %/Nm³ blast	–	1.72	3.44	6.9	10.3
Increase in bosh gas volume, %/Nm³ blast	–	0.81	1.62	3.25	4.87
Decrease in bosh gas volume, %/kg.C	–	0.85	1.75	3.40	4.92
Composition of bosh gas, % CO	34.7	35.04	35.34	35.94	36.52
% H_2	–	1.02	2.02	3.98	5.88
% N_2	65.3	63.94	62.63	60.08	57.6
Increase in volume of reducing gas ($CO + H_2$), %	–	4.68	9.38	18.72	28.1

The heat content of tuyere gas per kg.carbon and the flame temperatures for various blast temperatures and moisture and oxygen contents of blast can be calculated in the same manner as for dry blast with suitable modifications of Eqs. 6.10 and 6.14 and including the endothermic heat of Eq. 6.15. They are presented in Fig. 6.27 for 20 and 40 gm/Nm³ of moisture.

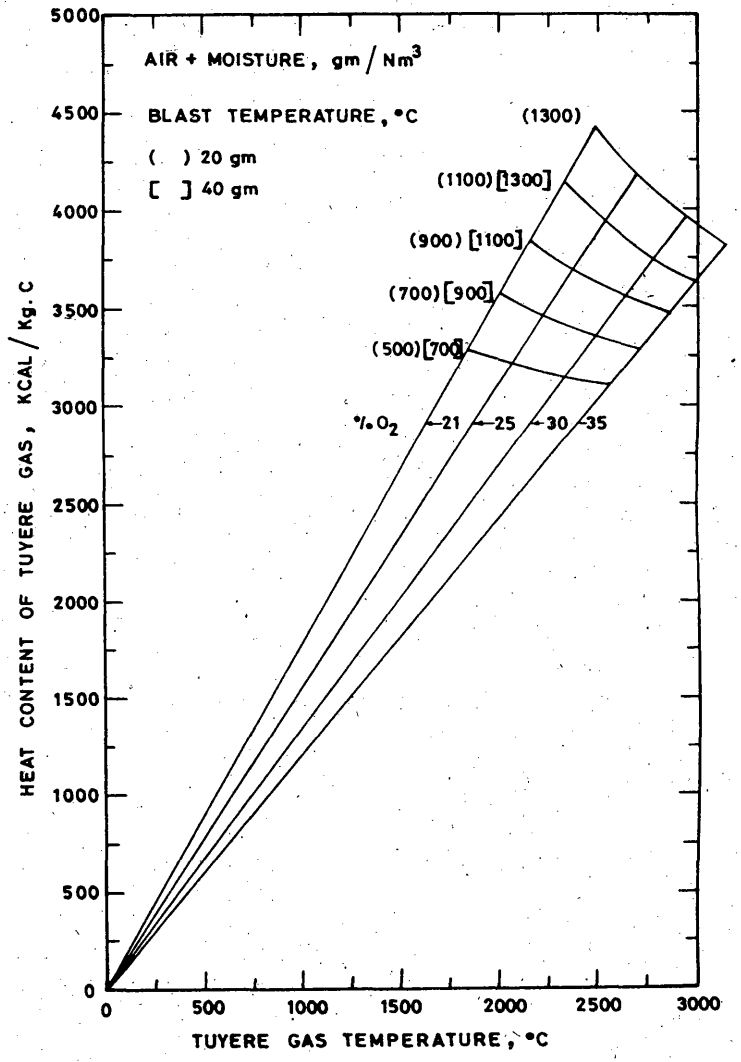


Fig. 6.27 Theoretical flame temperature and heat content of gas formed on combustion of 1 kg.C at 1400°C with air and oxygenated air containing 20 and 40 gm H_2O/Nm³ blast at temperatures 500–1300°C. As for example, for any oxygen content, the flame temperature and heat content for 500°C and 20 gm moisture in blast are the same as those for 700°C and 40 gm moisture in blast approximately.

The figure shows that for an increase of moisture in the blast by 20 gm/Nm³, the tuyere gas heat content and temperature are compensated by an increase of approximately 200°C in the blast temperature. This can be used as a thumb-rule for extrapolating to moisture contents above 40 gm/Nm³ blast. The calculated influences of moisture on fuel efficiency and productivity are illustrated in Secs. 10.7 and 11.3.3 respectively.

The variations in the theoretical flame temperature with increasing blast temperature for 21%-O_2 air and various moisture contents are shown in Fig. 6.28. As an example, for maintaining the same flame temperature as for dry air at 700°C, the blast temperature can be increased to 1300°C with 60 gm H_2O/Nm³ blast. Although its use is uneconomical because of heat absorption, blast humidification can be profitable under certain circumstances. The advantages are generation of hydrogen which is a more potent reducing agent and a smoother and faster furnace movement because of enlargement of the combustion zone (Sec. 7.6.6.6).

For keeping the flame temperature constant, it is necessary to increase the blast temperature by 8–10°C for each gm of H_2O per Nm³ blast.

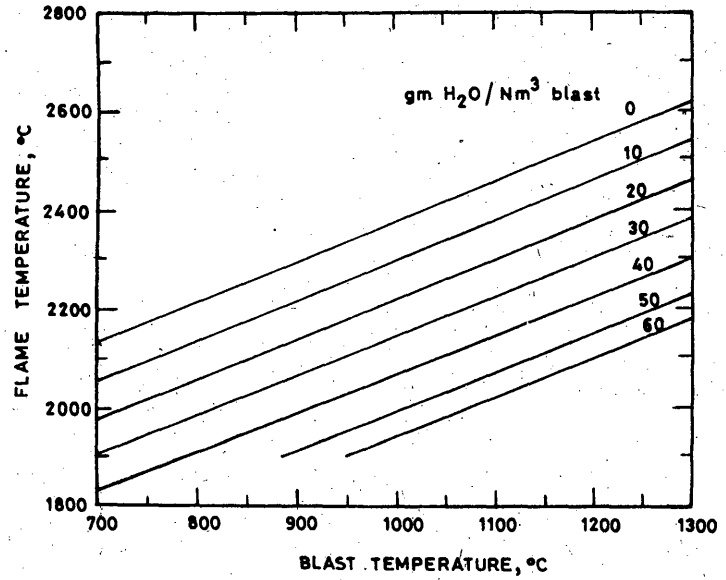


Fig. 6.28 Variations in the theoretical flame temperatures of the tuyere gas for blast of different temperatures and moisture contents.

6.8.2. Oxygenated-Humidified Blast

From Figs. 6.26 and 6.27 and Table 6.6, both oxygenated and humidified blast reduce the heat input as well as the heat content and volume of the tuyere gas per unit of carbon but the former increases and the latter decreases the flame temperature. From thermal viewpoint, fuel efficiency will be better if the flame temperature is kept constant by combined oxygenation-humidification. Very little, if any, savings in coke will be expected from such a combination although a higher degree of indirect reduction is expected from an enrichment of the tuyere gas with the reducing gases. However, the coke burning rate, i.e., furnace productivity increases greatly from such a combination. These have been discussed in Secs. 10.7 and 11.3.3.

6.9. Blast Furnace Fuels

Coke is the universal fuel used in the blast furnace. It acts both as a reductant as well as a supplier of heat. It also comprises the major portion of iron production cost. Now-a-days other fuels are also being used as part replacement of coke. These fuels cannot be charged from the top and as such they are injected into the furnace through the tuyeres along with the blast. They are described in brief in the succeeding sub-sections. In some countries, especially in Brazil, charcoal is used as a blast furnace fuel.

6.9.1. Coke

The function of coke in the blast furnace is five-fold, namely,

(i) it acts as a fuel by providing for the thermal requirements in the furnace, the reaction being,

$$2C + O_2 = 2CO: \Delta H^\circ = -2300 \text{ kcal/kg.C}$$

On complete combustion to CO_2 the heat evolved is 8150 kcal/kg.C. Thus only about 28 percent of the obtainable heat is supplied by coke;

(ii) it provides CO for the reduction of iron oxides;

(iii) it reduces the oxides of metalloids, such as, Mn, Si, P and others if present;

(iv) it carburizes the iron and lowers its melting point;

(v) it provides permeability (in the dry as well as the wet zones) and also mechanical support to the large charge column, permitting the

gases to ascend through the voids. The permeability of a coke bed can be 60–100 percent more than those of ores, sinters or pellets. It does not even soften and it is the only charge material that descends as solid up to the tuyere level where it is consumed by the air blast. The physical and chemical properties of coke are of utmost importance in the blast furnace. They are discussed below.

6.9.1.1. Physical properties of coke

(a) Coke size Coke comprises about 50–60 percent of the volume of the charge material. The importance of coke size for providing permeability in the dry as well as the wet bosh zone has been discussed in Sec. 5.4 and for increase in output in Sec. 11.3.2.3. In the former case, the size should be compatible with the ore size while in the latter it should be as large as possible to minimize flooding. Usually, a compromise is made and the coke should be about 3–5 times larger than the ore. Coke size must not be less than 40 mm (40–60 mm or 40–80 mm) although the burden material may be in the range 10–30 mm. The coke size should be particularly large in case of high slag bulk for minimizing flooding by providing more voidage and less surface area.

Since the coke size becomes smaller as it descends through the blast furnace due to mechanical breakdown, gasification, attrition, etc., the factor of prime importance is the strength of coke.

(b) Coke strength Mechanically considered, it is the quality *cohesion* that prevents the coke from collapsing and tends to avoid the formation of small particles. High cohesion or strength is related to several coke making properties, viz., proper crushing and blending, adequate swelling and coking during carbonisation, absence of strains and shrinkage cracks, etc. On the basis of breakage by impact, compression or abrasion, the coke strength should be assessed both at ambient as well as high temperatures. Studies of the structure of different coke samples show that the best varieties have a regular distribution of pores, with adequate thickness and hardness of the walls between the pores and are free from cracks generated internally. Such a structure ensures withstanding of high compressive forces and high temperatures in the all-important lower furnace. Factors of importance are fluidity and degree of coalification. The strength of coke produced in the coke-ovens is influenced by:[185,186]

(i) blending ratio of coals of varying caking components and proportion of the fibrous portion;

(ii) particle size and distribution of charging coal;
(iii) coke-oven temperature and combustion conditions;
(iv) moisture and addition of oil;
(v) soaking time;
(vi) width, height and method of heating.

As will be seen later, coke strength is related to its reactivity in the furnace. The oxidizing reaction of CO_2 on coke in the lower furnace at 1000°C and above, especially at temperatures above the carbonisation temperature, leads to a pitting type of attack on the cell walls extending even up to a depth of 5 mm. Surface pitting caused by carbon solution is a basic cause of increase in abradability. Hence, due to compressive load, abrasion and generation of weakness fissures by carbon solution, the coke as charged at the top arrives severely degraded at the tuyeres. The small and irregular sizes decrease the voidage of the coke grid in the bosh, increase propensity to choking and flooding and limit productivity. Powdery coke also results in coke mess and burning of tuyeres and slag notch. This assumes great importance in larger furnaces as shown[153] by the increase in coke breakdown with increasing hearth diameter for a given coke rate and with decreasing coke rate for a given hearth diameter. The latter is caused by the increased weight of burden per unit of coke.

The coke undergoes severe disintegration in the lower furnace due to high temperatures, gasification reaction, alkali attack, mechanical load, attrition caused by high velocity blast before the tuyeres, etc. There are various methods evolved for testing of coke strength. The most widely used are 'shatter' for impact and 'drum' test for abradability. Standard testing methods are available from ASTM or other sources. Because of degradation of coke all along the furnace height, both cold and hot strength should be determined. The measurements and their significance in blast furnace productivity have been emphasized by many recent investigators.[154–161]

6.9.1.2. Chemical properties of coke[160]

(a) Carbon Since coke is used as a fuel and reductant, its calorific value and carbon content should be as high as possible. More importantly, the carbon content should not vary to a great extent. If it does, variable amount of heat will be generated in the furnace which makes it difficult to control the quality of iron.

(b) Moisture Driving off the moisture needs additional heat which has to be supplied by additional coke or by increase in blast temperature.

Hence, for a lower coke rate and uniform running of the furnace, the moisture content of coke should be minimum and constant. It is surmised[162] that for every ± 1% change in moisture, the blast temperature increase needed is ± 25–50°C. However, it is the difficulty of control of the iron quality that is more important than the increase or decrease of the blast temperature. Ideally, the moisture and carbon contents of coke should be analysed before charging and the weight of coke adjusted to cater for the change in these contents.

(c) Coke ash Coke ash consists mostly of silica and alumina. Limestone is needed for fluxing the silica at the rate of approximately 1 kg for every kg of ash. The heat required for calcination and melting of the extra slag increases the coke requirement per tonne of iron at the rate of 2 percent for every 1 percent increase in coke ash.[162,163]

A high ash content, especially when smelting rich ore containing low silica, is very unfavourable for uniform furnace operation because the bosh slag becomes highly basic (Sec. 8.3). The liquidus temperature and viscosity of such limey slags are high which interfere with the smooth flow of the liquids and gases. Depending upon the ore quality, the ash content of coke should not exceed 10–15 percent.

(d) Sulphur About 80–95 percent of sulphur input in the blast furnace comes from coke. Sulphur removal through slag depends upon the slag bulk and basicity. If sulphur input is high, the removal is accomplished by higher slag basicity, higher slag bulk, higher temperature and desulphurization outside the furnace. All these increase the cost of production.

According to Schaefers and Winzer,[163] for a slag bulk of 300 kg/THM, a change of sulphur in coke of ± 0.1 percent changes the coke requirement by:

± 15 kg/THM, for change in slag bulk
± 4 kg/THM, for changing the basicity
± 2 kg/THM, for external desulphurization by soda.

(e) Coke reactivity Coke reactivity is measured by the reaction rate of C(coke) + CO_2 = 2CO at different temperatures. From a chemical standpoint, the coke should be of low reactivity. The vertical distance of the indirect reduction zone of 800–1000°C, i.e., the residence time of ore in this zone can be increased if the coke gasification temperature be raised which is possible by the use of less reactive coke. As for example, it is reported[165,166] that an increase of reactivity by 100% results in an increase

in the coke rate between 30–70 kg/THM. The reactivity is of little importance where the coke rate is so low as to require regeneration of CO by the gasification reaction for iron oxide reduction. Further, in the blast furnace the reactivity of the coke increases any way by the action of alkali metals (see next section).

According to Muller et al.,[167] the reactivity of coke depends to a great extent on the ash content, e.g., the reactivity at 10 percent ash is double that at 5 percent.

One of the methods[168] of reducing coke reactivity is to blend the coal mixture with petroleum coke.

The combustion of coke by air in front of the tuyeres can also be influenced by the use of compact, less reactive coke of large size with smaller surface area. Thus, the oxidizing zone in front of the tuyeres can be extended because of sluggish combustion of coke which facilitates the descent of the burden (Sec. 2.8.3). However, the reactivity of coke with CO_2 at 1000–1100°C is not affected by the size to any great extent because the rate is controlled mainly by pore diffusion for the coke size used in the blast furnace.

Apart from the above main properties, other constituents should also be taken into account while selecting suitable coke. They are: volatiles and oxygen, nitrogen, hydrogen, phosphorus, sodium, potassium, titanium, contents.

(f) Alkali attack[130,169–173] A great importance is attached to the action of the alkali metals which increase the reactivity of coke and decrease its strength. The alkali attack weakens the cell walls and increases the susceptibility of coke to breakdown under load. Alkalis impregnated on coke can greatly accelerate the Boudouard reaction (CO_2 + C = 2CO) in the 1000°C range when pore diffusion is the limiting factor in determining the carbon gasification rate. The gasification occurs in the shaft in the region where liquid K_2CO_3 is thermodynamically stable (Sec. 3.21). Both sodium and potassium catalyse the reaction by lowering the activation energy. A three or four fold increase in the percentage of coke gasified has been recorded.[130] Alkali-impregnated coke was found[171] to generate fines in about 10 minutes in the presence of CO_2 and reduced to ash in an hour whereas non-impregnated coke lost 50 percent of its carbon in about 3 hours and still retained its basic shape. Kojima[173] has found an increase of 5–10 times in coke reactivity from blast furnace samples than when charged due to alkali action. The high degree of breakdown, as determined by abradability tests both in static and dynamic apparatus, affects

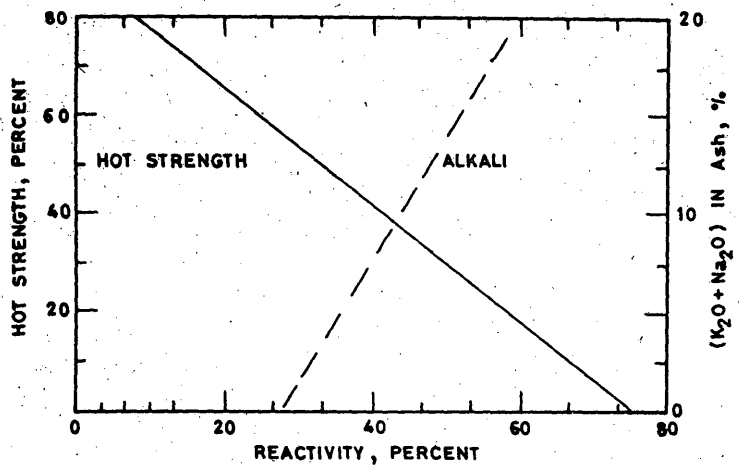


Fig. 6.29 The increase in the reactivity of coke with increasing alkali metal content of coke ash and the decrease in the hot strength of coke with increasing coke reactivity, after Sasaki et al.[157]

bed permeability in the blast furnace leading to hanging and non-uniform operation[157-159] (see also Sec. 11.3.2.4). Fig. 6.29[157] shows how the coke reactivity increases and hot strength decreases with increase in the alkali content of coke ash.

Coke strength is also severely affected at temperatures above 1000°C because of weakness in the matrix generated by preferential alkali attack according to:[130]

$$2K + 2C + N_2 = 2KCN \qquad 6.16$$

6.9.2. Form Coke

As good quality coking coal is becoming more and more scarce and costly, experiments are being done to use inferior, weak, non-caking coal suitable for blast furnace. In this process, various types of coal are ground to fines, blended, mixed with peech as bonding agent, briquetted into desired shapes and carbonised in coke-oven.[174] Such *form* cokes can be used as part replacement of the usual coke. Actual experiments in the blast furnace with 30 percent 'form' coke showed no adverse effect compared with 100 percent usual coke. Microscopic and X-ray investigations showed the structure of the 'form' coke to be similar to that of the usual coke.

Experiments[175] on resistance to flow of gases through mixtures 'form coke'-ore and 'usual coke'-ore showed higher resistance in the former case. However, the densities of the former and latter cokes are 1.1 gm/cm³ and 0.9 gm/cm³. This means that for the same weight of coke, a larger volume of the furnace remains at the disposal of ore in the former case. Since ores offer greater resistance to the flow of gases, the actual contribution of the 'form' coke to the resistance is much lower than in the case of the 'usual' coke.

Recently 100 percent 'form' coke has been used without any trouble.[176] Although the coke rate increased somewhat per THM, the output did not decrease since the coke consumption intensity t/m³/day increased.

A new method of making 'form' coke for blast furnace has been suggested.[184] It includes crushing of low-caking to high-volatile coals to <1 mm size, pelletising them to any desired size and coating them with hematite or lime prior to carbonising in normal coke-oven batteries.

6.9.3. Other Fuels

The changing price structure and availability of liquid and gaseous fuels are making them competitive with coke. All these fuels are hydrogen-bearers and carbonaceous. Since these fuels are burnt incompletely to CO and H_2 before the tuyeres, the full calorific value is not obtained from them. However, they all supply hydrogen which is a more potent reducing agent than CO for the reduction of iron oxides at higher temperatures. They are used at ambient temperatures and need a certain heat of dissociation of the C-H bonds. Thus their burning produces in the combustion zone a flame temperature which is lower than that obtained from the burning of coke because the latter arrives in the zone preheated to about 1400–1500°C. As the flame temperature increases with the blast temperature, a higher blast temperature (therefore, a larger heat input) can be utilized with the addition of such fuels maintaining, at the same time, a constant flame temperature. A larger heat input and better indirect reduction through hydrogen result in saving of coke in addition to the carbon which is already present in such fuels.

6.9.3.1. Hydrocarbons

Fuel oil can be assumed to consist of hydrocarbons of general formula $(CH_2)_n$, the natural gas almost 100 percent methane (CH_4) and coke-oven gas about 25 percent methane. The combustion reactions of fuel oil and methane with air are:

$$(CH_2) + \tfrac{1}{2}O_2 + \tfrac{1}{2}.\frac{(100-\%O_2)}{\%O_2}N_2 = CO + H_2 + \tfrac{1}{2}.\frac{(100-\%O_2)}{\%O_2}N_2 \quad 6.17$$

$$\Delta H^{177} = -1466 \text{ kcal/kg.oil} \quad 6.18$$

$$CH_4 + \tfrac{1}{2}O_2 + \tfrac{1}{2}.\frac{(100-\%O_2)}{\%O_2}N_2 = CO + 2H_2 + \tfrac{1}{2}.\frac{(100-\%O_2)}{\%O_2}N_2 \quad 6.19$$

$$\Delta H^{177} = -381 \text{ kcal/Nm}^3\text{.gas} \quad 6.20$$

The composition, calorific values, blast requirements per unit of fuel for air and 25%-O_2 air, tuyere gas volumes and compositions, of the above three additives (coke-oven gas is the least used) are compared with pure carbon in Table 6.8. Their theoretical flame temperatures for three levels of blast temperatures are shown in Table 6.7. Since the flame temperatures vary almost linearly, they can be determined for other blast temperatures.

Table 6.7. Flame temperatures of some blast furnace fuels, °C

Blast temp. °C	$\%O_2$	Carbon	Fuel oil	Natural gas	Coke-oven gas
900	21	2295	1315	671	518
900	25	2510	1360	651	505
1100	21	2458	1443	768	583
1100	25	2667	1497	740	566
1300	21	2621	1570	866	648
1300	25	2825	1598	830	627

In contrast to steam which is incorporated in the blast itself, the use of the fuel additives is depicted as kg.oil/THM or Nm³.gas/THM. Since the flame temperature depends upon the heat content of the total volume of the tuyere gas, therefore, when using these auxiliary fuels, it will depend upon the amount of tuyere carbon per THM as shown by the following example:

The heat input is given by (cf. Eq. 6.14):

$$K(2300 + 540 + 4.44C'_p t_b) + H(Q + V_b.C'_p t_b) \quad 6.21$$

which is equal to

$$(5.376K + V_a.H).C_p.t_f \quad 6.22$$

where,

K = tuyere carbon, kg/THM, with fuel addition
C'_p = 0.333 kcal/Nm³.°C, mean heat capacity of the blast
C_p = 0.338 kcal/Nm³.°C, mean heat capacity of the tuyere gas, assuming hydrogen does not change the heat capacity appreciably
t_f = tuyere gas temperature (flame temperature)
t_b = blast temperature
H = amount of additive, kg or Nm³/THM
Q = heat of combustion of additive to CO + H_2, kcal/kg or Nm³
V_b = blast volume required to gasify additive, Nm³/kg or Nm³
V_a = tuyere gas volume from additive, Nm³/kg or Nm³
2300, 540, 4.44, 5.376 = as in Eq. 6.14.

For the case of oil and normal blast,

$$Q = 1466 \text{ kcal/kg} \quad 6.23$$

$$V_b = 3.71 \text{ Nm}^3/\text{kg} \quad 6.24$$

$$V_a = 5.86 \text{ Nm}^3/\text{kg} \quad 6.25$$

Therefore, the flame temperature for any K, H and blast temperature can be calculated from Eqs. 6.21 and 6.22.

The flame temperatures for three levels of oil – 50, 100 and 150 kg/THM – and 250 and 350 kg of tuyere carbon per THM are given in Table 6.9 for 900 and 1300°C blast temperatures and 21% O_2 and 25% O_2-air. The flame temperatures for other fuels can be similarly calculated by substituting proper values from Table 6.8 in Eqs. 6.21 and 6.22.

It is evident from Table 6.9 that the higher the amount of tuyere carbon the less will be the blast temperature increment necessary for maintaining a constant flame temperature; or, employing the maximum possible blast temperature according to stove capacity, more of additives can be used and coke saved without endangering a smooth furnace operation. Because of their low heats of combustion, natural and coke-oven gases are inferior to oil from a thermal viewpoint and their amounts necessary for temperature compensation are smaller.

The complete combustion of the injectants into CO and hydrogen must be ensured for most favourable results. Too much an amount of injectants

Table 6.8. Properties of carbon, fuel oil, natural gas and coke-oven gas

	Carbon	Fuel oil	Natural gas	Coke-oven gas
Chemical composition,[177] %				
Carbon	100	84	–	–
Ash	–	0.5	–	–
Sulphur	–	2.5	–	–
Hydrogen	–	12.0	–	57.7
Oxygen	–	0.5	–	–
Nitrogen	–	0.5	–	6.9
Methane	–	–	100.0	26.0
Carbon monoxide	–	–	–	5.7
Carbon dioxide	–	–	–	2.0
Heavy hydrocarbons	–	–	–	2.4
Calorific value – kcal/kg(Nm³)[177]	8000	9600–9800	8580	4200
Gasification and cracking reaction	$C + \frac{1}{2}O_2 = CO$	$-CH_2- + \frac{1}{2}O_2 = CO + H_2$	$CH_4 + \frac{1}{2}O_2 = CO + 2H_2$	$CH_4 + \frac{1}{2}O_2 = CO + 2H_2$
Reaction heat, kcal/kg(Nm³)[177]	−2200	−1466	−381	−169
Percent oxygen in blast	21 25	21 25	21 25	21
Blast required to transform into CO and H_2, Nm³/kg(Nm³)	4.44 3.73	3.73 3.13	2.38 2.00	0.74
Tuyere gas amount:				
Carbon monoxide, Nm³/kg(Nm³)	1.87 1.87	1.57 1.57	1.00 1.00	0.42
Hydrogen, Nm³/kg(Nm³)	– –	1.34 1.34	2.00 2.00	1.17
Nitrogen, Nm³/kg(Nm³)	3.51 2.80	2.95 2.35	1.88 1.50	0.65
Tuyere gas total, Nm³/kg(Nm³)	5.38 4.67	5.86 5.27	4.88 4.50	2.24
Composition of tuyere gas:				
Carbon monoxide, %	34.70 40.00	26.80 29.80	20.50 22.20	18.70
Hydrogen, %	– –	22.90 25.40	41.00 44.40	52.30
Nitrogen, %	65.30 60.00	50.30 29.80	38.50 33.30	29.00

or inadequate atomisation of the liquid fuel into very minute particles may lead to incomplete combustion. The unburnt fraction, once it leaves the oxidizing zone in front of the tuyeres, gives rise to carbon soots in the burden, clogging the voids. It also results in carbon carry-over to the gas cleaning systems. As the force of the blast carries these soots to the furnace axis, the clogging of voids in the axial coke column lowers gas permeability; as we will see in Sec. 11.5 a pronounced central flow is very important for the productivity of modern blast furnaces. Also, the large reactive surface of the carbon soots helps to activate the Boudouard reaction at lower temperatures (<1000°C) with its consequent adverse effect on the coke rate. The formation of soots also reduces the effective utilization of oil carbon and hence deteriorates the replacement ratio (coke saved/kg oil). The oil can be atomised by steam.

To ensure complete combustion, generally, an excess oxygen input is necessary, the excess oxygen coefficient (u) being[178,179]

$$u = o_t/o_r \qquad 6.26$$

where,

o_t = total oxygen injected by blast through tuyeres (Nm³/min)

o_r = amount of oxygen required for complete combustion of the injected fuel oil (Nm³/min)

The coefficient (u) is usually 1.1.

Fuel oil is generally injected at the tip of oil nozzle placed inside near the tuyere. A great part of the oil burns simultaneously with the coke. Soot formation begins with increasing amount of oil. According to Inatani et al.,[180] in order to gasify the oil before the burning of coke, the nozzle should be shifted backwards by 750 mm. With this arrangement much oil is gasified without soot formation even at u = 0.9.

Oxygen utilization can be calculated assuming complete combustion of oil to CO_2 and H_2O and the amount of oil should be restricted to that amount which will consume 80 percent of available oxygen at the tuyeres (air or oxygenated air).[181] The use of homogenized oil minimises soot formation.[182]

6.9.2. Solid fuels

In addition to fuel oil, natural gas and coke oven gas, there are others which are not yet universally used. They are anthracite, lignite, coal, etc. In some cases, a mixture of oil-coal in the form of a slurry is used. The

Table 6.9. Theoretical flame temperatures with oil injection and oxygen-enriched blast and two levels of tuyere carbon (K)

Blast Temp.	K kg/THM	Oil kg/THM	Flame Temperature °C	
			21%-O_2 Blast	25%-O_2 Blast
900°C	250	50	2130	2310
	250	100	2005	2160
	250	150	1915	2050
	350	50	2175	2360
	350	100	2075	2240
	350	150	1995	2145
1300°C	250	50	2450	2615
	250	100	2315	2455
	250	150	2215	2340
	350	50	2495	2670
	350	100	2385	2540
	350	150	2300	2435

calorific values, blast requirements, tuyere gas volume and composition, etc, can be seen elsewhere.[6,183]

The calorific values of the solid fuels are much higher than those of natural or coke-oven gas. But, their hydrogen contents are much less. Hence the hydrogen-bearers are advantageous from the point of view of greater reducing power of hydrogen whereas the solid fuels are preferable from the thermal viewpoint. However, the injection of oil and gas in the tuyeres is much easier than that of the solids. For complete combustion, the solid particles must be as small as possible for exposure of large surface (0.05–0.1 mm). The solids also result in higher erosion of the tuyeres. Injection of a mixture of oil and pulverized coal in the form of a slurry is preferable to the use of solids alone. From the cost point of view, the solid fuel is more economical even including the high cost of their grinding to fines. Since they are at ambient temperature when injected, they lower the flame temperature. Hence, they can make considerable savings in coke if there is idle stove capacity and yet higher blast temperatures cannot be used for furnace irregularities (Sec. 10.7).

Ridgion[183] has calculated the amounts of gaseous, liquid and solid fuels per unit of blast necessary for compensating 100°C rise in the blast temperature for maintaining a constant flame temperature.

References

1. BALL, D. F., J. DARTNELL, J. DAVISON, A. GRIEVE and R. WILD: Agglomeration of iron ores, Amer.-Elsevier Pub Co., N.Y. 1973.
2. Blast Furnace – Theory and Practice – Vol. 1, Edt. J. H. Strassburger, Gorden and Breach Science Pub., N.Y. 1969, p. 165–324.
3. McLEOD, J. M.: Preparation of iron ore, Critical Rev. – IV, Metal Progress, Iron and Steel, London, 1954, p. 2–28.
4. NIKOL'SKII, N. A.: Stal in Eng., Aug. 1962, p. 593–594.
5. Economic aspects of iron ore preparation, UN Tech. Pub., Geneva, 1965.
6. BOGDANDY, L. v. and H.-J. ENGELL: The reduction of iron ores (in English), Springer-Stahleisen, 1971.
7. KOSMIDER, K. et al.: Stahl u. Eisen, 76, 1956, p. 858–870.
8. WENDEBORN, H. B.: J. Iron Steel Inst., Nov. 1953, p. 280.
9. WENDEBORN, H.: Stahl u. Eisen, 71, 1951, p. 121, 218.
10. SCHWABE, G. and H. RELLERMEYER: op. cit., 84, 1964, p. 327–349.
11. Agglomeration: Edt. W. A. Knepper, Interscience Pub., N.Y., 1962.
12. WENDEBORN, H. and F.. CAPPEL: Ref. 11, p. 1041–1065.
13. MEYER, K.: Stahl u. Eisen, 79, 1959, p. 222–225; see Ref. 6, p. 406.
14. ELLIOTT, G. and N. D. MACDONALD: J. Iron Steel Inst., 167, 1951, p. 261–272.
15. STERLING, H. T.: ref. 11, p. 177–206.
16. WILLEMS, J. and G. QUADE: Stahl u. Eisen, 81, 1961, p. 552–557.
17. EULER, R. et al.: op. cit., 86, 1966, p. 1465–1469.
18. WINZER, G. and K.-H. SCHMIDT: op. cit., 87, 1967, p. 432–438.
19. WILD, R.: J. Iron Steel Inst.: June 1953, p. 131–135.
20. MAZANEK, E. and I. JASIENSKA: op. cit., 201, 1963, p. 60–67; 202, 1964, p. 319–324.
21. PRICE, C. and D. WASSE: Developments in ironmaking practice, Proc. conf. 22–23 Nov. 1972, Iron Steel Inst., London, p. 32–52.
22. JAKUBEINER, N. M. et al.: Stal in Eng., March 1960, p. 161–168.
23. NEKRASOV, Z. I. et al.: op. cit., March 1970, p. 178–183.
24. NEKRASOV, Z. I. et al.: op. cit., Dec. 1966, p. 951–956.
25. MALYSHEVA, T. Y. et al.: op. cit., Oct. 1966, p. 773–776.
26. MURAV'V, V. N. et al.: op. cit., Aug. 1970, p. 290–294.
27. MURAV'V, V. N. et al.: op. cit., Oct. 1970, p. 768–771.
28. BAZILEVICH, S. V.: Agglomeratsiya, Metallurgiya, Moscow, 1967.
29. TIGERSCHIOLD, M.: J. Iron Steel Inst., 177, 1954, p. 13–24.
30. MICHARD, J.: 2nd Intern. sym. on agglomeration, Paris, 1, 1957, p. 34–61.
31. KOZIMA et al.: Tet-to-Hagane, 55, 1966, p. 1–7.
    KOSUGA et al.: op. cit., 59, 1966, p. 501–504.
32. POTEBNYA et al.: Steel in USSR, March 1972, p. 176–178.
33. FLEMING, G. et al.: Stahl u. Eisen, 95, 1975, p. 677–683.
    POOS, A. and J. LUCKERS: ibid., p. 683–689.
    KLEPPE, W. et al.: op. cit., 99, 1979, p. 1019–1027.
34. ASADA, et al.: Trans. Iron Steel Inst. Jap., 8, 1968, p. 245–250.
35. ENDELL, K. G. et al.: Arch. Eisenhuttenw., 10, 1936, p. 86.

36. WATANABE, S.: Ref. 11, p. 865–890.
37. RUDNEVA et al.: Stal in Eng., Jan. 1962, p. 3–6.
38. BAZILEVICH et al.: op. cit., Oct. 1966, p. 769.
39. KOPYRIN et al.: Steel in USSR, Sept. 1973, p. 771–776.
40. ENGEL, K. et al.: Stahl u. Eisen, 99, 1979, p. 891–896.
41. TRAICE, F. B. and R. L. LAPPIN: Developments in ironmaking practice, Proc. conf., 22–23 Nov. 1972, Iron Steel Inst., London, p. 17–31.
42. KOEN, W.: ibid., p. 12–16.
43. MEYER, K.: Stahl u. Eisen, 83, 1963, p. 1337–1346.
44. LOTOSH, V. E. and A. L. EFIMOV: Steel in USSR, March 1973, p. 169.
45. WENZEL, W. and H. W. GUDENAU: Stahl u. Eisen, 87, 1967, p. 933–938.
WENZEL, W. and H. W. GUDENAU: Klepzic Fachber., 75, 1967, p. 3–8.
GUDENAU, H. W.: Aufbereitungs Tech., 9, 1968, p. 2–8.
46. LOGINOV et al.: Stal in Eng., June 1969, p. 526–530.
47. KOLESANOV, F. F. and E. G. GAVRIN: Stal in Eng., April 1962, p. 247–250.
KHOKLOV, D. B.: op. cit., Aug. 1962, p. 557–562.
48. POCHVISNEV et al.: op. cit., Nov. 1966, p. 861–865.
49. NEKRASOV et al.: op. cit., Jan. 1970, p. 417–420.
50. NARITA Et al.: Tetsu-to-Hagane, 63, 1977, p. 1623.
51. KHOKHLOV, D. G.: Stal in Eng., Oct. 1970, p. 761–764.
52. KOVALEV, D. A. And Yu. G. EFIMENKO: Steel in USSR, Feb. 1971, p. 88.
53. TYAMA et al.: Trans. Iron Steel Inst. Jap., 18, 1978, p. 57–60.
54. BRATCHENKO et al.: Steel in USSR, June 1972, p. 421–423
55. SHIMOMURA et al.: Trans. Iron Steel Inst. Jap., 17, 1977, 381–390.
56. VOSKOBOINIKOV et al.: Stal in Eng., July 1969, p. 607–612.
57. MOROZOV et al.: Steel in USSR, Feb. 1972, p. 83.
58. NEKRASOV et al.: op. cit., Nov. 1976, p. 587–589.
59. ENDE, H. v. and K. GREBE: Stahl u. Eisen, 92, 1972, p. 303–314.
60. STARSHINOV, B. N.: Stal in Eng., Nov. 1970, p. 849–853.
61. WATANABE, S. and M. YOSHINAGA: Ann. Meeting AIME, Los Angeles, Calif., Feb. 1967; see U. Scheib, Stahl u. Eisen, 87, 1967, p. 1152–1156.
62. POCHVISNEV et al.: Stal in Eng., Feb. 1970, p. 85–91.
63. EDSTROM, J. O.: J. Iron Steel Inst., Nov. 1953, p. 289–303; Sym. on Sinter. London, 1955; Spl. Rep. Iron Steel Inst., No. 53, p. 10–25; Jernkont. Ann., 140, 1956, p. 116–129.
64. MEYER, K., H. RAUSCH and M. OTTOW: Stahl u. Eisen, 87, 1967, p. 654–660.
65. BRILLE-EDWARDS et al.: J. Iron Steel Inst., Dec. 1969, p. 1565–1577.
66. STONE, H. E. N. and B. I. DANIELL: op. cit., Ja. 1969, p. 7–11.
67. BARRIE et al.: op. cit., May 1969, p. 563–569.
68. GRIEVE, A.: op. cit., 175, 1953, p. 1–4.
69. BABARYKIN, N. N. and F. A. YUSHIN: Stal, 18, 1958, p. 1057–1065.
70. DICKENS, P. et al.: Stahl u. Eisen, 79, 1959, p. 905–917.
71. POOS, A. and A. DECKER: Rev. Univ. mines, Ser. 9, 102, 1959, p. 773–783.
72. SCHWABE, G. and H. RELLERMEYER: Stahl u. Eisen, 82, 1962, p. 449–457.
73. BRAUMANN, O.: Softening behaviour of ores, Dr. Ing. Thesis, Tech. Hochschule, Aachen, 1964.
74. BOGDANDY, L. v. et al.: Stahl u. Eisen, 84, 1964, p. 1561–1568.
75. BOGDANDY, L. v. and H.-J. ENGELL: Ref. 6, p. 436.
76. LECOMTE et al.: Met. Rep. CNRM, 21, Dec. 1969, p. 21–28.
77. DAVISON, J.: Recent developments in met. sci. and tech. Iron and Steel, Silver Jub. Sym., Ind. Inst. Metals, New Delhi, 1972, p. 1–36.

78. DAVISON, J.: J. Iron Steel Inst., Feb. 1973, p. 106–114.
79. BOGDANDY, L. v. and H.-G. RIECKE: Arch. Eisenhuttenw,. 29, 1958, p. 603–609.
80. PEPPER, M. D. and B. L. DANIELL: J. Iron Steel Inst., uly 1969, p. 972–978.
81. BOGDANDY, L. v. et al.: 3rd Jour. Int. de Siderur, Luxemburg, Oct. 1962, p. 142–156.
82. POOS, A. and R. LINDER: ibid., p. 117–126.
83. DICKENS, P. et al.: Stahl u. Eisen, 79, 1959, p. 905–917.
84. BOGDANDY, L. v et al.: op. cit., 83, 1963, p. 129–140.
85. SCHENCK, H. et al.: op. cit., 85, 1965, p. 963–970.
86. BEETON, T. B.: J. Iron Steel Inst., 201, 1963, p. 913–922.
87. BERG, B. et al.: Rev. univ. mines., 18, 1962, p. 284–287.
88. LINDER, R.: J. Iron Steel Inst., 189, 1958, p. 233–243.
89. KIKUCHI, T.: op. cit., 205, 1967, 606–624.
90. OLIVER, R. A.: op. cit., 205, 1967, 1131–1135.
91. IWASAKI, I.: The Gakhusin proposed procedures for testing iron ore pellet quality, Mines Expt. Sta., Univ. Minnesota, July, 1964, No. 8.
92. BONNIVARD, G. and A. RIST: Rev. de Met., 59, May 1962, p. 401; 60, 1963, p. 23.
93. BIRNBAUM, H.: Stahl u. Eisen, 80, 1960, p. 781–788.
94. JANKE, W.: Contribution to testing of iron ore in the laboratory and plant, Dr. Ing. Thesis, Tech. Univ., Berlin, 1960.
95. CALLENDER, W.: Ref. 11, p. 647–667.
96. CHESTERS, J. H.: Steel plant refractories, 2nd Edt., United Steel Co., Sheffield, 1957.
97. KISTER, H.: Stahl u. Eisen, 88, 1968, p. 1427–1428.
98. PEHLKE, B.: On the cause of decrepitation of iron ores, Dipl. Thesis, Bergakad. Clausthal, 1958.
99. DAVISON, J. et al.: BISRA Conf. Rep., IM/S/13/70.
100. GREBE, K. and H. KISTER: Stahl u. Eisen, 91, 1971, p. 825–833.
101. FORSTER, E. et al.: op. cit., 89, 1969, p. 1473–1480.
102. REUSS, J. L. and M. M. FINE: US Bur. Mines, Rep. No. 7060, 1968, p. 24.
103. SEATON, P. T. and T. A. HENDERSON: J. Iron Steel Inst., May 1973, p. 334–345.
104. LECOMTE et al.: Met. Rep., CNRM, 16 Sept. 1968, p. 3–9.
105. BURGHARDT, O. and K. GREBE: Stahl u. Eisen, 89, 1969, p. 561–573.
106. WATANABE, S. and M. YOSHINAGA: Trans. Met. Soc., AIME, 241, 1968, p. 1–15.
107. TIGERSHIOLD, M.: Stahl u. Eisen, 70, 1950, p. 397–403.
108. DANIELSSON, C.: J. Iron Steel Inst., 175, 1953, p. 152–154.
109. NOTINI, U.: Jour. Int. de Siderurg., 18–28 June 1958.
110. SETH, B. B. L. and H. U. ROSS: Canad. Met. Qrly, 2, 1963, p. 16–30.
111. TURKDOGAN, E. T.: Met. Trans., 9B, 1978, p. 163–179.
112. BIRNBAUM, H. And L. v. BOGDANDY: Stahl u. Eisen, 82, 1962, p. 785–796.
113. BOGDANDY, L. v. et al.: op. cit., 83, 1963, p. 129–139.
114. JOSEPH, T. L.: Trans. AIME, 120, 1936, p. 72–90; Metal Tech., 3, 1936, No. 688.
115. EL-MEHAIRY, A. E.: J. Iron Steel Inst., 179, 1955, p. 219–226.
116. TURKDOGAN, E. T. and J. V. VINTERS: Met. Trans., 2, 1971, p. 3175–3188; 3, 1972, p. 1561–1574.
117. TURKDOGAN, E. T. et al.: op. cit., 2, 1971, p. 3189–3196.
118. BUKLAN et al.: Stal in Eng., March 1970, p. 183–189.
119. KOHL, H. K. and H.-G. ENGELL: Arch. Eisenhuttenw., 34, 1963, p. 411–418.
120. PUTZIER, U.: Dr. Ing. Thesis, Tech. Hochschule, Aachen, 1966.

121. SCHENCK, H. et al.: Arch. Eisenhuttenw., 38, 1967, p. 577–584; Stahl u. Eisen, 87, 1967, p. 1065–1070.
122. BLEIFUSS, R.: Intn. conf. sci. tech., Iron and Steel, Tokyo, Sept. 1970; Prg. Rep. No. 19, Mines Expt. Stat., Univ. Minnesota, Jan. 1970; Trans. Met. Soc., AIME, 247, 1970, p. 225–241; Blast Fce. Tech., Edt. Szekely, Decker, 1972.
123. FUWA, T. and S. BAN-YA: Trans. Iron Steel Inst., Jap., 9, 1969, p. 137.
124. LU, W. K.: Scand. Metallurg., 4, 1974, p. 9.
125. ENDE, H. v. et al.: Stahl u. Eisen, 91, 1971, p. 815–824.
126. ENDE, H. v. et al.: op. cit., 90, 1970, p. 667–676; p. 694–697.
127. ENDE, H. v. and K. GREBE: op. cit., 92, 1972, p. 303–314.
128. WENZEL, W. and H.-W. GUDENAU: op. cit., 90, 1970, p. 689–694; 92, 1972, p. 689–696.
129. MOHLMANN, et al.: Arch. Eisenhuttenw., 47, 1976, p. 647–651.
130. DAVIES, J. et al.: Ironmaking Steelmaking, 5, 1978, p. 151–161.
131. WENZEL, W. et al.: Aufbereitungs Tech., 11, 1970, p. 154–157; p. 492–494.
132. NAKIBOGLU, F. et al.: Australia-Japan Sym. Ext. Met., Sydney, 1980.
133. WAHLSTER, M.: Tech. Mitting. Krupp Rheinhausen, 19, 1961, p. 1–16.
134. RICHARDSON, F. D. and E. DANCY: Trans. Farad. Soc., 4, 1948, p. 229.
135. GELLNER, O. H. and F. D. RICHARDSON: Nature, 168, 1951, p. 23.
136. FUWA, T. and S. BAN-YA: Trans: Iron and Steel Inst., Jap., 7, 1967, p. 137–147.
137. HASSLER, B.: Stahl u. Eisen, 95, 1975, p. 725–733.
138. EL-GEASSY et al.: Trans. Iron Steel Inst. Jap., 17, 1977, p. 629–635.
139. WIBERG, M.: Jernkont. Ann., 124, 1940, p. 172–212; see also B. Kalling, Phys. Chem. of Steelmaking, Edt. J. F. Elliott, MIT, Mass., p. 149–158.
140. SHEHATA, K. A. and S. Y. EZZ: Trans. Inst. Min. Met., 82, 1973, p. C38.
141. RIECKE et al.: Arch. Eisenhuttenw., 38, 1967, p. 249–255.
142. CORDIER, J. A.: J. Metals., Jan., 1961, p. 31.
143. KRAINER et al.: Stahl u. Eisen, 83, 1963, p. 578–585.
144. SHKODIN, K. K.: Stal in Eng., Feb. 1963, p. 85–90.
145. GRIEVE, A.: J. Iron Steel Inst., Jan. 1960, p. 37–43.
146. MILLER, V. Ya. and S. A. ELKIN: Stal, 3, 1958, p. 193–202.
147. SHAPOVALOV, M. A.: op. cit., 5, 1958, p. 385–396.
148. BOGDANDY, L. v.: Arch. Eisenhuttenw., 32, 1961, p. 275–296.
149. ULRICH et al.: op. cit., 36, 1965, p. 611–618.
150. DIEPSCHLAG, E.: Arch. Eisenhuttenw., 10, 1936, p. 179–181.
151. STRASSBURGER, J. H.: Iron and Steel, Oct. 1958. p. 491–496.
152. BELL, H. B. and J. TAYLOR: J. Iron Steel Inst., Nov. 1961, p. 261.
153. GIEDROYC, V. and W. HYSLOP: Proc. Sym. Blast Fce. Aerodynamics, Edt. N. Standish, Aus. I. M. M., Wollongong, 1975, p. 90.
154. PETERS, W.: Stahl u. Eisen, 84, 1964, p. 979–986.
155. ECHTERHOFF, H.: op. cit., 81, 1961, p. 992–1000.
156. SZURMAN, E.: op. cit., 97, 1977, p. 1.
157. SASAKI et al.: Trans. Iron Steel Inst. Jap., 17, 1977, p. 252–261.
158. NAKAMURA, N. et al.: Ironmaking Steelmaking, 5, 1978, p. 1–17.
159. DARTNELL, J.: ibid., p. 18–24.
160. BEER, H. and W. ZISCHKALE: Stahl u. Eisen, 188, 1968, p. 845–852.
161. MURAKAMI et al.: Coke cir., 23, 1974, p. 1.
162. ZISCHKALE, W. et al.: Stahl u. Eisen, 83, 1963, p. 1117–1125.
163. SCHAEFERS, W. and G. WINZER: op. cit., 85, 1965, p. 1509–1516.
164. ASAI, H.: Intn. congr. on coke in ironmaking, Charleroi, 19–22 Sept. 1966, Liege, 1967, p. 369–381.

165. HEYNERT, G. et al.: Stahl u. Eisen, 80, 1960, p. 981–990.
166. KAHLHOFER et al.: op. cit., 82, 1962, p. 547–556.
167. MULLER et al.: Blast Fce. Steel Plant, 53, 1965, p. 381.
168. TRISKA, A. A. and C. D. SCHUBERT: Steel Times, 193, 1966, p. 614.
169. Alkali in blast fce. – State of art – Proc. sym., McMaster univ., Hamilton, Ont., 1973.
170. MARSH, H.: J. Iron Steel Inst., 211, 1973, p. 334.
171. GEORGE, D. W. R. and j. A. PEART: Proc. Ironmaking Conf., 32, 1973, p. 40–59; Ref. 169, p. 4.1–4.25.
172. RANKIN, W. J. and J. B. SEE: Alkali in Blast fce., Rep. No. 1879, NIM, Johannesburg, S. Africa.
173. KOZIMA, K.: J. Iron Steel Inst. Jap., 16, 1976, p. 570.
174. STEFANESCU, I. et al.: Stahl u. Eisen, 88, 1968, p. 342–345.
175. ABEL and SHULTZ: op. cit., 92, 1972, p. 37–40.
176. NEKRASOV et al.: Steel in USSR, Nov. 1974, p. 861.
177. BOGDANDY, L. v. and W. SCHAEFERS: Stahl u. Eisen, 82, 1962, p. 1–18.
178. KASE, T: Recent dev. in met. sci. and tech., Iron and Steel, Silver Jub. Sym., Ind. Inst. Metals, New Delhi, 1972, p. 207–219.
179. HATANO et al.: Trans. Iron Steel Inst. Jap., 17, 1977, p. 102–109.
180. INATANI et al.: Tetsu-to-HAgane, 62, 1972, 1976, p. 514.
181. QUIGLEY, J. J. et al.: Ironmaking Proc., AIME, 32, 1973, p. 26.
182. ASHTON, J. D. and J. E. R. HOLDITCH: op. cit., 34, 1975, p. 265.
183. RIDGION, J. M.: J. Iron Steel Inst., Oct. 1961, p. 135–143.
184. WENZEL, W. et al.: Stahl u. Eisen, 97, 1977, p. 286–290.
185. KOZIMA, K.: Coke circ., 25, 1976, p. 301.
186. NAKAMURA, N. et al.: Ironmaking Steelmaking, 5, 1978, p. 49–60.
187. GERSTENBERG, B. and Th. KOOTZ: Stahl u. Eisen, 84, 1964, p. 1105–1120.

CHAPTER 7

REACTIONS IN THE BLAST FURNACE

7.1. General

Blast furnace is, from a physico-chemical point of view, a giant counter-current heat exchanger as well as a chemical reactor. The hot ascending gases heat up the descending charge materials, accompanied by a variety of physical changes and chemical reactions. We have seen in Chapter 4 that due to differential heat requirements at various temperature levels, the temperature profile assumes a shape like ≀ , the upper preheating zone (0–800°C) being separated from the lower melting zone (900–1500°C) by a vertical thermal reserve zone of considerable height where the temperature ranges between 800–1000°C and where very little heat exchange occurs between the solids and the gas. The idealized gas and solids temperature profile is redrawn schematically in Fig. 7.1(b).

The reduction profile, similar to that of Bülter and Klitzing,[1] is shown in Fig. 7.1(a). The nature of the counter-current process enables a highly reducing gas (high CO content) to come into contact with wustite having the lowest oxygen pressure of the three iron oxides, the other two, hematite and magnetite, having been reduced in the upper furnace with a gas of lower reducing potential (Sec. 3.6). In the direct reduction zone H_4', most of the CO_2 produced from the reduction of wustite and metalloid oxides is converted to CO by the Boudouard reaction. This CO together

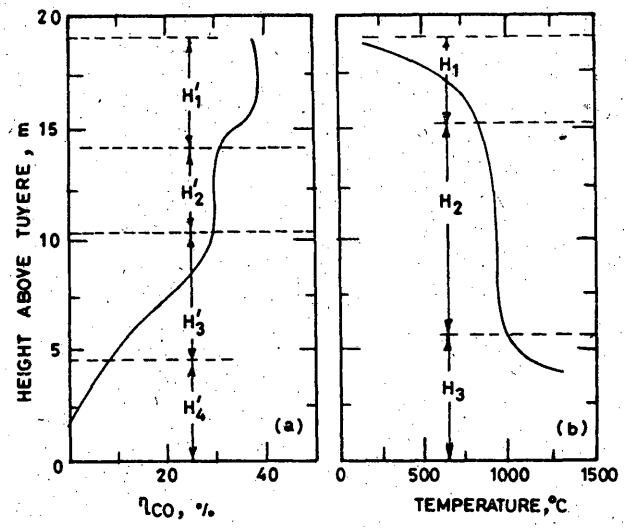


Fig. 7.1 A schematic representation of reduction and gas temperature profiles in a blast furnace; (a) shows variation of %CO-utilization and (b) gas temperature along the height of the furnace.

with that generated at the tuyeres travels up and the CO_2 generated from further reduction of wustite is preserved since the Boudouard reaction becomes sluggish below a temperature of about 1000°C. This zone is designated as indirect reduction zone of wustite, H_3' in Fig. 7.1(a). Only a part of wustite oxygen is reduced by direct reduction and if the total CO coming from zone H_4' is just sufficient to reduce the rest of the wustite oxygen in zone H_3' according to the equilibrium relation for 900°C, $FeO + 3.3CO = Fe + 2.3CO + CO_2$, there will arise a chemical inactive zone, H_2', where the gas composition does not change (η_{CO} = 30%, constant). In this zone the CO does not further react with the descending wustite which is formed in the pre-reduction zone H_1', where the magnetite and hematite are reduced to wustite, their equilibrium CO/CO_2 requirement being very small (η_{CO} = 80% for magnetite and nearly zero for hematite). The vertical length of the inactive zone depends upon the reduction rate of wustite. It would disappear completely if the reducibility and time of residence of wustite in the indirect reduction zone H_3' are insufficient for attainment of equilibrium with the reducing gas.

The temperature and reduction profiles in Fig. 7.1 more or less coincide and hence the blast furnace can be conveniently divided into three zones for a study of the physical and chemical reactions occurring therein. These

will be discussed in the following text. The formation of slags and removal of sulphur are subjects by themselves and will be treated in Chapters 8 and 9.

The three zones mentioned above are;

(i) The *upper* or *pre-heating* or *preparation* zone;
(ii) The *middle* or *indirect* reduction or *thermal reserve* or *isothermal* zone;
(iii) The *lower* or *processing* or *melting* or *direct* reduction zone.

7.2. Reactions in the Upper Zone

In this zone, the burden is rapidly heated from the ambient temperature to about 800°C within a distance of 4–6 m from the stock level and the gas coming from the middle zone cools down from 900°C to 100–200°C as it leaves the furnace top. The main reactions that occur in this zone are narrated below.

7.2.1. Reduction of Iron Oxides

Theoretically, hematite and magnetite should undergo reduction as soon as the ore is charged into the furnace since the reduction potential of the top gas is sufficiently high for the formation of wustite. The extent of actual reduction depends upon the size and nature of the ore and intensity of gas flow in the radial cross-section of the zone. If the ore size is large and/or if it is non-porous, the outer shell may be reduced to wustite while the inner core still containing hematite. There is considerable breakdown of hematite ores or even sinters in this low temperature region as we have seen in Sec. 6.5. Even in modern furnaces using well-prepared burden the reduction of hematite and magnetite to wustite is not complete in this zone, although the iron oxide which enters the zone H_2 should ideally be wholly wustite. Magnetite is reduced to wustite mainly[2] at 700–900°C. The reduction reactions are given by the following equations:

$$3Fe_2O_3 + CO = 2Fe_3O_4 + CO_2 + 10.33\ \text{kcal} \qquad 7.1$$

$$Fe_3O_4 + CO = 3FeO + CO_2 - 8.75\ \text{kcal} \qquad 7.2$$

$$FeO + CO = Fe + CO_2 + 3.99\ \text{kcal} \qquad 7.3$$

These reactions, as we are already aware (Sec. 3.6), are called indirect reduction.

7.2.2. Volatilization

This comprises mainly of the chemically uncombined water entering the furnace with moist ore, coke, limestone or any other charge material (water is also sometimes deliberately added to the ore to lower the top gas temperature when it is too high or to minimize dust nuisance when large amounts of fines accompany). The volatilization of water consumes about 580 kcal/kg water. The average moisture content of coke and ore is about 5 perent but can be as high as 15 percent in very moist ores.

A good variety of coke may contain up to 1.5–2 percent of volatiles. They also volatilize in this zone but the amount being small, they do not alter the top gas composition significantly.

7.2.3. Decomposition of Hydrates

Apart from the physical adherence of moisture with the charge materials, water is also present chemically combined as water of crystallization or hydration. The hydrated water is combined adsorptively with the solids and needs heat for breaking of the bonds in addition to that for vaporization of water. The decomposition of the hydrates of iron oxides may start around 300°C and continue to higher temperature levels. On the other hand, $Al_2O_3.2SiO_2.2H_2O$ gives up water at much higher temperatures and may even reach the middle zone before complete dehydration, although the decomposition starts at about 400°C. It needs 965 kcal/kg water in contrast to the heat of 580 kcal/kg water necessary for pure evaporation. The additional 385 kcal/kg is used up for breaking the bond of hydration.

The physically combined water escapes unchanged as steam at lower temperatures but the hydrated water which is released above 300–400°C may react with CO to produce CO_2 and H_2, known as *water-gas shift* reaction (or simply water-gas reaction).

7.2.4. Water-Gas Shift Reaction

The temperature dependence of the equilibrium constant of the homogeneous water-gas shift reaction,

$$CO + H_2O = CO_2 + H_2 + 9680\ \text{cal} \qquad 7.4$$

has already been dealt with in Sec. 3.9. The equilibrium constant of the reaction is 2.46 at 900°K and 0.8 at 1200°K. It is, therefore, thermodynamically possible for CO to reduce H_2O in the upper furnace to a certain extent while the reaction would be kinetically more favourable

in the middle zone where the temperature ranges between 800–1000°C. The reaction is influenced by catalysts and freshly reduced iron itself possesses catalysing properties.[3,4] This reaction as well as its effect on the utilization of CO and H_2 have been discussed in Secs. 3.11 and 7.3.4.

7.2.5. Carbon Deposition

We have already discussed this subject in Sec. 3.5. Thermodynamically, carbon deposition from CO by the reaction

$$2CO = CO_2 + C + 41210 \text{ cal} \qquad 7.5$$

is possible in any field left of the Boudouard curve (Fig. 3.4). Because of exothermic nature of the reaction, the formation of carbon should be preferred at low temperatures but the reaction velocity possesses the opposite tendency, that is, it increases with increasing temperature. Therefore, the deposition occurs predominantly in a narrow temperature range 450–600°C where the reaction velocity attains a reasonable rate (Fig. 3.5). The presence of iron and its oxides catalyses the reaction. According to Turkdogan and Vinters,[5] freshly reduced porous iron acts as a catalyst. The deposited carbon consists of graphite and cementite. Carbon deposition ceases when most of the iron is converted into cementite.

Carbon deposition can occur on the surface or in the pores of ores, sinters or pellets or inside refractory brickworks wherever reduced iron provides the active surface for catalysing the reaction. As the carbon-deposited materials descend to higher temperature regions, the direct reaction of carbon with ore oxygen liberates CO which causes bursting of the ore lumps and thus generates more ore surface and facilitates reduction. However, the deposition in the pores as well as the tendency to bursting lower the mechanical strength of the ore and may generate large quantities of fines which would adversely affect the bed permeability and gas distribution. On the other hand, deposition on the surface minimizes sticking of the ores and thus enhances the permeability of the bed.

Carbon deposition has some advantages. The deposited carbon can descend along with the burden and replace equivalent amount of coke and thereby economize fuel consumption. The deposition being exothermic helps in rapid heating of the charge materials. Because of fineness of deposition there is a danger of their being driven out of the furnace by the high velocity ascending gases. The danger will be less in high top pressure furnaces where the linear velocity and hence the kinetic energy of the gases are lower. Further, since reaction 7.5 is pressure dependent, an increased

average stack pressure in the pressurized furnaces will cause a larger deposition of carbon.

The disadvantage of carbon deposition is that the freshly formed highly active powdery carbon carried down with the burden is gasified by CO_2 at temperatures much lower than in the case of less reactive coke. Therefore, the Boudouard reaction would commence at a higher level in the furnace, shortening the vertical height of the useful indirect reduction zone (H_3', Fig. 7.1a) and thus increasing the direct reduction and coke consumption. Carbon also deposits in the brickworks of the shaft[6] and can cause its disintegration, dislocation as well as formation of bridges, accretions, etc. (Sec. 13.3).

We have seen that the reaction is catalysed by fine metallic iron produced during reduction of ores. The rate of formation of carbon depends upon the CO/CO_2 ratio as well.[7] The rate is large even at 450°C in a gas mixture of $CO + CO_2$ containing under 5% CO_2 but slows down greatly with CO_2 content of 10–25 percent. In modern furnaces, the occurrence of carbon deposition is not very excessive. This is perhaps because of more uniform gas distribution and very little formation of fresh metallic iron in the upper furnace. The higher temperature in the middle furnace is not so conducive to carbon deposition. Further, the residence time of the gas in the stack is very small, 9–10 seconds, which allows little time for the reaction to occur to any great extent.

It is possible to poison[8–11] the catalyst by very small additions of such compounds in the gas as sulphur dioxide, hydrogen sulphide, chlorine, cyanogen, ammonia, nitrogen dioxide. The former two act irreversibly[5,11] because of formation of pyrrhotite from cementite but the catalysts can be revived in other cases when they are removed from the system. Hydrogen acts as promoter.[12] Hydrogen adsorbed on iron catalyses the decomposition of CO in addition to $H_2 + CO = C + H_2O$. Water vapour catalyses the deposition of carbon in the absence and retards it in the presence of hydrogen.

7.2.6. Decomposition of Carbonates

Metal carbonates may accompany the ore or they are added deliberately for fluxing the acids of the charge materials. Spathic iron ore contains ferrous carbonate and sometimes calcium carbonate is also found in iron ores.

In this section we will confine to the carbonates of iron, manganese, magnesium and calcium-magnesium (dolomite) since calcium carbonate

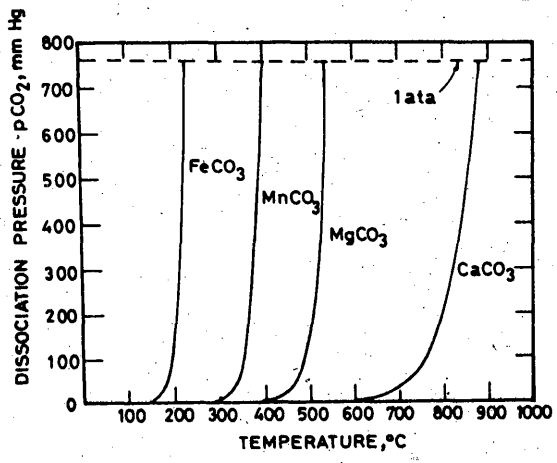


Fig. 7.2 The decomposition pressure of some carbonates as function of the temperature, according to Bogdandy et al.[13] (Copyright Verlag Stahleisen).

decomposes at much higher temperatures, 900–1100°C depending upon its lump size. The dissociation pressure (p_{CO_2}) of carbonates increases with increasing temperature, the decomposition temperature being that when $p_{CO_2} = 1$ atm. As can be seen from Fig. 7.2,[13] the decomposition of carbonates other than that of calcium occurs at relatively low temperatures, around 400°C. It should occur at still lower temperatures because the p_{CO_2} in the shaft gases is about 0.2–0.3 atm. but it does not do so due to the existence of a natural temperature gradient from the surface to inside of the lumps, which becomes steeper by the endothermic nature of the reaction. Again, especially in case of large lumps, the CO_2 produced in the interior may be pure, whereas outside, it is diluted.

These carbonates constitute a significant thermal load in the furnaces where run-of-mine ores are used. They are of very little importance now because most modern furnaces are using sinters or pellets and these carbonates as well as limestone are all calcined outside.

The volatile metals that accompany the charge materials are lead, zinc and alkalis in the form of their compounds. These compounds flux the refractories and cause extensive disintegration of the shaft brickwork (Secs. 3.21 and 13.3). Lead oxide is very easily reduced and the metal does not get reoxidized in the shaft. However, its vapours may penetrate the brickwork. The oxides of zinc and alkali metals are reduced in the lower furnace where the reduction potential and temperature of the gas are high. The

volatile metals are carried to the upper furnace by the fast moving gases, get reoxidized at lower temperatures by gases having higher oxygen potential (high CO_2 and H_2O content) and a part may escape with the top gas or penetrate the brickwork. The rest is carried down, gets reduced, the metals vaporize and the process repeated. Thus, a zinc and alkali cycle builds up in the furnace.

7.3. Reactions in the Middle Zone

This zone extends from the upper zone (4–6 m below the stock level) downwards to 3–5 m above the tuyere level. It is a moderate temperature zone where the temperature ranges between 800–1000°C. The height of this zone is considerable and may occupy 50–60 percent of the shaft height (about 75% of the shaft volume) in modern furnaces working smoothly

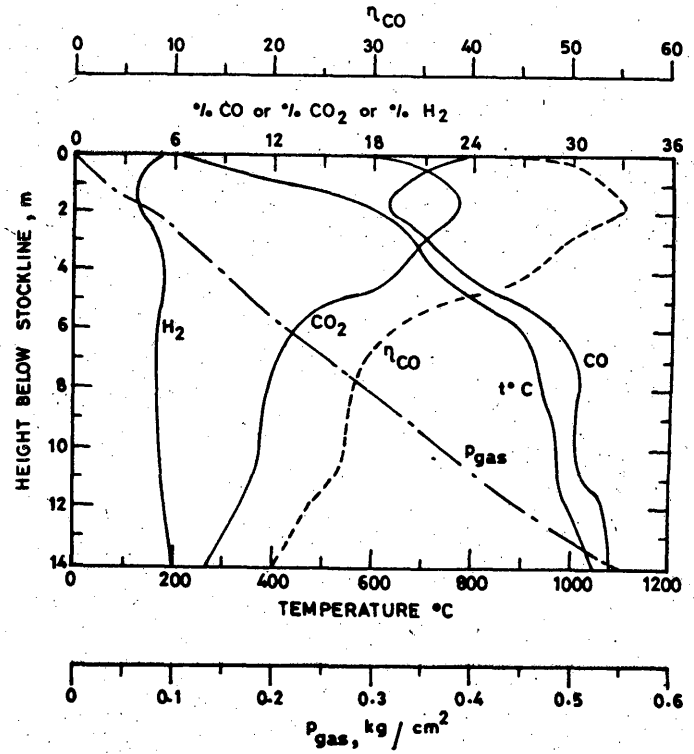


Fig. 7.3 The gas temperature, composition and pressure profiles in a 1700 m³ Magnitogorsk blast furnace using 100 percent pellet charge.

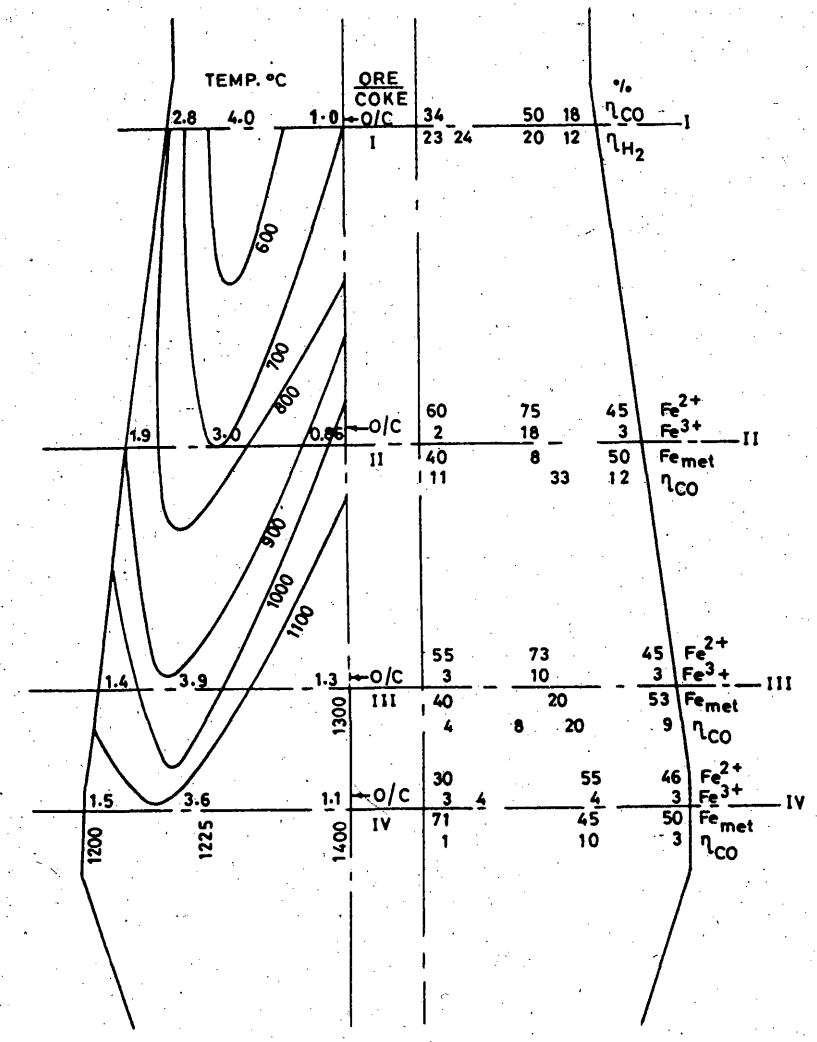


Fig. 7.4 A broad view of the variations in gas temperature, ore/coke ratio, CO-utilization and state of oxidation of iron in the radial and vertical cross-sections at four levels above the belly in a 2000 m³ Russian blast furnace.

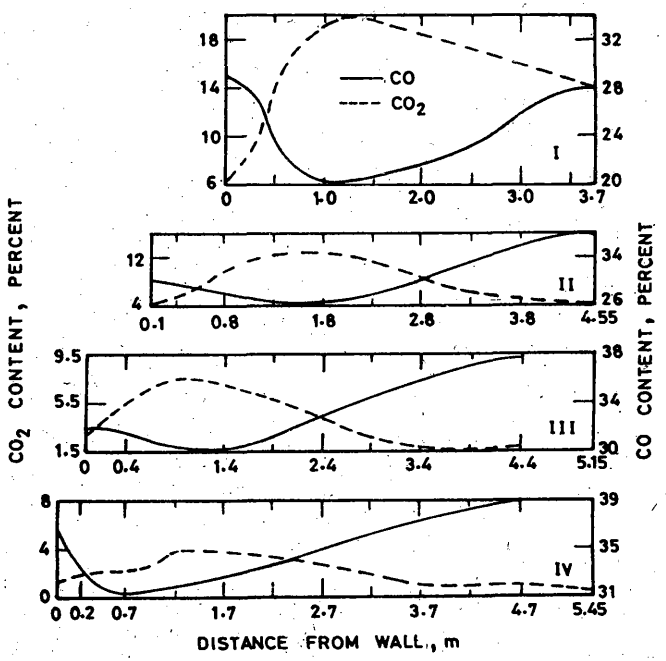


Fig. 7.5 Variations in the content of carbon monoxide and dioxide in a 2000 m³ Russian blast furnace at 4 levels shown in Fig. 7.4. (After Nekrasov and Buzoverya).[22]

with properly sized charge materials and uniform gas distribution. The charge passes through the zone[14] in 2.5–3 hours. From the kinetic point of view, this temperature range is very suitable for indirect reduction of wustite, the phase left after reduction of hematite and magnetite in the upper furnace. Within this zone, there may be present a chemical inactive zone where the gas composition does not change appreciably and the CO and CO_2 contents approach equilibrium with wustite ($\eta_{CO,FeO}$ = 25–30%). The temperature and gas composition profiles in the stack of a 1700 m³ furnace compiled from the plant data[15] at the Magnitogorsk combine working with 100%-pellet are shown in Fig. 7.3 which confirms the existence of a moderate temperature zone of considerable height as well as that of a chemical inactive zone where very little oxygen transfer occurs.[16–21]

However, in the middle zone itself there are peripheral, intermediate and central (or axial) zones where the temperature and composition of the gas can vary widely. The variation is due to non-uniform distribution of the charge materials at the top with the major portion of ores or agglomerates residing in the intermediate zone. It is an inevitable con-

sequence of the charging methods and is inherent in the use of the conventional two bell system. The temperature profile, ore/coke ratios, iron in various forms and CO-utilization in the various zones of a 2000 m^3 Russian furnace[22] at four levels above the belly are assembled in Fig. 7.4 and the gas compositions in Fig. 7.5.[22] Such variations were also obtained in the investigations of Kinney[23] and at the Magnitogorsk and Zaphorstahl works.[24]

Although for convenience we have divided the furnace into three different zones based on temperatures, these three zones may merge or overlap depending upon the gas and material distribution. In the schematic diagram 7.1(a), the lower furnace was designated as direct reduction zone where the temperatures are above 1000°C and where any CO_2 formed from the reduction of iron oxide would be reduced by carbon. Direct reduction, however, is not necessarily confined to the lower furnace but can occur at any place in the furnace where the temperature is above 1000°C. This is one of the reasons why the fuel efficiencies used to be so low in the older furnaces. From Fig. 7.4, the moderate temperature zone is of considerable height in the intermediate zone where the ores are more concentrated and where a considerable utilization of CO is expected.

Indirect reduction of all iron oxides takes place below 1000°C and that of wustite at 800–1000°C. Although the reaction should be fast at these temperatures, in fact it is retarded because of nearness of the gas composition to that necessary for equilibrium with wustite.

7.3.1. Direct/Indirect Reaction and Inactive Zone

The importance of the middle or indirect reduction zone in the blast furnace process can only be realized from an understanding of the role of direct/indirect reduction on the fuel economy. We have seen in Sec. 3.6.2 that direct reduction is economical of coke but results in a thermal deficit. The blast furnace works through an optimum balance between the thermal and reduction requirements. This has been detailed in Secs. 10.1–10.3. As a simple example, let us suppose that 280 kg of wustite oxygen (17.5 kg.atom O) is required to be removed per THM. (In blast furnace fuel calculations, the reduction of wustite *only* is important because of its low equilibrium CO-utilization or high equilibrium CO/CO_2 ratio). Suppose the total heat requirement (including an assumed amount of direct reduction) is supplied by burning 240 kg of carbon (20 kg.atom C) which provides 20 kg.mole of CO. According to wustite/iron equilibrium at 900°C (Eq. 3.14),

$$FeO + 3.3CO = Fe + 2.3CO + CO_2 \qquad 7.5$$

20 kg.mole of CO will remove 20/3.3 = 6 kg.atom O, leaving a further 11.5 kg.atom O to be removed. A part of this unreduced oxygen will descend to the lower zone and be reduced directly by C (through the Boudouard reaction) and the CO produced will be available for indirect reduction of the rest. To determine the optimum value whereby a part of the oxygen is reduced directly and the rest indirectly, let us assume y kg.atom O is removed directly which will produce y kg.mole of CO. Hence,

$$y = (11.5\text{-}y) \times 3.3$$

or $$y = 8.8 \text{ kg.atom O} = 140.8 \text{ kg.O}$$

That is, if about 141 kg of oxygen is removed directly, the CO evolved plus the CO generated from 240 kg of tuyere carbon will be just sufficient to reduce (280–140.8) = 139.8 kg of wustite oxygen indirectly, satisfying the above equilibrium relation. In such a case, the gas will be at equilibrium with wustite/iron and the composition will not change until it comes into contact with the higher iron oxides in the upper furnace. This zone where the gas composition does not change has been referred to as chemical inactive zone H_2' in Fig. 7.1(a). Now, if due to inadequate reduction velocity the entire 139.8 kg of oxygen is not removed during the residence of the wustite in the indirect reduction zone although the required amount of CO is still available, the amount not reduced will descend to the lower zone where the temperatures are higher than 1000°C. This oxygen will be removed no doubt by CO to form CO_2 but the latter will be reduced by carbon at this temperature,

$$FeO + CO = Fe + CO_2 \qquad 7.6$$

$$CO_2 + C = 2CO \qquad 7.7$$

adding, $$FeO + C = Fe + CO \qquad 7.8$$

Thus there will be more direct reduction than that necessary for the optimum and more unnecessary CO will be generated. Further, to cover the endothermal heat of direct reduction, an extra amount of carbon will need to be burned at the tuyeres which will produce an extra amount of CO. All these unwanted CO will pass through unused giving rise to high CO/CO_2 ratio in the top gas. The inactive zone will no longer appear. The coke rate will increase by an amount equal to the extra direct reduction and associated extra tuyere carbon. Circumstances similar to that above

will occur if any magnetite descends into the inactive zone from the pre-reduction zone (H_1').

In the above context, the importance of the temperature and vertical height of the middle zone and the reducibility of the ore are immediately evident. The larger the height of the 800–1000°C temperature zone, the longer the gas/solid contact time at these temperatures and the greater the degree of indirect reduction. Similarly, the higher the reducibility of the ore the more rapid the reduction. In short, the rate of reduction of the ore in the middle zone must not be a restriction for the attainment of optimum coke rate. It is for this reason that so much attention has been paid in recent years on the study of reducibility of ores and methods of increasing the rate of reduction which have already been described in Sec. 6.7. The optimum coke rate calculations in Sec. 10.2 assumed an infinite rate of reduction of wustite, i.e., the wustite will always be reduced as long as the gas is more reducing than the equilibrium composition.

Any furnace where the fuel efficiency is not at its optimum is obviously a badly working furnace. That is, there is an insufficient indirect reduction which can be caused by inferior reducibility of ore, inadequate residence time below 1000°C and non-uniform gas and temperature distribution in the furnace. Non-uniformity is best shown in Figs. 7.4 and 7.5. The temperatures and compositions of the gas vary widely at various levels and cross-sections.

7.3.2. Gas Utilization

As pointed out in Sec. 5.9, the gas temperature and CO-utilization in the vertical and horizontal cross-sections are functions of gas flow per unit of charge. In the intermediate zone where the ratio gas/ore is low, the extent of the moderate temperature zone and η_{CO} are both high. The gas composition comes close to equilibrium with wustite near the belly. Since iron forms from the reduction of wustite, metallic iron in the intermediate zone forms much later than in the other two zones. The softening of the ore also occurs much later because high temperatures are reached near the bosh parallel (cf. Figs. 5.1 and 11.24a).

The gas/ore ratios are high in the peripheral and central zones, the more so in the latter, especially in large furnaces where the ore/coke ratio is very small in the centre. However, the ore and the gas reach some sort of dynamic equilibrium in the centre.[21] Since the gas/ore ratio is high, the gas temperature becomes high resulting in a high degree of direct reduction. The endothermic direct reduction cools down the gas, facilitating

gaseous reduction which, being exothermic leads again to increased gas temperature. Thus an automatic and dynamic equilibrium is set up in the centre.

A typical example of investigations by Schürmann et al.[19] is shown in Fig. 7.6 where the compositions of the gas at various temperatures are drawn in terms of % η_{CO} along with the Fe-O and C-O equilibrium systems. The author has, for comparison, inserted in the figure approximate gas compositions of earlier (L) and modern (M) furnaces, as well as those expected from an ideal case (N) based on $\eta_{CO,FeO} = 30\%$ (Sec. 10.2). The Boudouard curve has been drawn for $p_{CO} + p_{CO_2} = 0.6$ atm. approximating the sum of their partial pressures in the shaft gas.

At temperatures above 1200°C the CO_2 content is negligible and rises to about 5 percent at 1000°C (curve ABC, Fig. 7.6), the equilibrium value at the temperature being less than 0.5 percent. Due to freezing of the Boudouard reaction at about 1000°C, there is a sharp rise in CO_2 thereafter and the η_{CO}-values range between 30–35 percent at 800°C (shaded area C-D) due to reduction of some hematite and magnetite. An oxygen balance shows that the gas did not reach equilibrium with wustite, the calculated $\eta_{CO,FeO}$ being only 15 percent. As the gas ascends and the temperature falls, further reduction of the two higher oxides occurs and the top gas finally

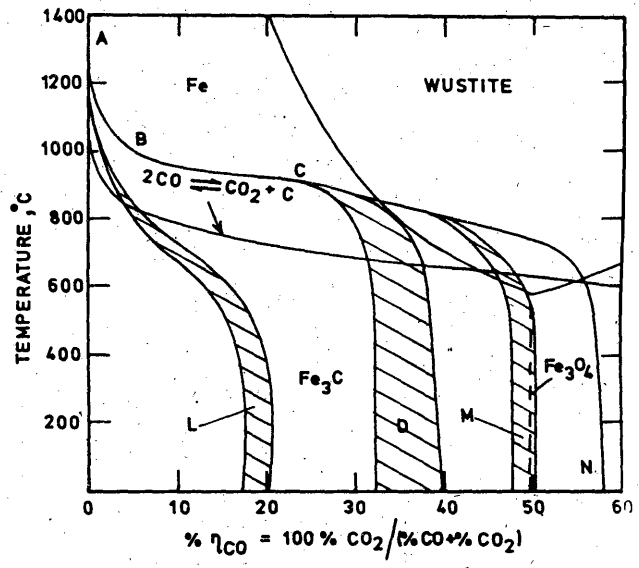


Fig. 7.6 Variations in the blast furnace gas composition in the iron-oxygen-carbon stability diagram. See text for L, D, M and N.

leaves the furnace with an overall η_{CO} of 32–40 percent. Apparently, the amount of CO generated from the tuyere carbon and direct reduction of part of wustite was much higher than the amount required for indirect reduction of the rest of the wustite oxygen. There obviously was a possibility of increasing the gaseous reduction of wustite and saving of coke.

It will be erroneous to think that indirect reduction is stabilized at temperatures above 1000°C because the presence of as much as 5% CO_2 is indicated. That CO_2 is present above 1000°C is indicative of its sluggish reactivity with coke. Whether the formation of CO_2 from the reduction of iron ore will exceed its reduction by carbon depends upon the relative kinetics of the reactions (Sec. 2.8). Hydrogen decreases the rate of the Boudouard reaction by chemisorption of active sites occupied by CO_2. The rate of the reaction $C + H_2O = CO + H_2$ is inherently faster. The carbon gasification rate may increase in the presence of H_2/H_2O because of rapid approach of the water-gas reaction to equilibrium whose rate is faster[25] than those of the reactions $C + CO_2$ or $C + H_2O$. In any case, the detection of CO_2 or H_2O in the high temperature region confirms that wustite in this zone is reduced indirectly and the CO_2 and H_2O evolved are reduced by carbon so that finally what we obtain is direct reduction, $FeO + C = Fe + CO$.

Fig. 7.6 summarizes the continuous improvements in CO-utilization with the improvement of burdening. The lines M and N show very high values of η_{CO} with high grade burden and low coke rates. They work with low gas/ore ratios with the attainment of chemical inactive zone. The maximum attainable limit appears to be about $\eta_{CO} = 60\%$ (line N).

7.3.3. Improving Indirect Reduction – Methods

We conclude that, except in cases where the presence of a chemical inactive zone is indicated from a thermal and reduction balance, it is possible to make savings in coke if indirect reduction can be increased before the onset of the Boudouard reaction. Thus, what happens in the middle zone becomes important from the point of view of fuel efficiency. An increase in indirect reduction can be achieved by:

(a) increased reducibility of the ore;
(b) extension and enlargement of the middle zone;
(c) longer gas/ore contact time;
(d) use of hydrogen bearers.

7.3.3.1. Reducibility of ore

The various factors that affect the reducibility of iron ores, sinters and pellets have been discussed in Sec. 6.7. They should be taken into account while selecting proper charge materials. Of prime importance are a large surface area/volume ratio and close size distribution (which assure a high reduction rate and a uniform gas flow) and pre-fluxing of sinters and pellets. The most suitable size for charging in the blast furnace is one where the rate of removal of oxygen from the ore exceeds 0.5%/min at 40 percent degree of reduction.

7.3.3.2. Size of middle zone

From Fig. 7.6, the gas composition above 1000°C, i.e., in the lower furnace, corresponds approximately to the curve ABC which runs parallel to the Boudouard curve but at temperatures about 200°C higher than the latter because of the inferior reactivity of blast furnace coke. The distance between the two can be varied by using coke of inferior or superior reactivity. Fig. 7.7[26] shows the difference. A less reactive coke shifts the Boudouard reaction to higher temperatures, i.e., to a lower level in the furnace and, therefore, vertically extends the zone of gaseous reduction of wustite. This will give more time to the ore for gaseous reduction and hence decrease the direct reduction and coke rate. In fact, a coke saving of 10–15 kg/THM has been obtained by the use of less reactive coke.[27]

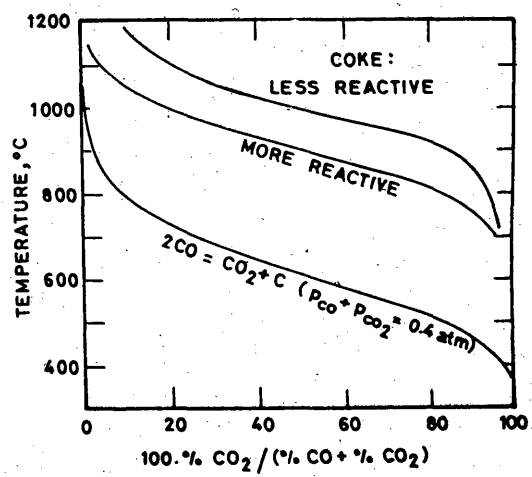


Fig. 7.7 The shift of the Boudouard curve with the change in the reactivity of coke, according to Heynert et al.[26] (Copyright Verlag Stahleisen).

On the other hand, the vertical distance will decrease with increasing reactivity of coke and the coke rate will increase. Heynert et al.[26] have shown that the fuel consumption increased by 8 percent (50–70 kg/THM) on increasing the coke reactivity by 100 percent. (See also Sec. 6.9.1.2).

The presence of limestone in the charge shortens the middle zone since the endothermic calcination reaction, which starts to occur at about 900°C, acts as a heat sink and the thermal reserve zone is stabilized at this temperature. The absence of limestone would extend the zone to higher temperatures because the Boudouard reaction (>1000°C) would be the first endothermic reaction occurring. Stabilization of the zone at higher temperatures should have a *further advantage* because the rate of wustite reduction increases with increasing temperature.

We have seen qualitatively in Sec. 4.3.3 that as the blast and hence the flame temperature increases the temperature gradient in the furnace becomes steeper, i.e., the high temperature zone in the lower furnace narrows down, elongating the thermal reserve zone vertically. This is confirmed in Fig. 7.8[28] which shows that with a blast temperature of 750°C the indirect reduction starts about 6–8 m above the tuyere axis whereas with a blast temperature of 1100°C it does so at 3–4 m. The middle zone is thus extended by about 3 m. This is presumably because an increased blast temperature reduces the coke rate and hence the bosh gas volume per THM, which decreases the ratio of gas/unit charge. The respective flame temperatures were 2020 and 2260°C.

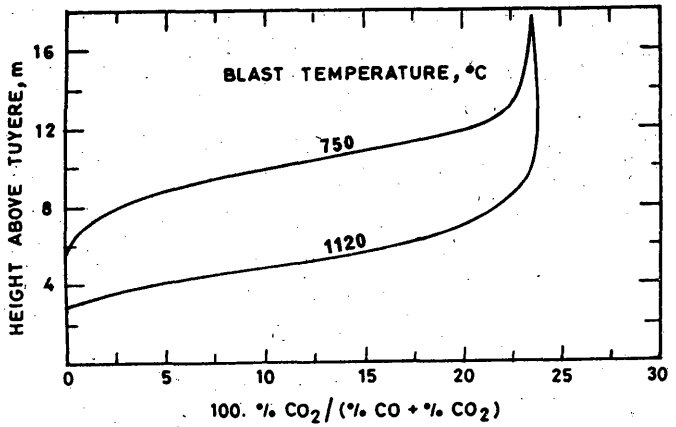


Fig. 7.8 The downward shift of the zone of beginning of indirect reduction at higher blast (flame) temperature in a blast furnace, according to Zischkale et al.[28] (Copyright Verlag Stahleisen).

As a corollary, the extent of the middle zone depends upon the quantity of gas generated. To supply the same amount of heat in the lower furnace, the gas volume must be larger the lower the flame temperature, i.e., more fuel needs to be burned. We have seen in Sec. 4.3.2 that because of a slower heating rate the high temperature zone shifts upwards in such a case. As a consequence, the middle zone narrows down vertically and, hence, the time of residence of the ore in this zone decreases. A stage may thus be reached when due to inadequate indirect reduction the chemical inactive zone, if present, would disappear. This is very clear from Fig. 7.9[29] which shows the influence of increasing amounts of reductants (which is directly related to the gas volume) on the temperature and reduction profiles. The terms H and H′ have the same significance as in Fig. 7.1. From Fig. 7.9, the inactive zone disappears at a reductant rate of about 575 kg/THM and thereafter the zones of indirect wustite reduction (H_3') and pre-reduction of hematite and magnetite to wustite (H_1') merge together. As long as the inactive zone exists the $\eta_{CO,FeO}$ should remain constant and the overall η_{CO} will slowly decrease because of higher gas volume for a constant removeable iron oxygen (cf. Fig. 3.8). Thereafter, with an increasing amount of the reductant, the η_{CO} for both the cases will fall steeply. These assumptions are confirmed by Fig. 7.10(b).[29]

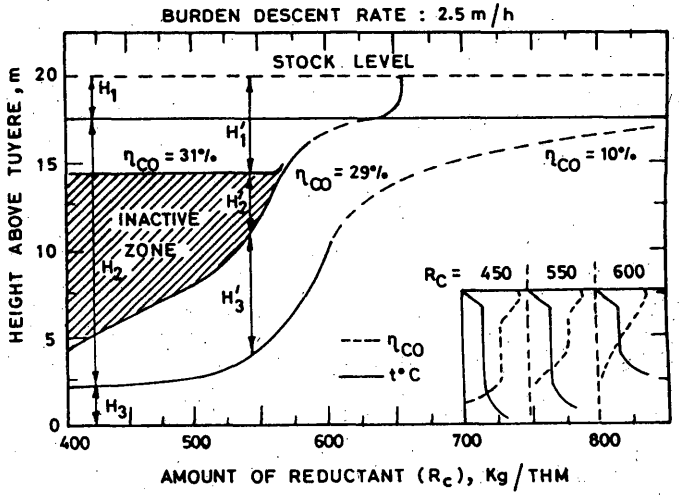


Fig. 7.9 The formation of temperature and gas utilization profiles along the furnace height and their dependence on the amount of reductants, according to Bülter and Klitzing.[29] (Copyright Verlag Stahleisen).

Fig. 7.10(a)[29] shows that indirect reduction increases with an increasing amount of the reductant as long as the inactive zone is present and falls after its disappearance. This is in accordance with Fig. 3.8 which shows that with an increasing amount of the reductant the indirect reduction should increase along the line *bc* in order that CO and CO_2 are at equilibrium with wustite. Only when the amount of reductant becomes large, the zone H_3' of Fig. 7.9 narrow and the wustite residence time short, will the indirect reduction start to decrease as is clear from Fig. 7.10(a). Obviously, the furnace will no longer be working at an optimum fuel rate. A very important conclusion which can be drawn from the above is that for an optimum coke rate, the thermal load of the burden should be decreased by pre-fluxing of sinter and pellets and for a given thermal load the blast temperature should be increased to a maximum possible extent. Both these steps lower the coke consumption rate and hence the amount of gas generated.

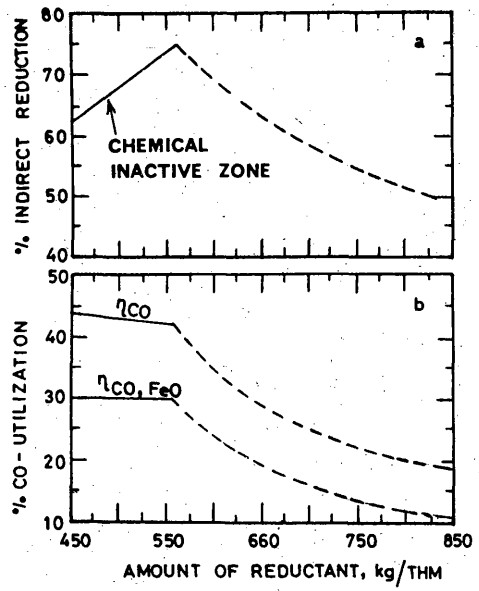


Fig. 7.10 The dependence of (a) indirect reduction and (b) gas utilization both overall and that for wustite, on the amount of reductant, according to Bülter and Klitzing.[29] (Copyright Verlag Stahleisen).

7.3.3.3. Gas-ore contact time

The above discussion points to the importance of the height of the indirect reduction zone or the transit time of wustite through the zone. This leads to item (c), i.e., gas/solid contact time. For the same burden and the same descent rate, the transit time of the ore would increase if the coke consumption rate per THM falls and *vice versa*. If the production rate (burden descent rate) and the height of the reduction zone are constant, the change in transit time can be estimated from the change in the coke rate and the burden/coke ratio by volume:[30]

$$\%\ \text{increase in transit time of ore} = \frac{\%\ \text{decrease in coke rate}}{\text{burden/coke ratio by volume}} \qquad 7.9$$

Suppose the total coke rate is brought down from 600 kg to 500 kg per THM by some means, the decrease amounting to 16.7 percent. Assuming a sinter burden with burden/coke ratio by volume of 0.72, the increase in transit time is 23 percent. Therefore, if the furnace has been operating with an inactive zone its presence is not likely to be affected if the production rate is increased by 23 percent, in case the transit time and not the resistance to gas flow is the limiting factor.

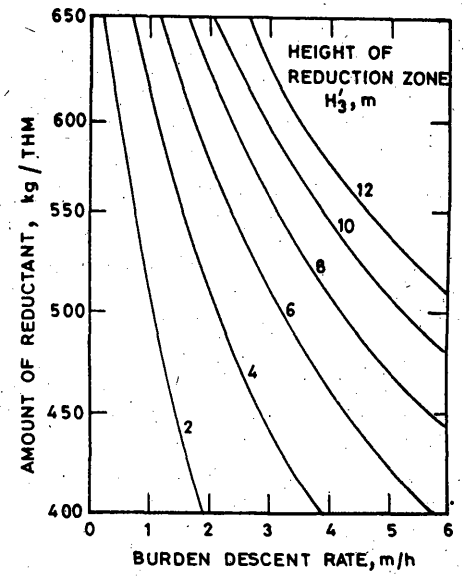


Fig. 7.11 The influence of stock descent rate and the amount of reductant on the height of the indirect reduction zone of wustite, H_3', according to Bülter and Klitzing.[29] (Copyright Verlag Stahleisen).

Bülter and Klitzing[29] have calculated the influence of burden descent rate and reductant rate on the height of the indirect reduction zone of wustite, H_3' (Fig. 7.11).[29] For any given height the inactive zone will be preserved with increasing burden descent rate if the reductant rate decreases correspondingly and *vice versa*. As for example, for an 8 m height of H_3', the corresponding figures are 550 kg/THM of reductant and 3 m/h burden descent rate. The same reduction profile will be maintained at a higher descent rate of 4 m/h if the reductant rate is brought down to 500 kg/THM. Fig. 7.11 should be read in conjunction with Fig. 7.9.

The influence of high top pressure on the height of the zones is not known. Probably, for a given reductant rate, the height of the reduction zone H_3' will be maintained even when the burden descent rate increases with increased production rate, if the linear velocity of the gas is kept constant by increasing the top pressure (Chapters 5 and 11). From the point of view of forcing the blast furnace, the inactive zone does not serve any useful purpose. Since, however, the existence of this zone denotes a minimum fuel rate, a furnace can be forced up to a point where the inactive zone just disappears, beyond which the fuel rate will start to increase.

7.3.3.4. Use of hydrogen-bearers

We have seen in Sec. 2.8 that the rate controlling steps in the reduction of iron ore are:[30]

(i) mass transfer through the pores of the particle by gaseous diffusion;
(ii) mass transfer through the solid product by diffusion.

Gaseous diffusion through pores depends upon the concentration gradient of the reductants and the products between the gas stream and inside of the particle, diffusion coefficients of the reductants and products and gas/solid contact time. Thus, porous diffusion will increase in the presence of hydrogen in the furnace gas because of higher diffusion coefficients of hydrogen and H_2O compared to those of CO and CO_2. This will be so also if the overall concentrations of CO and H_2 are higher, i.e., if the nitrogen content of the furnace gas is lower (use of steam, hydrogen-bearers and oxygenated blast).

If a major amount of wustite has already been reduced by gaseous diffusion, the rest is probably reduced by diffusion through solid reaction product, the rate being slow and dependent only on the gas/solid contact time. Therefore, in order to obtain an optimum indirect reduction, a high degree of efficiency of reduction according to item (i) above is desired.

As discussed at various places in the text, hydrogen is very effective in this regard.

7.3.4. Water-gas Shift Reaction

This subject has already been discussed in Secs. 3.11 and 7.2. The equilibrium H_2/H_2O ratio for FeO/Fe being lower than the corresponding CO/CO_2 ratio above 821°C, the regeneration of hydrogen by the water-gas reaction,

$$CO + H_2O = CO_2 + H_2$$

tantamounts to a catalytic effect of CO on iron oxide reduction. The role of hydrogen will be favourable according to the rapidity of attainment of the water-gas equilibrium. The fairly high temperature of 800–1000°C in the middle zone is favourable from the kinetic point of view, especially because of the presence of metallic iron which acts as a catalyst. In the blast furnace, the reaction is in equilibrium above 800°C.

According to Gol'dshtein and Khromchenko,[31] solid phases in the blast furnace, especially sinters of porous structure are good catalysts for the reaction above 800°C. The catalytic activity of sinter falls in the same order as its reducibility. The reaction proceeds faster than the decomposition of CO in the presence of sinter. The extent of conversion rises with decreasing H_2O concentration in the furnace gas. It has been confirmed by Bachinin et al.[32] that η_{CO} increases with η_{H_2}, η_{H_2} increases with increasing hydrogen content of the furnace gas and both η_{H_2} and η_{CO} increase with decreasing coke consumption.

According to Babarykin,[33] the water-gas reaction proceeds very feebly in the indirect reduction zone (below 1000°C). The satisfactory relationship of $(p_{CO_2} \cdot p_{H_2})/(p_{CO} \cdot p_{H_2O})$ with the equilibrium constant at 700–1000°C is not due to the approach of the water-gas reaction to equilibrium but it is due to the fact that the degree of approach to equilibrium for the reduction of iron oxide by CO and H_2 is the same.

The water-gas reaction becomes less important above 1000°C because any water formed from the reduction of iron ore is rapidly reduced by carbon,

$$C + H_2O = CO + H_2 \qquad 7.11$$

Reaction 7.11, under blast furnace conditions, proceeds much more slowly than the water-gas reaction.

It is very difficult to ascertain the extent of participation of hydrogen in the indirect reduction of ore. Various sources suggest an approximate 40 percent utilization.

7.3.5. Carburization of Iron

The temperature and oxygen potential of the gas in the middle zone are such that it is extremely unlikely that any CO will disintegrate to form carbon. On the other hand, carbon deposition will be facilitated since its activity is lowered in solution in iron. Even so, it is doubtful if iron is carburized in the middle zone to an extent exceeding 1 percent. Such absorption by the solid iron is possible (Sec. 3.7) according to:

$$2CO = CO_2 + C$$

$$3Fe + C = Fe_3C$$

$$\text{or} \quad 3FeO + 5CO = Fe_3C + 4CO_2 \qquad 7.12$$

The equilibrium carbon content of solid iron as a function of the CO/CO_2 ratio and temperature is shown in Fig. 3.9. The rate constant for carburization in the presence of hydrogen is 5 times higher than in CO alone at 900–1000°C. The presence of H_2O or H_2S in small amounts in the $CO + H_2$ atmosphere reduces the rate by a factor of 2 and 10 respectively.[34]

Most of the carbon is dissolved in the hearth where the coke column is submerged in a pool of hot liquid iron (Sec. 7.4.3).

7.4. Reactions in the Lower Zone

The temperature of the lower zone is above 900–1000°C. The zone extends from 3–5 m above the tuyere level to the hearth bottom. The temperature profile and its causes have been discussed in Sec. 4.2.1. The tuyere gas cools down from the flame temperature to 900°C if limestome is present or to 1000°C if it is absent. It takes 0.7–3 hours for the burden to descend from the belly to the tuyeres.[14] A variety of physical and chemical processes occurs in this zone, namely, calcination of limestone, direct reduction of iron from unreduced wustite and silicates, direct reduction of silicon, manganese, phosphorus, sulphur, alkali metals, lead, zinc, chromium and to a very small extent titanium, aluminium etc. The fusion of slag and metal, carburization of iron, burning of coke, oxidation of elements before the tuyeres etc. also occur in this zone. All these are narrated in the following sub-sections.

7.4.1. Calcination of Limestone

Limestone is used as a base for fluxing the acid components of the charge materials. The decomposition of the compound is endothermic:

$$CaCO_3 = CaO + CO_2 - 43350 \text{ cal} \qquad 7.13$$

From above, 1 kg $CaCO_3$ requires 430 kcal of heat for calcination and 1 kg CO_2 (2.3 kg $CaCO_3$) requires about 985 kcal. The partial pressure of CO_2 reaches 1 atm. at about 892°C. The evolution of CO_2 at this temperature is very rapid. The decomposition should occur at lower temperatures because the partial pressure of CO_2 in the shaft is usually in the range 0.15–0.25 atm. However, the evolution of CO_2 occurs in the range 900–1100°C because the limestone pieces, especially the larger ones, are heated up slowly.

Limestone lumps are initially dense and compact and as carbon dioxide is evolved the outer shell of CaO becomes porous with the core still undissociated and compact. According to Wuhrer and Radęmacher,[35] since the calcination reaction is endothermic and the relation between the time of calcination (t) and lump size (d) approximately obeys the parabolic law

$$t \propto d^2$$

the rate controlling step is the heat transfer to the reaction front across the porous CaO shell. This means that the time of calcination will increase four-fold with the doubling of the lump size. As for example, an increase of lump size from 20 mm to 40 mm will increase the time of calcination from 0.2 h to 0.8 h. Hence, for a rapid evolution of CO_2 a considerable superheating of the surface is required. In the blast furnace, the reaction may also be delayed because of coating of the lump surface with viscous semi-fluid slag.

The adverse effects of using raw limestone on fuel efficiency are three fold:

(i) increase in fuel requirement to meet the thermal deficit caused by the endothermic reaction (Sec. 10.4.2.4);
(ii) increased fuel requirement due to increase in direct reduction (Sec. 10.4.2.4); any CO_2 evolved from limestone above 1000°C takes part in the Boudouard reaction;
(iii) dilution of shaft gas with CO_2.

According to a rough estimate, for every 230 kg limestone charged the coke rate increases by 60–80 kg/THM. Calcination outside the furnace

(pre-fluxed sinters and pellets) leads to a considerable saving of coke (Sec. 10.4.2.4).

7.4.2. Reduction of Various Elements

Iron ores are not pure oxides of the metal nor is coke pure carbon. These and all other charge materials contain numerous impurities and most of them are reduced during ironmaking. They either dissolve in iron if soluble or escape out of the furnace with the flue gas or with the slag, or they are absorbed partly by the refractories.

The impurity compounds as well as wustite do not exist in the free state. During their descent they get intermixed and sintered together and later form a molten mass. Their reducibilities will depend upon their activities in the multicomponent liquid or solid mixture as well as on the temperature and reducing potential of the gas.

The negative free energies of formation of the oxides of Ni, Cu, Pb are small and they are reduced very easily. They (except Pb) dissolve in iron and may remain in the metal even during steelmaking as they are difficult to oxidize. Wustite is more difficult to reduce.

The reduction of phosphorus is a little more difficult than the reduction of wustite and occurs at a slightly higher temperature. Its reduction is more or less complete in the lower zone.

The reduction of manganese from its monoxide is much more difficult and occurs at a still higher temperature. Its extent of reduction varies between 50–75 percent depending upon the temperature and slag basicity. Chromium and vanadium behave in the same way as manganese.

The reduction of silicon and titanium require very high temperatures while the oxides of calcium, magnesium and aluminium are so stable that they are reduced to a very negligible extent.

The removal of sulphur and formation of slag are subjects by themselves and are treated in Chapters 9 and 8 respectively.

7.4.2.1. Reduction of unreduced iron

Most of the unreduced iron oxides descends into the lower zone as fayalite, calcium ferrites or intermixed in the primary slag. Ideally, they should all be reduced above the tuyere level before entering the hearth. Otherwise, their direct reduction in the hearth by the submerged coke column consumes an enormous amount of heat which disturbs the thermal state of the hearth and results in erratic metal temperature and composition.

We have seen in Sec. 6.7.1 that fayalite present in acid sinters or formed from the ore in the furnace does not get reduced as readily as limey sinters even at high temperatures. Probably because of this, the use of pre-fluxed burden results in a smoother furnace operation and steady metal qualities.

Direct reduction of iron oxide proceeds at temperatures above 1000°C according to:

$$\begin{aligned} FeO + CO &= Fe + CO_2 \\ C + CO_2 &= 2CO \end{aligned} \qquad 7.14$$

7.4.2.2. Reduction of silicon

Silicon in the form of silica and silicates invariably accompanies ores, agglomerates, flux and coke. From the free energy diagram, Fig. 2.4, it is possible for silicon to be reduced from silicate slags above 1300°C but as discussed in Sec. 3.15, the major pick-up of silicon by iron occurs above the tuyere zone *via* gaseous SiO and SiS. The final silicon content of pig iron depends upon any further reduction or oxidation of silicon undergone between the slag and iron in the oxidizing zone and in the hearth.

The equilibrium relations, the extent and the possible mechanisms of the silica reduction reaction have been discussed in Secs. 3.12 and 3.15. From thermodynamic considerations, the metal silicon will be the lower, the lower the activity of silica in the slag (i.e., the higher the slag basicity) and the lower the metal temperature. However, the actual silicon in the blast furnace iron is higher than that expected from the coupled reaction with manganese (Eq. 3.48) and lower than that expected from the reaction with C-saturated iron (Eq. 3.36 and Fig. 3.15).

Silicon has always been regarded as a barometer of pig iron quality and the thermal state of the hearth. The consistency of silicon analysis from tap to tap is of prime importance for the subsequent steelmaking processes. However, it is difficult in practice to control and, still more, to predict its amount in the final iron. For no apparent reasons it sometimes goes down or shoots up or varies from cast to cast and even from ladle to ladle. It is not even rare to find cold iron containing high silicon. The cause of this erratic behaviour has been attributed to combinations of such variables as: metal temperature; slag liquidus temperature; temperature, composition, basicity and viscosity of slag; blast and top gas temperature; ore/coke ratio; slag superheat (slag temperature above the liquidus); excess available heat (difference between the heat input and heat necessary in the lower furnace), etc. However, no significant correlations have been

detected amongst the variables except the general trend that silicon in iron increases with the increase in metal temperature, bosh slag acidity, slag superheat and excess lower furnace heat.

In order to understand the causes for the erratic behaviour, let us consider a few facts that have emerged from operational experience:

(i) an increase in blast temperature increases the temperature and silicon content of iron and they both take a long time, sometimes even up to 15–20 hours, to stabilize to the final values (Fig. 7.12).[36] However, the response to increase in silicon is much more and much quicker than the rise in metal temperature, the more so the lower the initial iron temperature when the blast temperature was raised;

(ii) the delay in response to any blast temperature increase for manganese (Fig. 7.12a) and for sulphur (not shown in the figure) is similar to that for the iron temperature;

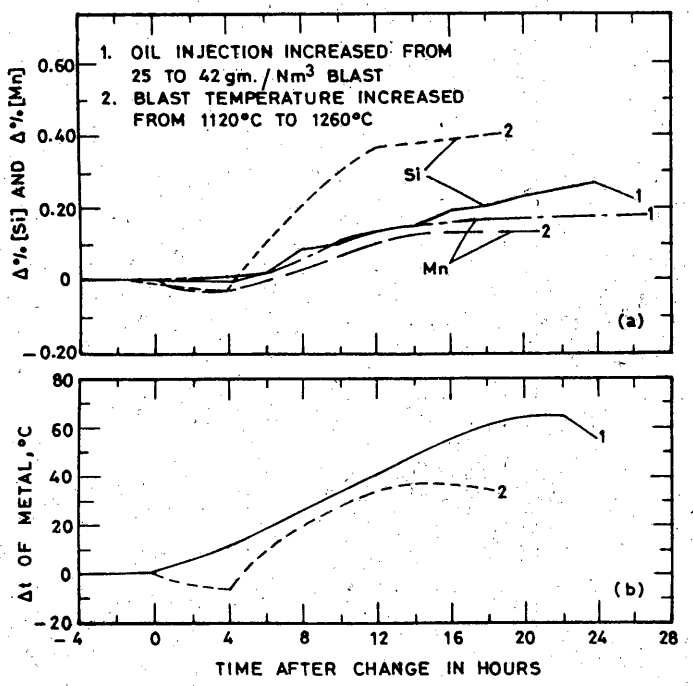


Fig. 7.12 The times for stabilization of the metal silicon, manganese and temperature on increase of the blast temperature and oil injection, according to Kootz.[36] (By permission, Indian Institute of Metals).

(iii) silicon content of iron is maximum above the tuyeres (Fig. 3.15);

(iv) the higher the bosh slag basicity, the lower the final silicon, in general; low-silicon iron is being consistently produced from iron-rich pre-fluxed burdens using up to 1250°C blast temperature, although high silicon iron is expected from the use of such high temperatures;

(v) the response to silicon and manganese reduction and iron temperature on blast temperature increases, with or without oil, are opposite (Fig. 7.12); with oil, there is a faster response to manganese reduction and iron temperature than is the case without oil.

It is obvious from above, how difficult it is to predict or even control the silicon content of pig iron. However, most of the erratic and inconsistent behaviour can be reasonably explained and, possibly, control measures taken on the basis that:

(a) silicon is predominantly reduced in the tuyere region by carbon[109] and/or ascends as gaseous SiO and SiS and is distributed between liquid iron and slag in the bosh according to the bosh slag basicity and prevailing temperature. That a low-silicon iron is produced with pre-fluxed burden even with high blast temperature is probably due to absorption of a smaller amount of silicon by iron in the presence of a highly basic slag. The iron, containing silicon in varying amounts depending upon the bosh slag basicity and tuyere (flame) temperature, descends to the hearth where silicon behaves as a poor reducing agent for slag oxides and fails to attain equilibrium with the slag components.[36]

In this respect, pre-fluxed burden is much superior to acid plus limestone burden since the dissolution of lime is a slow process and the bosh slag basicity is on the acid side compared to the pre-fluxed burden (Sec. 8.3). As a corollary, higher silicon irons will be expected as the slag volume increases, which is indeed what happens because the bosh slag basicity becomes lower (Fig. 8.2) and also because the blast furnace operators tend to work with lower slag basicity when the slag bulk is high in order to save coke.

(b) the response to any blast temperature increase for increasing the flame temperature and the consequent gasification of SiO and SiS and absorption of Si by iron are immediate but for iron temperature it is not so. The latter is dependent on the alteration of the thermal state of the hearth which is a slower process. We will see in Sec. 7.7 that considerable amounts of pig iron are re-oxidized while falling through the oxidizing zone in front of the tuyeres (the amount increasing with increasing blast temperature) and enter the hearth; in addition some unreduced iron oxides in the slag

descend into the hearth along the central coke column. Since all these iron oxides are re-reduced in the hearth endothermally, a considerable amount of sub-hearth heat is consumed in the process which affects the iron temperature. Hence, initially, a high silicon cold iron will be expected on raising the blast temperature. With the passage of time the iron will pick up temperature and more of MnO will be reduced by silicon resulting in a somewhat lower-Si, higher-Mn and lower-S metal (sulphur removal is closely associated with manganese reduction, Sec. 3.15).

(c) with blast additives like oil, natural gas or steam, the tuyere region is more reducing and more extended towards the centre than with the normal blast (Figs. 7.19 and 7.21). Hence, re-oxidation and re-reduction of the iron oxides are on a much smaller scale. In addition, the amount of iron oxides delivered to the hearth is also less since the overall reduction of iron oxides in the furnace above the tuyere level is much higher when injecting the hydrogen-bearers. All these result in a much quicker rise in the metal temperature on increasing the blast temperature (Fig. 7.12b), accelerating the reduction of MnO by silicon and hence aiding sulphur removal. However, an increased desiliconization of iron or a decreased Si-reduction due to decreased flame temperature does not necessarily mean that only low-Si iron can be made with such additives. The amount of silicon entering the hearth depends upon the amount reduced above the tuyeres and that re-oxidized in the oxidizing zone. In the case of additives, no doubt less silicon is reduced above the tuyeres but, on the other hand, less silicon is oxidized in this zone (Fig. 7.21). The final metal silicon depends upon the amount that enters the sub-hearth and that re-oxidized by the slag oxides.

7.4.2.2.1. Control measures

Models have been proposed[37-44] for computer control of silicon with changes in the various furnace parameters. For the reasons discussed above, these models have only had limited success. For obtaining low-silicon iron or for maintaining as consistent a metal analysis as possible, a few measures are suggested:

(1) use of pre-fluxed, preferably, super-fluxed agglomerates;
(2) avoid fluctuations of materials input; use of blended burden;
(3) use of mechanically strong agglomerates and coke to maintain uniformity of burden descent and gas throughflow;
(4) use of highly reducible materials (both at high and low temperatures) to maintain constancy of bosh temperatures; limey agglomerates possess better high temperature reducibility of residual wustite;
(5) maintain constancy of blast temperatures;
(6) use of hydrogen-bearing blast additives to maintain a reducing atmosphere in front of the tuyeres; they also extend the combustion zone, heat up the central zone and create more favourable thermal state of the hearth;
(7) use of blast additives rather than blast temperature for controlling the hearth temperature;
(8) use of high basicity and low viscosity bosh and hearth slags;
(9) operation above but as near to slag liquidus temperature as possible;
(10) use of magnesia for lowering the slag viscosity and liquidus temperature; very effective for 10–25 percent alumina slags;
(11) with normal blast, to lower or to increase metal silicon, the blast temperature should be decreased or increased slowly in stages, especially for large furnaces; in such furnaces, the heating up and cooling down of the hearth take place rather slowly;
(12) for making high silicon foundry iron, the slag liquidus temperature should be high and basicity low; high silicon iron can also be made with blast additives because the thermal state of the hearth can be maintained at high degree (decreased oxidation of iron in the oxidizing zone); the adverse effect of lowered flame temperature is amply compensated for by the high silica activity of the bosh slag and less re-oxidation of silicon in the oxidizing zone;
(13) a high peripheral descent results in inadequate preparation of the materials before reaching the hearth; it results in cooling down of the hearth, lower metal temperature and erratic metal analysis; this state can be corrected by changing the charging sequence, dumping more ore at the periphery and decreasing the tuyere diameter.

In addition or in combination with all these, in every plant the operators have acquired their own art of manipulating the silicon content of the blast furnace iron. They call it their *sixth sense*!

7.4.2.3. Reduction of manganese

Manganese oxides are present in or are deliberately added to the blast furnace charge materials. Manganese is also present as oxide, silicate, phosphate in the open hearth and converter slags, when charged. In its ore,

it is mainly present as dioxide, MnO_2. It is very unstable and forms Mn_3O_4 immediately as it is charged. Mn_3O_4 is reduced in the shaft by the reaction,

$$Mn_3O_4 + CO = 3MnO + CO_2 \qquad 7.15$$
$$\Delta H^\circ\ (1200^\circ K) = -13.25\ \text{kcal}$$
$$= -4420\ \text{cal/gm.atom Mn}$$

The equilibrium CO/CO_2 ratio between 700–900°C is 0.001–0.002 which is very much lower than that exists in the shaft. Therefore, Mn_3O_4 is completely reduced to MnO in the upper or middle zones before reaching the lower zone. The heat evolved from the reaction is 4400 cal/gm.atom Mn at 900°C compared to only 700 cal/gm.atom Fe during the reduction of Fe_2O_3 to FeO. Hence, if Mn_3O_4 is present in large amounts as it does in the ferro-manganese blast furnace, the temperature in the shaft may exceed 1000°C and the Boudouard reaction will occur up to a considerable height of the furnace. This is one of the reasons of very high coke consumption in the manufacture of the alloy. It is likely that the coke consumption due to the Boudouard reaction can be reduced considerably if the manganese ore is pre-reduced to MnO by the furnace exit gas before charging.

Reduction of MnO is difficult since even at 1200°C the equilibrium $CO/CO_2 = 10^4$. No such effective concentration gradient exists in the shaft or the bosh. Hence, MnO is reduced directly by carbon (*via* Boudouard reaction). The free energy of formation of MnO is more negative than that of wustite but more positive than that of silica and, therefore, its reduction temperature lies intermediate between them (Figs. 2.3 and 2.4).

The equilibrium relations, extent and possible mechanisms of manganese reduction reaction have been discussed in Secs. 3.13, 3.15 and 7.4.2.2. In contrast to the formation of gaseous SiO, SiS and other sulphurous compounds, manganese does not form any gaseous species. Some of it is reduced in the bosh or belly when the liquid manganous slag flows over the incandescent coke. Some further reduction from the slag by silicon occurs in the hearth. The manganese content of the final pig iron is below that expected from equilibrium with C-saturated iron or from the coupled reaction with silicon. From Eqs. 3.37–3.39 and 3.48–3.49, manganese reduction is facilitated by:

(i) lowering of the manganese activity through dissolution in iron;
(ii) increasing of the activity coefficient of MnO by using more basic slags; since MnO is basic in character, its activity coefficient in the slag is increased by lime and decreased by silica;

(iii) hotter slag and metal;
(iv) increasing metal silicon.

In the blast furnace, maximum manganese recovery is desired not only because it is costly but also because of its beneficial effect in the subsequent steelmaking processes. Although from the equilibrium relation (Fig. 3.13) a manganese recovery of about 85–90 percent is expected, the actual recovery ranges between 60–70 percent in the basic-steel iron, 50–60 percent in acid burdening, 85–90 percent in ferro-manganese and about 75 percent in the foundry practice.

In order to obtain a large reduction of both manganese and silicon, very high temperatures as in the electric furnace is necessary. The high exothermic heat of dissolution of silicon in iron aids the process.

During the descent of the burden some MnO always combines with silica to form less reducible manganese silicate. We will see in Chapter 8 that the formation of the silicate is not harmful but rather beneficial in the smooth running of the furnace.

7.4.2.4. Reduction of phosphorus

A major portion of phosphorus in the blast furnace comes from the coke and a little from the flux, iron ore and manganese ore. It is present as tri- or tetra-phosphate of calcium. Silica helps in breaking of the phosphate bond and promotes the reduction indirectly:

$$3CaO.P_2O_5 + 3SiO_2 = 3(CaO.SiO_2) + P_2O_5 \qquad 7.16$$

$$P_2O_5 + 5C = 2P + 5CO \qquad 7.17$$

In this case the reduction can occur either *via* the Boudouard reaction as in the case of SiO_2 and MnO or since P_2O_5 is gaseous it can directly come into contact with hot coke (Fig. 2.3). The reduction is nearly complete and no physical or chemical condition can alter it. More than 90 percent of the phosphorus load enters the iron and the rest is lost either in the slag or in the flue gas or is absorbed in the refractory linings.

7.4.2.5. Reduction of zinc

Zinc in small quantities is found in many ores mainly as difficultly reducible ferrites – $(Zn,Fe)O.Fe_2O_3$ or $ZnO.Fe_2O_3$; silicate, $2ZnO.SiO_2$; sulphides, (Zn,Fe)S or ZnS. The sulphides are probably transformed to complex oxides in the shaft. The silicate is more difficult to reduce than the ferrites. They are all reduced to metallic zinc vapour by CO in the

lower zone where the temperature is above 1000°C. The reduction of ZnO by CO is given by:

$$ZnO + CO = Zn(g) + CO_2 - 43130\,cal \qquad 7.18$$

$$\Delta G^\circ = 47870 + 10.35T \log T - 61.63T\,cal \qquad 7.19$$

$$K = \frac{p_{Zn} \cdot p_{CO_2}}{a_{ZnO} \cdot p_{CO}}$$

The equilibrium constant values are very small, especially below 1000°C:

t°C	600	800	1000	1200
K	0.00001	0.00014	0.03	0.2

The extent of reduction depends upon the activity coefficient of ZnO in the complex compounds. At the high temperatures where reduction occurs, zinc (b.p. 907°C) is obtained as a vapour which ascends along with the gas and is reoxidized in the cooler zone (reverse of Eq. 7.18), below 900°C. A part of the finely divided oxide thus formed escapes with the flue dust or forms scabs in the throat and offtakes,[46] whilst some remain in the shaft causing undesirable scaffolds which disturb stock descent (Chapter 13). The temperature of the start of condensation of zinc vapour is 520–580°C. Some zinc vapour may seep through the brick joints in the lining and condense around the cooling plates as metal. It does not pass through into the iron. The rest of the reoxidized zinc descends to the high temperature zone and gets reduced. Thus, a zinc cycle similar to the alkali cycle forms in the furnace.

7.4.2.6. Reduction of lead

Many ores contain some lead, usually along with zinc. It is completely reduced in the upper zone, the negative free energy of formation of its oxide being small.

$$PbO + CO = Pb + CO_2 + 15700\,cal \qquad 7.20$$

$$\Delta G^\circ = -14250 - 4.95\,T\,cal \qquad 7.21$$

At 300°C and 1250°C, the equilibrium p_{CO}/p_{CO_2} ratios are 0.001 and 0.06 respectively.

Since lead is not soluble in iron, it flows down and accumulates in the hearth bottom where it can seep through the refractory linings and destroy them. Although its vapour pressure is small, some of the metallic lead

can vaporize and attack the shaft lining or condense around the cooling plates.

7.4.2.7. Chromium[45,47]

It occurs in various ores as chromite ($FeO.Cr_2O_3$). In the highly reducing atmosphere in the hearth, chromium is presumably present as chromous oxide, CrO. The free-energy of formation of CrO was hitherto unknown but has been recently estimated to be:[48]

$$2Cr(s) + O_2(g) = 2CrO(s): \Delta G^\circ = -148800 + 33.4\,T\,cal \qquad 7.22$$

At 1400°C, the ΔG° value is −93 kcal as compared to Fe/FeO = −75 kcal and Mn/MnO = −125 kcal. Hence, it would be expected that CrO will be much more reducible than MnO in the hearth. In fact, while Mn recovery in the blast furnace ranges between 60–75 percent, the recovery of chromium is about 90 percent.

Since the recovery of chromium depends upon the activity of CrO which is amphoteric in nature, its recovery should decrease with increasing basicity of the slag. However, from Fig. 7.13,[49] the chromium recovery increases with increasing slag basicity. This is probably because, as in manganese equilibrium, silicon enters into coupled reactions as well as because the silica activity in the slag falls more rapidly than the activity of CrO with increase in basicity.

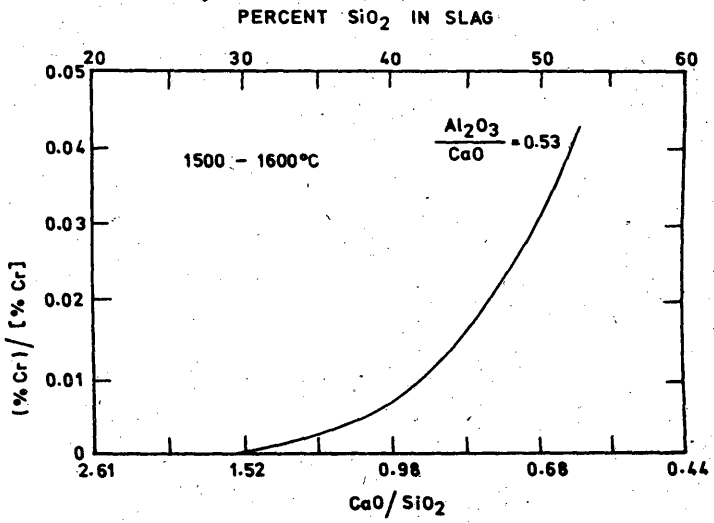


Fig. 7.13 The relationship between chromium distribution in carbon-saturated iron and slag basicity, according to McCoy and Philbrook.[49]

7.4.2.8. Titanium

It is usually present in the blast furnace raw materials as ilmenite ($FeO.TiO_2$) and rarely as rutile (TiO_2). Titanium dioxide is more stable than silica and is therefore reduced by much lesser extent at the prevailing hearth temperatures. Most of the oxide remains in the slag which increases its viscosity and may cause blocking of the slag notch. More serious trouble can arise because of the formation of titanium nitrides, carbides and carbo-nitrides in the hearth. Their solubilities in iron are very small, being 0.3% for carbides and 0.2% for carbo-nitrides[50] and they separate out to form incrustation on the bosh incline or on the hearth walls and hearth bottom. Their melting points are 3150°C and 2950°C respectively. Titania (TiO_2) is reduced in the hearth either by carbon or by silicon or by both.

$$TiO_2(s) + 2C(s) = Ti(l) + 2CO(g) \qquad 7.23$$
$$\Delta G^\circ = 165000 - 83.68\,T \text{ cal}$$

For carbon-saturated iron ($a_C = 1$) the equilibrium constant is:[45]

$$\log K = \log \frac{a_{Ti}.p_{CO}^2}{a_{TiO_2}} = \frac{-36000}{T} + 18.29 \qquad 7.24$$

At 1400°C, K = 0.0005.

It is most likely that the reduction of titania is intimately connected with the reduction of silica as is the case with MnO, similar to the relationship between Si and Mn described in Secs. 3.15 and 7.4.2.2. This is because in both the laboratory as well as in the plant, it has been found that the titanium content of iron increases with increasing silicon content of the iron and increasing basicity of the slag.[50–52] The relevant equation is:

$$(TiO_2) + Si = Ti + (SiO_2) \qquad 7.25$$

$$K = \frac{a_{Ti}.a_{(SiO_2)}}{a_{(TiO_2)}.a_{Si}} \qquad 7.26$$

or

$$\frac{a_{Ti}}{a_{(TiO_2)}} = K.\frac{a_{Si}}{a_{(SiO_2)}} \qquad 7.27$$

From the above equation, the higher the temperature (K increases with temperature) and the higher the basicity the greater will be the titanium reduction. The subject has been summarised recently by Hess et al.[52] and the results are shown in Fig. 7.14. It shows the laboratory[50] as well as actual plant data.[52]

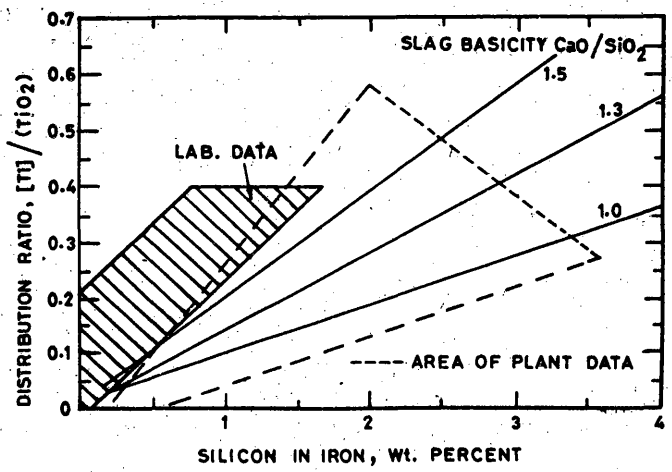


Fig. 7.14 The dependence of titanium distribution between slag and iron on the silicon content of iron. Laboratory[50] as well as plant data.[52]

The extent of titanium reduction from the slag depends upon the rate of its reduction by silicon in iron. As we have seen earlier, silicon enters the iron above the hearth slag level *via* gaseous SiO and SiS. Titanium does not form any such gaseous specious. Therefore, the reduction of titanium from the slag occurs during the passage of silicon-bearing iron droplets through the slag layer. However, since Si in iron is a poor reducing agent in the hearth, the titania reduction is restricted. Hence, the apparent linear relation between the titanium and silicon contents of the metal.

7.4.2.9. Aluminium

It has always been thought that alumina is not reduced in the blast furnace but the work of Sasaki and Nakazawa[53] and that of Stroup[54] suggest such a possibility. From free energy calculations, the possibility of formation of Al and Al_2O vapour exists in the tuyere region around 2000°C, the reactions being

$$Al_2O_3 + 3C = 2Al + 3CO \qquad 7.28$$

$$Al_2O_3 + 2C = Al_2O + 2CO \qquad 7.29$$

Such reactions are not possible with the alumina of the hearth slag since both the activity of alumina and the temperature are low. However, alumina activity is high in the coke ash which is released in the tuyere zone and since the flame temperature is also high and above 2000°C it

is possible that some alumina is reduced to vapours of Al_2O and Al in the same way as SiO_2 is reduced to gaseous SiO. As their vapours rise and the temperature falls, they are reoxidised by CO and CO_2 in the ascending stream. An increase in the ratio of Al_2O_3 and CaO in the sinter-originating granules at the belly level suggests the deposition of oxidized vapours of Al and Al_2O.

7.4.2.10. Calcium and magnesium

Direct evidence of generation of magnesium vapour in the tuyere region was obtained by Jon et al.[55] However, Sasaki and Nakazawa[56] have found indirect evidence of vaporization or dissociation of MgO and CaO from the presence of such unique components as bredigite ($2CaO.SiO_2$), periclase (MgO) and potassium-magnesium-aluminium silicate ($K_2O.MgO.SiO_2$-$K_2O.Al_2O_3.SiO_2$,S.S.) in the blast furnace scaffold.

7.4.2.11. Alkali metals

This subject has been discussed in Chapter 13 and Sec. 3.21.

7.4.3. Carburization of Iron

In the blast furnace a large amount of the ore is reduced in the shaft and the iron formed melts in the fusion zone above the tuyere. The iron in the solid or spongy state can absorb some carbon but seldom greater than 1 percent (Sec. 7.3.5). Since carbon lowers the melting point of iron, it is possible for iron in the belly region to absorb more carbon and iron samples from this region have often been found to contain carbon as high as 2.5–3 percent. Analysis of iron samples from the bosh right down to the hearth shows a continuous increase in the carbon content as the liquid metal flows over the hot coke. The final absorption to the tapping values occurs in the hearth itself where the metal is in intimate contact with the submerged coke column, the dissolution being quicker the smaller the coke size.

From the Fe-C phase diagram (Fig. 3.1) the eutectic at 1147°C contains 4.3% C and the carbon content increases by about 0.3 percent for every 100°C rise in temperature. At 1500°C, the solubility is about 5.2% C. But at the tapping temperatures, usually 1350–1450°C, the carbon content of the various grades of iron varies from 2.5 to 4.5 percent. This is because of the influences of the impurity elements on the solubility of carbon in iron as well as the fact that carbon never reaches saturation in pig iron.

Silicon lowers the solubility of carbon at an approximate average rate of 0.3% C for every 1 percent rise in silicon in iron.[57] However, since high silicon in iron is obtained by increasing the hearth temperature and the solubility of carbon increases simultaneously, the nett effect is very little variation in the carbon content. The carbon, however, separates out as graphite when the metal cools down in the launder or ladle, the combined carbon decreasing thereby. On the other hand, as a low-silicon iron is produced at lower temperatures, the carbon content will neither rise nor fall and be around 3.5 percent.

Phosphorus also lowers[57] the solubility of carbon at a rate of about 0.3% C for every 1 percent rise in P. Since high phosphorus basic bessemer iron is produced at lower temperatures, the carbon content in such irons varies considerably from the saturation values.

Manganese increases carbon solubility by about 0.1% C per 1 percent rise in Mn. Carbide forming elements like chromium, titanium increase the carbon content greatly (as much as 10 percent in ferro-chromium).

The average analysis of four grades of iron are given below in percent:

	%C	%Si	%Mn	%P	%S
Foundry	3.5–4	0.5–4.2	0.5–1.3	0.8–1.6	0.04
Hematite		2–2.5	1–1.3	0.1	0.04
Basic bessemer	3–3.5	0.4–0.8	1–2.5	1.7–2.2	0.1 max
Normal basic	3–3.5	1 max	1–2.5	0.1–1.2	0.07 max

7.5. The Combustion Zone

Coke is the only material of the blast furnace charge which descends to the tuyere level in the solid state. As mentioned in Sec. 5.1, it burns with air in front of the tuyeres in a 1–2 m deep raceway around the hearth periphery. Beyond the raceway there is a closely packed bed of coke, the central coke column or dead man's zone. The continuous consumption of coke and the consequent creation of an empty space permits the downward flow of the charge materials. The presence of the coke column effectively reduces the hearth area for the flow of materials. Hence, the size and shape, i.e., the depth of the raceway as well as its width between the neighbouring tuyeres, which determine the raceway area, are of great importance for a smooth and rapid burden descent, furnace productivity as well as the thermal state of the hearth.

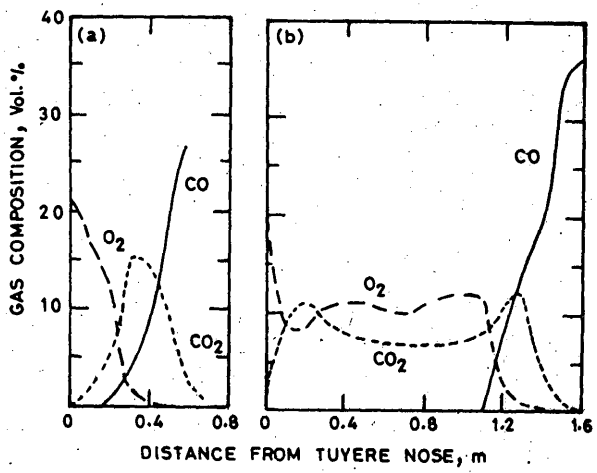


Fig. 7.15[58] Variations of gas composition along the tuyere axis with dry blast – **(a)** low blast volume; **(b)** high blast volume.

The oxygen of the blast reacts with coke to form initially CO_2 which, being unstable at the prevailing high temperatures of around 1800–2000°C, is endothermally reduced by carbon to CO. However, the blast oxygen does not disappear completely nor does the CO_2 content of the combustion gases reach a maximum in the immediate vicinity of the tuyeres. Their concentrations along the tuyere axis depend upon the kinetic energy of the blast. The variations[58,59] in the contents of oxygen, CO_2 and CO of the combustion gas along the tuyere axis are shown in Fig. 7.15(a)[59] for the case of a low and in Fig. 7.15(b)[59] for a high kinetic energy of the blast. These gas composition patterns have recently been broadly substantiated by investigations carried out[70] on a large scale in an experimental furnace composed only of the lower part of a commercial furnace. Numerous other investigations[59-69] also have been carried out by high speed photography and introduction of tubes in the combustion zone for taking gas samples as well as measuring the distance of the coke column from the tuyere nose. A broad picture of the combustion zone has emerged from these investigations which resembles the vertical section of the zone drawn schematically in Fig. 7.16.[70] The salient features are summarized below:

(a) the force of the blast forms a cavity the roof of which is formed of loosely packed or suspended coke lumps and the wall more closely packed. The CO_2 concentration tends to increase gradually from the

centre and reaches a maximum value just before the raceway boundary where most of the combustion of coke occurs according to:

$$C + O_2(air) = CO_2 + 94450\ cal \qquad 7.30$$

The entire region delineated by the CO_2-peak is known as *oxidizing zone*. This is named so because any metallic or slag iron including metalloids falling in this zone is re-oxidized in varying degrees;

(b) the temperature of the gas rises as the coke consumption proceeds and reaches a maximum just before the raceway boundary. Thereafter, it falls sharply as the endothermal reduction of CO_2 by C proceeds;

(c) due to above-mentioned reaction,

$$CO_2 + C = 2CO - 41000\ cal \qquad 7.31$$

the concentration of CO_2 falls rapidly from the raceway boundary and the gasification is completed within 200–400 mm from the starting point of the reaction.

In this short zone, no re-oxidation of the metal can occur. Rather, considerable reduction of the slag and metal oxides takes place. Hence, it is called *reducing zone*.

From the point of view of carbon, it is oxidized both in the oxidizing as well as in the reducing zones and hence Ostroukhov[59] has named them as 'oxygen' and 'carbon-dioxide' zones. The author prefers the use of the former two names for their distinguishing characteristics.

Carbon dioxide concentration is used as one of the indices to show the aspects of fuel combustion. Usually, 1–2% CO_2-concentration surface is regarded as the limit of the combustion zone;

(d) the raceway depth or blast penetration increases with increasing blast velocity. The raceway becomes smaller with smaller blast velocities but the broad pattern of coke combustion and CO_2-reduction remains;

(e) although coke and molten materials fall in the cavity from above, they are not seen immediately in front of the tuyeres in an active raceway. Presumably, they are diverted by the force of the blast. The liquids probably flow into the hearth along and through the voids of the central coke column or along the hearth wall or through the inter-tuyere space.

The coke pieces in the cavity are in constant spherical motion.[68,70] They are seen to move with tremendous speed in trajectories along the wall

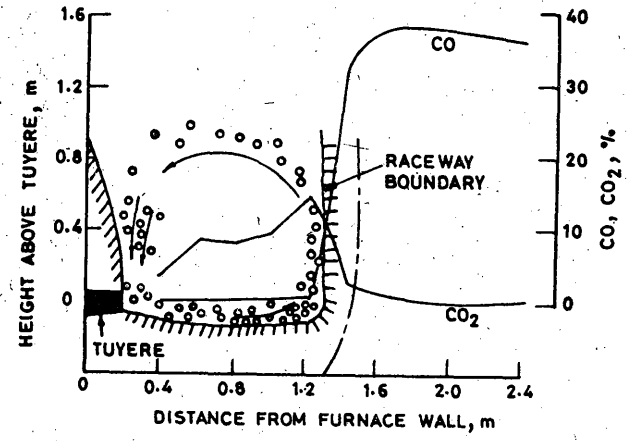


Fig. 7.16 A vertical cross-section of the combustion zone in an experimental truncated blast furnace, after Hatano et al.[70] (By kind permission).

of the cavity in an anti-clockwise fashion as shown in Fig. 7.16.[70] This is so because in commercial furnaces the tuyeres are inclined downwards by 8–10 degrees. The blast jet, projected downwards, finding no outlet rises with a circulatory motion and hence the said trajectory.

The gas analyses in Fig. 7.15(b) do not provide a true picture of the combustion process. Due to intensive circulatory motion there is widespread intermixing of the blast and combustion gases which stabilizes the analytical oxygen and CO_2-contents in the tuyere zone for a considerable distance.

Measurements[70] of burden descent rate show that the rate is much more above the raceway than at the middle or the centre of the furnace. This shows that an extended raceway is of vital importance for modern high capacity furnaces. According to Loginov et al.,[71] the rate of stock descent in the oxidizing zone is 1.5 times the average of the whole furnace. The rate at the throat is 2–2.5 times that in the lower stack and belly.

The material descent by gravity against the buoyancy and frictional forces is regulated by the size and shape of the raceway. The larger this zone the greater will be the charge movement and the more uniform the gas distribution in the entire cross-section of the furnace, with its attendant beneficial effects on heat and mass transfer, coke rate and smelting rate. If the combustion zone is confined only to a narrow region of the hearth

periphery, it will lead to a rapid peripheral descent with its attendant cold hearth and frequent burning of tuyeres. A uniform furnace operation, especially for larger furnaces, needs adequate development of both peripheral and central flow. The latter does not only ensure a uniform production of both slag and iron but also tends to increase and stabilize the hearth temperature. Also, since a major portion of the hearth cooling losses occurs at the tuyere level, a deeper penetration of the point of highest CO_2, i.e., the point of highest temperature, will mean lower hearth heat losses and savings in coke.

According to Tleugabulov et al.,[72] the effective vertical pressure of the charge column is not the factor that governs the increase in the blast furnace driving rate. The formation of ellipsoids of loose packing above the combustion zone decreases the lateral pressure of the charge in the lower furnace but increases it in the upper. Therefore, there is a sharp decrease in the effective vertical pressure of the stock column which approaches close to zero above the combustion zone. The movement of the stock into the raceway depends only on the periodic collapses of local arches formed above the combustion zone. This adds weight to the observation of periodic pulsations of the blast pressure in blast furnaces.

The size and shape of the raceway which are so important for the blast furnace operation are affected by various factors. They are:

(a) blast parameter (volume, velocity, pressure and temperature);
(b) diameter, length and shape of tuyeres;
(c) inter-tuyere space, i.e., number of tuyeres around the hearth periphery;
(d) nature of stock movement;
(e) coke size;
(f) blast modifications.

It must be remembered, as rightly pointed out by Ostroukhov,[59] that to obtain definite dimensions and configurations of the combustion zone is not an end in itself. The primary purpose is to provide adequate penetration of the hot gases to the axial part of the furnace in order to maintain at the centre of the hearth a temperature at which the slag is in a fluid state, to achieve regular peripheral and axial descent of the burden and to obtain as much of raceway area as possible. A judicious use of the following factors affecting the combustion zone will help to achieve the above objectives and result in high driving rates and fuel economy when smelting a given burden material.

7.6. Factors Affecting the Combustion Zone

7.6.1. Blast Parameter

The expansion of the combustion zone, especially the length of the oxidizing zone, depends upon the kinetic energy of the blast. As mentioned earlier, the combustion zone is delineated by 1–2% CO_2 surface. The kinetic energy of the blast is given approximately by:[59]

$$E = 1.6 \times 10^{-8} \frac{V^3}{n^3 A^2} \cdot \frac{T^2}{p^2} \qquad 7.32$$

where,

E = kinetic energy of the blast (kg force per second), kg.m/s
V = blast volume, Nm^3/s
n = number of blast tuyeres
A = free cross-sectional area of each tuyere, m^2
T = temperature, °K
p = blast pressure, ata, atm. absolute

From Eq. 7.32, the kinetic energy and hence the length of the combustion zone increases in proportion to the cube of blast volume. That the combustion zone in fact increases with the kinetic energy has been shown qualitatively by Möller[69] and is evident from Fig. 7.15(a) and (b). The existence of a clear relationship between the blast volume and dimensions of the combustion zone has also been shown experimentally.[73,74]

Modern blast furnaces operate at high driving rates and the kinetic energy ranges between 3000–8000 kg.m/s. The horizontal distance of the combustion zone is given by:

(a)[75] $D = 0.118\ 10^{-3}\ E + 0.77$ 7.33

(b)[76] $D = 0.120\ 10^{-3}\ E + 0.65$ 7.34

where,

D = depth of blast penetration, m
E = kinetic energy of the blast (kg force per second), kg.m/s

Eq. 7.32 does not cater for changes in the kinetic energy of gases in the combustion zone which can occur due to changes in the temperature and volume of the bosh gas, especially when fuel additives are used, as well as in the particle size of coke.

Similar to Wagstaff and Holman's equation,[62] dimensionless terms have been effectively used by Hatano et al.[70] assuming that the raceway depth is directly proportional to the momentum of the gas and inversely so to the gravitational acceleration of the charge materials. The terms are:

$$\text{Raceway factor (RF)} = \frac{\rho_{go} \cdot V_g^2}{g \cdot A^2} \cdot \frac{T_g}{T_o} \cdot \frac{P_o}{P} \cdot \frac{1}{d_k \cdot \rho_k} \qquad 7.35$$

$$\text{Penetration factor (PF)} = D/d_t \qquad 7.36$$

where,

V_g = volume of bosh gas, Nm^3/s
T_g = gas temperature in front of the tuyere, °K
T_o = standard temperature, °K
d_k = diameter of coke particle in the raceway, m
P_o = standard atmospheric pressure, kg/cm^2
P = atmospheric pressure, kg/cm^2
ρ_{go} = gas density under standard conditions, kg/m^3
ρ_k = coke density in the raceway, kg/m^3
A = free cross-sectional area of the tuyere, m^2
g = gravitational acceleration, m/s^2
D = raceway depth, m
d_t = tuyere diameter, m

Applying the Eqs. 7.35 and 7.36 in hot model experiments, Hatano et al.[70] obtained satisfactory correlations which are applicable to commercial blast furnaces provided the particle size and density of coke in the raceway are known and changes in the composition, volume and temperature of the gas in front of the tuyere are taken into account. The suggested equation for penetration depth is given by:[70]

$$D \text{ in (m)} = 1.37 \times 10^{-2} \cdot d_t \cdot (RF) + 1.55 d_t \qquad 7.37$$

From Eq. 7.37, the raceway depths of commercial furnaces range between 1.0 to 1.7 m. From Eq. 7.34, this range of depth is obtained with the kinetic energy of the blast between 3000–9000 kg.m/s. The depth is larger the larger the furnace. However, a small furnace sometimes can have a large raceway.

An increase of the combustion area between neighbouring tuyeres is also possible with increased kinetic energy of the blast.[69,73] Systematic experiments were carried out[69] in a blast furnace of 6.5 m hearth diameter and 210 mm tuyere diameter. The blast volumes were increased from 38000

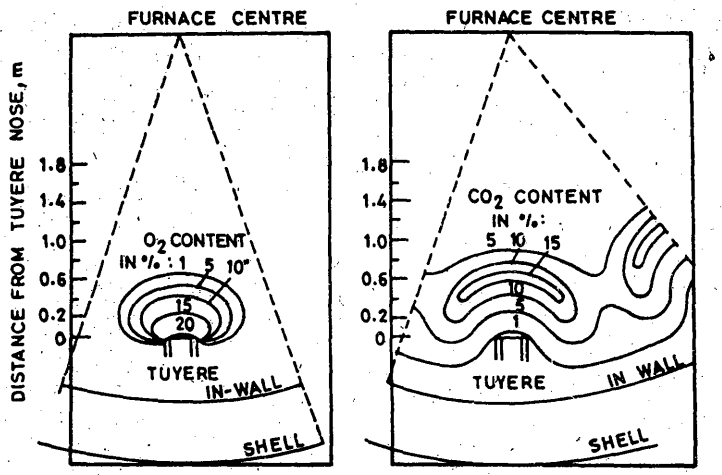


Fig. 7.17 Curves of equal oxygen and carbon dioxide contents at the tuyere level of a blast furnace, according to Möller.[69] (Copyright Verlag Stahleisen).

to 62000 and 85000 Nm^3/h at pressures of 0.34, 0.68 and 0.92 kg/cm^2 respectively. It was found that the distances of 1% CO_2, 1% O_2 and 30% CO surfaces from the tuyere nose as well as the horizontal surface areas bounded by them increased with increasing blast volumes. The shapes of the zones only for 62000 Nm^3/h blast are shown in Fig. 7.17.[69]

A high flow rate of the blast decreases the vertical height of the cavity above the tuyere axis but increases the vertical depth below, giving a more symmetrical zone;[77] (presumably because of downward inclination of the tuyeres).

From Eq. 7.32, the kinetic energy varies inversely as the square of the absolute blast pressure. Whether the raceway will shorten or expand depends upon the conditions under which the blast pressure is increased. If the blast pressure increases due to high top pressure or resistance to flow of gases for other reasons, it will result in the shortening of the raceway.[59,78] The result will be the opposite if the pressure drop between the tuyere and the raceway is high and the blast pressure artificially increased to supply the air by fitting special types of nozzles into the tuyeres. In such cases the kinetic energy actually increases due to transformation of the potential energy into kinetic energy. As a result the length of the raceway increases.

The oxidizing zone is generally shorter when the kinetic energy of the blast is low.[79]

An increase in blast temperature can affect the combustion zone both physically as well as chemically. The kinetic energy varies as square of the absolute temperature; as such an increase in the blast temperature should lengthen the zone and, in fact, it does so for the case of modern furnaces with high blast temperatures and high values of the kinetic energy. On the other hand, a high temperature affects the rate of the two chemical reactions, oxidation of carbon and reduction of CO_2, tending to shorten the zone.

Koval[80] has found a shortening of the combustion zone on increasing the blast temperature from 20°C to 320°C in a small furnace. In this case, because of high heat losses and low blast temperature, the gas temperatures must have been low and both the above two reactions probably were in the chemical reaction control region. Hence, the reaction rates increased greatly with temperature and shortened both the oxidizing as well as the reducing zones. The depth of the raceway may, however, increase due to the increase in the kinetic energy of the gases when using high blast temperatures.

Under raceway conditions and high flame temperatures in large furnaces, the combustion of carbon is in the diffusion range and the endothermal carbon gasification probably in the mixed control region. In the former case, the rate is not expected to increase greatly with the increase in blast temperature but in the latter the rate might increase by a greater extent. However, any shortening of the zones caused by increased blast temperature is more than compensated by the lengthening effect of increased kinetic energy. Thus, overall, the combustion zone expands or at least does not shorten with an increase in the blast temperature.[59,81,82]

7.6.2. Tuyere Dimension

From Eq. 7.32, a decrease in the tuyere diameter would increase the kinetic energy and hence the inward penetration of the gases. The depth of penetration is often manipulated by increasing or decreasing the tuyere diameter for obtaining peripheral or central flow respectively. Often, an increase in the tuyere diameter helps to expand the combustion zone vertically upwards.

A deep gas penetration not only heats up the axis and maintains the thermal state of the hearth but it also helps to loosen the central coke column when the gas permeability in this zone is lowered by an excessive accumulation of ores or coke fines. A deep penetration is obtained by lowering the tuyere diameter or, alternatively, by increasing the tuyere

length. Normally the tuyere nose should protrude (tuyere *overhang*) by at least 20–25 cm inside the hearth in order to minimize burning of the bosh lining. It can be increased to as much as 40 cm in order to increase the gas penetration to the axial part.

Experiments were performed[69] with auxiliary tuyeres of different lengths, diameters and nose shapes. According to the type of tuyeres used, the 1% CO_2 surface of the combustion zone could be enlarged horizontally, vertically and laterally (merging of inter-tuyere oxidizing zones). It is possible, by the use of these methods, to influence the zone dimensions and thereby peripheral running can be made to move to the centre or to the intermediate zone, or an uneven gas distribution corrected. By the use of these special tuyeres[69] it was possible in an experimental furnace of volume 818 m^3 and hearth diameter 6.5 m to reduce the coke rate by 6–10 percent and increase iron production by 10–30 percent. In practice, however, the use of auxiliary tuyeres is beset with difficulties, mainly on grounds of maintenance and increased downtime.

Even without the use of auxiliary tuyeres, considerable improvements in furnace running can be achieved by changing the charging sequence, blanking (partial or full blockage of one or more tuyeres by clay) or by changing the tuyere diameter. If the movement in front of a particular tuyere is slower than the others, the diameter of that particular tuyere can be decreased to obtain a higher kinetic energy and a more active zone. The diameter may also be narrowed if the peripheral flow is intense shown by high temperature and low CO_2-content of the peripheral gas or when the central flow is sluggish. In the case of formation of any scaffold or accretion on the wall, the diameter should be increased to encourage peripheral flow and melt them down, if possible. However, these modifications are helpful only when used judiciously in conjunction with appropriate variations in the charging sequence (Secs. 5.8.1, 11.3.2.10 and 13.3).

7.6.3. Inter-tuyere Space

A considerable amount of slag and iron descends to the hearth through the inter-tuyere zones. If they do so without having been adequately heated, the thermal state of the hearth may be disturbed with attendant high sulphur in iron, sluggish slag movement, erratic metal analysis, frequent tuyere burning, etc. The distance between the adjacent tuyeres around the hearth circumference should be such as to obtain, as far as possible, a merging of the individual combustion zones of each tuyere into a continuous ring. The consequent lateral enlargement of the raceway results in a smooth

counter-current gas and material flow over a wide peripheral area and minimization of any channel formation on this ground.

A lateral expansion can be obtained to a certain extent by an enlargement of the tuyere diameter or by the extension of tuyere overhang. Since the tuyeres are directed towards the centre of the circular hearth, any elongation will bring the tuyere noses nearer to each other. A venturi type of tuyere will also promote lateral expansion.

As regards the optimum inter-tuyere distance, in most large furnaces it ranges[59] between 1.45–1.55 m, the average value being about 1.5 m. The number of tuyeres generally is:

$$\text{number of tuyeres}^{73} = 2 \times \text{hearth diameter} + 1 \qquad 7.38$$

$$\text{or}^{83} = 2 \times \text{hearth diameter} \qquad 7.39$$

The use of number of tuyeres derived from the above equation is supposed to result in a coalescence of the neighbouring oxidizing zones. It should, therefore, provide a uniform gas and stock motion along the peripheral section of the charge column and enable a considerable forcing of the furnace when an adequate size and size distribution ensure bed permeability.

Modern large furnaces work with top pressures of up to 3 atm. which tend to shorten the combustion zone due to a decrease in the kinetic energy (Eq. 7.33). Eq. 7.32 further shows that one of the ways of increasing the kinetic energy is to decrease the number of tuyeres provided the continuity of the oxidising zone in the hearth annulus is ensured. In this regard the study of Manchinskii and Zaitsev[84] shows the relationship between the length and width of the combustion zone,

$$w_c = 0.83\, l_c,$$

where,

w_c = width of combustion zone
l_c = length of combustion zone

Using the above relationship Ostroukhov[59] suggests an inter-tuyere distance of 1.7 m instead of 1.5 m in order to reduce the number of tuyeres while at the same time not affecting the continuity of the raceway annulus. For large furnaces, the kinetic energy of the blast should range between 5000–8000 kg.m/s, depending upon the permeability of the stock and other relevant factors.

However, a smaller number of tuyeres has the disadvantage that if the kinetic energy is excessively high, it results in the breakage of coke due to high temperature attrition. Too much of coke fines form *kish* which floats up with the slag, increases its viscosity and promotes entrapment of the metal droplets which may ultimately lead to an increased burning of the tuyeres and slag notch.

Modern large furnaces should have a larger number of tuyeres in order to increase the raceway area and peripheral activity and at the same time *ensuring an adequate central flow with the use of prepared burden*. Large Japanese furnaces over 11 m hearth diameter have an inter-tuyere distance of slightly above 1 m,

$$\text{No. of tuyeres} = 3 \times \text{hearth diameter} - 1 \text{ or } 2 \qquad 7.40$$

Large Russian furnaces have,[85]

$$\text{No. of tuyeres} = 3 \times \text{hearth diameter} - 8 \qquad 7.41$$

Recent investigations of quenched blast furnaces show that the raceways of adjoining tuyeres are not inter-connected and lumpy coke exists between them.[111]

7.6.4. Nature of Stock and Gas Movement

The dimension and configuration of the combustion zone are also affected by the nature of stock and gas movement. A pronounced peripheral flow (periphery lightly loaded and centre over-loaded) hinders blast penetration and narrows down the combustion zone while a central flow enlarges it.[79] The oxygen and CO_2 contents of the tuyere gas for cases of peripheral and central flows are shown in Fig. 7.18.[68] The figure shows that in the case of peripheral flow the oxidizing zone shifts forward towards the tuyere nose. This occurs probably because of an intensified combustion of coke in front of the tuyeres as a consequence of an increasing amount of coke descending in front of the tuyeres.

In the case of increased peripheral resistance and faster central flow, the oxidizing zone widens towards the interior as shown by the oxygen and CO_2 contents. In such a case, a smaller amount of coke descends directly in front of the tuyeres than in a uniformly running furnace. The resistance to flow of the blast stream thereby decreases and, hence, the blast can penetrate deeper undisturbed. These irregularities can be rectified by changing the charging sequence and tuyere diameters.

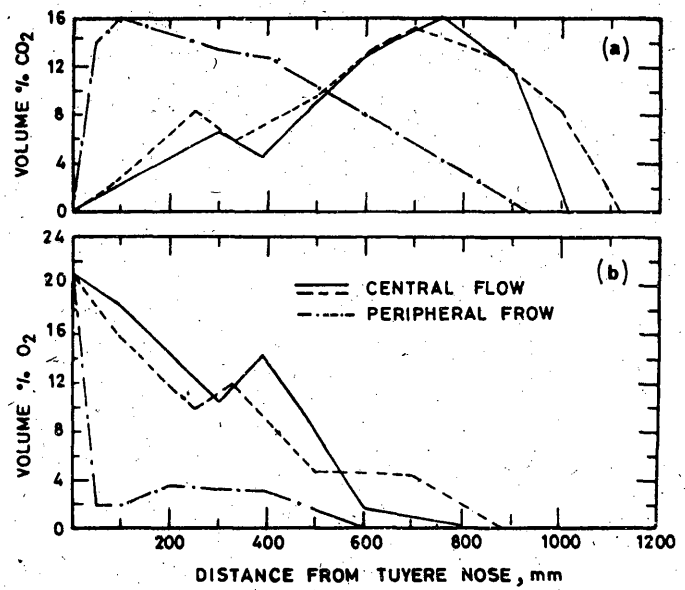


Fig. 7.18 Variation of gas composition in the combustion zone during peripheral and central flows, according to Wysocki and Pückhoff.[68] (Copyright Verlag Stahleisen).

The combustion zone is also affected by a sluggish stock descent or hanging (localised or more widespread).[59] In such cases, the amount of coke available in front of the tuyeres is comparatively small and it is also hotter because of a longer period of residence in the hot coke grid. The speed of movement of the coke pieces in the circulation zone as well as the depth of blast penetration are both smaller. However, because of the paucity of coke, less oxygen can combine with carbon and therefore the oxygen content of the gas is generally higher all along the axis of penetration. The combustion of coke occurs at a considerable distance from the tuyere nose.

When channels form in front of some tuyeres, more gas passes through them and a long raceway is formed in the zone. At other tuyeres, the blast is proportionately much less, the raceway is shorter and the coke lumps behave as a stationary bed. In the event the central part is choked with a dense mass of material, the combustion zone extends upwards. A high CO-content (70–80 percent) may be found at the boundary of the combustion zone.[59]

7.6.5. Coke Size

From Eqs. 7.35 and 7.37 the combustion zone is shortened if the coke delivered to the raceway is large in size. The resistance to flow of the blast stream increases as the coke size increases and the raceway becomes correspondingly narrower in horizontal depth but broader in width and vertical height.[77] On the other hand, the raceway is enlarged[68,77,86] if the coke is of small size but too small a size encourages flooding of the slag in the coke grid (Sec. 5.6). Breakdown of coke into fines affects gas permeability both in the dry and wet zones, causes coke mess and increases the frequency of tuyere burning (Secs. 13.9 and 13.10). Mechanically strong coke with size compatible with the free flow of gas is more important than the expansion of the raceway. The size of the combustion zone remains uniform if the size fraction of coke is narrow but the dimension and configuration of the zone vary in the case of a wide size range. If the coke is weak and extensive breakdown occurs, the fines deposit on the central coke column, enlarging its diameter and reducing the raceway depth.

The advantages and disadvantages of small coke size on furnace productivity will be seen in Sec. 11.3.2.3.

7.6.6. Blast Modifications

In the last two or three decades steam, oxygen and hydrocarbons are being increasingly used with the blast for decreasing the coke consumption and increasing the furnace output. It is important to find out the influence of these blast additives on the size of the combustion zone and smooth running of the furnace.

7.6.6.1. Oxygenated blast

Oxygen-enriched blast is seldom used without accompanying coolant blast additives. Oxygenated blast will presumably shorten the oxidizing zone because of a more intensive combustion of the coke and/or a diminution of the tuyere gas volume.

The effect of combined blast will be discussed in Sec. 7.6.6.3.

7.6.6.2. Natural gas[87-90]

The use of natural gas has invariably shown a much more extensive combustion zone than with the normal blast. The variations in the composition of the combustion gas along the tuyere axis for the two cases, normal and with natural gas blast, are shown in Fig. 7.19[87] for comparison.

Fig. 7.19(b) for natural gas shows that the oxygen content of the blast

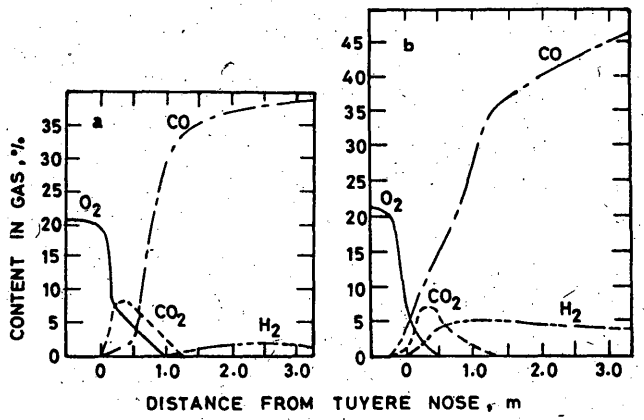


Fig. 7.19 Variation in the gas composition in the combustion zone along the tuyere axis for (a) normal blast and (b) natural gas injection, after Belevtsov et al.[87]

decreases even before emerging out of the tuyere since the gas is introduced inside the tuyeres at some distance from the tuyere nose. The oxygen reaches as low as 3 percent within 250 mm from the tuyere nose. The oxygen disappears and CO appears earlier than in the case of normal blast which can be traced to the burning of methane according to,

$$CH_4 + 1\tfrac{1}{2}O_2 = CO + 2H_2O \qquad 7.42$$

Fig. 7.19(b) also shows that the oxidizing zone as delineated by 1–2% CO_2 surface is elongated but Nekrasov et al.[88] report of a contraction when natural gas is injected. However, when injecting hydrogen-bearers, the depth of the combustion zone is not determined by the oxygen or CO_2 contents but by the reduction of water vapour by carbon,

$$C + H_2O = CO + H_2 \qquad 7.43$$
$$\Delta H(1400°C) = +\,3270\ \text{kcal/kg.C}$$

The above reaction is accelerated in the presence of hydrogen.[87,89]

The reduction of moisture apparently starts almost after the disappearance of CO_2 by carbon gasification. Hydrogen appears in considerable quantities at the outer surface of the CO_2 zone which suggests that the endothermic reaction 7.43 occurs preferentially at the outer surface of the oxidizing zone, thus extending the zone much farther (2–2.5 m from tuyere nose).[87] The sharp cooling effect of this reaction also reduces the volume and velocity of the gas in the axial neighbourhood. This, combined with an extensive penetration of the raceway towards the axis, promotes a

smooth ascent of the gas and descent of the charge materials over a wide area. Any hanging or retarded movement caused by the resistance to flow of gases in this region may therefore disappear.

A comparison of Figs. 7.19(a) and (b) shows that the gas in front of the tuyeres is much more reducing in the case of natural gas injection and this has a great influence on the re-oxidation of iron and metalloids in the oxidizing zone, reduction of slag iron oxides in the central zone and the maintenance of hearth temperatures. Although reaction 7.43 is highly endothermic, the temperature level even deep in the central zone is sufficiently high to keep the smelting products in a molten state and for the normal occurrence of metallurgical processes. The average temperatures of the gas along the tuyere axis were found to be:[88]

Distance from tuyere nose, m	0	1.5	2	2.5	3.1
Average temperature, °C	1670	1513	1447	1454	1411

7.6.6.3. Combined oxygen-natural gas

Gorshikov et al.[79] have shown using up to 30%-O_2 in the blast with natural gas injection that the oxidizing zone contracts. The shortening of the zone would tend to promote peripheral flow which was indeed detected.[87] A furnace running central changed to peripheral on oxygen-enrichment of the blast. A more uniform gas distribution and running of the furnace with great increase of driving rate was obtained.[91]

However, a more recent work[92] using 28–29%-O_2 blast and natural gas 140 Nm^3/THM shows that the combustion zone increased to more than 3 m. Steam formed from methane (Eq. 7.42) apparently continues to react farther, extending the zone of stock descent.

In any case, while using natural gas, the quality of the charge materials must be improved for better permeability, and both the axis and the periphery loosened by proper charging methods.

7.6.6.4. Fuel oil

The influence of fuel oil on the extent of combustion zone is controversial. According to Borusov and Fofanov,[93] fuel oil injection in the blast furnace lengthens the oxidizing zone and increases the raceway. It results in an increased looseness of the charge column which promotes smoother and more stable charge descent at higher driving rates. However, the tuyere gas is less reducing than in the case of natural gas since the CO appears much later with oil.

In a large scale investigation, Hatano et al.[70] observed a tendency of the raceway to shrink with fuel oil injection. The combustion zone was found to move towards the tuyeres raising the wall temperature around them. The CO_2 generated from the burning of coke reacted rapidly with the fuel oil carbon to form CO. In case the excess oxygen ratio (Sec. 6.9.3.1) was low and/or the blast velocity high, the oil flame lengthened considerably.

In any case, fuel oil helps to obtain a smoother and more uniform stock descent presumably because of lower flame temperature. A more reducing tuyere gas also ensures stabilization of the thermal state of the hearth.

7.6.6.5. Coke-oven gas

Coke-oven gas contains about 25 percent methane. Therefore, it is expected to behave as natural gas to some extent. The water-vapour initially formed from the combustion of methane reacts with the coke carbon later after the disappearance of CO_2 and hence the raceway penetrates more towards the axis. It thus contributes to the extension of the oxidizing and combustion zones to a greater hearth area.[94] Although the flame temperature falls, it improves the stability of the thermal conditions and smoothness of working and increases furnace productivity.[95]

7.6.6.6. Steam

Steam behaves more or less in the same way as natural gas does. The water-vapour reacts endothermically with coke at the raceway boundary after the reduction of CO_2 by coke has proceeded far. Steam contributes to the extension of the combustion zone to a greater hearth area.[96–98]

Blast temperature is generally increased to compensate for the cooling effect of steam (Sec. 6.9). An incomplete thermal compensation cools the tuyere gas, enlarges the combustion zone, raises the slag fusion zone upwards (Sec. 4.5) and thereby creates the conditions for a smooth running of the furnace.

7.6.6.7. Coal-dust

The length of the oxidizing and reducing zones decreases with coal-dust.[99–100]

According to K'rasavtsev and Sharkevich[110] the length of the raceway is not only influenced by the kinetic energy of the blast but also by the composition and volume of slag, thermal state of the furnace and the charging system. Since the slag is blown away from in front of the tuyere zone,

the resistance to penetration will increase with increasing slag bulk. The volume of the raceway zone determines the rate of removal of the gases from the combustion zone and the distribution and utilization of the gases in the furnace cross-section.

7.7. Re-oxidation of Metals

From the analysis of gas samples taken from the circulation zone it has been found that the oxygen content of the gas phase is not equal to the oxygen content of the input air along the tuyere axis towards the centre. With dry normal blast, the ratio $\Sigma O_2/N_2$ in the tuyere gas is expected to be 28.4 percent. However, as Fig. 7.20[68] clearly shows, the ratio is lower in the beginning and rises subsequently and finally exceeds the value. This finding makes it obvious that pig iron and its constituents absorb oxygen from the gas phase and are oxidized in the oxidizing zone. The removal of oxygen by the liquid phase dripping through the oxidizing zone is not reflected in the composition of the gas phase. The extent of oxidation of pig iron depends upon the length of the oxidizing zone, especially of the free oxygen surface. The figure also shows that with a blast temperature of 850°C the ratio is lower up to a distance of 500 mm and extends to 800 mm with 1000°C blast temperature. On the other hand, oxides (mainly unreduced iron oxides in the molten slag) flowing through the reducing zone and beyond get reduced in varying degrees and the gas phase becomes enriched with oxygen (as CO). Hence, the $\Sigma O_2/N_2$ ratio increases and exceeds 28.4 percent, the more so towards the centre where the %CO can

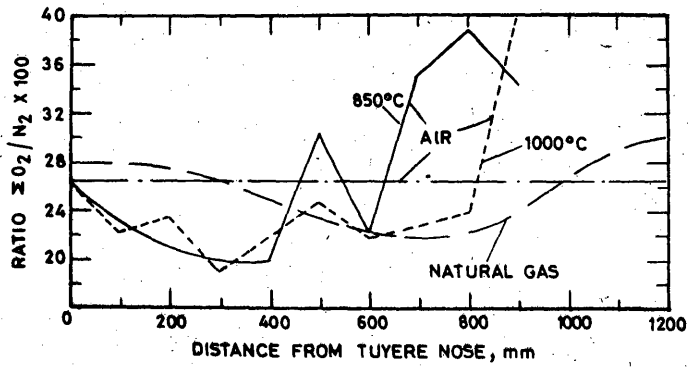


Fig. 7.20 Variation of oxygen content of tuyere gas in the combustion zone for 850°C and 1000°C blast temperatures[68] and also for natural gas.[89]

be much higher than the calculated tuyere gas value of 34.5 percent. The reduction of the slag oxides occurs directly by reaction with carbon while they percolate through the coke grid or *via* the Boudouard reaction producing excess CO. The variation in the ratio in the case of natural gas injection[89] is also inserted in Fig. 7.20.

The decrease in the contents of Si, Mn and S (also P and C) in the metal and increase in the FeO and Fe_2O_3 contents of the slag due to re-oxidation of the pre-reduced elements in the oxidizing zone in the case of normal blast as well as for natural gas injection are shown in Fig. 7.21.[88] The sulphur absorption by the slag (not shown in the figure) forms a mirror image, i.e., its content increases steadily after the boundary of the combustion zone, this being due to the decrease in the FeO content of the slag and consequent increase in its desulphurizing capacity (Sec. 9.2). For the case of natural gas (Fig. 7.21b), the decrease in the free oxygen content (cf. Fig. 7.19b) substantially limits the extent of oxidation of iron and metalloids. The oxidation occurs much less intensively compared to the normal blast. This, as will be seen in the next section, has great influence on the thermal state of the hearth.

The composition of the final metal for the two cases is shown in Table 7.2[88] which may be compared with that at the tuyere level (Fig. 7.21).

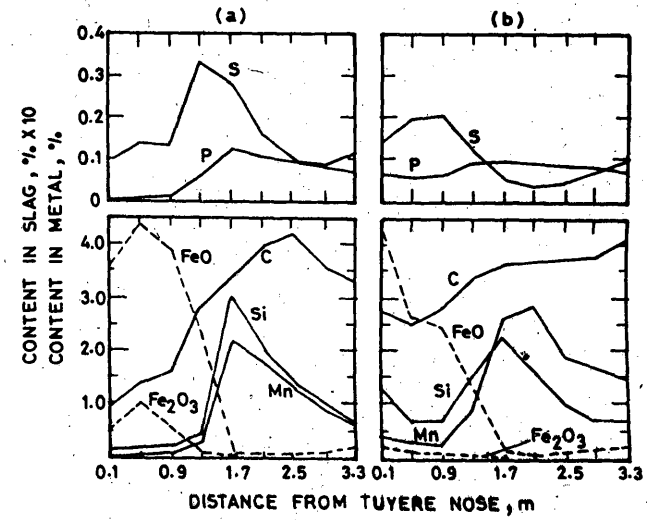


Fig. 7.21 Variations in the metal composition and slag iron contents along the tuyere axis in a blast furnace for (a) normal operation and (b) with natural gas injection, according to Nekrasov et al.[88]

It confirms the deductions in Secs. 3.15 and 7.4.2.2 that the metal entering the hearth contains more sulphur and silicon and less of manganese than the final metal. The metal is *desiliconized, desulphurized* and *remanganized* in the hearth.

Table 7.2[88]

	Si	Mn	S	P	C
Normal blast	0.64	1.22	0.039	0.112	4.51
With natural gas	0.64	1.61	0.037	0.092	4.10

7.8. Thermal State of Hearth

In Chapter 4 we have seen that the thermal capacity of the liquid smelting products becomes lower in the oxidizing zone ($W_s < W_g$) due to an enormous heat evolved during the re-oxidation of pig iron producing ferrous and ferric oxides. Therefore, there may exist an independent third heat-exchange zone[101] near the tuyere level where the temperature profiles of the burden and the gas will be similar to those in the upper furnace (convex type, Fig. 7.22).[101] The total quantity of iron oxidized may even

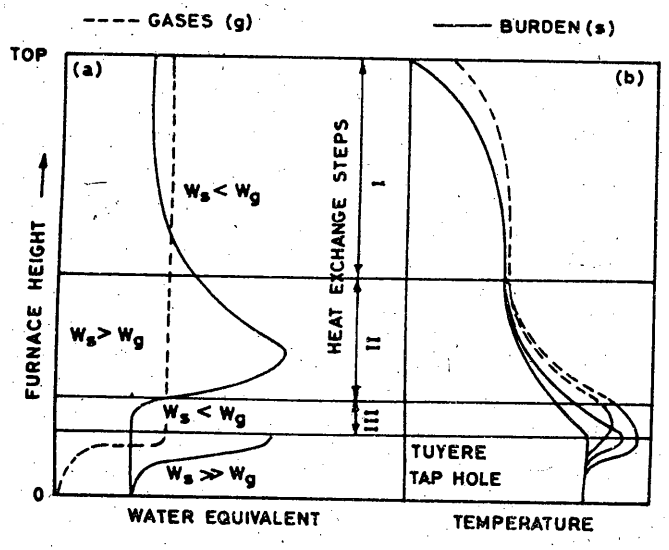


Fig. 7.22 (a) Schematic variation of water equivalents of the charge W_s and gas W_g from furnace top to tap hole; (b) temperature distribution along the furnace height. After Lavrent'ev.[101]

approach 25 percent of all the iron reduced in the furnace[101,102] and the iron oxide content of the slag[101,103] in the oxidizing zone reach even 75 percent. According to Gladyshev[104] about 75 percent of the iron and 25 percent of the slag pass through the oxidizing zone and the rest through the inter-tuyere and other zones. Therefore, the heat of re-oxidation may be so enormous that the temperature of the liquids may approach that of the combustion zone.

The re-oxidized iron flows down to the hearth in addition to the unreduced iron oxides in the molten slag running along the central coke column. Since the iron content of the final slag seldom exceeds 1 percent, all the iron oxides entering the hearth are reduced mainly by carbon with an enormous consumption of heat which greatly affects the temperature of iron and slag and the thermal state of the hearth. Since there is no outlet of the gas in the hearth, the combustion gas supplies very little heat (its thermal capacity is negligible) and hence the thermal capacity of the liquid products far exceeds that of the gas (Fig. 7.22). This required heat is compensated by the products themselves, superheated in the combustion zone. Since the input of the iron oxides into the hearth seldom reaches a steady state due to non-uniform stock descent, gas flow or iron oxide reduction, the heat supply and heat consumption in the hearth are different in sequence of time as well as at different sectors of the hearth cross-section. This reflects in erratic metal temperature and composition from cast to cast or sometimes even from ladle to ladle (depending upon from which sector the metal is withdrawn; lack of intermixing).

7.8.1. Metal Temperature and Composition

Under constant blast temperature and raw material condition and uniform furnace operation, the inter-relations between the processes of re-oxidation of pig iron and superheating of the liquids at the tuyeres, and the heat consumption of iron oxide re-reduction and its compensation by the liquids superheat, ensure an outwardly normal blast furnace operation.

In case an excess of unreduced iron oxides or re-oxidized pig iron enters the hearth due to accelerated stock descent or inadequate reduction, their re-reduction in the hearth will decrease the metal temperature, retard the reduction of slag-MnO by silicon and hence increase the metal sulphur. The final result will be a higher-Si, lower-Mn, higher-S and colder iron.

An increase in the blast temperature will increase the gasification of SiO and hence increase the metal silicon above the tuyeres. The re-

oxidation of iron will also increase due to the extension of the oxidizing zone which will tend to lower the hearth metal temperature initially until the metal picks up heat from the liquids with higher super-heat. Therefore, the initial effect of an increased blast temperature will be a high-Si, low-Mn and high-S cold iron. Later, with the passage of time, a hotter metal with higher-Mn and lower-S will be obtained (cf. Fig. 7.12).

We can see that the re-oxidation of pig iron and superheating of the smelting products are undesirable for the iron quality, especially of the steelmaking iron for its stringent requirements. The quality can be made better and more uniform with the injection of hydrogen-bearers or coal dust.

In the above context, the question of both low and high temperature reduction of iron ore or agglomerates needs re-examination. In order to lower the input of iron oxides in the hearth, they should be reduced as far as possible in the dry zone. In the wet zone, the remaining iron-oxygen should be removed before the slag enters the hearth. In Sec. 6.7.5 we have seen that in limey agglomerates the iron layer surrounding the residual wustite is porous and they are more easily reducible than the acid ones. This is one of the reasons why the temperature and quality of iron are more uniformly maintained in modern furnaces using pre-fluxed burden.

The silicon content is generally regarded as a measure of the metal temperature. But, we have seen it is possible for furnaces to produce *high silicon cold iron*. Also the reduction of slag-MnO by silicon is a function of temperature and the metal sulphur is intimately related with metal-Mn. Hence, it is expected that the metal temperature will be more closely related with the metal Mn and S. In fact, by statistical analysis, Pochvisnev and Kurunov[105] have determined that the highest correlation coefficient with the metal temperature is possessed by the (Mn)/[Mn], closely followed by the [Si]/[S] and (S)/[S] ratios. However, since the silicon in iron is easy to monitor, it can still be used as a measure[106] of the dynamics of the thermal state of a furnace making a given sort of iron from relatively constant raw materials.

7.8.1.1. Influence of additives

It is the experience of modern blast furnace operators that a hotter hearth can be more uniformly maintained with increased metal temperature and metal-Mn and decreased metal-S with the injection of natural gas (or coke oven gas, fuel oil, steam and pulverized coal). Although the flame temperature decreases with the use of additives, the thermal state of the hearth

improves because of a decrease in the input of iron oxide in the hearth which is thus relieved to a considerable extent from the highly endothermic work of re-reduction of the iron oxides. The decrease in the input of iron oxides in the hearth occurs due to one or more of the following reasons:

(i) use of hydrogen-bearers which increase the overall reduction of the iron oxides;[107,108] natural gas may decrease direct reduction by 10–15 percent;[108]
(ii) increase in the reduction of FeO-containing slag running down along the central coke column due to increased penetration of hydrogen towards the centre (Fig. 7.19b);
(iii) extension of the raceway, smoother and more uniform stock descent; less of inadequately preheated and pre-reduced burden entering the hearth;
(iv) lowered flame temperature and hence a decreased re-oxidation of pig iron;
(v) more reducing atmosphere in front of the tuyeres, smaller zone of free oxygen and hence decreased re-oxidation of pig iron (cf. Fig. 7.19b).

The effects of the above on the thermal state of the hearth are:

(i) decreased heat requirement in the hearth for re-reduction of iron oxides;
(ii) stabilization of the hearth heat;
(iii) increased metal temperature[107] (cf. Fig. 7.12b);
(iv) increased reduction of slag-MnO by silicon and hence higher-Mn iron;
(v) increased sulphur removal (lower-S iron) because of (iv) above, apart from a decreased sulphur input due to the lowered coke rate;
(vi) no decrease in metal silicon due to lowered flame temperature as expected because of decreased Si-reoxidation (Fig. 7.21b).

By manipulating the amount of the additive and blast parameters, it is possible to influence to a certain extent the thermal conditions of the hearth and regulate the temperature and composition of the metal. This is especially important when operating with a rich burden.[101]

References

1. BULTER, D. and A. KLITZING: Stahl u. Eisen, 88, 1968, p. 108–119.
2. LOGINOV et al.: Stal in Eng., 11, 1966, p. 868–874.
3. SCHURMANN, E. and D. BULTER: Arch. Eisenhuttenw., 35, 1964, p. 677–798.
4. BOGDANDY, L. v. and H.-J. ENGELL: The reduction of iron ores (in English), Springer-Stahleisen, 1971, p. 467.
5. TURKDOGAN, E. T. and J. V. VINTERS: Met. Trans., 5, 1974, p. 11.
6. See review by E. K. KOHLER: Stahl u. Eisen, 81, 1961, p. 1297–1301.
7. RIGBY, G. R. et al.: Bull. Brit. Refract. Res. Assoc., No. 59, 1941, p. 90; Trans. Brit. Cer. Soc., 43, 1944, p. 73–80.
8. CHUPAROV, G. L. and M. F. ANTOVA: Bull. Akad. Sci. URSS, Class Sci. Tech., 1942, p. 382.
9. KLEMENTASKII: J. Iron Steel Inst., 171, 1952, p. 176.
10. SCHENCK, H. and H. BARTH: Stahl u. Eisen, 80, 1960, p. 1681–1689. SCHENCK, H. et al.: Arch. Eisenhuttenw., 39, 1968, p. 101–107.
11. SCHENCK, H. and W. MASCHALANKA: op. cit., 31, 1960, p. 271–277.
12. BONE, W. A. et al.: J. Iron Steel Inst., 137, 1938, p. 85.
13. BOGDANDY, L. v., P. DICKENS, W. v. D. ESCHE and J. WILLEMS: Stahl u. Eisen, 83, 1963, p. 129–139.
14. KHODAK, I. Z. and Yu. I. BORISOV: Steel in USSR, March 1971, p. 182–185.
15. BABARYKIN, N. et al.: Stal in Eng., Aug. 1970, p. 583–590.
16. FIRKET, A. and T. MOLDEREZ: Rev. Univ. Mines, (2), 15, 1959, p. 93–106.
17. BONNAURE, E.: Rev. Met., Aug.-Sept. 1959, p. 141–154; Stahl u. Eisen, 79, 1959, p. 1105–1109.
18. ASTIER, J. E. et al.: J. Iron Steel Inst., Oct. 1961, p. 143–148.
19. SCHURMANN, E., P. ISCHEBECK, G. HEYNERT and W. ZISCHKALE: Stahl u. Eisen, 80, 1960, p. 854–861.
20. KITAEV, B. I., Yu. G. YAROSCHENKO and V. D. SUCHKOV: Heat exchange in shaft furnaces, Pergamon Press, Oxford, 1967.
21. KITAEV, B. I. and B. M. SHAVEL'ZON: Steel in USSR, June 1976, p. 300.
22. NEKRASOV, Z. I. and M. T. BUZOVERYA: Stal in Eng., Feb. 1969, p. 141–147. NEKRASOV, Z. I. et al.: op. cit., July 1970, p. 502–509.
23. KINNEY, S. P.: Tech. paper, Bur. Mines, No. 442, 1929, p. 148; see also G. Eichenberg and P. Oberhoffer: Arch. Eisenhuttenw., 1, 1927–28, p. 613.
24. PAVLOV, M. A.: Metallurgy of pig iron, vol. 2, Verlag Technik, Berlin, 1953, p. 183.
25. KORNEV, V. K. and S. V. SHAVRIN: Steel in USSR, Feb. 1971, p. 96–98.
26. HEYNERT, G., W. ZISCHKALE and E. SCHURMANN: Stahl u. Eisen, 80, 1960, p. 981–990.
27. PETERS, W. et al.: Proc. Blast Fce. Raw Mat., AIME, 20, 1961, p. 403–415.
28. ZISCHKALE, W., G. HEYNERT and H. BEER: Stahl u. Eisen, 83, 1963, p. 1117–1123.
29. BULTER, D. and A. KLITZING: op. cit., 88, 1968, p. 108–119.
30. BELL, H. B. and J. TAYLOR: J. Iron Steel Inst., Nov. 1961, p. 276–285.
31. GOL'DSHTEIN, N. L. and N. S. KROMCHENKO: Stal in Eng., March 1965, p. 172–175.
32. BACHININ, A. S. et al.: op. cit., March 1969, p. 211–215.
33. BABARYKIN, N. N.: Steel in USSR, Aug. 1973, p. 621–624.
34. FRUEHAN, R. J.: Met. Trans., 4, 1973, p. 2123–2132.

35. WUHRER, J. and G. RADEMACHER: Chem.-Ing. Techn., 28, 1956, p. 328; see also Physical chem of iron and steelmaking, Verlag Stahleisen, 1964, p. 86.
36. KOOTZ, Th.: Recent dev. in met. sci. and tech., Iron and Steel, Silver Jub. Sym., Ind. Inst. Metals, New Delhi, 1972, p. 247–271.
37. Intn. Eisenhüttentag: Automaton I, Amsterdam, 1965, p. 133–195.
38. STAIB, C.: Rev. Metallurg., 61, 1964, p. 1–26.
39. STAIB, C. et al.: op. cit., 65, 1968, p. 717–749.
40. GUILLEMAIN et al.: op. cit., 64, 1967, p. 961–986.
41. VAN LANGEN et al.: J. Metals, 17, 1965, p. 1379–1384.
42. LUCKERS et al.: Met. Rep., CNRM, No. 19, 1969, p. 51–64.
43. WOOD, B. I.: Developments in ironmaking practice, Proc. conf. Iron Steel Inst., London, 22–23 Nov. 1972, p. 146–151.
44. CASTORE et al.: ibid., p. 152–159.
45. BODSWORTH, C. and H. B. BELL: Phys. chem. of iron and steel manufacture, Longmans, London, 1972.
46. GOROKH, A. V. et al.: Stal in Eng., July, 1964, p. 509–512.
47. KORBER, F. and W. OELSEN: Mitt. Kaiser-Wilh. Inst. Eisenforch., 17, 1935, p. 231.
48. RANKIN, W. J.: Ph.D. Thesis, Univ. Queensland, Australia, 1975.
49. McCOY, C. W. and W. O. PHILBROOK: Phys: chem. of steelmaking, Edt. J. F. Elliott, MIT, Mass., 1958, p. 93–98.
50. DELVE, F. D. et al.: Phys. chem. of process met., Edt. G. St.-Pierre, Wiley, 1961, p. 1111–1139.
51. DELVE, F. D.: Trans. Met. Soc., AIME, 212, 1958, p. 226.
52. HESS, W., S. MEYER and H.-P. SCHULZ: Stahl u. Eisen, 93, 1973, p. 107–110.
53. SASAKI, M., and T. NAKAZAWA: Trans. Iron Steel Inst. Jap., 10, 1970, p. 464–472.
54. STROUP, R. T.: Trans. Met. Soc., AIME, 230, 1964, p. 356.
55. Jon et al.: Cent. Natn. de Rech. Metallurg., 15, 1968, p. 3.
56. SASAKI, M. and T. NAKAZAWA: Trans. Iron Steel Inst., Jap., 9, 1969, p. 413.
57. BURGESS, A. J. and B. G. BALDWIN: J. Iron Steel Inst., 186, 1957, p. 227–235.
58. BEER, H. and G. HEYNERT: Stahl u. Eisen, 84, 1964, p. 1353–1365.
59. OSTROUKHOV, M. Ya.: Stal in Eng., July, 1962, p. 512–515.
60. ELLIOTT, J. F. et al.: J. Metals, 4, 1952, p. 109–717.
61. WAGSTAFF, J. B.: op. cit., 5, 1953, p. 895–902.
62. WAGSTAFF, J. B. and W. H. HOLMAN: op. cit., 9, 1957, p. 370–376.
63. GARDENER, C. C.: Trans. Met. Soc., AIME, 218, 1960, p. 423–428.
64. BARDIN et al.: Neue Hutte, 1, 1955/56, p. 238–244.
65. McCUTCHEON, K. C.: Blast Fce. Steel Plant, 52, 1964, p. 1044–1049; p. 1075.
66. HUMPHREYS, K. K.: op. cit., 51, 1963, p. 1065–1069.
67. SUMAKOV, L. G.: Stal, 23, 1963, p. 202–205.
68. WYSOCKI, H. and U. PUCKHOFF: Stahl u. Eisen, 86, 1966, p. 761–770.
69. Possibilities of influencing the oxidizing of the blast furnace: op. cit., 66/67, 1947, p. 277–284; A. Moller, Dr. Ing. Thesis, Bergakad. Clausthal, 1947.
70. HATANO, M., B. HIRAOKA, M. FUKUDA and T. MASUIKE: Trans. Iron Steel Inst., Jap., 17, 1977, p. 103–109.
71. LOGINOV et al.: Stal in Eng., Nov. 1966, p. 868–874.
72. TLEUGABULOV et al.: op. cit., Nov. 1965, p. 861–864.
73. PAVLOV, M. A.: Metallurgy of pig iron, vol. 3, Verlag Technik, Berlin, 1953.
74. KOZLOVICH et al.: Soviet Metallurgy, (5–6), 1935.
75. BARDIN, I. P. et al.: Freiberg Forsch., ser. B, No. 25, 1958, p. 19–37.

76. BYALYI, L. A. et al.: Isv. Vys. Uce. Zav. cern Metallur., 4, 1963, p. 27–33.
77. TAYLOR, J. et al.: J. Iron Steel Inst., 187, 1957, p. 330–341.
78. SHCHERKOV, V. P.: Stal, 10, 1954.
79. GORSHIKOV et al.: Stal in Eng., Sept. 1965, p. 687–695.
80. KOVAL, I. F.: op. cit., June 1959, p. 421–424.
81. ZHEREBIN et al.: Stal, 5, 1956, p. 391–396.
82. VASIL'CHENKO et al.: op. cit., 10, 1958, p. 869–874.
83. LEONODOV, N. K. and M. N. LEONIDOVA: Stal in Eng., May 1967, p. 373–377.
84. MANCHINSKII, V. G. and A. F. ZAITSEV: op. cit., Sept. 1960, p. 629–633.
85. TIKHOMIROV, E. N. and Yu. I. GOKHMAN: Steel in USSR, April 1972, p. 264.
86. EBERT, R. and K. F. LUDEMANN, J. Iron Steel Inst., Sept. 1960, p. 46–50.
87. BELEVTSOV, G. A. et al.: Stal in Eng., June 1962, p. 410–413.
88. NEKRASOV, Z. I. et al.: op. cit., March 1962, p. 169–174.
89. NEKRASOV, Z. I. and F. N. MOSKALINA: op. cit., Sept. 1962, p. 664–667.
90. STARSINOV et al.: op. cit., May 1962, p. 337–341.
91. BIALYI, L. Y. and A. P. KOTOV: op. cit., Dec. 1966, p. 956–962.
92. NEKRASOV, Z. I. et al.: Steel in USSR, Oct. 1971, p. 770.
93. BORUSOV, Yu. S. and A. A. FOFANOV: Stal in Eng., June 1961, p. 397–402.
94. ZHEREBIN, B. N. et al.: op. cit., July 1961, p. 549–554.
95. ZHEREBIN, B. N. et al.: op. cit., April 1965, p. 256–260.
96. STRASSBURGER, J. H.: Am. Iron Steel Inst., Meeting, May 1956, N.Y.
97. MILLER, V. Ya. and S. A. EL'KIN: Stal, 3, 1958, p. 193–202.
98. GRIEVE, A.: J. Iron Steel Inst., Jan. 1960, p. 37–43.
99. ANDRONOV, V. N. anw Z. Sh. PLOTKIN: Steel in USSR, July 1974, p. 625.
100. LOGINOV, V. I. and E. I. BEKHTER: op. cit.: June 1975, p. 294.
101. LAVRENT'EV, M. L.: Stal in Eng., Feb. 1969, p. 135–140.
102. KRUGLOV, N. N.: Combustion process in front of blast furnace tuyeres, ONTI, 1936.
103. GOTLIEB, A. D.: The blast furnace process, Metallurgya, 1966.
104. GLADYSHEV, V. I.: Stal in Eng., Dec. 1965, p. 956–958.
105. POCHVISNEV, A. N. and I. F. KURUNOV: op. cit., April 1966, p. 257–260.
106. REBEKO, A. F. et al.: op. cit., 41, 1966, p. 260–262.
107. DUNAEV, N. E. and S. L. YAROSHEVSKII: op. cit., April 1962, p. 250–253.
108. PANEV, G. A. et al.: op. cit., March 1966, p. 171–175.
109. VIDAL, R. and A. POOS: Blast furnace technology, Edt. J. Szekely, Dekker, N.Y. 1972, p. 201–232.
110. K'RASAVTSEV, N. I. and L. D. SHARKEVICH: Steel in USSR, June 1975, p. 294.
111. NAKAMURA, N. et al.: Ironmaking Steelmaking, 5, 1975, p. 1–17.

CHAPTER 8

BLAST FURNACE SLAGS

8.1. Introduction

Iron blast furnace raw materials consist of gangue minerals and coke ash in combination with fluxes – usually lime and magnesia. The principal oxides of the minerals are alumina and silica and they are removed by the addition of flux, the resulting liquid slag being insoluble in and lighter than the molten iron forms a separate layer. Basic flux is necessary not only to lower the melting points of the acid constituents and thereby obtain a liquid or sufficiently fluid slag but it also takes part in the slag-metal reactions and controls the metal quality, viz., the Mn-, Si- and S-contents. Apart from the four main non-ferrous oxides (lime, magnesia, alumina and silica) which form about 95–96% of the total, there are other compounds present in minor quantities depending upon the raw materials and the type of iron smelted in the blast furnace. They generally are: FeO, MnO, FeS, CaS, alkali silicates, etc.

Although an ideal could possibly never be achieved, a proper slag should perform a variety of functions for maximum efficiency both in fuel as well as furnace performance; it should *determine*, *control* or *possess* the following:

(1) metal temperature;
(2) metal quality, i.e., the C, Si, Mn, S and FeO contents of iron;
(3) homogeneity, absence of crystalline phases, i.e., the melt should not undergo variations in its physical properties;
(4) tolerance of fluctuations in the temperature and physical and chemical properties of the burden which constantly occur even under the best operating conditions; the slag should cushion such shocks without materially affecting its properties and furnace performance;
(5) sulphur retention potentiality, i.e., a high (S)/[S] ratio under the operating conditions;
(6) low viscosity, i.e., the slag should be able to run out of the furnace freely and rapidly at the operating temperatures; as the coke rate is affected by the 'critical temperature' which will enable the slag to flow, the free running characteristic of the slag will affect fuel economy;
(7) free movement of the stock and furnace gases; these are determined by the physical properties and zones of fusion of the primary and bosh slags which greatly affect the productivity of the furnace and the quality of the products;
(8) suitability of the slag for use in cement manufacture, road ballast, etc.

On the other hand, the course of primary and bosh slag formation is itself affected by the operating and other conditions, namely, flame temperature, distribution of materials at the top, ore reducibility, burden yield (i.e., slag bulk), sinters and pellets (acid, fluxed or super-fluxed), softening temperatures of the ferrous charge, coke ash content, furnace lines, etc. When all the operating conditions are conducive to a smooth and regular furnace movement, the use of a slag of optimum composition may result in a maximum production and minimum of slag bulk, metal-sulphur and fuel costs.

The course of slag formation in the blast furnace can be divided into three zones:

(i) primary slag fusion zone;
(ii) bosh slag fusion zone;
(iii) final slag or hearth slag zone.

We have already followed the sequence of their formation in the descriptions of the FeO-SiO_2-Al_2O_3, CaO-Al_2O_3-SiO_2 and CaO-MgO-Al_2O_3-SiO_2 phase systems (Secs. 3.16–3.18).

8.2. Formation of Primary and Bosh Slag

We have seen in Sec. 3.16 that partially reduced iron oxide in combination with the gangue form easily fusible eutectics with alumino-silicates with or without lime, magnesia or MnO. The zone of softening and melting of the initial slag depends upon the temperature distribution in the vertical as well as horizontal cross-sections of the furnace (cf. Figs. 5.1, 7.4 and 11.24). The location, extent and temperature range of softening and melting are of great importance for gas throughflow, productivity and smooth running of the furnace (cf. Secs. 5.5, 6.5.2 and 11.5). The properties and behaviour of the initial slag formed depend upon the nature and mineralogy of the burden, i.e., whether the charge consists of raw ore or acidic or basic agglomerates. These are discussed briefly below:

8.2.1. Raw Ore

In raw ore plus limestone burden, the calcination and assimilation of the latter occur slowly and are complete only when very high temperatures are reached, i.e., in the bosh, tuyere and hearth zones. Therefore, the initial slag formed is acidic consisting essentially of unreduced FeO and gangue silica and alumina with some MnO, the fusion temperature depending upon the FeO-content (cf. Fig. 3.17). When the ore is lean and highly reducible, the %FeO-content of the slag is low and its fusion temperature high, 1200–1350°C. On the other hand, in rich ore with low slag bulk the %FeO is comparatively high even if it is highly reducible and its fusion temperature low, about 1200°C. The %FeO decreases due to direct reduction and the fusion temperature rises, as the primary slag flows down. The slag may resolidify if the rise in its temperature during its descent is not commensurate with the increase in its fusion temperature. However, in actual practice, the presence of MnO and absorption of lime and magnesia keep the slag molten during its passage to the hearth. The fluxing action of MnO is similar to that of FeO but the free energy of MnO being much smaller it is reduced at high temperatures in the bosh and the hearth, only partly, never to completion (Secs. 2.4 and 3.13 and 7.4.2.2).

The ferrous alumino-silicate slag is very viscous although its liquidus temperature is low. The dissolution of lime and absorption of heat by the viscous slag being slow, the burden in the raw ore practice heterogeneous and the temperature distribution non-uniform, there can be widespread variations in the slag composition and in the levels of the slag formation zones. The resulting changes in the viscosity and solidification temperatures

can cause the formation of scabs on the walls and non-uniform furnace operation. These variations may occur locally or may be the ultimate effect of non-uniform stock descent or gas flow, false burdening, wrong material distribution at the top, etc.

Ideally, the primary slag should start to soften, melt and contract in the belly with its wide transverse dimension designed specifically to allow gas flow through the semi-fused viscous pasty mass. However, as seen above, the melting temperature, melting zone or even the slag composition are not constant in time or place. As a rule, with our conventional charging system with two bells and a hopper, the concentration of the ore is the highest in the intermediate zone. The periphery and the centre being more permeable, the gas temperature there is high which softens and melts the gangue earlier. In the intermediate zone, the gas permeability and therefore the temperature of both the gas and the ore are low, causing reduction of the ore and melting of the slag to occur much later and at lower levels (cf. Figs. 5.1, 7.4 and 11.24).

Softening and melting of gangue may start even in the middle of the furnace in the case of a strong peripheral flow, centre overloaded with ore, use of fine ores or ores with low softening temperatures around 700–800°C. It will be seen in Sec. 11.5 that softenability may be a factor limiting productivity. Sintering of ores raises the melting temperature and narrows down its range as well.

8.2.2. Acid Sinter

The advantages and disadvantages of acid sinter have been seen in Sec. 6.4.4. In acid sinter, the primary slag is pre-formed and, therefore, its mineralogical composition, softening-melting temperatures and other physical properties are more or less predetermined. It softens gradually in a much narrower temperature range than in the case of raw ores because of greater homogeneity but otherwise the physical nature of the acid slag is similar. It, being less reducible, carries more FeO which together with MnO gives a low-melting slag. Such a slag is disadvantageous in the blast furnace, especially if it carries a lot of FeO, since it descends inadequately heated and prepared and disturbs the thermal state of the hearth. The wide fusion range and high fusion temperatures promote the formation of a pasty mass at a higher level of the furnace which hinders gas throughflow and causes an erratic stock descent. However, acid sinter is a much better feed material than the raw ore.

8.2.3. Basic Sinter

Basic sinter softens and melts almost simultaneously in a high and narrow range of temperature since its FeO content is low, it being very reducible. It acquires a high fluidity as soon as it melts. Since it does so at a high temperature and in a short zone in the belly or upper bosh, it promotes a high production rate and the adequate preheating ensures a stable furnace operation and metal quality. Its drawback lies in the fact that as it melts quickly it can also resolidify as rapidly during variations in the blast humidity and temperature. The advantages and disadvantages of the fluxed sinter have already been discussed in Sec. 6.4.4.2.

8.2.4. Liquidus Temperature and Viscosity

The liquidus temperature of the primary slag depends upon the various components present in the main ferrous alumino-silicate system. It needs to be ascertained by experiments since the liquidus is difficult to determine

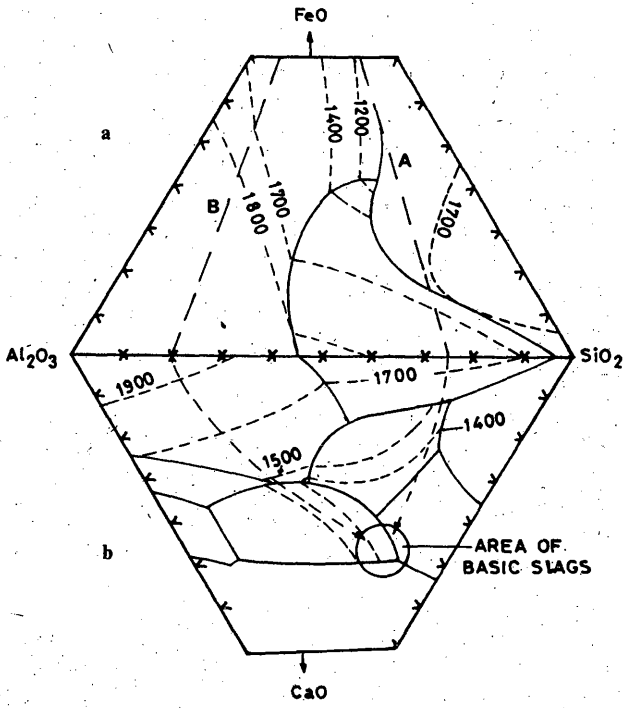


Fig. 8.1 A combination of FeO-Al_2O_3-SiO_2 and CaO-Al_2O_3-SiO_2 phase diagrams showing schematically the course of primary slag formation. Lines A and B are for high and low silica/alumina ratios in the ore respectively.

for multi-component systems from the values of three or four components. However, it is known that small amounts of lime and magnesia decrease the liquidus temperature which increases with their increasing amounts.

The liquidus temperature of the ferrous alumino-silicates depends not only upon the FeO-content but also on the silica-alumina ratio. The course of transformation of the primary slag to the final slag through the intermediate bosh slag is shown schematically in Fig. 8.1 which is a combination of Figs. 3.17 and 3.18. It is evident from the figure that the slag has to pass through high temperature regions near the alumina-silica binary. From Fig. 8.1(a), for any given %FeO in slag, the lowest melting points are obtained for silica/alumina ratios of 2.5–4.0:1 (line A). For a final slag silica of 35–40 percent, this corresponds to 10–15% Al_2O_3. In fact, such slags have been found to be most conducive to smooth furnace operation.[1–3]

The dissolution of lime and therefore the formation of the bosh and subsequently that of the hearth slags will be most smooth when the silica/alumina ratio is optimum. If not, a highly refractory slag and irregular furnace operation may result depending upon the %FeO-content, since the fusion temperatures rise with higher or lower ratios. One of the reasons why it is so difficult to work with Indian blast furnaces is the very low ratio, 0.25–0.5:1, in the Indian iron ores (line B, Fig. 8.1a). Hay[4] and Schraeder[5] have shown that both high and low alumina slags are more viscous than the medium ones (10–18% Al_2O_3). However, they can be thinned by the use of MgO.

The viscosity of the primary slag also plays a role in stock descent, rate of lime dissolution and stickiness in the bosh. It can range between 5–25 Poise for slags containing 10–30% FeO, the variations depending greatly on the composition. Some figures are given in Table 8.1.[6] Both FeO and MnO markedly thin the slag. The latter must be present in increasing quantities as the basicity increases in order to keep the slag fluid as otherwise the slag may resolidify as the FeO is progressively reduced. Since MnO is difficult to reduce, its presence (2–10 percent) helps to broaden the range of fluidity and stabilize the viscosity of the primary slag under the operating conditions. For making low-Mn iron, in the absence of sufficient MnO, the slag must be kept fluid with additions of MgO. Primary slags from self-fluxing sinters have viscosities of only 1–2 P even without FeO or MnO (slag No. 17,[7] Table 8.1).

MnO is also very helpful in retaining the fluidity of acid slags. It reduces the viscosity of slags of basicity $CaO/SiO_2 = 0.6–0.8$ by about 2–5 times.[8]

This allows working with extremely acid slags of basicity 0.3–0.9.

When the slag is excessively limey, it becomes very refractory as happens with rich Indian ores with high coke rate and high coke ash content. In case of any sudden reduction in temperature such slags are apt to solidify. They can be thinned to a certain extent by MgO or MnO but the latter in excessive amounts increases the cost as well as steelmaking difficulties. Acid slags are more immune in this respect since they retain their fluidity even at considerably lower temperatures. The formation of scabs arising from very limey slags can be minimized by keeping the limestone away from the walls by suitable charging sequence, e.g., OOLCCC or OOCLCC. The walls can also be washed with occasional use of hard-burnt acid sinter or by charging acid sinter first.

Modern furnaces working with low slag volume, pre-fluxed slag containing magnesia and comparatively high FeO seldom show furnace irregularity because of lower, uniform and narrow range of melting temperatures and very favourable fluidity (Table 8.1).

Table 8.1.[6] The viscosities of some primary slags

No.	Composition of primary slag, percent						Viscosity in Poise		
	SiO_2	Al_2O_3	CaO	MgO	FeO	MnO	1250	1300	1350°C
1.	43.2	16.2	23.9	8.8	7.8	–	73.6	40.5	23.2
2.	33.1	25.7	25.2	5.1	8.9	–	hard	65.5	30.0
3.	37.9	12.6	33.2	5.4	9.3	–	–	14.7	6.7
4.	31.6	16.0	38.5	7.0	10.3	–	–	25.0	10.0
5.	30.7	19.3	31.6	5.0	13.5	–	–	22.2	12.3
6.	27.0	15.0	21.0	4.7	28.4	–	5.3	3.7	2.5
7.	29.6	13.2	18.9	4.8	31.7	–	8.5	5.6	3.1
8.	32.9	13.1	31.8	4.6	10.1	–	24.0	7.6	5.2
9.	30.4	13.7	29.1	3.9	16.9	–	6.5	4.0	1.5
10.	47.2	7.0	28.6	4.1	11.9	7.7	6.2	3.5	2.6
11.	38.0	7.5	25.8	5.2	13.9	9.3	0.4	0.4	0.4
12.	35.4	7.9	27.8	3.1	15.0	9.9	4.4	2.8	2.2
13.	33.5	7.5	26.0	5.2	18.0	9.4	3.6	2.7	2.2
14.	31.8	8.2	27.4	3.0	24.0	4.3	4.7	2.9	2.6
15.	27.7	9.0	30.1	3.7	24.7	4.4	4.3	4.0	3.7
16.	25.6	8.5	27.9	3.2	25.4	8.8	3.2	2.2	1.5
17.*	40–45	10–15	45–50						1–2

* Primary slag from self-fluxing sinters[7] even without FeO or MnO

8.2.5. Effect of Blast Temperature[1-3,9]

We have seen that the formation of a molten slag and its subsequent resolidification can adversely affect gas throughflow and stock descent. Since high blast temperature lowers the slag fusion zone from the belly to the bosh region (Sec. 4.5), the danger lies more in the case of lean ores with high reducibility (very low %FeO) because of the formation of a low-FeO highly viscous primary slag in the bosh incline rather than in the belly.[1-3] This leads to increased viscosity and 'gumminess' of the bosh slag as well as late fusion and consequent late contraction of the material volume in the region. Plant experience shows that it is difficult to use high blast temperatures in the lean ore practice because of the tendency of the furnace to hang.[1-3] Such bosh hangings are removed by lowering the blast temperature (or by decreasing the flame temperature by any means) which moves the fusion zone to a higher level. Easily reducible American Mesabi ore is an example[3] where the furnaces could not take blast temperatures higher than about 450–500°C. The remedy for such ores presumably lies in changing the furnace lines and making a shorter bosh so that even with higher blast temperatures the fusion zone will confine to the belly region.

8.3. Formation of Bosh Slag

The course of bosh slag formation has been discussed in the preceding section as well as in Secs. 3.16–3.18. A reference to Table 8.1 shows that the lime content of the primary slags is low and is on the acid side. This is so because of the belated incorporation of lime in the primary slag. The absorption of lime may be slow but it is continuous and is complete only in the hottest parts, i.e., at the tuyere level. The reduction of FeO in the lower, hotter zones is very fast and is almost complete above the tuyeres (in the axial zone, however, there may be a considerable amount of slag-FeO due to inadequate penetration of the reducing gases). The resulting bosh slag is much more basic than the final slag because the acid constituents of the coke ash are only absorbed when released at the tuyeres. Bosh slag composition may vary widely depending upon the furnace movement as well as on the individual materials charged, namely, iron ore, manganese ores, sinters or fines, or limestone. Lime-coated slag is very frequently found. Iron oxide is usually low (5 percent) but may be as high as 10–20 percent. For graded ore, fluxed or super-fluxed agglomerates, the slag is substantially free from FeO (1–5 percent), about

90–95 percent of the iron having been reduced in the shaft, belly and upper bosh.

The bosh slag basicity is higher the richer the ore (i.e., the lower the slag volume), the higher the coke rate, the higher the sulphur load, the higher the metal silicon, and the higher the coke ash content. On the other hand, the difference between the bosh and final slag basicity is smaller the leaner the ore (i.e., the higher the slag volume). A simple calculation will show the differences. In the following calculations it has been assumed that no reduction of silica occurs and about 70 percent of the coke is burned at the tuyeres, i.e., about 30 percent of the coke ash is released above the tuyere level and is incorporated in the bosh slag.

Case I

(a) Iron ore = 64% Fe; 5.5% SiO_2; final slag basicity CaO/SiO_2 = 1.1; Coke = 600 kg/THM; coke ash = 10% with SiO_2 = 45% in ash.

Taking 92% Fe in pig iron, total ore required per THM is 1437 kg.
Total SiO_2 in ore/THM = 79 kg
Ash in coke = 60 kg and SiO_2 in ash = 27 kg
Total SiO_2 in ore + ash = 106 kg
Total lime to be added as CaO for final CaO/SiO_2 = 1.1 is $106 \times 1.1 = 116.6$ kg
Ash silica released above tuyere = $0.3 \times 27 = 8.1$ kg
Therefore, total silica in the bosh = 79 + 8.1 = 87.1 kg
or **bosh slag CaO/SiO_2 = 116.6/87.1 = 1.338.**

(b) Ash content in coke = 20% and coke consumption = 650 kg/THM

Total ash silica = $0.2 \times 650 \times 0.45 = 58.5$ kg
Total silica = 79 + 58.5 = 137.5 kg
Total CaO for final slag = $137.5 \times 1.1 = 151.25$ kg
Bosh ash silica = $0.3 \times 58.5 = 17.5$ kg
Total bosh silica = 79 + 17.5 = 96.5 kg
or **bosh slag CaO/SiO_2 = 151.25/96.5 = 1.566.**

Case II

(a) Iron ore = 50% Fe; 14% SiO_2; coke = 700 kg/THM
Coke ash = 10% with SiO_2 = 45%; Final slag basicity CaO/SiO_2 = 1.1

Total ore required per THM = 1840 kg
Total silica in ore = 0.14 × 1840 = 257.6 kg
Ash silica = 0.1 × 700 × 0.45 = 31.5 kg
Total silica = 257.6 + 31.5 = 289.1 kg
Total CaO required for final slag = 289.1 × 1.1 = 318 kg
Bosh ash silica = 0.3 × 31.5 = 9.4 kg
Total bosh silica = 257.6 + 9.4 = 267 kg
or **bosh slag CaO/SiO_2 = 318/267 = 1.19.**

(b) Ash content in coke = 20% and coke consumption = 750 kg/THM

Total ash silica = 0.2 × 750 × 0.45 = 67.5 kg
Total silica = 257.6 + 67.5 = 325.1 kg
CaO required for final slag = 325.1 × 1.1 = 357.6 kg
Bosh ash silica = 67.5 × 0.3 = 20.25 kg
Total bosh silica = 257.6 + 20.25 = 287.8 kg
or **bosh slag CaO/SiO_2 = 357.6/287.8 = 1.24.**

It will at once be clear from above calculations that the bosh slag basicity will be higher, the richer the ore and/or the poorer the coke. Although a higher slag basicity is beneficial for sulphur removal, the liquidus temperatures of such slags are higher and therefore normally they are more viscous which may lead to erratic furnace movement and consequently to lower production rate. Usually, the furnace can be made to move more uniformly by the use of MgO if the bosh slag basicity is not too high.

The changes in the composition of the bosh slag for the final slag A are shown by AB for slags of low MgO and AC for high MgO contents (Fig. 3.20). B lies in the field of dicalcium-silicate which is a solid at the operating temperatures. In fact, examples have been quoted[10] where hanging caused by the solid bosh slag has been removed by the incorporation of 8–10% MgO (line AC). The slag C lies in the liquidus field.

The bosh slag basicity is also a function of the final silicon content of iron, since most of the silicon is reduced from silica above the tuyere level. Hence, for a given final slag basicity, the higher the amount of silicon reduced above the tuyeres, the lower will be the amount of silica in the bosh and the higher will be the bosh slag basicity.

The variations in the bosh slag basicities with the slag volume for constant final slag basicities are shown in Fig. 8.2.[11] Account was taken of the increasing coke rate with increasing slag volume.

Taylor[1] has calculated the bosh slag compositions for several hypothetical final slag compositions in order to show the effects of slag weights, 4 levels

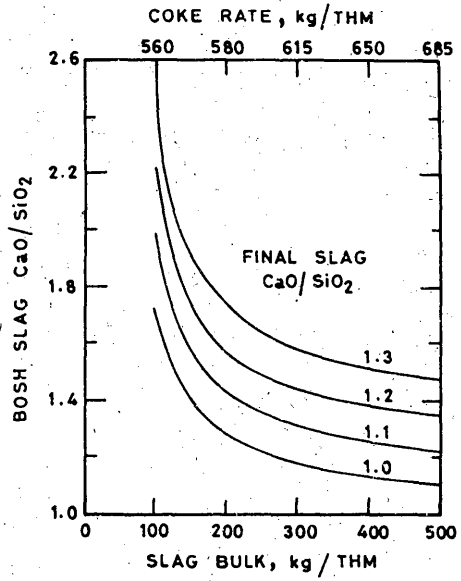


Fig. 8.2 Variation in bosh slag basicity with slag bulk for different isobasicities of the final slag, according to vom Ende and Winzer. (Copyright Verlag Stahleisen).

of alumina and 2 levels of magnesia contents on the liquidus temperatures of the slags. Table 8.2[1] shows three different bosh slag compositions A, B and C for each final slag having volumes of 250 kg, 500 kg and 1000 kg/THM respectively. The coke rate assumed in each case is 550 kg, 600 kg and 700 kg/THM respectively, the coke ash being 10 percent with 70 percent of alumina and silica in the ratio of 40:60. The desulphurizing capacities of the final slags are similar. The values, calculated from Eq. 9.14 have been introduced by the author. The viscosities range between 2–4 Poise at 1500°C.

Table 8.2 shows the deleterious effects of low and medium alumina (in cases of low slag weights) on the liquidus temperature of the bosh and, therefore, of primary slags. High alumina slags also have the same effect but their liquidus temperatures and those of the final slags are not very different. The disadvantage of the high alumina slags lies in their high liquidus temperatures. Although MgO has very little effect on the liquidus temperature of high alumina slags, it substantially lowers the liquidus in the low and medium alumina ranges. We have seen in the case of lean ore practice that high indirect reduction, high slag weight and high alumina are disadvantageous. In the case of super-fluxed sinters (in the absence

Table 8.2.[1] Calculated bosh slag compositions for given final or hearth slags

Slag	Composition				Liq. Temp.	Basicity		(%S)/[%S]† for γ'_s = 5
	CaO	MgO	Al_2O_3	SiO_2	°C	CaO/SiO_2	B*	
Final I	47	4	10	39	1400	1.205	1.296	90
Bosh A	52.6	4.5	4.7	38.2	1550	1.377	1.517	175
Bosh B	50.2	4.4	7.0	38.3	1500	1.311	1.416	129
Bosh C	49	4.1	8.3	38.7	1490	1.292	1.369	112
Final II	44	4	16	36	1435	1.222	1.274	85
Bosh A	49.6	4.5	10.7	35.2	1550	1.41	1.507	169
Bosh B	47.2	4.4	13.0	35.3	1470	1.334	1.419	130
Bosh C	46.0	4.1	14.3	35.7	1450	1.288	1.352	107
Final III	41.5	4	22	32.5	1490	1.279	1.254	80
Bosh A	47.1	4.5	15.7	31.7	1500	1.485	1.540	187
Bosh B	44.8	4.4	10	31.8	1500	1.408	1.437	138
Bosh C	43.5	4.1	20.3	32.1	1490	1.355	1.371	113
Final IV	39	4	28	29	1500	1.345	1.293	89
Bosh A	44	4.5	24.5	27	1510	1.629	1.582	212
Bosh B	42	4.4	26.2	27.4	1510	1.537	1.48	157
Bosh C	40.6	4.1	27	28.3	1510	1.434	1.381	117
Final V	41.5	10	10	38.5	1400	1.077	1.276	85
Bosh A	46.2	11.2	4.7	37.9	1550	1.218	1.482	157
Bosh B	44.1	10.7	7.2	38.0	1470	1.160	1.392	121
Bosh C	43.2	10.4	8.3	38.1	1440	1.134	1.355	108
Final VI	39	10	16	35	1430	1.114	1.285	87
Bosh A	42.7	11.2	11.5	34.6	1465	1.234	1.460	148
Bosh B	41.4	10.7	13.2	34.4	1445	1.212	1.378	115
Bosh C	40.7	10.4	14.3	34.6	1435	1.176	1.367	110
Final VII	36.7	10	22	31.5	1465	1.158	1.296	90
Bosh A	40.0	11.2	17.6	31.2	1445	1.282	1.472	153
Bosh B	39.0	10.7	19.0	31.3	1445	1.246	1.415	129
Bosh C	38.0	10.4	20.2	31.4	1450	1.210	1.366	111
Final VIII	33.5	10	28	28.5	1520	1.175	1.272	84
Bosh A	37.3	11.2	24.8	26.7	1500	1.397	1.527	180
Bosh B	35.8	10.7	26.2	27.0	1510	1.325	1.438	138
Bosh C	35.0	10.4	27.0	27.3	1515	1.282	1.383	117

B* = (%CaO + 0.7%MgO)/(0.94%SiO_2 + 0.18%Al_2O_3).

† $\log (\%S)/[\%S] = 1.3B^* + \log \gamma'_s - 0.43$ (cf. Eq. 9.14). Slags A,B,C correspond to 250;500 and 1000 kg/THM. Final slag composition of 2 levels of MgO and 4 levels of Al_2O_3 were selected having the same desulphurizing power. Coke ash assumed was 10% (with 70% of SiO_2 + Al_2O_3 in the ratio of 60:40). Coke rates were 550, 600 and 700 kg/THM for slag rates given above respectively. Assumed Si content of iron was 0.5%. Viscosity of final slag ranged between 2 to 4 Poise.

of FeO and the composition of bosh slag approaching the calculated one), it is the low slag weights and low alumina which are likely to cause trouble. An increase in magnesia to 10 percent lowers the liquidus temperature considerably.

The basicity and liquidus temperature of bosh slags have an influence on the final metal sulphur. We will see in Chapter 9 that low slag weights, i.e., high bosh slag basicities aid desulphurization. This is also apparent from Table 8.2. In each case, bosh slag A which has the highest basicity possesses the greatest desulphurizing potential. Iron made with such slags should possess the lowest sulphur content. For the same reason, low-silicon iron can be made with such slags when using very high blast temperatures (Sec. 7.4.2.2).

8.3.1. Bosh Slag Viscosity and Material Flow

Furnace productivity depends greatly upon the free flow of gases through the coke grid above the raceway against the mass of liquid metal and slag flowing downwards. The resistance to flow of gases increases with the viscosity and volume of the slag (Sec. 5.6). This is accentuated in the blast furnace process where the composition and the physical properties of the slag are continually changing at different levels.

A uniform furnace operation can only be maintained if the bosh slag is fluid which can be ensured by the presence of large amounts of FeO. In this respect hard-burnt sinter of low reducibility mixed with highly reducible ore or sinter should be helpful. However, the use of highly reducible fluxed sinters has been so successful that the trend at present is rather to work with fluxed or super-fluxed sinters. One of the difficulties of using fluxed sinter is its susceptibility to breakdown at temperatures 400–600°C at a basicity ratio of 1–1.5. From this point of view a mixture of proper proportions of acid and highly basic sinters in the charge will be beneficial.

The performance of large modern furnaces shows clearly that with FeO even as low as 1–5 percent in the bosh slag, the blast furnace operates smoothly. This is because the fluidity is not the only criterion for smooth gas flow but the furnace volume the slag occupies in the vertical cross-section plays an equally or more important role. Basic slags melt at higher but in a narrow range of temperatures and pass rapidly from the solid to liquid state. Therefore, the volume of the bosh occupied by the liquid slag is much smaller than in cases where the slag is acid or carries more FeO. The motion of the gases through the voids in the coke grid is facili-

tated because of the smaller distance it has to bubble through although the slag itself may be more viscous. The overall hydraulic resistance of the charge column is much lowered (cf. Eq. 5.22). The presence of MnO and/or MgO helps to keep the slag fluid in any practice.

An advantage of fluxed sinters over ores or acid sinters is that in the latter cases the incorporation of lime in slags originating from them occurs late which makes quality control more difficult because of local irregularities in the bosh slag composition.

8.3.2. Importance of Bosh Slag

The properties of the bosh slag are of utmost importance for furnace productivity and metal quality. The more important properties are:

(i) high fluidity: it ensures free movement of the bosh gas through the coke grid (cf. Sec. 5.6);
(ii) narrow fusion range: it lowers the pressure drop in the lower furnace (cf. Eq. 5.22);
(iii) high fusion temperature: for adequate pre-heating before entry of the smelting products into the hearth (high residence time of slag in the bosh);
(iv) high basicity: for low-Si low-S iron (cf. Secs. 7.4.2.2 and 9.4.1); addition of MgO to thin any excessively limey slag;
(v) items (ii–iv) above permit the use of highest blast temperatures without affecting the metal silicon or smooth furnace operation.

8.4. Final or Hearth Slag

As already mentioned, the hearth slag is formed on dissolution of the lime which was not incorporated in the bosh and on absorption of the coke ash released during combustion. The formation is more or less complete in the combustion zone. This slag runs along with the molten iron into the hearth and accumulates there and forms a pool with the molten metal underneath. During the passage of iron droplets through the slag layer, the slag reacts with the metal and a transference of mainly Si, Mn and S occurs from or to the metal, tending to attain equilibrium between themselves as far as possible (Secs. 3.12–3.15).

The nature, composition and bulk of the hearth slag ultimately control the composition of the pig iron and the productivity of the blast furnace. It should be noted that the most important purpose of slag control is the control of sulphur, since sulphur is the key to iron quality. It is

uneconomical to produce a low-P, low-Si and high-S iron. There is a wide range of slag composition in terms of CaO, SiO_2, Al_2O_3 and MgO, where the slag is a homogeneous liquid of low viscosity at the hearth slag temperatures (1450–1500°C) but the difficulty arises when the slag has to have certain minimum basicity and bulk for the control of sulphur. The use of optimum slag composition would give minimum sulphur in iron and minimum slag volume, resulting in maximum production and minimum fuel costs.

It is now required to consider the various aspects of proper choice of slag constituents for obtaining an effective hearth slag for the desired iron quality and efficient furnace production.

8.4.1. Liquidus Temperature and Viscosity

In order that a blast furnace slag be practicable and most effective, it must be a completely homogeneous liquid at the operating temperatures. It must also have sufficient fluidity so that it can run out of the hearth freely without any loss of production time.

As sulphur is the key to iron quality and the basicity of the slag is the key to low sulphur iron, it is important to ascertain the limitations of the basicity on slag properties. We are aware that the viscosity decreases with increasing basicity while, on the other hand, the melting temperature of the slag increases with increasing lime content. Therefore, the permissible slag basicity is limited by the provision of adequate fluid properties of the slag at the hearth temperatures. The liquidus temperature of the hearth slag should be below the desired minimum slag temperature because the appearance of any crystalline phase may result in a sharp increase in viscosity if the slag temperature is close to the liquidus temperature.

The hearth slag belongs mainly to the $CaO\text{-}SiO_2\text{-}Al_2O_3$ and $CaO\text{-}MgO\text{-}SiO_2\text{-}Al_2O_3$ systems and the relevant liquidus temperatures can be seen from Figs. 3.18 and 3.20. For the latter system, Osborn et al.[12] have measured the liquidus temperatures at various alumina levels from which the optimum slag compositions based on an assumed slag liquidus temperature of 1500°C and maximum desulphurization power, at intervals of 5 percent alumina, can be deduced. They also assumed that the liquidus temperatures of the actual slags are about 100°C lower because of the fluxing action of the minor constituents like MnO, FeO, TiO_2, S, etc. The optimum slag compositions from the point of view of sufficient slag fluidity and desulphurization at 1500°C are shown in Table 9.3 and discussed in Sec. 3.18.

However, a comparison of the measured liquidus temperatures of some slags studied by Baldwin[13] with the values obtained from the four-oxide diagrams show that the measured values lie, on average, only 10°C lower than the calculated ones. Therefore, the Osborn diagrams can only be used with confidence for selection of the blast furnace slag compositions if the calculated liquidus temperatures of the selected slags are lower than 1500°C. But how much lower, as a safeguard against operational fluctuations of the hearth temperature and slag composition which might result in the appearance of crystalline phases, requires investigation.

Recent data[13,14] obtained from measurements of temperatures of flushing slags (slag notch), roughing slags (iron notch) and that of iron show that while the liquidus temperatures of both the former are the same, the actual temperatures of the flushing slags are about 100°C higher than the roughing ones and the temperatures of the roughing slags about 10°C higher than those of iron (about 1435°C). On an average, the temperature of the flushing slag is about 1500°C. To avoid the appearance of crystalline phases, it is essential that the liquidus temperature of the slag lies below the mean roughing slag temperature, i.e., below about 1445°C, so that there is a reasonable assurance that in most cases the temperatures of the slags inside the furnace would be well above the liquidus temperature.

If any periodical fluctuation in temperatures takes the slag temperatures to below the liquidus, it may result in an increase in the viscosity and appearance of crystals. As discussed in Sec. 3.18, melilite is the primary phase in most of the slags and di-calcium silicate, merwinite and even periclase may separate out from slags of extreme compositions. The sulphur carrying capacity of the residual acidic liquid being low, the sulphur distribution coefficient of operational slags with the calculated liquidus temperatures exceeding 1450°C may be variable and lower than those for slags of a corresponding basicity but with liquidus temperatures below 1450°C (Sec. 3.18).

Osborn et al.[12] assumed that, for the slag to run freely, it should be above its liquidus temperature. The basicity ratio $(CaO + MgO)/(SiO_2 + Al_2O_3)$ determines the slag viscosity above the liquidus and it is progressively lower as the basicity increases. The term *above the liquidus* is to be noted since the melting point of the slag may increase with increasing lime content. The mutual influence of silica and alumina on slag viscosity is apparent from Sec. 2.9.

The selection of slags should be based on the calculated liquidus temperature of about 1450°C from the Osborn diagrams, keeping in mind

the basicity for proper desulphurization (Chapter 9). Unless direct viscosity and liquidus measurements are available, this would provide sufficient safety for any periodical unintentional variations in the temperature and composition of the slag which may occur in practice.

The selection of the final slag composition should be made bearing in mind the composition, liquidus temperature, basicity and viscosity of the bosh slag. The importance of the bosh slag has already been seen in Sec. 8.3.2.

A special mention needs to be made regarding the difficulties with Indian raw materials. An important factor for Indian conditions is the very high content of alumina in the blast furnace slags. While the Indian ores may have alumina/silica = 2–3:1, the coke ash which is rather high, about 25 percent, has high silica and low alumina (alumina/silica = 0.5). The resulting slag contains 25–30 percent alumina, with high viscosity and liquidus temperatures. Normally, a good, fluid slag is obtained when the alumina in slag is around 10–15 percent. There are, however, furnaces in UK and USSR working with alumina as high as 20 percent. The raising of the hearth temperature for lowering the slag viscosity results in a simultaneous increase of silicon in iron which renders the iron incapable of being used directly for steelmaking especially because of the presence of about 0.3% P in the Indian irons. It is, however, possible to obtain a fluid slag with requisite viscosity and desulphurizing power by the addition of dolomite in the flux charge which will give 8–10% MgO in the slag. For foundry irons with 3% Si, the slag temperature requirement is higher and the corresponding MgO in the slag may be lower (5–6%). Two typical slags capable of producing basic pig iron (1% Si, <0.05% S, 1% Mn and 0.3% P)

Table 8.3.[15] Two typical slags for producing basic and foundry grade irons under Indian raw material conditions

Slag composition	Basic iron	Foundry iron
% CaO	34	27
% MgO	9	6.2
% SiO_2	31.5	32
% Al_2O_3	22	22
$(CaO + MgO)/(SiO_2 + Al_2O_3)$	0.80	0.80
$(CaO + MgO)/SiO_2$	1.37	1.04

and foundry grade pig iron (3% Si) as suggested are shown in Table 8.3.[15]

It is also possible to operate with fluid slags high in alumina when the alumina/silica ratio in the slag is 2:1 (cf. Sec. 3.17). Although Indian ores have high content of alumina, the cokes contain high silica (52%) and low alumina (28%) in the ash. These make it impossible to obtain an alumina/silica ratio of 2:1 in the slag unless the coke silica can be reduced or a major portion of coke replaced by silica-free fuels.[16]

8.4.2. Practical Slag Composition

Depending upon the sulphur load, a satisfactory desulphurization can be obtained generally with $(CaO + MgO)/(SiO_2 + Al_2O_3) = B$ between 0.90 to 1.10. Slags of basicity of this range and of adequate viscosity are shown in Tables 8.2, 9.4 and 9.5. It should, however, be noted that in day-to-day practice it is difficult to control closely the basicity ratio B since the four oxides do not vary proportionately with the change in raw materials. Where alumina input from ores is low and it comes mainly from the coke ash, the alumina plus magnesia becomes more or less fixed and the furnace operators are left to work practically with the lime/silica ratio, varying the lime as the silica in the ore changes. Hence it is difficult to work[17] with a fixed B.

When working with only a fixed CaO/SiO_2 ratio, any decrease in silica of the ore means charging of less CaO but the percentage of alumina in the slag (coming mainly from the coke ash) would increase, rendering it necessary to increase the hearth temperature for obtaining a fluid slag – the slag thus becoming less suitable for producing low-Si low-S irons. When working with a fixed B, the amount of lime to be reduced for keeping B fixed, when silica in the ore decreases, is not as much as in the case of a fixed CaO/SiO_2 ratio and hence the slag will remain sufficiently fluid.

8.5. Slag Composition and Utilization

In addition to restrictions on slag composition imposed by the furnace operational requirements, there is a further restriction by the slag users for blast furnace aggregates and cement making.

8.5.1. Blast Furnace Aggregate[13,14,18]

Slags which are used for aggregates should be free from lime unsoundness. As seen in Sec. 3.19, 'dusting' is caused by the breakdown of slag when the lime content exceeds certain limits causing crystallization of dicalcium silicate. Under certain conditions, the crystallized dicalcium silicate is stabilized in its high temperature β-form and therefore does not transform at low temperatures to the γ-form which causes volume expansion and consequently dusting.

There are some recognized standards based on chemical analysis of slags which should be free from 'dusting', the most rigorous of which being:[18]

$$\%CaO < 0.9\%SiO_2 + 0.6\%Al_2O_3 + 1.75\%S$$

Giedroyc et al.[14] used this formula for calculating the maximum permissible basicities of slags which should be free from lime instability. From the table put forward by them, it can be seen that below 17 percent alumina in the slag, the basicity is restricted by lime instability and above 17 percent alumina, the operational requirements restrict the slag basicities. However, in either case, slag basicities above 0.9 can be achieved by increasing the MgO content of the slags. Their table also contains the composition of some slags with high desulphurizing power and stability as well.

8.5.2. Blast Furnace Cement

Blast furnace slags having at least 12 percent alumina, provided they remain a glass after quenching, are suitable for cement making. For good hydraulic properties, there should not be any crystals present while quenching. In other words, the slags must be a true liquid, i.e., the slag temperature must be above the liquidus temperature before they enter the quenching plant. There should not be any difficulty with flushing slags since they are on an average at a temperature about 100°C higher than the liquidus and would quench to glass without crystallization. Roughing slags, on the other hand, are only 20–50°C higher than the liquidus and may not be suitable for cement, especially when they come out immediately after opening the iron notch. Initially, they are usually cold and viscous, with the possibility of the presence of crystals.

Some Russian works as mentioned by Baldwin[13] suggest that with high alumina slags (30–50%) it is necessary, in order to obtain hydraulic properties, to have crystals present in the slag after quenching. That means, that the slag should have a temperature below the liquidus before it enters the quenching plant.

For further details in this subject, the works of Keil,[19] Lee[18] and Kühl[20] may be referred to.

References

1. TAYLOR, J.: J. Iron Steel Inst., Sept. 1962, p. 701–703.
2. TAYLOR, J.: op. cit., 164, 1950, p. 129.
3. TAYLOR, J.: Ironmaking, Met. Progress-3, Iron and Steel, London, 1953, p. 2–22.
4. HAY, R.: J. West Scot. Iron Steel Inst., 49, 1941–42, p. 89.
5. SCHRADER, H.: Arch. Eisenhuttenw., 22, 1951, p. 275.
6. BARDIN, I. P. et al.: Academy of Sciences, SSSR, 1951.
7. POTEBNYA, Yu. M. and T. I. LITVINOVA: Stal, 1959, p. 485.
8. STRUVE, G. v.: J. Iron Steel Inst., Sept. 1960, p. 50–56.
9. KOZLOVICH, I. Z.: Stal, Nos. 4, 5, 6, 1929; Leningrad Research Inst., 6, 1938, p. 123–132.
10. LOWING, J.: Ironmaking Steelmaking, 5, 1978, p. 239–252.
11. ENDE, H. v. and G. WINZER: Stahl u. Eisen, 84, 1964, p. 1366–1380.
12. OSBORN, E. F. et al.: J. Metals, 6, 1954, p. 33–45.
13. BALDWIN, B. G.: J. Iron Steel Inst., 186, 1957, p. 388–395.
14. GIEDROYC, V. et al.: op. cit., 202, 1964, p. 11–22.
15. NIJHAWAN, B. R.: Trans. Ind. Inst. Metals, 16, June 1963, p. 120.
16. RAUSCH, H.: Sym. Pilot Plant, Natn. Met. Lab., Jamshedpur, India, July 1960.
17. HOUGHTON, J. W.: Summ. Proc. 26th Blast Fce. Conf., BISRA, 1958, p. 59–67.
18. LEE, A. R.: Blast furnace and steel slag, Edw. Arnold, 1974.
19. KEIL, F.: Blast furnace slags, Stahleisen, Dusseldorf, 2nd Ed. 1963.
20. KUHL, H.: Cement chemistry, vol. 2, Berlin, 1958.

CHAPTER 9

THE REMOVAL OF SULPHUR

9.1. General

Sulphur is carried into the blast furnace by the burden materials. In coke, the ash contains most of it, in the form of iron sulphide, calcium sulphide as well as organic sulphur. In the ores it is present as iron sulphide and in the fluxes both as sulphide and sulphate. The amount of sulphur brought in by the ores and fluxes is much less compared to that brought by the coke. Depending upon the origin, the ore and the coke may contain sulphur ranging respectively from 0.05–0.10 percent and 0.6–1.5 percent. Thus, while the sulphur brought in by the ores and fluxes may range from 1 to 2 kg/THM, that accompanying the coke may be as large as 4 to 10 kg/THM with a moderate coke rate of around 700 kg/THM. In the blast furnace, most of the sulphur is removed by the slag. Depending upon the sulphur load and the sulphur content of pig iron, the slag may carry as much as 80–90 percent of the total sulphur while about 10–15 percent is removed in the flue dust and top gas, the rest 2–5 percent entering the iron. A typical sulphur balance is shown in Table 9.1.

Table 9.1. A typical blast furnace sulphur balance

Material	Sulphur input		Sulphur output	
	kg	%	kg	%
Coke (1%S) 600 kg/THM	6.0	80		
Charge materials	1.5	20		
Iron (0.03%S)			0.3	4
Flue dust and gas			0.37	5
Slag			6.82	91

During the descent of the stock, the sulphur in the charge materials is absorbed in the shaft and the bosh by the metal and the slag and the final transfer of sulphur from the metal to slag occurs in the hearth. The coke starts giving off its sulphur in the shaft itself.[1-7] Depending upon the character of the coke, about 5–20 percent of the sulphur can be liberated which is aided by an increasing hydrogen content of the stack gas and decreasing size of the coke.[7] The bulk of the coke sulphur is, however, transformed by chemical reactions, mainly during the combustion of coke in front of the tuyeres.

9.2. Chemistry of Sulphur Reactions

Sulphur in iron may be assumed to be present as [FeS] or [S]. Whatever its form may be, it enters the metal from the raw materials, where it is present as sulphides or sulphates, through one or more of the following reactions:

(1) MS (metal sulphide) + Fe = (FeS) (burden) 9.1

(FeS) = [FeS] 9.2

(2) $FeS + 10Fe_2O_3 = 7Fe_3O_4 + SO_2$ 9.3

$SO_2 + 2C = \frac{1}{2}S_2(g) + 2CO$ 9.3a

$[Fe] + \frac{1}{2}S_2(g) = [FeS]$ 9.3b

(3) $CaSO_4 + [Fe] + 3C = [FeS] + CaO + 3CO$ 9.4

(4) $CaSO_4 + 4C = CaS + 4CO$ 9.5

$CaS + FeO = CaO + [FeS]$ 9.6

(5) $CaS + SiO(g) = SiS(g) + CaO$ 9.7

$SiS(g) + 2[Fe] = [Fe\text{-}Si] + [FeS]$ 9.8

In the oxidizing zone before the tuyeres,[8] where the p_{CO_2}/p_{CO} ranges between 0.26–26.0, sulphur is mainly present as SO_2. Farther towards the centre, in the reducing zone, it is present as CS_2 (1600°C). With the fall in temperature near the axis and in the upper levels where $p_{CO} \gg p_{CO_2}$, the sulphur in the gas is mainly in the form of COS and H_2S. The following reactions can occur before the tuyeres:[9]

Gasification of coke sulphur:

$$0.5S_2 + O_2 = SO_2;$$
$$SO_2 + C = 2CO + 0.5S_2;$$
$$SO_2 + 2C = 2CO + CS;$$

In the reducing zone:

$$SO_2 + 1.5C = 0.5CO_2 + COS$$

When natural gas is present:

$$SO_2 + 3H_2 = 2H_2O + H_2S$$
$$SO_2 + CH_4 = CO + H_2O + H_2S$$

Sulphur reaction has already been discussed in Secs. 3.14, 3.15 and 7.7. Assuming, in the first instance, that sulphur removal from the metal to slag occurs according to reverse of Eq. 9.6, i.e.,

$$[S]_{Fe} + (CaO) = (CaS) + (FeO) \quad 9.9$$

$$K = \frac{a_{CaS}.a_{FeO}}{a_{[S]}.a_{CaO}} \quad 9.10$$

or,

$$K' = \frac{(\%S).a_{FeO}}{[\%S].\gamma'_s.a_{CaO}} \quad 9.10a$$

The sulphur distribution ratio, η_s, is given by (cf. Eq. 9.10a),

$$\eta_s = (\%S)/[\%S] \propto K' \frac{\text{basicity}}{\text{oxygen potential}} . \gamma'_s \quad 9.11$$

From Eq. 9.11, η_s will be higher,

(i) the higher the slag basicity

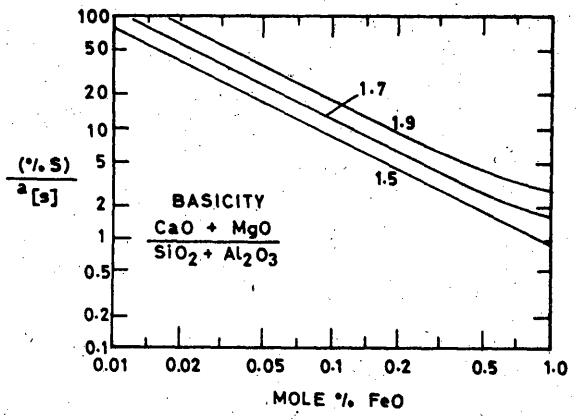


Fig. 9.1 Influence of basicity and iron oxide content of slag on the distribution of sulphur between slag and metal.[10,11]

(ii) the higher the γ'_s

(iii) the lower the oxygen potential of the slag.

Figure 9.1, reassembled by Ward[10] from the results of Rocca et al.,[11] shows the influence of oxygen potential (FeO content of slag seldom exceeds 1 percent in the hearth slag) and basicity on the equilibrium sulphur distribution ratio $(\%S)/a_{[S]}$. The ratio increases as the FeO-content decreases and/or the basicity increases. The η_s depends upon the composition of the metal, i.e., on γ'_s, which increases greatly in the presence of Si, P and C (Fig. 2.2).

The oxygen potential is controlled by the carbon and/or silicon and manganese reactions (Secs. 3.14–3.15). We can write the overall desulphurizing reaction as

$$[S] + (CaO) + C = (CaS) + CO \qquad 9.12$$

Taking $a_C = 1$ and $p_{CO} = 1$ atm., we can write

$$\eta_s = \frac{(\%S)}{[\%S]} \approx K' \times \text{basicity factor} \times \gamma'_s \qquad 9.13$$

Sulphur reaction has been studied by various workers[11–20] and for our purpose we would employ the most used equilibrium relationship which gives values similar to those of others. This relationship, given by Kalyanraman et al.[14] and valid for slag sulphur up to 1.5 percent, is:

$$\log (\%S)/[\%S] = 1.3B^* + \log \gamma'_s - 0.43 \qquad 9.14$$

B^* = basicity index

$$= \frac{\%CaO + 0.7\%MgO}{0.94\%SiO_2 + 0.18\%Al_2O_3} \qquad 9.14a$$

The distribution ratio given by Giedroyc et al.[15] is,

$$\log (\%S)/[\%S] = 1.60 \frac{(\%CaO + \%MgO)}{(\%SiO_2 + \%Al_2O_3)} - 0.38 + \log \gamma'_s \qquad 9.15$$

The actual sulphur ratio in the blast furnace ranges usually between 20–50 percent of the equilibrium values given by Eq. 9.14, for reasons discussed in Secs. 3.14–3.15.

It appears the temperature has little effect on the equilibrium relation. The rate of desulphurization, however, increases with temperature and slag basicity. Eq. 9.14a shows that wt.% silica is about 5 times more effective than alumina in decreasing the desulphurizing capacity of the slag and MgO is 0.7 times as effective in increasing it compared to lime.

9.3. Sulphur Reactions in the Shaft

The sulphur movement in the shaft comprises of liberation of sulphur from the coke and its absorption by the burden components from the gases.

Sulphur liberated by chemical or gasification reactions enters the gas phase as compounds or as vapour and combines with the burden components. About 50–70 percent of the coke sulphur enters the gas phase before the tuyeres, the rest having been already liberated in the upper regions. Therefore, a major amount of the coke sulphur is carried by the ascending tuyere gas, an overwhelming portion of which is absorbed by the descending burden and reduced iron, the relative amounts depending upon the nature of the burden material like, Mn-ore, limestone, sinter, pellet – the absorption by the burden being more the higher the basicity. Analysis of iron samples taken from not far below the stock level shows[3,4] 0.2–0.4%S and further down the iron analysis has shown[21] even as high as 0.9%S.

The pattern of sulphur removal in the blast furnace is shown schematically in Fig. 9.2. Sulphur both in the slag as well as in the metal increases continuously up to the tuyere level. In front of the tuyere zone there is a slight decrease of iron sulphur because of oxidation to SO_2 (Fig. 7.21). Thereafter, the iron sulphur decreases greatly in the hearth up to the iron

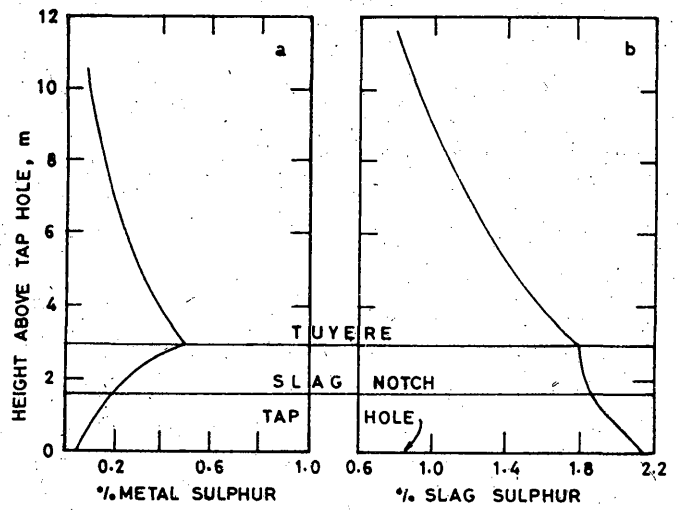


Fig. 9.2 **(a)** Variation of metal sulphur along the furnace height (author); **(b)** variation of slag sulphur along the furnace height (Galatonov and Chernyatin).[22]

notch. The sulphur in the slag increases only a little in the tuyere zone because of an oxidizing atmosphere. Thereafter, there is a rapid rise of sulphur in slag between the slag notch and the tap hole[22,23] (Fig. 9.2b).[22]

In ordinary operations the gas phase contains about 0.4 gm.S/Nm³. In the case of fuel oil injection it is about 0.6 km.S/Nm³ but the final sulphur in iron does not decrease. Most of the gasified organic sulphur leaves with the top gas.[24]

9.4. Sulphur Reactions in the Bosh

Above 1100–1200°C, the formation of primary slag starts with the softening, melting and absorption of flux by the gangue. Thus, a separation of the slag and metal begins in the semi-liquid state which reaches completion when the slag and the metal are both completely molten. Limestone also dissociates in this region and the lime absorbs some of the sulphur. About 2%S has been detected in lime samples from this region.[25] As lime dissolves, sulphur absorption increases with the rise in the basicity of the primary slag. The metal and the slag in their spongy and viscous states absorb in the primary slag formation zone most of the sulphur liberated from the coke and that present in the gas and they do so according to their

absorption capacities, which depend greatly on the lime and the FeO-content of the slag (Eq. 9.6).

Iron samples from the region between the tuyere and the bosh show sulphur contents[5,26,27] ranging from 0.05–0.5 percent, the lower values being obtained when the bosh slag has high basicity and low FeO. Such reducing slags are obtained at places with increasing horizontal distance from the tuyere nose since the tuyere gas is more reducing, the farther away it is from the nose (cf. Fig. 7.15). It is more so with hydrogen-bearing additives. As a corollary, because of a more reducing atmosphere prevailing in the regions between the neighbouring tuyeres, the sulphur in iron will be lower in these regions.[27]

A considerable amount of sulphur (2 percent or even more) can be absorbed by the bosh slag if it is sufficiently basic and reducing. At constant sulphur load, this means that the higher the sulphur absorption by the bosh slag the lower will be the sulphur in iron. Since desulphurization is never complete in the bosh region and reaches finality only in the hearth, it is obvious the higher the sulphur in the bosh slag, the lower will be the load on the hearth slag for the final desulphurization of iron. Therefore, for efficient desulphurization, the primary importance should be attached to the formation of a fluid, highly basic and reducing bosh slag.

According to Tsuchiya et al.,[28] sulphur in iron in the bosh zone can be removed to the gas phase as S_2 or CS_2 and to the slag phase as sulphides by the gaseous alkali and alkaline earth metals produced at high temperatures.

9.4.1. Importance of Bosh Slag

The final sulphur in iron depends greatly upon the character of the bosh slag. Apart from its fluidity, the major role is played by the basicity and FeO content. Since the basicity of the bosh slag is directly related to slag bulk, especially for iron-rich burdens, and the basicity increases with decreasing slag bulk (Fig. 8.2), it is obvious that a very good desulphurization can be obtained with low slag quantities, as is being experienced at present in various blast furnaces. The influence of iron in slag and that of the slag volume and basicity are discussed below.

9.4.1.1. Slag iron

Since sulphur transfer to the bosh slag is facilitated by low FeO content, the materials in the shaft should reach the bosh zone sufficiently reduced. This presupposes a good reducibility of the ore, if necessary obtained by

crushing to smaller size, narrow sizing for good permeability, use of coke and ore of sufficient strength and abrasive resistance, use of prefluxed sinters and pellets, use of hydrogen-bearers, etc. An increased reducibility means a lower endothermal direct reduction and a hotter hearth which increases the rate of sulphur transfer from metal to slag (Sec. 3.15). Starsinov et al.[23] cite an experiment with 3 different burdens with increasing basicity where sulphur removal by the slag up to the tuyere level increased with increasing basicity. This may have been partly due to an increased reducibility of the sinters with increasing basicity.

In most of the experiments with fuel oil injections, it has been found that desulphurization does not deteriorate and in many cases it has rather improved although the oil contains more sulphur (~3%) than does the coke. This can be traced to the higher degree of indirect reduction obtained by the powerful reducing action of hydrogen, more uniform operation with fuel oil and stabilization of the thermal state of the hearth. It is reported[29] that the sulphur distribution ratio between the slag and metal is 1.2 times higher in the case of fuel oil injection than without oil.

9.4.1.2. Slag volume and basicity

We have seen in Fig. 8.2 that, for the same basicity of the final slag, the bosh slag basicity increases as the slag volume decreases. It is obvious,

Table 9.2. Approach of sulphur distribution ratios to equilibrium in three steel plants

Steel-works	Slag bulk kg/THM	log γ_s'	(S)/[S] Theor.	(S)/[S] Actual	% appr. to equil.	Final slag basicity (Eq. 9.14a)
Stelco	329	0.85	82	28	34	1.14
(OH iron)	252	0.85	104	49	47	1.24
	168	0.83	107	83	78	1.25
Italsider	355	0.74	106	54	51	1.32
(OH iron)	275	0.76	114	54	47	1.33
	201	0.79	108	72	68	1.28
Mannesmann	558	0.69	101	23	23	1.34
(Thomas iron)	382	0.68	99	31	32	1.34
	327	0.69	106	35	33	1.36

therefore, that desulphurization should increase with decrease in slag volume as corroborated in Table 9.2. Because of increased basicity the slag would absorb more sulphur and thereby decrease the sulphur content of iron above the tuyere level and hence lighten the load of the hearth slag from its desulphurizing work. Table 9.2 shows the approach to equilibrium in percent with decreasing slag bulk in three different steel works.[30] Above 300–400 kg slag/THM, the approach to equilibrium is less than about 40 percent. The percentage increases rapidly below a slag bulk of 300 kg. The equilibrium sulphur distribution ratios have been calculated by Eq. 9.14.

Although a rich ore with lower slag bulk results in an increased bosh slag basicity and, therefore, in an increased desulphurization, the process is limited by the increasing liquidus temperature of the slag with increasing basicity. In the CaO-Al_2O_3-SiO_2 system, the viscosity rises with increasing CaO/SiO_2 from the minimum at a ratio[31,32] of 1.35. An increased refractoriness of the bosh slag results in disturbed stock movement and bosh hanging. The cause of the non-uniform stock descent and hanging can be traced to resolidification of the fluid FeO-rich highly basic bosh slag whose melting temperature increases progressively with the rapid reduction of slag-FeO as the slag flows over the incandescent coke.

Even if, from the standpoint of desulphurization a reduction in the slag bulk (i.e., enrichment of the ore) is permissible in specific cases, a lower limit is set because of operational difficulties and consequent loss of production. However, the slag bulk can be reduced and the bosh slag basicity lowered if, simultaneously, the coke rate and/or coke ash could also be reduced. In this respect, the use of silica-free fuels such as fuel oil or natural gas should be ideal. It has indeed been seen that very low sulphur iron could be produced even when using fuel oil having 2–3% S.

Even if the desulphurizing capacity of a slag is very high, the extent of desulphurization depends also upon the solubility of sulphur in the slag which has been discussed in Sec. 9.5.1.2. If the solubility limit is reached, the only way to achieve low sulphur in iron is to increase the slag bulk.

9.4.1.3. Importance of pre-fluxing

We can conclude that the bosh slag plays a paramount role in the removal of sulphur. If the slag is fluid and highly basic containing little FeO, an extensive mass exchange of sulphur can occur when the sulphur-laden gases churn through the emulsified foamy slag dripping through the coke grid. If the slag is viscous, it may be made fluid by increasing the

manganese input. If a low-Mn iron is sought for, the slag should be made thin by MgO.

In the case of raw ore or acid agglomerate plus limestone burden, the lime dissolution in the belly and the bosh is slow and hence the slag formed therein is less basic than when the lime is incorporated in the burden itself as happens when pre-fluxed agglomerates are used. We have seen such burdens give a highly reduced fluid bosh slag of uniform and high basicity and promote a smooth furnace operation, which are ideally suited for an efficient mass exchange of sulphur.

According to Yupko et al.,[33] the use of 100% sinter of basicity 1.19–1.26 results in active sulphur absorption by the slag all over the path of its formation and increases the (S)/[S] ratio which approaches closer to equilibrium.

9.5. Sulphur Reactions in the Hearth

On leaving the tuyere zone the liquid iron droplets trickle down through the hearth slag. The final metal sulphur depends upon the extent of exchange of sulphur between the iron droplets and the hearth slag during the passage of the former through the latter and, therefore, upon:

(i) sulphur reaction rate of the slag;
(ii) reaction surface between slag and metal;
(iii) contact time;
(iv) slag composition;
(v) slag bulk, slag basicity and sulphur load;
(vi) metal composition;
(vii) slag and metal viscosities.

These and others are discussed hereafter.

9.5.1. Reaction Rate[7,18,34–37]

The reaction rate of sulphur transfer from metal to slag depends upon various factors, they being mainly, viz.,

(i) basicity and temperature of slag;
(ii) slag bulk;
(iii) contact surface and time.

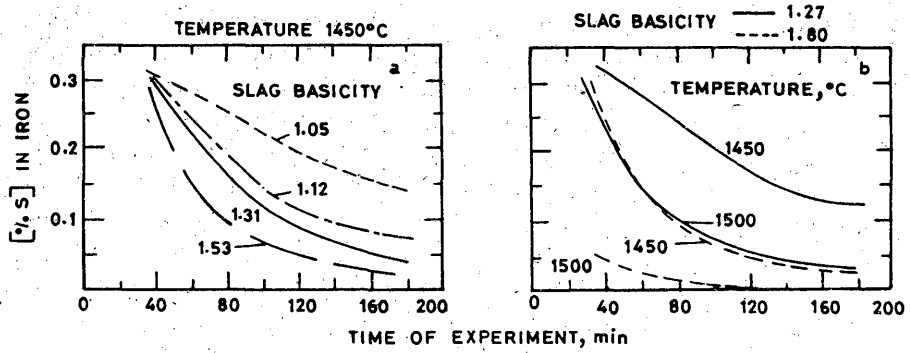


Fig. 9.3 (a) Variation of sulphur in iron with experimental time for different slag basicities at constant temperature; (b) influence of temperature on sulphur in iron at two levels of slag basicities. After Neuhaus et al.[7] (Copyright Verlag Stahleisen).

9.5.1.1. Slag basicity and temperature

Laboratory experiments show that the sulphur transference rate increases with increasing basicity and temperature of the slag. Fig. 9.3[7] shows the influence of basicity and temperature on desulphurization of pig iron where the greater effect of temperature than of the basicity is at once apparent. An increase of temperature from 1450 to 1500°C for a slag basicity of $B^* = 1.27$ (Eq. 9.14a) has the same effect as an increase of basicity to $B^* = 1.80$. Apart from basicity, the absolute contents of alumina and magnesia also affect the rate.

We have seen in Sec. 3.15, the sulphur transfer rate depends upon the manganese reduction rate according to $2(MnO) + [Si] = 2[Mn] + SiO_2$. The manganese reduction rate is increased by higher temperatures, higher basicity (higher γ_{MnO}) and higher MnO content of the slag.

9.5.1.2. Slag bulk

It is to be expected that with richer ores and decreasing slag bulk per THM, the desulphurization rate should decrease because of an increased sulphur concentration in the slag (smaller quantity of slag carrying the same amount of sulphur from iron). However, it has been shown that the extent of desulphurization with time is not influenced by the slag bulk at each basicity level.[7] The determining factor appears to be the sulphur exchange rate which is affected very little by sulphur transport inside the slag phase.

In this context a study of the solubility of sulphur in slag appears to be important. Although solubility values of 3.5–5 percent sulphur have

been quoted,[13,38] they are considerably higher than those found in practice where usually the range is between 1.5 to 2.5% S. As the solubility of sulphur in slag decreases with temperature, the sulphur content of colder slags (Thomas iron slags) should be low since if the solubility is exceeded calcium sulphide will start crystallizing out at lower temperatures. The slag will become viscous, will be apt to carry metal droplets and the furnace operation will be disturbed.[39] The average S-content of Thomas slag should not therefore exceed 1.8–2 percent. The furnace can be corrected by increasing the slag temperature which, on the other hand, is likely to increase the Si-content of the metal. An increase in the slag bulk appears to be the only other solution when the sulphur load is high. This may be the reason why the open-hearth iron, which is smelted at higher temperatures (more silicon in iron), shows a higher sulphur content of the slag.[40]

9.5.1.3. Contact time and surface

The contact surface between the iron and the slag appears to be of considerable importance and, within wide limits, a rate determining factor. Sulphur transference increases with increasing phase contact surface and this has some significance in blast furnace desulphurization. It has been shown by Neuhaus et al.[7] that the greater the thickness of the slag layer through which the iron droplets pass, i.e., the greater the contact time, the greater the desulphurization. With a viscous slag the residence time of iron droplets passing through the slag and, therefore, the reaction time will be higher. On the other hand, according to Kulikov,[41] a thin slag of higher sulphur holding capacity has the greatest desulphurizing power.

It is doubtful if increasing the contact time by increasing the thickness of the slag layer has any substantial effect since we have seen that low slag volume gives the highest desulphurization. Substantial sulphur removal occurs in the hearth as shown by increasing the amount of roughing slag, i.e., by more frequent tapping of the iron. Ideally, the metal and the slag should flow together, dispensing completely with the flushing of slag.[42,43]

The above discussions show that the essential influences in the kinetics of desulphurization are:

(i) basicity, temperature and FeO-content of slag;
(ii) slag-metal reaction surface;
(iii) MnO-Si reaction rate.

There being limits to increase in the basicity and temperature, the reaction can be accelerated by:

(i) holding the slag longer in the hearth;
(ii) decreasing the amount of flushing slag, i.e., tapping iron and slag together;
(iii) more frequent tappings;
(iv) a good and uniform furnace run with high degree of indirect reduction. This would ensure a longer period of contact of the metal with the highly reduced slag in the lower bosh while they flow down together. This will also lower the input of slag-FeO in the hearth, stabilize the thermal state of the hearth and increase the metal temperature. Indirect reduction can be increased by the use of hydrogen-bearers which reduce the re-oxidation of pig iron, decrease the FeO-input and enhance desulphurization (Secs. 3.15 and 7.6.6).

9.5.2. Slag Composition

The most effective method of restricting sulphur in iron is by controlling the slag basicity. There is, however, a permissable limit of basicity beyond which the slag itself may become unsound and non-saleable. On the other hand, an increasing amount of lime (i.e., high CaO/SiO_2 ratio) would raise the slag liquidus temperature and the formation of any primary crystals would increase the viscosity of the slag. Any attempt to decrease the viscosity by increasing the temperature would result in an increased silicon in iron. Both these negative manifestations can be somewhat counter-acted by increasing the magnesia content of the slag. In the case of fluxed sinters, the replacement of lime should be done by incorporating dolomite in the sinter strand itself since the use of any raw dolomite will be associated with increased fuel rate.

Considering a sufficient slag fluidity and maximum possible desulphurization, the optimum slag compositions for different alumina levels have been suggested by Osborn et al. (Table 9.3).[44]

According to Table 9.3, the permissible basicity (CaO/SiO_2) increases with increasing alumina and the magnesia required for optimum desulphurization decreases slightly. However, the total base to acids ratio, i.e., $(CaO + MgO)/(SiO_2 + Al_2O_3)$ does not vary much. These optimum slag compositions are much more basic than the usual blast furnace slags and therefore a much better desulphurization is expected. However, these slags are unstable and prone to 'dusting' due to the danger of crystallization of periclase and dicalcium silicate. They are also unsuitable for cement-making because of high magnesia content. There are other favourable slag compositions possible without the danger of 'dusting' as suggested by vom

Table 9.3.[44] Optimum slag composition for optimum desulphurizing capacity

Al_2O_3	SiO_2	CaO	MgO	$\frac{CaO}{SiO_2}$	B*	$\frac{CaO + MgO}{SiO_2 + Al_2O_3}$
5	36	43	16	1.20	1.58	1.43
10	32	44	14	1.38	1.68	1.38
15	28.5	44	12.5	1.54	1.79	1.30
20	24	45	11	1.88	1.93	1.27
25	19	48	8	2.52	2.40	1.27

$$B^* = \frac{\%CaO + 0.7\%\ MgO}{0.94\%\ SiO_2 + 0.18\%\ Al_2O_3}$$

Ende and Winzer.[6] They are given in Table 9.4 for 10 percent and 15 percent alumina and increasing MgO content and they have liquidus temperatures below 1500°C with highest possible CaO/SiO_2 ratios. These compositions are at a safe distance from the primary crystallization fields of the pseudo-ternary system $CaO\text{-}MgO\text{-}SiO_2\text{-}Al_2O_3$ (cf. Fig. 3.20).

In Table 9.4, the equilibruim sulphur distribution based on Eq. 9.14 is also given in terms of $(S)/a_{[S]}$, and (S)/[S] for γ'_s of 5.0 for cases of open-hearth irons (OH). From Table 9.4 and a 25 percent approach to equilibrium in the case of Thomas iron with $\gamma'_s = 4.5$, an (S)/[S] ratio of 40 is expected from favourable slag compositions. With open-hearth iron and a 40 percent approach to equilibrium, the expected ratio is about 75. These ratios are much better than those usually obtained in practice.

9.5.3. Sulphur Load, Slag Volume and Slag Basicity

The theoretical sulphur content of iron depends on the sulphur distribution ratio, sulphur load and slag bulk. The relation is given by:

$$[\%S] = \frac{0.1\ S}{1 + 0.001\ \eta_s.q} \qquad 9.16$$

where,

S = sulphur load in kg/THM
q = slag bulk, kg/THM
η_s = (%S)/[%S]

The relationship is shown in Fig. 9.4[6] for two sulphur loads and η_s varying from 20 to 100. From Fig. 9.4, in the case of Thomas iron with 300 kg slag, a sulphur load of 8 kg/THM and (S)/[S] = 40, a 0.06% [S] in iron can be achieved. However, in such a case the sulphur in slag will be about 2.4 percent which might disturb the furnace operation, especially because of low slag temperatures. Therefore, in such cases, an increase in the slag bulk is necessary. On the other hand, with a sulphur load of 6 kg/THM and 300 kg slag, the desulphurizing capacity will still be sufficient. As for example, in this case with $\eta_s = 40$, the [%S] will be 0.045 and (%S) in slag = 1.85. The slag bulk can be lowered if the sulphur load is brought down still further.

Table 9.4.[6] Composition and desulphurizing capacity of physically stable blast furnace slags for $CaO + MgO + SiO_2 + Al_2O_3 = 95$ wt.%. OH = open-hearth iron

Chemical composition				Basicity			Equilibrium	
$\%Al_2O_3$	%MgO	%CaO	$\%SiO_2$	$\frac{CaO}{SiO_2}$	B**	B*	$\frac{(\%S)}{a_{[S]}}$	$^{\dagger}\eta_s$ OH
10	0	45.0	40.0	1.12	0.90	1.14	11.5	57
10	2	43.4	39.6	1.10	0.91	1.14	11.7	58
10	4	43.3	37.7	1.16	0.99	1.24	15.1	75
10	6	42.6	36.4	1.17	1.04	1.30	18.2	91
10	8	42.0	35.0	1.20	1.10	1.39	22.4	112
10	10	41.0	34.0	1.20	1.16	1.42	26.3	132
10	12	39.8	33.2	1.20	1.20	1.46	29.5	148
10	14	38.7	32.3	1.20	1.27	1.50	33.9	170
15	0	44.6	35.4	1.26	0.88	1.24	15.1	75
15	2	43.7	34.3	1.27	0.92	1.29	17.8	89
15	4	42.5	33.5	1.27	0.96	1.32	19.5	98
15	6	41.4	32.6	1.27	1.00	1.37	22.4	112
15	8	40.2	31.8	1.27	1.03	1.40	25.1	126
15	10	39.4	30.6	1.29	1.08	1.47	30.9	155
15	12	39.1	28.9	1.35	1.18	1.59	43.6	218
15	14	37.1	28.9	1.28	1.18	1.57	40.7	204

$B^{**} = \frac{\%CaO + \%MgO}{\%SiO_2 + \%Al_2O_3}$; $B^* = \frac{\%CaO + 0.7\%\ MgO}{0.94\%SiO_2 + 0.18\%Al_2O_3}$; $^{\dagger}\gamma'_s = 5.0$

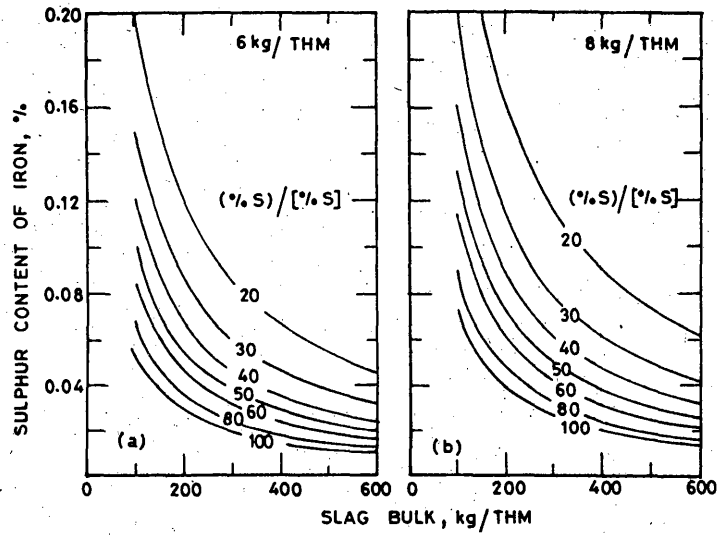


Fig. 9.4 The dependence of sulphur in iron on the slag bulk and sulphur distribution ratio for 2 levels of sulphur load, according to vom Ende and Winzer.[6] (Copyright Verlag Stahleisen).

Again, from Fig. 9.4, a sulphur content of 0.04% can be attained in the case of open-hearth iron with a slag bulk of 300 kg/THM, sulphur load of 8 kg/THM and $\eta_s = 70$ to 75. The slag sulphur amounts to 2.5%. Such a slag is expected to flow because the slag temperature of such irons is higher. For still lower metal sulphur, the sulphur load should be decreased or the slag bulk increased.

In Sec. 3.17, a slag field has been mentioned which is aluminous but less siliceous (<20% SiO_2) than normal slags. The author has recently investigated the desulphurizing capacity of such slags. Such slags were found to be possessing enormous desulphurizing power and iron with as low as 0.006%S can be obtained.

Apart from increasing the slag bulk or lowering the sulphur load or countering any increase in the sulphur content of coke, the same aim can be achieved by increasing the slag basicity (i.e., high η_s), the limiting condition in the latter case being the sulphur solubility of the slag. For a good desulphurizing slag with good stability for use as road aggregates, the sulphur content should not exceed about 2 percent. If the slag has already reached this limit, a further desulphurization can only be obtained by increasing the slag bulk. On the other hand, where (%S) is below 2,

it is more economical to obtain the required further desulphurization by an enhancement of the basicity.

In practice, however, there is a limit to an increase of the basicity in order to maintain a sufficient fluidity of the slag. The composition of the slag and therefore its basicity has to be within limits so that the liquidus temperature of the slag is below about 1450°C. Any basicity increase would not help if the sulphur in slag has already reached the solubility limit (2–2.5 percent).

Since the slag basicity and η_s are inter-related, the influence of slag bulk, basicity and sulphur load on the final sulphur in iron can be easily estimated from Eqs. 9.14 and 9.16. Giedroyc et al.[15] have shown that, ordinarily, increasing the slag basicity solely for controlling sulphur is more economical than by increasing the slag volume for the purpose. Increasing the slag basicity ($CaO + MgO/SiO_2 + Al_2O_3$) by 0.05 would cost about 7–10 times less than that by increasing the slag volume, for the same final sulphur. In the latter case, however, if a suitable and cheap lean ore is available which will cover the extra cost of smelting, a higher slag bulk may be advantageous especially because the furnace moves more smoothly and uniformly with slags of low basicities. According to calculations by Schaefers and Winzer,[45] to counter an increase of 0.10%S in coke by increasing the basicity would cost 0.5–1.3 percent of extra coke; whereas, by increasing the slag volume, the extra coke necessary will be about 3 percent.

The slag compositions of some important blast furnaces producing various grades of iron along with their viscosities, liquidus temperatures, basicities and desulphurizing potentials, both actual and theoretical, are given in Table 9.5. The ratio $(S)/_{[S]}$ has been calculated from eq. 9.14 and the γ'_s for calculating the sulphur ratio has been derived from the actual metal compositions (not shown) by methods discussed in Sec. 2.3. The approach to equilibrium has been calculated from,

$$\% \text{ approach to equilibrium} = \frac{(S)/[S] \text{ actual}}{(S)/[S] \text{ theoretical}} \times 100.$$

Table 9.5. The composition, basicities, bulk, viscosity and liquidus temperatures of some commercial blast furnace slags along with the actual and theoretical sulphur distribution ratios and percent approach to equilibrium

Works	Slag kg/THM	Slag composition, %				Basicity*				(S)/[S] Actual	(S)/[S] Theor.**	% Appr. to Equil.	Liq.. Temp. °C of slag	Viscosity Poise 1500°C
		SiO_2	CaO	MgO	Al_2O_3	A	B	C	[S]					
Thomas Iron														
Phoenix-Rhein Rohr	513	33.44	43.22	5.39	12.67	1.29	1.05	1.39	0.050	24	104	23	1460	3.0
Mareimelle	535	32.45	45.85	3.95	14.85	1.41	1.05	1.47	0.067	18	122	15	1490	10.0
ARBED	1340	33.62	42.26	2.85	14.52	1.38	0.95	1.41	0.051	15	119	13	1490	8.0
Hoesch	350	33.20	35.10	8.30	14.60	1.06	0.91	1.21	0.149	11	63	18	1420	3.8
Appleby-Frodingham	1265	33.27	40.15	3.80	18.94	1.21	0.84	1.23	0.065	22	69	32	1480	4.5
Mannesmann	558	34.63	41.70	6.74	11.57	1.20	1.05	1.34	0.053	23	101	23	1430	3.0
	327	33.10	40.93	6.58	13.33	1.24	1.02	1.36	0.049	35	106	33	1450	3.5
Basic Iron														
Italsider	201	31.47	36.39	8.11	18.89	1.16	0.88	1.28	0.022	72	105	69	1450	3.0
Mannesmann	416	31.53	38.36	13.17	13.69	1.22	1.13	1.48	0.017	75	158	48	1460	2.6
Steel Co. of Wales	587	33.30	36.20	9.80	16.60	1.09	0.92	1.26	0.020	68	117	58	1460	2.9
Armco	484	36.96	38.86	9.52	11.56	1.05	1.00	1.21	0.027	42	89	47	1380	3.2

Bethlehem	286	35.80	34.20	18.00	10.50	0.96	1.13	1.32	0.036	47	100	47	1440	1.7
National tube	479	35.20	46.60	6.10	10.90	1.31	1.14	1.45	0.018	101	202	50	1480	2.7
Gary Works	448	37.60	37.70	6.90	14.90	1.00	0.85	1.12	0.037	30	70	43	1400	4.8
Dzerzkensk	909	37.80	47.80	4.20	7.70	1.27	1.14	1.40	0.035	57	125	46	1470	3.5
Krivoj-Rog	865	40.20	47.10	4.00	5.30	1.17	1.12	1.29	0.043	37	76	49	1440	3.0
Magnitogorsk	450	34.34	39.52	11.47	13.61	1.15	1.06	1.37	0.018	57	141	40	1420	2.8
Stelco	168	37.61	38.94	10.92	9.92	1.04	1.05	1.25	0.021	83	107	78	1390	2.4
Youngstown	328	40.35	39.38	12.11	6.58	0.98	1.10	1.22	0.033	26	94	28	1450	2.0
Jones and Laughlin	342	34.60	39.41	13.02	11.79	1.14	1.13	1.40	0.031	74	170	44	1440	1.7
Foundry Iron														
National Steel	437	38.13	41.13	7.78	11.13	1.08	0.99	1.23	0.027	61	113	54	1480	3.0

*$A = CaO/SiO_2$; $B = (CaO + MgO)/(SiO_2 + Al_2O_3)$; $C = (CaO + 0.7\,MgO)/(0.94SiO_2 + 0.18Al_2O_3)$;
**Eq. 9.14.

Data obtained from Ende and Winzer.[6]

9.5.4. Metal Composition

As we have seen, the sulphur distribution coefficient is a function of sulphur activity in iron, e.g., $(\%S)/a_{[S]}$ or $(\%S)/([\%S].\gamma'_s)$. Since impurity elements influence the sulphur activity coefficient and the higher the γ'_s the lower the [%S] for a given $a_{[S]}$, it is natural that Si, Mn, P and C will determine to a certain extent the sulphur content of iron. The influence of iron composition on the sulphur distribution cannot, however, be traced to the effect of these elements on the sulphur activity alone. Any increase or decrease of sulphur in iron is not only due to the effect of the individual components on γ'_s but also greatly due to the effect of temperature and oxygen potential on the slag-metal system, the variations in the iron composition being manifestations of the temperature and oxygen potential.

We have seen in Secs. 3.15 and 7.4.2.2, that the absorption of Si and S by iron is maximum above the tuyeres due to their gasification, the extent depending upon the temperature, fluidity and basicity of the bosh slag. Unlike Si and S, manganese does not gasify and its amount in the final iron depends upon the extent of slag-metal reaction undergone in the hearth. Since the sulphur removal rate depends upon the manganese reduction and the latter depends upon silicon in iron, slag-MnO, slag basicity and temperature, the final sulphur becomes a function of silicon and manganese in iron and slag-metal temperature. The latter depends upon the thermal state of the hearth.

9.6. Sulphur Control

In the blast furnace the sulphur distribution ratio is much lower than the equilibrium values. This may be traced to various factors, they being mainly: temperature, basicity and oxygen-potential of the slag both in the bosh and hearth regions, slag bulk, slag viscosity, contact time and contact surface between the molten slag and metal, etc.

The control of sulphur in iron is based on the following:

(1) an extensive pre-reduction of ore before it reaches the bosh; it ensures a hotter bosh;
(2) high basicity and low-FeO content of bosh slag;
(3) fluid bosh slag; thinning by MgO and/or MnO, the latter aids desulphurization in the hearth;
(4) for rich ores and consequent low slag volume, the coke rate, coke sulphur and coke ash should all be low; a low coke rate and low coke ash take care of excessive bosh slag basicity and a low coke rate and low coke sulphur do so of sulphur solubility in slag;
(5) part replacement of coke with hydrocarbon lowers the input of coke ash;
(6) lower sulphur load by decreasing the coke rate;
(7) use of pre-fluxed burden; highly reducible, both at high and low temperatures; more uniform and higher bosh slag basicity and fluidity compared to acid burden plus limestone; more intensive mass exchange of sulphur between the slag and sulphur-laden gases;
(8) lower input of slag-FeO into the hearth; use of hydrogen-bearers for extensive reduction of slag-FeO around the hearth axis and minimization of re-oxidation of pig iron; use of highly reducible, mechanically strong charge materials for gas penetration and smooth running of the furnace; gives hotter hearth and accelerates manganese reduction and sulphur transfer;
(9) excessive lime in bosh slag to be replaced by MgO for lowering the viscosity as well as for maintaining the desulphurization capacity;
(10) increase in slag basicity; it is cheaper if sulphur solubility in the slag is not exceeded; if it does, increase the slag volume by using cheap siliceous ores;
(11) for high-ash coke, avoid refractory bosh slag by replacing part of the coke by hydrocarbon; injection of lime-powder through the tuyeres or use of lime-bearing coke (if practicable);
(12) more frequent tappings to increase the amount of roughing slag; the more the slag flows together with iron, the better the sulphur removal.

There may be cases when the raw materials are such that the making of a low sulphur iron is not possible or economical, e.g., high sulphur in coke, too siliceous an ore requiring the use of large amounts of limestone with consequent high coke rate or when an optimum slag composition cannot be used for the fear of formation of a highly basic or refractory slag. In such cases, a desulphurization of iron outside the furnace can be resorted to. This will be described in the next section.

9.7. External Desulphurization

Under certain circumstances discussed in the preceding section, it may be more economical to resort to desulphurization of pig iron outside the blast furnace. The methods used fall broadly into two categories:

(i) use of soda ash (Na_2CO_3) or caustic soda (NaOH);
(ii) use of lime (CaO), calcium carbide (CaC_2) and calcium cyanamide (CaNCN) with or without soda.

9.7.1. Desulphurization by Soda

Soda ash is usually employed for ladle desulphurization. Bags of soda are thrown in the casting ladle prior to or during casting of hot metal. It can also be used for continuous desulphurization in separate ladles, like siphon-ladle.

Sodium possesses great affinity for sulphur and forms sodium sulphide in contact with FeS either in metal or in slag, according to:

$$[FeS] + Na_2CO_3 \text{ (or } 2NaOH) = Na_2S + FeO + CO_2(H_2O) \quad 9.17$$

Na_2S is obtained in a liquid state above 900°C, a temperature much below that of hot metal. Reaction 9.17 is facilitated by the removal of FeO which is possible by reaction with carbon and silicon present in the hot metal. Writing Na_2O instead of carbonate or hydroxide,

$$[FeS] + Na_2O + [C] = Na_2S + [Fe] + CO \quad 9.18$$

$$2[FeS] + 2Na_2O + [Si] = 2Na_2S + 2[Fe] + SiO_2 \quad 9.19$$

Silicon on the one hand reduces the oxygen potential but on the other it consumes Na_2O by forming sodium silicate. The lowering of the activity coefficient of Na_2O in the silicate as well as dilution of the silicate in the slag which accompanies the hot metal in the ladle can lead to a substantial loss of the oxide. In view of its low efficiency, danger of attack on the ladle refractories, health hazard due to alkali fumes and erratic reproducibility of metal sulphur, the use of soda is generally confined to intermittent use when a cast is anticipated to produce sulphur higher than the specification.

Investigations of Shanahan[46,47] in British blast furnaces show a removal of 0.005–0.010%S for addition of 1 kg soda/THM. Since soda desulphurization is not very efficient, it is difficult to bring down the sulphur content greatly if the initial sulphur is high. In such a case, by repeating the process in two or three stages 0.025%S can be removed by every 1 kg soda/THM. Although the process is simple and cheap, only a limited amount of sulphur can be removed. Also, the thermal losses are very high. Recently, using pneumatic injection[48] of soda ash, the sulphur content has been brought down to 0.015–0.005 percent. This is due to the formation of an Na_2O-SiO_2 slag finely dispersed in the iron bath. Only 4 kg/THM of soda ash is required to bring down sulphur from 0.02 to 0.01 percent.

9.7.2. Desulphurization by Lime

An extensive sulphur removal can be achieved by injection of burnt powder lime with nitrogen or other inert or reducing carrier gases in the hot metal. By this process, the sulphur content can be brought down to a very low level required for making high quality iron and steel. The injection produces turbulence and ensures intimate solid-liquid contact as does the large surface area of the finely powdered lime (lime size: 90 percent, 0.080–0.500 mm and 10 percent 0.250–0.500 mm).

Similar to Eqs. 9.18 and 9.19, the lime reacts with sulphur according to:

$$[FeS] + CaO(s) + C(gr) = CaS(s) + CO(g) + [Fe] \quad 9.20$$

$$2[FeS] + 2CaO(s) + [Si] = 2CaS(s) + SiO_2(s) + 2[Fe] \quad 9.21$$

The standard free energy of Eq. 9.20 is given by,[49]

$$\Delta G^\circ = 27050 - 27.55\ T \text{ cal.}$$

$$K = \frac{a_{CaS} \cdot p_{CO}}{a_{CaO} \cdot a_C \cdot [\%S] \cdot \gamma'_s} \quad 9.22$$

At an average hot metal temperature of 1300°C, K = 183. Assuming that CaO and CaS are solids and the hot metal is carbon-saturated, their activities are equal to unity; further if $p_{CO} = 1$ atm. and $\gamma'_s = 5$ in the hot metal, the equilibrium metal sulphur will be

$$[\%S] = \frac{1}{183 \times 5} \approx 0.001 \quad 9.23$$

The theoretical sulphur in iron will be much less when using a carrier gas since the CO will be diluted and p_{CO} less than 1 atm.

Since silicon is always present in the iron, Eq. 9.21 should be more relevant. For Thomas pig iron, according to Eketorp,[50] the equilibrium sulphur content is about 0.000025%.

Thus, thermodynamic calculations show that extremely low residual sulphur can be obtained provided an intimate lime/iron contact is ensured. With a lime consumption of about 2 percent of the weight of metal (20 kg/THM), Trentini et al.[49] could bring down the sulphur from 0.1 percent to as low as 0.01, i.e., by 90 percent in about 3 minutes, using nitrogen as carrier gas containing less than 0.5 percent oxygen. By increasing the lime blow rate, a desulphurization as high as 95 percent could be achieved with a final sulphur of 0.005 percent. In all experiments the decrease in

carbon and silicon contents was minimal. However, when compressed air was used, there was considerable desiliconization, from 1.6 to 1.4 percent, but it was difficult to attain sulphur below about 0.01 percent.

By adding a powerful reducing agent like aluminium powder,[49] only 2 percent mixed with lime, there was an extremely sharp decrease in the sulphur content, dropping from 0.300 to 0.004 percent in 4.5 minutes with a desulphurization efficiency of 99 percent. Similar results were obtained using magnesium powder. Injection of granulated magnesium[51] with nitrogen produced a final sulphur of 0.001 percent:

$$Mg(g) + [S] = MgS(s) : \Delta G^\circ = -104100 + 44.07\ T\ cal \quad 9.24$$

The estimated temperature drop of the metal during the experiment was about 15°C.

A mixture of finely powdered 80 percent lime and 20 percent soda was used by Esche et al.[52] Employing compressed air as carrier gas, they succeeded in bringing down the sulphur from 0.17 to 0.05 and from 0.043 to 0.02 percent.

Kalling and Eketorp[53] have developed a process where a refractory lined rotating cylinder is used for the intermixing of liquid metal and lime powder (<1.5 mm) with some soda instead of injection with carrier gas. The capacity of the cylinder is 25–30 THM with inner diameter 2.5 m, length of metal bath 3.5 m and rotation speed 20 rpm. A 90–95 percent desulphurization has been achieved, the sulphur falling from 0.1 to 0.01 percent in 20–30 minutes. The lime consumption varies from 1 to 2.5 percent with the initial sulphur ranging from 0.1 to 0.3 percent.

Theoretically, a very high degree of desulphurization can be obtained using a rotating cylinder if, instead of lime powder, a liquid slag of composition 50% CaO, 40% Al_2O_3 and 10% SiO_2 is used (cf. Secs. 9.5.3 and 3.17). The desulphurizing capacity of such slags is very high. Even blast furnace slags with a residual desulphurizing capacity can be used, thus saving the cost of lime without the danger of a fall in the metal temperature or iron loss in the slag. There is a further possibility of regenerating the desulphurizing capacity of the slag by blowing air or oxygen through the slag as shown by the thermodynamic calculations of Richardson and Fincham.[54] Very high rates of desulphurization by this method have been shown experimentally by Schürmann and Nedelikovic.[55]

Whittenberger et al.[56] have investigated the use of lancing of powdered calcium carbide with nitrogen as carrier. The reaction

$$CaC_2 + [S] = CaS + 2[C] \quad 9.25$$

shows a theoretical consumption of 2.5 kg carbide for every 1 kg S at 100 percent efficiency. Results show about 50 percent desulphurization. With initial sulphur in the range 0.02 to 0.06 percent, the carbide consumption is more economical at higher initial sulphur, being about 2–2.5 kg for every 0.01%S at the lower and 1–1.5 kg at the higher initial sulphur contents.

Nolle et al.[57] have investigated the possibility of using mechanical stirring with simultaneous injection of lime powder and methane through the stirrer dipped in the metal bath. With 30 litres of methane and 9 kg CaO per THM a sulphur content below 0.01 percent could be obtained.

References

1. BURGESS, A. T. and B. G. BALDWIN: J. Iron Steel Inst., 186, 1957, p. 227–235.
2. ESS, T. J.: Iron Steel Eng. Year Book, 1946, p. 185–241.
3. STARSHINOV, B. N. et al.: Stal in German, 1, 1961, p. 437–444.
4. VOLOVIK, G. A.: op. cit., 2, 1962, p. 412–417.
5. VOSKOBOINIKOV, V. G.: Stal, 15, 1955, p. 582–591.
6. ENDE, H. v. and G. WINGER: Stahl u. Eisen, 84, 1964, p. 1366–1380.
7. NEUHAUS, H. et al.: op. cit., 85, 1965, p. 1578–1587.
8. GALAMIN, I. M. and S. M. NARTOV: Stal in Eng., Nov. 1966, p. 865.
9. VOLOVIK, G. A. et al.: Steel in USSR, Oct. 1975, p. 532–533.
10. WARD, R. G.: Physical chemistry of Iron and Steelmaking, Ed. Arnold, 1962.
11. ROCCA, R. N. et al.: J. Metals, 3, 1951, p. 319–326.
12. HATCH, G. G. and J. CHIPMAN: op. cit., 1, 1949, p. 274–284; 831–832.
13. TAYLOR, J. and J. J. STOBO: J. Iron Steel Inst., 178, 1954, p. 360–367.
14. KALYANRAMAN, M. R. et al.: op. cit., 195, 1960, p. 58–64.
15. GIEDROYC, V. et al.: op. cit., 202, 1964, p. 11–21.
16. KULIKOV, J. S.: Desulphurization of iron, Moscow, 1962.
17. BOSLEY, J. J. et al.: J. Metals, 11, 1959, p. 610–615.
18. WARD, R. G. and K. A. SALMON: J. Iron Steel Inst., 190, 1960, p. 393–403.
19. SCHENCK, H. et al.: Arch. Eisenhüttenw., 31, 1960, p. 11–17.
20. TURKDOGAN, E. T.: Met. Trans., 9B, 1978, p. 163–179.
21. CHOLZAKOV, V. I. et al.: Stal in German, 3, 1963, p. 961–963.
22. GALATONOV, A. L. and A. N. CHERNYATIN: Stal in Eng., June 1966, p. 425–428.
23. STARSINOV, B. N. et al.: op. cit., Aug. 1960, p. 542–548.
24. GALAMIN, I. M. and S. M. NARTOV: op. cit., Nov. 1966, p. 865.
25. STARSINOV, B. N. et al.: Stal in German, 3, 1963, p. 239–244.
26. GONCAROV, B. F.: ibid., p. 961–965.
27. GONCAROV, B. F.: Stal in Eng., 1960, p. 168–171.
28. TSUCHIYA, T. et al.: Tetsu-to-Hagane, 59, 1973, p. 33.
29. KUSUNO, K. et al.: Trans. Iron Steel Inst. Jap., 9, 1969, p. 297–305.
30. Data from Ref. 6.
31. KOZAKEVITCH, P.: Rev. de Metallurg., Mem., 51, 1954, p. 569–587.
32. HOFMANN, E. E.: Stahl u. Eisen, 79, 1959, p. 846–854.
33. YUPKO, D. et al.: Stal in Eng., July 1965, p. 512.
34. RAMACHANDRAN, S. et al.: J. Metals, 8, 1956, p. 1549–1558.

35. SAITO, T. and Y. KAWAI: Sci. Rep. Resear. Inst., Tokohu Univ., Ser. A., 7, 1955, p. 402–410.
36. SCHULZ, H. P.: Arch. Eisenhüttenw., 35, 1964, p. 803–825.
37. CHANG, L. C. and K. M. GOLDMAN: Trans. Met. Soc., AIME, 176, 1948, p. 309–329.
38. FILER, F. W. and L. S. DARKEN: J. Metals, 4, 1952, p. 253–257.
39. GLANERT, G. et al.: Neue Hütte, 7, 1962, p. 658–664.
40. NEKRASOV, Z. I. et al.: Stal in German, 3, 1963, p. 1063–1068.
41. KULIKOV, J. S. op. cit.: 2, 1962, p. 407–421.
42. GAVRILYUK, L. Ya. and V. N. PROKHOROV: Stal in Eng., Aug. 1964, p. 593.
43. BABARYKIN, N. N. et al.: op. cit., Dec. 1964, p. 934–939.
44. OSBORN, E. F. et al.: J. Metals, 6, 1954, p. 33–45.
45. SCHAEFERS, W. and G. WINZER: Stahl u. Eisen, 85, 1965, p. 1504.
46. SHANAHAN, C. E. A.: Iron and Steel, 29, 1956, p. 9–14; 45–48.
47. SHANAHAN, C. E. A.: J. Iron Steel Inst., 180, 1955, p. 140–144.
48. BAHOUT, B. et al.: Ironmaking Steelmaking, 5, 1978, p. 162–167.
49. TRENTINI, B. et al.: J. Iron Steel Inst., June 1956, p. 124–133; Rev. de Metallurg., Mem., 53, 1956, p. 388–399; J. Metals, 9, 1957, p. 1133–1139.
50. EKETORP, S.: Rev. de Metallurg., No. 9, 58, 1955, p. 718–724.
51. VORONOVA, N. A. et al.: Steel in USSR, April 1974, p. 261–265.
52. ESCHE, W. vor dem et al.: Stahl u. Eisen, 83, 1963, p. 270–281.
53. KALLING, B. and EKETORP, S.: Blast Furn. Steel Plant, 45, 1957, p. 494–497; p. 410. See also Stahl u. Eisen, 79, 1959, p. 815.
54. RICHARDSON, F. D. and J. B. FINCHAM: J. Iron Steel Inst., 178, 1954, p. 4–15.
55. SCHÜRMANN, E. and L. NEDELIKOVIC: Arch. Eisenhüttenw., 48, 1977, p. 323–328.
56. WHITTENBERGER, E. J. et al.: Blast Furn. Steel Plant, 44, 1956, p. 644–647; 689; 747–754. See also Stahl u. Eisen, 78, 1958, p. 910–913.
57. NOLLE, U. v. et al.: Stahl u. Eisen, 92, 1972, p. 1085–1090.

CHAPTER 10

THE COKE RATE AND FUEL EFFICIENCY

10.1. General

Coke constitutes a major portion of the production cost of iron. Therefore, it is the aim of blast furnace operators to lower the coke rate (kg coke/THM) and burn it faster to increase the productivity. Attempts to lower the coke rate can only be usefully undertaken when we are aware of the factors that govern the coke rate. Estimation and prediction of the coke rate are also useful for ascertaining whether smelting of any particular variety of ore would be economical or the use of any auxiliary fuel as part replacement of coke would result in blast furnace economy. It is, however, extremely difficult to correctly estimate the coke rate of any burden by theoretical calculations without the ore having been actually smelted in the furnace. This is mainly because of the variations in the rate of reduction of wustite. The proportions of direct reduction of wustite by carbon and indirect reduction by CO or H_2 have a great bearing on the thermal requirements, the extent of which for any given ore cannot be predicted with any reliability. Moreover, such calculations should also take into account the overall material and thermal balance, flame temperature, temperature and composition of top gas, heat requirements at various temperature levels and supply of the required heat by the ascending hot furnace gas. The gas must at least be at a slightly higher temperature potential in order to avoid any thermal imbalance.

Apart from providing mechanical support and permeability to the burden, especially in the wet bosh zone, the coke is necessary in the blast furnace for the following four purposes:

(i) carburization of iron, C_c, kg;
(ii) production of heat on burning at the tuyeres for covering the thermal requirements; on combustion it also provides CO for gaseous reduction of iron oxides; the amount burnt may be termed as tuyere carbon, C_t kg;
(iii) direct reduction of iron oxide, direct reduction carbon, C_d kg;
(iv) direct reduction of metalloids carbon, C_m kg.

We have seen in Sec. 3.6.1 that although item (iii) needs less carbon than in the case of indirect reduction, yet because of its endothermal nature an additional carbon has to be burnt before the tuyeres for replenishing the heat thus consumed. For every kg of carbon entering into direct reduction FeO + C = Fe + CO, 3000 kcal of heat is consumed which, as we will see later, would need burning of more than a kg of carbon to provide the heat.

The number of kg of carbon (or coke, converted from carbon) for each of the above items on adding on the basis of one THM constitutes the coke rate, i.e., kg carbon/THM

$$\text{kg.C/THM} = C_c + C_t + C_d + C_m \qquad 10.1$$

All reactions in the blast furnace (except gaseous reduction of iron oxides, carbon deposition and slag formation) give thermal deficiency, viz., evaporation of moisture and hydrated water, calcination of carbonates, heating and melting of iron and slag, direct reduction of oxides of iron and metalloids, sensible heat of the flue dust and top gas, radiation and cooling losses. The sensible heat lost in the top gas varies between 5–10 percent of the total heat generated at the tuyeres and 90–95 percent of the heat is utilized showing the blast furnace to be an extremely efficient countercurrent apparatus. Cooling losses are minor, about 5 percent. However, a large portion of the chemical heat of carbon is lost due to its incomplete conversion to CO_2. As shown in Fig. 10.1,[1] even in the most efficient furnaces about 50 percent of the total heat input remains unutilized. The CO-utilization is seldom 50 percent.

For the purpose of coke rate calculations, the blast furnace has been divided by many into several zones. Thermal requirements and supplies in each of these can be calculated and the minimum carbon required to

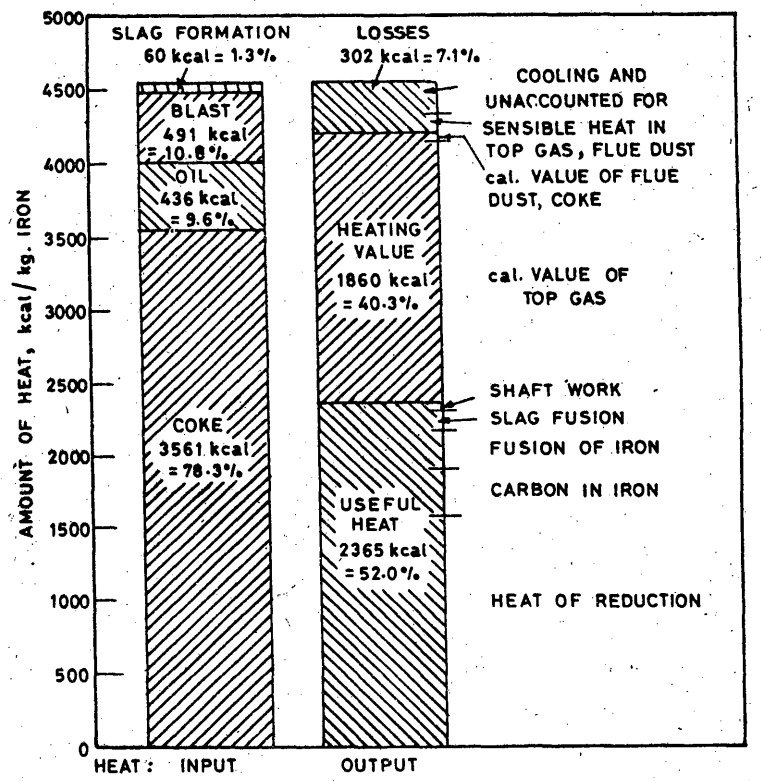


Fig. 10.1 Heat balance of a blast furnace using a particular burden, according to Bogdandy et al.[1] (Copyright Verlag Stahleisen).

satisfy the overall demand as well as the demands of each zone would give the most efficient coke rate. The highest heat consumption takes place in the lower furnace where the direct reduction of FeO and the calcination of limestone occur at 900–1150°C and the melting of iron and slag and direct reduction of metalloids at 1200–1400°C. Direct reduction accounts for 35–50 percent of the high potential heat required in the lower furnace and about 20–35 percent of the total heat requirement in the blast furnace process. As heat can only travel from the gas to the stock if a temperature gradient exists between them, it must be ensured that the thermal capacity and flame temperature of the tuyere gas are such that the heat transfer can occur in the hearth and the bosh for the maintenance of these two temperature levels.

However, we have seen in Chapter 4 the existence of a thermal reserve zone where the temperature of both the gas and the solids is about 900°C. Therefore, the blast furnace can be conveniently divided into two zones, each in equilibrium with the other, for the purpose of coke rate calculations. They are, one above 900°C and the other below 900°C. One temperature level of 900°C has been selected for simplicity in the calculation but is also acceptable on thermodynamical grounds. The amount of carbon burned at the tuyeres C_t for meeting the thermal deficits at temperatures >900°C should correspond to the maximum and the thermal capacity of the gas leaving this temperature level should satisfy the thermal requirements in the upper furnace, <900°C. If it does not, which is rather rare, the C_t should correspond to upper part thermal requirement. The difference between the heat supplied at 900°C by the gas and that required in the upper furnace (<900°C) would give the sensible heat and therefore the temperature of the top exit gas. This has already been discussed briefly in Chapter 4. Provided a value of direct reduction is assumed, the lower furnace heat requirement per THM can be easily estimated. Hence, in a simple mathematical form the calculation of tuyere carbon C_t can be made as follows:

The raceway flame temperature and the heat available from burning 1 kg of hot carbon at 1400°C in front of the tuyeres have been seen in Sec. 6.9. If the raceway flame temperature is t_f, and h_f and h_{900} are the heat contents of the gas at t_f and t_{900} evolved from the combustion of 1 kg.C_t, then the heat transferred during cooling of the gas from t_f to t_{900} per kg.C_t is h_f-h_{900} (h = volume of tuyere gas, Nm^3/kg.C × mean specific heat of gas, kcal/Nm^3.°C × temperature, °C; for normal blast the volume of the tuyere gas = 5.376 Nm^3/kg.C_t). Therefore, the total carbon burned at the tuyeres is,[2]

$$C_t = \frac{Q>900}{h_f - h_{900}} \qquad 10.2$$

where Q >900 is the thermal requirement per THM above 900°C. As the flame temperature and, therefore, h_f increases with the blast temperature it is apparent that C_t will decrease correspondingly. As C_t becomes less, the tuyere gas generated and hence the thermal capacity of the gas at 900°C per THM entering the upper zone will be less. Since the thermal requirement in the upper zone remains approximately constant, the top gas temperature will fall. As for example, if Q<900 be the heat requirement in the upper furnace and h_i the heat content of the gas based on

1 kg of tuyere carbon at the top temperature of t_i, then

$$C_t = \frac{Q<900}{h_{900} - h_i} \qquad 10.3$$

From Eq. 10.3, for the C_t calculated from Eq. 10.2, the top temperature will vary according to the values of Q<900 since, at a given blast temperature, C_t fixes the total available heat <900°C. (This is only an approximation. Actually, the volume of the gas produced by C_t increases in the shaft because of direct reduction, FeO + C = Fe + CO, calcination of carbonates giving CO_2, evaporation of water, etc; direct reduction occurs according to Eq. 7.7; for calculations, FeO has been taken as $Fe_{0.95}O$, Sec. 1.3).

For adequate heat transfer and operational reasons the top temperature should not fall below 100–150°C. Otherwise, due to an inadequate heat transfer rate, the preheating zone will extend vertically, shorten the middle indirect reduction zone, increase direct reduction and, therefore, enhance the coke rate. Hence, (h_{900}-h_{100}) is the maximum heat available per kg.C_t. If C_t(h_{900}-h_{100}) is less than Q<900, then more C_t needs to be burned to increase the value of the expression to satisfy Q<900. If the value is more than Q<900, the top temperature will be more than 100°C. In cases where Q<900 is small, as in rich prepared burden, the top temperature can be very high if the C_t is not lowered by increasing the term (h_f-h_{900}) in Eq. 10.2 (by using higher blast temperature) to satisfy the heat requirement of the lower furnace.

A sample calculation of the coke rate is shown in Sec. 10.2. It must be understood that C_t provides not only the heat but also a part of the reduction requirement. The CO evolved from direct reduction and from C_t must satisfy the reduction requirement of the FeO-oxygen remaining from direct reduction, according to

$$FeO + 3.3\ CO = Fe + 2.3\ CO + CO_2 \qquad 10.4$$

necessary for equilibrium (cf. Eq. 3.14). In our calculation, Q>900 was based on a fixed assumed quantity of direct reduction oxygen. If C_t is lowered by increasing the flame temperature or by any other means and the CO evolved therefrom is not sufficient for the equilibrium requirement, then more of direct reduction must perforce occur which will need more C_t to supply the endothermal heat. The CO generated from the extra direct reduction and extra C_t would slightly decrease the need for the extra direct reduction. This adjustment will go on and on until both the thermal as

well as the reduction requirements are satisfied. In actual practice, the furnace operator decreases or increases the ore/coke ratio in the charge in order to attain a specified silicon content of metal. If the furnace needs heat, the hearth temperature falls lowering the silicon content. If the coke rate is higher than that necessary, the hearth overheats increasing the silicon content.

Since the extent of the direct reduction of wustite is an unknown quantity, the coke rate calculation becomes easier if it is assumed that the reduction rate of wustite is not limiting and that the CO evolved from direct reduction and tuyere carbon reduces the rest of the wustite, with simultaneous satisfaction of the equilibrium and thermal requirements. The calculation shown in Sec. 10.2 is based on this principle. A few other results of such calculations are also shown in this chapter.

A logical approach should be to calculate the optimum carbon requirement by the above method and if it is not practically possible to operate with the calculated rate (because of inadequate reduction rate of FeO, i.e., the actual extent of direct reduction of FeO is higher than the optimum), to consider increase in the blast temperature and/or burning of more coke. Direct reduction of wustite varies between 40 to 70 percent from furnace to furnace. Even in the best operating furnaces the average is 40–45 percent.

As the coke rate is intimately connected with the tuyere carbon, direct/indirect reduction and, therefore, with CO-utilization η_{CO}, they will be discussed together in Sec. 10.3.

10.2. Optimum Coke Rate Calculation

We have seen in Secs. 3.6 and 7.3 the methods of calculation of the optimum reduction carbon requirements without the heat balance considerations. The method here is based on the heat balance and optimum wustite reduction by the CO produced from tuyere carbon (C_t), direct reduction carbon (C_d) and metalloids reduction carbon (C_m). These values added to the carburization carbon C_c give the total carbon rate. An assumed upper and lower furnace heat requirements is given in Table 10.1. The effective heat obtainable per kg of tuyere carbon from the flame temperature to 900°C can be read from Fig. 6.26 for 1300°C blast temperature and it is about 3130 kcal/kg.C. The lower furnace heat requirement does not include the endothermal heat of an unknown quantity of direct reduction (3000 kcal/kg.C) and the heat content of tuyere carbon from

900–1400°C which is approximately 215 kcal/kg.C_t. The latter must be taken into account since the heat content of the tuyere carbon has been taken as 540 kcal/kg.C_t for the calculation of the flame temperature (cf. Eq. 6.14) and the rest 325 kcal/kg.C_t will need to be satisfied for the upper furnace heat balance. The oxygen content of wustite has been taken as 280 kg/THM.

At first, the tuyere carbon C_t' required to satisfy the minimum lower furnace heat requirement of 322000 kcal/THM is calculated:

$$3130 \times C_t' = 215\, C_t' + 322000$$

or

$$C_t' = 110.45 \text{ kg} = 9.20 \text{ kg.atom}$$

$$\text{Metalloids carbon, } C_m = 8 \text{ kg} = 0.67 \text{ kg.atom}$$

Since 1 kg.atom of carbon gives 1 kg.mole of CO whether from direct reduction of wustite or metalloids or from tuyere carbon, the total CO formed is:

$$C_t' + C_m = 9.87 \text{ kg.atom} \equiv 9.87 \text{ kg.mole of CO.}$$

This amount of CO is available for indirect reduction of wustite. The number of kg.atom oxygen removed, according to Eq. 10.4, is

$$\text{kg.atom O} = 9.87/3.3 = 2.99 \equiv 47.85 \text{ kg.O}$$

Therefore, the amount of oxygen left in wustite

$$= (280 - 47.85) \text{ kg.O}$$
$$\equiv 14.51 \text{ kg.atom O.}$$

Suppose y kg.atom of oxygen is removed directly from the 14.51 kg.atom left in the wustite. This will consume y kg.atom C, provide y kg.mole CO and consume (3000 × 12y) kcal of heat. To provide the heat, C_t'' kg.atom of tuyere carbon needs to be burned which will need a further (215 × 12 × C_t'') kcal to satisfy the heat content of C_t''. Again, C_t'' will generate C_t'' kg.mole CO which will also take part in indirect reduction. To satisfy the heat and reduction requirement,

$$y \text{ kg mole CO} + C_t'' \text{ kg.mole CO} = (14.51 - y) \times 3.3 \text{ kg mole of CO} \qquad 10.5$$

and

$$3000 \times 12 \times y + 215 \times 12 \times C_t'' = 3130 \times 12 \times C_t'' \qquad 10.6$$

From Eq. 10.6, $C_t'' = 1.03y$ kg.atom.
Substituting the value of C_t'' in Eq. 10.5, we get

$$y + 1.03y = 47.88 - 3.3y$$

or

$$y \equiv 8.98 \text{ kg.atom C} \equiv 107.8 \text{ kg.C} \equiv 143.74 \text{ kg.O}$$

and

$$C_t'' = 9.25 \text{ kg.atom} = 111 \text{ kg.C}.$$

Therefore, the final tuyere carbon,

$$C_t = C_t' + C_t'' = 110.45 + 111 = 220.45 \text{ kg}.$$

Direct reduction carbon, $C_d = y$ kg.atom $= 107.8$ kg.
Total reduction carbon, $C_d + C_t + C_m = 336.25$ kg.
Hence, total carbon requirement $C_t + C_d + C_m + C_c = 376.25$ kg
Converted to coke (85% C), the coke rate = 442.65 kg/THM.
Percentage direct reduction of total oxygen

$$= 100 \times 143.7/400 = 36\%.$$

Percentage direct reduction of wustite oxygen = 51%
Total CO formed from C_t, C_d and C_m = 28.02 kg moles
Total oxygen indirectly removed = (400/16)–8.98
= 16.02 kg.atom
and CO_2 formed = 16.02 kg mole

Hence, $\eta_{CO} = CO_2/(CO + CO_2) = 57\%$
and $CO/CO_2 = 0.75$
Total gas produced $= 5.376 \times C_t + 1.87 \times C_d + 1.87 \times C_m$
$= 1402$ Nm³/THM
Heat requirement, upper furnace $= 23900 + 325 \times C_t$
$= 310645$ kcal
Total heat available in gas $= 1402 \times 900°C \times 0.337$
$= 429015$ kcal

Hence, the heat requirement in the upper furnace is more than satisfied.

$$\text{Top gas temperature} = \frac{429016 - 310645}{1402 \times 0.337} = 246°C$$

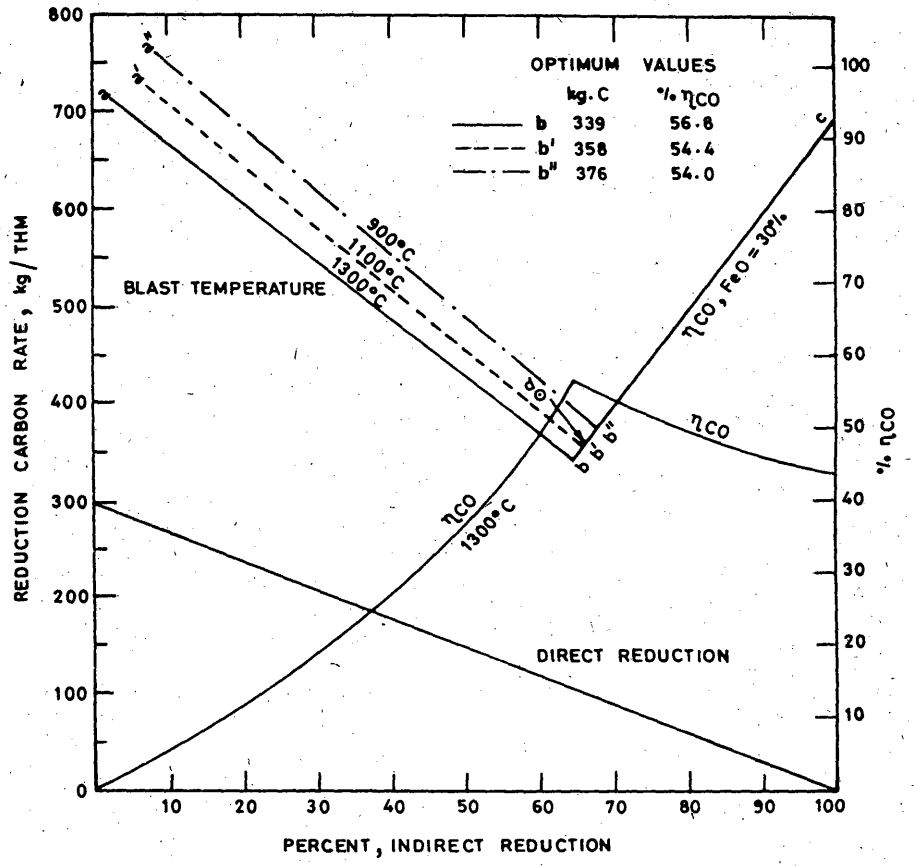


Fig. 10.2 Variation of reduction carbon rate with indirect reduction for three blast temperature levels for the burden shown in Table 10.1. The course of CO-utilization for 1300°C blast temperature is also shown.

Similar calculations can be done for other blast temperatures with the help of Fig. 6.26. The optimum reduction carbon requirements for blast temperatures of 900(b″), 1100(b′) and 1300°C(b) are shown in Fig. 10.2. The reduction carbon requirements increase on either side of the optimum to 0 percent indirect reduction (lines ab, a′b′, a″b″) and 100 percent indirect reduction (line bc). Line (bc) obviously represents equilibrium with FeO/Fe and $\eta_{CO,FeO} = 30$ percent (representing chemical inactive zone in the furnace). The lines (ab, etc., and bc) were calculated assuming a fixed percentage of direct reduction of wustite oxygen. (See also Fig. 3.8).

The overall CO-utilization values for all the 400 kg of oxygen in iron are also drawn in the figure for 1300°C blast temperature against percentage indirect reduction. Again, the η_{CO} values decrease on either side of the maximum.

Table 10.1. A simple thermal balance in a blast furnace

1.			
Description			
Ore oxygen	kg/THM		400
Wustite oxygen	kg/THM		280
Slag bulk	kg/THM		300
Blast temperature	°C		1300
2.			
Pig-iron Composition			
C	%		4.0
Si	%		0.5
P	%		0.2
Mn	%		0.8
3.			
Heat requirement, <900°C			
Description	**Unit values**	**Unit, kg/THM**	**Heat, kcal/THM**
Heat content of iron	130 kcal/kg.Fe	1000	130000
Heat content of slag formers	230 kcal/kg.slag	300	69000
Shaft work (assumption)	10 kcal/kg.Fe	1000	10000
Radiation losses (assumption)	30 kcal/kg.Fe	1000	30000
Heat content of tuyere carbon (To be added according to requirement)	325 kcal/kg.C	?	?
		Total	239000
4.			
Heat requirement, >900°C			
Heat content of iron	165 kcal/kg.Fe	1000	165000
Heat content of slag (including heat of formation)	150 kcal/kg.slag	300	45000
Heat of dissolution of carbon and metalloids (assumption)	8 kcal/kg.Fe	1000	8000
Reduction FeO + C = Fe + CO (to be added according to C_d)	3000 kcal/kg.C	?	?
Reduction of Si by C	5500 kcal/kg.Si	5	17500
Reduction of Mn by C	1200 kcal/kg.Mn	8	9600
Reduction of P by C	3600 kcal/kg.P	2	7200
Cooling losses (assumption)	80 kcal/kg.Fe	1000	80000
Heat content of tuyere carbon (to be added according to requirement)	215 kcal/kg.C	?	?
		Total	322000

10.3. Direct Reduction, Tuyere Carbon and Thermal Efficiency

The role of direct and indirect reductions in the fuel efficiency of the blast furnace can be best appreciated from a consideration of Fig. 10.2. For each carbon consumption line *ab*, *a'b'*, *a''b''* in Fig. 10.2, the optimum carbon efficiency is given by the proportion of direct and indirect reductions where these lines meet the line *bc*. Any attempt to further increase indirect reduction would mean unnecessary increase in the carbon rate along *bc*. Although C_d will decrease but C_t will increase proportionately much more because indirect reduction is more expensive of carbon. On the other hand, suppose the optimum carbon rate for the given burden is at *b'* but because of an inadequate reducibility of wustite it is working at a carbon rate at *d*. If now, say through ore preparation, the reducibility and hence the indirect reduction increase, the furnace will no longer be working at optimum efficiency. The balance will be restored gradually by decreasing the carbon rate along *a'b'* towards the line *bc* and the furnace will now work at higher η_{CO} or lower CO/CO_2 ratio and hence with higher fuel efficiency (cf. Fig. 3.8).

On the other hand, suppose an ore is being smelted in a furnace with optimum efficiency at a given proportion of direct/indirect reduction and the thermal deficit increases due to, viz., higher slag bulk, additional limestone requirement, decreased blast heat, higher cooling losses, etc. To compensate for the increased thermal load, an increased burning of tuyere carbon will be necessary. If the proportion of direct/indirect reduction remains the same, the CO formed from the extra carbon burned at the tuyeres will pass unchanged through the furnace, thus decreasing the CO-utilization. As the carbon will burn only to CO, it will supply much less heat than if it had been partially converted to CO_2. This is an inefficient utilization of carbon. It can be partially compensated by an increased degree of indirect reduction obtained by ore preparation, e.g. by crushing the ore to small sizes. As a result, the $C_d + C_t$ will decrease and CO-utilization will increase.

From the above discussion, it follows that if the CO-utilization or CO/CO_2 ratio is a measure of *fuel efficiency* and percent indirect reduction that of *operational efficiency*, the latter must increase with increasing thermal deficit (along bc) in order to maintain an optimal fuel efficiency.

For optimum efficiency under any given set of conditions, indirect reduction should rise or fall respectively according as the thermal deficit increases

or decreases. As the burden gets increasingly leaner and the thermal requirement larger, indirect reduction should increase correspondingly and approach Gruner's ideal of 100 percent at point *c*. Thereafter, any CO produced from carbon burned at the tuyeres does not take any part in the reduction reactions. It only burns to produce heat and is therefore used very inefficiently. The importance of decreasing the thermal requirement through burden preparation is immediately obvious and has been discussed in Sec. 10.4.2.

The fuel efficiency is increasing with constant improvement of burdening and the attainable CO/CO_2 ratio is also decreasing. Most modern furnaces working with almost ideal burdens run about a ratio of 1.5 or $\eta_{CO} = 40$ percent although in a few furnaces ratios as low as 1–1.3 or $\eta_{CO} = 45$–50 percent have been achieved. In badly working furnaces, ratios as high as 4 or $\eta_{CO} = 20$ percent have been reported. For the idealized burden in Sec. 10.2, the CO/CO_2 ratio was 0.75 and $\eta_{CO} = 57$ percent.

The line *bc* in Fig. 10.2 is valid for $\eta_{CO,FeO} = 30$ percent. The line in reality shows that wustite is in equilibrium with CO generated from the

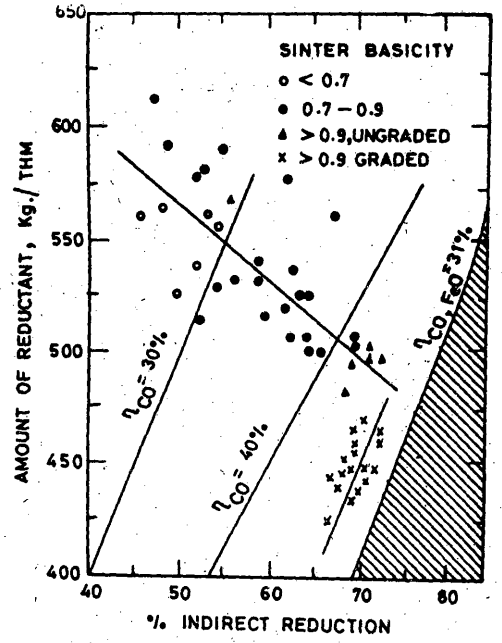


Fig. 10.3 The influence of increasing basicity and grading of sinter on the amount of reductant consumed and percent indirect reduction achieved, according to Schulz et al.[3] (Copyright Verlag Stahleisen).

tuyere carbon and direct reduction carbon. In Sec. 7.3.1, we mentioned the existence of a chemical inactive zone in the furnace when the CO-utilization for wustite reaches 30 percent and the gas composition does not change in this region. However, since the rate of reaction decreases as the gas composition approaches the FeO/Fe equilibrium value, it may be presumed that furnaces showing a value of 25–30 percent are operating with an inactive zone and optimum fuel efficiency. Fig. 10.3[3] shows the approach to the inactive zone with improvements in the burden preparation (close size fraction, increased reducibility of fluxed sinter, etc.).

The existence of the chemical inactive zone can be used as a barometer of fuel efficiency. As will be seen in Sec. 11.4, the blast volume can be increased without any detrimental effect of reduced mass transfer rate as long as this zone exists in the blast furnace.

10.4. Reduction of Coke Rate-Methods

The coke consumption rate per THM can be decreased by any method which increases indirect reduction, decreases the thermal load, increases the sensible heat supply and decreases its outflow or replaces coke with other fuel. These can be realized broadly by:

(a) increased blast temperature
(b) burden preparation
(c) stack gas injection (seldom used in practice)
(d) super-burden (pre-reduced ore)
(e) blast additives
(f) high top pressure, HTP.

It should be noted here that most of the coke savings are realized by the replacement of valuable metallurgical coke with cheaper and easily available fuels. The economy depends upon the relative prices of fuels and, therefore, on the local fuel cost conditions. As for example, in the 1960s it was fashionable to use an increasing amount of oil to replace coke because the use of the former was cheaper. After the 1973 oil price hike, it is no longer an economical proposition. The real coke saving can only occur from a lowering of the top gas temperature as well as that of radiation and cooling losses. The increase in indirect reduction and the use of higher blast temperatures are possible but partly at least at the cost of inferior calorific value of the top gas, lower top gas volume, cost of burden preparation and the expenditure of fuel for developing higher

blast temperatures. Sinter and pellet require an additional fuel for their preparation and so do the processes of crushing, screening, concentration, etc. The economics of physical and chemical burdening depends upon the prevalent price of metallurgical coke in relation to those of other direct and indirect fuels (including electrical energy) used for the purpose of lowering the coke rate.

10.4.1. Blast Temperature

It is well-known that the use of higher blast temperature results in a saving of coke and in an increase in productivity. The saving is mainly due to an increased supply of sensible heat through the blast in order to reduce the tuyere coke consumption. This has other consequential effects which can be traced to a decrease in the amount of tuyere gas CO as the amount of tuyere carbon per THM decreases. The diminution of available CO for indirect reduction would need direct reduction for the removal of wustite oxygen.

As for example, for every 100 kg of tuyere carbon, an increase of 100°C blast temperature means an extra supply of heat equivalent to:

$$100 \times 4.44 \times 0.333 \times 100 = 14785 \text{ kcal}$$

where,

4.44 = Nm^3 blast/kg.C
0.333 = heat capacity of air, kcal/Nm^3.°C

Taking an average of 2500 kcal/kg.C supplied by the tuyere gas while cooling down from the flame temperature to 900°C, the carbon equivalent of the extra heat supplied is 6 kg which should be saved. However, for a burden operating at an optimum carbon rate, this means a supply of less CO for indirect reduction necessitating an extra direct reduction with its heat requirement of 3000 kcal per kg of direct reduction carbon. Following the principle of coke rate calculation in Sec. 10.2, it can be easily shown that instead of 6 kg.C, about 4 kg.C can be saved for every 100 kg of tuyere carbon per 100°C rise in blast temperature. As will be seen later, this is also borne out in actual blast furnace operations. A consideration of the above effects of increased blast temperature will show that the following changes occur in the furnace:

(a) a decrease in the amount of tuyere gas CO per THM;
(b) an increase in direct reduction;
(c) a decrease in the tuyere gas and hence top gas volumes;

(d) an increase in (CO + CO_2) and hence a decrease of nitrogen in the furnace gas caused by increased direct reduction;
(e) an increase in the η_{CO}, for both overall and that for wustite (for non-optimum cases);
(f) an increase in the top gas calorific value because of lowered nitrogen content although the η_{CO} increases;
(g) a decrease in the top gas temperature because of a smaller volume of gas reaching the 900°C level in the stack.

All these are apparent from Figs. 10.4–10.6. The decrease in indirect reduction with increasing blast temperature is apparent from Fig. 10.2 (shifting of b″ and b′ towards the left). The calculated increase in the direct reduction carbon and decrease in the tuyere carbon with increasing blast temperature are compared in Fig. 10.7 with those obtained in the actual blast furnace practice.[5] The influence of blast temperature on the furnace output will be seen in Chapter 11.

However, the blast temperature and, therefore, the flame temperature cannot be increased arbitrarily. If the flame temperature is increased over a certain optimum, the furnace starts to show erratic movement or results in hanging. Even an increase in the coke rate is possible. It is not known exactly why the stock descent becomes irregular but some suggestions as to the causes have been put forward in Sec. 4.5. In any case, experience shows that the optimum flame temperature is limited by the quality of the burden, furnace profile and method of operation. A decrease in the

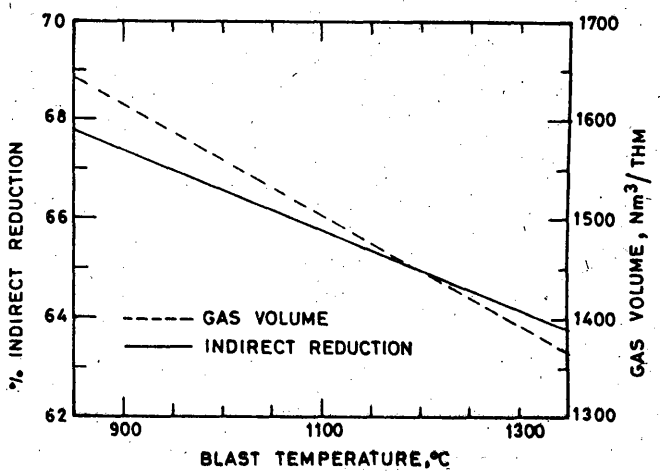


Fig. 10.4 Calculated decrease in indirect reduction and top gas volume with increase in blast temperature for the burden given in Table 10.1.

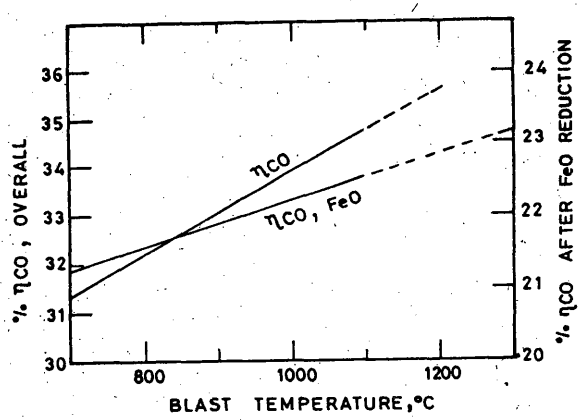


Fig. 10.5 The influence of blast temperature on CO-utilization, both for overall and that for wustite, according to Zischkale et al.[4] (Copyright Verlag Stahleisen).

blast temperature or injection of coolants like steam or natural gas invariably removes the *hot* hanging.

The adverse influence of high flame temperature on stock descent is more the more unprepared the burden. According to Bell and Taylor,[66] on changing from raw ore to a fluxed burden, the latter can accept a much higher blast temperature than the former. This is because, in the latter case, the gas/solid temperature difference is much smaller which together with the fact that the slag is pre-formed, permits the use of higher blast temperatures.

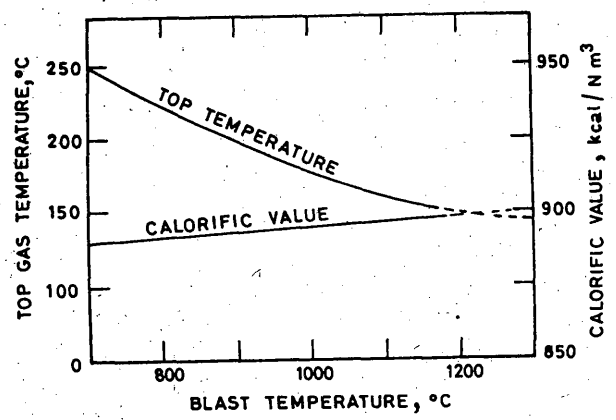


Fig. 10.6 The influence of blast temperature on the temperature and calorific value of the top gas, according to Zischkale et al.[4] (Copyright Verlag Stahleisen).

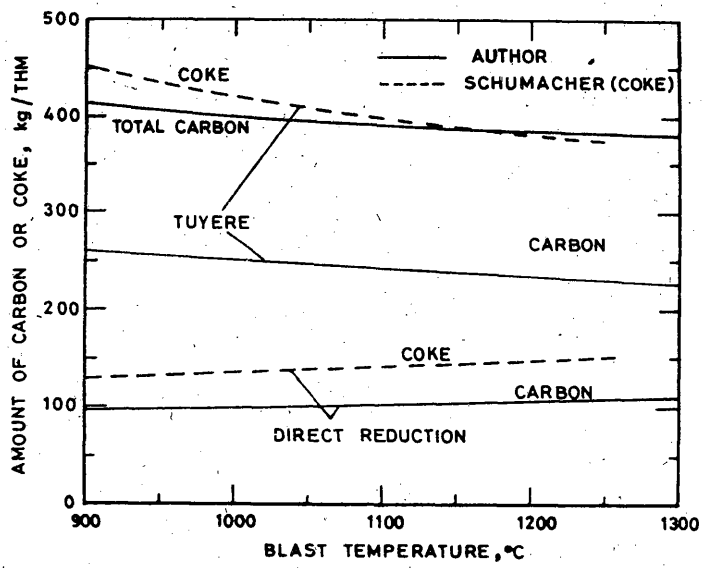


Fig. 10.7 Theoretical changes in the amounts of direct reduction carbon, tuyere carbon and total carbon with increasing blast temperature (author). The changes in the direct reduction and tuyere coke according to Schumacher[5] are also shown.

If the thermal load in the upper furnace is low (rich, pre-fluxed burden), the low-temperature heat requirement is low and, therefore, the heat carried by the ascending gas can also be correspondingly lower without any danger of thermal imbalance in the stack. Hence, an increased blast temperature can be used although this produces a smaller quantity of gas per THM (due to lowered tuyere carbon). With such burdens, blast temperatures as high as 1250°C have been used successfully without any significant furnace irregularity. It is not possible to do so with unprepared burden but blast temperatures higher than the optimum can be used in such cases with simultaneous coolant injections to keep the flame temperature constant.

There are different opinions as to the amount of coke saved in practice by increasing the blast temperature. They are summarized[4-9] in Fig. 10.8. It is generally believed that the savings are more at lower blast temperatures than at the higher ones. Eq. 10.2 can be used for an approximate estimation of coke savings:

$$C = C' \cdot \frac{t_f - 900}{t'_f - 900} \qquad 10.7$$

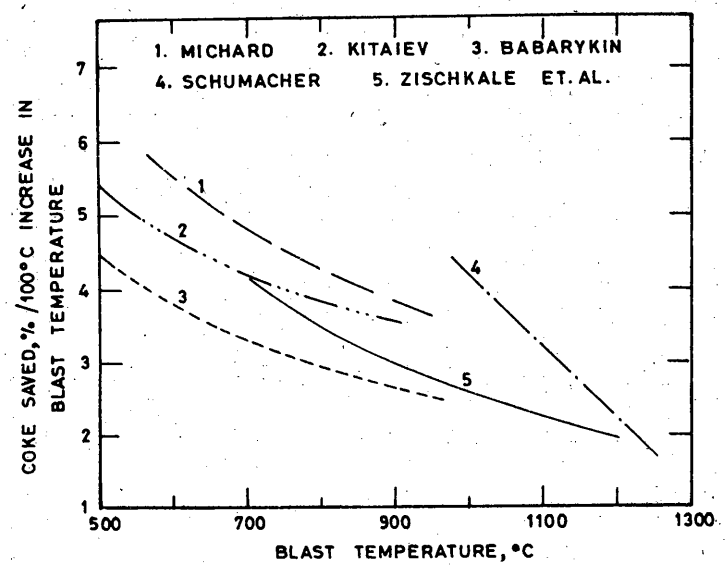


Fig. 10.8 The influence of blast temperature on savings in coke in actual practice, according to various investigators.[4-9]

where,

C = coke rate after blast temperature increase, kg/THM
C′ = coke rate before blast temperature increase, kg/THM
t_f = flame temperature before blast temperature increase, °C
t_f' = flame temperature after blast temperature increase, °C.

Zischkale et al.[4] found a saving of coke of 3%/100°C at 900°C and 2%/100°C at 1200°C whereas more recent experiments[5] show a saving of about 4%/100°C at 900°C, 3%/100°C at 1000°C and 2%/100°C at 1100°C. At a coke rate of 635 kg/THM, the total savings amounted to 12 percent on raising the blast temperature from 850 to 1250°C with a simultaneous increase in iron output by about 27 percent.[5] The overall cost saving from the increase in the blast temperature by 400°C was calculated at about 1 dollar/THM at 1966 price levels.

10.4.2. Burden Preparation

The primary purpose of burden preparation is to use blast furnace charge materials which are optimum in size, easily reducible and possess a thermal load as low as possible in order to achieve a maximum production with a minimum of coke rate, production cost and capital outlay. The burden

preparation includes: crushing, screening, washing, concentrating, roasting, sizing, sintering, pelletising, pre-fluxing, pre-reducing, etc., of the charge materials. The objects of the measures are:

(i) a uniform size distribution of the materials to obtain uniform permeability and minimum resistance to gas flow and thus to ensure a uniform gas distribution throughout the horizontal and vertical cross-sections of the furnace;
(ii) a decrease in particle size and increase in surface area by crushing in order to augment heat transfer and reducibility of the ore;
(iii) an increase in the burden yield by upgrading the ore and removal of coke ash to relieve the thermal load;
(iv) roasting of hydrated, carbonated and magnetic ores; sintering and pelletising the fine concentrates;
(v) calcination of limestone and dolomite outside the furnace and charging them in the form of pre-fluxed agglomerates; super-fluxing to take care of coke ash acids;
(vi) pre-reduction of ores or pellets into a super-burden prior to charging.

In order to properly appreciate the effect of ore preparation on the coke rate, Mintrop[10] has calculated the burden composition and heat requirements of various ores and derived relationships between the burden yields (percentage iron in the charge materials without coke), total heat requirements, indirect reduction and coke rate.

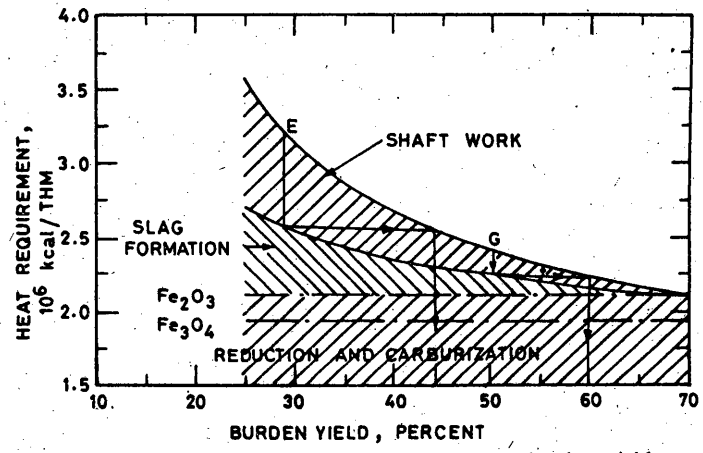


Fig. 10.9 The dependence of burden heat requirements on burden yield, according to Mintrop.[10] (Copyright Verlag Stahleisen).

Fig. 10.9[10] shows the heat requirements for calcination of carbonates and evaporation of moisture and hydrated water, designated as *shaft work*. It is clear that the heat requirements for the 'shaft work' and that for melting of correspondingly lower amount of slag decrease as the burden yield increases. If an ore E of burden yield 28 percent is smelted, the coke rate is about 1250 kg/THM at 60 percent indirect reduction and with 600°C blast temperature. The same ore converted to fluxed sinter and its burden yield correspondingly increased (as shown by the arrow), would give a coke rate of 850 kg/THM for the same degree of indirect reduction and at the same blast temperature. Thus, a nett gain of 400 kg/THM is expected. The actual saving during smelting will be much more because of an increased degree of indirect reduction expected from a better gas distribution, an increased reducibility of fluxed sinter and a higher blast temperature that can be used with enriched burden having a smaller low temperature thermal load.

In contrast, a rich burden G with 50 percent yield shows a decrease in the coke rate of only 100 kg/THM when sintered. Therefore, for rich ores, it is better to reduce the size and narrow down the size fraction (for uniform permeability, enhanced heat transfer, better gas/solid contact and increased indirect reduction) than to resort to agglomerating methods. However, the present trend appears to be to upgrade even the rich ores and pelletise the concentrate fines to achieve a stupendous production rate. These have been discussed in Sec. 11.3.2.2.

The primary factor governing burden preparation is profitability. Rich, abrasion resistant, lumpy and highly reducible ores could easily be used for direct smelting after crushing, screening and grading them into different size fractions and charging them separately (Sec. 11.3.2.1). Less reducible ores may either be crushed to small sizes for increasing the reducibility and smelted directly or ground to fines and then converted to fluxed sinters or pellets, whichever is more economical. Magnetites should be sintered or pelletised and converted to hematite during firing for higher reducibility. Ores having large amounts of carbonates, moisture or hydrated water should all be prepared.

The influence of the various factors is discussed below.

10.4.2.1. Size

Experience shows that for a good operating value, the reducibility must not be below about 0.5% oxygen/min at 40 percent reduction. Different ores should be crushed to different sizes to obtain a similar reducibility

(Fig. 6.14). The ideal size range for ores, depending upon the reducibility, is 10–15 mm or 20 mm above which size the heat and mass transfer both deteriorate, mainly the latter. For providing a good permeability to gas flow, size below 6 mm should be screened out and agglomerated. In Oberhausen,[11] operational results with physical burden preparation showed a decrease in the coke rate of about 144 kg/THM by crushing and screening into two size fractions, 6–20 mm and 20–60 mm and sintering sizes below 6 mm. The fines in the charge were all eliminated.

Birnbaum et al.[12] have cited an example of greatly decreased coke rate using 6–20 mm Kiruna ore, which is difficult to reduce, in place of 20–60 mm size used previously. The coke rate fell by 100 kg/THM due to indirect reaction alone which increased from 42 to 60 percent. The CO-utilization factor increased from 18.4 to 26.3 percent.

The phenomenal decrease in the coke rate and increase in the associated production rate obtained through only crushing, screening and sizing are too numerous to quote. The reader is referred to the literature.[10,13–25]

Size of coke compatible with the size of other charge materials yields a further improvement (Secs. 6.9.1.1 and 11.3.2.3). A comparative study in an experimental furnace showed that the use of small size of coke improved the radial distribution of the gas resulting in a marked decrease of direct reduction and better reduction efficiency.[26] It was also possible to utilize higher blast temperatures and the cumulative effect of all these was a lowered coke rate. By using coke size of 40–60 mm or 30–50 mm and sinter 15–50 mm, a fall in the coke rate by 6.5 percent has been reported.[27]

As the discussions in Secs. 5.6 and 11.3.2.3 will show, too small a coke size hinders gas throughflow in the wet bosh zone and decreases furnace productivity. Coke fines cause coke mess during casting, choking of the hearth, burning of tuyeres and slag notch, etc. By the use of stabilized coke, roll-crushed and screened, the coke rate fell by about 4.8 percent and the output increased by over 1 percent.[28]

10.4.2.2. Gas distribution

The influence of uniform gas distribution on the coke rate apparently far outweighs that of ore reducibility. Although the reducibility of the sinter is generally much less than that of the ore (especially if the sinter is hard burnt, its degree of oxidation low and fayalite content high), in practice it gives a much lower coke rate presumably because of more uniform material distribution[29,30] and hence more uniform gas distribution. As for

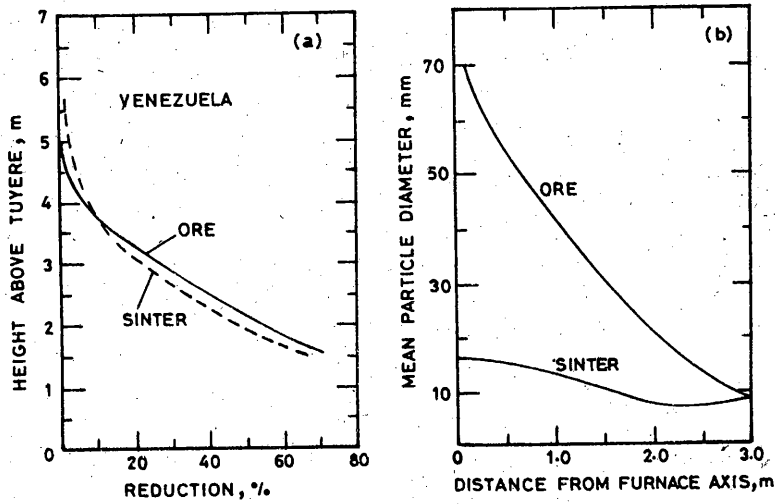


Fig. 10.10 (a) The reduction of Venezuela ore and sinter above the tuyere axis in an experimental furnace, after Bosley et al.[31] (Copyright The Metallurgical Society of AIME); (b) particle size distribution of mixed ore and 100 percent sinter in model experiments, according to Heynert et al.[29] (Copyright Verlag Stahleisen).

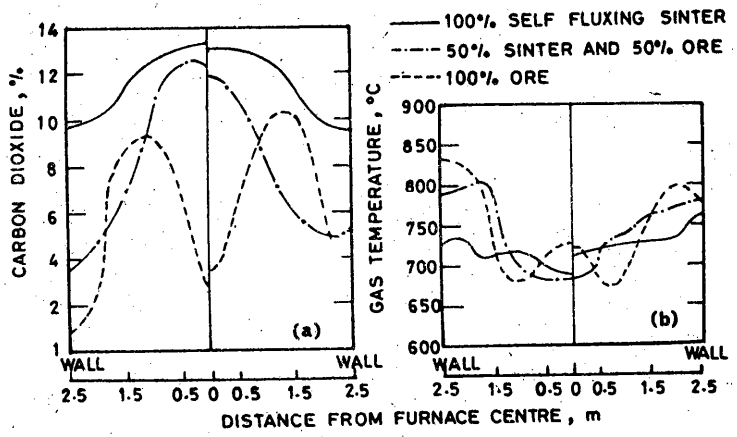


Fig. 10.11 The distribution of temperature and carbon dioxide in the stack gas at approx. 6 m below the top with varying amounts of raw ore and sinter in the burden, according to Doi and Kasai.[32] (Copyright The Metallurgical Society of AIME).

example, the reducibility of Venezuela ore is much higher than that of its sinter but during an experimental smelting both showed a very similar degree of reduction along the height of the furnace (Fig. 10.10a).[31] That the uniformity of gas and material distribution when using sinter is much better than when using ore is clear from Figs. 10.11[32] and 10.10b.[29] The uniformity of gas temperature and that of $\%CO_2$ in the gas along the horizontal axis is shown in Fig. 10.11 which was made possible by the uniformity of material distribution[33] (cf. Fig. 10.10b). Such a behaviour has also been confirmed by Wolf.[22]

The decrease in the coke rate and increase in productivity may be as high as 20–25 percent when using a major quantity of sinter in the blast furnace. Further discussions on this subject will be found in Chapter 11 (Sec. 11.3.2.2).

The benefits obtained from crushing of ores to small sizes and from uniform gas distribution are mainly due to an achievement of increased degree of indirect reduction, an overall higher CO-utilization factor and, to some extent, a decrease in slag weight. Fig. 10.12 shows that in practice the η_{CO} varies between 25–45 percent depending upon the burden weight and the richer the burden the higher the CO-utilization.

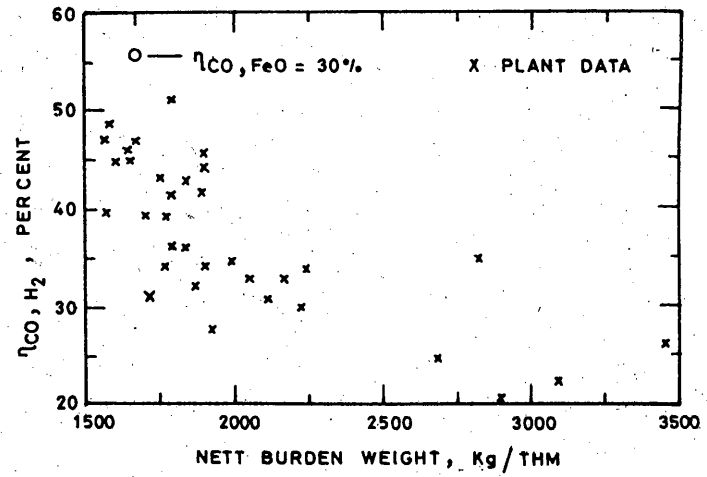


Fig. 10.12 The relationship between CO- and H_2-utilization and nett burden weight from plant data. The theoretical value of 57 percent for the burden in Table 10.1 is also shown.

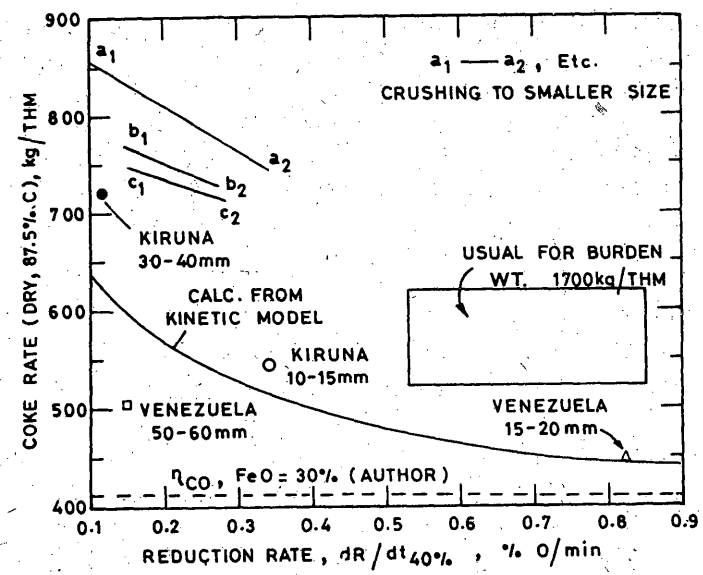


Fig. 10.13 Relationship between burden reducibility and coke rate in a blast furnace; comparison of results obtained in practice with a mathematical/kinetic blast furnace model, according to Bogdandy et al.[1] The optimum coke rate of a particular burden assuming wustite/iron equilibrium and infinite reaction rate has been introduced by the author.

The coke rate falls with increasing burden enrichment. According to Nekrasov et al.,[34] the coke rate falls by 1.4 percent for each 1 percent increase in the Fe-content and the productivity increases by 2.5 percent.

10.4.2.3. Reducibility

The prospect of decreasing the coke consumption for a given burden and blast temperature is very little if the furnace possesses a chemical inactive zone. The saving of coke becomes possible only when the coke rate deviates from the optimum, i.e., the extent of direct reduction is much more than necessary although the furnace gas possesses sufficient reduction potential for further indirect reduction. One of the ways to decrease direct reduction is to increase the rate of reduction of the iron oxides. Fig. 10.13[1] shows the relationship between the coke rate and reduction rate of the ferrous charge in %O/min at 40%-degree of reduction. The decrease in the coke rates and increase in the reduction rates shown by *a*, *b* and *c* from points 1 and 2 for three cases are due to size reduction. The enclosed area applies to the range of good reducibility and coke consumption for

a burden weight of 1700 kg/THM. The horizontal line, inserted by the author, shows the calculated coke consumption for a burden weight of 1700 kg/THM and blast temperature 1300°C based on a gas utilization of wustite at $\eta_{CO,FeO} = 30\%$ and infinite rate of wustite reduction. The solid curve calculated from a mathematical-kinetic model shows the expected decrease in the coke rate with increased rate of reduction of ore. The figure shows that Venezuela ore of size 15–20 mm reaches the predicted coke rate.

The amount of extra carbon required to be expended for an increase in direct reduction can be calculated approximately. As for example, if due to inadequate reducibility, direct reduction increases by 1 percent, i.e., 4 kg more of oxygen is removed by direct reduction on the basis of 400 kg.O/THM, then 3 kg more of carbon will be consumed. Since $3 \times 3000 = 9000$ kcal of extra heat will be necessary for covering the endothermal reaction, a further $9000/2500 = 3.6$ kg.C will need to be burned at the tuyeres, assuming that 1 kg tuyere carbon delivers 2500 kcal in the lower zone. Thus, on an average, the carbon rate increases by 6–7 kg for every 1 percent decrease in indirect reduction and *vice versa*.

Acid burdens are less reducible, very expensive of coke and seldom produce a chemical inactive zone. In contrast, basic sinters and pellets are very reducible and provided the gas distribution is uniform, their coke rates are increasingly approaching the optimum line *bc* of Fig. 10.2 and many furnaces around the world are indeed operating very near the line. The immense benefits obtained from using pre-fluxed burden are discussed below.

10.4.2.4. Fluxed burden

The coke savings from fluxed burden emanate from the following causes in addition to those discussed earlier:

(i) better reducibility and enhanced indirect reduction (6–7 kg.C saved from every 1 percent increase in indirect reduction);
(ii) use of higher blast temperatures because the thermal load is smaller and the slag is pre-made; the primary slag melts at higher temperatures and does so within a vertically narrow softening zone;
(iii) avoidance of carbon dioxide generated from limestone in the stack which adversely affects indirect reduction;
(iv) transference of heat of calcination from the furnace to the agglomerating plant.

Items (i) and (ii) have already been discussed in Secs. 6.7.2 and 10.4.1.

Regarding item (iii), the liberation of CO_2 in the stack increases its partial pressure in the stack gas and decreases the rate of reduction of wustite in the indirect reduction zone since the rate depends upon the difference between the actual and the equilibrium p_{CO_2} (Eq. 6.2). A further disadvantage is the possibility of CO_2 taking part in the endothermic Boudouard reaction since the calcination of limestone continues from 900°C to about 1100–1150°C. This is more harmful than the direct reduction of wustite if the CO generated from the Boudouard reaction does not take part in any indirect reduction and leaves the furnace unused.

$$CO_2 + C = 2CO \quad : \Delta H = +3500 \text{ kcal/kg.C}$$
$$FeO + C = CO + Fe \quad : \Delta H = +3000 \text{ kcal/kg.C}$$

Regarding item (iv), calcination of limestone in the furnace is most expensive of carbon. A conservative estimate puts the saving at 60–70 kg.C for every 100 kg.CO_2 (230 kg.$CaCO_3$) driven out outside the furnace which can be performed by much cheaper variety of carbon. A precise calculation of the savings can be seen elsewhere.[14,23] It is based on operational experience with the gradual replacement of limestone by CaO through fluxed sinter. The result showed that the degree of CO-utilization in the top gas as represented by

$$\eta_{CO} = CO_2/(CO + CO_2)$$

was independent of the amount of limestone charged in the furnace. This means that for every mole of CO_2 produced from limestone, the indirect reduction is suppressed by an equivalent amount (carbon consumption increases by 6–7 kg for every 1 percent decrease in indirect reduction). Thus a carbon saving of 55–65 kg can be made for every 100 kg.CO_2 calcined outside. Added to this is the extra tuyere carbon necessary to supply the endothermic heat of calcination which, on an average, is about 70000 kcal/100 kg.CO_2 taking into account the heat capacities, heat of slag formation, etc. Considering again an effective heat supply of 2500 kcal/kg.C in the lower furnace, an extra expenditure of about 30 kg.C is necessary, the total thus being 85–95 kg.C/100 kg.CO_2. However, assuming that the extra CO produced at the tuyeres will take part in indirect reduction, about 20–25 kg of carbon will be saved, the total saving being about 60–70 kg.C/100 kg.CO_2. A statistical study of the contribution of limestone to coke consumption (Eq. 10.10) approximately confirms the above figure.

Since the use of fluxed burden lowers the coke rate enormously the amount of slag made also decreases correspondingly. For a normal slag containing 40–50% CaO, a carbon saving of 20–25 kg/100 kg of slag can be made by charging pre-fluxed burden. Added to this is the heat of melting of slag, 150 kcal/kg, which means a further saving of about 5 kg.C, a total saving of about 25–30 kg.C per 100 kg slag.

The advantages of pre-fluxing will be evident from Fig. 10.14.[35] But the use of beneficiated fluxed sinter is not so advantageous as far as the coke rate is concerned since an extra slag of 100 kg would mean an extra expenditure of only 20 kg.coke (85% C). On the other hand, from the productivity point of view, a lower slag volume is very advantageous.

The benefits of fluxed burden are more the higher the silica in the ore, i.e., the larger the amount of limestone transferred to the sinter strand. The benefit of pre-fluxing can be increased by changing over from self-fluxing to superfluxed sinters to flux the coke acid as well. The benefit will be higher the higher the coke rate and/or the larger the amount of coke acids. In addition, a higher blast temperature can be used provided the bosh slag is not so basic and refractory as to cause an irregular furnace movement. Theoretically, a smooth furnace operation with possibly higher sulphur removal can be obtained if a part of the lime is transferred to the coke ovens for making lime-incorporated coke or lime powder injected along with the blast.

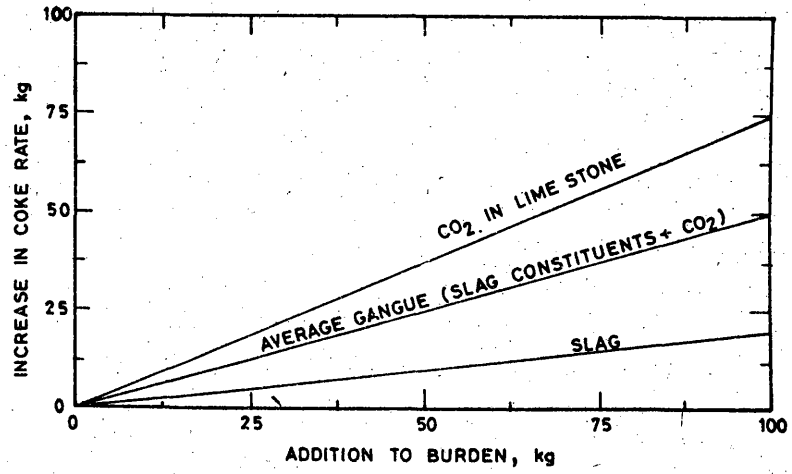


Fig. 10.14 Schematic representation of increase in coke rate due to different additions to the burden, after Astier et al.[35] (Copyright Iron and Steel Institute).

The overall coke savings by the use of self-fluxing or super-fluxed burden depends upon the lime requirement of the burden, the proportion of the fluxed material in the charge and the basicity of the fluxed agglomerates that can be attained without impairing their strength. It must, however, be remembered that the mechanical stability of sinters deteriorates at basicities of $CaO/SiO_2 = 1$–1.5. Sinters of higher basicities (2.5–3) with adequate mechanical strength can be used successfully provided they are cooled slowly and screened before charging in the furnace.

Two cases will be cited here and some others will be discussed in Chapter 11 about the immense decrease in the coke rate achieved on switching over from raw lean ores to self-fluxing sinters. An outstanding example[36,37] is the working in Appleby-Frodingham where lean ores were slowly converted to self-fluxing sinters. The burden weight of 3590 kg for raw ore steadily decreased to 2650 kg/THM for 94 percent sinter and the coke rate fell from 1185 kg to 890 kg/THM. In 1960, the reported coke rate touched a figure as low as 725 kg/THM with 100 percent self-fluxing sinter, a total saving of almost 450 kg/THM. At the same time, the production of iron increased by more than 50 percent.

Table 10.2.[35] Slag volume and coke rate of some furnaces

Location	Slag volume kg/THM	Coke rate, kg/THM
1. Unprepared Lorraine ore	1200	1200
2. Prepared Lorraine ore (crushed and fines sintered)	—	950
3. 100% self-fluxing Lorraine		
Dillingen	892	720
Hayange	820	633
4. Appleby-Frodingham (unprepared)	—	1200
Appleby-Frodingham (100% self-fluxing)	1200	725
5. Domnarvet (Sweden)	430	605
6. Armco, USA (85% pellet)	367	591
7. Stelco, Canada (ore)	—	800
Stelco, Canada (self-fluxing)	—	535
8. Kokura, Japan	440	548

Results similar to that at Appleby-Frodingham have been obtained with lean French Lorraine ores.[35] Radical changes in ore preparation through crushing, screening and sintering of fines have brought down the French coke rates from 1200 to 950 kg/THM. Self-fluxing sinters from the Lorraine ores show a much decreased coke rate ranging from 630 to 720 kg/THM and slag weight 800–890 kg/THM. These benefits and some such figures from other parts of the world are shown in Table 10.2.[35] Other more recent figures are available from Bogdandy et al.[1]

The benefits obtained by changing over from a limestone burden (completely screened and/or sintered) to one of self-fluxing sinter can be seen from the following regression equations:

(a) limestone burden (about 113 kg.CO_2/THM)[14]

$$K = 200 + 0.257\ B \qquad 10.8$$

Percent explained = 82%

(b) self-fluxing sinter

$$K = 175 + 0.247\ B \text{ (Percent explained} = 92\%) \qquad 10.9$$

[14]

$$K = 200 + 0.200\ B \qquad 10.9a$$

[38]

where,

K = coke consumption rate, kg/THM
B = nett burden weight, kg/THM

Bogdandy et al.[1] have suggested Eq. 10.10 for the calculation of the coke rate target from a regression analysis of about 200 modern furnaces operating all over the world, with a standard variation of ± 28.5 kg coke/THM.

$$K = 470 + 0.164\ B + 0.249\ L - 1.006\ S - 1.142\ P - 0.093\ t°C \qquad 10.10$$

where,

K = coke (87.5% C) consumption rate, kg/THM
B = nett burden weight, kg/THM
L = weight of limestone charged, kg/THM
S = sinter percentage of gross burden weight
P = pellet percentage of gross burden weight
t° = blast temperature, °C.

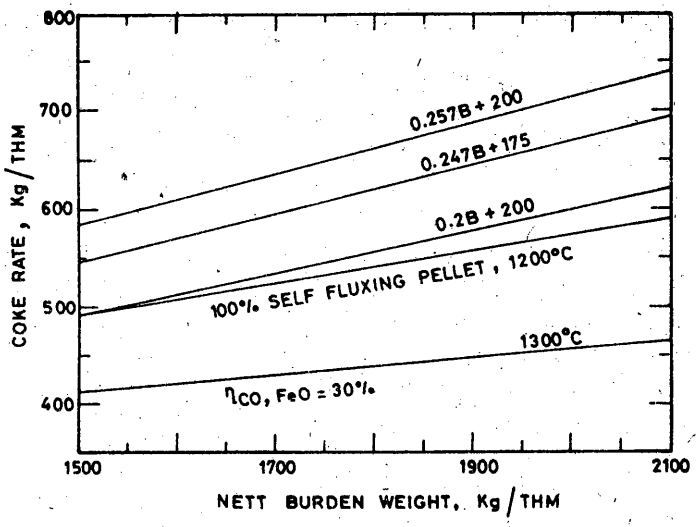


Fig. 10.15 Relationship between coke consumption and nett burden weight, according to equations 10.8–10.10. The optimum values assuming wustite/iron equilibrium calculated by the author are also shown.

The plots of Eqs. 10.8–10.10 (for 100 percent super-fluxed sinter) are shown in Fig. 10.15 where the nett burden weight is drawn against the dry coke consumption (85.5% C). The minimum coke consumption based on wustite/iron equilibrium is also drawn for comparison.

The theoretical coke rates for different CO-utilization factors for Fe_2O_3-Fe and wustite-Fe and for 200 and 600 kg of slag volumes are shown in Fig. 10.16.[1] The thermodynamic limits[39] are also shown. The immense importance of gas utilization and, hence, of ore reducibility is at once clear from the figure. The thermodynamic limit was calculated assuming an infinite rate of iron oxide reduction, CO-utilization of about 70 percent and an overall heat balance. It is doubtful whether such an assumption is permissible since the total heat requirement rather than the heat balance in stages was the basis of calculation. A more realistic approach would be to endeavour to obtain the coke rates given by wustite/iron equilibrium. Best Japanese furnaces have reached coke rates approaching within 40–50 kg/THM of the thermodynamic limit.

Manganese ore is usually charged in the raw state which decreases the bed permeability to a certain extent. By incorporating the ore in the sinter along with MgO, a 2–4 percent decrease in the coke rate and 1.5–2 percent increase in output have been reported.[40]

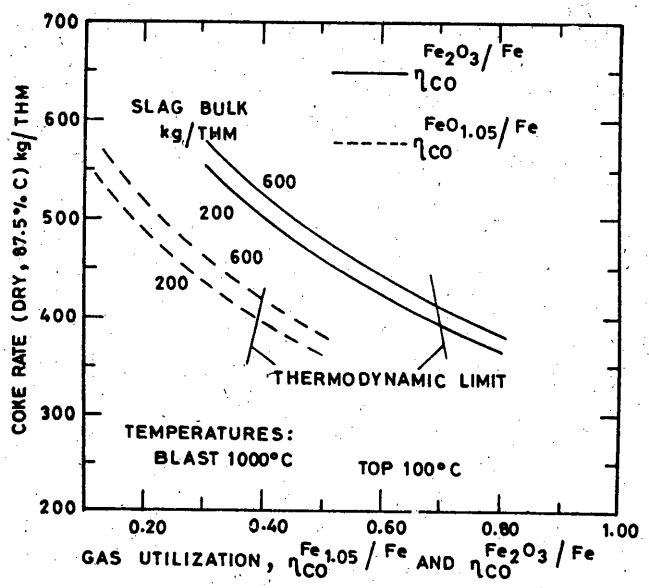


Fig. 10.16 Relationship between coke consumption and slag volume as well as CO-utilization, both overall and that for wustite/iron, according to Bogdandy et al.[1] The thermodynamic limits are also shown. (Copyright Verlag Stahleisen).

10.4.3. Acid Burdening[41–43]

An alternative to transference of limestone to the sinter strand is not to charge it at all or to work with a very low slag basicity. A total elimination of lime, however, would not be workable because of the high viscosity and refractoriness of the mainly silica-alumina slags. Siliceous lean ores can be smelted successfully at low basicity provided the resulting high sulphur in metal is removed by external desulphurization (Sec. 9.7). With normal basic slags of CaO/SiO_2 = 1.1–1.4, such lean ores lead to very high slag volume and the coke rate reaches an economically inadmissible level. Beneficiation with accompanied agglomeration is equally uneconomical. A possible solution is acid smelting. A region of acid smelting slags is shown in Fig. 3.18. Lennings[41] worked with a slag basicity of 0.8. Paske[43] lowered the basicity to an ultra-acid slag of basicity 0.22 by reducing the limestone in stages. A ratio of 0.3 showed the lowest cost. The viscosity of the slag increased greatly below a ratio of 0.82 and it was made thin by adding soda desulphurization slag.

Struve[42] smelted a burden with yield of only 23.4 percent. The limestone requirements for basicities of 1.12 and 0.69 were 916 and 87 kg/THM re-

spectively. An actual coke saving of 250 kg was made although that estimated from the heat balance was 436 kg/THM. The slag was workable because of its high FeO and MnO contents. The manganese input was doubled to obtain a high MnO-slag which has a beneficial effect on slag viscosity.

10.4.4. Summary

Summarizing, the beneficiation of ores and subsequent agglomeration of the fines and concentrates may now be reconsidered in the light of fore-going deliberations. An increase in indirect reduction by 1 percent decreases the coke rate by 7–8 kg. Gas/solid contact and, therefore, proper sizing and size distribution are as important as the chemistry of the burden for decreasing the coke rate and increasing the production. Limestone is the most expensive of the blast furnace charge materials; an elimination of 230 kg can save 70–80 kg coke/THM. Lowering of the slag volumes may not be as economical for the coke rate as is often believed (100 kg slag ≡ 20 kg coke) but it certainly permits the use of higher blast rate and increases the iron output.

At present, the world trend is towards 100 percent raw materials preparation involving crushing, grinding, sizing, concentrating, sintering and pelletizing of fines, self-fluxing, super-fluxing, super-burdening, use of high blast temperatures and blast additives, etc. These, as will be seen in Chapter 11, have led to a phenomenal increase in the iron output and decrease in the coke rate and contributed immensely to the overall furnace economy. It is now an accepted fact that optimum gas distribution/utilization and optimum bed permeability achieved through strictly adhering to small and uniform size of burden materials as well as coke of compatible size – all result in a minimum coke rate and maximum production. The output has increased by 25–50 percent, sometimes even by 100 percent, with the coke rate decreasing by 20–40 percent.

10.5. Super-burden

We have seen the impossibility and inadvisability of removal of the entire wustite oxygen in the furnace by indirect reduction because of the sluggish reaction rate of wustite and an excessive requirement of tuyère carbon for producing the requisite amount of reducing gas (Sec. 3.6). In the former case, in the later stages of reduction the reaction rate is controlled by solid diffusion which is dependent only on the transit time and very little on

gas composition. In the blast furnace, with an overall 60–70 percent indirect reduction, some 30–40 percent of the total oxygen and 45–55 percent of wustite oxygen is removed by direct reduction which because of its endothermal nature may account for, depending upon the burden, 25–50 percent of the lower furnace heat requirement. Hence, for the same extent of direct reduction, if the amount of total oxygen to be removed from wustite is decreased by pre-reducing the burden, it is possible to lower the coke rate correspondingly. A decreased tuyere carbon requirement will produce a smaller volume of bosh gas and result in an increase in iron production and hence in an additional fuel saving arising from lowered radiation and cooling losses per unit of iron produced.

The theoretical total carbon rates for various degrees of wustite reduction at 1300°C blast temperature have been calculated for the case in Sec. 10.2 and are shown in Fig. 10.17. The fuel saving is larger the higher the degree of pre-reduction. One should not, however, over-reduce as this could result in a waste of energy since a minimum amount of tuyere carbon is necessary in any case for the melting of iron and slag, etc. The optimum percentage of pre-reduction that would give the minimum overall energy requirement per unit of iron should be determined for each stage of partial reduction.[44–46] The theoretical values in Fig. 10.17 show that the optimum is

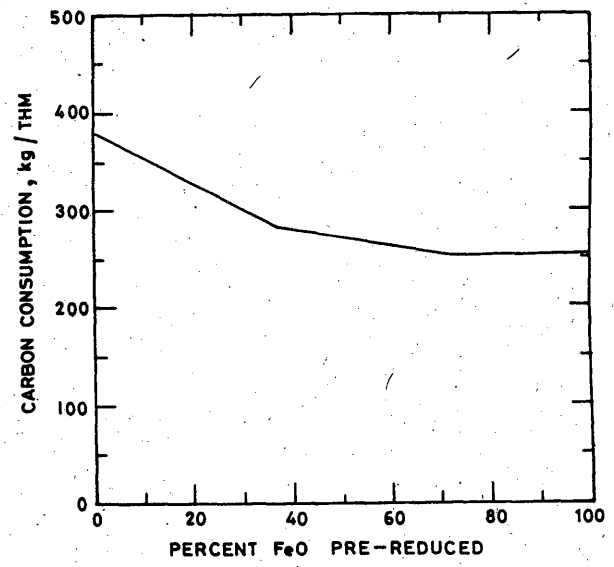


Fig. 10.17 Relationship of carbon consumption and percent wustite pre-reduced before charging (calculated).

at about 50–60 percent of partial reduction. The figure also shows that the total carbon requirement for 100 percent pre-reduction is 250 kg/THM. The carburization carbon being 40 kg, the reduction carbon is 210 kg. However, in the absence of any direct reduction requirement except that of metalloids, the carbon necessary to produce the necessary high temperature heat plus metalloids reduction is about 119 kg. But, the gas produced from this amount of carbon does not satisfy the low temperature heat requirement in the upper furnace and hence a much larger amount of carbon is consumed giving a high CO/CO_2 ratio in the top gas. The increase in the ratio is not due to any inferior utilization of CO but due to an increased volume of gas available compared to Fe-oxygen.

For every 10 percent metallization of the burden, the estimated[47,48] decrease in the coke rate is about 5.6 percent with associated increase in output by the same amount. Metallized pellets have greater strength than sinters or oxidized pellets. Metallization is profitable when the coal dust used for the pre-reduction is 60–65 percent cheaper than the blast furnace coke.[48]

It should be noted that the pre-reduction of oxygen from *wustite only* is of primary importance. Wustite constitutes 70 percent of the available oxygen in iron. No gain in the coke rate can be expected if only 30 percent of the total oxygen is removed, for the CO generated from the tuyere carbon would in any case be sufficient to reduce hematite and magnetite to wustite.

10.6. Stack Gas Injection

Instead of pre-reducing the ore to metallic iron outside in a separate batch process, the reduction can be performed continuously inside the furnace itself by injecting a reducing gas in the shaft. The purpose of such injection is to achieve any desired degree of indirect reduction, even up to 100 percent, by using cheaper gaseous reductant in order to save costly metallurgical coke. The savings are derived both from the direct reduction carbon as well as from the tuyere carbon needed to supply the endothermal heat of direct reduction. The productivity should increase simultaneously since the amount of bosh gas produced becomes smaller, the gas throughflow in the bosh zone being more frequently the limiting factor in iron production than that in the stack.

The stack gas can be obtained by reforming natural gas or oil or by

any other method. In order that the reaction products (CO_2 and H_2O) do not undergo any Boudouard reaction, the place of injection should be at the base of the thermal reserve zone and the temperature of the injectant gas about 1000°C so as to maintain the furnace temperature profile. For the case of 100 percent indirect reduction, the carbon requirement (for metalloids reduction and supply of high-temperature heat) as given in Example 10.2 and in the preceding section will be about 119 kg. The low-temperature heat requirement will be supplied by the hot injected gas. Including the carburization carbon of 40 kg, the calculated coke rate (85% C) will be about 200 kg/THM, a figure predicted by Decker and Poos.[49] However, because of various difficulties, the process is seldom used in practice.

The amount of stack gas necessary to obtain 100 percent indirect reduction in addition to the bosh gas generated from 119 kg.C is about 925 Nm^3/THM, assuming a CO/H_2 volume ratio of 1:2 (e.g., $CH_4 + \frac{1}{2}O_2 = CO + 2H_2$).

The amounts of bosh gas produced for the two cases (pre-reduced and stack gas) show a possibility of increase in the production by 90 percent providing 'flooding' in the bosh is the limiting factor. Taking a factor[49] of 0.7 in Sherwood's equation, the expected increase in production is about 60 percent. No increase in the production is possible, rather it may even decrease, if the limiting factor is the fluidization of the materials in the stack. This is because of an overall increase in the amount of furnace gas to satisfy the requirement of indirect reduction.

The difficulty of using stack gas lies in the proper distribution and utilization of the gas in the entire cross-section of the stack. According to Jeschar et al.,[50] the approximate depth of penetration of the stack gas is given by:

$$\text{depth of penetration} \propto \frac{\text{mass of stack gas}}{\text{mass of bosh gas}}$$

The above factor substantiates the favourable results obtained from experimental furnaces.

Table 10.3[49] shows the results of experimentations by AIRBO (Ougree) with and without oil injection through the tuyeres. The coke savings were not as much as expected because of higher cooling losses per THM and the presence of about 20 percent of CO_2, H_2O and nitrogen in the reformed gas.

Table 10.3.[49] Stack gas injection with and without oil

Items		Base	Without oil	With oil
Coke rate (85% C)	kg/THM	660	515	375
Stack gas, quantity	Nm^3/THM	0	730	751
Oil	kg/THM	0	0	155
Blast temperature	°C	1.020	1020	920
Oxygen content	%	21	21	40
Blast quantity	Nm^3/THM	1802	1297	785
Top gas temperature	°C	235	355	235
Top gas composition				
CO	%	24	27.2	36
CO_2	%	15.9	14.3	17
H_2	%	1	12	19.5
N_2	%	59.1	46.5	27.5
Hot metal				
Silicon content	%	1	0.99	0.95
Production	THM/h	1.248	1.54	1.85
Replacement ratio,	kg.coke/Nm^3 gas	—	0.199	0.174
	kg.coke/kg oil	—	—	1.15

Cost calculation shows that the stack gas injection process may be economical if a replacement ratio of 0.25 kg.coke/Nm^3 stack gas is obtained.

Yatsuzuka et al.[51] have used oil partially oxidized to gas and injected in the stack to reduce the tuyere gas volume. With a fuel oil rate of 70 kg/THM injected through the tuyeres and 30 kg/THM of oil injected in the stack as gas, the replacement ratio obtained is 0.9–1.0 kg.coke/kg of gasified oil. The ratio decreases with increasing amount of gasified oil.

10.7. Blast Additives

The primary purpose of using injectants with the blast is profitability which depends upon the relative price of coke and injectants and the amount of coke that can be saved per unit of the latter, i.e., upon the replacement ratio:

$$\text{Replacement ratio} = \frac{\text{kg.coke saved/THM}}{\text{kg or } Nm^3 \text{ of injectant/THM}}$$

In addition, such injections generally cause a smoother furnace movement especially when coolant additives are used (Sec. 7.6.6) and give rise to a higher productivity especially with oxygen-containing additives, e.g., humidified or oxygenated air or oxygen plus fuel additive.

The additives used as part replacement of coke are those which cannot be charged from the top. They may be:

(i) gaseous, such as, oxygen, steam, natural gas, coke-oven gas, reformed gas;
(ii) liquids, such as, fuel oil, tar, oil-coal slurry, naphtha;
(iii) solids, such as, pulverized coal, anthracite etc.

These additives obviously cannot play the role of coke for providing bed permeability in the dry zone or mechanical support to the charge column in the wet bosh zone but otherwise they perform the same chemical and thermal functions, the latter however at a much reduced scale. This is because, except oxygen, all the above additives lower the flame temperature.

The blast furnace works through a happy marriage between the thermal and chemical (reductant) energy requirements. Since the amount of removable oxygen from iron oxides per THM (of prime importance being wustite oxygen) is more or less a fixed quantity and hence the minimum amount of reductant necessary for its elimination is also fixed, the optimum fuel rate is obtained *only when* the heat requirement is satisfied along with the minimum reduction requirement. In the blast furnace, the fuel supplies the both, the sensible heat of the blast supplying part of the thermal energy.

The properties, composition and products of combustion of some blast furnace fuels have been discussed in Sec. 6.9. The hydrocarbons are combusted to CO and H_2 before the tuyeres. Hydrogen is better than CO as a reductant and it also gives a better utilization factor for wustite. At 900°C, for wustite/iron equilibrium (Eqs. 3.14 and 3.28),

$$FeO + 3.3\ CO = Fe + 2.3\ CO + CO_2;\ \eta_{CO,FeO} = 30\% \qquad 10.11$$

$$FeO + 2.7\ H_2 = Fe + 1.7\ H_2 + H_2O;\ \eta_{H_2,FeO} = 37\% \qquad 10.12$$

From the above two equations, 1 kg of hydrogen will remove the same amount of wustite oxygen as will be done by CO evolved from 7.2 kg

carbon. Because of the higher reduction rate and utilization factor obtained with hydrogen, hydrocarbons are expected to increase indirect reduction and hence decrease both the direct reduction as well as the tuyere carbon rates. Against this credit in heat, a debit is occasioned through the lowered flame temperature. Since the lower furnace heat requirement per THM, Q kcal, is supplied by

$$Q_{>900^\circ C} = \text{gas vol.}(Nm^3/THM) \times \text{sp heat } (kcal/Nm^3.^\circ C) \times t_f\text{-}900 \qquad 10.13$$

the gas volume must increase (if Q is constant) in order to compensate for the fall in flame temperature, t_f. Further, the gas volume is made up of the tuyere gas produced from tuyere carbon and the additive and Q decreases with the increase in indirect reduction (by hydrogen). Hence, for a fixed amount of any blast additive per THM, the tuyere carbon saved will decrease or increase according as the ratio $Q/(t_f - 900)$ increases or decreases. The replacement ratio will depend upon the sum of the tuyere and direct reduction carbon saved.

Although the bosh gas enriched with hydrogen increases indirect reduction, the extent depends upon the temperature gradient $(t_f - 900)$. The heat transfer rate decreases as the gradient becomes smaller, with the ultimate result that the 900°C level in the lower furnace shifts vertically upwards, shortens the thermal reserve zone and deteriorates the otherwise obtainable degree of indirect reduction of wustite. Although the overall indirect reduction increases, when the gas volume is large it may result in an inferior gas utilization. Also, a larger volume of gas carries more sensible heat at 900°C level, and the upper furnace heat requirement remaining the same, it will lead to an increase in the top gas temperature. Some of these and other related aspects have already been discussed in Chapter 4 and Sec. 7.3.3.

From above, depending upon the value of the term $(t_f - 900)$, a part replacement of coke by coolant injectants lowers the fuel efficiency. The gradient can be increased and the furnace temperature profile maintained by an increase in the flame temperature (through heat input, e.g., by increasing the blast temperature) which will lower the necessary gas volume, i.e., a smaller volume of tuyere gas will be needed for carrying the required quantity of heat. In other words, for a given quantity of additive per THM, the tuyere carbon rate will decrease which means an increase in the replacement ratio. Again, we have seen in Sec. 6.9.3 that the flame temperature itself depends upon the amount of tuyere carbon in blast addi-

tive cases. Thus, we can see that there are so many complicated interdependent variables, they render a prediction of the fuel rate for a given burden virtually impossible. However, it is still possible, as has been done in the coke alone case in Sec. 10.2, to calculate the fuel (coke + additive) rate for a given thermal requirement assuming that the hydrogen and CO from the additive and the CO from the tuyere and direct reduction carbon reach equilibrium with wustite/iron at their respective gas utilization factors at 900°C (Eqs. 10.11 and 10.12). Some such optimum fuel rate calculations will be shown at proper places.

The heat content of the tuyere gas per unit volume is a measure of the flame temperature. A constant flame temperature is maintained if the heat content of the tuyere gas per Nm^3 remains constant. However, with the use of blast additives, the amount of the tuyere gas as well as the flame temperature change with the changing amounts of tuyere carbon. For a simple case, assuming that Q>900°C remains constant, it is possible to calculate the blast temperature necessary to compensate for additive fuels if the amount of tuyere carbon for the coke alone case is known.[23,52] From Eqs. 6.14, 6.21 and 6.22, the heat content of the tuyere gas, Q_g kcal/Nm^3, for the coke alone case is given by:

$$Q_g = \frac{C_t\,(2840 + 4.44\,C_p.t)}{5.376\,C_t} \qquad 10.14$$

and that for the coke plus additive, Q'_g kcal/Nm^3, given by:

$$Q'_g = \frac{C'_t\,(2840 + 4.44\,C_p.t') + H\,(Q_c + v_b.C_p.t')}{5.376.C'_t + v_a.H} \qquad 10.15$$

where,

C_t = tuyere carbon, kg/THM, without additive
C'_t = tuyere carbon, kg/THM, with additive
H = amount of injected fuel, kg/THM
t = blast temperature, °C, without additive
t′ = blast temperature, °C, with additive
Q_c = heat of combustion of fuel additive, kcal/kg(Nm^3)

The other quantities are obtainable from Eqs. 6.14, 6.21 and 6.22.

For constant flame temperature,

$$Q_g = Q'_g \qquad 10.16$$

Hence, from Eqs. 10.14 and 10.15, it is possible to calculate t′, necessary for maintaining a constant flame temperature, if C_t' and H, i.e., the tuyere carbon replacement ratio, R′,

$$R' = \frac{C_t - C_t'}{H},$$

is assumed or desired. The term $C_t - C_t'$ or the ratio will obviously be smaller if the blast temperature remains constant and they will increase with the increase in blast temperatures.

In actual fact, Q>900°C will be smaller in the case of additives because of increased indirect reduction by hydrogen, lower slag volume due to reduced input of tuyere coke ash, etc. Therefore, the values of C_t' and t′ of Eq. 10.15 will change accordingly. If $(C_d - C_d')$ be the direct reduction carbon saved, then, based on one THM,

$$\begin{aligned} R \text{ (replacement ratio)} &= \frac{\text{total carbon saved}}{\text{oil input}} \\ &= \frac{(C_t - C_t') + (C_d - C_d')}{\text{oil input}} \\ &= \text{kg.C saved/kg.oil} \end{aligned} \qquad 10.17$$

From Table 6.7, for a fixed blast temperature and amount of hydrocarbon, the flame temperature is higher the higher the tuyere carbon. Therefore, a larger amount of fuel can be injected to maintain a constant flame temperature. That means, the additive fuel will be more profitably utilized the leaner the ore. Further, lean ores are usually smelted with lower blast temperature than the rich ones and hence more sensible heat can be utilized by using higher blast temperatures without the danger of erratic furnace movement. For rich ores working with highest blast temperatures, additive fuels are less attractive from the point of view of replacement ratio but still they are widely used because of smoother furnace operation and maintenance of metal quality for reasons already discussed in Sec. 7.8.1.1. Coolant injectants appear to be of utmost importance for achieving high productivity in super-large blast furnaces.

The comparative evaluation of the hydrogen-bearers in their use in the blast furnace has been dealt with excellently by various workers.[23,52-54] The effect of steam, oil and natural gas on the carbon consumption rate for the cases of constant blast temperature, temperature compensation and oxygenation are described below. The operational data of these and other additives will be narrated later.

The use of blast additives may affect the fuel rate of a burden in several ways, they being mainly due to changes in:

(i) flame temperature;
(ii) bosh gas composition and volume;
(iii) thermal efficiency, i.e., the CO/CO_2 ratio and temperature of the top gas;
(iv) operational efficiency, i.e., proportion of direct/indirect reduction;
(v) slag volume and basicity;
(vi) iron quality;
(vii) production efficiency.

These variations and their effects on operational results are discussed in the following.

10.7.1. Effects of Blast Additives

10.7.1.1. Flame temperature

It is our experience that the blast furnace can operate at widely varying flame temperatures, the upper limit being the beginning of erratic burden movement and the lower one, the maintenance of free-running temperature of the hearth slag as well as a specified metal silicon. Operation at low temperatures needs generation of a large amount of tuyere gas and hence can be performed at the cost of high fuel consumption. As the cost of preheating the blast is relatively cheap, the use of maximum flame temperature conducive to smooth running of the furnace is most economical. Therefore, a maximum possible blast temperature should be employed before contemplating any introduction of blast additives.

There are two separate cases for consideration:

(i) operation at constant blast temperature (decrease in tuyere gas heat content/Nm^3; lower flame temperature);
(ii) operation at constant flame temperature (constant tuyere gas heat content/Nm^3; increase in blast temperature).

10.7.1.1.1. Steam

Steam is not injected separately but is incorporated in the blast and hence is introduced as a fixed quantity per unit of blast volume. A fixed amount of tuyere gas is produced per kg.C and the flame temperature is independent of the amount of tuyere carbon (Fig. 6.27). The flame tem-

perature and the available heat per kg.C are also fixed. They depend upon the blast temperature and the degree of oxygen-enrichment.

The optimum tuyere carbon and direct reduction carbon rates for various blast moisture contents at three temperature levels are summarized in Fig. 10.18. The values for dry blast (0% moisture) in Fig. 10.18 are assembled from Fig. 10.7 for the burden of Table 10.1. The method followed is the same as cited in Sec. 10.2 except that the amount of indirectly reduced wustite-oxygen per kg of tuyere carbon has been calculated from the amount of CO and H_2 evolved per kg.C and employing Eqs. 10.11 and 10.12. The heats available from the tuyere gas per kg.C cooling down from the flame temperature to 900°C has been taken from Fig. 6.27 and other similar figures for higher moisture contents not included in the text. Fig. 10.18 shows that, for any fixed blast temperature, the total carbon rate increases with moisture injection because the tuyere carbon rate increases while the direct reduction carbon does not decrease proportionately. The increase in the tuyere carbon is due to fall in the flame temperature (Fig.

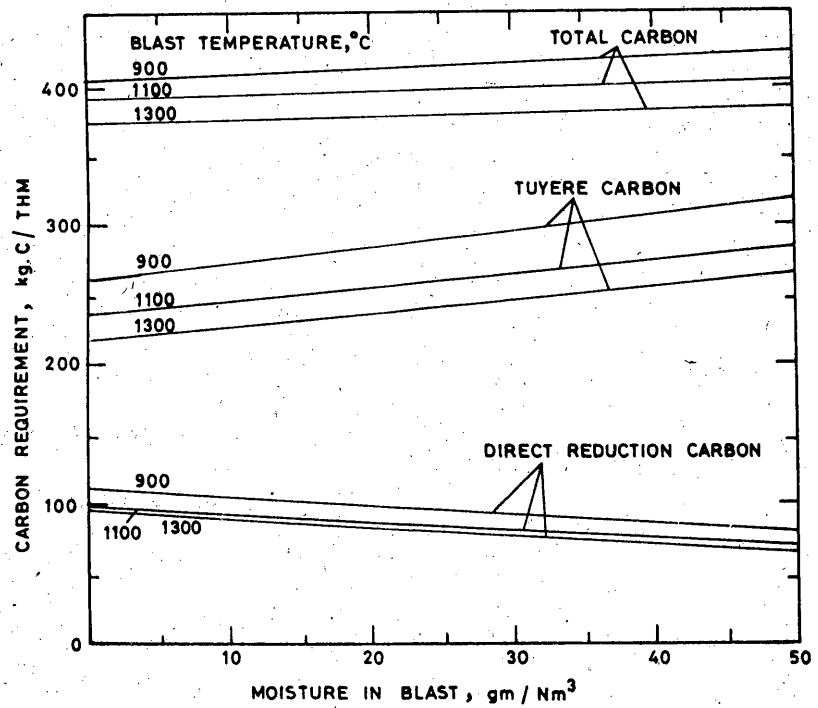


Fig. 10.18 The influence of blast temperature and blast moisture on the total, direct and tuyere carbon requirements (calculated).

6.28) and tuyere gas volume per kg.C (Table 6.6), the combined effect of both being less available heat in the lower furnace.

From Sec. 6.8.1, for maintaining a constant flame temperature, an increase of 8–10°C in blast temperature is necessary for every gm of steam per Nm^3 of blast. The heat content of the tuyere gas remains more or less constant if the decrease in the flame temperature is fully compensated (cf. Fig. 6.27). Most of the savings in carbon is due to the higher utilization of hydrogen compared to CO with respect to wustite. Carbon savings expected can be estimated from a comparison of Figs. 10.18 and 10.7.

For furnaces not working at optimum carbon rates, a further carbon saving can be realized due to:

(i) increased rate of wustite reduction with hydrogen; decreased direct reduction carbon;
(ii) extended and more reducing combustion zone; more uniform gas and stock movement; maintenance of hearth and metal temperature and metal quality (Sec. 7.8.1.1).

Although oxygen-enrichment of the blast can be used for raising the flame temperature, the heat content of the bosh gas decreases (Figs. 6.26 and 6.27). The increase in the flame temperature is due to a lower volume of bosh gas produced per kg.C and not due to any increase in the heat input. Therefore, a saving in coke is not expected but a great increase in the production rate can be achieved.

10.7.1.1.2. Oil

The variations of the optimum reduction carbon rates with indirect reduction for the same burden (Table 10.1) and 0, 50, 100 kg.oil/THM at blast temperatures of 900 and 1300°C are shown in Fig. 10.19. The variations of the optimum tuyere, direct reduction and final carbon rates for oil rates 0–100 kg/THM and three levels of blast temperature are drawn in Fig. 10.20. The method of calculation is based on the total amount of CO and H_2 generated from the given quantity of oil (Table 6.8) and the amount of wustite-oxygen they will remove according to Eqs. 10.11 and 10.12. Added to this is the wustite-oxygen removed by CO evolved from direct reduction of the metalloids. The amount of heat evolved from oil (Table 6.8) is added to the heat evolved from the tuyere carbon. The latter is not a fixed quantity and hence the flame temperature changes as the tuyere carbon changes. Computer iteration was used to determine the tuyere carbon and direct reduction carbon necessary to remove the

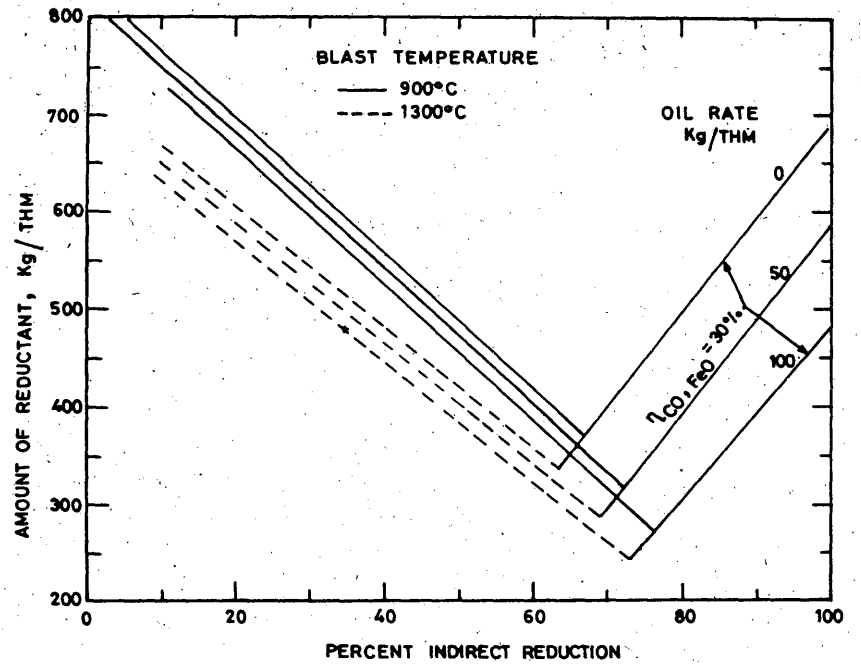


Fig. 10.19 Variation of reduction carbon rates with indirect reduction for two levels of blast temperature and oil injections (calculated).

rest of the wustite-oxygen and at the same time satisfying the lower furnace heat requirements along with the changing direct reduction and changing heat supply (because of changing flame temperature).

Since the flame temperature decreases with oil additions at constant blast temperature, the replacement ratio kg.C/kg.oil suffers and it varies from 1.0 to 1.5 in non-compensated cases (Fig. 10.22).

For determining the influence of temperature compensation, the flame temperatures at optimum carbon rates (optimum tuyere carbon) for each level of oil 0–100 kg/THM and three blast temperature levels are drawn in Fig. 10.21. From comparison with no-oil case of Fig. 10.7, the replacement ratios are drawn in Fig. 10.22 showing the variations with the change in flame temperature. For the temperature compensated case, $\Delta t_f = 0$, the ratio is about 1.5 and becomes higher as Δt_f increases. It is evident that a large amount of coke can be saved by increasing the blast temperature if the furnace can accept a flame temperature beyond the optimum.

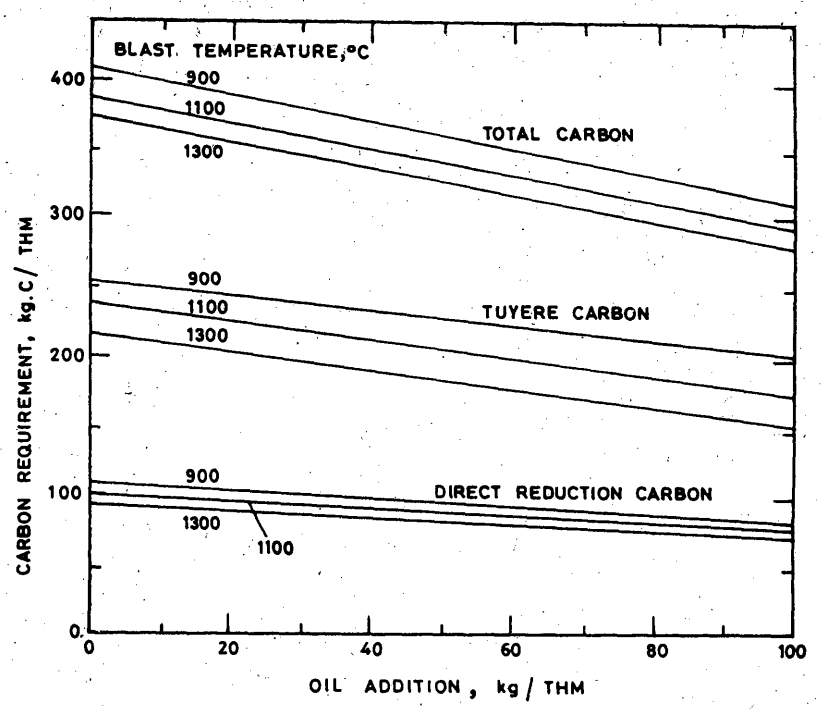


Fig. 10.20 Variation of the total, direct reduction and tuyere carbon requirements with oil additions at three levels of blast temperatures (calculated).

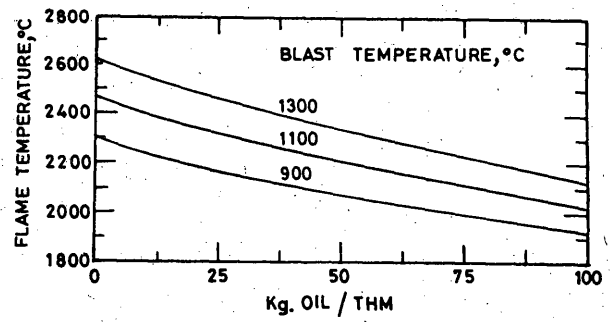


Fig. 10.21 Variation of flame temperature with oil rates at three levels of blast temperature calculated from Figs. 10.19 and 10.20.

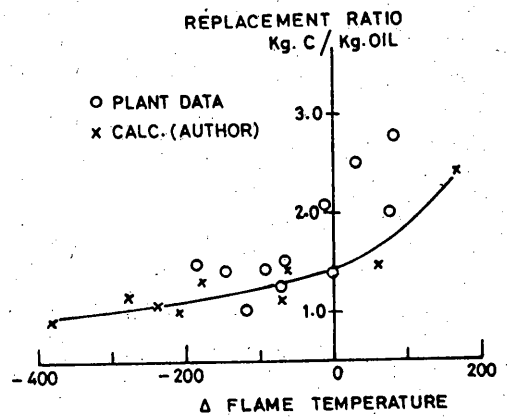


Fig. 10.22 Variation of replacement ratio kg.C/kg.oil with change in flame temperature.

Some actual replacement ratios from plant experience are included in Fig. 10.22. A few show very high ratios. The plausible reasons are:

(i) more uniform and extended gas and stock movement (Sec. 7.8);
(ii) higher degree of indirect reduction because of (i) above;
(iii) lower input of iron oxides in the hearth; improvement of its thermal state (Sec. 7.8);
(iv) coke rate already high due to tightness of the furnace caused by high blast temperatures; restoration of temperature gradient by use of coolants; initially, a higher coke saving per unit of additive fuel.

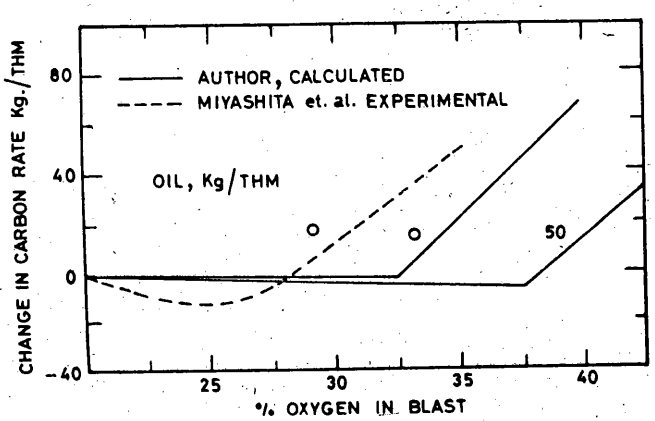


Fig. 10.23 Change in carbon rates with oil injection and oxygen-enrichment of blast.

Most modern plants using pre-fluxed burden operate at optimum stove capacities and hence it is seldom possible to increase the blast temperature. Although the flame temperature increases with oxygen-enrichment, for reasons seen in the preceding sub-section, very little gain in the carbon rate is expected from theoretical considerations (Fig. 10.23) as well as plant experiments.[55] The figure shows that after an initial small decrease, with further oxygenation, the carbon rate actually increases both with and without oil.[56] However, oxygenation of the blast increases furnace productivity.

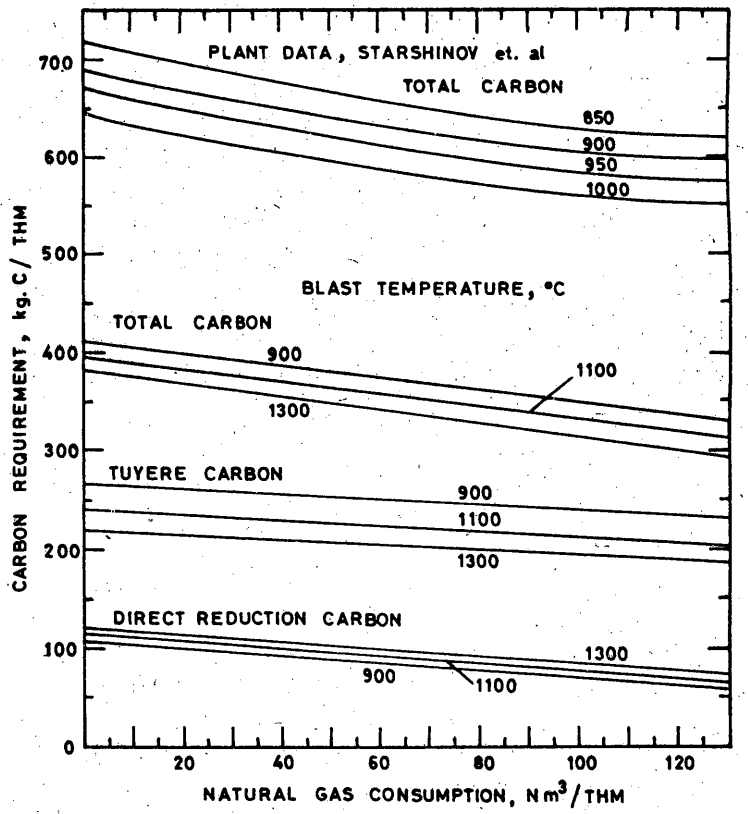


Fig. 10.24 Variation of total, direct reduction and tuyere carbon requirements with natural gas injection at three levels of blast temperatures (calculated). The variation of estimated total carbon requirement from the results of Starshinov et al.[57] is also shown.

10.7.1.1.3. Natural gas

The optimum final, tuyere and direct reduction carbon rates for various levels of gas injection and blast temperature are shown in Fig. 10.24 for the same burden (Table 10.1). The same method as in the case of oil has been used for the calculation taking the heat values and gas compositions from Table 6.8. The variations in the final carbon rates from the investigations of actual plant practice by Starshinov et al.[57] are also included in the figure, assuming that the coke contained 86% C.

Natural gas has a lower C/H ratio and it decreases the flame temperature much more than oil does (Table 6.7). Hence, a larger increase in the blast temperature is necessary for compensating the fall in flame temperature. Calculations, similar to those for oil, show that the replacement ratios vary from 0.86–0.94 for blast temperatures 900–1300°C and gas injection rates 70–140 Nm^3/THM. As expected, oxygenation has very little effect on the ratio.

10.7.1.2. Bosh gas composition and volume

We have seen in Eq. 10.13 that an adequate heat content of the bosh gas is necessary for satisfying the heat requirement of the lower furnace. Even if the heat is supplied by a very high temperature bosh gas, the volume per THM may become so small that the upper furnace heat requirement $Q<900°C$ is not satisfied which would increase the carbon rate and the replacement ratio will suffer.

The additives enrich the bosh gas with reductants, extend the combustion zone, reduce re-oxidation of pig iron and improve the thermal state of the hearth (Sec. 7.8). All these result in a further saving of coke for operational reasons (decreased direct reduction, stable operation, use of blast temperature to the maximum without keeping any reserve heat, etc.).

10.7.1.3. Top temperature. Thermal efficiency

The top gas temperature and CO/CO_2 ratio depend upon the bosh gas volume which itself depends upon the replacement ratio and hence upon the flame temperature. This again shows that maximum coke saving is obtained by the use of maximum flame temperature obtained from blast temperature increase. According to Trense and Rosborough,[58] the top gas CO/CO_2 ratio increases by 1 percent for a 40°C decrease in the flame temperature below the base case and decreases by 5 percent for each 40°C increase above the base case.

The top gas volume, calorific value and temperature increase while the thermal efficiency suffers, in general, with increasing additive injection. With oxygen-enrichment the top gas temperature decreases because of lower gas volume and the calorific value increases due to a lower nitrogen content but the coke rate and reduction conditions remain more or less the same.

10.7.1.4. Operational efficiency

Hydrogen-bearing additives give rise to a bosh gas richer in hydrogen and CO and they are expected to increase indirect reduction and operational efficiency.

In actual practice also, direct reduction carbon decreases greatly with additives. The contribution arises mainly from hydrogen, the utilization of which increases with increasing amount of additives while that of CO remains more or less constant.[55,59] Since additives induce a smoother and more uniform and extensive stock descent, the actual savings in coke may be much more than the calculated ones.

10.7.1.5. Slag volume and basicity

The coke-ash input decreases with savings in coke and results in decreased slag volume. In the case of raw burden, considerable coke can be saved from the decreased input of limestone. Further savings arise because with fuel additives, a lower basicity of the slag can be used without affecting the efficacy of sulphur removal (Sec. 9.4.1.2).

10.7.1.6. Iron quality

For reasons already seen in Sec. 7.8, fuel additives promote and maintain better hearth conditions and metal quality. Some coke savings are expected from this, especially when the metal analysis is erratic and needs additions of coke and changing of the blast temperature to obtain the metal within specifications.

10.7.1.7. Production efficiency

The uniformity of the furnace movement and the lower density and higher heat transfer coefficient of hydrogen permit a higher blast volume to be blown without upsetting the temperature and reduction profiles of the furnace. Therefore, a higher rate of production can be realized without impairing the gas efficiency. Since the radiation and cooling losses are constant in time, a higher production will mean savings in coke per THM. The limit of forcing is discussed in Sec. 11.5.

10.7.2. Plant Data

10.7.2.1. Oil

Coke saved depends upon the blast temperature increase and any gain in direct reduction and heat associated with it. For constant blast temperature, replacement ratios between 2.0 kg.coke/kg.oil for small oil additions to 1.0 for 100 kg.oil/THM have been obtained. The productivity increases[59] by about 2 percent up to 50 kg.oil/THM and falls by 6 percent with 100–120 kg/THM because of an excessive increase in the bosh gas volume. Figures of similar order have been obtained.[5] Ratios up to 3.0 have been obtained with high blast temperatures. In the experimental furnace at Bruceton,[60] replacement ratios of 2.73–1.13 have been obtained for oil rates 0–158 kg/THM and blast temperatures 1000–1330°C. By the use of oil 87–95 kg/THM, decrease in the blast humidity by 4–5 gm/Nm^3 and increase in the blast temperature by only 50°C, a decrease in the coke rate by 14.2–15.7 percent, and increase in productivity by 6.1–8.8 percent have been reported.[61] Suggested blast temperature compensation is 4–6°C/gm oil/Nm^3 blast.

According to Malvaux et al.,[62] for oil rate of 14.7 kg per 1000 Nm^3 blast the temperature compensation required is 100°C. At this rate, a replacement ratio of 2.8, a decrease in the coke rate by 22 percent and an increase in output by 23 percent were obtained. Although the volume of the bosh gas increased, the output increased because the daily consumption of coke was maintained.

Oxygen-enrichment of blast up to 25% O_2 at 1025–1125°C with heavy oil injection up to 100 kg/THM has been investigated.[59] Compared to the normal blast, the effect was negligible on the replacement ratio, indirect reduction or on CO-H_2-utilization. The productivity increased by 2.5 percent for every 1 percent increase in oxygen. In all cases, with or without enrichment, the productivity rose up to 50 kg oil/THM and then started to decrease with increasing oil (Fig. 11.18) because the bosh gas volume increased with decreasing replacement ratio. According to Vakulin et al.,[63] with heavy oil up to 100 kg/THM and 30% O_2 blast, the coke rate fell by 13.8 percent and the productivity increased by 10.4 percent. Further details of the theory and practice of fuel injection can be obtained from the literature.[52–54,64–73]

Modern high capacity furnaces working with higher blast temperatures employ oil or natural gas without temperature compensation although the replacement ratio suffers. The benefits of smoother furnace movement and

maintenance of metal quality far outweigh any loss in coke due to the reduced flame temperature.

10.7.2.2. Natural gas

The calculated replacement ratio is about 1.0 kg coke/Nm^3 natural gas.[74] Injection of 80–200 Nm^3 natural gas per THM has been investigated.[75] Natural gas has the same beneficial effects as oil, perhaps more. Even without temperature compensation a replacement ratio of 0.8 kg coke/Nm^3 has been obtained with 6–10 percent savings in coke and 0.5–2 percent increase in productivity. Depending upon the ore quality, blast temperature and amount of natural gas, coke savings up to 10 percent can be expected with a slight increase in productivity.

Large furnaces work smoother with natural gas than the smaller ones. An injection of 75–80 Nm^3/THM saved 65–75 kg coke with a replacement ratio of 0.86 and increased the productivity[76] by 4.5 percent. In USSR, with suitable charge preparation and natural gas plus 30–35% O_2-blast, the average decrease[74] in the coke rate is 20–25 percent.

10.7.2.3. Coke-oven gas

According to calculations of Bogdandy and Schaefers,[52] the replacement ratio kg.C/Nm^3 coke-oven gas is about 0.8 for constant flame temperature. The results of investigation[77] in a 6.25 m blast furnace with 80 Nm^3/THM of the gas shows a ratio of 0.5–0.8 for blast temperatures 680–880°C.

Without temperature compensation and with a gas consumption of 99 Nm^3/THM, a decrease in the coke rate by 9.6 percent with a replacement ratio of 0.62 kg.coke/Nm^3 and an increase in productivity by 4.2 percent have been reported.[78] Coke-oven gas reduces the flame temperature much more than oil or natural gas does. It improves the stability of the thermal conditions, extends the combustion zone and promotes smoothness of furnace operation.

10.7.2.4. Coal-dust

The calculated replacement ratio of 0.68 kg.coke/kg.coal-dust agrees well with that in practice.[74] In USSR, with coal containing 31–34%-ash and an injection rate of up to 80 kg/THM, the ratio is 0.61–0.64 and an increase in productivity of 1.2–2 percent. A ratio of 1.02 kg coal dust/kg.carbon has also been reported.[79,80]

10.8. High Top Pressure (HTP)

HTP can influence the coke rate mainly because:

(i) an increased gas pressure in the furnace increases the rate of reduction of iron oxides (Sec. 6.7.10), decreases direct reduction and hence reduces the coke rate;

(ii) a decrease in the linear gas velocity caused by HTP increases the gas-solid contact time, decreases direct reduction and hence reduces the coke rate; HTP improves gas permeability in the furnace and promotes a more uniform gas distribution which in its turn further decreases direct reduction.

Fig. 10.25[81] shows the decrease in direct reduction carbon with increasing top pressure for constant productivity and increase in direct reduction carbon with increasing productivity at constant top pressure. Since productivity increases with increasing top pressure because of increased gas mass flow rate, the extent of coke saved will depend upon the linear gas velocity. Generally, coke can be saved if the gas velocity with HTP is kept below the base case without HTP. At all events, HTP improves furnace permeability, decreases the number of slips and flue dust emission and promotes stable operation for long periods in both large and medium capacity furnaces. The subject is further discussed in Secs. 11.3.2.9 and 11.4.

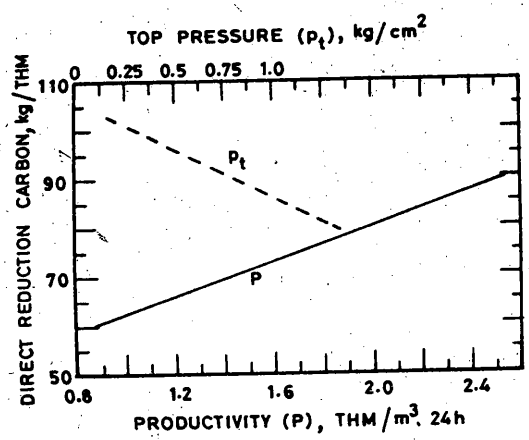


Fig. 10.25 Productivity (P) against direct reduction carbon with top pressure of 0.8 kg/cm^2; top pressure (P_t) against direct reduction carbon with productivity 2.3 THM/m^3.24h. After Higuchi et al.[81] (Copyright Iron Steel Institute).

References

1. BOGDANDY, L. v., G. LANGE and P. HEINRICH: Stahl u. Eisen, 88, 1968, p. 1177–1188.
2. REICHARDT: op. cit., 78, 1958, p. 748.
3. SCHULZ, D., D. BULTER and G. ESFELD: op cit., 89, 1969, p. 905–917.
4. ZISCHKALE, W., G. HEYNERT and H. BEER: op. cit., 83, 1963, p. 1117–1123.
5. SCHUMACHER, H.: op. cit., 86, 1966, p. 313.
6. KITAEV, B. I.: Stal, 8, 1954, p. 684–690.
7. KITAEV, B. I. et al.: Trans. Ind. Inst. Metals, No. 12, 11, 1958, p. 3–30.
8. MICHARD, J.: Cahiers du CESSIS, 18, 1960, p. 78.
9. BABARYKIN, N. N. and F. A. YUSIN: Stal in Eng., 5, 1960, p. 314.
10. MINTROP, R.: Stahl u. Eisen, 78, 1958, p. 633–644.
11. BIRNBAUM, H. and L. v. BOGDANDY: op. cit., 82, 1962, p. 785–796.
12. BIRNBAUM, H. et al.: op. cit., 80, 1960, p. 781–788.
13. KAHLHÖFER, H.: op. cit., 78, 1958, p. 644.
14. BOGDANDY, L. v.: op. cit., 81, 1961, p. 12–22.
15. MARSHALL, W. E.: J. Metals, 13, 1961, p. 308–313.
16. Economic aspects of iron ore preparation – UN Technical Publication, Geneva, 1966, No. ST/ECE/Steel/14.
17. KAHLHÖFER, H. et al.: Stahl u. Eisen, 79, 1959, p. 1461–1470.
18. DOBSCHA, H. F.: Blast Furn Steel Plant, 34, 1946, p. 979–983.
19. SQUARCY, C. M. and R. J. WILSON: Steel, No. 21, 139, 1958, p. 150–160; No. 22, p. 100–110.
20. SMEDSTAM, J. A.: J. Metals, May 1965, p. 465–472.
21. SQUARCY, C. M. and R. J. WILSON: Steel, 19 Nov. 1956, p. 150; 26 Nov. 1956, p. 98.
22. WOLF, W.: Stahl u. Eisen, 81, 1961, p. 558.
23. BOGDANDY, L. v. and H.-J. ENGELL: The reduction of iron ores (in Eng.), Springer-Stahleisen, 1971.
24. Blast Furnace – Theory and Practice, Edt. J. H. Strassburger, Gordon and Breach Sci. Pub., N.Y. 1969, Vols. 1 and 2.
25. MACDONALD, N. D.: Future of ironmaking, Spl. Rep. 72, Iron Steel Institute, 1962, p. 149–153.
26. KNEPPER, W. M. and C. M. SCIULLE: J. Metals, Feb. 1966, p. 228–230.
27. ZHEREBIN, B. N. et al.: Steel in USSR, Jan. 1972, p. 6–13.
28. KAZANSKII, M. F. et al.: op. cit., June 1971, p. 421–426.
29. HEYNERT, G. et al.: Stahl u. Eisen, 80, 1960, p. 473–483.
30. DANIELSSON, Ch.: J. Iron Steel Inst., 175, 1953, p. 152–154.
31. BOSLEY, J. J., N. B. MELCHER and M. M. HARRIS: J. Metals, 11, 1959, p. 610–615.
32. DOI, Y. and K. KASAI: ibid., p. 755–759.
33. WILLEMS, J. and G. QUADE: Stahl u. Eisen, 81, 1961, p. 556.
34. NEKRASOV, Z. I. et al.: Stal in Eng., March 1970, p. 178–183.
35. ASTIER, J. E., J. MICHARD and P. DANCOISNE: J. Iron Steel Inst., Oct. 1961, p. 143–148.
36. ELLIOTT, G. D. et al.: op. cit., Nov. 1953, p. 241–247.
37. ELLIOTT, G. D.: op. cit., 181, 1955, p. 1–16.
38. VOICE, E. W. and K. G. DIXON: op. cit., 200, 1962, p. 438–443.
39. SCHIERLOH, U.: Stahl u. Eisen, 90, 1970, p. 709–712.
40. STARSINOV, B. N.: Stal in Eng., Oct. 1969, p. 865–867.

41. LENNINGS, W.: Stahl u. Eisen, 58, 1938, p. 25–34; 52–58; 623–630.
42. STRUVE, G. v.: J. Iron Steel Inst., Sept. 1960, p. 50–56.
43. PASKE, M. and P. HAHNEL: Stahl u. Eisen, 61, 1961, p. 385–392.
44. AGARWAL, J. C. and H. R. PRATT: J. Metals, 1966, p. 226.
45. ASTIER, J. E. and J. RAGUIN: Blast Furn. Steel Plant, 56, 1968, p. 319–322.
46. ASTIER, J. et al.: In: Ironmaking tomorrow, London, 1967; Iron Steel Spl. Rep. No. 102, p. 108–135.
47. MIKHALEVICH, A. G.: Steel in USSR, May 1971, p. 327–331.
48. VOSKOBOINIKOV, V. G. and A. G. MIKHALEVICH: Stal in Eng., July 1969, p. 612–615.
49. DECKER, A. and A. POOS: Stahl u. Eisen, 92, 1972, p. 1077–1084.
50. JESCHAR, R. et al.: op. cit., 91, 1971, p. 665–678.
51. YATSUZUKA, T. et al.: Trans. Iron Steel Inst. Jap., 13, 1973, p. 115–124.
52. BOGDANDY, L. v. and W. SCHAEFERS: Stahl u. Eisen, 82, 1962, p. 1–18.
53. Blast furnace injection: Proc. Sym., Ed. N. Standish, Aus. I.M.M., Wollongong, 1972.
54. The future of ironmaking in the blast furnace: Spl. Rep. 72, Iron and Steel Inst., 1962.
55. BRANDI, H. Th. et al.: Stahl u. Eisen, 83, 1963, p. 1541–1546.
56. MIYASHITA, T. et al.: Trans. Iron Steel Inst. Jap., 13, 1973, p. 1.
57. STARSHINOV, B. N. et al.: Stal in Eng., May 1962, p. 337–341.
58. TRENSE, R. V. and D. F. ROSBOROUGH: Ref. 53, p. 53–58.
59. ISCHEBECK, P., G. HEYNERT and H. BEER: Stahl u. Eisen, 82, 1962, p. 1476–1485.
60. WOOLF, P. L. and W. M. MAHAN: Blast Furn. Steel Plant, 49, 1961, p. 1189–1196.
61. BORUSOV, Yu. S. and A. A. FOFANOV: Stal in Eng., June, 1961, p. 397–402.
62. MALVAUX, T. et al.: Ref. 53, p. 59–71.
63. VAKULIN, V. N. et al.: Steel in USSR, July 1976, p. 349–353.
64. RIDGION, J. M.: Ref. 53, p. 1–9.
65. HAZARD, P.: Ref. 53, p. 24–30.
66. BELL, H. B. and J. TAYLOR: Ref. 53, p. 10–23.
67. SCIULLI, C. M. and D. G. WHITE: Ironmaking Proc., 74, 1975, p. 243–264.
68. ASHTON, J. D. and J. E. R. HOLDITCH: ibid., p. 265–284.
69. QUIGLEY, J. J. et al.: op. cit., 32, 1973, p. 26–35.
70. LUNN, H. G. and G. W. WATERHOUSE: J. Inst. Fuel, June 1976, p. 70–78.
71. ASHPIN, B. I. et al.: Steel in USSR, Oct. 1974, p. 784.
72. HIGUCHI, M. et al.: Trans. Iron Steel Inst. Jap., 15, 1975, p. 516.
73. BORUSOV, Yu. S. and A. A. FOFANOV: Stal in Eng., June 1961, p. 397–402.
74. VOSKOBOINIKOV, V. G. and A. G. MIKHALEVICH: op. cit., July 1969, p. 612–615.
75. VOLKOV, Yu. P., op. cit., May 1960, p. 337–341.
76. LEVIN, L. Ya. et al.: op. cit., Jan. 1965, p. 7–12.
77. LOORZ, W. and D. WINZER: Stahl u. Eisen, 87, 1967, p. 185–187.
78. ZHEREBIN, B. N. et al.: Stal in Eng., April 1965, p. 256–260.
79. EMUSHINTOV, V. V. et al.: op. cit., June 1969, p. 531–534.
80. AKBERDIN, A. A. et al.: op. cit., Sept. 1966, p. 683.
81. HIGUCHI, M., M. IIZUKA and T. SHIBUYA: Dev. in ironmaking practice, Proc. Conf. Iron Steel Inst., London, Nov. 22–23, 1972, p. 98–108.

CHAPTER 11

BLAST FURNACE PRODUCTIVITY

11.1. General

The development of blast furnace technology between the years 1860 and 1960 was relatively slow but steady. During these years the diameter of the furnace increased from smaller than 1 m to 8 or 9 m with production of 25–150 THM and 1500–2000 THM per day respectively. However, since the 1960s the expansion in technology has been so rapid that the furnace diameters have almost doubled and the production increased about five fold. Today, especially in Japan, furnaces with diameters 14–15 m are producing 10,000–12,000 THM per day. As the furnace diameter increased, so did its height and inner volume. Since the growth in height is limited by the mechanical strength of the ferrous burden as well as that of the coke, especially the latter, the modern high capacity furnaces grew outwards rather than upwards in order to increase the inner volume for adequate heating and reduction of the burden. The working volume has increased from 64 m^3 in 1860 producing 25 THM/day to 5000 m^3 in 1975 producing 13000 THM/day with future planning for 5500 m^3 with rated capacity of 14000 THM/day.

Theoretically, such high productivity figures may not be surprising since the higher the blast volume, i.e., the higher the oxygen input the greater will be the amount of coke burned and, therefore, the larger will be the

production. In practice, the crux of the problem lies in making the furnace accept the enormous volume of air. A host of physical, chemical and mechanical (mainly aerodynamical) factors determines the limit to forcing of the furnace and, therefore, to production, apart from the economics of an optimum productivity beyond which forcing would not pay. In this chapter we will deal with, or rather summarize, the effects of the physico-chemical and mechanical factors that govern iron production, most of them having already been discussed at various places in the text.

Productivity depends upon the amount of carbon burned in unit time at the tuyeres and the tuyere carbon (coke) consumed for producing a unit of iron. In other words, productivity is a function of the gas generated at the tuyeres in unit time and that required to produce a unit of iron. The amount of coke burned is usually called the *coke throughput* or *coke burning rate* or *driving rate* per day. The coke consumed for a unit of iron is termed as *coke consumption rate* or simply *coke rate* in kg or tonnes per THM. The production rate, also known as *smelting rate or output* is denoted as[1]

$$P = Q/K \qquad 11.1$$

where,

P = productivity, THM per day
Q = coke burned, tonnes per day
K = coke consumed, tonnes per THM.

From Eq. 11.1, P increases as Q increases and/or K decreases. These can be achieved by various measures as discussed in Secs. 11.3 and 11.4.

The production rate P can also be determined from the following:

$$P\ (\text{THM/day}) = \frac{\text{Total heat input per day}}{\text{Heat required to produce one THM}} \qquad 11.2$$

Since now-a-days a considerable amount of coke is replaced by hydrogen-bearing fuels, the productivity should be given by

$$P \approx \frac{\text{Total tuyere gas produced per day}}{\text{Tuyere gas generated to produce one THM}} \qquad 11.3$$

11.2. Blast Furnace Production Index

The blast furnace production index, B.P.I., is denoted as a percentage ratio of the actual production to an accepted production target,[2]

$$\text{B.P.I.} = \frac{\text{actual production}}{\text{production target}} \times 100 \qquad 11.4$$

The production target has no absolute value and is continuously improving with the improvement of blast furnace technique. The target itself can be derived from Eq. 11.1 from the average performance of the world's best blast furnaces with regard to their coke throughput and coke consumption rate.

11.2.1. Coke Rate Target

The target of coke rate can be derived from a statistical study of the best modern practices. It is a function of nett burden weight and other variables like the amount of limestone, sinter, pellet etc. in the charge. According to Eq. 10.9a, for 100% self-fluxing sinter, the coke rate varies linearly with the nett burden weight, given by[2]

$$K = 200 + 0.200\ B \qquad 11.5$$

More recent figures from an analysis of about 200 blast furnaces all over the world are given by the following equation:[3]

$$K = 470 + 0.164\ B + 0.249\ Z - 1.006\ S - 1.142\ P - 0.093\ t_b^\circ \qquad 11.6$$

Percent explained = 71.3%;
Standard deviation = 28.5 kg/THM

K = coke rate in kg/THM (87.5%C)
B = nett burden weight, kg/THM
Z = limestone charged, kg/THM
S = percentage of sinter based on gross burden weight
P = percentage of pellet based on gross burden weight
t_b° = hot blast temperature, °C

11.2.2. Coke Throughput Target

The coke burning rate is usually referred to as the amount of coke burned per day per m² hearth area. Also, the furnace productivity is often expressed in the same manner. However, on the basis of the assumption that the coke burns only in the raceway, the effective hearth area where the coke burns is therefore less than the total hearth area. We have seen in Sec. 5.2 that the proportion of the effective hearth area to the total hearth area decreases with increasing hearth diameter. Thus, the smaller furnaces

would be in a more advantageous position than the larger ones on the basis of total hearth area. A calculation of the coke burning rate per m^2 of the effective hearth area would therefore be a more realistic measure for comparing the coke throughput of various furnaces. Rice[4,5] put forward the idea from a statistical study of 130 world furnaces that the coke burns in a 6 feet wide annulus in front of the tuyeres and the optimum coke burning rate was about 6000 lbs of 86% C-coke per ft^2 of the active perimeter.

On conversion[6] of Rice's values to metric system, the width of annulus = 1.83 m and tuyere overhang = 0.23 m and hence the effective hearth area is given by,

$$A = 5.746\ (D - 2.29) \qquad 11.7$$

where,

D = hearth diameter, m
A = effective hearth area, m^2

Rice's coke burning rate is about 30.753 t coke/m^2/day. Therefore the coke throughput is,

$$Q = 30.753 \times A \qquad 11.8$$

$$= 177\ (D - 2.29), (t\ coke/day) \qquad 11.9$$

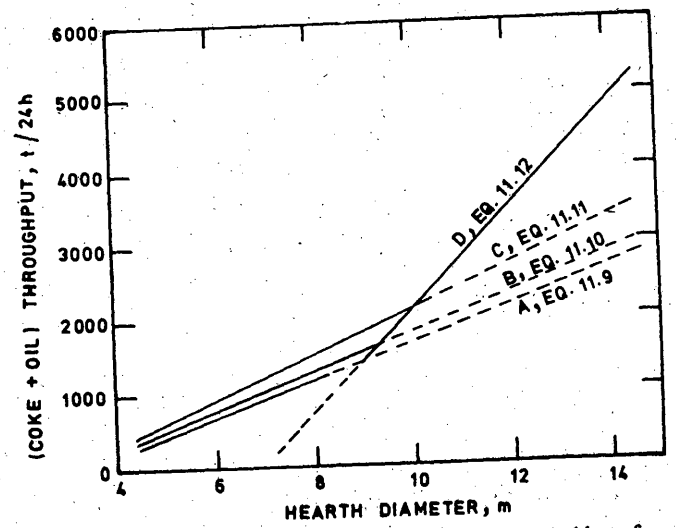


Fig. 11.1 Relationship between coke plus oil throughput and blast furnace hearth diameter.

Blast furnace performance has increased tremendously since Rice's statistical study and the coke throughput has risen steeply due to continuous improvements in the physical, chemical and mechanical properties of the raw materials. The comparative coke throughput values according to hearth diameters are shown in Fig. 11.1. Line A is after Rice;[4] Line B was calculated from 100 blast furnaces and Line C from 15 of the world's best furnaces up to 1962 (by Petersen et al.)[7] which was confirmed by Beer and Heynert.[1] A regression analysis by the author of the modern high capacity furnaces with diameters between 10–15 m is shown by Line D. The equations for Lines A to D are:

$$\text{Line A, } Q = 177\ (D - 2.29) : D = 4 - 6\ m \qquad 11.9$$

$$\text{Line B, } Q = 218\ (D - 2.83) : D = 4 - 8\ m \qquad 11.10$$

$$\text{Line C, } Q = 307\ (D - 3.15) : D = 4 - 9\ m \qquad 11.11$$

$$\text{Line D, } Q = 735\ (D - 7.25) : D = 10 - 14\ m \qquad 11.12$$

The Rice index is based on the width of the raceway of 1.83 m which approximates the value actually determined (range of 0.75–1.75 m). How-

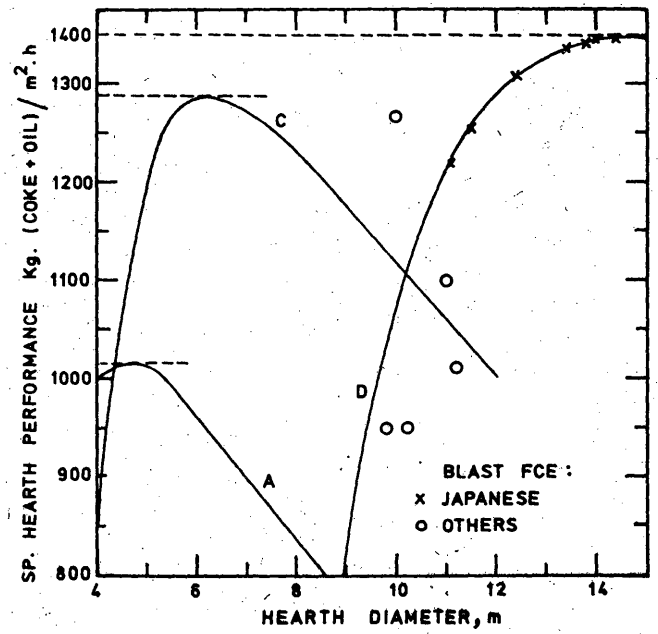


Fig. 11.2 Relationship between blast furnace hearth diameter and specific hearth performance.

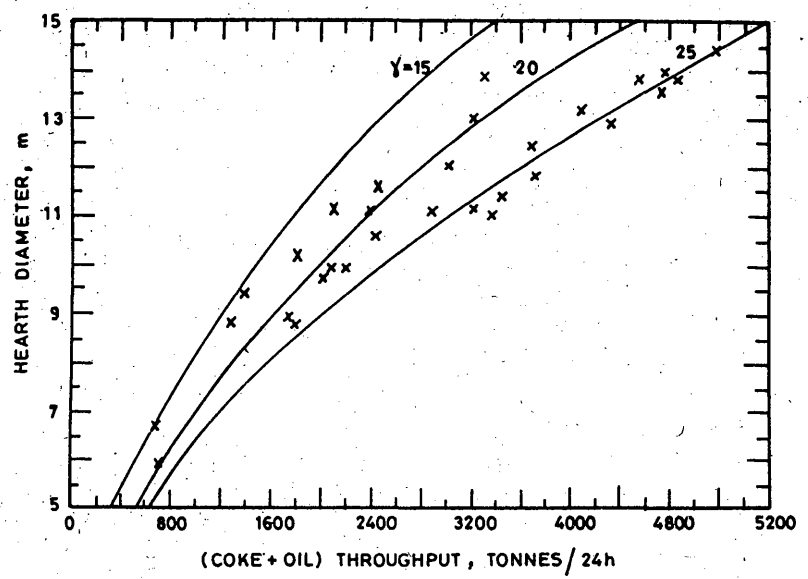


Fig. 11.3 Parabolic relationship between blast furnace hearth diameter and coke plus oil throughput.

ever, from Eqs. 11.10–11.12, the productivity of high capacity furnaces does not show any close relationship with the size of the raceway.

The coke throughput is also depicted as specific hearth performance which is number of kg coke/m².h. The lines calculated from Eqs. 11.10–11.12 are drawn in Fig. 11.2 against the hearth diameter. It is clear that after a certain diameter, the specific performance decreases as the hearth diameter increases. The coke throughputs for various furnaces range between 1–1.5 t/m².h or 24–36 t/m².24h. Eq. 11.12 has been calculated from furnaces all over the world. The performance of Japanese furnaces is much higher than others as shown in Fig. 11.2.

According to Schenck and Küpperbusch[8] the width of the raceway increases progressively as the hearth diameter increases and they derived a parabolic relationship between the coke throughput and hearth diameter as shown in Fig. 11.3. The relationship is given by

$$Q = \gamma.D^2 \qquad 11.13$$

The relationship of Q and D for various values of γ are shown in Fig. 11.3 together with the actual performance of various modern furnaces. The higher the value of γ the better the furnace performance.

The relative productivity of the furnaces is difficult to judge because the coke throughput and the coke rate depend so much upon the size and size distribution of the charge materials, quality and reducibility of the ore, sinter or pellet and slag volume and slag basicity. However, although a production index of 100 percent is difficult to achieve, all blast furnaces should endeavour to prepare their burden in order to approach the target.

11.2.3. Other Performance Indices

Three other indices are also used to indicate blast furnace performance based on iron production. They are:

(i) THM/m².24h used mostly in Europe and America, based on unit area of the hearth;

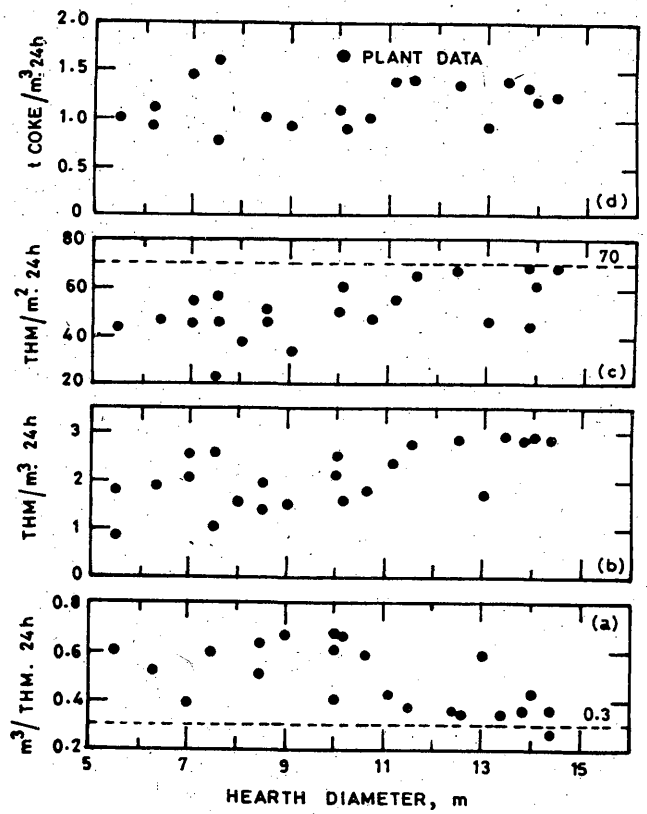


Fig. 11.4 Various hearth performance indices and their relation with the hearth diameter.

(ii) volume efficiency, THM/m³ 24h used mostly in America and Soviet Union, based on furnace volume calculated from the height taken from tuyere axis to 1 m below the tip of the bell in open position (America) or from the iron notch to the tip of the bell in open position (Soviet Union);
(iii) furnace volume utilization coefficient (KIPO), m³/THM.24h, used in the Soviet Union.

According to the above, the best performance is given by furnaces with highest values according to (i) and (ii). Their values with increasing furnace diameter are shown in Fig. 11.4(c) and (b) respectively. In case (i), in the last couple of decades, the value has increased from about 30–40 to about 65–70 THM/m².24h. In case (ii), it has done so from 1.4 to 3.5 THM/m³.24h.

In case (iii), the best performance is given by the least KIPO value (Fig. 11.4a). The values have decreased from 0.7 to 0.28 m³/THM.24h.

Since iron production depends upon the coke rate per THM, it is not fair for those using inferior variety of burden if the efficiency is based on tonnes of metal produced. It will be more appropriate to use the coke throughput based on useful furnace volume, tonnes coke/m³.24h. (Fig. 11.4d).

11.3. Methods of Increasing the Productivity

From Eq. 11.1, blast furnace production can be increased by measures which would increase the coke throughput and decrease the coke consumption rate. The methods for achieving a high production rate are shown in Fig. 11.5 and summarized below.[2]

The coke throughput can be increased by:

(a) increased oxygen supply (increased blast volume, oxygenated blast, humidified blast, high top pressure);
(b) decreased volume, viscosity and increased density, surface tension of slag;

The coke rate can be decreased, as narrated in Sec. 10.4, by:

(a) preparation and concentration of charge materials;
(b) increase in blast temperature;
(c) blast modifications;
(d) super (metallized) burden;

(e) stack gas injection (not used);
(f) fuel additives.

11.3.1. Increase in Coke Throughput, Q

The coke burning rate can be increased by an increased oxygen supply. Since most furnaces are blown with normal blast an increased gas throughflow would depend upon the aerodynamics of the bed.[57] These will be apparent from the following discussions.

11.3.2. Increase in Blast Volume

An increased blast volume rate means an increased oxygen input in unit time which results in an increased coke burning rate. The coke burning rate is approximately proportional to oxygen input.

A large blast volume will be accepted by the furnace if the permeability of the stock column is increased simultaneously so that the material descent and gas distribution are uniform throughout the vertical and horizontal cross-sections. This is ensured by the use of mechanically strong, abrasive resistant, graded and sized ore, limestone and coke and their proper distribution at the top.

The very high production rates in modern high capacity furnaces have been made possible by the maintenance of suitable size and size fraction of the charge materials; blending, concentration and agglomeration of ores; washing of ash and increase in strength of coke, etc. We have seen in Chapter 5 that fines are most harmful for gas throughflow and the ferrous burden should not contain any − 6 mm. The resistance to gas flow due to smaller particles increases the blast pressure, especially in large furnaces with high charge column and large transverse dimensions. A considerably high blast pressure is needed for overcoming the resistance causing high flue dust emission, channelling, hanging, slipping, etc. and resulting in increased coke rate and decreased production. In large furnaces, therefore, the need for the charge to be coarser, mechanically strong, closer in size fraction with proper screening before charging and having high reduction strength on load both at low and high temperatures, is much greater than in the smaller furnaces.

Although the driving rate can be increased greatly with large particle size because of the high rate of gas flow permitted, two other factors governing the coke rate are affected, viz., reduction and heat transfer rates. Large particles with comparatively small surface are heated or reduced less rapidly. An inadequate heat transfer also shortens the 800–1000°C indirect

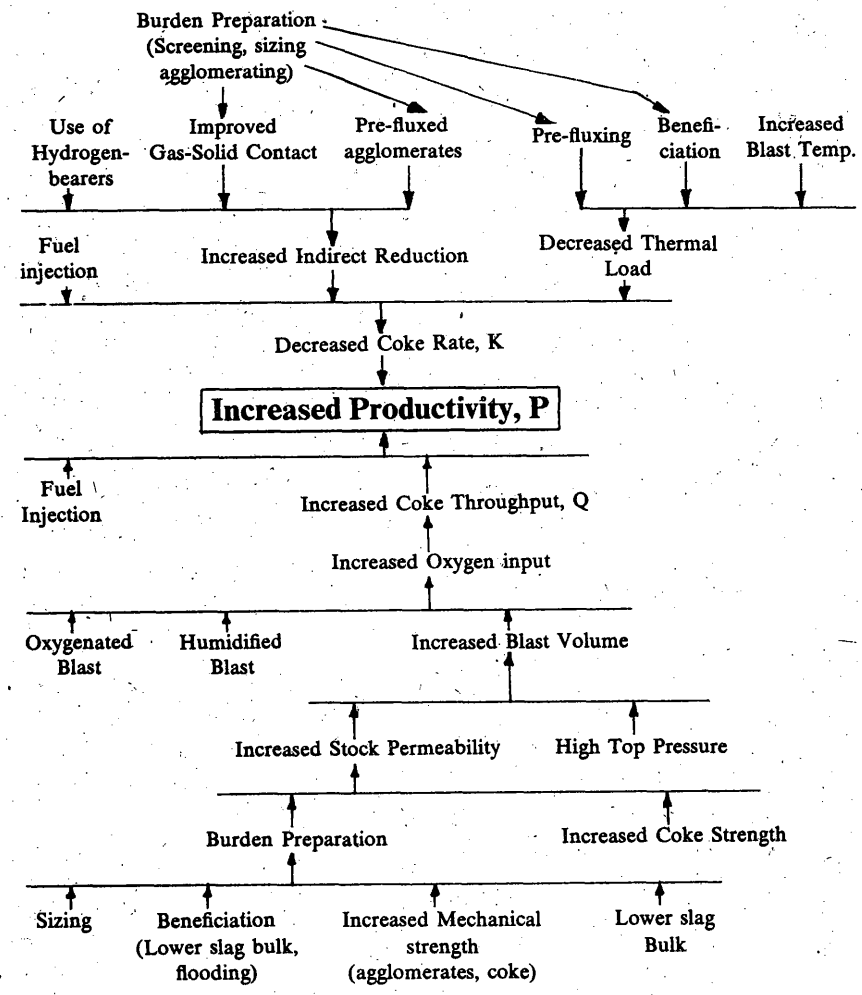


Fig. 11.5 Some of the methods by which the productivity of the blast furnace can be increased.

reduction zone (Fig. 4.2b). The reduction is therefore affected on both counts. With smaller size the driving rate decreases but the heat transfer and reduction rates increase. For optimum production, usually a compromise is made; for low reducibility a size range 10–20 mm and for high reducibility 20–40 mm appear to be most appropriate. It should, however, be pointed out that large lumps are more susceptible to breakdown than the smaller ones.

The influence of various factors on the blast volume rate is described in the following sub-sections.

11.3.2.1. Size distribution

We have seen in Fig. 5.9 that the pressure drop is the smallest in a bed of materials of uniform size. It is smaller the larger the size. But the pressure drop increases steeply in a mixed bed containing smaller and larger sizes. The figure also shows that if the two materials are charged separately in layers, the pressure drop is much smaller. Thus the improvements in blast furnace productivity and coke rate that can be obtained by the use of crushed and screened ores are obvious. It is particularly important for large furnaces with extended transverse dimensions in order to obtain good permeability for stable gas flow.

Table 11.1 illustrates the actual improvement obtained from screening out −10 mm size ore in Krivoi Rog.

Table 11.1.[9] Effect of percentage content of +10 mm fraction of ore on blast furnace performance

	Base	1	2	3
+10 mm size in ore, %	54.25	71.36	88.20	89.17
Coke saved (kg/THM)	—	58	77	90
Flue dust (kg/THM)	254	241	187	137
Performance, %	100	106.5	109.5	110
Volume utilization, m^3/THM.24h	0.918	0.865	0.840	0.834
Coke burning rate, t/m^3.24h	1.140	1.190	1.220	1.230

A much larger improvement in permeability, performance and coke rate would be expected if the ores, after crushing and screening, are graded into 2 or 3 narrow size ranges (−10 mm sizes being sent for sintering) and each size range charged separately after an interval of 2 or 3 hours

to avoid an intermixing in the furnace. This is shown in Table 11.2. The great increase in indirect reduction due to better gas utilization is obvious.

Table 11.2.[10] Effect of charging different sizes in layers

Types of charge	$\%CO_2$ in top gas	Coke rate kg/THM	%, expected output increase
Mixed ore	11.0	1180	–
Ore sized into 2 categories	12.1	1070	+9.3
Ore sized into 3 categories	16.1	960	+18.5

An illustrating example of increase in the productivity of blast furnaces on changing from mixed to graded burden has been cited by Boland.[11] The test was carried out at Ougree works, Belgium, crushing a mixed ore to an optimum size and then screening and grading it into three sizes, +50 mm, 10–50 mm and −10 mm. The latter was sent for sintering. The results of the base period April 1960 and the final testing May 1961 are shown in Table 11.3. The charging cycle shows a change from ore in the axis to a moderate opening up of the axis.

Table 11.3.[11] Tests with mixed ore at Ougree, 1960 and 1961.

Results	April 1960 unprepared ore	May 1961 prepared ore
Iron production, THM/24h	495	815
Coke throughput, t/24h	478	578
Coke rate, kg/THM	965	709
Coke burning rate, $t/m^2.24h$	16.91	20.45
Iron productivity, $THM/m^2.24h$	17.51	28.83
Blast temperature, °C	811	838
Top gas temperature, °C	319	179
Top gas CO/CO_2 ratio	3.9	2.1
Indirect reduction, %	54.45	61.7
Flue dust, kg/THM	151	33
Charging cycle	CC/OO/CC	OC/SC/CO/SC

Innumerable examples may be quoted for benefits in output and coke rate when −6 mm or −10 mm sizes are screened out prior to charging. The increase in output can be as high as 30–40 percent and decrease in the coke rate as much as 15–20 percent simply by screening out the fines and charging narrow size fractions separately. The effect of burden sizing on the blast furnace performance has been amply demonstrated by Trognitz[12] and Mintrop.[13]

11.3.2.2. Sinters and pellets

The development of sintering and pelletizing originated from a desire or need of making use of an enormous amount of fines generated from ore beneficiation processes. However, these two agglomeration processes have become such a tremendous success both in the increase of production and savings in coke that they are almost universally accepted as the ideal blast furnace charge material. The role these two agglomerates played in the reduction of coke rate has already been discussed in Sec. 10.4.2.4. Their use has also resulted in a phenomenal increase in productivity. In fact, the growth of the furnaces in dimension in the last two decades has been made possible by the mechanical and aerodynamic properties, high and uniform softening temperature and range, high reducibility and porosity of the sinters and pellets. We should again note that agglomeration not only converts the fines into larger lumps but also in the process removes some of the impurities and volatile matters, and converts different varieties of ores of different physical and chemical compositions into a single, homogeneous, strong, porous, high grade blast furnace burden of uniform size.

11.3.2.2.1. Sinter

The benefits of sinter as obtained in Appleby-Frodingham have been mentioned in Sec. 10.4.2.4. Another example will be cited here on the performance at the Stanton plant.[14] When using run-of-mine ores, the average iron production was 2100 THM/week per furnace at an average coke rate of 975 kg/THM. The furnaces were then switched over to screened rubble which brought about more regular furnace working, faster driving rate, larger outputs, lower coke rates and more consistent metal analysis. The average output increased by 13.3 percent to 2380 THM/week and the coke rate fell by 8.2 percent to 895 kg/THM.

When the sinter plant came into operation, the burden was gradually changed from rubble to 100 percent non-fluxed sinter. The output increased by 41 percent from the base period to 3077 THM/week and the coke rate

dropped by 19 percent to 790 kg/THM. It was noticeable that when − 3 mm size increased beyond 10 percent, the blast pressure and flue dust losses increased.

Subsequently, on switching over to fluxed sinter the overall output increased by 56 percent to 3275 THM/week and the coke rate dropped by 26.5 percent to 715 kg/THM.

Trends in the production figures show that an increase in the sinter content of burdens from small values to 40–60 percent has a greater influence on furnace performance than has a subsequent increase from 60 to 100 percent. Depending upon the ore quality and the physical and chemical properties, in the lower ranges every one percent increase in the proportion of sinter raises the output by about 0.35 percent and reduces the coke rate by about 0.3 percent, while changing from 50–60 percent to 100 percent sinter, the respective values are 0.14 percent and 0.14 percent.

From the mathematical analysis of data obtained from southern Russian plants the following relationships between the daily output and coke rate within the limits of 0 to 60 percent sinter in the burden were derived:[9]

(i) $P = 0.0065\ A^2 - 0.065\ A + 3.085$
(ii) $K = 0.305\ A - 0.05$

where,

P = increase in daily output, percent
K = reduction in coke rate, percent
A = sinter content of the charge, percent.

The output can be increased and the coke rate decreased considerably by the use of fluxed or super-fluxed sinters. Such sinters soften or melt at higher temperature and in a narrower vertical zone, facilitate gas flow and permit the use of higher blast temperatures. The enormous savings in coke (60–70 kg coke/100 kg CO_2 transferred to sinter strand) lower the slag volume which in its turn increases the flooding limit.

From tests in southern Russian plants, it has been found that the coke rate and KIPO index both decline as the sinter basicity increases according to the following equations:[9]

(i) $K = 12.3221\ B + 3.182$
(ii) $V = 12.105\ B + 2.174$

where,

K = reduction in coke rate, percent
V = reduction in volume utilization coefficient, KIPO, percent
B = sinter basicity

It follows from the above equations that the volume coefficient, m^3/THM.24h, improves by 12.1 percent and the coke rate falls by 12.3 percent if the sinter basicity increases from 0.1 to 1.0.

Calculations[9] show that the production cost and capital outlay are reduced by 14.8 percent and 16.8 percent when the sinter basicity is increased from 0.01 to 1.19.

An increasing basicity, on the other hand, increases the brittleness and reduces the abrasion resistance of the sinter. It generates a lot of fines during handling, transport and also in the furnace itself which tend to clog the voids, hampering gas throughflow. The maximum loss of strength occurs at CaO/SiO_2 ratio 1–1.5 and temperatures 400–600°C in a reducing atmosphere (Figs. 6.4 and 6.5). Since the strength increases both at low and high basicities, it is advisable to charge acid and high basicity sinters in suitable proportions so as to obtain the desired final slag basicity. Even then, for optimum production, the sinter must undergo additional screening just prior to charging in the furnace. The improvement in production by screening out varying proportions of −9.5 mm sinter at Appleby-Frodingham is apparent from Fig. 11.6[15] where a 30 percent increase in the output was achieved.

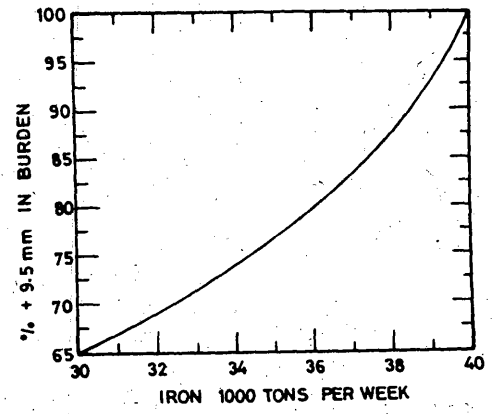


Fig. 11.6 Increase in blast furnace output with increasing degree of screening, after Macdonald.[15] (Copyright Iron and Steel Institute).

An increase in the blast rate by 1.3 percent has been obtained by the removal of each 1 percent of 0–5 mm sinter. A very uniform running of the furnace was achieved by re-screening 5–40 mm sinter to 5–15 and 15–40 mm and charging them separately.[16] A rise in the output of 0.5 percent for each 1 percent fines removed with a total rise of 3.7 percent in the output and 4.3 percent decrease in the coke rate have been reported.[17] A higher output can be achieved if the sinter is stabilized in vibrating screens. Such sinters gave 14 percent increase in output and 6 percent decrease in the coke rate.[18]

Russian tests[19] show an increasing strength and reducibility as the ratio $MgO/(CaO + MgO)$ in the sinter increases, for constant basicity $(CaO + MgO)/(SiO_2 + Al_2O_3)$ of 1.35.

Astier et al.,[20] have shown that an increase in the productivity by 150–200 percent was achieved by crushing low-grade French Lorraine ores and agglomerating them into 100% self-fluxing sinters.

11.3.2.2.2. Pellets

As already mentioned in Chapter 6, the pellet came into being only in an attempt to agglomerate very fine concentrates not amenable to sintering. Now it has assumed the role of an ideal blast furnace burden because of its valuable properties (Sec. 6.4.8).

Pellets give a more permeable stock column than is possible with raw ores or unscreened sinters, resulting in a more uniform pressure drop across the entire furnace cross-section, virtual elimination of channelling, better gas/solid contact with consequent better utilization of the thermal and chemical energies, lower top gas CO/CO_2 ratio and temperature, lower coke rate and very high coke burning rate, i.e., higher production. These are obvious from Tables 11.4 and 11.5.

As against the above favourable properties, a great disadvantage is that the pellets are prone to catastrophic swelling which tends to reduce the voidage and lower the strength. This drawback does not give as high a production as would be expected from the charging of pellets. The swelling is intimately connected with the presence of lime and alkali metals (Sec. 6.7.6). Also, self-fluxing pellets with adequate strength are difficult to make. Hence, the ideal charge sometimes is acid pellet plus very high basicity sinter. Pellets that swell more than 20 percent should be restricted in their use and mixed with other non-swelling charge materials (Table 6.3). Because of high energy cost of pelletising and inferior physico-chemical properties compared to those of basic sinters, the latter are being increasingly preferred by the blast furnace operators.

We will summarize here the enormous output obtained during large scale experimentations with pellets at Armco's blast furnace at Middletown during the period May 1954–June 1961 (Table 11.4) and Mannesmann Works – Huckingen, 1962 (Table 11.5).

Attention was first drawn to the future potential of pellets by the startling production figures at Armco's Middletown plant in a blast furnace of 8.53 m hearth diameter with a useful volume of 1750 m^3. By changing over from a burden of raw ore containing 10 percent to 80 percent pellets in the course of seven years from 1954 to 1961, the coke rate was reduced by about 19 percent and the iron production increased by 100 percent.[21–23] This is apparent from Table 11.4.[23] It will be seen that the actual production increased from 1462 with raw ore charge by 100 percent to 2942 tons/24h with pellets. The blast rate increased from 83000 to 123000 ft^3/min and the coke rate decreased by 19 percent from 1623 to 1304 lbs per ton of iron. Comparing two figures having an almost identical blowing rate of 83000 ft^3/min for non-pellet and pellet charge, the iron made increased by 60 percent from 1462 to 2344 tons/24h and the coke rate fell by 27 percent from 1623 to 1182 lbs. The top gas CO/CO_2 ratio decreased from 2.13 to 1.14.

For attaining very high blowing rates, the pellets must be screened to eliminate all −6 mm. They must be sufficiently strong and resistant to degradation during transportation and not susceptible to low temperature breakdown or swelling in the furnace.

Another large scale experiment with pellets has been reported by Petersen et al.,[7] which attracted widespread attention because the results were so favourable and convincing. The success is apparent from Table 11.5.[7] Two varieties of pellets were used (i) Swedish pellets of size 10–35 mm in amounts about 50 percent of the charge in the 1st and 4th test periods and (ii) US-Reserve pellets of size 9–15 mm in amounts of 83 and 85 percent of the charge in the 2nd and 3rd periods. The reducibility of US pellets, dR/dt (40%), was 0.82% O as against that of the sinter used, 0.43% O/min. The coke sizes were 40–60 mm and 60–80 mm in the two periods respectively. The influence of coke size on the iron output was not discernible. The materials were carefully pre-screened, fines removed and then charged in layers. The output increased by about 50 percent to 2091 THM/24h from a base output of 1400 THM/24h using only a mixture of sinter and lumpy ores. The productivity figure was about

54 THM/m².24h and the volume utilization factor 0.45 m³/THM.24h compared to most modern figures of 65–70 THM/m².24h and 0.28–0.30 m³/THM.24h respectively.

Table 11.4.[23] Effects of pellets on iron production. Hearth diameter 8.53 m

	May 1954	May 1960	Nov. 1960	June 1961
Burden, lb/nett ton hot metal				
Ore	2594			
Pellets	649	2975	2902	3080
Miscellaneous	754	547	505	430
Limestone	676	429	421	440
Blast volume, ft³/min	83000	109500	84000	123000
Blast temperature, °F	1125	1390	1491	1300
Top gas temperature, °F	380	349	200	300
Top gas CO/CO_2	2.13	1.24	1.11	1.28
Top pressure, lb/in²	7	4.5	4.5	7.2
Actual production, tons/24h	1462	2804	2344	2942
Coke rate, lbs/ton iron	1623	1276	1182	1304
Specific production, tons/m².24h	25.6	49.1	41.0	51.5

Table 11.5.[7] Smelting performance with pellets at Huckingen. Hearth diameter 7 m. Base production (sinter + lumpy ore) = 1400 THM/24h

	42% Swed. pellets + 35% sinter + 18% US pellets	83% US pellets	85% US pellets	35% Swed. pellets + 30% US pellets + 35% sinter
Iron production, THM/24h	1856	2040	2091	1974
Coke rate, kg/THM	592	590	571	564
Specific iron productivity, THM/m².24h	48.2	53.0	54.3	51.3
Specific coke burning rate, kg/m².h	1187	1301	1308	1235
Volume utilization coefficient, m³/THM.24h	0.51	0.46	0.45	0.48
Volume efficiency, THM/m³.24h	1.96	2.17	2.22	2.08
Blast rate, 1000 Nm³/h	128	138	143	140
Blast temperature, °C	857	862	882	847
Top gas temperature, °C	163	116	87	117
Indirect reduction, %	58.6	62.9	61.2	57.9

11.3.2.3. Coke size and strength

A proper size consist should be 40–60 mm or 60–80 mm depending upon the ore size. Smaller sizes, provided the coke is sufficiently resistant to abrasion and attrition at high temperatures, help in the enlargement of the raceway (Sec. 7.6.5). However, in the wet zone, the slag will be less liable to flooding the larger the coke size and smaller the surface area/volume ratio. In the dry zone, the bed permeability is better the more compatible the coke and ore sizes and the closer the size ratios to 0.65–0.75 are (Sec. 5.4). For optimum gas throughflow, both in the dry as well as wet zones, the coke size should be 3–5 times larger than the ores.[24] (This should be valid only when the ore size is small, 10–20 mm).

In an experiment[25] lasting for several months in Youngstown Sheet and Tube Co., the production increased from 642 to 698 THM and the coke rate dropped from 696 to 638 kg/THM with the average coke size decreasing from 58 to 48 mm. With graded coke of 20–50 mm size, an increase of blast intake of 5 percent has also been reported.[26]

An excellent example of the influence of classifying the ore and coke into closer size consist on the smelting output is seen in Fig. 11.7.[27] The iron production increased continuously as the percentage of 20–50 mm size fraction of coke increased and the size distribution of the ore became narrower, e.g., for the same 20–50 mm percentage of coke the production with ore size 9–50 mm was more than in the case of ore size 9–75 mm. With ore size 9–150 mm the size spectrum is so broad compared to that of the coke that there was actually a fall in the production. Similar conclusions[28–30] have been drawn in the operation of experimental blast furnaces with sized

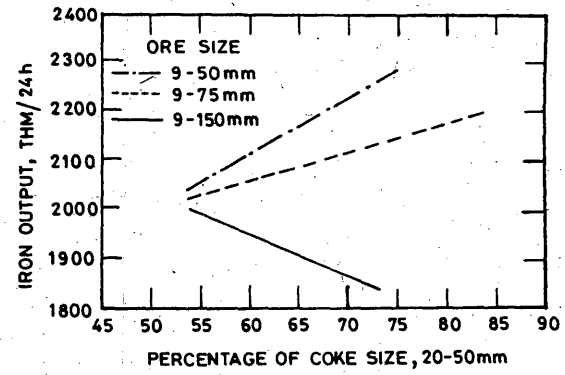


Fig. 11.7 Variation of furnace output with changes in the size distribution of ore and coke, according to White.[26] (Blast Furnace Steel Plant).

coke. Because of uniform furnace operation, the hearth temperature is more uniform, sulphur in iron is lower and the metal analysis less erratic. According to Henkel[31] about 2–10 percent increase in iron output and fall in the coke rate of 10 kg/THM can be obtained by using <80 mm coke in the range 40–80 mm. Size 40–60 mm can be used under special circumstances, e.g., in smaller furnaces or where the burden size is small. Under no circumstances the size 20–40 mm should be used because of the tightness in running and deterioration of gas flow in the wet zone.

An interesting case of flooding of particular tuyere regions where the coke size is small has been cited by Giedroyc and Hyslop.[32] The furnace showed operating difficulties which had been identified by pressure differential tests and attributed to gas flow restrictions in the bosh. The flooding diagram (Fig. 11.8)[32] shows that unusually small coke on one side of the furnace (No. 11 tuyere) as tested from tuyere probes had given operating characteristic close to the flooding limit line.

Whether the coke will maintain its size in the furnace depends upon its mechanical and chemical properties described in Sec. 6.9.1 and in the next sub-section. The degradation of the coke in the furnace results in flooding, choking of the hearth, increased burning of tuyeres and slag notch, all of which limit furnace output. The use of pre-stabilized and screened coke increases the output by over 1 percent.[33]

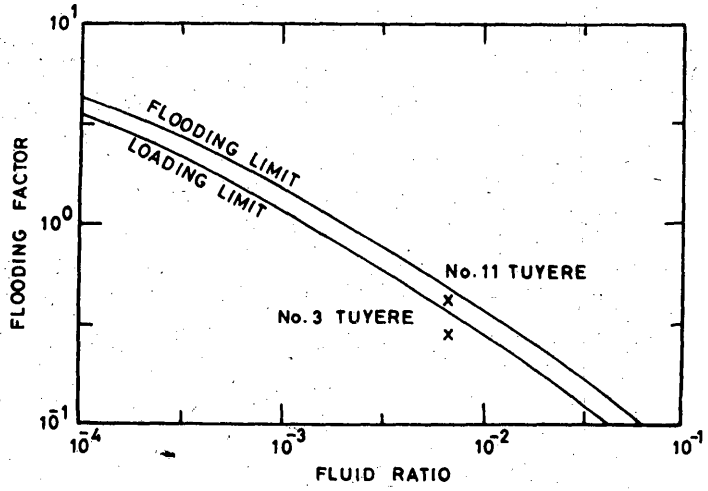


Fig. 11.8 The influence of small-sized coke at No. 11 tuyere on flooding in a blast furnace, according to Giedroyc and Hyslop.[32] (Copyright Australasian Institute Mining Metallurgy).

The need for coke of high quality for use in the blast furnace, especially in the large ones, is being increasingly emphasized as a result of investigations carried out to ascertain the internal state of the furnace quenched while in operation.[34–37] It has been revealed that the mean size of coke tends to become increasingly fine from the lower part of the shaft to the tuyere level (cf. Fig. 11.9).

The loss of strength of coke and its degradation into fines in the lower furnace resist gas flow in four important regions, viz., softening-melting or cohesive zone, dropping zone, combustion zone and the hearth zone. These are discussed briefly below:[34]

(1) **Softening-melting zone** In Figs. 1.3 and 11.24 we can see that in the cohesive zone where the ore layer becomes compacted due to softening-melting, the gas passes predominantly through the sandwiched coke layer (coke slit). If the coke voids are choked with fines, the gas flow is deflected to other more permeable coke slits and when the gas velocity becomes excessive, fluidization of the fines commences which may ultimately lead to channelling. If the flow resistance is excessive, hanging and loss of productivity will occur.

(2) **Dropping zone** This zone refers to formation of liquid globules of molten metal and slag which when sufficiently fluid drop through the coke slits and subsequently descend to the hearth through the central coke column. The diminution of voidage and large surface area of the coke fines result in liquid hold-up in the coke slits and hence in loss of production. The viscosity of the slag also increases greatly because of intermixing with the coke fines, accentuating the slag hold-up.

(3) **Combustion zone** Very fine coke (−5 mm) has been found to exist between the lumpy coke in the central coke column and the cavity wall in front of the tuyeres. Such fine particles resist blast penetration, decrease the raceway depth and more of the gas flows along the wall. The slag viscosity increases due to intermixing with the coke fines which promotes stickiness and slag hold-up, entraps metal droplets in the slag, causes burning of tuyeres and slag notch and the slag flows into the tuyeres. The gas flow along the wall increases wall-heat losses and hence increases coke consumption.

(4) **Hearth zone** Intermixing of ash generated in the combustion zone and the coke fines with the liquid metal and slag increases their viscosities, promotes accumulation of kish around the tuyeres and slag notch resulting in their burning. The diminution of voidage of the coke bed which floats

on the iron layer in the hearth retards separation of the metal and slag and results in an uneven drainage of the liquids to the tap hole and erratic metal analysis from tap to tap or even from ladle to ladle.

The effects of coke breakdown in the furnace on productivity are apparent from above. Therefore, to ensure adequate and uniform permeability, greatest importance should be attached to making of coke of highest quality bearing in mind that the size of the coke in the lower furnace is determined by the strength and size at the charging stage, mechanical breakdown during descent through the shaft, embrittlement by CO_2 and alkali attacks and breakdown due to high temperature and attrition in the highly turbulent zone in front of the tuyeres.

The behaviour of coke and methods of improving the coke quality have been discussed by various workers.[34-39]

11.3.2.4. Flame temperature and alkali metals

We have seen in Secs. 10.4.1 and 4.5 that although an increase in the flame temperature saves coke the furnace behaves irregularly above a certain optimum which depends upon the burden quality and furnace characteristics. Several plausible reasons for such a behaviour have been discussed, the more important of them being:

(i) production of large amounts of gaseous SiO which is reoxidized to SiO_2 at lower temperatures and in more oxidizing atmospheres in the bosh; deposition of SiO_2 and clogging of voids;
(ii) the slag fusion zone comes down from the belly to the bosh incline and the viscous mass there hinders burden descent and gas throughflow;
(iii) an excessive volatilization of alkali metals at higher flame temperatures which contributes to the breakdown of burden and coke, excessive gasification of coke, formation of scabs and scaffolds and glueing together of materials by liquid cyanides and carbonates which reduces the bed permeability (Sec. 3.21).

When alkali is the cause of productivity limit the blast temperature should be reduced but that would lead to a higher coke rate. If possible, the alkali input must be controlled to within 2–3 kg/THM in the burden. If the major source of alkali is the ore gangue, such ores should be beneficiated. On the other hand, if it is the coke ash, the coke input should be reduced by increasing the use of oil, natural gas etc. Alternatively, when the alkali build-up in the furnace is high (the sign being erratic furnace

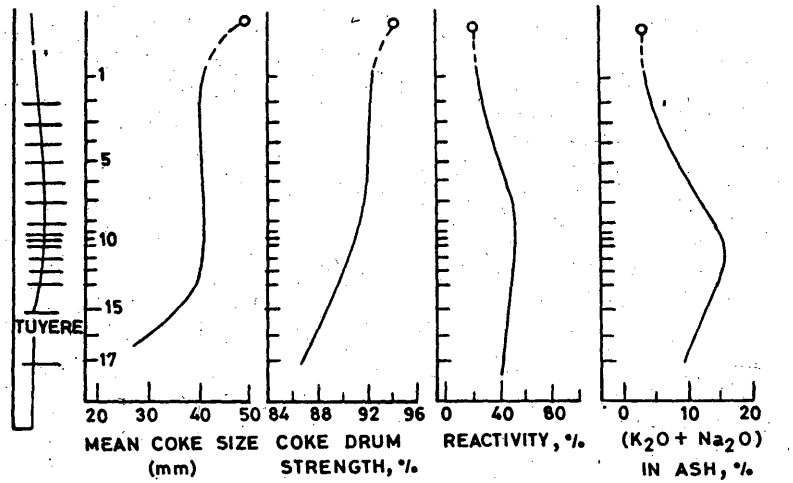


Fig. 11.9 Variations of size, strength and reactivity of coke and the alkali content of coke ash along the height of the furnace, according to Sasaki et al.[35] (By kind permission).

movement), the slag should be made more acidic to decrease the activity coefficient of the alkali oxides so that more of the alkali metals may be removed through the slag. During these temporary measures, the sulphur in iron will increase which can be removed by external desulphurization.

Fig. 11.9[35] shows the actual effects of alkali metals in the coke ash on coke reactivity (with CO_2), abradability and mean size of coke in the belly region of the blast furnace. The relationship between the amount of alkali oxides, and the reactivity and hot strength of coke has already been seen in Fig. 6.29. The breakdown of the coke affects furnace output and increased reactivity deteriorates indirect reduction, increases the coke rate and hence further limits the output. The reaction of coke with CO_2 weakens its structure and makes it porous.[40] The embrittled coke becomes powdery due to load and abrasion during descent and due to attrition in the combustion zone by the impingement of high velocity blast. This may result in increased fluidization of coke fines in the dry zone, slag hold-up in the wet zone, choking of the hearth, burning of tuyeres and slag notch, uneven tapping of metal, etc.

The relationship between alkali input, stock permeability and production is clear from Fig. 11.10.[41] Production and permeability of the stock both decrease with increasing alkali input.

If the slow movement of the charge is due to lowering of the slag fusion zone, the zone should be raised by reducing the blast temperature or by

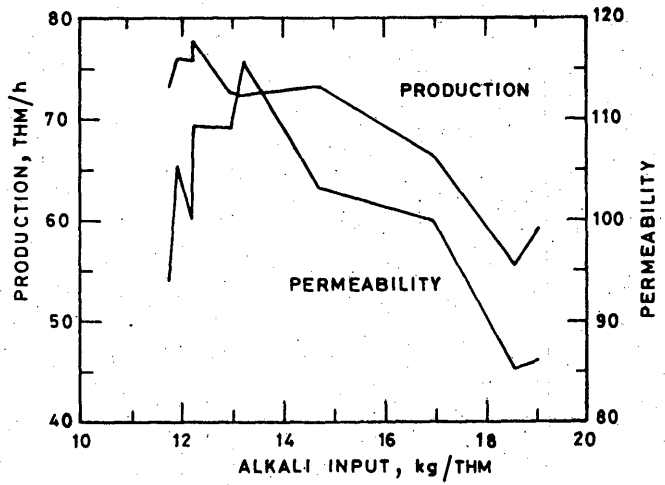


Fig. 11.10 Effect of alkali input on permeability and blast furnace production, according to Davies et al.[41]

lowering the flame temperature at the same blast temperature by the use of steam, oil or other injectants (Sec. 4.5). The other long term measures are upgrading of the ores and the use of rich fluxed sinters and pellets. Lean ores with high slag volumes are averse to the use of high flame temperatures. The primary slag must also contain sufficient MnO to minimize any danger of resolidification of the slag during the rapid reduction of FeO in the bosh (Sec. 8.2.4). In this respect pre-made slag, as is present in fluxed sinters, is more immune from this danger and hence high basicity sinters permit the employment of high blast temperatures, even up to 1250°C.

The lowering of the slag fusion zone can also be countered by suitable furnace design. A short and steep bosh would eliminate the possibility of formation of a viscous mass on its incline even if the fusion zone descends with the use of high blast temperatures.

11.3.2.5. Bosh slag

A highly limey bosh slag is very refractory and hence interferes with smooth descent of the burden. Such limey bosh slags are expected when the burden is rich and the coke contains a large amount of ash (Sec. 8.4). The remedy is either beneficiation of the coal or use of an increasing amount of oil or natural gas as part replacement of coke. Injection of lime powder through the tuyeres or use of lime-incorporated coke or part replacement of lime by MgO are other possibilities (line AC, Fig. 3.20).

11.3.2.6. Softening-melting temperatures

The burden, during its descent in the furnace undergoes reduction, softens and ultimately melts and drops in the form of molten metal and slag into the hearth through the interstices of coke. The softening-melting zone consists of the temperature range from the start of softening of the ore or agglomerate to the formation of liquid globules of the molten material. Therefore, depending upon the temperature distribution of the gas, the flow properties of the burden change continuously in place and time along the entire vertical and horizontal cross-sections, especially from the belly to the middle of the shaft.

We have seen in Secs. 5.5 and 6.5.2 that premature softening of the burden materials results in an increase in the pressure fall because of diminution of voidage. A decrease in the voidage by 10–20 percent can increase the pressure fall by 300–400 percent. Such a softening in the stack can hinder gas throughflow and hence adversely affect furnace productivity. Ideally, the softening-melting range of the burden should be narrow and coincide with the melting temperature of the primary slag. But raw ores, depending upon their nature, soften and melt in a wide range of temperature, the semi-molten viscous mass choking the voids. However, on sintering and pelletising, the zone narrows down between 1000–1350°C for acid sinter, 1100–1350°C for basic sinter and 1200–1400°C for pellets, compared to 700–1350°C for raw ores. For a mixed charge like basic sinter plus acid pellets, the range may be much wider than for the individual ones. If the range is narrow, the gas passes through a short vertical distance of viscous mass and the resistance to flow of gas will be minimal (Eq. 5.22). The beneficial effects of basic sinters with low reduction-softening index on furnace productivity are evident from Fig. 11.23 and Sec. 11.5.

Recently, the internal states of some blast furnaces have been examined by quenching them while in operation.[34–37] Two distinct softening-melting patterns have been revealed by the investigations, viz., a W-type shape extending right down to the lower furnace and an inverted-V type extending almost to the tuyere level. The distribution of the softening-melting layers appears to be a function of the gas temperature distribution. The softening-melting regimes are not uniform radially in the furnace cross-section. In the former case, the zones are higher in the periphery and centre where the temperatures are high (cf. Fig. 7.4). In the intermediate zone where the ore hump is located, the materials soften much lower down in the furnace. These are shown schematically in Figs. 5.1 and 11.24(a). The W-profile was obtained in a furnace where a large quantity of oil

was used and the productivity was comparatively low with a low coke rate.

The inverted-V type (Fig. 11.24b) presumably emanates from a pronounced central flow. This shape was obtained in a furnace with a high productivity and relatively high coke rate.

The probable course the gas takes during its ascent and the influence of softening-melting temperatures of burdens on productivity are discussed in Sec. 11.5. It is difficult to surmise the effect of the softening-melting pattern on furnace productivity since the pattern itself evolves from the gas temperature distribution which is greatly dependent upon the methods of operation. However, it appears plausible that the inverted-V shape, which presumably is a result of a predominant central flow, is more conducive to higher productivity. In large furnaces the ore/coke ratio in the centre is minimum (Fig. 7.4) which stimulates a central gas flow. Whatever the shape of the zone, large furnaces should have horizontally extended belly to minimize the pressure fall.

A softening-melting contour which gives an optimum productivity in a furnace smelting a particular burden can only be determined by experimentation and simulation techniques. An appropriate contour of the softening-melting zone can be obtained by an appropriate burden distribution. The latter can be achieved by the use of deflecting ring or movable armour (NKK) in the bell-type charging system or, more effectively, by bell-less top which permits charging of the burden selectively throughout the furnace cross-section. They are discussed in Sec. 11.5.

11.3.2.7. Slag volume, viscosity and surface tension

The pressure drop between the tuyeres and the belly is greatest compared to other portions of a blast furnace (Fig. 5.21). The hydraulic resistance to the motion of gas in this region increases because its entry in the coke grid is resisted by the liquids in the interstices of the coke lumps. We have seen in Sec. 5.6 that when a critical gas velocity is reached, initially loading and later flooding of the coke voids by the slag can occur, resulting in hanging. The gas motion in this region is of critical importance in forcing of the blast furnace since with increasing coke throughput and hence iron output, the gas velocity and the mass of the liquids (iron and slag) both increase.

The influence of the liquids mass and gas velocity on loading and flooding has been seen in Fig. 5.12. The influence of slag bulk on the smelting intensity has been investigated in two Chinese blast furnaces.[42] It is reported

that the production increased by about 35 percent when the slag bulk decreased from 700 to 500 kg/THM. However, one should bear in mind that the coke rate decreases with decreasing slag bulk, albeit not to a great extent (about 20–50 kg/100 kg slag, Fig. 10.14), which helps in boosting of the output to some degree. These will be clear from Fig. 11.22.

Hydraulic resistance to gas flow is likely to increase with decreasing surface tension of the slag. No data appeals to be available in this respect. It is merely a deduction from Fig. 5.15. Therefore, it is possible that the greater the surface tension of slag the higher the critical gas velocity before flooding is indicated. In the blast furnace, slag offers more resistance to gas flow than the liquid iron because of the former's lower density and higher foaming tendency (Sec. 5.6).

Apart from the volume and surface tension of the slag, its viscosity, range of softening-melting temperature and the position in the furnace where the melting starts are all important. The position where the slag melts should be high (not higher than the belly) and the vertical height through which it flows as short as possible. This means that the belly should be broad and the bosh short, which are ensured by the profile of modern furnaces. From the burdening point of view, the softening temperatures of the ore and the liquidus temperatures of the primary slag should be close and narrow so that the entire fusion occurs in the belly where the diameter is the largest. In this respect pre-fluxed burden is very suitable because the pre-made slag softens and melts almost simultaneously.

The pressure drop increases as the slag viscosity increases. The resistance to gas flow increases because of an increased retention of a more viscous slag in the voids of the coke grid and consequent decrease of free passage. The influence of slag viscosity on the productivity and flooding limit is shown in Fig. 11.22. The burden composition should be such that the slag is fluid not only in the hearth but in the bosh as well. The bosh slag is more limey than the hearth slag and it is more so the lower the slag bulk, the higher the coke rate and the higher the coke ash (Sec. 8.3). If the bosh slag is very limey, it becomes very viscous and refractory with liquidus temperatures greater than 1600°C. In such cases, beneficiation of coal, injection of oil and natural gas which are ashless, or the use of magnesia for thinning the slag are necessary.

In the case of fluxed sinters where limestone is added only for fluxing the coke ash, the operation is smooth since the stone is not wholly absorbed in the bosh. However, for super-fluxed sinters where all the flux for the ore as well as coke acids are incorporated, the actual and calculated bosh

slag compositions are of the same order. In such cases, especially when the slag bulk is small and the alumina content too high or too low, the bosh slag will be viscous, pasty or refractory and a high resistance will be offered to gas flow. Because the tolerance of the slag composition lies within a narrow range, an extreme carefulness is needed in the selection of slag composition as well as in the operation of the blast furnace.

The flooding limit can be increased by HTP which decreases the linear gas velocity (Sec. 11.3.2.9).

11.3.2.8. Gas residence time

We have seen at various places in the text that both heat and mass transfer deteriorate at high rates of counter-flow of solids and gas. From Fig. 4.2(b), at high blast rates, the solids and gas temperature profiles become flatter and the indirect reduction zone vertically shorter, resulting in a deterioration of CO-utilization. Depending upon the reducibility of the ore, for each furnace there is a maximum blowing rate and hence, a minimum residence time of gas in the furnace below which utilization of the chemical energy will suffer and the coke rate start to increase. According to Bogdandy et al.,[3] for well-prepared burdens, the minimum gas residence time is about 9 seconds (Fig. 11.11),[3] below which the CO-utilization suffers.

In a series of experiments to determine the effect of blast volume on the smelting output, Brandi et al.,[1,43] increased the volume from 126000 to 162000 Nm³/h. From Fig. 11.12,[1] the smelting output increases linearly and the coke rate remains stationary with increasing coke throughput up to about 1250 t/24h. Thereafter, the former decreases due to the increase

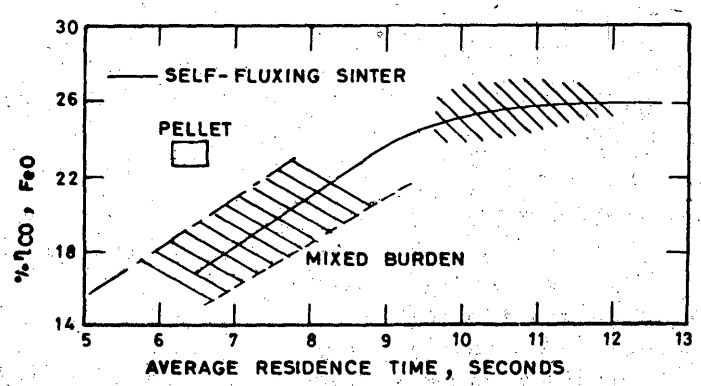


Fig. 11.11 Dependence of CO-utilization for the wustite/iron stage on the average time of residence of gas in a blast furnace. Taken from Bogdandy et al.[3]

of the latter from 580 kg/THM to 640 kg/THM at a coke throughput of 1600 t/24h.

A study of the heat and material balance shows that the increase in the coke rate was due to an increase in the direct reduction carbon from 122 to 138 kg/THM and in the tuyere carbon from 332 to 365 kg/THM. The trends are shown in Fig. 11.13.[1,43] The extra tuyere carbon almost exactly covers the thermal requirement of the higher direct reduction. Presumably because of a decrease in the residence time, indirect reduction decreased from 56 to 48 percent and CO-H_2-utilization from 32 to 25 percent for the total oxygen and from 17 to 13 percent for the wustite oxygen.

11.3.2.9. High top pressure (HTP)

We have seen in Sec. 5.7 that an increase in counter-pressure at the top decreases the linear velocity of the gas (for the same blast volume). The beneficial effects of HTP have been discussed in Sec. 5.7.1. As for example, the linear increase in output in Fig. 11.12 can be maintained along the dotted line with the use of HTP to a higher coke throughput instead of its starting to decline at 1250–1300 t/day.

The purpose of HTP is to introduce more oxygen to burn more carbon by blowing more air and at the same time maintaining the linear gas velocity (and pressure drop) identical to that in the conventional practice without any formation of channels, maldistribution of gas, increase in coke

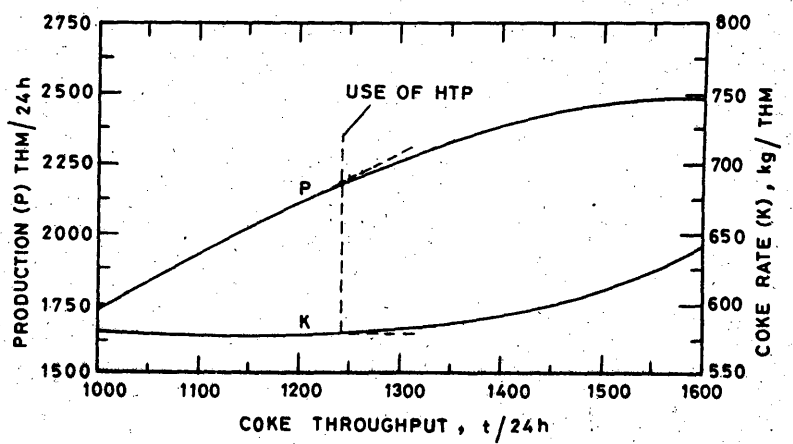


Fig. 11.12 Dependence of furnace production and coke rate on coke throughput, according to Beer and Heynert.[1] The use of high top pressure (HTP) has been introduced by the author.

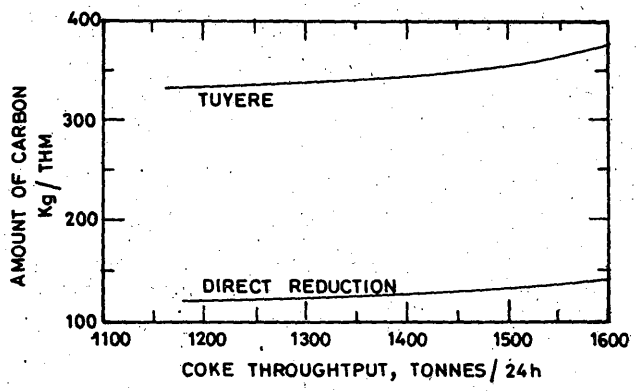


Fig. 11.13 Variations in direct reduction and tuyere carbon rate with increasing coke throughput, according to Brandi et al.[43] (Copyright Verlag Stahleisen).

rate or in flue dust emission. It is the linear gas velocity and not the mass flow rate that determines the pressure drop in the furnace.

The volume of blast that can be blown for the same pressure drop has been calculated in Sec. 5.7. Theoretically, the percentage increase in coke throughput should be equivalent to the percentage increase in the blowing rate. But in practice the throughput is somewhat lower because of increased repair downtime with HTP operation and increased blast leakage due to increased blowing pressure. With a moderate pressure at the top, the increase in production is about 80 percent of the change in the blast rate.[44] An extra 10–15 percent air can be blown easily with 8–12 percent of extra production. With HTP of about 1.85 ata and a blast pressure of 3 ata, approximately 25–30 percent more air can be blown and 20–25 percent more coke burned before the tuyeres without increasing the linear gas velocity.

The benefits of HTP in large modern furnaces need special mention since the larger the furnace the more unstable the gas flow. Although the furnace height has increased only marginally by about 4 percent, for diameters 9 m to 14 m, the pressure loss given by (blast pressure – top pressure) has increased with the furnace diameter as shown in Fig. 11.14.[45,46] This is detrimental to stable furnace conditions and obtaining of an optimal productivity. The pressure drop decreases with increased counter-pressure at the top.

Measurements[45,46] of static pressures show that the gas movement at the axis in the lower furnace is comparatively very slow. This results in a high gas velocity and hence in a high pressure loss around the raceway in larger

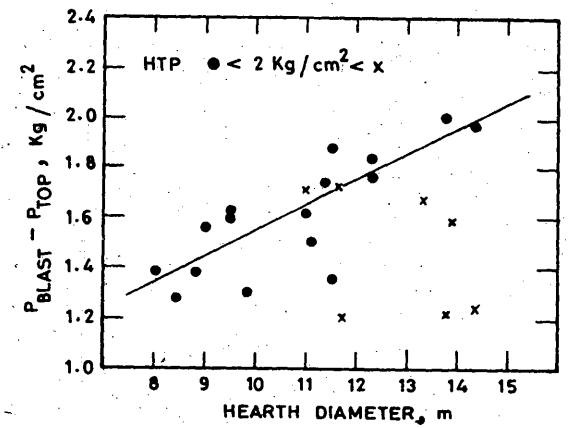


Fig. 11.14 Relation between hearth diameter and pressure loss between the blast and top pressures, after Higuchi et al.[45,46] (By kind permission).

furnaces, although the average gas velocity based on the hearth area remains the same as in the smaller furnaces. This is aggravated by the fact that the diameter of the dead man's zone increases or the proportion of active hearth area decreases with increasing hearth diameter (Table 5.1) and hence the portion that does not contribute to gas flow increases both in the horizontal as well as in the vertical cross-sections of the lower furnace.

With the normal charging system, in large furnaces, the ores tend to confine away from the axis because of large throat diameter. The consequent blockage of the periphery results in a preferential flow in the centre where most of the coke resides. Both the deviation of gas flow and the

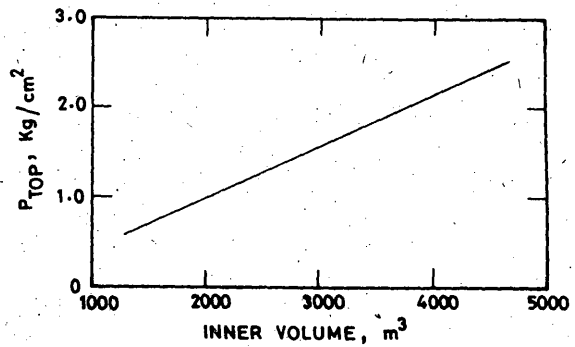


Fig. 11.15 Relation between top pressure and inner volume of blast furnaces, according to Higuchi et al.[45] (Copyright Australasian Institute Mining Metallurgy).

high pressure loss above the raceway can be corrected by the use of HTP which ensures a reduction in the gas velocity.

Fig. 11.15[45] indicates the need of increasing the top pressure with the increase in furnace volume because the volume has been increased by extending the furnace horizontally rather than vertically. In fact, in super-HTP, a smaller pressure drop is observed as a result of reduced gas velocity probably in order to increase the gas residence time and save fuel.

Most Japanese furnaces are equipped with HTP with top pressures of 2–4 ata while in the Soviet Union of about 3 ata. The almost linear increase in (coke + oil) throughput in Japanese furnaces of diameters greater than 7 m are shown by Eqs. 11.14 and 11.15 for HTP of about 1.45 ata and conventional cases.[47] The average increase in throughput is 11 percent compared to the conventional process.

$$\text{For HTP, } y = 26.6\,x - 63.3 \qquad 11.14$$

$$\text{For conventional, } y = 26.6\,x - 313.3 \qquad 11.15$$

where,

y = coke + oil throughput in tonnes/day
x = hearth area, m^2.

An increase in coke throughput of 17 percent and hence an increase in iron output of 17 percent have been obtained with an HTP of 1.7 ata. Very little decrease in the coke consumption rate has been noted. However, the flue dust emission decreased up to 40 percent.

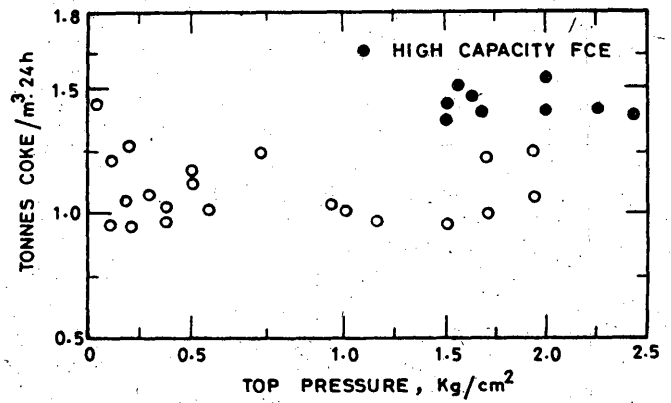


Fig. 11.16 The influence of top pressure on the amount of coke burned per m^3 of furnace volume per day for medium and large furnaces (author).

The increase in coke throughput per unit of furnace volume with increasing HTP is shown in Fig. 11.16.

The drawback of HTP furnaces is the damage to the big bell and valves and consequent gas leakages. The life span of the big bells made with hard special alloys is about 2 million THM.

11.3.2.10. Top control

In small diameter furnaces the gas flow is more uniformly distributed in the horizontal cross-section than in the larger ones because of proportionally larger raceway area compared to the hearth area in the former. In large furnaces, the central flow is of extreme importance for uniformity of gas distribution, heat exchange and stock descent as well as for smooth and regular operation. In addition to a pronounced central flow, a moderate peripheral flow is also necessary which must be ensured, especially when the periphery is loaded with fines.

As mentioned before, in large furnaces with large throat area the ores tend to confine towards the periphery, loosening the axis and thus impairing gas efficiency. Fig. 11.17(a)[46] shows the temperature distribution at the stockline of Fukuyama No. 5 furnace. With normal charging there is a wide high temperature zone in the centre of the furnace which suggests

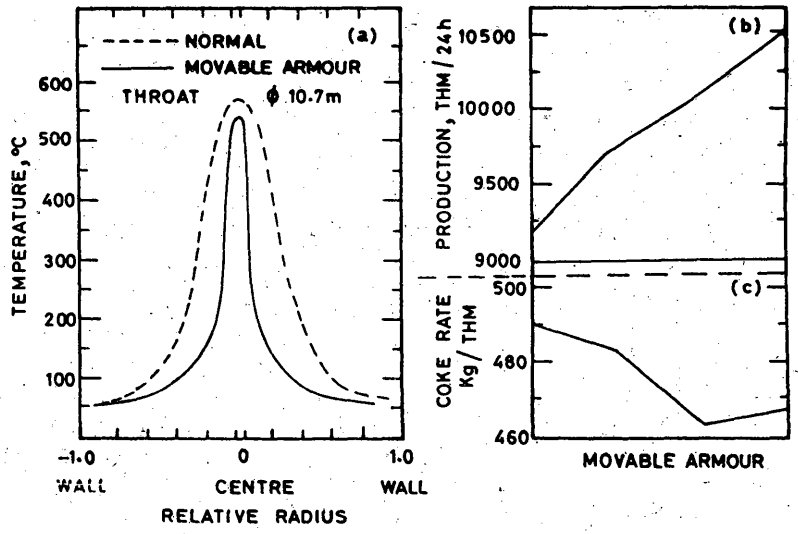


Fig. 11.17 (a) Radial temperature distribution at the stock level in Fukuyama No. 5 furnace with and without movable armour; (b) increase in production and (c) decrease in coke rate with the introduction of movable armour. After Higuchi et al.[45,46] (By kind permission).

that in this region the gas flow is very strong which is not suitable for high productivity, probably because of too high a coke rate.

In order to obtain a more efficient gas utilization, an NKK type movable armour (Fig. 5.18) was used to dump one ore charge towards the centre for promoting utilization of the high temperature reducing gas in the axis and the second ore charge distributed in the periphery without using the armour to utilize the peripheral gas, protect the wall and reduce wall heat losses. The armour is set at distances 0.8 and 1.0 m from the wall as desired in order to obtain an optimum result. By using such a charging sequence, a very sharp central gas flow with a narrow high temperature zone was realized (Fig. 11.17a), the gas efficiency improved, the coke rate fell from 490 to 460 kg/THM (Fig. 11.17c) and the production increased from 9600 to 10900 THM/day (Fig. 11.17b).[45]

The flow pattern of the gas in the furnace can be changed greatly from the top by attention in the charging technique and sequence as already discussed in Secs. 5.8 and 13.3. With sinters and pellets, especially the latter because of more uniform size, the changes in the flow pattern cannot be as striking as in the case of run-of-mine ores with their very broad size fraction and widely varying densities. Along with the changes in charging technique and sequence, stockline level, coke quantity per charge, etc., for attaining a smooth operation with optimum blast intake, it is necessary to keep a close watch on the blast pressure, inwall temperature and the temperature and composition of the gas at various levels of the stack.

11.3.2.11. Bottom control

Blast control at the bottom is as important as charge control at the top. The flow of gas through the stock column and the peripheral blast distribution are usually not uniform. It is possible to regulate the flow pattern to a limited extent by judicious alterations of the tuyere diameter and/or length. A preferential axial flow can be obtained by lengthening the tuyeres which also induces a more continuous combustion zone between the neighbouring tuyeres (Sec. 7.6.3). Where the peripheral flow is unduly large in some area, the relevant tuyeres may be replaced by smaller diameter ones, e.g., a 200 mm dia. tuyere may be replaced by a 150 mm one. These changes are reflected within a few hours in the temperature changes shown by the inwall thermocouples. A non-uniform flow is evidenced by the differences in the inwall temperatures at various levels along the stack circumference as well as by the differences in pressures shown by pressure gauges on blow-pipes or by pressure falls at various levels. The blast distribution

differences can also be controlled manually or automatically by adjusting valves in the goose neck. In the case of a pronounced axial flow, the peripheral activity can be increased by enlarging the tuyere diameter, say, from 180 to 190 mm. A decrease in the gas velocity permits the use of an increased blast volume. A decrease in the coke rate by 20 kg/THM and an increase in the output by 8.5 percent have been recorded.[48]

Maximum blast intake is limited by hanging, slipping, channelling, excessive flue dust, irregular stock descent, non-uniform metal composition, cold hearth etc., apart from an excessive coke rate. Such irregularities should be corrected at the top as well as at the bottom by the adjustment of blast temperature and moisture or hydrocarbons where used. The blast volume which determines the iron output should be lowered as a last resort when all the other methods fail. For the removal of channelling, reduction of the blast pressure to 1.1–1.2 ata is perhaps the only remedy. Choking of the lower furnace, the sign being increased pressure drop between the tuyere zone and the foot of the stack, can be remedied by lowering the blast temperature or increasing the additive input.

Many furnaces are run at optimum blast rates and therefore they work hard. They need to be checked at regular intervals, often every 30 minutes. Lowering of the blast temperature also smoothens the furnace but ultimately it lowers the output because of an increase in the coke rate.

Optimum volume and temperature of the blast are determined from experience for each furnace using a particular burden and making a particular iron. The blast temperature is generally high if the low temperature thermal load is low, the slag volume low, the iron ore rich, the sinter prefluxed, etc.

11.3.3. Oxygenation and Humidification of Blast

Incorporation of oxygen and/or steam increases the percentage of oxygen in the blast and therefore increases the coke burning rate per unit volume of blast, i.e., per unit time. This will obviously lead to an increased production provided the furnace runs smoothly and the coke rate does not rise or, if it at all rises, it does not do so at a rate to offset the increase in production. Both give a bosh gas richer in the reducer components CO and H_2.

We have seen in Secs. 4.4 and 6.8 that oxygenated blast increases the flame temperature which, if the optimum is surpassed for any given furnace and burden quality, leads to hanging. On the other hand, moisture in the blast reduces the flame temperature which again, if it crossed the lower

limit, would cause all the troubles inherent in the cold furnace. A judicious use of both can give a higher production at any flame temperature within the two limits. However, the economics of using a combined oxygen plus steam will be a determining factor. The costs of steam and oxygen and the capital outlay for the auxiliary plants needed for injection should be counter-balanced by the higher heating value of the top gas and increased output.

11.3.3.1. Oxygenated blast

Oxygen-enrichment lowers the nitrogen content of the blast and decreases the blast volume per unit of carbon burned as well as the bosh gas volume per THM. For the same blast volume or the volume of bosh gas generated per unit time, oxygenation would give increased coke driving rate. However, as seen in Sec. 4.3, the heat transfer aspect becomes unfavourable when a limiting oxygen in the blast is reached. It varies between 21–30 percent depending upon the burden and its acceptance of high flame temperature.

In cases where the heat requirement of the hearth is high and that of the stack is low, e.g., in the making of ferro-alloys, oxygenated blast may be profitably used. In these cases, the coke rate is usually high and the amount of gas evolved is in excess and even with high oxygen-enrichment the amount of gas is usually sufficient for the necessary heat transfer in the upper heat exchange zone. Since the use of high flame temperature reduces the tuyere carbon rate, a great increase in productivity is realized. According to Pochvisnev et al.,[49] in the manufacture of ferro-silicon with oxygen in the blast, the production increased from 100 to 160–180 THM/day and the coke rate fell from 2300 to 2000 kg/THM when oxygen was increased from 25 to 27 percent. With further increase of oxygen to 33 percent, the production rose to 218 THM/day and the coke rate sank to mere 1670 kg/THM.

In ironmaking, oxygenation does not reduce the coke rate especially when high blast temperature is used. However, the coke burning rate increases in proportion to the increase in oxygen. An increase from 21 to 26 percent would increase the burning rate by $5 \times 100/21 = 24$ percent. The productivity would increase by approximately the same amount. According to Stapleton,[50] with 27 percent oxygen in the blast the average production increased by 29 percent. The coke rate decreased simultaneously by 9 percent and the dust emission by 8 percent.

11.3.3.2. Humidified blast

Like oxygenation, the humidification increases the coke burning rate and produces a bosh gas richer in $CO + H_2$, the volume being smaller per unit weight of carbon burned (Table 6.6). Thermally, however, the moisture reduces the flame temperature while oxygen increases it (Fig. 6.27).

Since moisture lowers the flame temperature, it is necessary to increase the blast temperature, the compensating temperature increase being about 8–10°C per 1 gm H_2O/Nm^3 blast. The effect of moisture content and temperature of the blast on the coke rate is shown in Fig. 10.18. If the flame temperature is adequately compensated, the increase in production can be approximately calculated from the decrease in tuyere gas volume per unit of blast volume (Eq. 11.3 and Table 6.6). As for example, with 20 gm H_2O/Nm^3 and blast temperature of 1100°C, the calculated production increase is about 5–6 percent compared to the base case of blast temperature 900°C with no moisture.

Steam can be profitably used where there is idle stove capacity but hanging prevents the use of high blast temperature. Steam increases the production rate for the following reasons:

(i) higher gasifying power which intensifies coke consumption in the raceway;
(ii) smoothens the temperature gradient and facilitates stock descent (Sec. 4.6);
(iii) enlarges the combustion zone and accelerates stock descent; heats up the axial zone; maintains thermal state of the hearth (Sec. 7.6.6.6);
(iv) even with incomplete temperature compensation, the coke rate may not rise because of higher reducing power and higher heat transfer coefficient of hydrogen;
(v) decreases pressure loss due to lower density and viscosity of hydrogen. The blast pressure may drop even by 0.1–0.2 atm. which means the furnace can be blown at a higher blast rate.

Giedroyc[51] reports from single correlations in Colville No. 3 furnace that the increase in the daily output of iron was 50 tonnes, i.e., 8.1 percent. Of this, 7.1 percent could be attributed to increased driving rate and smoother operation and the rest 1 percent to decreased coke rate. A reduction in the number of checks by 50 percent showed a smoother operation.

11.3.3.3. Combined oxygenation and humidification[52,53]

For maintaining constant flame temperature, it is necessary to introduce steam with oxygen-enrichment.

Table 11.6 illustrates the combined effect of oxygenation and humidification of the blast on the relative driving rates and composition of the bosh gas based on 1 Nm^3 of dry or modified air. The flame temperature for all the cases is about 2620°C based on pure carbon at 1400°C and blast temperature of 1300°C. The amount of carbon gasified or the driving rate is increased by 50 percent on changing from dry normal blast to a blast containing 29% O_2 + 50 gm H_2O/Nm^3 at a constant blast volume. The relative increase in the bosh gas volume is 1.1 with the increase of ($CO + H_2$) from 34.7 to 50.1 percent. Such an increase in the reductant content is advantageous for increasing the wustite reduction rate to compensate for the decreased gas/solid contact time resulting from the increased throughput rate of 50 percent. The furnace should be able to take up the excess 10 percent bosh gas volume since hydrogen with its lower density and viscosity would encounter less resistance to flow. If it cannot, the blowing rate has to be brought down and the productivity would decrease correspondingly and range between 140 to 150 percent of the original.

11.3.4. Fuel Injection

We have seen in Secs. 6.9.3.1 and 10.7 that all injectants are coolants and need a compensating increase in the blast temperature for obtaining high replacement ratios. The total amount of gas produced depends upon the relative amounts of tuyere carbon and injectants. As for example, from Table 6.8, the decrease in bosh gas volume is about 6 percent when the tuyere carbon is 350 kg/THM in the coke alone case compared with 275 kg/THM plus 50 kg oil/THM, the replacement ratio being 1.5. In such a case the productivity will increase by at least 6 percent if the blowing rate is increased.

In the case of fuel injection, the bosh gas becomes enriched in the reductant gases CO and H_2 and they increase the rate of iron oxide reduction. On the other hand, the transit time of the ore through the zone of indirect reduction also affects the kinetics of reduction. For the same iron production rate, the transit time of the ores increases because of decreased coke rate with blast additives (Sec. 7.3.3.3). Therefore, an equivalent increase in the production rate could be achieved if the transit time, and hence the reduction rate, of the ore is the only limiting factor.

Suppose the transit time increases by 20 percent. Therefore, an increase in the productivity of 20 percent will be expected if the transit time of ore is the limiting factor. However, since the decrease in bosh gas volume is only 6 percent, the expected increase in production will be about 6 percent instead of 20 percent since the gas flow rate through the stock column is in most cases the limiting factor in the rate of production.

It is true, because of much lower viscosity and density of hydrogen, a hydrogen-rich bosh gas will encounter smaller resistance to gas flow (lower pressure drop and smoother furnace operation) and, therefore, a high production rate can be expected but at the same time a higher ore/coke ratio increases the permeability factor (Sec. 5.9.1) and offers greater resistance to gas flow. The cumulative effect of these opposing influences is extremely difficult to predict or evaluate.

On the basis of the bosh gas volume produced per kg or Nm^3 of the additives (Table 6.8), the volume will decrease (i.e., the output will increase for the same volume) if the replacement ratios based on carbon exceed 1.1 in the case of oil, 0.91 with natural gas and 0.42 with coke oven gas. In furnaces already using highest possible blast temperature of 1250–1300°C, the fuel/coke ratio is very unfavourable and no increase in the output is expected except that from a possible higher blowing rates permitted by the presence of hydrogen. As for example, with small additions of oil, the replacement ratio is high and the bosh gas generated smaller in volume and hence the productivity will increase. With increasing amounts of oil, the replacement ratio decreases and the bosh gas volume increases. The productivity will start to fall when the volume exceeds the volume in the coke alone case. The trends are shown in Fig. 11.18.[54] The figure also shows the increase in output with the oxygenation of the blast.

We have seen in Eq. 11.1, the productivity increases only when the ratio Q/K increases. The coke throughput Q is dependent upon the resistance of the charge material to gas flow. In the conventional operation, the coke driving rate is a measure of the gas flow rate but in the case of modified blast this is not so since a part of the bosh gas available from the combustion of coke is replaced by the gas formed from the additives. Hence, the introduction of Eq. 11.3 as a measure of productivity.

There are two criteria to judge the effect of oxygen-enrichment on production when using blast additives. They are:

(i) oxygen-enrichment at constant amount of blast additives (increased flame temperature);

Table 11.6. Effect of oxygenated-humidified blast on the driving rate and bosh gas composition based on 1 Nm^3 blast volume

$\%O_2 + \frac{gm.H_2O}{Nm^3}$	Blast composition, % by volume			kg.C burned by		Total C kg	Relative driving rate
	O_2	N_2	H_2O	O_2	H_2O		
21.0 + 0.0(air)	21	79	–	0.225	–	0.225	1.0
24.5 + 20.0	23.9	73.6	2.49	0.256	0.0132	0.27	1.2
26.0 + 30.0	25.0	71.25	3.72	0.280	0.02	0.30	1.3
27.5 + 40.0	26.14	68.90	4.96	0.294	0.027	0.321	1.4
29.0 + 50.0	27.2	66.60	6.20	0.31	0.033	0.343	1.5

	Composition of bosh gas and relative volume					
$\%O_2 + \frac{gm.H_2O}{Nm^3}$	% CO	% N_2	% H_2	% (CO + H_2)	Relative volume	
21.0 + 0.0	34.70	65.30	–	34.70	1.0	
24.5 + 20.0	39.80	58.25	1.95	41.74	1.04	
26.0 + 30.0	41.74	55.33	2.91	44.68	1.06	
27.5 + 40.0	43.65	52.50	3.79	47.46	1.08	
29.0 + 50.0	45.43	49.88	4.71	50.12	1.10	

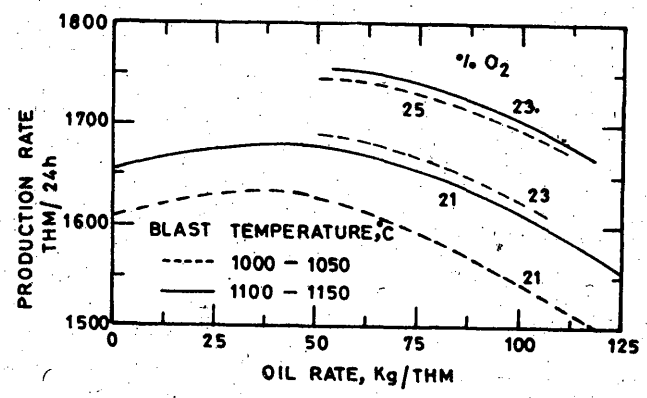


Fig. 11.18 Productivity and oil rate per THM for various oxygen contents of air at two levels of blast temperature; injection of heavy oil with high blast temperature, fully prepared burden and oxygen-enrichment, after Brandi et al.[54] (Copyright Verlag Stahleisen).

(ii) oxygen-enrichment keeping the flame temperature constant (increase in the amount of blast additives).

Recent investigations of Henkel et al.[55] in blast furnaces show that in the former case the production increased by 2.5–3.5 percent for every 1%O_2-enrichment and in the latter it did so by 1.0–1.3 percent. However, in the latter case, more of additives can be used and there will be less fear of furnace irregularities because of constancy of the flame temperature.

The increase in productivity with the use of fuel additives, oxygenation, use of metallized burden, etc., have already been seen in Sec. 10.7.1.6.

11.4. Decrease in Coke Rate

The methods by which the coke rate can be reduced have been narrated in Chapter 10. In this chapter the dependence of the coke rate on coke throughput will be discussed. The savings in coke with the use of hydrocarbons may also lead to an increased output if the furnace permeability is sufficient to accept any increase in the bosh gas volume occasioned therefrom. Productivity will increase according to Eq. 11.3 if the tuyere gas volume per THM is decreased and/or the gas throughflow increased by any means. A decreased coke rate decreases the slag bulk which raises the flooding limit and hence increases the productivity.

The influence of coke throughput on the coke rate can be two fold:

(i) influence on indirect reduction caused by inadequate heat and mass transfer as the velocity of the gas and that of burden descent increase with increasing blast volume (cf. Fig. 11.13);

(ii) influence on radiation and cooling losses. For a given furnace the heat losses are constant per unit time. Therefore, the heat losses per THM will decrease with increasing output and the coke rate will correspondingly fall. On the other hand, with increasing blast volume there will be a deterioration in the coke rate when a critical velocity of the ascending gas and descending burden is surpassed (cf. Fig. 11.12). Therefore, with an increasing blast volume or coke throughput (i.e., iron output), there will be a fall in the coke rate initially and above an optimum the coke rate will register an increase because of (i) above. In between these two lower and upper limits there is a stage where the coke rate will remain more or less constant.[56] This is shown schematically in Fig. 11.20.

At low blow rates, it is not only the heat losses per THM that are disadvantageous but the ascending gas develops a preferential flow and hence does not have the opportunity to come into intimate contact with all the ore pieces of the charge. With increased forcing of the blast the gas enters the formerly inaccessible regions, resulting in a more efficient utilization of the thermal and chemical energies of the gas and hence in a decreased coke rate. The pattern of the gas flow at low and high blast rates is shown

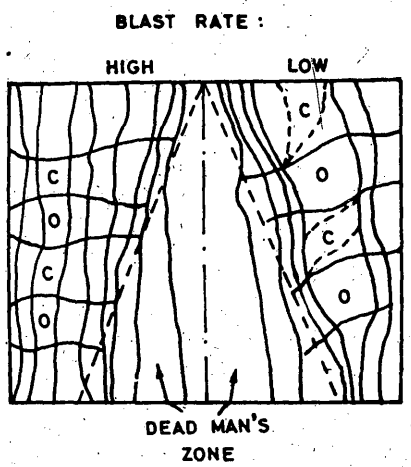


Fig. 11.19 A schematic representation of gas flow pattern in the lower furnace with high and low blast rates. C = coke and O = ore.

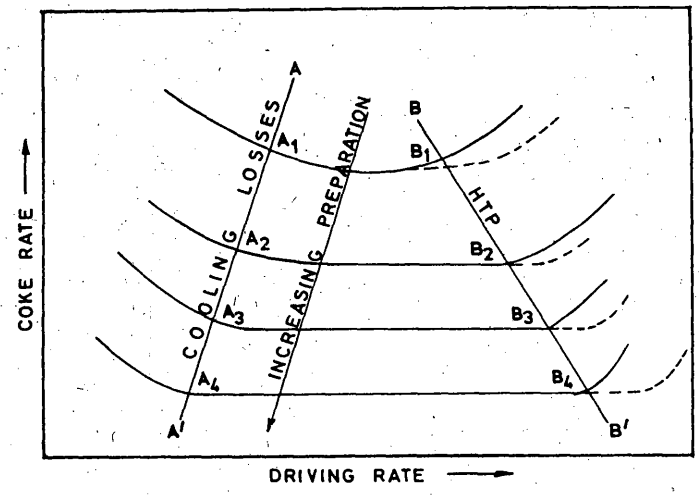


Fig. 11.20 A schematic diagram of dependence of coke-rate on the driving rate and degree of ore preparation.

schematically in Fig. 11.19. This is also borne out from the blast furnace data of the 1930s in the U.S.A. where the furnaces were perforce blown at only 10–20 percent of the capacity because of lack of demand for pig iron. During the period it was found to be more economical in coke rate to blow the furnace alternately at full and about one-tenth of the usual blast rate after a lapse of certain predetermined intervals (so-called *fanning*) rather than blowing continuously with medium blast.

In Fig. 11.20, the lines of constant coke rate range from run-of-mine ore (A_1B_1) to 100 percent prepared burden (A_4B_4). Between these two ranges, the coke rate virtually remains constant due to adequacy of residence time of the gas. In the case of unprepared burdens, due to inadequate reducibility of the ore and maldistribution of the gas, the horizontal distance is short. With an increasing burden preparation, the consequent even gas distribution and the presence of the chemical inactive zone elongate the horizontal distance to much higher coke throughput. In modern furnaces, as long as the inactive zone exists there is very little increase in the coke rate with increasing blowing rate. Even if the inactive zone disappears and/or CO-utilization deteriorates the coke rate may not increase as long as the increased direct reduction heat is compensated by lower cooling losses per THM with increasing production. The optimal zone disappears along BB′. In contrast to unprepared burden where much of the shaft volume is utilized for 'shaft' work, in modern furnaces almost

the entire shaft volume is utilized for gaseous reduction. In all cases, the time of residence of the gas can be increased, a more uniform gas distribution obtained and the furnace volume better utilized with the help of HTP. From Fig. 11.20, it appears that HTP is only necessary when desiring to work beyond BB′ and it is more useful when working with unprepared burdens than in the case of prepared ones.

The installation of HTP is very costly. As the residence time decreases, the heat transfer and burden reducibility must increase correspondingly in the absence of HTP in order to maintain the horizontal scope of the coke rate in Fig. 11.20. They can be increased by better material distribution, reduction of ore size, narrow size fraction, use of highly reducible pre-fluxed sinters and pellets, etc. However, in modern high capacity furnaces the HTP forms an essential part in order to distribute the gas evenly as well as to decrease the linear velocity of the gas to avoid fluidization or flooding.

We have seen in Fig. 10.15 that with prepared burdens, there is an approximately linear relationship between the coke rate and burden weight. This relationship is apparently independent of the time of residence of the ore or gas in the furnace. This is so presumably because the operators generally work their furnaces uniformly aiming at a minimum coke rate and therefore they work within the horizontal scope of Fig. 11.20.

11.5. Factors Limiting Productivity

The solids to gas ratio in the blast furnace is determined by the energy requirements of the process. Hence, a maximum productivity is achieved when the gas flow rate is maximum since it is the gas that makes available the thermal and chemical energies. However, the maximum gas rate is determined by the resistance it encounters during its ascent. This maximum is limited by various factors which have already been discussed in Chapter 5. They are:

(i) fluidization of bed in the dry zone. This happens when the gas velocity equals or exceeds a critical velocity which depends upon the size and density of the particles (Figs. 5.1 and 5.10);

(ii) loading and flooding of slag in the coke grid. This happens when the gas velocity in the lower furnace equals or exceeds a critical velocity which depends amongst others upon the slag bulk and slag viscosity (Sec. 5.6);

(iii) decrease in bed voidage due to softening, swelling or breakdown of ores or coke.

The calculated minimum particle size for the onset of fluidization is illustrated in the nomogram, Fig. 11.21,[3] which shows the relationship with the blast volume (i.e., iron production for given coke rates) per m^2 of hearth area and top pressure (which determines the empty tube velocity of gas in the throat). The nomogram shows that for an iron production of 50 THM/m^2.24h without HTP, ore sizes below 6 mm and coke sizes below 23 mm will be blown out. Since the coke size as used is always much larger, it is the fine ore that becomes vulnerable. A few other maximum productivity figures derived from Fig. 11.21 for fluidization are given in Table 11.7.[3]

Fig. 11.21 and Table 11.7 illustrate the importance of screening out of all fines, resistance to breakdown of both ore (sinter, pellet) and

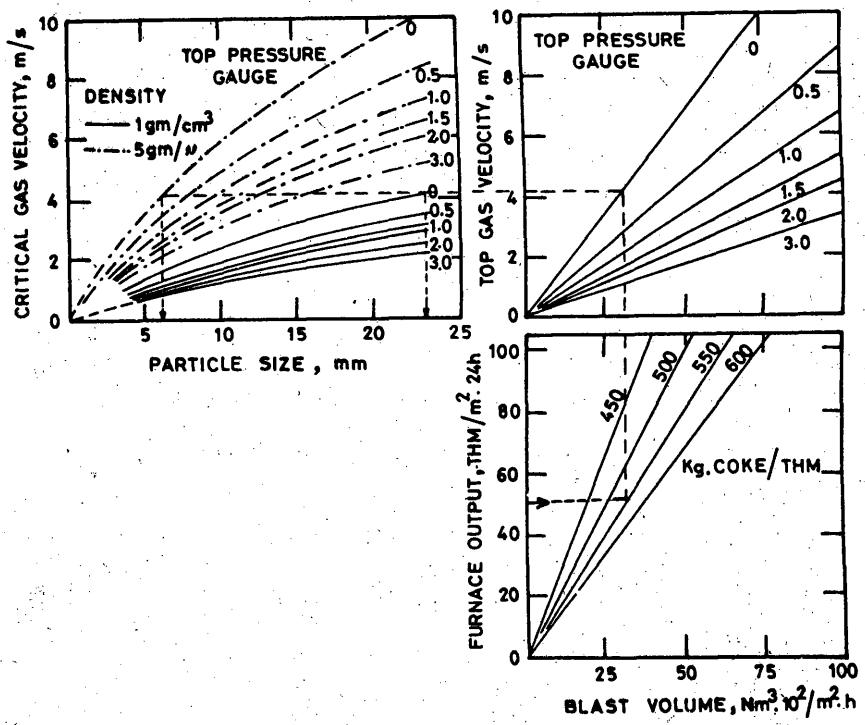


Fig. 11.21 The limit of productivity caused by fluidization at the blast furnace top and the effect of high top pressure, according to Bogdandy et al.[3] (Copyright Verlag Stahleisen). Densities of coke and ore are 1 gm and 5 gm/cm³.

coke as well as of high top pressure for lowering the minimum size of fluidization.

Table 11.7.[3] Dependence of productivity per m² hearth area per 24h on particle size of ore of density 5 gm/cm³ and HTP

Assumptions: Fluidization in the throat to be limiting. Coke rate 500 kg/THM, coke = 87.5% C

HTP, atm. gauge	minimum ore size mm	highest productivity THM/m².24h
0	6	50
0	8	60
3	6	95
3	8	116

The flooding limits calculated with the help of Eq. 5.30 and by substituting proper values therein are shown in Fig. 11.22[3] for blast volumes, coke rate, production rate, slag bulk, slag viscosity, etc. taking into consideration the relationships between the blast volume, coke rate and CO-utilization. Further assumptions made are:

ε = 0.35 = voidage in the coke grid
F_s = 90 m²/m³ = surface area of coke/m³
d = 40 mm = coke size
η = 10, 15P = slag viscosity
η_{co} = 0.45 = CO-utilization
Carbon content of coke = 87.5 percent
Bosh gas pressure = 1 atm., gauge
Bosh gas temperature = 1600°C
O = 400 kg/THM = removable oxygen in iron.

The approximate maximum productivities, where flooding is limiting, are shown in Table 11.8[3] for a few cases. Comparing Figs. 11.21 and 11.22 and Tables 11.7 and 11.8, the productivity limit for flooding is reached at lower output than in the case of fluidization of the solid particles. However, it must be borne in mind that fines much below 6 mm accompany pellets, in the case of sinters considerable breakdown occurs in the furnace itself between temperatures 400–600°C and in the case of ores the fines are generated by breakdown and decrepitation below 500°C. The cause

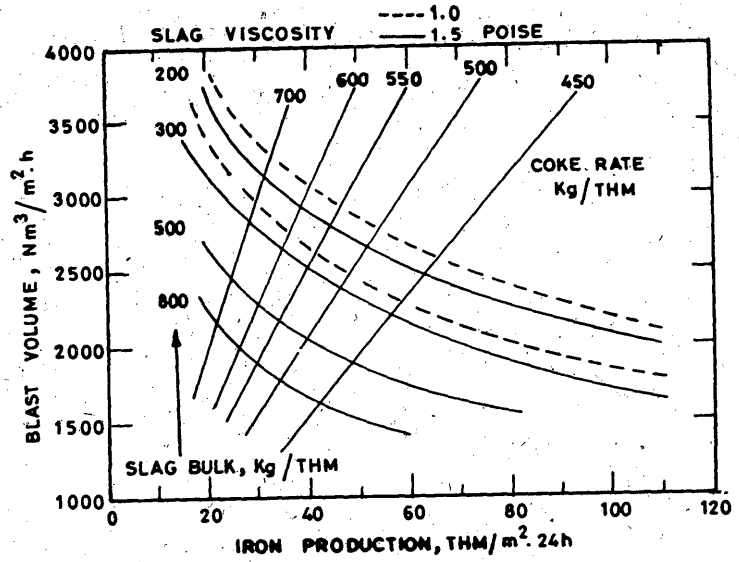


Fig. 11.22 The limit of productivity caused by loading and flooding in the blast furnace without high top pressure, according to Bogdandy et al.[3] (Copyright Verlag Stahleisen).

of the loss of strength in reducing atmospheres is not known but its extent is lower the smaller the residence time of sinter in this temperature zone and the higher the basicity and ($MgO + Al_2O_3$) content of the sinter. In high productivity furnaces, the residence time in the 400–600°C zone is comparatively small and hence the danger of breakdown is minimized. Since the strength of sinters is the lowest at basicity of 1.0–1.5, it is preferable to charge partly low-flux and partly high-flux sinters in order to avoid

Table 11.8.[3] Dependence of productivity limit on coke rate, slag bulk and top pressure with respect to flooding of slag

Bosh gas pressure, atm. gauge	Top pressure, atm. gauge	Coke rate, kg/THM	Slag bulk, kg/THM	Productivity, THM/m².24h
1	0	500	300	46.7
1	0	700	800	22.0
5	3	500	300	73.2
5	3	700	800	34.3

sinter breakdown and, therefore, avoid fluidization limiting the productivity.

The other factor which limits gas throughflow is softening of the ore, sinter or pellet. We have seen before that the higher the basicity the greater the softening temperature and narrower the temperature range.

Recent blast furnace operational results[57] show that the productivity may possibly be limited by the compaction of bed due to softening of the ferrous burden. From Fig. 11.23(a),[58] the actual production of iron was less than half of that calculated for charge instability from the material size as charged. However, the ferrous burden, especially the sinters, undergo considerable breakdown between 400–600°C. Taking into account the possible extent of breakage from laboratory experiments, a new productivity limit was calculated which was also 20–30 percent higher than the actual production as shown in the figure.

The maximum production trend estimated on the assumption that the limiting factor was flooding is also shown in Fig. 11.23(a). The results show that with increasing proportion of basic sinter the actual production approached the flooding limit. However, as the percentage of basic sinter was decreased (replaced by essentially acidic ore or pellet, which are more easily softened), the gap between the two increased.

The marked reduction in the actual production may have been caused by a greater degree of compaction during the reduction of acidic material

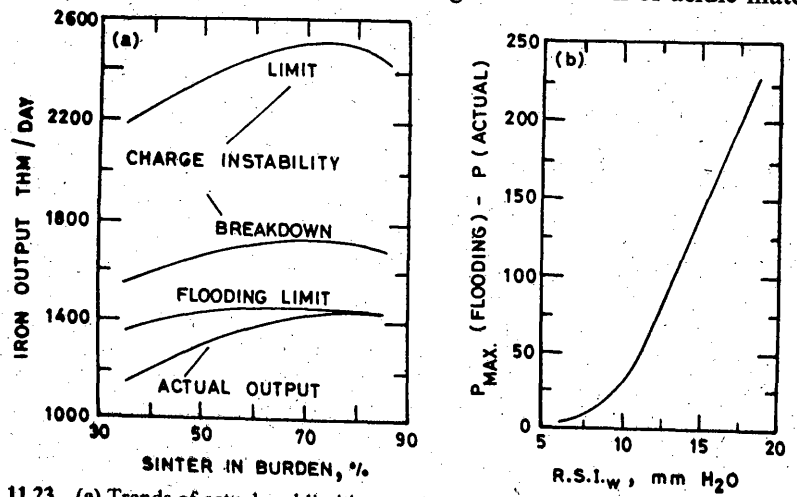


Fig. 11.23 (a) Trends of actual and limiting production of iron; (b) difference between maximum flooding production and actual production related to burden reduction softening index (RSI). After Pallela et al.[58] (Copyright Australasian Institute Mining Metallurgy).

under load. This is substantiated in Fig. 11.23(b)[58] where the difference between the flooding limit and actual production [P_{max} (flooding) − P_{actual}] in THM/24h is plotted as a function of reduction softening index*, RSI. The RSI decreases with increasing basicity of the sinter. The small difference at low index between 5 and 10 is probably due to the irregularity of liquid flow in the bosh zone. The sharp increase thereafter is connected with softening.

The zone where the ores and agglomerates soften and melt is of paramount importance for gas flow in the lower furnace. As we have seen in Fig. 5.1, the softening and compacting of the ferrous burden do not occur in a particular horizontal section of the furnace but follow a pattern which is similar to the gas temperature profile in an operating furnace (cf. Fig. 7.4). Recent investigations by dissecting furnaces quenched while in operation show broadly two different patterns of the softened and compacted materials;[35–37] the W-type and the inverted-V type. They are named as cohesive zones and are shown schematically in Fig. 11.24. The types depend upon the pattern of gas flow and hence on the gas temperature distribution. The latter depends upon the ore/coke distribution in the furnace cross-section and hence is related to charging techniques.

The cohesive zone consists of permeable coke layers (coke slits) interspersed with viscous semi-fused ores and iron which resist the passage of gas. The gas can pass horizontally through the coke voids and then ascend taking the path of least resistance through the dry granular bed composed of alternate layers of ore and coke (cf. Fig. 1.3). The softened materials form liquid globules on melting and descend through the interstices of coke. The central coke column above the tuyere axis is relatively loosely packed and active through which the molten metal and slag flow as in a counter-current liquid-gas exchanger, the coke pieces providing the mechanical support. The coke slits act more or less as gas distributors.[59–60] If the coke breakdown is excessive, the slits also resist gas throughflow (Sec. 11.3.2.3).

The distribution of gas and hence the furnace performance depend greatly on the location of the cohesive zone and the magnitude of resistance to gas flow offered by the zone. If the liquid hold-up in the active coke column is small (low liquid flow rate), the gas will flow preferentially through the column. If the hold-up is large, the increased resistance will

* The pressure drop through a defined sample bed after 2 hours of testing is taken as reduction softening index (RSI),[58] mm H_2O.

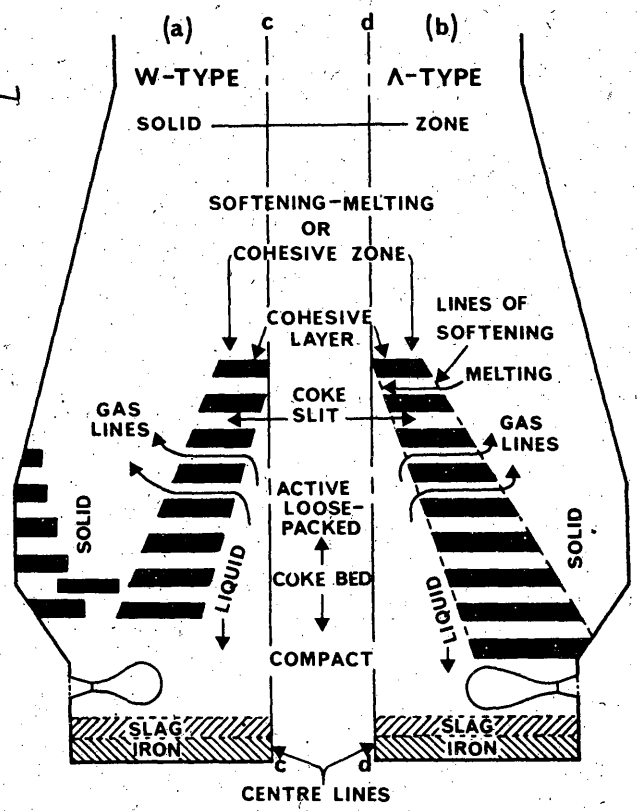


Fig. 11.24 Schematic representation of the internal state of a quenched blast furnace showing (a) W-type and (b) V-type softening-melting zones. Only sections through the centre lines c-c and d-d are shown. The gases pass horizontally through the permeable coke slits interspersed with relatively impervious layers of fusing slag and iron. The coke bed above the tuyere axis is loose-packed because of the upward thrust of the high velocity combustion gases.

force the gas to seek more permeable regions in the periphery. Therefore, whether the gas will flow preferentially through the central or the peripheral regions will depend upon the resistance offered by the coke column and the coke slits in the cohesive zone.

Recently Gudenau et al.[60] have studied the effects of different softening and melting properties of ore agglomerates on gas permeation in the blast furnace and optimization of these properties for maximum productivity. According to their findings, horizontal gas streams seem to exist between the individual agglomerate layers of the cohesive zone. The investigations show that highly basic sinter with $CaO/SiO_2 > 1.5$ has inferior high temperature properties but a part replacement of lime in the sinter by about 2.5% MgO has a markedly favourable effect.

It is surmised that a pronounced central flow of gas gives an inverted-V pattern of the cohesive zone which is preferable to the W-type for higher productivity, although the former is associated with less efficient gas utilization and higher coke rate. Whatever the type, of most decisive importance is the temperature and range of the softening-melting transformation. If the transformation of solid to liquid is quick and occurs in a high and narrow range of temperature, the cohesive zone will be more permeable, the gas flow more uniform, the furnace more stable and the iron production higher.

Recently, Wakayama et al.[61] have determined the relationship between burden distribution and blast furnace operation from a series of studies using a model furnace and paraffin coated particles as well as results obtained from the internal state of quenched commercial blast furnace. The difference in the configuration of the softening-melting zones (i.e., the W and inverted-V types) is the result of the difference in burden distribution. The results of their investigations are summarized below:

(a) W-type is obtained if the mode of charging or the ore/coke ratio is such that the central ore layers become thick which offer increased permeability resistance in the centre;
(b) the pressure loss in the lower furnace is high in the case of W-type;
(c) the inverted-V type is obtained if the ore/coke ratio in the furnace centre is relatively lower than at the furnace walls presenting a thick, more permeable layer of coke in the centre;
(d) the pressure loss in the lower furnace is low in the case of inverted-V type;
(e) the inverted-V type is a desirable pattern for obtaining good permeability, steady burden descent and lower heat losses at the wall;
(f) if the top of the inverted-V type zone rises too high in the furnace, it may result in inferior gas utilization or channelling; the level at the furnace centre can be lowered if the ore/coke ratio distribution across the furnace diameter is made more flat;
(g) the sharper the inverted-V shape, the greater the amount of gas flowing towards the wall *via* the coke layer in the lower part of the zone, the greater the gas utilization because of better gas/ore contact at the wall, the more stable the burden descent but the larger the gas flow resistance;

(h) a sharp inverted-V shape narrows down the high temperature gas-flow region in the furnace centre which increases gas utilization; the narrower the zone, the better the gas utilization and the lower the coke rate (cf. Fig. 11.17);
(i) a narrow central high-temperature zone is obtained by the use of movable armour, bell-less top or spiral charging; spiral charging enables the coke layer to be progressively thickened towards the centre from the wall and ensures a pronounced central flow.

11.6. Summary

Maximum productivity is obtained by using the following measures:

(i) small size and narrow size fraction for adequate heat and mass transfer and optimum permeability as the gas and stock residence time decreases with increasing output;
(ii) size of coke should be 3–5 times the size of ore, sinter or pellet for optimum gas flow in the dry as well as the wet zone;
(iii) slag bulk and viscosity should be low for minimizing flooding;
(iv) all −6 mm or preferably −10 mm should be screened;
(v) sinters should be highly fluxed preferably having some MgO for increasing the softening temperature and narrowing down the range and minimizing the low temperature reduction breakage;
(vi) coke and ferrous burden should be resistant to breakage due to abrasion, compression and impact under reducing conditions;
(vii) channelling must be controlled because it reduces the useful volume of the furnace;
(viii) use of HTP;
(ix) control of the shape and size of the cohesive zone by proper charging technique;
(x) control of alkali metals input and their vaporization in the furnace.

References

1. BEER, H. and G. HEYNERT: Stahl u. Eisen, 84, 1964, p. 1353–1365.
2. VOICE, E. W. and K. G. DIXON: J. Iron Steel Inst., 200, 1962, p. 438–443.
3. BOGDANDY, L. v., G. LANGE and P. HEINRICH: Stahl u. Eisen, 88, 1968, p. 1177–1188.
4. RICE, O. R.: Blast Furn. Steel Plant, 40, 1952, p. 513–521; 657–662; 787–792.
5. RICE, O. R.: J. Iron Steel Inst., 170, 1952, p. 89–108.

6. BRANDI, H. Th. et al.: Stahl u. Eisen, 80, 1960, p. 65–73.
7. PETERSEN, W. et al.: op. cit., 83, 1963, p. 1397–1407.
8. SCHENCK, H. and H. KUPPERBUSCH: op. cit., 83, 1963, p. 1345–1348.
9. Economic aspects of iron ore preparation: United Nations Tech. Pub., Geneva, 1966, p. 48–78.
10. FURNAS, C. C.: Blast Furnace, vol. 29, 1941 (see Ref. 9).
11. BOLAND, J.: J. Iron Steel Inst., Nov. 1961, p. 253–258.
12. TROGNITZ, W. R.: Blast Furn. Steel Plant, No. 4, 1964, p. 315–319; (see Ref. 9).
13. MINTROP, R.: Stahl u. Eisen, 78, 1958, p. 633–646.
14. HODSON, T. P. and G. R. SPRING: Future of ironmaking in the blast furnace, Spl. Rep. 72, Iron Steel Inst., 1962, p. 155.
15. MACDONALD, N. D.: Ref. 14, p. 151.
16. BABUSHKIN, N. M. et al.: Steel in USSR, Sept. 1973, p. 707–710.
17. VOSKOBOINIKOV, V. G. and A. G. MIKHALEVICH: Stal in Eng., July 1969, p. 612–615.
18. MIGUTSKII, L. R.: op. cit., Jan. 1967, p. 3–6.
19. GAMAJUROV, A. I. and A. G. NEJASSOV: Stal, 17, 1957, p. 20–24; see also Stahl u. Eisen, 79, 1959, p. 1470.
20. ASTIER, J. E. et al.: Ref. 14, p. 160.
21. MARSHALL, W. E.: J. Metals, 13, 1961, p. 308–313.
22. HALEY, K. R.: Operating results of using taconite pellets in Armco's Middletown blast furnace, Blast Furn., Coke-oven and Raw Mat. Conf., AIME, April 1961.
23. OLTS, T. F.: Ref. 14, p. 171–179.
24. BREDEHÖFT, R. and R. JESCHAR: Stahl u. Eisen, 93, 1973, p. 55–60.
25. WRENN, Th. K.: Blast Furn. Steel Plant, 1962, p. 518–522; see A. Send, Stahl u. Eisen, 83, 1963, p. 1053.
26. WHITE, R. H.: Recent advances in iron production tech., AIME, Minnesota Div., Jan. 1962; see A. Send, Stahl u. Eisen, 83, 1963, p. 1053.
27. WHITE, R. H.: Blast Furn. Steel Plant, 54, 1966, p. 241–245; see Stahl u. Eisen, 86, 1966, p. 1606.
28. KNEPPER, W. A. and C. M. SCIULLI: J. Metals, Feb. 1966, p. 228–230.
29. TEICHERT, E. and V. N. GUPTA: Stahl u. Eisen, 96, 1976, p. 662–676.
30. EISENHUT, W. et al.: op. cit., 99, 1979, p. 1–6.
31. HENKEL, S.: op. cit., 88, 1968, p. 1129–1131.
32. GIEDROYC, V. and W. HYSLOP: Ref. 57, p. 86–93.
33. KAGANSKII, M. I.: Steel in USSR, June 1971, p. 421–426.
34. NAKAMURA, N. et al.: Ironmaking Steelmaking, 5, 1978, p. 1–17.
35. SASAKI, K. et al.: Trans. Iron Steel Inst. Jap., 17, 1977, p. 252–261.
36. SASAKI, M. et al.: ibid., p. 391–400.
37. KANBARA, K. et al.: ibid., p. 371–380.
38. NAKAMURA, N. et al.: Ironmaking Steelmaking, 5, 1978, p. 49–60.
39. Coal, Coke and Blast furnace: Proc. Intnl. Conf., The Metals Soc., Middlesborough, 15–17 June, 1977.
40. KOZIMA, K. et al.: Trans. Iron Steel Inst. Jap., 17, 1977, p. 401–409.
41. DAVIES, J., J. T. MOON and F. B. TRAICE: Ironmaking Steelmaking, 5, 1978, p. 151–161.
42. DU-CHO-GUI: Theory and practice of forcing of blast furnace: Rep. North-east Polytech. Inst. of Chin. Peop. Replic., 1959; see Stahl u. Eisen, 82, 1962, p. 1062.
43. BRANDI, H. Th., G. HEYNERT and H. BEER: Stahl u. Eisen, 84, 1964, p. 1169–1174.
44. MELCHER, N. B. et al.: J. Metals, Feb. 1967, p. 41–45.

45. HIGUCHI, M. et al.: Ref. 57, p. 129–138.
46. HIGUCHI, M. et al.: Trans. Iron Steel Inst. Jap., 17, 1977, p. 452–464.
47. TAKEODA, K.: Revista Latino-Americana de Siderurgia, Oct. 1967, p. 54–62 and 74; see also E. Krebs, Stahl u. Eisen, 89, 1969, p. 1422.
48. SEN'KO, G. E. and B. N. STARSHINOV: Stal in Eng., Feb. 1970, p. 93.
49. POCHVISNEV, A. N. et al.: Blast furnace practice, Verlag Technik, Berlin, 1954, p. 357.
50. STAPLETON, J. M.: 25th Blast Furn. Conf., BISRA, 1957, p. 26.
51. GIEDROYC, V.: 26th Blast Furn. Conf., BISRA, 1958, p. 47–58.
52. STRASSBURGER, J. H.: Iron and Steel, Oct. 1958, p. 491–496.
53. STRASSBURGER, J. H.: Blast Furnace – Theory and Practice, Vol. 1, Gordon and Breach Sci. Pub., N.Y., 1969, p. 51.
54. BRANDI, H. Th., P. ISCHEBECK and G. HEYNERT: Stahl u. Eisen, 83, 1963, p. 1541–1546.
55. HENKEL, S. et al.: op. cit., 90, 1970, p. 321–328.
56. BONNAURE, E.: op. cit., 79, 1959, p. 1115.
57. Blast Furnace Aerodynamics: Proc. Sym. Aus. I.M.M., Ed. N. Standish, Wollongong, 25–27 Sept. 1975.
58. PALLELA, P. et al.: Ref. 57, p. 75–85.
59. PROPSTER, M. A. and J. SZEKELY: Ironmaking Steelmaking, 6, 1979, p. 209–220.
60. GUDENAU, H. W. et al.: Stahl u. Eisen, 99, 1979, p. 1204–1210.
61. WAKAYAMA, S. et al.: Ironmaking Steelmaking, 5, 1979, p. 261–267.

CHAPTER 12

PRODUCTIVITY AND FURNACE PROFILE

12.1. Introduction

Blast furnace productivity depends upon an optimum gas throughflow as well as smooth and rapid burden descent. The character of the gas and stock movements is intimately associated with the furnace lines. The solid materials expand due to heating as they descend and their volume contracts when they begin to soften and ultimately melt at high temperatures in the lower furnace. A further volume contraction occurs when the solid coke burns before the tuyeres. An enormous volume of the combustion gas has to bubble through the coke grid irrigated with a mass of liquid metal and slag. An optimum furnace profile should cater to the physical and chemical requirements of counterflow of the descending solid, viscous pasty or liquid stock and the ascending gases at all places from the hearth to the top. Only then, an optimum utilization of the chemical and thermal energies of the gases as well as a smooth, uniform and maximum iron production with minimum coke rate will be realized.

12.2. Influence of Furnace Lines

The furnace profile has undergone a profound change in the last century. It was realized from the earliest that, for a smooth stock descent, the diam-

eter of the shaft should increase up to the softening or fusion zone to provide for the thermal expansion of the materials and smooth passage of the gas the volume of which increases with increasing temperature. Thereafter, in the primitive furnace, the shaft narrowed down in the bosh meeting ultimately the top of the cylindrical hearth (Fig. 12.1a).[1] The belly or bosh parallel has been introduced later and in-between the broadening shaft and narrowing bosh. Ideally, the softening, fusion and contraction of the burden materials should occur in the cylindrical belly. Coke is the only solid material present in the bosh and the coke grid in the narrowing bosh provides the mechanical support, lest the burden should collapse prematurely, block gas passage and chill the hearth.

A study of the evolution of the furnace profile (Fig. 12.1) shows an initial long bosh without its belly to the introduction of the latter with gradual shortening of the bosh (Fig. 12.1). We have recognized in Sec. 4.5 that the slag fusion zone descends with increasing blast temperature and also in Sec. 8.2.3 that the pre-fluxed burden softens at high temperatures and in a narrow temperature range. If the charge fuses in the bosh,

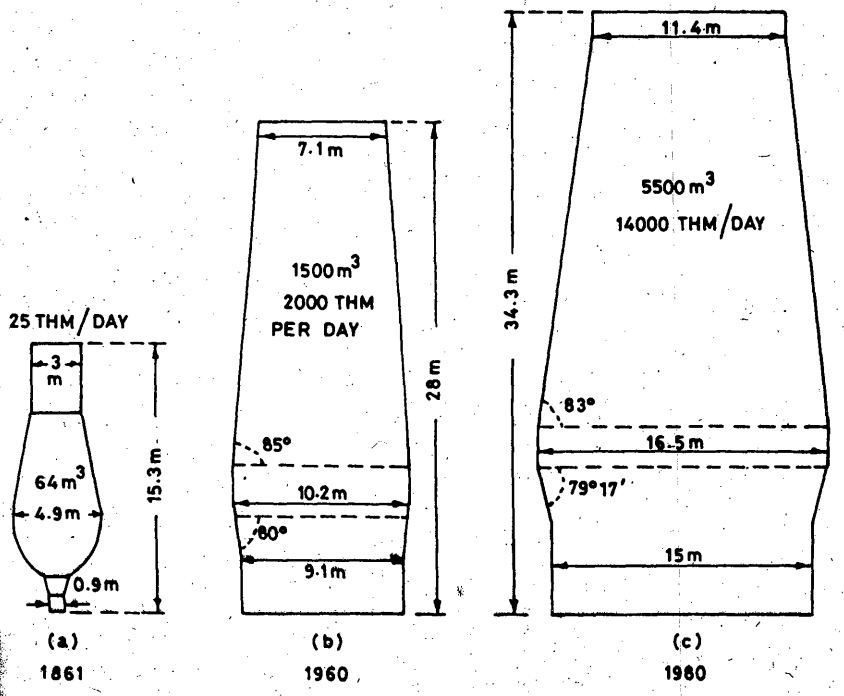


Fig. 12.1 Growth of blast furnace during the last 100 years.

the sticky mass hinders the passage of the gas and smooth descent of the burden through the narrowing bosh. As the modern tendency is for large furnaces using pre-fluxed burden and high blast temperatures, it is imperative that the furnace should have a short bosh so that the slag can fuse in the belly.

12.3. Profile Calculation

The blast furnace profile has evolved through experience and, therefore, the calculation of the furnace dimensions is more or less empirical in nature. Most furnace measurements follow some simple relationships which, however, are changing with the changing nature of the charge materials. The major dimensions which are inter-related are: useful furnace height and volume, the diameters of the hearth, belly, throat and big bell, the tapers of the shaft and bosh and the heights of the throat, belly and bosh.

In any furnace, a substantial portion of the total reduction of the iron oxides occurs in the lower shaft and below.[3] The profile must therefore be such that the stock remains the longest possible time in the lower furnace and where the gas velocity should also be relatively sluggish. This implies largest possible volume of this region which is achieved by widening of this zone in the transverse direction by the introduction of larger diameter and height of the belly and a shorter bosh. In fact, modern high capacity furnaces are expanding horizontally rather than vertically in order to provide sufficient volume for adequate processing of the charge materials. Since the combustion zone is localized along the hearth periphery, gas penetration deeper in the furnace is ensured by the use of mechanically strong and properly sized charge materials. As the horizontal cross-section increases it results in an uneven distribution of the materials. An uneven stock distribution is not a disadvantage because forcing of the modern furnaces is achieved through a pronounced peripheral and central flow.

It is not intended in this chapter to go into details of the furnace design. Only the relationships between the various dimensions and their influence on stock and gas movements are described briefly below.

12.3.1. Hearth Diameter and Height

For a given burden with a coke rate, the coke throughput determines the iron production rate. In Sec. 11.2 equations have been suggested relating the coke throughput with the hearth diameter based on the size of

the active hearth annulus. However, the depth of the raceway is not constant and it increases with increasing hearth diameter. The determining factors are the kinetic energy of the blast and burden permeability. With increasing diameter of the hearth, the gas penetration must be ensured by providing adequate bed permeability with the use of mechanically strong, rich, pre-fluxed burden of uniform size and low slag bulk as well as strong lumpy coke.

12.3.1.1. Hearth diameter

A very approximate relationship between the coke burning rate and hearth diameter is given by Eq. 11.13 from which the following equation is derived:

$$D = c\, Q^{1/2} \qquad 12.1$$

where,

D = hearth diameter, m
Q = coke throughput, tonnes/24h
c = throughput coefficient which varies between 0.2–0.3 depending upon burden preparation.

For highly prepared burden, the value of $c = 0.2$ has been achieved in modern large furnaces ($c = 0.2$ is equivalent to $\gamma = 25$ in Eq. 11.13). Therefore, for a furnace planned to produce 10,000 THM per day with a coke rate of 500 kg/THM, i.e., a coke throughput of 5,000 tonnes per day, the hearth diameter should be about 14.1 m.

Productivity is intimately associated with the furnace volume. The volume of super-large furnaces has been increased by increasing the hearth diameter without changing the height significantly, maintaining at the same time a constant gas velocity. As for example, the diameters of the 2000 m³ and 4000 m³ furnaces are approximately related by:[4]

$$D_l^2 = 2\, D_s^2 \qquad 12.2$$

where D_l and D_s are the diameters of the large and small furnaces.

Since the gas velocity is approximately proportional to G/D^2 where G is the blast volume and assuming that the production rate THM/m³.24h and the blast volume required to produce one THM are the same for both smaller and larger furnaces, then

$$G_l = 2\, G_s \qquad 12.3$$

or, from Eq. 12.2,

$$\frac{G_l}{D_l^2} = \frac{G_s}{D_s^2} \qquad 12.4$$

Hence, the gas velocity for the two types of the furnace are the same, i.e., the furnace capacity has been increased only by enlarging the diameter.

12.3.1.2. Hearth height

The hearth height is measured from the tap hole to the tuyere axis or from the floor to the upper rim which joins with the bosh incline. The latter has the disadvantage because the floor gets eroded by the metal with the passage of time. The floor is generally 0.5–1.5 m below the tap hole and the upper rim 0.5 m higher than the tuyere axis. The latter facilitates building of the tuyere brickwork and coolers. If it is too high and away from the coolers, the bricks can burn away very rapidly.

The hearth height is not increasing with increasing furnace capacity probably because of provision for more tap holes which are used alternately for almost continuous tapping of the metal and slag together for obtaining low-S iron. Although provision is made for slag notch, it is seldom used in the super-large furnace.[2]

The hearth volume and, therefore, the hearth height (from the tap hole to tuyere centre line) should be based on the number of m³ for each THM made in a day. On the basis of practical data from large Japanese furnaces of diameters 9.8–14.4 m, the values for the hearth volume range between 0.085–0.055 m³/THM.24h. The hearth height from the tap hole to the tuyere axis ranges between 3.5–4.2 m and the total height 5–6.2 m (Table 12.1).[5–9]

12.3.2. Useful Volume

The pre-reduction of the iron oxides, adequate preheating of the burden and, therefore, the smelting intensity depend upon the stock residence time and hence on the furnace volume. Furnace productivity is directly related with the furnace volume. According to Gipromez calculations,[2] an increase in furnace volume from 2000 m³ to 5000 m³ under comparable conditions increases iron production by 2.3 times, lowers the coke rate by 21 kg/THM, increases labour productivity by 1.4 times and reduces capital and operating costs by 6 and 4 percent respectively.

Table 12.1. Some blast furnace dimensions

Dimensions	Fukuyama Furnaces,[5] Japan							USSR[2]	USSR[2]	USSR[7]	USSR[8]	USA[9]	Japan Oita No. 1[6]
	No. 1	No. 1	No. 2	No. 2	No. 3	No. 4	No. 5						
Inner volume, m^3	2004	2323	2626	2828	3016	4197	4617	5000	5500	3200	2700	–	4158
Useful volume, m^3	1735	2012	–	2431	2605	3614	3923	–	–	–	–	–	3466
Hearth dia. D, m	9.8	10.5	11.2	11.5	11.8	13.8	14.4	14.7	15.7	12.0	11.0	7.6	14.0
Belly dia. d_b, m	10.8	11.6	12.0	12.7	13.0	15.2	15.9	16.1	16.5	13.1	12.35	8.54	15.0
Throat dia. d_t, m	7.3	8.0	8.4	8.6	9.0	10.5	10.7	10.8	11.4	8.9	8.1	5.78	10.2
$(d_b/D)^2$	1.214	1.220	1.148	1.200	1.214	1.213	1.219	1.200	1.190	1.192	1.261	1.263	1.148
$(d_t/D)^2$	0.555	0.580	0.563	0.559	0.582	0.579	0.552	0.540	0.570	0.550	0.542	0.580	0.531
$(d_t/d_b)^2$	0.457	0.476	0.490	0.459	0.479	0.477	0.453	0.450	0.477	0.462	0.430	0.458	0.462
Bottom – tap hole, m	1.0	1.1	1.0	1.1	1.5	1.35	1.5	–	–	–	2.2	–	1.987
Tap hole – tuyere, m	3.5	3.6	3.7	3.8	3.7	3.9	4.2	3.9*	4.7*	3.9*	3.4	2.285	4.5
Tap hole – slag notch, m	2.2	2.3	2.3	2.4	2.3	2.5	2.8	–	–	–	1.8	–	–
Hearth height, m	5.0	5.2	5.2	5.45	5.7	5.75	6.2	–	5.2**	–	6.1	3.6	7.2
Bosh height, m	3.5	3.7	3.5	2.7	3.5	4.0	4.3	3.7	3.7	3.4	3.4	2.74	3.5
Belly height, m	3.0	2.8	3.0	2.8	3.0	2.75	2.5	1.7	1.7	2.3	2.2	3.96	1.9
Shaft height, m	16.4	16.3	17.0	16.8	17.0	16.75	17.0	20.7	21.2	19.6	18.7	15.47	17.6
Throat height, m	1.5	1.5	1.5	1.5	1.5	2.0	2.0	3.0	2.5	2.99	3.0	2.95	1.4
Tuyere – stock level, m (useful height)	24.9	24.8	25.5	25.3	25.5	26.0	26.3	–	–	–	27.3	25.42	25.1
Inner height, m	28.4	28.4	29.2	29.1	29.2	29.9	30.5	33.5	34.3	32.19	30.6	27.2	29.6
Shaft angle	83°54′	83°49′	83°57′	83°02′	83°17′	82°01′	81°18′	82°42′	83°08′	83°53′	84°14′	84°54′	–
Bosh angle	81°51′	81°30′	82°27′	80°47′	80°16′	80°04′	80°06′	79°17′	79°17′	80°49′	78°14′	80°32′	–
Estimated iron, THM/day	3800	5700	–	6400	5600	10000	11000	12900	14000	–	–	–	10000
Big bell dia., m	5.1	–	–	6.5	7.0	8.3	–	–	–	–	6.2	–	–

* Probable ** Probably from tap hole

The useful volume comprises of that volume of the blast furnace which is full of charge materials and smelting products. Therefore, it is the volume measured from the tap hole to the stock level (or a fixed distance from the bell rim, in open or closed position). In Europe and America, it is taken between the tuyere centre line and 1 or 1.83 m below the open big bell and is named as *working volume* as well. The former, a Russian convention, is more correct since the hearth plays an active role and determines the quality of the smelting products. In Sec. 7.8 we have seen that a considerable extent of direct reduction of iron oxides occurs in the hearth. In order to differentiate between the two, the author has used *useful volume*, V_u, after European convention and *inner volume*, V_i, after the Russian.

The required useful volume can be approximately calculated on the basis of the total hearth area. The mean value of V_u is about 24–26 m^3/m^2 hearth area. On this basis a 10 m diameter furnace should have a V_u of about 2000 m^3, a 12 m one a V_u of 2800 m^3 and a 15 m one a V_u of 4400 m^3.

The coke burning efficiency of the furnace is also related to the furnace volume, $m^3(V_u)$/tonnes coke per day. The figures for modern furnaces vary between 0.7–0.9 depending upon the furnace profile and burden quality. Thus, a furnace designed to produce 10,000 THM per day with a coke rate of 500 kg/THM should have a useful volume of about 3500 m^3.

The furnace volume and hearth diameter should be inter-related through the production rate per m^3 of V_u and per m^2 of the hearth area per day. A large hearth diameter without corresponding furnace volume will not produce the iron calculated on the basis of Eq. 12.1 or THM/m^2.24h since inferior materials preparation in the inadequate volume would increase the coke rate per THM. On the other hand, a smaller hearth diameter with an excessive furnace volume would mean an inadequate utilization of the volume and loss of optimum productivity because of associated smaller number of tuyeres, blast volume, bosh volume, etc.

Again, for the same hearth diameter and furnace volume, the latter can be obtained by having a narrow and high furnace which will give rise to excessive pressure loss, or, by having a short height with horizontal enlargement of the belly which necessitates the use of almost ideal burden for gas penetration. The latter feature is being adopted by the modern furnace designers. However, any increase in the belly diameter without simultaneous increase of the hearth diameter or the bosh height will decrease the bosh angle. Therefore, the furnace height, belly and bosh diameters and heights, bosh and shaft angles, all become inter-related.

The ratio of the useful volume to hearth diameter V_u/D has increased

from 130–160 for small furnaces to 230–270 for the larger ones and that for belly diameter V_u/b_d, it has done so from 100–160 to 160–250.

12.3.3. Useful Height

The useful height is measured between two fixed levels, i.e., between the lowered big bell and the centre lines of the tuyere or tap hole. Most countries use the former, H_u, while the USSR uses the latter which, in order to differentiate between the two, the author has named 'inner height', H_i, corresponding to inner volume.

An increased height of the stock column causes an increase in the gas pressure fall in the furnace. In addition to a normal increase in the resistance to gas flow due to increased bed thickness, there may be a further reduction of bed permeability caused by the breakage of the charge materials which accompanies with the increase in load. The contribution of the latter is, however, small.[10] The important point is, in order to decrease the pressure fall and maintain adequate gas flow in high furnaces, materials of larger size need to be used and the larger the size the more susceptible they are to breakage in the shaft. The height increase has only been nominal compared to the increase in furnace volume (cf. Table 12.1).

12.3.4. Shaft Angle

The angle or the outward taper or *batter* of the shaft is not only the outcome of the shaft height and belly and throat diameters but it has a functional importance. Pavlov[11] suggested long ago the following shaft angles for different ore varieties:

(i) 85° for weak and powdery ores;
(ii) 86° for mixture of strong and weak, lumpy or fine ores;
(iii) 87° for strong, lumpy ore and coke.

The variations in the angles are necessary for obtaining an adequate peripheral flow which is an essential pre-requisite for forcing of the blast furnace. Since the ore hump is located in the intermediate zone and it moves almost vertically downwards pushing the lighter coke towards the wall and the axis, a smaller shaft angle in the case of weak and powdery ore helps to loosen the periphery. However, the super-large furnaces are run on pronounced peripheral and axial flows. Therefore, the shaft angles have been lowered to 81–83° (cf. Table 12.1) even though mechanically strong lumpy agglomerates are being used.

The shaft angle can be adjusted within limits by changing the heights

of the cylindrical throat and belly since they together can be varied up to 3–4 m without any adverse effect on furnace operation. The angle can be increased or decreased by shortening or elongating respectively the throat and the belly. However, an excessively high throat can cause hanging in the upper furnace.

A deficiency in the taper can be overcome to a certain extent by the charging practice. If the angle is too small with excessive peripheral activity, it can be counter-acted by concentrating the ore on the wall by OOCCO/, resulting in coke saving and minimization of channelling. On the other hand if the angle is too steep, the periphery can be loosened by putting the ore away from the wall by CCOOC/-- or COOCC/- although this may somewhat increase the coke rate.

12.3.5. Throat Diameter

The throat diameter of the old furnaces used to be small. Later, as the usefulness of high-volume furnaces became apparent and the hearth and belly diameters increased correspondingly, the throat diameter also had to increase progressively to allow the enormous volume of gas to pass through at a reasonably low velocity to maintain adequate gas/solid contact and to decrease dust emission, throat hanging or channelling. However, too wide a throat may compact the charge. A certain velocity and lifting power of the gas is necessary for loosening the charge at the top.

On the basis of the necessity to maintain a uniform gas velocity in the throat and the shaft, the throat area should vary with the belly area according as the gas volume varies in the respective regions. Assuming a mean gas temperature in the belly of 1100°C and 400°C in the throat, the gas volume decreases by a factor of 0.5. Hence, the ratio of the throat to belly area should be about 0.5. From Table 12.1, the ratios indeed vary between 0.45 to 0.62. The corresponding diameter ratios are

$$d_t/d_b = 0.66\text{–}0.79 \qquad 12.5$$

where d_t and d_b are the throat and belly diameters respectively. The large furnaces have ratios between 0.66–0.70.

The throat and belly dimensions are intimately related with the shaft angle. The angle can, depending upon the shaft height, vary even when d_t/d_b is kept constant. For loosening the periphery whether in large furnaces or when using powdery ore, the ratio should be small with shaft angle 82–85°. If the ratio is too high the throat will be too wide and the furnace operation may be irregular due to overloading of the periphery

or the shaft being too steep. The periphery, however, can be led by reverse charging or by the use of deflecting ring or movable armour (Fig. 5.18).

As with the belly, the throat and hearth diameters should be interrelated. In modern high capacity furnaces the ratio d_t/D is 0.74 and for smaller furnaces it is 0.78–0.88.

The throat diameter also depends upon the nature of the charge. For furnaces designed to use hot sinter, the throat should be wider because of higher gas volume. On the other hand, the ratio can be lower if the furnace is provided with HTP.

12.3.6. Throat Height

The purpose of the cylindrical throat is to provide a porous stock for intimate gas-solid contact. The height varies between 1.5–3.0 m. A very tall cylinder, >3 m, will no doubt give a greater utilization of the thermal energy but the gas flow will be retarded, leading to non-uniform operation. If it is too short, the heat and mass transfer will suffer. However, modern furnaces have small height, 1.5–2 m, because it facilitates gas flow and the burden gets well-prepared in the shaft in any case because of the use of selected raw materials.

12.3.7. Throat and Bell Diameters

The ratio of the throat and big bell diameters determines the clearance between the bell rim and throat inwall, the importance of which has been discussed in Sec. 5.8. The clearance in small furnaces ranges between 0.6–0.9 m. For large furnaces a clearance of 1.0–1.1 m is advocated. The purpose is to locate the ore hump at such a place in the throat as to make the periphery and the axis permeable. This enables forcing of the furnace at a higher rating with uniform operation.

12.3.8. Belly Diameter

The belly is the cylinder that connects the tapers of the shaft and the bosh. Its diameter, d_b, and the ratio of this diameter to the useful or inner height of the furnace as well as to the diameter of the hearth play an important role in the operation and forcing of the furnace. The correct descent of the stock, ascent of the gas and efficient utilization of the chemical and thermal energies of the gas depend greatly upon these ratios. The importance of an adequate belly diameter lies in the fact that softening and melting of the gangue and formation of the slag occurs in this region.

An increase in the diameter facilitates gas passage through the sticky mass and also slows down stock movement, thus increasing the residence time for indirect reduction. However, the belly diameter cannot be increased arbitrarily as it is directly related to bosh angle, bosh height, hearth and throat diameters and useful height.

Any increase in the differential area of the throat and the belly increases the permeability of the periphery which facilitates peripheral flow of gases resulting in a higher coke burning rate. The differential area increases with the belly diameter even at constant d_t/d_b ratio, and, therefore, the wider the belly the greater the extent the furnaces can be forced. In smaller furnaces the amount of coke burned per hour per m^2 of the differential area is about 1.5–1.8 tonnes and in the super-large furnaces it is about 2.0–2.1 tonnes.

12.3.9. Inner Height and Belly Diameter

The principle behind the volumetric enlargement of the blast furnace by increasing the transverse dimensions is based on maintenance of the volumetric operating intensity in terms of the amount of gas per m^3 of the useful volume.[10] If the gas velocity is retained at the former level, the heat and mass transfer do not fall and the coke rate does not rise. As the furnace height has risen only marginally with increasing volume, the ratio of inner height to belly diameter, H_i/d_b, has decreased greatly as advocated by Lenonidov.[12] The ratio has decreased from 3.1–4.9 in very small furnaces to 1.92–2.10 for furnaces of over 4000 m^3 in volume. According to Leonidov et al.,[10] the maintenance of the volumetric intensity when the ratio is lowered reduces the average gas flow rates over the furnace cross-section and ensures a more uniform gas distribution. The net result is a more intensive heat and mass transfer, fall in the coke rate and increase in productivity.

12.3.10. Belly Height

The belly is the place where the major portion of the gangue and flux is in a softened and semi-fused state which interferes with the free ascent of the gas. The belly height depends upon the softenability of the ferrous burden and also on the shaft angle desired. If the slag fusion occurs at higher temperatures and in a narrow temperature range as in the case of pre-fluxed burden, the hydraulic resistance decreases in the vertical cross-section and the belly height can be correspondingly reduced. In modern furnaces the height ranges between 2.5–3 m while in furnaces using raw ores it can be considerably higher.

12.3.11. Bosh Angle and Height

The bosh angle and height determine the hearth diameter and *vice versa*. For a constant bosh height an increase in the hearth diameter is necessarily accompanied by an increase in the bosh angle, i.e., the bosh becomes steeper, if not compensated by a corresponding increase in the belly diameter. We have seen in Sec. 5.9.2 that the bosh angle should decrease as the hearth diameter increases. If it increases, the bosh will approach the form of the cylindrical hearth. The confinement of the combustion zone near the bosh wall promotes intensive peripheral activity. This affects fuel consumption because of lack of adequate gas-solid contact in the lower heat-exchange regime. The hearth and belly differential area governs the stock flow and heat-exchange in the lower furnace. Location of the combustion zone intermediate between the axis and the bosh wall ensures a uniform gas distribution and stock descent.[10,13,14] The bosh angle has decreased from 82° for 1000 m^3 furnaces to about 79–80° for 4000–5000 m^3 furnaces.

The bosh height is a function of the belly and hearth diameter ratio and the desired bosh angle. In order that the slag fusion is confined to the belly only and the slag descending to the bosh is completely liquid, the bosh height should be decreased as the fusion zone descends to the lower level by the use of larger diameter furnaces, higher blast temperatures and higher softening and fusion temperatures of the pre-fluxed burden. With the decrease in the bosh height and only a slight flattening of the bosh, the belly and hearth diameter ratios, d_b/D, have decreased from 1.15–1.20 for smaller furnaces to 1.09–1.10 for the larger ones.

12.4. Role of Lining Wear[10]

In principle, it is not the furnace lines as built but the working lines as determined by the wear of the refractories in the first months of use that should be designed. As a result of wear the useful furnace volume rises substantially. The top of the bosh can rise by 1.5 m, the belly diameter increases with d_b/D increasing by 0.1–0.2 and d_t/d_b decreasing by 0.08–0.17 and the H_i/d_b by 7–15 percent. The slope of the shaft and bosh decreases. Because of the wear, the furnace volume increases with the consequent improvement of the operating indices. The increased volume increases the ore residence time and improves indirect reduction and reduces the coke rate.

The increase in the cross-section of the shaft promotes rise in the vertical pressure of the charge materials and facilitates the movement of gas and

stock. The increase in the volume of the peripheral zone delays descent at the periphery, while the increase in bosh height intensifies axial descent of the charge materials in the middle and lower parts of the furnace.

References

1. SPRINGORUM, F. A.: Stahl u. Eisen, 80, 1960, p. 1838–1853.
2. GUBERT, S. V. et al.: Steel in USSR, Jan. 1976, p. 1–7.
3. KINNEY, S. P.: Tech. Paper, US Bur. Mines, No. 442, 1929.
4. HIGUCHI, M. et al.: Blast furnace Aerodynamics, Proc. Conf. Aus. I.I.M., Wollongong, 25–26 Sept. 1975, p. 130.
5. HIGUCHI, M. et al.: Trans. Iron Steel Inst. Jap., 16, 1976, p. 453–464.
6. KAWAMURA, M. et al.: ibid, p. 569–580.
7. SHUKORUKOV, A. E. et al.: Steel in USSR, June 1972, p. 427.
8. LEONIDOV, N. K.: Stal in Eng., Nov. 1962, p. 837–844.
9. BRANDI, H. Th. et al.: Stahl u. Eisen, 80, 1960, p. 65–73.
10. LEONIDOV, N. K. et al., Steel in USSR, June 1976, p. 289–293.
11. PAVLOV, M. A.: Metallurgy of pig iron, vol. 3, Verlag Technik, Berlin, 1953, p. 95.
12. LEONIDOV, N. K.: Stal, 9, 1948, p. 775–779.
13. STEFANOVICH, M. A. and V. K. KROPOTOV: Steel in USSR, June 1974, p. 442–444.
14. SHVIDKII, V.: ibid., Aug. 1974, p. 622–624.

CHAPTER 13

FURNACE IRREGULARITIES AND THEIR CONTROL

13.1. General

In the preceding chapters the conceptions and practice for optimum production of iron in the blast furnace have been systematically developed. However, furnace production is beset with numerous difficulties and irregularities, a successful counter-action of which only can give rise to smooth operation and high production. The hindrance to smooth counter-flow of solids, liquids and gases occurs due to changes or abnormalities in the physical character of the burden materials, which themselves may arise on chemical grounds. The usual difficulties and the counter-measures generally adopted are detailed below.

13.2. Channelling[1]

We have seen in Chapter 5 that in a mixed bed of different sizes of materials, the resistance to gas flow increases as the proportion of small particles or fines increases with simultaneous decrease in gas permeability and increase in the gas pressure fall. This causes differential gas flow in the bed, uneven gas distribution and differential gas velocities. Where the gas velocity is excessive, fluidization may start, smaller particles lifted up and the gas will increasingly rush into these regions which become more

and more unstable until the majority of the particles are in a suspended state. The suspended layer may extend to a considerable depth. The lifting up of the particles is the beginning of channelling and the gas starts to show an active, direct influence on the structure of the burden in the affected areas.

According to Shur,[1] although channelling is generally caused by unevenness of gas distribution but in characteristic cases it is directly connected with aerodynamic transfer and not with unevenness. It is rather caused by the gas bursting through a layer of fine materials and not as a result of increased gas permeability in an area. The increased gas permeability in the region of the channel occurs later as a result of the action of the lifting power of the gas.

Channelling can be detected by one or more of the following indications:

(1) rise and closer approach of the top gas temperature;
(2) sharp rise in peripheral gas temperature in the neighbourhood of the channel;
(3) sharp fall in the CO_2 content of the top gas;
(4) larger blast volume entering tuyeres that are close to the channel;
(5) high flue dust losses;
(6) collapse of one or both of the stock-line indicators into the suspended layer;
(7) severe and erratic gas pressure pulsations during lowering of the big bell;
(8) drop in blast pressure (especially when channels are large).

In contrast to above, uneven gas distribution is indicated by:

(1) non-uniform (not excessive) blast distribution at the tuyeres;
(2) sudden changes in the stock-line contour;
(3) difference in the temperature and CO_2 content of the uptake gas samples.

While unevenness can be tackled by manipulating charging techniques, channels can be eliminated by reducing the blast pressure to as low as 0.2 atm. gauge by opening the snort valve or sometimes by frequent checking to cause artificial slips. Sometimes it is also possible to control channelling by changing the charging sequence to encourage or discourage peripheral flow or by lowering the blast temperature or increasing the moisture content of the blast.

Contrary to usual belief, charging of fine ores in the channel does not remove channelling. Rather it helps the channel to maintain itself because the fines are blown out by the high velocity gas, are deposited in less permeable areas and thereby promote an enhanced gas flow through the already formed channel. If any fine ore does enter the channel, it is melted by the hot gases and the fused mass strengthens the channel wall. Due to transfer of ore from one place to another, it is possible for several channels to ultimately merge into a large single one.

13.3. Scaffolding[2-8]

The smooth running of the blast furnace is often disturbed by the formation of scaffolds that are accretions of materials which build up on the furnace wall and project towards the furnace centre. A *wedging* or *bridging* of the charge materials occurs across the horizontal cross-section as well as vertically along a part of the lining which interrupts smooth descent of the stock. This build-up of a solid impervious mass can occur at any place, from the bosh to the upper parts of the shaft. A typical example is shown in Fig. 13.1.

In general, the build-ups are divided into two varieties which are different in position, composition as well as in their formation. In the low temperature regions where liquid phases do not normally occur, the accretions are formed in the middle and upper shaft; we will name them as *scaffolds*. In contradistinction, we have *scabs* which are formed of viscous semi-fluid or liquid phases at higher temperatures, in the belly and bosh zones. As the cause of their formation may be different from those of scaffolds, the scabs will be discussed in the next section.

The diminution of the cross-sectional area at the place of scaffold formation leads to slow-down or interruption of stock descent and to an increased gas velocity in the unaffected regions. As a result, higher top gas temperatures in general and at the uptakes above the scaffold-free portion in particular are experienced. In an actual case,[6] the CO_2 content of the top gas fell from 13.3 to 11.9 percent, CO-utilization from 33.8 to 30.1 percent and indirect reduction from 55.6 to 50.8 percent, with an average increase of top temperature by 25°C. All these resulted in an increased coke rate of 3.5 percent and the higher linear gas velocity increased the flue dust emission by 70–100 percent.

Numerous investigations have been made in running but mostly in blown-out furnaces, for finding the cause of scaffold formation. It has been

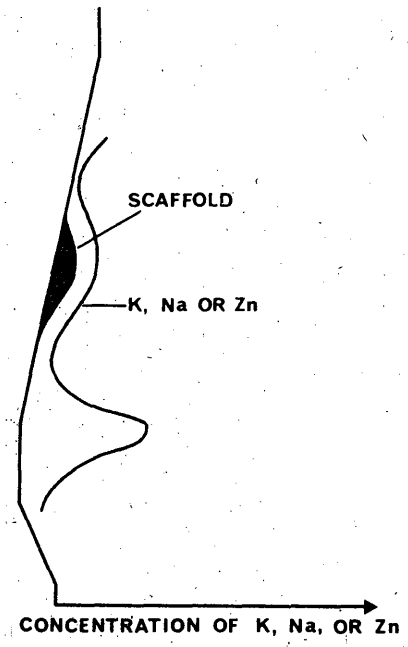


Fig. 13.1 Accumulation of sodium, potassium and zinc in the recirculating zone and formation of scaffold (schematic).

variously attributed to the action of volatile alkali metals, zinc, lead, tin and their compounds, low and wide softening range of ores, fines in sinter, carbon deposition, furnace operation (flow of gases) and even to cooling plates. Chemical analysis of the samples obtained from such scaffolds shows the presence of compounds of sodium, potassium, zinc, lead as well as that of powdery coke along with other burden constituents.

The formation of alkali metal compounds like cyanides, oxides, carbonates and silicates and their build-up in the temperature range 800–1100°C (alkali cycle) have been discussed in Sec. 3.21. The build-up is shown schematically by the bulge in Fig. 13.1. Zinc also builds up in a similar fashion (Sec. 7.4.2.5). Metallic zinc has also been found to condense around stack cooling plates. At higher levels where the oxygen potential is high and the temperature low, zinc is re-oxidized to ZnO. It not only slags the bricks and burden materials as the alkali compounds do but its deposition increases the volume of the bricks and cause their disruption. Lead is easily reducible and it accumulates as metal partly in the wall and the rest in the hearth. Carbon deposition ($2CO = C + CO_2$) occurs in the medium temperature range 400–600°C and is catalysed in

the presence of iron and its oxides as well as oxide of zinc. According to Diemers et al.,[6] it can also occur according to:

$$4/3\ KCN + O_2 = 2/3\ K_2CO_3 + 2/3\ N_2 + 2/3\ C$$

According to Chesters et al.,[7] carbon deposited within and around the bricks pushes them out and a wedge is formed where the descending materials can accumulate, facilitating adhesions between the ore and the lining.

Various mechanisms of slagging of the brick lining by the alkali metals and zinc have been suggested,[2-15] e.g., through formation of cyanides, silicates, carbonates or oxides. Whatever the mechanisms involved, it is believed that slagging and softening of bricks are caused predominantly by alkali metal compounds with a contribution from zinc oxide. The volatile metals on re-oxidation in the belly and the shaft flux the bricks on coming into contact or on deposition in their pores and crevices and initiate scaffold formation. The burden materials adhere to the softened bricks where further deposition occurs and the slagged materials create another sticky film. The scaffold builds up in this self-accelerating process and continues to project more and more inwards towards the shaft axis as well as along the wall. The presence of powdery coke emanates from carbon deposition reaction and pulverisation of coke weakened by the alkalis. Since the build-ups are maximum at 800–1100°C it is presumed the 'scaffold-foot' forms somewhere in the upper belly and lower shaft.

13.3.1. Controlling of Scaffolds

The scaffold can be kept under control firstly, by controlling the input of materials that cause it or by facilitating their exit from the furnace and secondly, by taking such actions as to minimize its formation and promote its removal, when formed, as early as possible. They are all discussed together in the following. To mention again, the indications of scaffold formation are:

(1) sudden increase within a few days in flue dust emission by 100–200 percent or even more;
(2) higher top gas temperature;
(3) lower gas temperature above the scaffold with low inwall temperatures in the neighbourhood of the scaffold;
(4) higher CO/CO_2 ratio in the top gas;
(5) hanging, slipping and non-uniform burden descent.

13.3.1.1. Methods of control

(1) decreasing the concentration of alkali metals in the 800–1100°C zone by increasing their exit in the slag; this can be achieved by decreasing the activity coefficient of the alkali oxides by lowering the CaO/SiO_2 ratio of the slag; however, the basicity cannot be lowered below a certain limit in view of desulphurization considerations unless external desulphurization is resorted to;
(2) control by flame temperature; the recirculating load of the alkalis at 800–1100°C increases with increase in the flame temperature (Sec. 11.3.2.4) and it is accentuated by the fact that high flame temperature produces high-silicon iron which increases the basicity of the bosh slag; lowered flame temperature decreases the alkali build-up and facilitates its removal through the slag but on the other hand it increases the coke rate;
(3) lowering of zinc input through sintering of the ores;
(4) a steep bosh with not too thick brick lining fitted with cooling plates may result in less hanging of the furnace;
(5) very compact bricks with lowest possible porosity so as to resist[16] seepage of alkalis and CO; high alumina bricks fired at high temperatures are less susceptible to alkali attack than the low-alumina ones; carbon deposition can be inhibited by the use of bricks where any iron present is converted into non-reactive compounds like fayalite and hercynite during their manufacture in a slightly reducing atmosphere and at very high temperatures;[15]
(6) a substantial peripheral flow of the gases discourages scaffold formation and if one is already formed, its further growth is kept under control; usually, a peripheral flow is obtained with an M- rather than a V-profile and the former can be obtained by suitable adjustments of the bell-throat diameter ratio, charging distance, use of deflecting ring or movable armour, etc., as discussed in Sec. 5.8.1; a change in the charging sequence with coke first, such as, CCCOOO/ or CCOOC/ would also result in loosening of the periphery; through such methods, the gas temperature along the wall increases and scaffold formation is either prevented or raised to higher levels and broken down;
(7) enlargement of the tuyere diameters on the side of scaffold formation for encouraging peripheral flow;
(8) avoidance of use of ores with large softening range;

(9) avoidance of use of fines in the burden; use of coke with high resistance to mechanical breakage and chemical reaction;
(10) sinters promote scaffold formation; should be screened before charging;
(11) suitable blending of ores to reduce alkali input and softening temperature range;
(12) destruction of scaffold with explosives; the furnace is blown to a low level, borings made into the scaffold and the explosives detonated (dangerous);
(13) burning of scaffold by oil burners introduced through the lining (after boring) at the proper place;[16]
(14) the use of calcium chloride as a cleaner; the procedure[17] involves calculation of the alkali deposited in the furnace from mass balance and addition of stoichiometric amount of calcium chloride according to:

$$Na_2O\ (K_2O) + CaCl_2 = 2\ NaCl\ (2KCl) + CaO$$

13.4. Scabs[18]

Scab is formed in the bosh region due to changes in the physical properties of the primary and bosh slags caused by faulty burdening or irregular operation. The primary cause is a sudden lowering of the slag fusion zone, increase in slag viscosity and re-solidification of the slag. As a result, an incrustation of pasty mass forms tending to adhere to the bosh incline, a projection of which inside the furnace obstructs the ascent of the gas and the descent of the stock. In addition, the blast would tend to channel, if the scab is not removed, leading to one-sided drive and damage to linings. The changes in the temperature, viscosity and solidification zone of the slags may be caused by:

(1) increase in flame temperature (lowering of the slag fusion zone, Sec. 4.5);
(2) reduction in blast humidity;
(3) change in the chemical composition of slag (irregular composition of ore and/or coke);
(4) non-uniform gas distribution, i.e., non-uniform direct reduction which means erratic supply of wustite (a fluxing agent) to the bosh whose rapid removal by reduction in the bosh results in the re-solidification of the bosh slag.

In short, any variation in the practice which would thicken the primary or the bosh slag may result in the formation of scab. In this respect, highly basic slags are more dangerous than the acid ones because the latter remain fluid even after considerable reduction in temperature (Sec. 8.4). The fluidity of the primary slag is controlled by the FeO content. As the FeO is progressively reduced, the slag melting temperature increases simultaneously and the rise is steeper the higher the basicity. The slag may freeze if, due to any reason, a sudden lowering of the temperature occurs, e.g., due to any sudden increase of endothermal direct reduction.

13.4.1. Controlling of Scabs

Scab formation can be prevented or removed by the following countermeasures:

(1) charging of extra coke for melting down the incrustation;
(2) temporary reduction of blast temperature for the same purpose; it raises the slag fusion zone upwards;
(3) if the hanging of the furnace is severe due to the formation of arches towards the centre of the furnace, checking of the furnace (lowering of blast pressure) may be necessary; this reduces the buoyant effect of the blast and the weight of the stock column would break the incrustation;
(4) charging of limestone away from the periphery to avoid formation of limey slag on the walls; this can be achieved by such chargings as, OOCCLC or CCLCOO;
(5) for loosening the periphery and cleaning the scabs, fillings like CCCOO/ can be used for a short time; with such a filling the coke preceding the ore forms a depression (funnel) in the axis and the ore rolls down the funnel slope to the centre;
(6) when the furnace production is not smooth and regular, the scabs should be washed and cleaned from the walls occasionally; this can be achieved by the use of hard-burnt sinters containing a lot of fayalite; such sinters, which are reduced at 1100–1150°C, ensure the presence of a sufficiently fluid slag up to a considerable distance in the lower furnace, dissolve the limey incrustations and promote a uniform furnace operation;
(7) use of pre-made slag with a high softening temperature and narrow softening range (pre-fluxed sinters or pellets) which reduces the occurrence of scabs.

13.5. Hanging

Hanging occurs when the stock meets with resistance in its downward flow or the gas in its upward flow. These can occur due to:

(1) physical obstruction to burden descent due to the formation of scaffolds, scabs or sticky bosh slag;
(2) increased gas support due to the presence of a lot of fines;
(3) blocking of drainage of liquids in the coke grid;
(4) blocking of gas passage in the bosh due to highly viscous or resolidified slag or frozen iron.

These are all discussed in the following sub-sections.

13.5.1. Scabs and Scaffolds

Formation of scabs, scaffolds, bridges, arches and the like on the walls offer physical resistance and obstruction to material flow downwards, slowing down or even stopping stock descent. Measures for prevention of their formation or for their removal have been discussed in the two preceding sections. In extreme cases, where the arch formed in the bosh or belly is of hard, impervious mass, it may be necessary to charge extra coke and thereafter blow full cold blast alternating with reduced blast volume. When the incrustations break, there is a suddent descent of the stock, known as *bosh slip*.

13.5.2. Peripheral Overloading

Overloading of the periphery with a large quantity of fine ores lowers the bed permeability. Such furnaces work hard, the rate of stock descent slows down and the blast pressure increases rapidly. In extreme cases, the furnace may start to hang. The CO_2-content of the peripheral gas just above or below the stock level records an increase. Such hangings can be minimized by the use of coke-first charging sequence or by screening out the fines.

13.5.3. Hot Hanging

It has been seen in Sec. 4.5 that an increase in the flame temperature results in an irregular stock descent and hanging. Such hanging is invariably removed by the lowering of blast temperature or using any coolant injectants. The probable cause of the sluggish flow has been suggested in Sec. 4.5. The flame temperature can increase if the blast temperature is increased or the blast humidity decreases or the C-content of coke increases.

13.5.4. Cold Hanging

Cold hanging is caused by high viscosity or solidified slags in the interstices of the coke grid in the bosh. The high viscosity may be caused by low bosh and hearth temperatures which may arise from:

(1) leaking bosh or hearth cooling plates;
(2) sudden decrease in C-content of coke;
(3) sudden increase in blast humidity.

The remedies are:

(1) isolating the leaking plates and changing them when possible;
(2) decreasing the ore/coke ratio in the charge; it takes 6–8 hours to have the desired effect; in the meantime, increase the blast temperature if possible or reduce the blast volume temporarily.

In addition, a decrease in indirect reduction can also cause cold hanging. The endothermic heat requirement of the increased direct reduction of wustite may result in the freezing of iron in the voids, hindering gas throughflow. If the freezing occurs on the wall refractories, it would resemble scabs. The remedy lies in increasing the blast temperature and/or the coke/ore ratio of the charge temporarily and improving the gas distribution through charging control.

13.6. Slips

Slips are sudden rapid downward movements of the stock column resembling collapse. They occur due to the formation of an initial arch or bridge inside the furnace or due to hanging in the upper furnace as a result of which the materials below continue to descend and be smelted while the materials above continue to hang. A void is thus created underneath which continues to increase in size until the weight of the hanging charge materials causes collapse and sudden downward movement. A sudden collapse may in extreme cases develop explosive dimension and cause damage to the top gear. The hanging and subsequent slipping may be traced to:

(1) condensation of oxidized alkali metal and zinc vapours in the upper shaft and formation of a hard impervious mass protruding inwards;
(2) hindrance to counter-flow of solids and gases due to carbon deposition or landing of powdery coke or ore fines in the interstices of the lumpy materials; the impervious bed resembles an arch;

(3) resolidification of previously fused slag due to operational variations, forming an impervious solid mass interfering with the smooth passage of the stock.

Slips may also occur due to differential rates of descent of the stock as a result of channelling. The more compact and denser regions descend at much slower rates than the rest resulting in the creation of voids underneath with occasional collapses. Such collapses may be beneficial and channels may be removed because of the loosening of materials, facilitating a free flow of gases. The loosening of materials occurs due to rushing up of the compressed gases released from the cavity underneath. In cases of highly compressed gases, it might cause emission of large pieces of ore and coke. If the collapsing materials during slips fill up the channels without increasing the permeability elsewhere, hanging may re-start after a period.

The occurrence of local hangings or slips depends upon the type of the softening-melting zones formed in the furnace (cf. Fig. 11.24). According to Wakayama et al.,[19] slips occur frequently in the W (or V) type zones whereas they seldom occur in furnaces with inverted-V type zones. In the former case, a solid arch tends to form between the central coke column and furnace wall and the furnace hangs because the arch does not collapse easily. In the case of inverted-V zones, the arch tends to form between the furnace centre and the intermediate zone and is small in size and disappears very easily. Therefore, for a uniform and optimum furnace production, an inverted-V type of the softening-melting zone is desirable apart from other reasons discussed in Sec. 11.5.

Slips lead to an increase in the temperature and pressure of the top gas as well as dust emission. The CO and CO_2 contents may show a decrease because of dilution of the gases by nitrogen released suddenly from the cavity.

According to Körber and Meyer,[20] the evolution of the gas at very high pressures (6–12 atm.) during slipping may be the cause of the loosening of materials. The explosive reaction occurs probably between the iron oxide (ore) with the carbon deposited inside when it collapses into a high temperature zone or between the oxide with alkali cyanides, resulting in a voluminous evolution of gas,

$$Fe_2O_3 + 3C = 2Fe + 3CO$$

$$Fe_2O_3 + 2\,KCN = 2\,Fe + K_2O + 2CO + N_2$$

Slips hinder a uniform furnace movement, deteriorate uniform gas distribution, decrease the production rate, increase the coke rate and give rise to non-uniform metal quality. They also affect the thermal state of the hearth. The excessive emission of dust containing a lot of coke dust and the collapse of the thermally unprepared and unreduced ore into the lower furnace result in erratic metal quality (low-Si, low-Mn and high-S) as well as furnace irregularities like chilled hearth.

13.7. Ore Shift

The shifting of fine ores from regions of higher permeability to those of lower one has been mentioned in Chapter 5 as well as in this chapter. This can happen because of non-uniform distribution of gas velocity arising from differential permeabilities in different radial cross-sections. A high gas velocity in certain regions will physically lift the fines below a critical size (Sec. 5.5) which will deposit in areas where the velocity is comparatively low.

In case of an overloading of the periphery with ore fines or the charge forms a thin and compact layer, the gas movement is obstructed and the gas pressure increases. The gas, in its attempt to force through the dense layer, throws the finer particles towards the centre or elsewhere where the gas velocity is low. Such shifting of the ore may form channels as well as blockages, resulting in non-uniform gas and stock movement, insufficient utilization of the thermal and chemical energies of the gas and higher coke rate. Because the entire gas flows through a narrow permeable area, both the temperature and pressure of the top gas rise. The stock level increases (at least it does not decrease) due to sluggish movement whereas in the case of slips the top temperature and pressure increase but the stock level decreases greatly. Direct reduction and hence the ($CO + CO_2$) content of the gas increase in both the cases but in the case of ore shift it is due to preferential flow and inadequate utilization of CO whereas in the case of slips it is due to collapse of unreduced oxides into the hot lower furnace.

The transference of the fines (due to differential gas velocity or pressure) from regions of higher to lower permeability can be remedied by trial and error methods, viz., reducing the blast volume, changing of charging depth or altering the charging sequence with careful watch on the top gas temperature and analysis, flue dust emission and radial shaft wall temperatures.

13.8. Choking of Hearth[21]

In broad terms, choking is ascribed to disturbance of furnace working due to blocking of drainage of liquids through the coke grid into the hearth and build-up of frozen solids on hearth walls. Choking may be caused by:

(1) attainment of the flooding limit with excessive gas velocity (i.e. high blast rate) and excessive liquids throughflow in the coke grid;
(2) use of high melting viscous slags;
(3) use of small-sized and/or weak coke; breakage of coke due to excessive accumulation of recirculating load of alkalis;
(4) use of excessive amount of raw limestone and small-sized sinter;
(5) accumulation of graphite, e.g., during making of high silicon iron.

Choking results in sluggish stock movement, delayed charging and in the appearance of slag in the tuyeres quickly after tapping. Liquid iron may be entrapped in the slag and burn the tuyere and slag notch. Iron temperature usually becomes low and the sulphur content high. Due to choking of the coke grid, more iron passes around the tuyeres and burns them.

Due to deposition of solids on the hearth wall, the hearth volume decreases and the level of the liquids rises quickly after tapping. The small coke pieces float just above the hearth floor and the liquids percolate through the voids towards the tap hole. The slag and metal leave the hearth in separate layers due to low voidage.

The following measures may be adopted to counter choking:

(1) improve mechanical strength of coke; breakdown of coke is the most important cause of choking and burning of tuyeres;
(2) if breakdown of coke is due to alkali attack, lower the alkali input if possible or operate with lower flame temperature or use less basic slags to decrease alkali build-up in the furnace;
(3) lower the blast temperature in order to increase the coke/ore ratio;
(4) use of sinter at the periphery, e.g., SSCCC/charge;
(5) blank charge of coke every 5–7 charges;
(6) increase manganese charge for higher slag and metal fluidity and reduce graphitization of iron;
(7) make low-Si iron to reduce graphite separation;
(8) use more fluid bosh and hearth slags.

13.9. Chilled Hearth

Chilling of the hearth occurs when the hearth becomes cold and the iron temperature falls steeply. It can happen because of the following reasons:

(1) sudden and massive slips when relatively cold materials fall into the hearth;
(2) a pronounced development of peripheral descent;
(3) a pronounced variation in the ore/gas ratio in one or more tuyere sectors;
(4) collapse of relatively cold materials through large channel;
(5) leaking of bosh and hearth cooling plates;
(6) sudden lowering of the fixed coke carbon without prior warning (rare cases).

We have seen in Sec. 13.6 that when an arch is formed and a void is formed underneath, the arch may break due to heavy load over it. The collapse of the cold materials may cool down the hearth, especially if the slip is massive. More frequent checking of the furnace may avoid a massive slip. The remedies have already been discussed in Sec. 13.6.

If a burden of greater permeability accumulates in any sector, the ore/gas ratio decreases and this particular sector heats up. But the ratio in the other sectors would increase and those sectors would cool down resulting ultimately in the cooling down of the hearth. Such cooling can occur for the same reasons if the blast consumption in a particular tuyere increases because of development of various processes in the furnace. Enlargement of the tuyere diameters will have the same effect as a result of excessive peripheral flow and cooling down of the axial portions.

In the event of formation of a pronounced channel, coarse unprepared lumpy materials may collapse through the suspended bed.[1] If the rate of descent of materials in the channel zone increases to a great extent, they do not become adequately heated up in spite of the fact that a large volume of hot gas passes through the zone. In addition, the other sectors will also cool down because of inadequacy of gas supply. All these contribute to a severe cooling and chilling of the hearth.

The remedies for channelling, uneven gas distribution and preferential flow of gases which sometimes leads to chilled hearth have already been discussed at various places in this chapter.

13.10. Burning of Tuyeres

The burning of tuyeres (and also slag notches) can occur due to:[21]

(1) choking of the bosh due to high melting viscous bosh slags and flowing of the slag over the tuyeres with some liquid iron entrapped therein as well as due to more metal passing around the tuyeres;
(2) choking of the hearth and bosh due to the presence of powdery coke, accumulation of slag rendered viscous by powdery coke or graphite under the tuyeres, resulting in their burning;
(3) a pronounced peripheral flow which may chill the bottom part of the furnace; the slag becomes viscous and the FeO-content rises; the temperature falls at the hearth periphery and the freezing of the metal occurs between and under the tuyeres and burns the tuyeres; a temperature fall of the peripheral gas by 50–100°C and a difference in the temperature of 100–150°C with the opposite tuyere is a warning of the probability of the burning of tuyeres.

The usual remedies are:

(a) making of a fluid, less viscous bosh and hearth slag;
(b) improving the quality of the coke; more resistant to mechanical breakdown and chemical attack, especially at high temperatures;
(c) use of low alkali burden; use of more acidic slag if the alkali content is high in the burden;
(d) eliminating channelling or preferential flow;
(e) continuous blowing without interruption as far as possible.

13.11. Coke-mess

Occasionally, during casting of iron or even flushing of the slag, a large amount of coke comes out from the hearth along with the metal and slag. Such a phenomenon is called *coke-mess* and it creates serious operating troubles and delays, especially because the tap hole is obstructed and cannot be sealed by the mud gun until the trough is cleaned.

The coke-mess may be caused by:

(1) entrapment of small pieces of coke in slag rendered viscous by the incorporation of coke fines generated from a weak and/or unscreened coke; these coke pieces are ejected along with the slag through the slag notch while flushing or through the tap hole along with the slag and iron during casting;

(2) coke-mess can occur even with strong cokes if the operation is not continuous;[22] under normal working conditions, the large coke pieces become progressively smaller in the combustion zone as they burn and are totally consumed in the tuyere raceway; in the event of any interruption in blowing causing the raceway to collapse, these small pieces enter the hearth and cannot re-enter the raceway when the blowing is resumed; these small pieces are ejected in the same way and for the same reasons as in item (1) above.

The coke-mess can be avoided or its frequency minimized by:

(a) use of mechanically and chemically strong coke to withstand breakdown due to abrasion, compression, impact, attrition and chemical attack by CO_2 and alkali metals at high temperatures;
(b) uninterrupted blowing as far as possible; casting and sealing of tap hole without reducing the blast pressure;
(c) screening out coke below 20–25 mm;
(d) ensuring good and strong tap hole with suitable clay mixtures.

References

1. SHUR, A. B.: Steel Times, 19 June 1964, p. 832–835; Metallurg, No. 8, 7, 1962, p. 2–5.
2. Alkalis in blast furnace – State of the art: Proc. Sym. McMaster University, Hamilton, Ont., 28 June 1973.
3. RANKIN, W. J. and J. B. SEE: Alkalis in the iron blast furnace, Rept. No. 1879, Natn. Inst. Met., Johannesburg, S. Africa, 1977.
4. ABRAHAM, K. P. and L. I. STAFFANSSON: Scand. J. Met., 4, 1975, p. 193–204.
5. WILLEMS, J. et al.: Stahl u. Eisen, 84, 1964, p. 57–62.
6. DIEMERS, H. et al.: op. cit., 85, 1965, p. 1240–1247.
7. CHESTERS, J. H. et al.: J. Iron Steel Inst., 159, 1948, p. 23–30.
8. RIGBY, G. R.: op. cit., 161, 1949, p. 295–300.
9. RICHARDSON, F. D. and J. H. E. JEFFES: op. cit., 163, 1949, p. 397–420.
10. ELLIOT, G. D.: Iron Steel Inst. Spl. Rept. No. 30, p. 217–230.
11. LOGELING, P.: Circ. Inform. techn., 10, 1953, p. 465–492.
12. RIGBY, G. R. and H. M. RICHARDSON: Trans. Brit. Cer. Soc., 52, 1953, p. 405.
13. STRUVE, G. V.: Neue Hütte, 1, 1955/56, p. 515–524.
14. POPOW, A. P. et al.: Stal, 13, 1953, p. 313–321.
15. TAYLOR, J.: Iron and Steel, London, April/May 1955.
16. KAHLHÖFER, H. et al.: Stahl u. Eisen, 74, 1954, p. 1714–1723.
17. ARMATORIO, G. G. et al.: Amer. Iron Steel Inst., Region. techn. meetings, Nov. 1971, p. 15–41.
18. LUGANIN, N. and I. G. LUGANINA: Izv. Vuz. Chern., Met., 6, 1971, p. 43–45.
19. WAKAYAMA, S. et al.: Ironmaking Steelmaking, 5, 1979, p. 261–267.
20. KORBER, F. and H. MEYER: Arch. Eisenhüttenw., 6, 1932, p. 173.
21. BABARYKIN, N. N. et al.: Stal in Eng., May 1962, p. 341–345.
22. DARTNELL, J.: Ironmaking Steelmaking, 5, 1978, p. 18–24.

INDEX

Accumulation of charge materials, factors influencing 171
Accretions 498
Activation energy 27
  Boudouard reaction 45
  diffusion, solid state, iron 40
  iron oxide reduction 35, 238
  S-O bond 89
Activity 15
  Henrian 16
  Raoultian 15
  wt. percent scale 16
Activity coefficient 15
  Henrian 16
  Raoultian 15
  wt. percent scale 17
Adsorption 30
  Boudouard reaction 44–46
  iron oxide reduction 33
Aerodynamics, blast furnace 137
Agglomerates (see Sinters, Pellets)
Agglomeration 194–208
  aims of 194
  pelletising 204
  sintering 194
  usefulness 203, 207
Air blast (see Blast air)
Air proportioning, tuyere 463
Alkali metals (see alkalis, potassium, sodium)
Alkalis 110–115
  alkali cycle 114
  control measures 115
  effect, on bed permeability 114, 452
    burden breakdown 211
    coke reactivity 253, 451
    coke strength 254, 451
    productivity 450–452
    refractories 110
      scabs and scaffolds 498–501
    swelling 233
  reduction of, in furnace 110–115
    influence, temperature 450
    slag basicity 451
  sources of, furnace 110
  thermodynamics, 110–115
Alumina,
  effect of, on iron quality 345
    slag liquidus temperature 339–345
    slag viscosity 339–345
    sinter quality 201
Alumina-silica-wustite system 98
Alumina-lime-silica system 100
Alumina-lime-magnesia-silica system 105
Alumino-silicate refractories 5
Alumino-silicate slags
Angle of repose 171
  coke, ore, agglomerates 171
Anisotropy, reduction 210
Arrhenius equation 27
Auxiliary fuel injection 316, 410–425, 466
Auxiliary tuyeres 312

Basicity, of slag 50–53
  ratio 53
Batter, stack 490
Bed instability 153
Bells, charging system 3
  four-bell 3
  large 3–5
  small 3
Bell-less top 454, 480
Belly 3
  dimensions 492
  function of 493
Beneficiation, iron ores 192
  effect of, on coke rate 394
    economics 194
    productivity
Blast air (see also Blast) 243
  humidified 245
  oxygenated 243–249
  penetration 308–312
  preheat 243
  effect, on coke rate 387–392, 413–421
    productivity 192
Blast additives 415–425
  effect on,
    bosh gas composition 422
      volume 422
    coke rate 411–425
    flame temperature 415
    iron quality 423
    operational efficiency 423
    production efficiency 423
    slag basicity 423
    slag volume 423
    thermal efficiency 422
    top temperature 422
Blast furnace,
  an outline 1–13
  belly dimension 492
  bosh dimension 182, 494
  charging systems 3, 169–177
  coke rate 375–426
  dimensions 485
  fuels for 249–261
  hearth dimensions 485
  height 490
  high capacity
  installation costs 12
  numbers, worldwide 12
  performance, indices 431
  productivity 429–481
  profile calculations 483
  raw materials 188–261
  reactions in 266–325
  slags 48, 98–107, 330
  temperature profile 118–135
  thermal efficiency 376, 385
  thermal requirements 119, 384
  throat dimensions 491–493
  volume 487
Blast furnace lines 485
  modern designs 488
Blast furnace refractories 5
Blast humidification 245
Blast moisture,
  effect, on coke rate 415
    flame temperature 245
    productivity 463–466
    stock movement 134
    thermal state of hearth 322
Blast, oxygen-enriched (see oxygenated blast)
Blast penetration, raceway 308
Blast pressure,
  factors influencing 310
  influence on raceway 308
Blast requirements 258
Blast temperatures,
  effect, on coke rate 388
  flame temperature 244
    productivity 392
    replacement ratio 414
    stock movement 134, 336
Blending, usefulness 193
Bo-Rist test 218
Bosh,
  design 182, 494
  flow conditions, in 157
  importance of 182
Bosh (tuyere) gas,
  composition and volume 258
    effect of,
      coke oven gas 258
      fuel oil 258
      moisture 246
Bosh parallel (see belly)
Bosh slag 9
  basicity 336
    role of coke ash 337
    role of Fe in ore 337
    role of slag volume 339
  characteristics of 331–342
  importance of, in
    material flow 341
    silicon control 291–295
    sulphur control 354–358
  liquidus temperature,
    role of alumina 339
Bottom control 462
Boudouard reaction 7, 44, 70
  activation energy 45
  effect of pressure 71
  rate,
    role of alkalis, on 253
    role of coke reactivity 46, 252
    role of hydrogen 280
    role, in coke rate 6, 252, 281
      extent of middle zone 46, 281
Boundary layer diffusion 30
Breakdown, burden 208
  alkali attack 211
  anisotropy 210
  other causes 208–211
Bridging, charge materials 498
Bulk burden reducibility index 218
Burden, blast furnace,
  beneficiation 192
  blending 193
  charging sequence 176
  coke size range 250
  evaluation, heat balance 377, 384
  fines in 194
  fluxes for 329
  heat transfer 125
  iron ore 190
  limestone in, 100, 289, 334, 399
  magnesia in 105, 334

movement 178
non-uniform distribution 169
optimum 152, 190
relation, coke size 152
particle size 190, 228
pellets in 441, 445
pre-fluxed 203, 206
preparation of 192, 392
prepared 392
effect on, coke rate 392
productivity 439–446
raw materials 188–261
reducibility 215, 222
index, bulk 218
sinters in 394, 441
size consist, optimum 152
sized, advantages of, 394
effect on, coke rate 394
gas flow 151, 395
productivity 439
temperature profile 118–135
unprepared 393–396, 439
Burden and gas lines 122
Burden descent rate 12, 275
extent, middle zone 283
Burden materials (see also Raw materials) 188
characteristics 189
degradation 208
distribution of 169
physical testing 218
reduction testing 216
stabilization of 219
strength,
cold and hot 219
Burden permeability,
effect, on coke rate 394
production rate 439
Burghardt test 222
Bustle pipe (main) 5

Calcination,
limestone 289
other carbonates 272
rate of 289
temperatures of 272, 288
Calcium chloride, use for scaffold removal 502
Calcium ferrites 109, 200
as sinter bond 200
formation in sinter 200
reducibilities 201, 225
viscosity 201
Calcium silicates 102–108
Calcium sulphide,
formation in slag 351
solubility in slag 359
$CaO-Al_2O_3-SiO_2$ system 100
$CaO-Al_2O_3-MgO-SiO_2$ system 105
$CaO-FeO-SiO_2$ system 107
$CaO-FeO-Fe_2O_3$ system 109
Carbon,
burning of, at tuyeres 243, 305
in sintering process 195
consumed in direct reduction 79
consumption, determination 380
deposition reaction 70, 270
advantages 270
catalysts 72, 270
disadvantages 270
poisons 271, 288
refractory attack 500
Carbon dioxide,
in top gas 8
role of, in direct reduction 400
in reduction rate 215, 399
Carbon gasification reaction 7, 46
Carbon monoxide,
as reducing agent 6, 74
reduction equilibria,
in CO/CO_2 mixtures 72
in CO-hydrogen mixtures 85
requirement, for iron reduction 75
Carbon-saturated iron,
reaction with slag 87–98
Carbon solubility in iron 65, 302
effect of metalloids 65, 302
Carburization,
liquid iron 302
solid iron 81
Channelling 496–498
formation, removal 497
harmful effects 156
Charge (see Burden)
Charging 169–178
cycle or sequence 170, 176
control 172–178
effect of sequence 176
on gas flow 171
on stock profile 177
in centre,
effect of charge weight 177
influence, stock and gas movement 178
gas distribution 183
mechanisms 3, 174
methods, influence on cohesive zone 479
Checking 463, 497
Chemical kinetics (see Kinetics)
Chemical reactions,
gas-solid 26
heterogeneous,
rate control factors 30
homogeneous,
rate constant 27, 31
Chemical inactive zone, 11, 75–78, 267, 273–286, 387
influence, gas quantity 284
Chiba test 218
Chilled hearth 509
Choking of hearth 508
causes and remedies 508
Chromium,
recovery 90
reduction reaction,
with C-saturated iron 90
with silicon 90
C.N.R.M. test 217
CO-utilization 6, 74
definition 6
equilibrium, wustite-iron 6, 74
wustite-magnetite 6, 74
magnetite-hematite 6, 74
overall, in furnace 386, 397
Coal,
as blast additive 260, 319
coal-oil slurry 261, 411
Cohesive zone 9, 449, 447
Coke (see also coke rate)
ash 252
alkali attack 253, 450
blending 250
breakdown 253, 447
effect, productivity 447–451
choking of hearth 508
tuyere burning 510
form coke 254
moisture 252
pelletised 255
quality 250
reactivity 252
size, importance of 250
strength, importance of 250, 447
sulphur 252, 368
Coke mess 510
Coke rate, blast furnace 375
acid burden 405
calculations 376–384
decrease in, methods 387–426
effects on, of
blast additives 410
blast temperature 388
burden quality 393
burden size 394
burden reducibility 398
coal-dust injection 425
coke ash 252
coke oven gas injection 425
Fe-content, burden 398
fuel oil injection 417, 424
gas-burden distribution 395
gas-solids ratio 283
high top pressure 426
improved burden 280
limestone addition 400
moisture injection 415
natural gas injection 422, 425
ore quality 280
pellet charge 403
pre-fluxed burden 399
pre-reduced burden 406
pre-stabilized burden 219, 448
reserve zone size 281
residence time, gas-solid 458
silica in burden 193
slag bulk 401
smelting rate 469
stack gas injection 408
sulphur load 365
factors, influencing 387
influence, gas distribution 395
Coke savings,
blast additives 410
blast temperature increase 388
uniform gas distribution 395
Coke rate target 431
Coke size,
effect of narrowing 447
effect on combustion zone 308, 316
productivity 447, 451
importance of 447
optimum 447
Coke strength,
effect on hearth choking 508
productivity 447, 451
tuyere burning 510
Coke throughput (see Productivity and production rate)
Coke throughput target 431
Cold or chilled hearth 509
Combustion,
at tuyeres, of coke 303
heat, of carbon 69, 249
heat, of coke 70
heat, of additive fuels 258
Combustion zone (see also Raceway)
dimensions 308–319
effect of,
blast parameters 308
coal dust 319
coke size 308, 316
hydrogen-bearers 316
oxygen and additives 318
stock movement 314
tuyere dimensions 311

tuyere numbers 314
shape and size 312
Concentration, iron ores 193
Critical gas velocity,
flooding 158
fluidization 153
Critical hearth temperature 10, 102
Critical residence time,
gas 456
effect, inactive zone 126–131
ore 218
Counter-current process,
heat exchange 125
reduction 76
Coupled reactions 94

D'arcy's equation 141
Dead man's zone 139, 303
effect on production 431
extent of 303
gas flow through 157
liquids flow through 157
Decrepitation 220
Decreased reducibility 24
Deflecting ring 175
Degree of oxidation 198, 216
effect on reducibility 229
Degree of reduction 216
Desorption 33, 46
Desulphurization (see Sulphur removal)
Diffusion,
as transport phenomenon 31
coefficient 31
Knudsen 38
porous 35
control, reduction 34
slag-metal reaction 57
Fick's 1st Law of 31
gaseous 35
effect of,
molecular weight 39
total pressure 38
temperature 37
solid state 40
Diffusive flux 32
Diffusivity,
CO and hydrogen 40
Distributors, top 175
Direct-indirect reduction 77, 380
calculations 80
fuel efficiency 385
Direct reduction 7, 73–81, 276, 380, 416
and CO-utilization 385
effect on fuel efficiency 385
optimum, for minimum fuel rate 383
Dissociation pressure,
iron oxides 69
metal carbonates 273
Dissociation temperatures,
iron oxides 69
limestone 272
other carbonates 273
Distribution, burden materials 169
effect on gas flow 183
gas temperatures 183
Distributors, furnace top 175
Driving rate 430
Dropping zone 449
Dumping 170
Dusting (falling) 201, 347
Dwight-Lloyd sinter machine 194
Dynamic equilibrium, furnace centre 180, 279

Electro-chemical nature, slag-metal reactions 51
Energy, activation 27
free 18
Equation,
Arrhenius 27
Boudouard reaction rate 45
D'arcy's 141
Ergun's 143
Fick's 1st Law 31
Sherwood 158
van't Hoff 22
Wagner 17
Equilibrium 15
constant 15
distributions 87–97
dynamic, furnace centre 278
in hearth reactions 94
Equilibrium systems,
C-O 69
C-O-H 82
$CaO-Al_2O_3-SiO_2$ 100
$CaO-Al_2O_3-MgO-SiO_2$ 105
Fe-C 64
Fe-C-Metalloids 65
Fe-O 66
Fe-O-C 72
Fe-O-H 83
Fe-O-C-H 85
Fe-O-C-Mn-Slag 91
Fe-O-C-S-Slag 92
Fe-O-C-Si-Slag 87
Fe-O-C-Mn-S-Si-Slag 94
$FeO-Al_2O_3-SiO_2$ 98
$FeO-CaO-Fe_2O_3$ 109
$FeO-CaO-SiO_2$ 107

Ergun's equation 143
External desulphurization, effect of various reagents 369–373

Falling (dusting) 201, 347
Fanning 471
Fayalite,
formation, in sinter 200
furnace 233
melting point 108
reducibility of 224
Fe-systems (see equilibrium systems)
Ferrites (see calcium ferrites)
Ferro-manganese 296
Ferro-silicon, use of oxygenated blast
coke requirements 464
productivity 464
Ferrous oxide (see wustite)
Fick's Law, diffusion 31
Fines,
effect on channelling 496
coke rate 395
gas distribution 156
pressure fall 144–151
productivity 443
generation, in furnace 208, 220
Flame temperature,
calculations 243, 257
effect on, of
blast oxygen 243, 260
blast temperature 244, 257
coke oven gas 255–257
coke rate 415–425
fuel oil 255–257, 260
moisture 245
natural gas 255–257
stock flow 134, 336, 450
Flooding 158
cause of hanging 160
diagrams 158, 162
effect on production 454, 474
equation 158, 162
factor 158
in bosh 158
parameters 158–164
surface tension of slag 163
Flue dust,
effect of, on
channelling 497
scaffolds 500
slips 506
Fluid ratio 158
Fluidization 153–157
influence of,
gas velocity 154, 473
particle size and density 154, 473
top pressure 473
productivity limit 473
Flux 2, 329
Fluxed burden 197, 206, 399
Free energy,
change, in reactions 18
with standard state 19
compounds 20
diagrams 20, 28, 111, 113
Friction factor,
and pressure fall 142
and Reynolds number 141, 148
Fuel, auxiliary, as control tool 134, 452
Fuels, in blast furnace 249
Fuel injectants 255
Fuel injection,
aerodynamic limitations 180
amounts used 424
coal pulverized 425
coke oven gas 425
effect of, on
coke rate 425
combustion zone 319
flame temperature 256
gas-solids ratio 180
permeability 180
fuel oil 424
in stack 408
natural gas 425
replacement ratio 420, 424
Fuel oil injection,
atomisation 259
blast requirement 258
carbon soot 259
effect of, on
coke rate 417
flame temperature 256
productivity 466
shaft efficiency 417
tuyere gas composition 258
operational data, with 424
replacement ratio 420, 425
with oxygenated air
coke rate 420
productivity 466
Fuels, blast furnace 249
Fusion zone 7, 122, 268, 453
and bosh height 494
lowering of 123, 131, 134, 281, 336, 452
metal and slag 336
movements of 336

Gakushin test 218
Gangue minerals 1

Gas composition,
  actual in furnace 273–280
  and temperature 273
  effect, gas-solid ratio 283
  equilibrium,
    in C-O system 71
    in Fe-O-C system 74
    in Fe-O-H system 84
  profile 273–275
  top 8
  tuyere region 258
Gas distribution 172
  coke savings by controlling 397
  control 173
  effect on coke rate 395, 461
    productivity 461
  factors influencing 169–177, 461, 477
  in stock column 275
  variations in 184, 275
  velocity, actual 183
Gas flow,
  at tuyeres 470
  control 169–184, 461
  excessive 461
  inadequate 470
  in various zones 183
  particle size resistance to 148
  patterns of 172
  through, axial zone 180
    equigranular bed 140
    intermediate zone 180
    multigranular bed 147
    peripheral zone 180
    wet bosh zone 157
  variations in 184
Gas flow and pressure drop 142
Gas movement 183, 184
Gas-solid contact time 285
  effect on reduction rate 285
Gas-solid residence time 285
  effect on coke rate 458, 471
    gas utilization 283, 456
    heat transfer 125
    mass transfer 280
    productivity 457
    temperature profile 125
Gas-solid equilibrium 75
  approach to Fe/FeO 273, 386, 456
Gas-solid reactions 26
  rate control mechanism 30
  diffusion, gaseous 35
    solid state 40
  growth of iron 40
  influence on swelling 42
  nucleation of iron 40
  phase boundary control 33
Gas-solids ratio 184
Gas temperature 183
  and gas-solids ratio 184
Gas temperature profile 127, 267
Gas utilization 75, 278, 386, 461
  and reduction 75, 386
Gas velocity 183
  dependence of, on
    furnace pressure 167
    voidage 141
  distribution 183
Gaseous fuels (see coke oven and natural gas)
Gases,
  behaviour in furnace 183
  channelling of 156, 496
  density and pressure fall 145
  diffusivity and hydrogen 40
  influence, temperature profile 184
  viscosity 143
Gruner's ideal 386

Hanging 504
  causes and control 390, 504
  factor, critical condition 159
Hearth,
  choking 508
  dimensions 485
  heat exchange in 123, 322
  heat losses 384
  slag 343
    composition 40, 366
    liquidus temperature 343
    permissible basicity 343
    viscosity 343
  slag-metal reactions 87–98
    approach to equilibrium 95
    kinetics 97
  temperature
    control 324
    critical temperature 10, 102
  thermal state 322
    and metal analysis 323
    control 325
Heat,
  bosh gas as source 120
  generation of 243, 256
  sensible,
    top gas 377
    tuyere gas 243
Heat balance,
  and reduction 414
  burden-gas lines 120
  calculations 120–130
  lower and upper furnace 120–130, 378–384

  overall 119
  Reichardt, use by 133
  use in,
    coke rate estimation 378–384
    flame temperature 245, 256
Heat exchange,
  countercurrent, gas-solid 125
Heat flux, convective 125
Heat input,
  calculations 245
    blast additives 245, 257
    dry blast 245
Heat losses,
  effect of coke throughput 469
  effect on coke rate 469
  major sources of 118
Heat of combustion (see under combustion)
Heat of reaction,
  iron oxides, with CO 73
    with hydrogen 83
  carbon, with air 245
    with CO_2 70
    with steam 83
Heat of vaporization,
  hydrated water 269
  moisture 269
Heat of hydration 269
Heat requirements 118
  high and low temperatures 384
Heat transfer,
  coefficient 125
  equation 125
  efficiency, effect on
    temperature profile 125
  in hearth 123, 322
  in stack 180
Heated air (see Blast Air)
Hematite 66
  breakdown 208, 223
  oxygen pressure 69
  reduction 28, 73, 83
  structure 66
Hematite-lime-wustite system 109
Henrian activity 15
  coefficient 16
Henry's Law 15
Heterogeneous reactions 30
  rate control mechanism 30, 33
High blast temperature, effects of 388
High pressure drop,
  lower furnace 181
High pressure operation (see high top pressure)
High temperature bed permeability test 217, 221
High top pressure 165–169
  advantages of 168
  calculations 165
  effect of, on
    coke rate 426
    productivity 457
    temperature profile 286
  equipment 169
  increased mass flow 167
  life of bell 461
  linear gas velocity 167
  pressure drop in 166
Humidification (see Blast)
  and oxygenated blast 245, 463
    effect on production 463
Hydrocarbon fuels 255
  injection 316, 415, 466
Hydrogen,
  and CO, ore reduction 239
  as reducing agent 28, 83
  diffusivity 240
  effects of, on
    coke rate 410
    CO-utilization 86
    fuel efficiency 87
    heat transfer 423
    pressure drop 145
    productivity 465
    reduction efficiency 85
    reduction rate 238
      effect, pressure 241
  reduction equilibria 84
  sources, in furnace 245, 255
  use in blast furnace 463
  viscosity 143
Hydrogen-bearers (see Fuels)
  effect, flame temperature 256

Impurities, effect on iron oxide reduction 41
Indian coke, ash silica 345
Indian ore, silica/alumina 334
Indirect reduction 7, 76, 276–287, 380
  calculation 80, 276
  effect on, of
    burden descent rate 285
    coke rate 78, 284, 385
    fuel efficiency 76, 385
  improving of 280
  zone, of wustite 8, 267
Indirect-direct reduction 77, 380
  dynamic equilibrium 278
Induction period, reduction 40
Injection, fuel (see Fuel injection)
Interaction coefficient 17
Interaction parameter 18

Interface reaction 28
  phase boundary 33
Iron,
  carbon in 65, 303
  chromium in 299
  manganese in 295
  phases of 64
  silicon in 291
  sulphur in 349
  titanium in 300
Ironmaking costs 12
Iron notch, burning 510
Iron ore beneficiation 192
Iron ore blending 193
Iron ore analyses 190
Iron ore fines,
  effect of 153, 473, 502, 504, 507
Iron ore reduction 223
Iron ores,
  agglomeration 194
  analyses of 190
  beneficiation 192
  blending 193
  chemical properties 224
  effect, alumina/silica 334
  high grade, effect of 191, 394
  pelletising of 204
  physical properties 224
    breakdown 208
    decrepitation 220
    reducibility 222
  sintering 194
  size, optimum 191
  size uniformity 191
  softening temperature 191
    range, importance 212
  sulphur in 349
Iron oxides reduction 28–43
  by CO 6, 72–79
  by hydrogen 83–87
  equilibrium CO/CO_2 6, 74
    H_2/H_2O 85
  kinetics 28–43
    effect, alkalis 41
  mechanism 32–43
Iron production (see Productivity)
Isothermal zone (see Middle zone and Reserve zone, thermal)

Kinetics of reaction,
  Boudouard 44–46
  calcination, limestone 289
  chemical 27
  combustion, coke 47
  effect, diffusion 35–43
    temperature 33
  hearth 87–97, 290–300, 358
  heterogeneous 30–43
    nucleation, iron 40
  iron oxide reduction 28
  slag-metal 57
Kitaev, heat exchange zones 122
Knudsen diffusion 138
  and reduction rate 38
    effect, pressure 39

Labyrinth factor 36
Laws,
  Fick's 1st, diffusion 31
  Henry's 15
  mass action (LMA) 15
  parabolic 32
  Raoult's 15
Lead, reduction 298
Lime,
  as flux 53
  effect on,
    pellet strength 206
    reducibility 227
    sinter strength 203
    sintering rate 204
    slag formation 100–110, 329
    slag-metal reaction 87–94
    slag viscosity 100–110, 336–345
    sulphur removal 350–353
  reduction in hearth 302
Lime systems (see CaO)
Limestone,
  as flux 53
  calcination 272, 289
    kinetics 289
  effect, on coke rate 400
  heat, reaction 289
Linder test 217
Lines (profile), blast furnace 483
Lining, blast furnace,
  carbon deposition 72, 270, 499
  cooling plates,
  effect on, of
    alkali 499
    lead 499
    zinc 499
  wear of 494
Loading 158, 160
Low silica slag 104
Low temperature breakdown (LTB)
  causes 201, 208
  properties 201
  tests, importance 221
Lower zone, reactions in 7, 288–325

Magnesia,
  as flux 53
  effect on viscosity,
    bosh slag 334, 339–342
    hearth slag 106
  limits, addition 106
  reduction, hearth 302
Magnesia-alumina-lime-silica system 105
  viscosity 107
Magnesium, effect on external desulphurization 372
Magnesio-wustite 206
Magnetite 67
  composition 69
  in pellet 205
  in sinter 198
  oxidizing roasting 223
    effect, coke rate 223
  reduction rate,
    in CO 42, 223
    in hydrogen 42
Maldistribution,
  charge and gas 169–184, 274
Manganese,
  coupled reactions 60, 94
  distribution, slag-metal 91
    equilibrium constant 91
  effect, sulphur transfer 60, 97, 294
  recovery 297
  reduction of 91, 292, 295
Manganese ores,
  in sinter 404
  reduction, shaft 296
Manganese oxide,
  usefulness in slags,
    bosh 342, 358
    hearth 344, 360
    primary 334
Mass flow rate,
  gas-solids 184
    temperature 184
  pressure fall 165
Mass transfer,
  coefficient 57
  dependence, particle size 146
  in slag-metal 57
  in reduction 286
Mechanisms,
  Boudouard reaction 44–47
  coke combustion 47
  iron oxide reduction 32–44
  silica reduction 87–91, 94–98, 291
  slag-metal reaction 51, 59, 87–98
  silicon absorption 87
  sulphur transfer 94–98, 341, 349–373
  swelling of pellets 41, 233

Melting zone (see Fusion zone)
Methane (see Natural gas)
$MgCO_3$, dissociation 272
MgO, equivalence to CaO 53
Middle zone, reactions in 11, 273–288
  size 281
Mineralogy of,
  iron ore 224
  pellet 205
  sinter 198
Moisture content, blast,
  effect on coke rate 415
    driving rate 463
    flame temperature 245
    heat content, gas 247
Molecular diffusion (see Diffusion, gaseous)
Movable armour 175
  ring 175

Natural gas 255
  composition 258
  heat, combustion 258
  injection 316, 422, 425
    effect on
      coke rate 422, 425
      flame temperature 256
      metal analysis 321
      oxidizing zone 316
      replacement ratio 422, 425
      thermal state, hearth 324
      tuyere gas composition 258
Nitrogen, as ballast,
  usefulness 128
Nucleation of iron 40
Nusselt number 125

Oil injection (see fuel oil injection)
Oil-coal slurry 261, 411
Operational efficiency 385, 423
  direct/indirect reduction 385
Olivines 109
Operational slag viscosity 161
Ore shift (transfer) 155, 507
  causes and control 507
Ore/coke ratio, in stack 180
Overall heat balance 119
Oxides,
  acidic and basic 53
  stability of 23
Oxidizing zone, tuyeres 305
Oxygen,
  content, iron oxides 69
  dissociation pressure 69
  potential, in furnace 23

Raw materials, blast furnace 188–261
(see also Burden materials)
blast air 243
distribution, top 169–178
effect on coke rate 392
effect on productivity 439
moisture, blast 245–249
oxygen, blast 243–249
Reaction kinetics (see kinetics of reaction)
Reaction mechanism (see Mechanism)
Reducibility 215
BoRist test 218
Burghardt test 222
Chiba test 218
C.N.R.M. test 217
decreased 24
determination of 215–222
factors affecting 222–243
agglomerate quality 225
degree of oxidation 229
fluxed agglomerates 225
gas composition 238
gas pressure 241
gas velocity 236
impurities 41
ore quality 223
porosity 230
swelling 233
temperature 237
time of contact 242
high temperature 238
bed permeability 217, 221
importance, coke rate 398
increased 24
indices 218
iron ore 223
isothermal test 217
Linder test 217
low temperature 238
LTB test 220
other testing methods 217–222
pellets 225
sinters 225
Reduced pressure drop 151
Reducing zone, tuyere 305
Reduction,
agglomerates 225–230
direct 7, 73–81, 276, 380, 416
improving of 280
indirect 7, 76, 276–287, 380
limey pellets 233
iron oxides 28–44
velocity of 26
Reduction rate (see under Kinetics of reaction)
Reformed gas 408
Refractories,
alkali effect 110, 498
blast furnace 5
fluxing of 100, 499
high alumina 5
Refractory damage, causes 110, 498
Reichardt diagram 133
Replacement ratio 441, 467
direct reduction coke 414
tuyere coke 414
Reserve zone,
chemical 11, 275–279, 387
factors affecting extent 280–286
importance, coke rate 77, 277–286, 387
thermal,
factors influencing extent 124–135, 252, 280–286
importance, coke rate 46, 252, 281
indirect reduction 280–286
Resistance concept in transport phenomenon 26, 58
Reynolds number 141
calculations 141–145
relation, friction factor 141, 143
values, in furnace 143
Rist-Schürmann diagram 77
reduction carbon, optimum 78
Residence time,
burden 12, 275
gas 143, 456

Scabs 335, 502
causes, formation 502
in lower furnace 502
in upper furnace 298
harmful effects 298, 502
removal and control 335, 503
Scaffolding,
causes, formation 498
control 501
harmful effects 498
Screening,
ores,
effect on,
coke rate 439
productivity 439
pellets,
effect, productivity 446
sinters,
effect, coke rate 444
productivity 443
Shaft,
burden residence time 276
chemical reactions in 268–288
dimensions 488

gas distribution 275
indirect reduction 273–286
volume 273
Shatter test 219
Sherwood equation,
flooding 158
use, productivity 474
Silica,
behaviour as acid 53
reduction 87, 91
slag formation 48
structure 48
Silica-alumina-lime system 100
Silica-alumina-lime-magnesia system 105
Silica-alumina-wustite system 98
Silica-lime-wustite system 107
Silicates, primary slag 99
Silicon,
alloy (see ferro-silicon)
content, effect of temperature 90
control 294
thermal state of hearth 322
coupled reaction 94–97
with manganese 94–97
with sulphur 94–97
with titania 300
distribution, slag-metal 87–90
equilibrium content, in iron 88
effect of, pressure 90
slag basicity 90
temperature 90
high, in cold iron 294
causes 294, 323
remedies 323–325
reduction 87–90, 291–295
re-oxidation, raceway 294, 321
sulphide 351
Sinter 194
acid 197, 202
advantage 202
primary slag 332
angle of repose 171
basic 197–202
advantage 203
breakdown 201, 209
slag formation 333
strength 201
basicity ratio 200
bonding of 198–202
breakdown of basic 209
causes 201
in reducing gas 221, 209
low temperature 221
composition 199
degree of oxidation 198
effect on, of basicity 226
coke rate 223
effect of, on
coke rate 442
productivity 442
scaffold formation 499, 502
fluxed 442
hard-burnt 200, 503
limestone in 197
mineralogy 198–204
effect of, alumina 199, 201
magnesia 199, 201
lime 198–204
performance, in furnace operation 395, 441
quality 198–204
reducibility 225
self-fluxing 197
strength (see sinter strength)
super-fluxed 197
types of 197
use, in cleaning accretions 503
voidage, in bed 150
Sinter strength 198–203
basicity and fuel rate 200–204
effect, alkali metals 211
low temperature breakdown 208–212
effect, CO and hydrogen 209, 210
testing of 214–222
Sintering,
arsenic removal 202
bed depth 194
coke size 197
combustion zone 195
description, process 194
dew point 195
ferrite formation 200–202
fuel rate 197
heat generation 195
moisture, optimum 196
preheating zones 195
return sinter, use of 195
size of mix 196
temperature of bed 194
theory of 194
wustite formation 200
zones of 195
SiO, free energy of formation 87
Size, effect on burden reducibility 228
Size consist, importance 152
Size ratio,
effect on, gas flow 147–152
voidage 148, 152
Slag basicity (see Slag)
Slag, blast furnace,
alumina content 362, 366
acid/base ratio 9, 53

and metal reactions,
electro-chemical nature 51
kinetics 57
basicity,
effect, coke ash 337
richness of ore 337
importance, furnace movement 98–107, 333–346
sulphur removal 95, 353, 361
optimum 344
bosh,
basicity 337
calculation 337
dependence on coke ash 337
amount 337
silica content 338
formation, course 331, 336
importance 338, 342
liquidus temperature 338–342
effect of MgO 342
MnO 342
prefluxing 203, 334, 342
viscosity 341
constituents 100–107
flushing 344
hearth 343
alumina content 345
composition 346, 363
commercial 366
effect on aggregate 347
cement 347
dusting 347
sulphur removal 361
critical temperature 10, 102
importance, liquidus temperature 343
viscosity 343
magnesia content 361
volume, effect on,
bosh slag basicity 339
bosh slag viscosity 335
operational 161
material flow 157–163
sulphur removal 362
primary 331
effect, furnace movement 100, 336
formation, course 331
liquidus temperature 334
effect, alumina/silica ratio 334
viscosity 334
effect, alumina/silica ratio 334
MgO, MnO contents 334
roughing 344
structure 48
breakdown 49
Slag-metal reactions 51, 57, 87–98
Slag properties 54, 330
low silica 104
Slips, causes and control 505
Smelting intensity or output (see Productivity)
Sodium oxide (see alkalis)
Softening of ores and agglomerates 212
effect on,
gas throughflow 212
pressure fall 213
productivity 473, 476
voidage 212
temperatures 191, 214, 453
testing 221
Softening-melting zone 9, 449, 453, 477
and productivity 453, 476
Softening-melting temperatures 453
Solution loss 7
Stabilization,
coke 219, 448
sinter 219
Stack (see also Shaft),
dynamic equilibrium in 180, 279
scabs 335
scaffolds in 498
temperature profile 267
Steam injection, variation of composition and tuyere gas volume 246
Stock column,
permeability 181
rate of descent 179, 275
influence, various factors on 184
Stock distribution, shape 172–176
Stock movement, influence of various factors 178
Sulphur,
activity coefficient, in iron 17, 362
balance in furnace 350
contents, estimation 362
control of 368
coupled reaction 94
distribution, slag-metal 92
approach to equilibrium 365
coefficient 93, 352
equilibrium 92
effect of, on
coke rate 365
slag volume 362
mechanism, pick up 350
reactions 92, 94, 351
chemistry of 350
in bosh 354
in hearth 358
in shaft 353
mechanism 97, 293, 323
Mn-reduction, importance 97, 294, 323
role, temperature 92, 294, 323

solubility in slag 359
Sulphur compounds,
in charge materials 349
in furnace gas 350
Sulphur content, in iron,
effect of,
bosh slag basicity 356
hearth slag basicity 359–367
metal composition 368
reaction rate 358
slag composition 361
slag volume 362
tapping method 360
temperature 359, 368
Sulphur control 368
Sulphur removal 349–373
effect of,
burden quality 353–358
distribution coefficient 352
metal composition 368
Mn-reduction rate 97, 294, 323
reducing atmosphere 352
silicon 97, 294, 323
slag basicity,
bosh 356
hearth 359–368
slag bulk 359, 362
slag iron 355
slag viscosity 356–367
solubility in slag 360
temperature 93, 359, 364
extent, commercial irons 356, 366
external desulphurization 369
mechanism of 92–97, 294, 323
rate 358
reactions 92, 350–353
Surface to volume, relationship 157
Swelling 41, 206, 233
factors influencing 235

Temperature,
blast furnace 7
burden, profile 127
combustion zone 7, 304, 318
difference, gas-solid 122
effect of, on
diffusivity 37
reaction rate 27
reduction rate 33, 237
slag viscosity 54–56
flame 245, 256
gas 127
higher blast, effect on,
coke rate 388
fusion zone 134, 336
furnace movement 136, 336, 389, 450
oxidizing zone 311
productivity 450
raceway, effect,
fuel addition 255
moisture addition 245
oxygenation 244, 247, 260
relation to Mn, S, Si contents 292
Temperature profile, furnace 118–135
Testing methods 215–222
physical 218–222
reducibility 215–222
Thermal balance 119, 380
and coke rate 380
Thermal conductivity 125
Thermal efficiency, blast furnace 376
Thermal reserve zone (see Reserve zone)
Thermodynamics limit 404
Thermodynamics, blast furnace,
hearth reactions 288–305
slag-metal reactions 87–97
TiC-TiN precipitation 300
Titania,
mechanism, reduction 300
reduction rate 300
slag-metal equilibrium 300
Top control 461
Top gas,
analyses 8
available energy 126
CO/CO_2 ratio 8, 386
CO-utilization 386, 397
sensible heat in 126, 377
temperature 8
cause, variation 375–380
Top pressure (see High top pressure)
Top temperature 8
Top, blast furnace 5, 172–175
Topochemical reaction 28
Transit time, ore 285
burden 12
gas 143, 456
Transport,
gaseous 31
heat 125
mass 57
mechanisms 31, 35, 57
reaction steps 30
Transport control, in
gas-solid reaction 34
slag-metal reaction 57
resistance concept 30, 58
Tumbler (drum) test,
cold and hot 219
reducing gas 217, 220
Tuyere burning 510

Tuyere zone (see also Raceway and Combustion zone) 303
combustion reactions 305
dimensions and control 308–320
heat exchange in 122, 322
re-oxidations in 320
temperatures,
gas 318
smelting products 119
Tuyeres,
additions at 255
effect on gas temperature 255
auxiliary 312
combustion at 306
gas analysis from 304
fuel injection at 316

Upper zone, reactions in 12, 268–272

Vaporization,
alkali metals 112
aluminium 301
lead 298
lime 302
magnesia 302
moisture 269
phosphorus 297
SiO 88
SiS 293, 351
zinc 297
Variations, stock and gas movements 184
Velocity of reaction (see Kinetics of reaction)
Viscosity,
blast furnace gas 143
hydrogen 143
slags,
hearth 53, 98–107
primary 335
Void fraction (see Voidage)
Voidage,
effect of, on pressure drop 142
effect of size ratio on 148–151
Volume ratio, spheres 157

Wagner,
half-cell reaction 57, 97
interaction coefficient 17
Water,
reaction with coke 83, 287
Water cooling, lining 5
Water equivalent,
gas and solids 120
Kitaev's theory 122
ratio, influence on gas-solids temperature 122
Water gas (shift) reaction 85, 269, 287
approach to equilibrium 86, 287
catalysts in 86, 270
effect of, on
wustite reduction 287
overall fuel efficiency 87
in middle furnace 288
in upper furnace 269
Wind (see Blast)
Whisker, formation 41, 233
Wustite 68
composition 69
formation, in sinter 200, 207
melting point 68
non-stoichiometry 68
oxygen content 69
oxygen pressure 69
reduction equilibria,
importance, coke rate 78
with CO/CO_2 mixture 74
with H_2/H_2O mixture 85
reduction rate, importance in coke rate 243, 276, 385
Wustite-alumina-silica system 98
Wustite-lime-silica system 107
Wustite-hematite-lime system 109

Zinc,
and scaffolds 499
cycle in furnace 298
reduction of 297
source of 297

Jai Haranath Jai
Kusum Kumari Jai